

Regulation of Mec1 (ATR) signaling in budding yeast

Inauguraldissertation

zur Erlangung der Würde eines Doktors der Philosophie
vorgelegt der
Philosophisch-Naturwissenschaftlichen Fakultät
der Universität Basel

von

Nicole Hustedt

aus Deutschland

Basel, 2014

Originaldokument gespeichert auf dem Dokumentenserver der Universität Basel
edoc.unibas.ch

Dieses Werk ist unter dem Vertrag „Creative Commons Namensnennung-Keine kommerzielle Nutzung-Keine Bearbeitung 3.0 Schweiz“ (CC BY-NC-ND 3.0 CH) lizenziert. Die vollständige Lizenz kann unter creativecommons.org/licenses/by-nc-nd/3.0/ch/ eingesehen werden.

**Genehmigt von der Philosophisch-Naturwissenschaftlichen Fakultät
auf Antrag von**

Prof. Dr. Susan Gasser

Prof. Dr. Philippe Pasero

Basel, den 16.09.2014

Prof. Dr. Jörg Schibler (Dekan)

THESIS OVERVIEW

This PhD thesis is based on the following publications:

Hustedt, N., Seeber, A., Sack, R., Bhullar, B., Vlaming, H., van Leeuwen, F., Guenole A., van Attikum, H., Srivas, R., Ideker, T., Shimada K., Gasser, S.M. Yeast PP4 interacts with ATR homologue Ddc2-Mec1 and regulates checkpoint signaling. *under revision at Molecular Cell*

Hustedt, N., Gasser, S.M., and Shimada, K. (2013). Replication checkpoint: tuning and coordination of replication forks in s phase. *Genes* 4, 388-434.

Hegnauer, A.M*, Hustedt, N*, Shimada, K., Pike, B.L., Vogel, M., Amsler, P., Rubin, S.M., van Leeuwen, F., Guenole, A., van Attikum, H., et al. (2012). An N-terminal acidic region of Sgs1 interacts with Rpa70 and recruits Rad53 kinase to stalled forks. *EMBO J* 31, 3768-3783.

* These authors contributed equally to this work

This thesis consists of five chapters. Each chapter starts with a title sheet stating if and where parts or the whole chapter were published. When projects were collaborative I list my contributions, clarifying as well the contributions of others.

In the first chapter, the current knowledge of the replication checkpoint with a specific focus on *S. cerevisiae* is summarized. A large part of this chapter (Sections 1 – 5 and 6.2) is published as a review in *Genes (Basel)*, 2013. 4(3): p. 388-434. Small updates and modifications were added when appropriate. Section 6.1 called “Phosphatases downregulate the checkpoint” was modified and extended because of its special relevance to my thesis.

Chapters 2, 3 and 4 are experimental chapters. In chapter 2 the relationship between the PP4 phosphatase complex Psy2-Pph3 with the checkpoint kinase Ddc2-Mec1 is investigated. Data is presented supporting the idea that PP4 negatively regulates Mec1 checkpoint signaling. The work presented in this chapter is under revision for publication in *Molecular Cell*.

Chapter 3 contains additional data on characterization of the S-phase defective allele *mec1-100*. Several hypotheses about the cause of the specific defect are developed and tested. Furthermore, intragenic mutations that suppress the sensitivity of *mec1-100* to hydroxyurea (HU) are characterized and studied.

Chapter 4 focuses on the role of the RPA-interacting domain in the RecQ helicase Sgs1 in replication checkpoint signaling and replication fork stabilization. We show that this domain is targeted by Mec1 and once phosphorylated, can serve to recruit Rad53. Thus, we propose that Sgs1 acts as a checkpoint mediator, recruiting Rad53 to stalled replication forks for activation. This project was started by a former PhD student, Anna Maria Hegnauer, and finished as part of the PhD work presented here. It was published in *EMBO J*, 2012. 31(18): p. 3768-83.

In the last chapter, the main conclusions from this work are summarized and future directions for this research are discussed.

SUMMARY

Cells are continuously challenged by various sources of DNA damage that can contribute to cancer formation if not appropriately repaired. To cope with this threat, cells have conserved mechanisms called the DNA damage checkpoints that sense damaged DNA, stop the cell cycle, and upregulate DNA repair. Central players in these checkpoints are the PI3K-like kinases ATM and ATR (*S.c.* Tel1 and Mec1). Mec1 senses single stranded DNA (ssDNA) that is exposed at stalled replication forks and activates the S phase checkpoint. However, ssDNA, which is generated at the lagging strand during normal replication, does not cause detectable checkpoint activation. It is unknown how Mec1 is regulated in S phase. To study this, we took advantage of a mutant allele of MEC1, *mec1-100*, which is proficient for the G2 DNA damage checkpoint, but is compromised in G1-S and intra-S-phase checkpoints.

In the first part of this thesis we aimed at identifying regulatory factors. We screened for spontaneous survivors on a lethal dose of the replication fork-stalling agent hydroxyurea (HU) for *mec1-100* cells. We mapped additional mutations in *mec1-100* or mutations in either *PPH3* or *PSY2*, which form a highly conserved phosphatase (PP4) complex. In a second, more unbiased, high-throughput screen we combined *mec1-100* with a collection of 1525 gene deletions involved in chromatin processes and scored double mutants for HU sensitivity. *pph3Δ* and *psy2Δ* were among the top *mec1-100* suppressor hits, confirming a strong genetic interaction. Suppression by *pph3Δ* was correlated with the phosphorylation of the downstream kinase Rad53. However, it did not depend exclusively on Rad53, because residual suppression of *mec1-100* by *pph3Δ* could also be observed in *rad53Δ* cells. We tested whether Psy2-Pph3 might regulate Mec1 directly, and found a physical interaction between Psy2 and Ddc2-Mec1. Moreover, we found that a phosphorylation site within Mec1 (S1991) is downregulated in *mec1-100* cells and restored when Pph3 is also lost. However, we were unable to demonstrate that Pph3 dephosphorylates Mec1 directly *in vitro*. Phosphorylation required both Mec1 kinase activity and Rad53. Thus, we speculate that Mec1 phosphorylation is achieved through Rad53, which is in turn regulated by Pph3, indicating the existence of a feedback loop from Rad53 back to Mec1. Mutation of the phosphorylation site renders cells sensitive to the radiomimetic drug Zeocin, indicating an important role in the survival of DNA damage. Finally, we applied quantitative phosphoproteomics to identify Mec1 and Pph3 targets. We found that the levels of the majority of the phosphopeptides that are affected by a *tell1Δ mec1-100* mutation but not by *rad53Δ* can be rescued due to additional deletion of *PPH3*. The data presented here support a model in which Pph3 is a major regulator of Mec1 signaling.

In a second part *mec1-100* was further characterized in order to understand the mechanism by which its two point mutations outside of the catalytic domain (F1179S, N1700S) cause defects in the replication checkpoint. We find that the mutations leave kinase activity *in vitro*, oligomerization and Ddc2-Mec1 interaction intact. Genetic analysis shows that *mec1-100* is additive, rather than epistatic with mutation or deletion of any of the canonical checkpoint activating proteins Ddc1, Dna2, Dpb11, Rad24, Mrc1, Rad9, Tel1 or Chk1. Thus, we conclude that *mec1-100* does not impair function of any of these proteins. We hypothesized that the mutated region might constitute a regulatory domain that is bound by a yet unknown factor. IP experiments followed by mass spectrometry analysis did not show reproducibly decreased interaction of any protein. Additional detailed biochemical analysis is needed to fully understand the mechanism of the two *mec1-100* mutations.

We further characterize intragenic *mec1-100* suppressor mutations by mapping them to a homology model. While some mutations reside within the kinase domain, and could influence catalytic activity, others might as well be involved protein-protein interactions. We asked whether

suppression would involve Rad24 dependent Mec1 activation. Interestingly, we find that suppression by mutations in residues that might make protein-protein contacts completely requires Rad24. Other suppressor mutations relied less on Rad24. Thus, we conclude that intragenic suppression of *mec1-100* HU sensitivity employs at least two different mechanisms: one that is Rad24-dependent and a second that is Rad24-independent. These unpublished results will help in understanding Mec1 function and regulation once structural data is available.

The third experimental part resolves the role of the RecQ helicase Sgs1 in replication checkpoint signaling. It was shown before that Sgs1 and Mec1 synergistically contribute to replication fork stabilization under replication stress. Both interact with the ssDNA binding protein RPA. Here, we created a mutant, *sgs1-rl*, which lacks the RPA interaction domain. While *sgs1-rl* is proficient to stabilize stalled forks under replication stress, it is synthetic lethal with *mus81Δ*, *slx4Δ*, *slx5Δ* and *slx8Δ*. These could provide alternative means to recover stalled forks by resolving crossover structures, DNA repair or break induced replication. Sgs1 was previously shown to promote Rad53 activation in a manner independent of its helicase activity. We show here that Sgs1 checkpoint function requires the R1 domain. Mec1 phosphorylates Sgs1 in this domain and Sgs1 phosphorylation allows its binding to Rad53 *in vitro* and *in vivo*. We thus propose that Sgs1 serves as a mediator in checkpoint signaling by recruiting Rad53 to stalled replication forks for activation.

This work provides new insights into Mec1 signaling by elucidating the checkpoint function of Sgs1 and defining Psy2-Pph3 as a major regulator of this pathway.

TABLE OF CONTENTS

Thesis overview	3
Summary.....	4
Chapter 1: Introduction	7
1. Introduction	8
2. Replication Checkpoint Initiation.....	11
3. Activation of Effector Kinases	17
4. Targets of the Replication Checkpoint.....	20
5. Coordination between ATR ^{Mec1} and ATM ^{Tel1}	29
6. Checkpoint Recovery.....	31
7. Scope of my projects	36
References.....	38
Chapter 2: Yeast PP4 interacts with ATR homologue Ddc2-Mec1 and regulates checkpoint signaling.....	57
Introduction.....	58
Results.....	60
Discussion	78
Experimental Procedures	81
Author Contributions	82
Acknowledgements.....	82
References.....	83
Supplemental Material To Chapter 2	87
Chapter 3: Characterization of <i>mec1-100</i>, an S-phase defective allele of <i>MEC1</i>.....	105
Introduction.....	106
Results and Discussion.....	107
Experimental procedures.....	115
Acknowledgements.....	120
References.....	121
Chapter 4: An N-terminal acidic region of Sgs1 interacts with Rpa70 and recruits Rad53 kinase to stalled forks.....	123
Chapter 5: Concluding Remarks And Future Prospects.....	141
Chapter 6: Appendix	155
List of abbreviations	156
Tables 2.1-2.4 and 2.6 (related to Chapter 2).....	163
Curriculum Vitae	253
Acknowledgements.....	259

CHAPTER 1: INTRODUCTION

Hustedt, N., Gasser, S. M., and Shimada K.

Friedrich Miescher Institute for Biomedical Research, Maulbeerstrasse 66, CH-4058 Basel, Switzerland

Based on the published review

Hustedt, N., S.M. Gasser, and K. Shimada, Replication Checkpoint: Tuning and Coordination of Replication Forks in S Phase. *Genes (Basel)*, 2013. 4(3): p. 388-434.

(part of a special issue on DNA replication)

CONTENT AND AUTHOR CONTRIBUTIONS

Sections 1 to 5 and 6.2 from this chapter were published in *Genes (Basel)*, 2013. 4(3): p. 388-434, but slightly modified and updated where appropriate. Section 6.1 was extended and modified because of special interest to this work. NH independently wrote the introduction (Section 1), sections on Replication checkpoint initiation (Section 2), Effector kinase activation (Section 3) and phosphatases (Section 6.1). KS contributed to sections on checkpoint targets (Section 4), ATM/ATR coordination (Section 5), and phosphatase-independent checkpoint downregulation (Section 6.2) and SMG made editorial corrections.

SUMMARY

Checkpoints monitor critical cell cycle events such as chromosome duplication and segregation. They are highly conserved mechanisms that prevent progression into the next phase of the cell cycle when cells are unable to accomplish the previous event properly. During S phase, cells also provide a surveillance mechanism called the DNA replication checkpoint, which consists of a conserved kinase cascade that is provoked by insults that block or slow down replication forks. The DNA replication checkpoint is crucial for maintaining genome stability, because replication forks become vulnerable to collapse when they encounter obstacles such as nucleotide adducts, nicks, RNA-DNA hybrids, or stable protein-DNA complexes. These can be exogenously induced or can arise from endogenous cellular activity. Here, we summarize the initiation and transduction of the replication checkpoint as well as its targets, which coordinate cell cycle events and DNA replication fork stability.

1. INTRODUCTION

Dividing cells go through cycles of cell growth, DNA replication, chromatin condensation, chromosome segregation, and cell division. All these highly complicated processes need to be accurately performed and tightly controlled in order to produce viable offspring. Checkpoints were initially characterized as mechanisms that ensure that a certain process is started only after the previous one has been successfully completed (Hartwell and Weinert, 1989). Originally, yeast genetic studies identified checkpoint genes that ensured cell survival and delayed the onset of mitosis during DNA replication arrest, yet many of these factors are now known to be involved in the DNA damage response (Allen et al., 1994; Friedel et al., 2009; Weinert et al., 1994). Thus, in addition to preserving the order of events, checkpoint factors contribute to the maintenance of genome stability (Harper and Elledge, 2007). The loss of genome stability has extremely deleterious consequences, including malignant transformation or cell death (Haering and Nasmyth, 2003).

Cells are exposed to many types of exogenous and endogenous stress that can modify or damage the DNA. These include oxidative stress, ionizing or UV-light mediated irradiation, and chemical damage, as well as inherent DNA compaction, tightly bound DNA binding proteins, and transcription. Even excessive or premature initiation of replication can cause replicative stress (Halazonetis et al., 2008), arguing that normal DNA metabolism itself can interfere with DNA replication (Aguilera and Gomez-Gonzalez, 2008). This is particularly true in cells with perturbed G1/S control, such as oncogene-transformed cells. In response to excessive DNA damage, wild-type cells arrest the cell cycle in G1 phase, before starting DNA replication, or in G2 phase before entering mitosis (Elledge, 1996). On the other hand, replication fork-associated damage provokes a response that delays progression through S phase, by controlling forks and initiation events (Santocanale and Diffley, 1998; Shirahige et al., 1998; Tercero and Diffley, 2001).

At the heart of all DNA damage checkpoint responses, are the two kinases Tel1 (telomere maintenance 1; ATM in mammals, see Table 1.1 for an overview of checkpoint protein names in several model organisms) and Mec1 (Mitosis Entry Checkpoint 1; ATR in mammals) (Figure 1.1) (Friedel et al., 2009). Both are phosphoinositide 3-kinase (PI3K)-related kinases (PIKKs) that share significant sequence homology and phosphorylate an overlapping set of substrates. Both show a preference for serine or threonine residues followed by glutamine ([S/T] Q) or a hydrophobic residue (Chan et al., 1999; Cortez et al., 1999; Kim et al., 1999; Sweeney et al., 2005). Often these target sites are found in SQ/TQ cluster domains (SCDs) (Traven and Heierhorst, 2005). All PIKKs, not only Mec1 and Tel1, share a common domain architecture in which the kinase domain is flanked by both FRAPP, ATM, TRRAP (FAT), and FAT C-terminal (FATC) domains (Figure 1.2A), all being conserved alpha-helical regions (Bosotti et al., 2000; Cimprich and Cortez, 2008). Because FAT and FATC domains are always present in combination, it has been suggested that these two domains interact with each other, potentially providing a scaffold or binding sites for other proteins (Bosotti et al., 2000).

In budding yeast, Mec1 is active even in an unperturbed S phase, as it can regulate dNTP levels and replication initiation without blocking cell cycle progression (Randell et al., 2010; Zhao et al., 2001). ATR^{Mec1} becomes hyperactivated in response to a wide variety of DNA insults and is essential for cell viability, whereas ATM^{Tel1} is activated primarily by double-strand breaks (DSBs) and its loss in budding yeast is not lethal. Nonetheless, in mammalian cells, mutation of either homolog leads to an elevated predisposition towards cancer (Cimprich and Cortez, 2008). Once localized to the site of DNA damage and activated by DNA damage sensing proteins, either kinase can initiate a signaling cascade that transduces the signal through mediator proteins Mrc1 and Rad9 (Claspin, BRCA1, MDC1 and 53BP1 in mammals) to the effector kinases Rad53 and Chk1 (CHK2 and CHK1 in mammals) (Figure 1.1) (Alcasabas et al., 2001; Pelliccioli et al., 1999; Sanchez et al., 1999; Sanchez

et al., 1996). Effector kinases are transiently recruited to sites of DNA damage and are released after their activation (Gilbert et al., 2001; Katou et al., 2003), allowing transmission of the checkpoint response to a range of effector proteins (Gardner et al., 1999). In addition to the effector kinases, Mec1 and Tel1 also phosphorylate proteins bound at sites of damage, such as budding yeast histone H2A (the H2AX variant in mammals), generating γ H2AX, to provoke local chromatin changes (Downs et al., 2000).

DNA damage occurs in all stages of the cell cycle, yet cells are particularly vulnerable to insults during DNA replication, when the double helix is unwound. Indeed, in S phase, defects in one strand can have serious consequences on the integrity of the daughter chromosome. Moreover, the single-stranded DNA (ssDNA) that is generated during replication, is intrinsically more labile than double-stranded (dsDNA) (Lindahl, 1993). To cope with this danger, cells provide a surveillance mechanism called intra-S-phase or DNA replication checkpoint (Figure 1.1A). This checkpoint slows genome replication by inhibiting the firing of late origins (Santocanale and Diffley, 1998; Shirahige et al., 1998), and protects stalled replication forks by preventing their conversion to DSBs and/or reducing recombination events (Cobb et al., 2005; Sogo et al., 2002; Tercero et al., 2003). Consistently, it has been shown that the loss of replication checkpoint factors provokes high levels of spontaneous gross chromosomal rearrangements in budding yeast (Myung et al., 2001). The factors involved in this checkpoint are highly conserved and many, including ATR itself, have tumor suppressor roles in mammals (Aguilera and Gomez-Gonzalez, 2008).

Table 1.1: Conserved checkpoint proteins and their functions.

<i>S. cerevisiae</i>	<i>S. pombe</i>	<i>H. sapiens</i>	Function
Rad24-RFC	Rad17-RFC	RAD17-RFC	RFC-like complex, 9-1-1 clamp loader
Ddc1-Rad17-Mec3	Rad9-Rad1-Hus1	RAD9-RAD1-HUS1	9-1-1 complex, DNA damage checkpoint clamp, Mec1 activation
Dpb11	Cut5/Rad4	TOPBP1	Mec1 ATR activation
Dna2	Dna2	DNA2	Mec1 activation in S phase
Mre11-Rad50-Xrs2	Mre11/Rad32-Rad50-Nbs1	MRE11-RAD50-NBS1	MRX/MRN complex, DSB resection, Tel1/ATR recruitment
Mec1-Ddc2	Rad3-Rad26	ATR-ATRIP	checkpoint signaling kinase
Tel1	Tel1	ATM	checkpoint signaling kinase
Mrc1	Mrc1	Claspin	fork-associated, checkpoint mediator
Rad9	Crb2	53BP1, BRCA1	checkpoint mediator
Sgs1	Rqh1	BLM, WRN	fork-associated, Rad53 activation
Rad53	Cds1	CHK2	effector kinase
Chk1	Chk1	CHK1	effector kinase

Gene name abbreviations: Rad24 (radiation sensitive 24), RFC (replication factor c), Ddc1 (DNA damage checkpoint 1), Mec3 (Mitosis entry checkpoint 3), Hus1 (hydroxyurea sensitive 1), Dpb11 (DNA polymerase B.11), Cut5 (cell untimely torn 5), TOPBP1 (DNA topoisomerase 2 binding protein 1), Dna2 (DNA synthesis defective 2), Mre11 (meiotic recombination 11), Xrs2 (X-ray sensitive 2), Nbs1 (Nijmegen breakage syndrome 1), ATR (ATM and Rad3-related), ATRIP (ATR interacting protein), Tel1 (telomere maintenance 1), ATM (Ataxia telangiectasia mutated), Mrc1 (mediator of the replication checkpoint 1), Crb2 (cut5 repeat binding 2), 53BP1 (tumor suppressor p53 binding protein 1), BRCA1 (breast cancer 1, early-onset), Sgs1 (slow growth suppressor 1), rqh1 (RecQ-type DNA helicase 1), BLM (Bloom syndrome protein), WRN (Werner syndrome ATP-dependent helicase), Cds1 (checking DNA synthesis 1), CHK2 (checkpoint kinase 2), CHK1 (checkpoint kinase 1).

Here we review recent findings on the replication checkpoint. We will first discuss the nature of the DNA lesions that provoke a checkpoint response. We then describe the mechanism of ATR^{Mec1} activation and summarize the functions served by the replication checkpoint, especially with respect to replication fork stability. We will discuss how cells downregulate the checkpoint signal to resume the cell cycle after the insult has been removed, and finally examine the coordination between two checkpoint PIKK kinases, ATR^{Mec1} and ATM^{Tel1}. Although we focus primarily on insights from studies in budding yeast, we relate those findings to results obtained from other organisms.

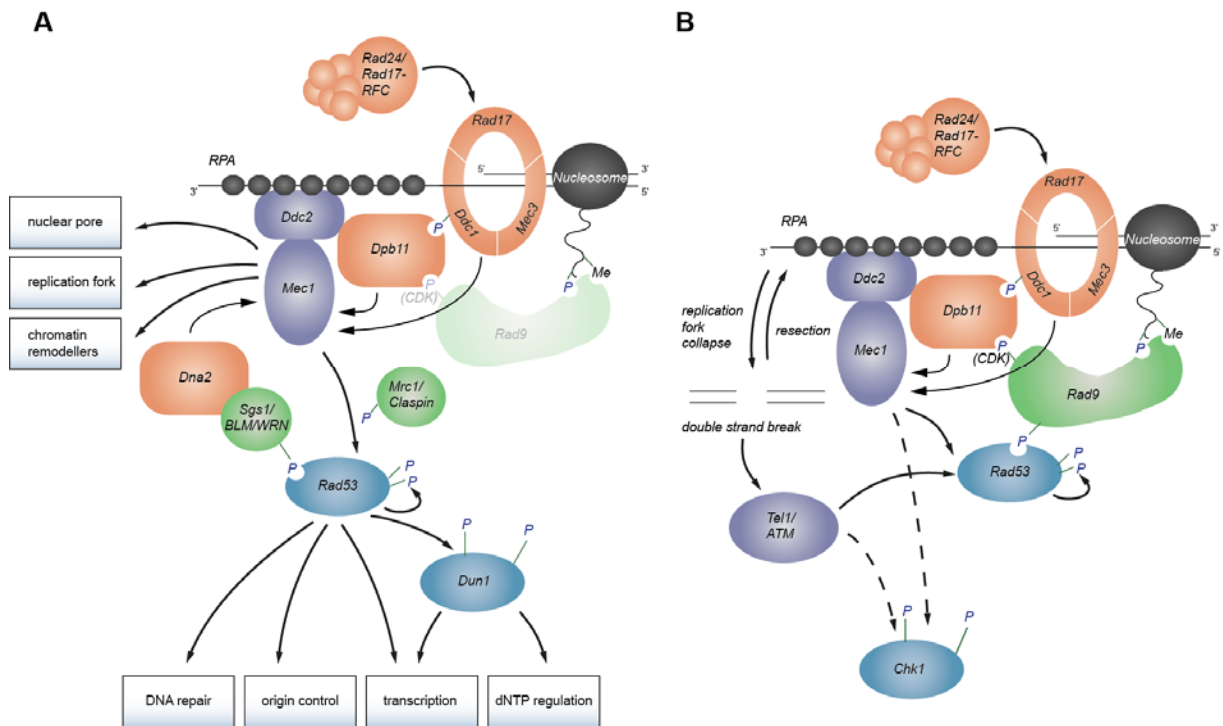


Figure 1.1: Checkpoint signaling network. (A) Replication checkpoint signaling. The yeast equivalent to ATRIP, Ddc2, binds ssDNA that is covered with RPA, while the 9-1-1 checkpoint clamp is loaded onto ds/ssDNA junctions. Dpb11, 9-1-1, and Dna2 (checkpoint sensors, orange) can activate Ddc2-Mec1 (checkpoint kinase, purple). Checkpoint mediators like Mrc1 and Sgs1 (green) help activate Rad53 (checkpoint transducing kinase, blue). Rad53 activates Dun1 and other downstream responses. (B) DNA damage checkpoint signaling. Crosstalk between Mec1 and Tel1 (DSB response) can occur, if stalled replication forks collapse, since they can generate DSBs. These are resected to generate ssDNA which activates Mec1. Rad9, the DNA damage checkpoint mediator, can be recruited by histone modifications and also binds, once phosphorylated by CDK, to Dpb11. In addition, both Mec1 and Tel1 can activate the Chk1 kinase.

2. REPLICATION CHECKPOINT INITIATION

2.1 LESIONS THAT ACTIVATE THE CHECKPOINT

Replication forks themselves play a critical role in inducing a checkpoint signal. Only when a critical number of replication forks initiate and encounter lesions, will the replication checkpoint signal become robust (Shimada et al., 2002; Tercero et al., 2003). This has seeded the notion of a threshold for activation of the replication checkpoint. After treatment with a replication stress-inducing drug (hydroxyurea, HU), long stretches of ssDNA (about 200 nucleotides) are exposed at stalled forks (Sogo et al., 2002). These extended stretches of ssDNA themselves contribute to the induction of the checkpoint response, but they are not sufficient: a double-stranded primer with a free 5' end is also required (MacDougall et al., 2007). The ds-ssDNA junction structure can arise from a variety of replication and repair processes, such as lagging strand DNA synthesis, nucleotide excision repair (Huang et al., 1992), or from resection at DSBs. This structure is recognized by the 9-1-1 checkpoint clamp and its loading factor (see below and Figure 1.1AB). At DSBs ATM^{Tel1} is recruited and activated initially by the Mre11-Rad50-Nbs1^{Xrs2} complex, which then promotes resection. Resection generates ssDNA and a ds-ssDNA junction, which in turn activate ATR^{Mec1} (Costanzo et al., 2001; Jazayeri et al., 2006; Myers and Cortez, 2006; Shiotani and Zou, 2009) (see also Section 5). Both at resected DSBs and at stalled replication forks, ssDNA is rapidly coated with the trimeric ssDNA binding complex RPA (replication protein A) (Alani et al., 1992). RPA-bound ssDNA interacts with ATRIP^{Ddc2}, an essential cofactor of the ATR^{Mec1} kinase (Ball et al., 2005; Zou and Elledge, 2003) (Figure 1.1). Mutations in RPA that disrupt its interaction with ATRIP^{Ddc2} reduce checkpoint activation (Ball et al., 2007; Dubrana et al., 2007; Kim and Brill, 2001; Zou and Elledge, 2003). In budding yeast, the RPA-Ddc2 interaction also requires Mec1, suggesting either that there may be an independent RPA binding surface on Mec1, or that Mec1 changes Ddc2 conformation in a way that favors RPA interaction (Nakada et al., 2005).

The ds-ssDNA junctions are recognized by the Rad24-RFC complex that loads the 9-1-1 checkpoint clamp (Ddc1, Rad17 and Mec3 in *S. cerevisiae*). *In vitro* analysis argues that 9-1-1 can be loaded at both 3' and 5' junctions, although if RPA is bound to the ssDNA, the 9-1-1 complex prefers to load at 5' junctions. These structures, together with RPA, are sufficient to activate the ATR^{Mec1} checkpoint in a cell-free system (MacDougall et al., 2007; Majka et al., 2006a). In budding yeast, Mec1 phosphorylates the Ddc1 subunit (human RAD9) of the 9-1-1 complex, which can then recruit Dpb11 (human TopBP1). TopBP1^{Dpb11} further stimulates ATR^{Mec1} kinase activity (Delacroix et al., 2007; Furuya et al., 2004; Lee et al., 2007; Mordes et al., 2008a; Mordes et al., 2008b; Paciotti et al., 1998; Puddu et al., 2008). This indicates that in addition to its loading onto ssDNA, ATR^{Mec1}-ATRIP^{Ddc2} needs to contact an activator in order to induce the checkpoint response (see Section 2.3). In addition to this, several studies have suggested that mismatch repair factors at the site of DNA damage provide an alternative means to recruit and activate ATR^{Mec1} (Liu et al., 2010; Pabla et al., 2011; Wang and Qin, 2003)¹.

2.2 DRUGS USED TO INDUCE AND STUDY CHECKPOINT RESPONSES

As mentioned above, special DNA structures initiate the ATR^{Mec1} checkpoint response. To study the replication checkpoint and downstream responses *in vivo*, a variety of DNA-damaging and fork stalling agents are used, and these provoke the checkpoint response in different ways (summarized in Table 1.2). Natural replication fork stalling can also occur, generally due to secondary

¹ Moreover, a recent study suggested that ATR^{Mec1} can localize to the nuclear envelope independently of RPA or DNA damage (Kumar, et al., 2014).

DNA structures (e.g. G-quadruplexes), RNA-DNA hybrids found at genes, tightly bound transcription complexes (e.g. at rDNA or tRNA genes) or specific protein-DNA complexes, like that formed by the replication fork barrier protein (Fob1), which prevents forks from colliding with RNA PolII in the rDNA repeats (Azvolinsky et al., 2009; Lambert and Carr, 2005). Natural fork pausing, however, does not provoke a global checkpoint response. We note that the proteins involved in a chemically induced checkpoint response depend on the type of damage induced and can vary with the dose applied, as demonstrated recently for camptothecin (Ray Chaudhuri et al., 2012). Further complexity in the checkpoint network stems from differences in cell type or genetic background. For example, the checkpoint response is more prone to be activated in cells deficient for DNA repair, such as the *rad18* mutant, which is deficient for post-replication repair (Hishida et al., 2009; Huang et al., 2013). Other lesions that expose primed ssDNA and activate the replication checkpoint arise when replicative helicase and polymerase functions are uncoupled (Byun et al., 2005) (Figure 1.3A, B). Here we summarize commonly used treatments that induce the checkpoint response, and highlight differences in the responses they elicit.

Table 1.2: *S. cerevisiae* checkpoint responses differ, depending on the treatment.

Treatment/Impediments	Mode of action	Result	Responders (<i>S.cerevisiae</i>)
hydroxurea (HU)	inhibits ribonucleotide reductase—dNTP pools become depleted	uncoupling of helicase and polymerase function; ssDNA is exposed	Mec1, Mrc1, Sgs1
aphidicolin	inhibits DNA polymerases	uncoupling of helicase and polymerase function; ssDNA is exposed	Mec1, Mrc1
methylnmethanesulfonate (MMS)	alkylates DNA	uncoupling of helicase and polymerase function; ssDNA is exposed; in addition DNA repair takes place, that also leads to ssDNA; requires replication forks to induce checkpoint response	Mec1, Rad9 (Mrc1, Sgs1)
ultraviolet light/4-NQO	induces Thymidine dimerization	induces DNA repair, that leads to ssDNA	Mec1, Rad9, Mrc1
crosslinking agents (cisplatin/nitrogen mustard)	causes DNA inter-strand crosslinks	both helicase and polymerase are blocked; in addition DNA repair takes place, that also leads to ssDNA	Mec1/Tel1, Rad9
ionizing irradiation (IR)/bleomycin	causes single and double strand breaks	breaks are directly recognized by MRX-Tel1; resection leads	Mec1/Tel1; Rad9

		to ssDNA	
camptothecin (CPT)	inhibits Topoisomerase I, keeps it in a DNA-bound confirmation	both helicase and polymerase are blocked; double strand breaks are actively induced by DNA repair machinery	Mec1/Tel1, Rad9
natural fork barriers (rDNA, t-RNA genes, transcription)	slow down replisome progression	both helicase and polymerase are slowed down	-

One commonly used means to trigger the replication checkpoint is to treat cells with either hydroxyurea (HU) or aphidicolin. HU inhibits ribonucleotide reductase (RNR) by reducing the reactive tyrosyl radical in the active center of the enzyme (Eklund et al., 2001). When replication is initiated, dNTP pools are rapidly depleted if RNR is inhibited (Poli et al., 2012), and this leads to a stalling of DNA polymerases. Aphidicolin, on the other hand, directly inhibits DNA polymerases (Ikegami et al., 1978) without affecting the replicative helicase (Pacek and Walter, 2004). Accordingly, polymerases are blocked, but MCM helicases continue to move, generating long stretches of ssDNA that trigger the replication checkpoint (MacDougall et al., 2007). It should be noted that HU also induces an oxidative stress and a transcriptional response to DNA damage, even in G1 phase.

Interstrand crosslinks (ICs), such as those caused by cisplatin, do the opposite: they tend to block the MCM helicase in front of the replication fork. There is no uncoupling of helicase and polymerase, and hence no immediate activation of the replication checkpoint. However, often the replication forks pause 20-40 nucleotides before reaching the IC lesion, and often structure-specific nucleases will process the template or nascent strand, generating ssDNA (Lambert et al., 2003; Raschle et al., 2008), which in turn leads to checkpoint activation.

Methyl methane sulfonate (MMS) creates bulky lesions by alkylating DNA. Alkylation alone does not elicit the checkpoint response, but requires that the replication fork collides with the DNA adduct. Therefore, MMS-induced checkpoint responses are restricted to S-phase cells (Tercero et al., 2003). Although both MMS and HU activate an S-phase checkpoint, it is important to note that they do not provoke equivalent responses (Ball et al., 2007; Emili, 1998; Liu et al., 2003; Pelliccioli et al., 1999). In response to MMS, cells activate several repair pathways, including base excision repair (BER), DNA damage tolerance pathways such as trans-lesion synthesis (Vazquez et al., 2008), and homologous recombination (HR). However, since DSBs are not detected on MMS, it is not clear whether it is the repair process itself, or an uncoupling of leading and lagging strand synthesis, that provokes what appears to be a combined replication/DNA damage checkpoint response (Lundin et al., 2005).

Ionizing radiation (IR) or treatment with bleomycin or its derivatives (e.g. Zeocin®) cause DSBs, which activate the DNA damage response initially through the ATM^{Tel1} kinase, and after processing, through ATR^{Mec1} (Povirk, 1996). It should be kept in mind that IR or bleomycin derivatives induce oxidative damage and single-strand nicks much more efficiently than DSBs. At sufficiently high doses, UV light also provokes an ATR^{Mec1}-dependent response (Jazayeri et al., 2006), for the pyrimidine dimers caused by UV treatment are recognized by the nucleotide excision repair (NER) machinery, which itself creates a ssDNA patch during the repair process which is extended by Exo1 (Giannattasio et al., 2010; Huang et al., 1992). While these lead to ATR^{Mec1} activation, the

pathway involves Rad9 (homologue of 53BP1 or BRCA1), a mediator typically implicated at DSBs (Neecke et al., 1999). In mammals, Mre11-Rad50-Nbs1^{Xrs2} (MRN) nuclease has been shown to be involved in UV-dependent ATR^{Mec1} activation, possibly again by creating a single-strand patch (Olson et al., 2007).

Camptothecin inhibits topoisomerase I (Top1) by blocking religation after the enzyme has made a ssDNA nick and becomes covalently linked to the DNA end (Hsiang et al., 1985). These structures arrest replication forks and are cytotoxic (Hsiang et al., 1989), yet they only provoke a mild checkpoint response (Redon et al., 2003), presumably because the lesion is not accompanied by helicase-polymerase uncoupling nor extensive resection. The so-called replication run-off model (Strumberg et al., 2000) has indicated that replication forks running into these ssDNA nicks are converted into DSBs, which generally depend on a recombination-dependent mechanism for replication fork restart (Ray Chaudhuri et al., 2012; Regairaz et al., 2011). Recent data indicate that torsional stress generated by Top1 inhibition may lead to fork slowing, and suggest that the formation of a DSB is an active process involving cleavage by the endonuclease Mus81. An artificial system that generates a similar lesion uses a mutant form of the site-specific Flp recombinase to generate a covalent protein-DNA complex, adjacent to a ssDNA nick (Nielsen et al., 2009). This lesion, like the Top1-camptothecin complex, does not induce a checkpoint response in wild-type yeast, but recruits the recombination machinery for repair following collision with a replication fork (L. Bjergbaek, personal communication). This illustrates the broad range of responses elicited by exogenous agents, and underscores the importance of highlighting the type of damaging agent used.

2.3 MEC1/ATR ACTIVATION

An accumulation of RPA-coated ssDNA recruits ATR^{Mec1}-ATRIP^{Ddc2}, just like a DSB bound by MRN^{MRX} recruits ATM^{Tel1}. However, whereas MRN^{MRX} also activates ATM^{Tel1}, ssDNA-RPA is not sufficient to induce ATR^{Mec1} activation. As discussed above, ds-ssDNA junctions that recruit the 9-1-1 checkpoint clamp are also required for activation (see Section 2.1). In budding yeast, Ddc1, a subunit of the 9-1-1 complex that binds the ds-ssDNA junction, has been shown to be capable of activating Mec1 alone under low salt conditions *in vitro* (Majka et al., 2006b; Navadgi-Patil and Burgers, 2009), just as the artificial juxtaposition of multiple Ddc1 and Ddc2 molecules can activate Mec1 *in vivo* (Bonilla et al., 2008). In higher organisms, on the other hand, RAD9^{Ddc1} instead creates a binding site for the ATR^{Mec1} activator TopBP1^{Dpb11} (Delacroix et al., 2007; Furuya et al., 2004; Lee et al., 2007). TopBP1^{Dpb11} contains eight BRCA1 C-terminal (BRCT) domains (Figure 1.2A) and interacts with phosphorylated RAD9^{Ddc1} through its BRCT domains 1 and 2. In addition, the MRN^{MRX} complex has been shown to recruit TopBP1^{Dpb11} through its BRCT domains 3-6 (Figure 1.2B) (Duursma et al., 2013). Overexpression of a domain of TopBP1^{Dpb11} that sits between its BRCT motifs 6 and 7 (called AAD for ATR activation domain), also leads to ATR^{Mec1} activation. Indeed, one can bypass the need for the intact 9-1-1 clamp by tethering the AAD to PCNA or histone H2B (Delacroix et al., 2007; Kumagai et al., 2006). TopBP1^{Dpb11} itself binds to ATRIP^{Ddc2}, and mutations within its TopBP1^{Dpb11} binding region can block ATR^{Mec1} activation. Finally, a region of ATR^{Mec1}, between the kinase and the FATC domain, is important for TopBP1^{Dpb11}-mediated ATR^{Mec1} activation (Mordes et al., 2008a) (Figure 1.2A, B). Here, however, molecular details are scarce, as there are no structural data available for ATR^{Mec1}. This RAD9^{Ddc1}-TopBP1^{Dpb11} pathway for ATR^{Mec1} activation is also found in budding yeast. Dpb11 is recruited by Ddc1, which is phosphorylated by Mec1 (Puddu et al., 2008), although either Ddc1 or Dpb11 can activate Mec1 on its own (Mordes et al., 2008b; Navadgi-Patil et al., 2011; Wang and Elledge, 2002). The responsible regions of Dpb11 and Ddc1 have been mapped to their unstructured C-terminal tails, within which two conserved hydrophobic residues are important for Mec1 activation (Navadgi-Patil and Burgers, 2009; Navadgi-Patil et al., 2011; Pfander and Diffley, 2011).

How Ddc1 and Dpb11 act together to activate Mec1 is still under debate, and it may vary in a cell-cycle dependent manner (Figure 1.2C). Burgers' laboratory suggests that whereas the 9-1-1 subunit Ddc1 is responsible for the activation of Mec1 in response to DNA damage in G1 phase, 9-1-1 and Dpb11 cooperate to activate Mec1 in G2/M phase (Navadgi-Patil and Burgers; Navadgi-Patil et al., 2011). Dpb11 interacts with phosphorylated Rad9, which is modified by a cell-cycle regulated Cyclin-dependent kinase (CDK). Since CDK is not active in G1, this could explain why Dpb11 function is cell-cycle specific (Pfander and Diffley, 2011). In contrast, Puddu et al. have shown that Dpb11 and 9-1-1 act together in G1, while 9-1-1 is the predominant Mec1 activator in G2 (Puddu et al., 2011). Fission yeast Rad4/Cut5^{Dpb11} similarly assists Rad3^{Mec1} activation in G1, when DSB resection is restricted (Lin et al., 2012). This observation suggests that Rad4/Cut5^{Dpb11} compensates for limited ssDNA to promote full Rad3^{Mec1} activation in G1 phase (Lin et al., 2012).

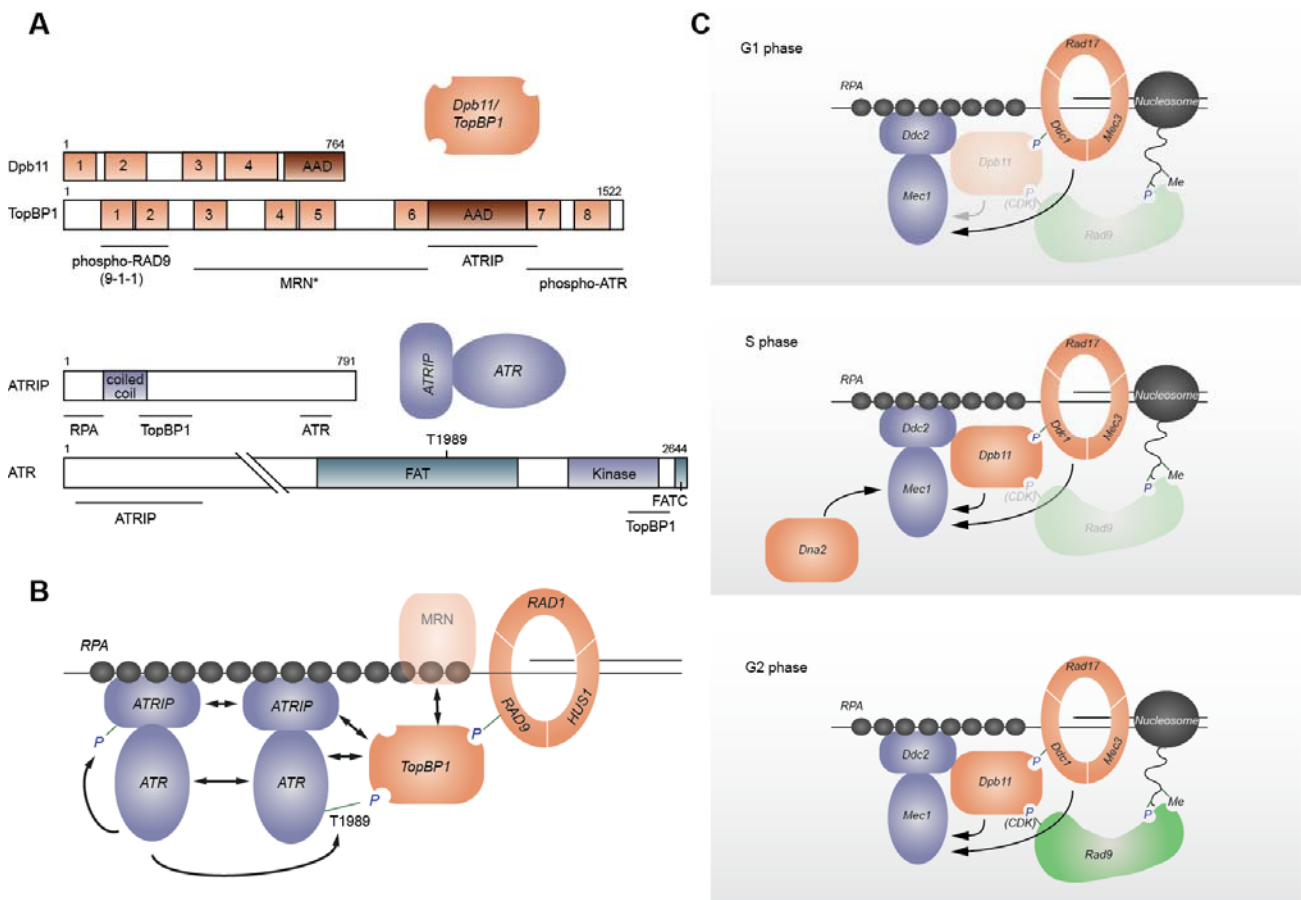


Figure 1.2: ATR/Mec1 activation. (A) Domain architecture of *S. cerevisiae* Dpb11, human TopBP1^{Dpb11}, human ATRIP^{Ddc2}, and human ATR^{Mec1}. Numbered brown boxes indicate BRCA1 C-terminal (BRCT) domains. Underlined regions interact with indicated proteins. *MRN^{MRX} interaction shown for *Xenopus* TopBP1^{Dpb11}. (B) Mammalian ATR^{Mec1} activation. TopBP1^{Dpb11} is recruited by RAD9^{Ddc1} phosphorylation and interacts with ATRIP^{Ddc2} and ATR^{Mec1}. *Xenopus* TopBP1^{Dpb11} may be recruited through MRN^{MRX}. ATR^{Mec1} autophosphorylates, and this may also contribute to interaction with TopBP1^{Dpb11}. ATRIP^{Ddc2} and ATR^{Mec1} form higher-order oligomers. (C) Cell cycle specific *S. cerevisiae* Mec1 activation. In G1 phase Ddc1, a subunit of the 9-1-1 checkpoint clamp, is the predominant Mec1 activator. In S phase, Ddc1, Dpb11, and Dna2 are able to activate Mec1. In G2 phase, both Ddc1 and Dpb11 can activate Mec1. Dpb11 is recruited through phosphorylated Ddc1 and CDK-mediated phosphorylation of Rad9, which in turn binds to modified histones. AAD—ATR/Mec1 activation domain; FAT—FRAP, ATM, TRRAP domain; kinase—kinase domain; FATC—FAT C-terminal domain.

In S-phase cells, several proteins have been reported to activate Mec1, apparently in a redundant manner. The 9-1-1 complex is recruited to stalled replication forks, and facilitates Rad53 phosphorylation (Bjergbaek et al., 2005; Katou et al., 2003). However, *dpb11* or *ddc1* mutations that

interfere with Mec1 activation (or a mutation defective in 9-1-1 loading such as *rad24Δ*), alone or in combination, show only mild defects in Rad53 phosphorylation in response to replication stress (Berens and Toczyski, 2012; Navadgi-Patil and Burgers, 2009; Navadgi-Patil et al., 2011). Recently, Burgers' laboratory has reported that Dna2, a conserved nuclease-helicase that is essential for Okazaki fragment maturation, has a role in Mec1 activation in S phase. *TEL1* and *DDC1* deletions (which also compromises Dpb11-mediated Mec1 activation) were combined with a mutation in the Mec1 activation domain of Dna2, and this eliminated Rad53 activation upon HU treatment in S phase (Kumar and Burgers, 2013). These data indicate that Dna2 functions as a third factor contributing to Mec1 activation in S phase. Here it is important to note that Dna2 binds the yeast RecQ helicase Sgs1, and that the two factors co-activate each other (Cejka et al., 2010). Sgs1 also promotes replication stress-dependent checkpoint activation, and the checkpoint defects of a *SGS1* deletion are strongly aggravated by mutations in 9-1-1 or the *RAD24* gene (Bjergbaek et al., 2005; Frei and Gasser, 2000; Fu et al., 2008). Sgs1 directly binds Rad53 in a Mec1-dependent manner, arguing that its loss does not simply generate structures that activate and require Mec1 (Hegnauer et al., 2012).

Whereas Ddc1, Dpb11 and Dna2 were all shown to enhance Mec1 catalytic activity *in vitro*, the molecular details of how they act on Mec1 are unclear. Rather than stimulating Mec1 through its kinase domain, they may serve as scaffolds that bring factors closely together. Indeed, Berens and Toczyski have shown that an artificial co-localization of Ddc2 and the replication checkpoint mediator Mrc1 elicits a downstream Rad53 kinase response in the absence of Dpb11 and Ddc1 (Berens and Toczyski, 2012). It remains possible the Dna2 serves as the crucial activator in this case, and it would be interesting to see how a *dna2* mutant defective for Mec1 activation, or the *dna2 dpb11* and *dna2 ddc1* double mutants, would behave in the Toczyski assay.

Another level of ATR^{Mec1} regulation may be inherent to the kinase itself. Recently it has been reported that human ATR^{Mec1} can autophosphorylate *in trans*, and that this phosphorylation correlates with ATR^{Mec1} activation (Liu et al., 2011; Nam et al., 2011b). It has been suggested that ATR^{Mec1} autophosphorylation assists its binding to TopBP1^{Dpb11}, which further activates the kinase (Liu et al., 2011) (Figure 1.2B). However, another study concluded that mutation of the same autophosphorylation site does not have a strong impact on ATR^{Mec1} function (Nam et al., 2011b), and the relevant target residue, Thr 1989, is not conserved in budding and fission yeast (Nam et al., 2011b). Indeed, a study that mutagenized all [S/T]Q sites in checkpoint proteins in fission yeast did not find a single [S/T]Q residue in Rad3^{Mec1} critical for its function (Yue et al., 2011). However, since the ATR^{Mec1} autophosphorylation site does not match the [S/T]Q consensus (Liu et al., 2011; Nam et al., 2011b), these results are inconclusive. It remains to be seen whether a similar autophosphorylation mechanism exists for Rad3^{Mec1} in fission yeast or for Mec1 in budding yeast.²

ATR^{Mec1} may be also controlled by regulated protein complex formation. It has recently been determined that Nek1 (Never in mitosis A-related kinase 1) promotes ATR^{Mec1}-ATRIP^{Ddc2} association in a DNA damage independent manner. The responsible phosphorylation site is unknown, but Nek1 does not seem to target ATR^{Mec1} Thr 1989 directly (Liu et al., 2013). Functional complexes may require disruption of dimers. ATM^{Tel1} forms inactive dimers, which dissociate upon autophosphorylation after DSB induction (Bakkenist and Kastan, 2003). ATR^{Mec1}-ATRIP^{Ddc2} can also form oligomers (Ball and Cortez, 2005; Itakura et al., 2005; Lee et al., 2004; Lindsay et al., 1998;

² Mec1 serine 38 phosphorylation was shown to depend on Mec1 (Chen et al., 2010). and fits to the ATR consensus ([S/T]Q), thus it is likely an autophosphorylation site. However, serine 38 mutation does not show a phenotype (Chapter 2). In Chapter 2 we show that Mec1 is also phosphorylated on serine 1991, which is important for resistance to the Zeocin. However, serine 1991 phosphorylation requires not only Mec1 but also Rad53 and thus is unlikely to be a site of autophosphorylation (Chapter 2).

Paciotti et al., 2001) and it has been speculated that the oligomerization of ATR^{Mec1}-ATRIP^{Ddc2} regulates kinase activity, even though oligomerization is independent of DNA damage or replication stress (Itakura et al., 2005; Paciotti et al., 2001). There are conflicting reports on the size of ATR^{Mec1}-ATRIP^{Ddc2} complexes, ranging from 300 to 1000 kD in size (Itakura et al., 2005; Kim et al., 2005; Majka et al., 2006b). In humans, both the coiled-coil domain of ATRIP^{Ddc2} and ATR^{Mec1} contribute to oligomerization (Ball and Cortez, 2005) (Figure 1.2A). Mutation of the human ATRIP^{Ddc2} coiled-coil domain does not impair chromatin binding, but impairs foci formation and signaling. Interestingly, this coiled-coil mutation shows stronger defects in the replication checkpoint than in the G2/M damage checkpoint (Ball and Cortez, 2005; Itakura et al., 2005). In contrast, it has been reported that in *Xenopus* the ATRIP^{Ddc2} coiled-coil domain is dispensable for both oligomerization and CHK1^{Chk1} phosphorylation (Kim et al., 2005), indicating species or cell-type specific differences.

3. ACTIVATION OF EFFECTOR KINASES

Once ATR^{Mec1} and ATM^{Tell} have been activated, these kinases signal to the downstream effector kinases, Rad53 and Chk1 (Figure 1.1). Although Rad53 is more closely related to CHK2^{Rad53} by sequence, its function is taken over by CHK1^{Chk1} in higher organisms. In response to stalled replication forks, the signaling of the replication checkpoint is mediated primarily through Rad53 in budding yeast, or by its functional homolog CHK1^{Chk1} in mammalian cells. Rad53 contains a kinase domain which is flanked by two Forkhead associated (FHA) domains, that can bind phosphorylated proteins (Durocher and Jackson, 2002). Mutations of critical residues in the FHA domains have revealed that full Rad53 activation requires at least one functional FHA domain, and that mutations of FHA2 show slightly stronger defects (Pike et al., 2003; Schwartz et al., 2003; Sweeney et al., 2005). N-terminal of each FHA domain is an [S/T]Q cluster domain (Lee et al., 2003), which becomes modified at multiple residues by either Mec1 or Tel1 (Pelliccioli et al., 1999; Sanchez et al., 1996; Sun et al., 1996). Nonetheless, genetic evidence indicates that either Mec1 or Tel1 is required, but not sufficient, for Rad53 activation (de la Torre-Ruiz et al., 1998; Emili, 1998). Rad53 activation is facilitated by at least two mediator proteins: the budding yeast Rad9 fulfills this role in the DNA damage checkpoint, while Mrc1 serves as mediator during replication checkpoint activation (Alcasabas et al., 2001; de la Torre-Ruiz et al., 1998; Navas et al., 1996; Sweeney et al., 2005). Interestingly, Rad53 also appears to be phosphorylated in a cell-cycle dependent manner, and this phosphorylation may fine-tune the checkpoint response (Schleker et al., 2010). Here we will first summarize the well-characterized molecular mechanism of Rad53 activation by Rad9, and then review current knowledge about Mrc1.

3.1 RAD53 ACTIVATION IS MEDIATED BY RAD9 IN RESPONSE TO DNA DAMAGE

Rad9 was the first cell-cycle checkpoint protein identified in budding yeast, and it has a key role as an adaptor for activating Rad53 in the DNA damage response, yet it has little or no role in the replication checkpoint triggered by HU-arrested forks (Weinert and Hartwell, 1988; Weinert et al., 1994). Rad9 does not possess enzymatic activity, but contains both tandem Tudor and BRCA1 C-terminal (BRCT) domains. Thus, the mammalian proteins BRCA1, MDC1 and 53BP1 are all considered to be functional homologs of Rad9. The Rad9 tandem Tudor domains can bind to histone H3 methylated on lysine 79 (Grenon et al., 2007), which is deposited throughout the genome by the methyltransferase Dot1 (van Leeuwen et al., 2002). In addition, Rad9 binds histone H2A phosphorylated on serine 129, using its tandem BRCT domains (Hammet et al., 2007). The H2A phosphorylation is mediated by both Tel1 and Mec1 at sites of DNA damage (Cobb et al., 2005; Downs et al., 2000; van Attikum et al., 2004), and both H3K79 methylation and phosphorylated H2A are thought to recruit Rad9 to damaged sites. Consistently, strains bearing *dot1*Δ or phospho-acceptor

mutations in H2A show defects in the G1 checkpoint activation (Giannattasio et al., 2005; Grenon et al., 2007; Hammet et al., 2007; Wysocki et al., 2005). The G2 checkpoint, on the other hand, still functions in the *dot1* mutant. Because the G2 checkpoint activity is lost in a *dpb11 dot1* double mutant, it appears that Dpb11 may also recruit Rad9 in G2 (see Section 2.3) (Pfander and Diffley, 2011; Puddu et al., 2008).

Rad9 becomes phosphorylated by Mec1/Tel1 in response to DNA damage, and is required for efficient Rad53 activation (Emili, 1998). It has been shown that phosphorylated Rad9 can bind to the Rad53 FHA domains, with a preference for FHA2 (Emili, 1998; Schwartz et al., 2002; Schwartz et al., 2003; Sun et al., 1998; Sweeney et al., 2005). This, together with the observation that the autophosphorylation of Rad53 is concentration-dependent, has led to the hypothesis that phosphorylated Rad9 locally increases Rad53 concentration, providing a scaffold for efficient Rad53 autophosphorylation and activation (Gilbert et al., 2001; Ma et al., 2006). In this model, Mec1 would be only required for initial Rad9 phosphorylation, and might not necessarily act directly on Rad53. However, more recent studies have shown that direct phosphorylation of Rad53 by Mec1/Tel1, and not only of Rad9, is required for Rad53 activation (Ma et al., 2006; Sweeney et al., 2005). Indeed, the mutation of Mec1/Tel1 target sites in Rad53's N-terminal [S/T]Q cluster domain reduced viability, replication and damage checkpoint functions, as well as its kinase activity (Lee et al., 2003).

Activation of the mammalian Rad53 homolog CHK2^{Rad53} or *S. pombe* Cds1^{Rad53} requires phosphorylation of one specific residue by upstream kinases (threonine 68 or 11, respectively) (Matsuoka et al., 2000; Tanaka et al., 2001). In the case of Rad53, the [S/T]Q sites in the N-terminal SCD seem to be redundant, and phosphorylation at multiple sites is important for activation (Lee et al., 2003; Sweeney et al., 2005). Once Rad53 has been primed by Mec1/Tel1 and fully activated through autophosphorylation, Rad9 seems to release Rad53, enabling the transduction of the checkpoint responses throughout the nucleus (Gilbert et al., 2001). Mec1/Tel1 phosphorylation of Rad9 also leads to oligomerization of Rad9. The oligomerization may be dispensable for Rad53 activation, whereas it is needed for maintenance of the checkpoint (Usui et al., 2009). Intriguingly, phosphorylation of Rad9 by Rad53 disrupts Rad9 oligomerization, providing a negative feedback mechanism for checkpoint regulation (Usui et al., 2009).

3.2 MRC1 SERVES AS A MEDIATOR IN THE REPLICATION CHECKPOINT

Whereas Rad9 acts in response to DNA damage in G1 and G2, Mrc1 is a key mediator protein for Rad53 activation in the context of DNA replication (Alcasabas et al., 2001; Osborn and Elledge, 2003; Tanaka and Russell, 2001). Mrc1 is a component of the replisome, and it travels along with replication forks (Katou et al., 2003; Osborn and Elledge, 2003). Mrc1 enhances Rad53 activation during replication stress, but does not activate Mec1 kinase activity per se. Rather, it seems to positively influence the enzyme-substrate interaction between Mec1 and Rad53, and could, therefore, recruit Rad53 to stalled forks to facilitate Rad53-Mec1 interaction (Chen and Zhou, 2009). Analogously, Claspin, the Mrc1 homolog in higher eukaryotes, contributes to replication checkpoint activation by interacting with CHK1^{Chk1}, a functional homolog of Rad53, and facilitating its activation (Chini and Chen, 2003; Kumagai and Dunphy, 2000; Kumagai et al., 2004).

In addition to its checkpoint function, Mrc1 appears to have a structural role in replication fork maintenance, as it binds to the replisome via the Csm3-Tof1 fork protection complex (Bando et al., 2009). Mrc1 interacts with Pol ϵ and Mcm6 (Komata et al., 2009; Lou et al., 2008), and Tof1 and Csm3 interact with Mcm2 (Bando et al., 2009). Thus, it has been suggested that this complex forms a bridge between the leading strand polymerase ϵ and the replicative helicase (Lou et al., 2008). Consistently, replisome structure is aberrant in the *mrc1* Δ mutant; *mrc1* Δ cells proceed faster through S phase, show an uncoupling of the replisome from the site of DNA synthesis and have impaired

recovery from HU arrest (Alcasabas et al., 2001; Katou et al., 2003; Szyjka et al., 2005; Tourriere et al., 2005). Mrc1 becomes phosphorylated by Mec1 and a mutant in which all Mrc1 [S/T]Q sites are mutated to AQ, shows a defect only in checkpoint signaling, but not in replisome progression (Alcasabas et al., 2001; Osborn and Elledge, 2003). By using this *mrc1*-AQ mutant, an alternative function for Mrc1 in the replication checkpoint has been suggested, namely, phosphorylation of Mrc1 may stabilize the association of Mec1 with sites of stalled replication forks, thereby creating a positive feedback for Mec1 function (Naylor et al., 2009). Although Mrc1 activates the replication checkpoint in response to replication stress, loss of it can be compensated by Rad9 (Alcasabas et al., 2001). Indeed, Rad9 accumulates at stalled replication forks in *mrc1* Δ cells on HU (Katou et al., 2003). It is therefore likely that loss of Mrc1 checkpoint function creates DSBs or damage structures that provoke Rad9-dependent Rad53 activation. This is a much more likely option than that Mrc1 and Rad9 are equivalent in their mode of action, given that Mrc1 is part of the replisome, and Rad9 clearly is not.

3.3 A ROLE FOR SGS1 IN RAD53 ACTIVATION

Another factor that has been shown to be involved in replication checkpoint signaling and which helps activate Rad53, is the budding yeast RecQ helicase, Sgs1 (Bjergbaek et al., 2005; Hegnauer et al., 2012). Sgs1 interacts with Dna2, RPA and Rad53, and is constitutively associated with replication forks (Cejka et al., 2010; Cobb et al., 2003; Hegnauer et al., 2012). The deletion of *sgs1* alone destabilizes DNA polymerases α and ϵ when replication forks are stalled by HU (Cobb et al., 2003), and this effect is far more pronounced when combined with either *mrc1* Δ or the S-phase specific mutant allele of *MEC1*, *mec1-100* (Cobb et al., 2003; Cobb et al., 2005; Lopes et al., 2001; Lucca et al., 2004; Paciotti et al., 2001). This leads to a synergistic arrest of growth and failed fork recovery in response to HU, and a loss of dNTPs incorporation, as both polymerases α and ϵ are lost from the replisome (Cobb et al., 2003). One explanation of the observed synergy, may be that *mec1-100* generates fold back structures that need Sgs1 for resolution. However, Sgs1 also participates in the activation of Rad53, particularly in response to HU arrest (Bjergbaek et al., 2005). Sgs1 itself contains a [S/TQ] cluster that is phosphorylated in a Mec1-dependent manner *in vivo* and *in vitro* (Hegnauer et al., 2012) (Chapter 4). When phosphorylated, this domain of Sgs1 binds Rad53, again both *in vivo* and *in vitro* (Bjergbaek et al., 2005; Hegnauer et al., 2012) (Chapter 4). Therefore, Sgs1 serves as a replication checkpoint mediator that recruits Rad53 to stalled forks, acting in much the same way as Rad9 acts at DSBs (Chapter 4). Mrc1 and Sgs1 have been found to be epistatic for their function in Rad53 phosphorylation, although Sgs1 functions in parallel with Rad24 and 9-1-1, and the double mutants are highly compromised for the activation of Rad53 at stalled forked (Bjergbaek et al., 2005; Fu et al., 2008). A RecQ homologue in mammals, the WRN^{Sgs1} helicase, has also been shown to facilitate the ATR^{Mec1}-CHK1^{Chk1} checkpoint pathway in response to camptothecin (Patro et al., 2011), indicating that RecQ function in checkpoint signaling may be conserved.

4. TARGETS OF THE REPLICATION CHECKPOINT

An activated replication checkpoint cascade transduces a multitude of stimuli that control cell-cycle and replication-fork recovery. Here, we summarize the downstream pathways that are influenced by the checkpoint. We focus on relevant replication fork targets at the end of this section, to the extent that they are known.

4.1 CELL CYCLE REGULATION

In all eukaryotic species, checkpoint effector kinases play a central role in cell-cycle arrest upon checkpoint activation, even though the mechanism of arrest differs. In fission yeasts and higher eukaryotes, $\text{CHK1}^{\text{Chk1}}$ and $\text{CHK2}^{\text{Rad53}}$ negatively regulate $\text{CDC25}^{\text{Mih1}}$ phosphatases that remove inhibitory phosphorylation on cyclin-dependent kinase (CDK) (Karlsson-Rosenthal and Millar, 2006; Rhind and Russell, 1998; Sanchez et al., 1997; Sorensen and Syljuasen, 2012). Checkpoint-dependent phosphorylation of $\text{CDC25}^{\text{Mih1}}$ down-regulates its activity through inhibition of its nuclear localization by binding 14-3-3, a nuclear-cytoplasmic shuttling protein, and through degradation by the $\text{SCF}^{\text{BTrcp}}$ ubiquitin ligase (Busino et al., 2003; Jin et al., 2003; Peng et al., 1997). Therefore, DNA replication and the damage checkpoint down-regulates the CDK cell cycle engine, thereby blocking G2/M transition. In *S. cerevisiae*, however, this cell-cycle arrest by CDK inhibition does not occur (Sorger and Murray, 1992). Nonetheless, checkpoint mutants exhibit a cytologically typical mitotic arrest defect, with elongated spindles in response to blocked replication forks (Allen et al., 1994; Paulovich and Hartwell, 1995; Weinert et al., 1994). Budding yeast cells transmit the checkpoint signal to inhibit progression of mitosis by stabilizing securin^{Pds1}, which inhibits the metaphase to anaphase transition, and by stimulating the Bub2/Bfa1 GAP complex which inhibits the mitotic exit network (Clarke et al., 2001; Hu et al., 2001; Sanchez et al., 1999). Microtubule elongation is also blocked (Krishnan et al., 2004).

4.2 ESSENTIAL FUNCTION FOR CELL VIABILITY—dNTP POOL REGULATION AND FORK MAINTENANCE?

Intriguingly, *Mec1* and *Rad53* and their functional homologs ATR^{Mec1} and $\text{CHK1}^{\text{Chk1}}$ are essential for cell proliferation, but this is not due to their checkpoint function (Brown and Baltimore, 2000; de Klein et al., 2000; Desany et al., 1998; Liu et al., 2000; Takai et al., 2000; Zhao et al., 1998). In *S. cerevisiae*, the lethality of *mec1* or *rad53* deletions can be bypassed by up-regulating the dNTP pool with another mutation (Desany et al., 1998; Zhao et al., 1998). In *S. pombe*, on the other hand, neither $\text{Rad3}^{\text{Mec1}}$ nor $\text{Cds1}^{\text{Rad53}}$ are encoded by essential genes, raising the question of whether the critical dNTP regulating function of these checkpoint kinases is conserved. In mammalian cells NTP pool control through c-Myc appears to be a determinant of dNTP levels (Bester et al., 2011).

In *S. cerevisiae* dNTP levels increase 8-fold in response to DNA damage, an increase that facilitates cell survival, even as it increases the mutation rate (Chabes et al., 2003). Given the pleiotropic effects of dNTPs, it is reasonable that cells have multiple pathways that regulate dNTP concentrations, one of which is through the Dun1 kinase, a target of *Rad53* (Nordlund and Reichard, 2006) Dun1 phosphorylates *Sml1* and *Dif1*, which inhibit ribonucleotide reductase (RNR), priming them for degradation (Lee et al., 2008; Zhao and Rothstein, 2002). Dun1 also induces RNR gene transcription by inhibiting the transcriptional repressor *Crt1* (Huang et al., 1998). Given that the failure to regulate dNTPs is lethal, these pathways are obviously very important in budding yeast.

A recent study from the Longhese laboratory has revealed that the essential functions of *Mec1* and *Rad53* can also be bypassed by lowering the activity of *Cdc28*, the budding yeast CDK (Manfrini

et al., 2012). Similarly, a delayed entry into S or M phase provoked by lowered levels of G1- or M-phase cyclins, improves the survival of *mec1Δ* or *rad53Δ* cells on low doses of HU. This suggests that either extending G1, prior to S phase entry, or a reduction in the number of active replication forks, compensates for the lethal effects of checkpoint kinase ablation. Most likely, this suppression is explained by the fact that cells have sufficient time both to generate dNTPs and to complete replication. Surprisingly, lowered rates of microtubule elongation provoked by *cin8* mutation, also suppresses the lethality of *mec1Δ* or *rad53Δ* cells. Both survival on HU and the ensuing completion of replication improve in the *cin8* mutant, suggesting that centromere segregation by a premature mitotic spindle, is another lethal consequence of *mec1* or *rad53* ablation. Similarly, the inhibition of microtubule elongation through nocodazole diminishes Rad52 repair foci, which are induced in cells bearing the temperature-sensitive *mec1-14* mutation at elevated temperatures in S phase (Manfrini et al., 2012). Together, these data suggest that checkpoint kinases also coordinate the completion of replication with microtubule elongation, in line with the original concept of checkpoints: that is, to preserve the order of cell-cycle events. We note, however, that the experiments in the cited study used either no or low dose HU. Indeed, after treatment with a high doses of HU or MMS, the essential function of the replication checkpoint was shown to be its ability to facilitate the restart of replication forks once the lesions have been removed (Desany et al., 1998; Tercero et al., 2003). This may act by preventing the accumulation of aberrant DNA structures and/or fork collapse (Cobb et al., 2003; Cobb et al., 2005; Lopes et al., 2001; Lucca et al., 2004) (see Section 4.6).

Mec1 and ATR^{Mec1} are known to prevent chromosome breakage at fragile sites where replication forks frequently slow down, even in the absence of exogenous damage (Casper et al., 2002; Cha and Kleckner, 2002). Given the fact that ATR^{Mec1} is an essential protein in mammalian cells, and given that there are many more obstacles that impair fork progression in higher eukaryotes, it may well be that overcoming intrinsic replication stress is the essential role for ATR^{Mec1}/CHK1^{Chk1} in higher organisms.

4.3 ORIGIN CONTROL

DNA replication is initiated by a series of steps that proceed in a sequential manner. In the first step, known as licensing, the pre-replicative complex (pre-RC) is loaded onto DNA at the origins of replication in G1 phase, when CDK activity is low. The pre-RC consists of ORC, Cdc6, Cdt1, and Mcm2-7. In the second step, the essential helicase components Cdc45 and GINS, together with DNA polymerases, are brought onto pre-RC by the bridging factors Sld3-Sld7 and Dpb11-Sld2 in a CDK- and DDK- (Dbf4 dependent kinase, CDC7^{Cdc7}-DBF4^{Dbf4}) dependent manner (Tanaka and Araki, 2010; Zegerman and Diffley, 2009)³. Finally, Mcm10 functions in the unwinding step, together with the CMG helicase complex (Cdc45-MCM-GINS), thus initiating DNA replication (Kanke et al., 2012; van Deursen et al., 2012; Watase et al., 2012).

In eukaryotes, there are multiple origins of DNA replication (in *S. cerevisiae* ~500 in a haploid genome), and those initiation events are regulated temporally (Barberis et al., 2010; Gilbert et al., 2010). In budding yeast cells, several factors essential for the initiation of DNA replication are limiting, and those factors appear to be recycled for later initiation events (Mantiero et al., 2011; Tanaka et al., 2011). Recent studies have shown that Rad53 targets and inactivates two of the limiting

³ DDK promotes DNA replication by phosphorylating Mcm4 (Sheu and Stillman, 2006). In a domain of Mcm4 that integrates multiple kinase signals important for replication initiation and elongation (Sheu et al., 2014). Recently, it was shown that PPI^{Glc7}, which is recruited by Rif1, regulates and prevents premature Mcm4 phosphorylation, thus suggesting a role for Rif1 in regulation of replication initiation in budding yeast (Hiraga et al., 2014).

replication factors, Sld2 and Dbf4 (the DDK regulatory subunit). Thus, late-origin firing is suppressed by an activated replication checkpoint (Lopez-Mosqueda et al., 2010; Zegerman and Diffley, 2010). Regulation of replication initiation by the checkpoint also occurs in higher eukaryotic cells, although the targets appear to be different (Karnani and Dutta, 2011). It is interesting to note that in *S. pombe* and mammalian cells, DDK has been shown to have a positive role in replication checkpoint activation (Kim et al., 2008b; Matsumoto et al., 2010; Tenca et al., 2007). DDK also modulates the checkpoint response to facilitate DNA repair and recovery from checkpoint arrest (Furuya et al., 2010; Tsuji et al., 2008) (see Section 4.5).

4.4 TRANSCRIPTION CONTROL

Genome-wide gene expression analyses in budding yeast have revealed that hundreds of genes are up- or down-regulated upon treatment with genotoxic reagents that induce stalled replication forks (Benton et al., 2006; Gasch et al., 2001; Jelinsky and Samson, 1999; van Attikum et al., 2004). This transcriptional regulation is controlled by two branches in the replication checkpoint pathway; one directly by Rad53, the other by Dun1 (Bastos de Oliveira et al., 2012; Huang et al., 1998; Travesa et al., 2012). Dun1 phosphorylates and inhibits Crt1, which recruits repressors Ssn6 and Tup1 to the promoters of DNA damage response genes. Dun1 thereby up-regulates genes involved in DNA repair and ribonucleotide biosynthesis (Gasch et al., 2001; Huang et al., 1998). Two recent studies have revealed that the cell-cycle dependent genes that are transcribed at the G1/S boundary are also induced as a part of the DNA replication and damage response in *S. cerevisiae* (Bastos de Oliveira et al., 2012; Travesa et al., 2012). Over 200 G1/S genes are regulated by the heteromeric transcription factors SBF (Swi4-Swi6 cell-cycle box (SCB) binding factor) and MBF (*Mlu*1 cell-cycle box (MCB) binding factor) (Iyer et al., 2001). While SBF activates transcription in G1, MBF down-regulates transcription outside of G1 through the co-repressor Nrm1, thereby restricting the expression of the target genes in late G1 (Bean et al., 2005; de Bruin et al., 2006). The studies revealed that MBF target genes are up-regulated upon replication stress by inactivation of Nrm1 in a Rad53-dependent Dun1-independent manner (Bastos de Oliveira et al., 2012; Travesa et al., 2012). This transcriptional regulation is also conserved in *S. pombe*, as the Rad53 homolog Cds1^{Rad53} inhibits Nrm1 and promotes G1/S transcription in response to replication stress (de Bruin et al., 2008; de Bruin et al., 2006).

4.5 COORDINATING DNA REPAIR

It seems obvious that the DNA damage checkpoint should be coupled with the up-regulation of DNA repair, and various forms of damage provoke both a checkpoint response and DNA repair. Since ssDNA coated by RPA initiates both checkpoint activation and the loading of Rad51 for repair by HR, the cell has to carefully coordinate these events, particularly at the replication fork where ssDNA exists constitutively. Importantly, studies in budding and fission yeasts have shown that the replication checkpoint actively suppresses the initiation and processing required for HR (Alabert et al., 2009; Barlow and Rothstein, 2009; Meister et al., 2005). Rad52 foci are absent in cells treated with HU, even in the presence of DSBs, as long as the replication checkpoint is intact (Alabert et al., 2009; Barlow and Rothstein, 2009). Consistently, the ATR^{Mec1}-p53 pathway has been shown to suppress the formation of RAD51^{Rad51} foci in response to HU in mammalian cells⁴ (Sirbu et al., 2011), although in other cases it has been reported that CHK1^{Chk1} phosphorylates RAD51^{Rad51} and positively regulates HR in response to HU or CPT (Huang et al., 2008; Sorensen et al., 2005). These discrepancies suggest that the checkpoint regulation of HR is fine-tuned with respect to the type and level of damage.

⁴ One recent study suggested that hyperphosphorylated RPA2 sequesters Rad51 in the soluble nuclear fraction, thus impairing homologous recombination (Lee et al., 2010).

In addition to the role of 9-1-1 in ATR^{Mec1} activation described above, it has been well documented that 9-1-1 functions in various aspects of DNA repair (see review (Helt et al., 2005)). Indeed, cells may use the multi-tasking capacity of 9-1-1 to coordinate the checkpoint activation with DNA repair. In both *S. cerevisiae* and *S. pombe*, it has been suggested that 9-1-1 functions in DNA damage tolerance pathways (Kai and Wang, 2003; Karras et al., 2013; Paulovich et al., 1998). The budding yeast 9-1-1 complex also contributes to the resection of DSBs, as *rad24* mutants that impair 9-1-1 loading have reduced ssDNA formation and impaired recruitment of Mec1 at HO-induced breaks (Aylon and Kupiec, 2003; Dubrana et al., 2007). Finally, human 9-1-1 physically interacts with factors involved in base excision repair (BER), such as MYH, Pol β , TDG, Fen1, and DNA ligase I, and stimulates their enzymatic activities (Balakrishnan et al., 2009; Chang and Lu, 2005; Gembka et al., 2007; Guan et al., 2007; Toueille et al., 2004; Wang et al., 2004).

How then is 9-1-1 function regulated? Recent studies have indicated that post-transcription modification of 9-1-1 is crucial for its regulation. *S. pombe* Rad9^{Ddc1}, a component of checkpoint clamp, is phosphorylated at multiple sites by Rad3^{Mec1}, and two phosphoacceptor sites in the C-terminal tail that promote Rad9^{Ddc1}-Cut5^{Dpb11} interaction are required for Chk1^{Chk1} activation (Furuya et al., 2004) (see Section 2.1). Interestingly, Rad3^{Mec1}-dependent phosphorylation at T225 on Rad9^{Ddc1} has been shown to facilitate the interaction with Mms2^{Mms2}-Ubc13^{Ubc13}, a ubiquitin-conjugating enzyme, to promote error-free repair (Kai et al., 2007). Finally, a study in human cells has indicated that RAD18^{Rad18} facilitates RAD9^{Ddc1} recruitment at IR-induced damage through an unknown mechanism, although this mode of RAD9^{Ddc1} recruitment has little impact on checkpoint activation: no loss of CHK1^{Chk1} or CHK2^{Rad53} activation was scored in cells depleted for RAD18^{Rad18} (Inagaki et al., 2011).

As mentioned above, Dbf4-Cdc7 also modulates checkpoint activity (Kim et al., 2008b; Matsumoto et al., 2010; Tenca et al., 2007; Tsuji et al., 2008). A recent study by Furuya et al. has shown that the *S. pombe* DDK phosphorylates Rad9^{Ddc1} (Furuya et al., 2010), thereby reducing interaction between Rad9^{Ddc1} and RPA and releasing 9-1-1 from chromatin. This phosphorylation appears to be important for the repair of CPT-induced lesions, as the number of Rad22^{Rad52} repair foci increase in DDK phospho-acceptor site mutants (Furuya et al., 2010). Together, the above studies argue compellingly that 9-1-1 functions at the interface of repair and checkpoint pathways.

4.6 REPLICATION FORK STABILITY

As briefly discussed in Section 4.2, maintenance of replication fork integrity is the crucial function of the replication checkpoint in response to replication stress (Figure 1.3). Control of the cell cycle, transcription, and origin firing, while important, are non-essential events based on the following considerations: (1) Blocking the transition through M phase by nocodazole is not sufficient to rescue the lethality of high doses of MMS or HU in *rad53* or *mec1* mutant cells (Desany et al., 1998; Tercero and Diffley, 2001); (2) De novo protein synthesis does not contribute to cell viability, nor is it required for the resumption of replication forks after HU treatment (Tercero et al., 2003); and (3) HU treatment of cells that cannot suppress late-origin firing due to phospho-site mutations in both Dbf4 and Sld3, is not lethal (Lopez-Mosqueda et al., 2010; Zegerman and Diffley, 2010). On the other hand, checkpoint mutants fail to resume DNA replication after transient exposure to HU or MMS, and replisome components are not detected by chromatin immunoprecipitation (ChIP) at early origins on HU in *mec1* mutants (Cobb et al., 2003; Cobb et al., 2005; Lucca et al., 2004; Tercero et al., 2003). Finally, upon fork stalling, checkpoint mutants show aberrant DNA structures, such as the formation of reversed forks (so-called chicken-foot structures) and an accumulation of ssDNA (Lopes et al., 2001; Sogo et al., 2002). These observations led to the notion that the replication checkpoint maintains the stable association of replication polymerases at stalled forks.

An important aspect of the replication checkpoint is the fact that the roles of ATR^{Mec1} and the effector kinase, CHK1^{Rad53}, are not equivalent, particularly with respect to fork recovery. This is well-documented, yet often overlooked. In *S. cerevisiae* it has been shown that the function of Rad53 that is essential for viability on MMS is largely rescued by deletion of the exonuclease, *EXO1* (Segurado and Diffley, 2008). This suggests that the down-regulation of Exo1 at arrested forks is a major function of Rad53 (Segurado and Diffley, 2008). Interestingly, however, an *EXO1* deletion does not suppress *mec1Δ* lethality, indicating that Mec1 has functions that are crucial for cell survival on MMS, other than the activation of Rad53 (Segurado and Diffley, 2008). Indeed, when forks are arrested by high concentrations of HU, quantitative CHIP assays showed that leading and lagging DNA polymerases are displaced in *mec1* mutant cells, although their association is intact in the absence of Rad53 (Cobb et al., 2003; Cobb et al., 2005; Lucca et al., 2004). Similarly, in *mec1* mutants Cdc45 becomes undetectable at early origins (Cobb et al., 2005; Katou et al., 2003). In *rad53* mutants, on the other hand, CHIP signals for DNA polymerases stay high, yet the distribution of the MCM helicase is altered, underscoring again the distinct roles played by Mec1 and Rad53 at stalled forks (Cobb et al., 2003; Cobb et al., 2005). The exact mechanisms are unclear, yet it appears that Mec1 activity keeps replication polymerases engaged in the presence of HU, while Rad53 acts primarily through the MCM helicase to ensure replication restart (Cobb et al., 2003; Cobb et al., 2005).

Whereas the outcome of checkpoint activation is clear, it is not clear exactly what happens to the stalled replisome complex in the absence of a functional replication checkpoint. CHIP data led to the conclusion that the replication checkpoint stabilizes the replisome and preserves its integrity (Figure 1.3C). Recent biochemical approaches, on the other hand, have shown that intact replisome complexes can be recovered by Sld5-(GINS) pull-down even in *mec1* and *rad53* checkpoint mutants arrested with HU. The replisome complex, even though it is not functionally engaged, may stay chromatin-associated in both checkpoint-proficient and -deficient cells (De Piccoli et al., 2012). CHIP coupled with deep sequencing suggests that the replisome moves away from the last site of DNA synthesis in an uncoordinated manner in checkpoint mutants, possibly still unwinding double-stranded DNA by the helicase, but not incorporating dNTPs (Figure 1.3D). This random sliding of the replisome could explain the apparent “loss” of polymerases from early initiating sites, as well as the accumulation of ssDNA observed by CHIP and electron microscopy analyses (Cobb et al., 2005; De Piccoli et al., 2012; Katou et al., 2003; Lucca et al., 2004; Sogo et al., 2002). This movement, however, was only detected at the very earliest origins (De Piccoli et al., 2012), did not correlate with the incorporation of nucleotides (Crabbe et al., 2010; Katou et al., 2003), and could not account for the majority of forks where both polymerase and helicase seem to persist even in checkpoint mutants (De Piccoli et al., 2012). One model that could reconcile these results suggests that the replication checkpoint keeps the replisome engaged at sites of stalled forks in an as yet undefined way, rather than simply tethering the replisome factors together. Further work is needed to address the molecular mechanisms of how the replication checkpoint facilitates the restart of stalled forks and recovery from replication stress.

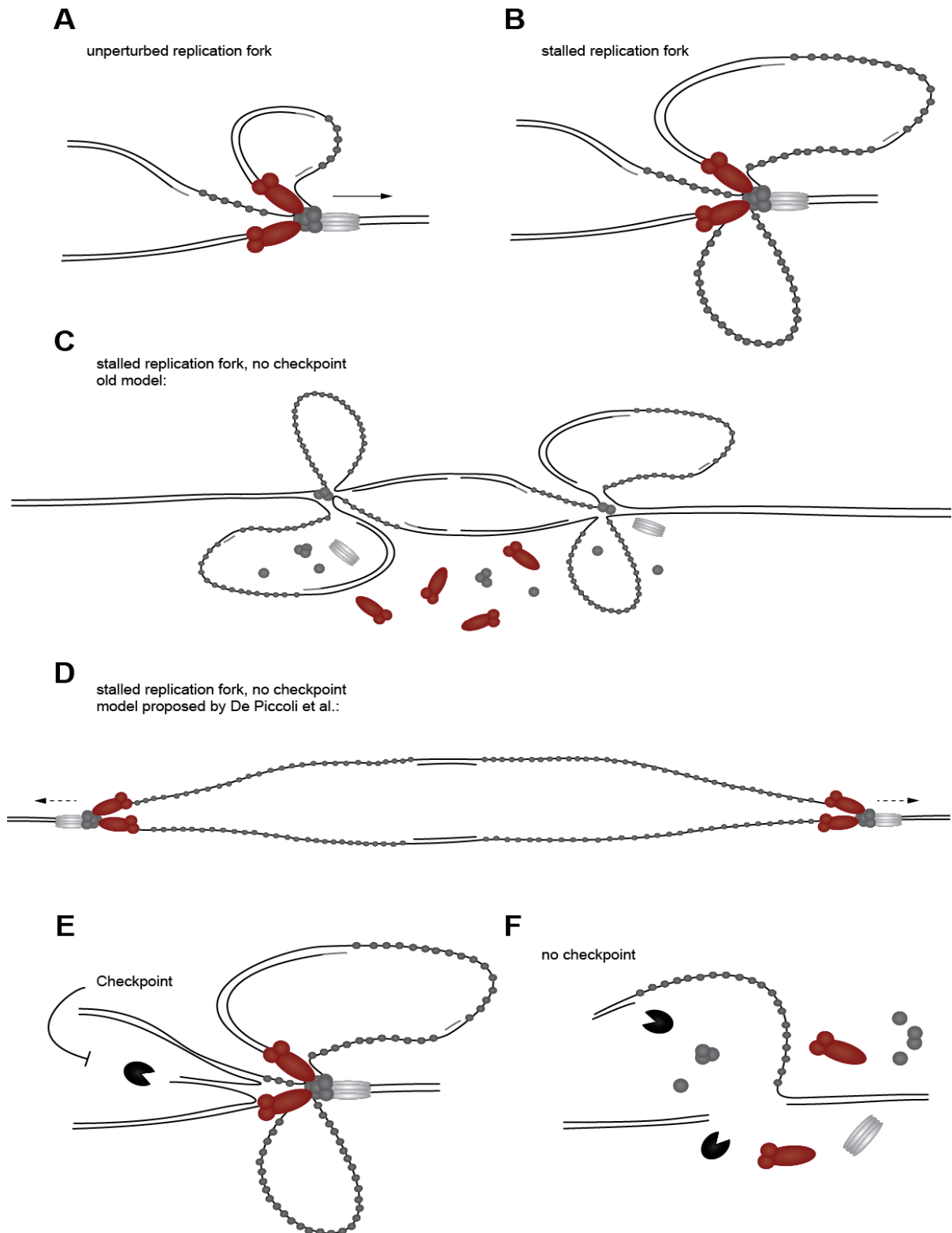


Figure 1.3: Replication fork stabilization. (A) A normal replication fork with leading and lagging strand polymerases, replicative helicase, and short ssDNA stretches coated with RPA. (B) When replication forks stall and helicase and polymerases become functionally uncoupled, long ssDNA stretches are exposed that lead to checkpoint activation. (C) ChIP experiments have indicated that replisome factors are lost from stalled replication forks if the replication checkpoint is not functional. (D) New data suggest that replisomes stay intact, but move away from replication origins without incorporating nucleotides. This leads to long ssDNA stretches. (E) The checkpoint regulates nucleases that may target structures (e.g. reverse forks) that arise at stalled replication forks. (F) If nuclease regulation fails due to checkpoint dysfunction, this may lead to uncontrolled processing and could result in double-strand breaks.

Several studies have indicated that the checkpoint regulates the action of nucleases and helicases at stalled forks (Figure 1.3E, F). Indeed, in *S. cerevisiae* the exonuclease Exo1 is modified and inhibited by the DNA damage checkpoint (Morin et al., 2008; Segurado and Diffley, 2008), and deletion of *EXO1* has been shown to suppress the accumulation of ssDNA in checkpoint-deficient cells on HU (Cotta-Ramusino et al., 2005). Similarly, human EXO1 undergoes ubiquitin-mediated degradation on HU, in a manner partly dependent on phosphorylation by ATR^{Mec1} (El-Shemerly et al., 2008). Recently it has also been shown that the nuclease/helicase Dna2 is a target of the replication checkpoint, and that phosphorylation facilitates its association to DNA following exposure to HU (Hu et al., 2012). Dna2 nuclease activity is thought to prevent ssDNA formation by cleaving off ssDNA tails that arise from stalled fork regression (Hu et al., 2012). A structure-specific nuclease Mus81-Eme1 is also a target of Cds1^{Rad53} in *S. pombe*, and is released from chromatin upon fork stalling (Kai et al., 2005). Finally, as mentioned above, the Sgs1 helicase is a target of Mec1, and its helicase activity has an important role in replication fork stability (Cobb et al., 2003; Cobb et al., 2005; Frei and Gasser, 2000; Hegnauer et al., 2012). Specifically, when *sgs1Δ* is combined with either *mrc1Δ* or *mec1-100*, an S phase-specific *mec1* mutant (Paciotti et al., 2001), then total fork collapse occurs in the presence of HU, and neither DNA polymerases nor RPA can be detected at the collapsed fork by ChIP analysis (Cobb et al., 2003; Cobb et al., 2005; Frei and Gasser, 2000; Hegnauer et al., 2012). This results in a dramatic increase in gross chromosomal rearrangements and high levels of cell lethality. The mammalian RecQ helicases BLM^{Sgs1} and WRN^{Sgs1} are also phosphorylated by ATR^{Mec1} and ATM^{Tel1} (Davies et al., 2004; Pichierri et al., 2003), and are implicated in replication fork recovery after stress (Ammazzalorso et al.; Davies et al., 2004; Davies et al., 2007). Whereas Sgs1 helicase does help transduce the checkpoint signal by activating Rad53, the prevention of fork collapse requires its helicase activity, and not simply its ability to bind Rad53. (Cobb et al., 2003; Cobb et al., 2005; Frei and Gasser, 2000; Hegnauer et al., 2012). Together, these data suggest that ATR^{Mec1} and CHK1^{Rad53} target distinct sets of nucleases and helicases to suppress the formation of pathological fork structures that impair replication fork resumption after removal of the damage.

A number of studies has been carried out to identify the targets of the replication and DNA damage checkpoints, and to determine their relevance for the checkpoint response. In Table 1.2, we list the replication fork associated factors in addition to those mentioned above, that are phosphorylated upon checkpoint activation (Bennetzen et al., 2010; Blasius et al., 2011; Chen et al.; Matsuoka et al., 2007; Mu et al., 2007; Smolka et al., 2007; Stokes et al., 2007). While phosphoproteomic studies have identified many, only a few checkpoint targets have been elucidated in depth. For example, RPA1^{Rfa1}, the large subunit of RPA, is crucial for ATR^{Mec1} recruitment at the site of damage and is a documented Mec1 target (Brush et al., 1996), yet the function of its phosphorylation remains unclear. In human cells, the second RPA subunit, RPA32^{Rfa2}, is phosphorylated by ATR^{Mec1} and by another PIKK, DNA-PK, upon replication stress, and this phosphorylation is required for a robust checkpoint response and for recovery from fork arrest (Liu et al., 2012b). DNA polymerase α , the lagging strand polymerase, is a checkpoint target (Pellicioli et al., 1999), and has an important role in the initiation of the replication checkpoint (Michael et al., 2000). Interestingly, the gap-filling lagging strand polymerase, DNA polymerase δ , has been shown to be a target of Mec1 in response to MMS (Chen et al., 2010), although the importance of its phosphorylation in replication fork stability is unclear. The active replicative helicase CMG complex (Cdc45-MCM-GINS) is one of the common targets of the replication and damage checkpoint in different organisms; MCM2^{Mcm2} (primarily a target of ATR^{Mec1} (Cortez et al., 2004; Trenz et al., 2008; Yoo et al., 2004)), MCM3^{Mcm3} (primarily a target of ATM^{Tel1}-CHK2^{Rad53} (Cortez et al., 2004; Ilves et al., 2012; Shi et al., 2007)), MCM4^{Mcm4} (a target of both ATR^{Mec1} and ATM^{Tel1} pathways (Bailis et al., 2008; Ilves et al., 2012; Ishimi et al., 2003)), GINS component Psf1 (a Mec1 target (De Piccoli et al., 2012)), and PSF2^{Psf2} (a CHK2^{Rad53} target (Ilves et al., 2012)) are all phosphorylated upon checkpoint

activation. CHK2^{Rad53} phosphorylation of the CMG inhibits its helicase activity (Ilves et al., 2012), whereas phosphorylation of Mcm2 has been shown to recruit Plk1^{Cdc5} (polo-like kinase 1) on chromatin and promote checkpoint recovery (Trenz et al., 2008) (see also Section 6). Finally, analyses in both budding yeast and human cells have identified specific phosphopeptides of the GINS complex and DNA polymerase ϵ targeted by ATR^{Mec1} and/or ATM^{Tel1}, and not by downstream effector kinases CHK1^{Rad53} (see Table 1.3 (Chen et al., 2010; Matsuoka et al., 2007)), consistent with the distinct roles played by ATR^{Mec1} and the downstream effector kinase CHK1^{Rad53}. It is of utmost relevance to find out whether, and how, phosphorylation of these factors impacts replication fork integrity and fork restart.

Table 1.3: Replication factors modified by replication and damage checkpoint kinases.⁵

	Function	References
<i>S. cerevisiae</i> (targeted by)		
Rfa1 (Mec1/Tel1)	a subunit of RPA	(Brush and Kelly, 2000; Chen et al., 2010; Smolka et al., 2007)
Rfa2 (Mec1/Tel1)	a subunit of RPA	(Brush et al., 1996; Chen et al., 2010)
Pol1 (Rad53)	a subunit of DNA pol α	(Chen et al., 2010)
Pol31 (Mec1/Tel1)	a subunit of DNA pol δ	(Chen et al., 2010)
Dpb4 (Mec1/Tel1)	a subunit of DNA pol ϵ and ISW2	(Chen et al., 2010; Smolka et al., 2007)
Mcm4(Mec1)	a subunit of MCM	(Randell et al., 2010)
Mcm6 (Mec1)	a subunit of MCM	(Randell et al., 2010)
Psf1 (Mec1)	a subunit of GINS	(De Piccoli et al., 2012)
Mrc1 (Mec1, Rad53)	checkpoint mediator	(Alcasabas et al., 2001; Chen et al., 2010)
Tof1 (Rad53)	fork protection complex	(Smolka et al., 2007)
Ctf4 (Rad53)	pol α interactor	(Smolka et al., 2007)
Dbf4 (Rad53)	a subunit of DDK	(Chen et al., 2010; Lopez-Mosqueda et al., 2010; Weinreich and Stillman, 1999; Zegerman and Diffley, 2010)
Sgs1 (Mec1)	Rec Q helicase	(Hegnauer et al., 2012)
Higher eukaryotes		
RPA1 (ATR/ATM)	a subunit of RPA	(Matsuoka et al., 2007; Stokes et al., 2007)
POLE (ATR/ATM)	a subunit of pol ϵ	(Matsuoka et al., 2007)
POLEE4 (ATR/ATM)	a subunit of pol ϵ	(Matsuoka et al., 2007)
POLL (ATR/ATM)	a subunit of pol λ	(Matsuoka et al., 2007)
MCM2 (ATR/ATM)	a subunit of MCM	(Bennetzen et al., 2010; Matsuoka et al., 2007; Stokes et al., 2007)
MCM3 (ATR/ATM)	a subunit of MCM	(Matsuoka et al., 2007)
MCM4 (ATR/ATM, Chk1)	a subunit of MCM	(Bennetzen et al., 2010; Ishimi et al., 2003; Matsuoka et al., 2007)
MCM5 (Chk1)	a subunit of MCM	(Blasius et al., 2011)
MCM6 (ATR/ATM,	a subunit of MCM	(Bennetzen et al., 2010; Matsuoka et al., 2007)

⁵ Many additional checkpoint kinase substrates are known from large scale phosphoproteomics studies from this work (Chapter 2) and other laboratories (Marcus Smolka, unpublished data, Chen et al., 2010) that have not been directly located at replication forks yet may also help to keep polymerases engaged and enable replication fork restart.

MCM7 (ATR/ATM)	a subunit of MCM	(Matsuoka et al., 2007)
POLDIP3 (ATR/ATM)	Pol δ interacting factor	(Matsuoka et al., 2007)
MCM10 (ATR/ATM)	replication initiation factor	(Matsuoka et al., 2007)
HELB (ATR/ATM)	DNA helicase B	(Matsuoka et al., 2007)
RFC1 (ATR/ATM)	clamp loader	(Bennetzen et al., 2010; Matsuoka et al., 2007; Stokes et al., 2007)
RFC3 (ATR/ATM)	clamp loader	(Matsuoka et al., 2007)
PSF2 (ATR/ATM)	a subunit of GINS	(Ilves et al., 2012; Matsuoka et al., 2007; Stokes et al., 2007)
ORC3 (ATR/ATM)	a subunit of ORC	(Matsuoka et al., 2007)
ORC6 (ATR/ATM)	a subunit of ORC	(Matsuoka et al., 2007)
DBF4 (ATR/ATM)	a subunit of DDK	(Matsuoka et al., 2007)
Claspin (ATR/ATM)	checkpoint mediator	(Matsuoka et al., 2007; Stokes et al., 2007)
CAF-1B (ATR/ATM)	histone assembly	(Stokes et al., 2007)
CTF18 (ATR/ATM)	POLH interactor	(Matsuoka et al., 2007; Stokes et al., 2007)
TopBP1 (ATR/ATM, Chk1)	initiation and ATR activation	(Blasius et al., 2011; Matsuoka et al., 2007; Stokes et al., 2007)
WDHD1 (ATR/ATM)	Pol α interactor	(Stokes et al., 2007)
BLM (ATR/Chk1)	RecQ helicase	(Blasius et al., 2011; Davies et al., 2004)
FEN1 (Chk1)	5' flap endonuclease	(Blasius et al., 2011)
DNA Ligase 1 (Chk1)	DNA ligase	(Bennetzen et al., 2010; Blasius et al., 2011)
TIPIN (ATR/ATM)	fork protection complex	(Matsuoka et al., 2007)
WRN (ATR/ATM)	RecQ helicase	(Matsuoka et al., 2007; Pichierrri et al., 2003)

In addition to direct fork-associated proteins, enzymes that modulate long-range chromatin organization are also shown to be targets of the replication checkpoint. For instance, the Ino80 and Isw2 chromatin remodelers are confirmed targets of the DNA damage checkpoint (Chen et al., 2010; Morrison et al., 2007). These ATP-dependent chromatin remodeling complexes are shown to be recruited at the stalled replication forks and to promote the recovery of stalled forks (Falbo et al., 2009; Papamichos-Chronakis and Peterson, 2008; Shimada et al., 2008; Vincent et al., 2008). Loss of Ino80 chromatin remodeling activity results in a poor resumption of stalled forks and an increase in DNA repair response (Falbo et al., 2009; Papamichos-Chronakis and Peterson, 2008; Shimada et al., 2008). This correlates with a proposed action of removing nucleosomes to allow fork progression, although INO80 contains a 5' to 3' DNA helicase activity in its Rvb1 and Rvb2 subunits, which may also be involved in altering fork structure (Shen et al., 2000). Another study has suggested a role in checkpoint down-regulation, although how chromatin remodeling reduces a checkpoint response is unknown ((Au et al., 2011) see also Section 6.2).

A recent study has proposed that the replication checkpoint releases topological tension generated by a transcribed gene that is tethered to components of the nuclear pore (Bermejo et al., 2011). DNA replication forks frequently pause at transcribed genes, and this pausing is independent of the directionality between replication and transcription (Azvolinsky et al., 2009). Bermejo et al. (Bermejo et al., 2011) have determined that mutations in THO, TREX-2, or inner basket nucleoporins enhance the survival of *rad53* mutants on HU, and rescue fork reversal, which occurs in the checkpoint mutants on HU (Bermejo et al., 2011). The replication checkpoint appears to target Mlp1, a nucleoporin, and

counteracts its function for gene tethering to the nuclear pore. A phospho-mimicking *mlp1* mutation suppresses *rad53Δ* lethality on HU, suggesting that releasing topological impediments generated by gene gating is one task of the replication checkpoint. However, the interpretation may be rather complicated since loss of Mlp1 also releases and alters the activity of the SUMO-protease Ulp1 which plays a key role in DNA repair (Palancade et al., 2007).

A bioinformatics approach has also indicated that ATR^{Mec1} and ATM^{Tel1} may be involved in regulating a broad range of cellular structures, such as the spindle pole body/centrosome and actin cytoskeleton (Cheung et al., 2012). It will be interesting to explore whether those less canonical Mec1/Tel1 targets function at replication forks to ensure genome stability.

5. COORDINATION BETWEEN ATR^{MEC1} AND ATM^{TEL1}

While ATR^{Mec1} and $CHK1^{Chk1}$ serve distinct roles in the replication checkpoint, it is also clear that ATR^{Mec1} and ATM^{Tel1} do not have identical roles. ATM^{Tel1} initiates the DSB checkpoint response, while ATR^{Mec1} is the first responder to the replication-associated DNA damage. As mentioned above, MRX/MRN recognizes DSBs and recruits ATM^{Tel1} kinase. However, there are also a range of overlapping functions between ATM^{Tel1} and ATR^{Mec1} . At DSBs, budding yeast Tel1 phosphorylates Mre11, Xrs2, and Sae2. Sae2 activates MRX nuclease activity, which initiates 5'-3' end resection (Mimitou and Symington, 2011). Extended ssDNA formation is followed by Exo1, Sgs1-Top3-Rmi1, and Dna2 helicase/nuclease activity, with the aid of Fun30 (SMARCAD1), a recently identified chromatin remodeler (Chen et al., 2012; Costelloe et al., 2012; Eapen et al., 2012; Mimitou and Symington, 2011). Extended RPA-coated ssDNA leads to the recruitment and subsequent activation of ATR^{Mec1} - $ATRIP^{Ddc2}$ (Jazayeri et al., 2006) (see Figure 1.1). Recently, Peterson et al. have shown that ATR^{Mec1} in mammals also phosphorylates CtIP^{Sae2}, and this phosphorylation stimulates CtIP^{Sae2} chromatin interaction and end-resection (Peterson et al., 2011). Thus, checkpoint signaling after DSB induction involves both the ATR^{Mec1} and ATM^{Tel1} pathways. A recent biochemical analysis has suggested a mechanism for a consecutive switch from ATM^{Tel1} to ATR^{Mec1} through swapping the recruiter MRN^{MRX} for RPA at the DSB damage site during end-resection (Shiotani and Zou, 2009). We note that in higher eukaryotes another PIKK, DNA-PK, also participates in the signaling of the DSB damage response (Hill and Lee, 2010).

Although ATR^{Mec1} - $ATRIP^{Ddc2}$ is the major regulator of the replication-associated checkpoint, the vulnerable nature of replication forks can generate DSBs through fork collapse (Figure 1.1), which then might require ATM^{Tel1} activation to protect the break and facilitate fork restart. In a *Xenopus* replication system, both ATM^{Tel1} and ATR^{Mec1} appear to play an important role in preventing DSB formation during replication (Trenz et al., 2006). In the absence of ATM^{Tel1} and ATR^{Mec1} , DSBs accumulate and DNA polymerase ϵ is displaced from CPT- or mitomycin C-damaged chromatin. It has also been demonstrated that MRN^{MRX} is redistributed to the restarting forks, in a manner dependent on ATM^{Tel1} and ATR^{Mec1} . This appears to be important for preventing persistent DSB formation (Trenz et al., 2006). Consistently, Doksani et al. have shown that in the absence of Tel1 or MRX function, abnormal DNA intermediates accumulate when the replication fork encounters an induced DSB. They suggest that the MRX-Tel1 pathway prevents the formation of cruciform structures at the fork-DSB junction (Doksani et al., 2009), a pathway that may depend on crosstalk between ATR^{Mec1} and ATM^{Tel1} .

The mechanism of ATR-ATM crosstalk is somewhat lesion specific. For instance, ATR^{Mec1} phosphorylates ATM^{Tel1} at serine 1981, which promotes the dissociation of inactive ATM^{Tel1} dimers

into active monomers, in response to HU or UV. This results in $\text{CHK2}^{\text{Rad53}}$ activation and a robust G2/M arrest (Stiff et al., 2006). In contrast, in the presence of IR-induced damage, ATM^{Tel1} auto-phosphorylates this same residue, resulting in self-activation (Bakkenist and Kastan, 2003; Stiff et al., 2006). A screen for novel *tel1* mutations in budding yeast has shown that there are overlapping functions between Mec1 and Tel1 with respect to stalled forks, and that some *tel1* gain-of-function mutants can even compensate for Mec1 functions. These dominant *TELI-hy* mutants suppress *mec1Δ* deficiency in respect to Rad53 activation and cell survival to different extents, in response not only to DSBs but also to UV, MMS, and HU in S phase (Baldo et al., 2008). Some *Tel1-hy* proteins have higher catalytic activity than the wild-type *Tel1*, yet others show equivalent or even lower activity, suggesting that changes in specificity can also result in suppression. In addition, checkpoint restoration by *TELI-hy* mutants in response to DSBs requires Xrs2 interaction, suggesting that *Tel1-hy* recruitment to damage through MRX is still crucial for the suppression phenotype (Baldo et al., 2008).

In agreement with the above observations, MRX has been shown to have a role in replication checkpoint signaling, in parallel to its well-characterized function in the DSB response (D'Amours and Jackson, 2001; Olson et al., 2007). Indeed, budding yeast *mre11* mutants show reduced Rad53 activation in response to HU (D'Amours and Jackson, 2001). In mammals, as well, MRN^{MRX} has been shown to function upstream of ATR^{Mec1} in response to UV and HU, and to interact with ATR^{Mec1} - $\text{ATRIP}^{\text{Ddc2}}$ through the FHA and BRCT domains of $\text{Nbs1}^{\text{Xrs2}}$ (Olson et al., 2007). These data would suggest that MRN^{MRX} functions as a regulator for both ATM^{Tel1} and ATR^{Mec1} . Recently, MRN^{MRX} has also been found to assist in $\text{TopBP1}^{\text{Dpb11}}$ recruitment to ssDNA-dsDNA junctions, explaining how this complex might help activate ATR^{Mec1} in *Xenopus* egg extracts (Duursma et al., 2013; Lee and Dunphy, 2013). It is proposed that MRN^{MRX} recruits $\text{TopBP1}^{\text{Dpb11}}$, after which the interaction between 9-1-1 and $\text{TopBP1}^{\text{Dpb11}}$ subsequently exposes the ATR^{Mec1} activation domain (AAD) of $\text{TopBP1}^{\text{Dpb11}}$ to fully activate ATR^{Mec1} (Duursma et al., 2013). On the other hand, the *Mre11* nuclease activity has also been implicated in checkpoint activation, possibly by generating ssDNA (Lee and Dunphy, 2013). In budding yeast MRX is also recruited to stalled replication forks, where it contributes to the maintenance of stalled polymerases (Tittel-Elmer et al., 2009). Another study by the same group has demonstrated that MRX has an important role in cohesin association behind the fork in response to HU, which is necessary for fork restart (Tittel-Elmer et al., 2009; Tittel-Elmer et al., 2012). Whereas the full molecular details of how MRX contributes to fork stability and cohesin recruitment remain to be clarified, current results suggest that it may be its structural properties, rather than its nuclease activity, that are crucial (Tittel-Elmer et al., 2009; Tittel-Elmer et al., 2012). In mammalian cells cohesin is also important for $\text{CHK2}^{\text{Rad53}}$ activation in the intra-S and the G2/M damage checkpoints, and this role is independent of cohesin's role in sister chromatid cohesion (Watrin and Peters, 2009). In *S. pombe*, the N-terminus of the MRN component $\text{Nbs1}^{\text{Xrs2}}$ is required for the $\text{Rad3}^{\text{Mec1}}$ - $\text{Rad26}^{\text{Ddc2}}$ -dependent telomere recruitment of *Tel1*, while the well-studied *Tel1*-binding C-terminal $\text{Nbs1}^{\text{Xrs2}}$ domain is not needed (Subramanian and Nakamura, 2010). These observations further emphasize the significant cooperation that exists between ATR^{Mec1} and ATM^{Tel1} , and the important role MRN^{MRX} plays in coordinating their interplay.

6. CHECKPOINT RECOVERY

6.1 PROTEIN PHOSPHATASES DOWN-REGULATE THE CHECKPOINT

The kinase cascade of DNA replication and damage checkpoints must be down-regulated to continue the cell cycle once the impediment is removed (Figure 1.4). This process is known as recovery, and correlates with the disappearance of hyper-phosphorylated Rad53 in *S. cerevisiae* (Pelliccioli et al., 2001). Recovery is distinct from “adaptation”, which refers to the down-regulation of the checkpoint despite the persistence of unrepaired DNA damage (see review (Clemenson and Marsolier-Kergoat, 2009)). A reasonable way to counteract the kinase cascade would be through protein phosphatases.

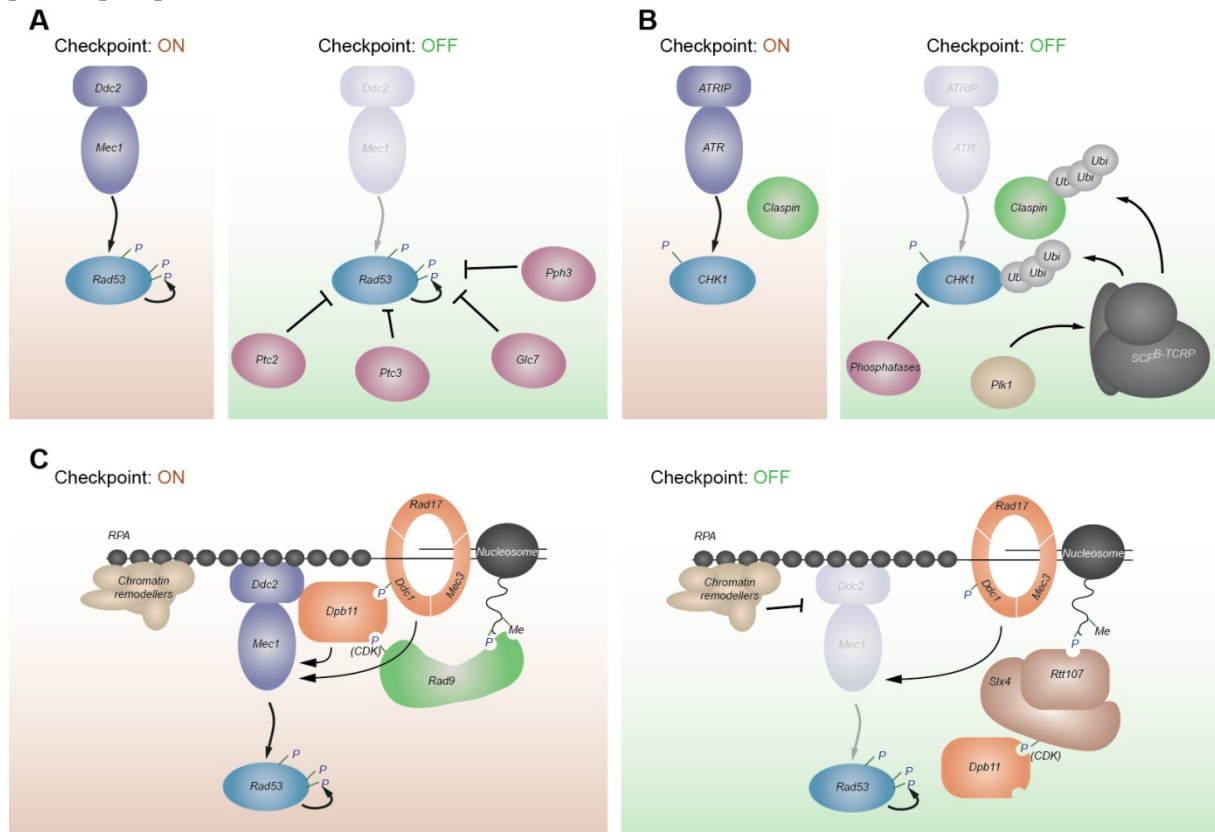


Figure 1.4: Checkpoint down-regulation. (A) The phosphatases Ptc2, Ptc3, Glc7, and Pph3 have been implicated in dephosphorylating Rad53 in *S. cerevisiae*. (B) In the mammalian replication checkpoint, $\text{CHK1}^{\text{Chk1}}$ activation by ATR^{Mec1} is facilitated through the checkpoint mediator $\text{Claspin}^{\text{Mrc1}}$. During checkpoint down-regulation, both $\text{CHK1}^{\text{Chk1}}$ and $\text{Claspin}^{\text{Mrc1}}$ are targeted for ubiquitin-mediated degradation, which is promoted by $\text{Plk1}^{\text{Cdc5}}$. In addition, phosphatases lead to $\text{CHK1}^{\text{Chk1}}$ dephosphorylation. (C) Phosphatase-independent down-regulation in *S. cerevisiae*. Left: The Mec1 activator Dpb11 interacts with phosphorylated Rad9. Rad9 is recruited by chromatin modifications like histone H2A phosphorylation and methylated histone H3, and assists in Rad53 activation. Right: A complex of Slx4 and Rtt107 down-regulates the checkpoint. Slx4 competes with Rad9 for Dpb11 binding, and may sequester Dpb11 away. Rtt107 can interact with phosphorylated H2A, and may compete with Rad9 for that. Chromatin remodelers may also have a role in checkpoint down-regulation. Ubi—Ubiquitin.

42 yeast genes are annotated as having protein phosphatase activity (Figure 1.5). Protein phosphatases can be subdivided into protein tyrosine phosphatases (PTPs), serine/threonine phosphatases and dual specificity phosphatases (see reviews (Moorhead et al., 2007; Stark, 1996)). Since all the checkpoint kinases belong to the family of serine/threonine kinases, we will focus on serine/threonine phosphatases here. Serine/threonine phosphatases were initially classified into either class I (PP1) and class II (PP2A, PP2B and PP2C). While PP1 enzymes are sensitive to the endogenous protein inhibitor-1, all class II enzymes are insensitive (Ingebritsen and Cohen, 1983). Unlike PP2A, PP2B enzymes are calcium and PP2C enzymes magnesium dependent. Thus, PP2C

enzymes are also called “phosphatases, magnesium-dependent” (PPMs), in contrast to phosphoprotein phosphatases (PPPs), which refer to PP1, PP2A and PP2C (see reviews (Moorhead et al., 2007; Shi, 2009)). Both PPPs and PPMs employ ions for their catalytic mechanisms (see review (Shi, 2009)). Three histidine, two aspartate and one asparagine residue, all highly conserved, coordinate two metal ions (e.g. Mn^{2+} and Fe^{2+} for PP1) that are thought to activate a water molecule for the nucleophilic attack on the phosphorous atom (Egloff et al., 1995; Goldberg et al., 1995). Subsequent cloning of phosphatase genes led to the discovery of additional PPPs. PP4 and PP6 are closely related to PP2A, while PP5 and PP7 are slightly distinct. An additional class of serine/threonine phosphatases represents aspartate-based phosphatases. They do not employ metal ions but instead use aspartate residues for catalysis. Two subclasses of aspartate-dependent phosphatases have been described. The first subclass is comprised of FCP/SCP (TFIIF-associating component of CTD phosphatase / small CTD phosphatase), which predominantly target the C-terminal domain (CTD) of RNA polymerase II. A second, less characterized subclass consists of several enzymes of the HAD (halocacid dehalogenase) enzyme superfamily with phosphatase activity (see review by (Moorhead et al., 2007)).

Most PPPs and PPMs are conserved in yeast (see Figure 1.5). While one or two genes encode for the PPP enzymes PP1 (*GLC7*), PP4 (*PPH3*), PP5 (*PPT1*), PP6 (*SIT4*), PP2A (*PPH21* and *PPH22*) and PP2B (*CNA1* and *CMP2*), seven genes encode for PP2C enzymes (*PTC1-7*). Yeast does not have a PP7 homolog, but has several reported PP1-related enzymes (Ppq1, Ppz1 and Ppz2) and Ppg1, which seems to be closely related to PP4^{Pph3} and PP6^{Sit4} (Stark, 1996). While PP2C^{Ptc1-7}, PP5^{Ppt1} and PP7 enzymes contain both catalytic and regulatory domains in the same protein, PP1^{Glc7}, PP2A^{Pph21/22}, PP4^{Pph3} and PP6^{Sit4} rather employ additional regulatory subunits, which confer substrate specificity. Most PP1^{Glc7} regulatory subunits have an RVXF motif in common, through which they bind the catalytic subunit (Terrak et al., 2004; Zhao and Lee, 1997). However, the probably best studied phosphatase complex is PP2A^{Pph21/22}, which besides the catalytic subunit (subunit C) contains two regulatory subunits, a HEAT repeat containing scaffolding subunit A (Tpd3 in yeast) and a third regulatory subunit B. Distinct B subunits (e.g. Cdc55, Rts1 and Rts3 in yeast) (and additional A subunits in mammals) lead to a variety of PP2A complexes, even though only two genes encode for PP2A catalytic subunits. PP6^{Sit4} and PP4^{Pph3} also associate with additional subunits. Sit4 binds to Sit4-associated proteins (SAPs). Human PP4^{Pph3} was found in three distinct complexes with R1, Tap42^{Tap42} and CCT, and R2^{Psy4} and R3^{Psy2} (Gingras et al., 2005). In the same study, yeast Pph3 was found to interact with Psy2, Psy4 and Tap42. Tap42 in combination with Tip41 also interacts with Sit4 and Pph21/22, the latter complex playing a role in TOR signaling.

Additional proteins seem to assist in phosphatase complex assembly. Rrd2 interacts with PP2A^{Pph21/22} during holocomplex biogenesis (Hombauer et al., 2007). Rrd2 is one of two yeast homologs (i.e. Rrd1 and Rrd2) of phosphotyrosyl phosphatase activator (PTPA). While Rrd2 preferentially interacts with Pph21/22, Rrd1 can bind to Pph3, Sit4 and Ppg1 (Van Hoof et al., 2005). Rrd2 is thought to assist in Pph21/22 activation through ATP-dependent cis/trans prolyl isomerization (Jordens et al., 2006). PTPA^{Rrd2} was also shown to stimulate a normally weak PP2A phosphor tyrosine phosphatase activity *in vitro* (Cayla et al., 1990). However, the relevance of PTPA^{Rrd2} in PP2A^{Pph21/22} activation *in vivo* remains unclear. More recently, Rrd1 was shown to act on the same pathway as Pph3 in promoting telomere formation at a DSB site, indicating that it may function in Pph3 activation (Zhang and Durocher, 2010). In contrast, in Chapter 2 we show that *rrd1Δ* is not epistatic with *pph3Δ* in suppressing *mec1-100* HU sensitivity.

Several phosphatases have been implicated in the process of checkpoint recovery in *S. cerevisiae*. Among them are the two PP2C enzymes Ptc2 and Ptc3 (Leroy et al., 2003; Marsolier et al., 2000), the PP1 enzyme Glc7 (Bazzi et al., 2010) and the PP4 enzyme Pph3 (O'Neill et al., 2007; Szyjka et al., 2008). Interestingly, distinct phosphatases are employed depending on the type of

damage that led to Rad53 activation (reviewed by (Heideker et al., 2007)). Ptc2, Ptc3 and Pph3 have been shown to function in the recovery from and repair of a HO endonuclease-induced single DSB response (Guillemain et al., 2007; Keogh et al., 2006; Kim et al., 2011; Leroy et al., 2003). Rad53 down-regulation requires Pph3 and Ptc2 in response to MMS (O'Neill et al., 2007; Szyjka et al., 2008) and another PP1 phosphatase, Glc7, in response to HU (Bazzi et al., 2010) (Figure 1.4A). Dephosphorylation of Rad53 is important for the resumption of stalled replication forks after removal of the drugs (Bazzi et al., 2010; Szyjka et al., 2008). It has been suggested that the phosphatases non-redundantly target Rad53 in response to different types of damage (DSBs vs. MMS) (Heideker et al., 2007). However, the loss of several of those phosphatases at the same time impairs cell growth, suggesting that they have overlapping functions that support cell viability (Bazzi et al., 2010; Szyjka et al., 2008; Travesa et al., 2008). In addition to Rad53, regulation of γ H2AX (phosphorylated H2AX, or H2A in budding yeast) phosphorylation has been well studied in both budding yeast and mammalian cells and a conserved function of PP4^{Pph3} was found in γ H2AX dephosphorylation (Chowdhury et al., 2008; Keogh et al., 2006; Nakada et al., 2008). Although this role of PP4 is conserved, additional phosphatases have been implicated in H2AX^{H2A} dephosphorylation in mammalian cells (i.e. PP2A^{Pph21/22}, the PP2C-type phosphatase Wip1 and PP6^{Sit4}) (reviewed in (Shimada and Nakanishi, 2013)).

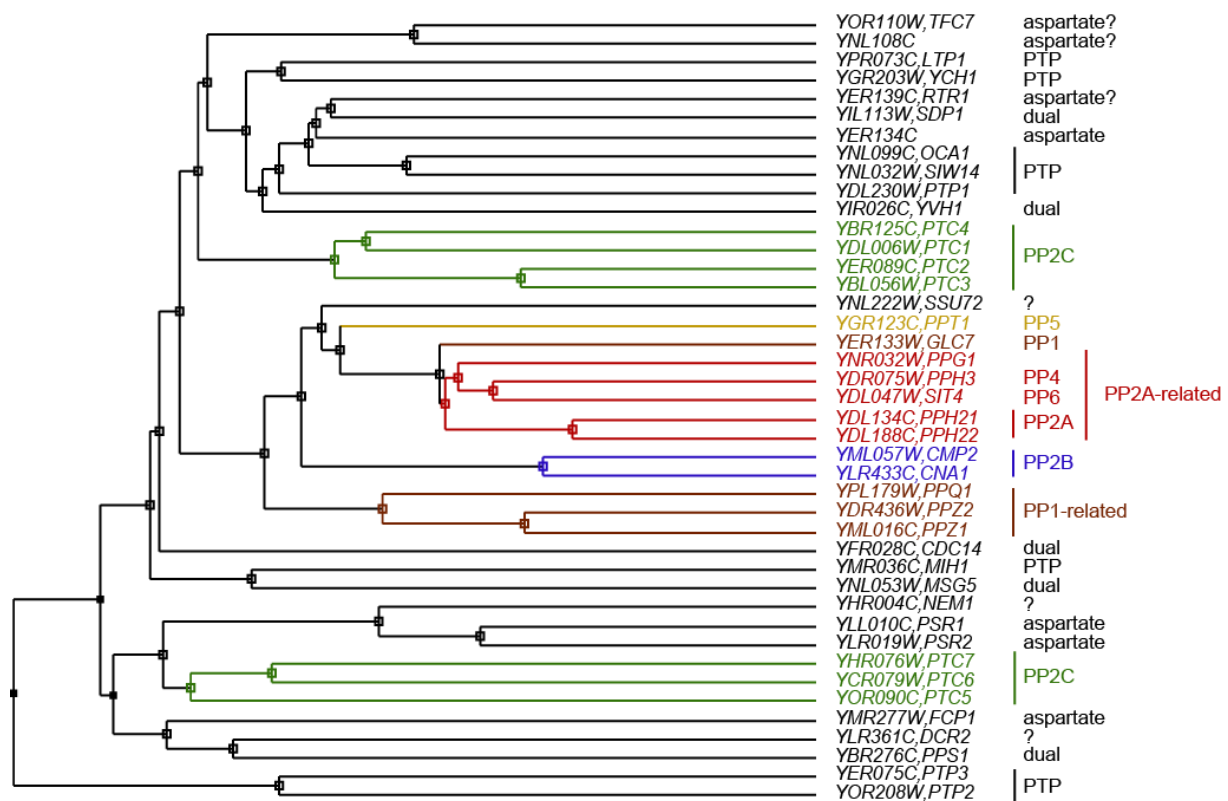


Figure 1.5: Relationship between yeast phosphatase catalytic domain genes. All yeast genes annotated with phosphatase activity (list downloaded from SGD (Saccharomyces Genome Database, <http://www.yeastgenome.org/>) were manually filtered for phosphoprotein phosphatase catalytic domains, multiple sequence alignment of protein sequences performed with Clustal Omega (Sievers et al., 2011) and a phylogenetic tree generated using jalview (Waterhouse et al., 2009). Phosphatases were classified depending on their annotation in the SGD database and based on a previous review (Stark, 1996). Phosphoprotein phosphatase (PPP) and metal-dependent phosphatase (PPM) classes are color coded. Aspartate: aspartate based phosphatase; PTP phosphotyrosyl phosphatase; dual: dual specificity phosphatase; question marks indicate unclear annotation.

Much more about the role of phosphatases in checkpoint down-regulation can be learned from other organisms than budding yeast: PP1 phosphatase Dis2^{Glc7} negatively regulates Chk1^{Chk1} in *S. pombe* (den Elzen and O'Connell, 2004) and, in metazoans, various phosphatases have been found to function in checkpoint down-regulation (see reviews (Freeman and Monteiro, 2010; Shimada and

Nakanishi, 2013)). ATM^{Tel1} is targeted by PP2A^{Pph21/22}, PP1^{Glc7} and the PP2C-type phosphatase Wip1 (Wild-type p53-induced phosphatase 1) (Goodarzi et al., 2004; Peng et al., 2010; Shreeram et al., 2006). While PP2A^{Pph21/22} and PP1^{Glc7} seem to dissociate from ATM^{Tel1} upon DNA damage (Guo et al., 2002; Peng et al., 2010), Wip1 is constitutively ATM^{Tel1}-associated (Shreeram et al., 2006). However, its activity is cell-cycle regulated by both protein level and phosphorylation, and thus it has been suggested that Wip1 protein regulation fine-tunes the global DDR response (Macurek et al., 2013). In contrast to the other phosphatases, PP5^{Ppt1} rather promotes ATM^{Tel1} as well as ATR^{Mec1} activation and signaling through an unknown mechanism (Ali et al., 2004; Zhang et al., 2005). CHK1^{Chk1} and CHK2^{Rad53} are also targeted by PP2A^{Pph21/22} and Wip1 (Fujimoto et al., 2006; Liang et al., 2006; Lu et al., 2005; Oliva-Trastoy et al., 2007), while PP4^{Pph3} has been further implicated in dephosphorylation of the ATM/ATR^{Mec1/Tel1} targets KAP1, 53BP1 and RPA2^{Rfa2} (Lee et al., 2014; Lee et al., 2012; Lee et al., 2010; Liu et al., 2012a). Also, genetic interactions of Pph3 with deletions of checkpoint proteins have been described (Bandyopadhyay et al., 2010; O'Neill et al., 2007). In particular, pph3Δ shows positive (suppressive) interactions with deletions of upstream checkpoint proteins and negative interactions with loss of proteins known to negatively regulate checkpoint signaling, like *sae2Δ* and *ptc2Δ* (Bandyopadhyay et al., 2010; Clerici et al., 2006; Guenole et al., 2013; Keogh et al., 2006; Marsolier et al., 2000; O'Neill et al., 2007). Thus both in budding yeast and other organisms several different phosphatases are employed to prevent untimely checkpoint protein phosphorylation and provide rapid checkpoint recovery after the checkpoint trigger has been removed. ATR^{Mec1} and Mec1 are phosphorylated as well (Chen et al., 2010; Liu et al., 2011; Nam et al., 2011b). However, the role of phosphatases in the control of Mec1/ATR^{Mec1} themselves is largely unexplored. In Chapter 2 we show that Psy2-Pph3 (PP4) regulates not only Mec1 phosphorylation but also phosphorylation of many of its targets.

6.2. PHOSPHATASE-INDEPENDENT MECHANISMS OF CHECKPOINT DOWN-REGULATION

In addition to the phosphatase-dependent down-regulation, the ubiquitin proteasome pathway also plays a role in checkpoint recovery in higher organisms (Figure 1.4B). CHK1 has been shown to be targeted by cullin 1—(CUL1) or cullin 4A—(CUL4A) dependent proteolysis (Leung-Pineda et al., 2009; Zhang et al., 2009). Claspin^{Mrc1} is also targeted by SCF^{B-TRCP} for degradation⁶ (Mailand et al., 2006; Mamely et al., 2006; Peschiaroli et al., 2006), and this effect is counteracted by USP7, a deubiquitylating enzyme, called ubiquitin-specific protease 7 (Faustrop et al., 2009). PLK1^{Cdc5} (polo-like kinase 1) promotes Claspin^{Mrc1} degradation by promoting SCF^{B-TRCP}-dependent ubiquitination (Mailand et al., 2006; Mamely et al., 2006; Peschiaroli et al., 2006), and this PLK1^{Cdc5} activity is prompted by Aurora A and Greatwall kinases (Macurek et al., 2008; Peng et al., 2011). The role of PLK1^{Cdc5} in checkpoint down-regulation may be conserved, since the *S. cerevisiae* PLK1 homolog, Cdc5, is important for adaptation from an irreparable DSB, although the action of Cdc5 appears to be different (Donnianni et al., 2010; Schleker et al., 2010; Toczyski et al., 1997; Vidanes et al., 2010). PLK1^{Cdc5} has also been shown to facilitate DNA replication under replication stress. Namely, the *Xenopus* PLK1^{Cdc5}, Plx1^{Cdc5}, is recruited to chromatin through ATR^{Mec1}-dependent phosphorylation of MCM2^{Mcm2} at serine 92 upon fork stalling, and Plx1^{Cdc5} recruitment is important for origin firing near stalled forks (Trenz et al., 2008). In human cells, it has been shown that PLK1^{Cdc5} phosphorylates ORC2^{Orc2} on serine 188. This phosphorylation promotes DNA replication under replication stress (Song et al., 2011). In summary, checkpoint recovery is promoted by two opposing enzymatic activities; multiple phosphatases directly quench the checkpoint kinases and the effectors, while polo-

⁶ Similarly, yeast Mrc1 was recently shown to be degraded in a SCF^{Dia2}-dependent manner during checkpoint recovery (Fong, et al., 2013).

like kinase promotes the degradation of checkpoint factors and facilitates the initiation of replication to complete S phase.

Srs2 helicase and Sae2 in *S. cerevisiae* appear to facilitate checkpoint recovery by eliminating or reducing the source of the sensor kinase activation. Srs2 restrains homologous recombination by dislodging the Rad51 recombination protein from ssDNA (Krejci et al., 2003; Veaute et al., 2003). Consistently, *SRS2* deletion impairs the down-regulation of the checkpoint after repair of HO-induced DSBs (Jain et al., 2009; Vaze et al., 2002). A recent study has demonstrated that *srs2Δ* cells retain Ddc2- and RPA-focus formation and chromatin association, even when the bulk of the DSB repair has been completed (Yeung and Durocher, 2011). Yeung and Durocher suggest that Srs2 dismantles Rad51, which results in elimination of ssDNA and a suppression of Mec1 signaling. Sae2 (CtIP in vertebrates) is involved in meiotic and mitotic DSB processing, together with the Mre11-Rad50-Xrs2 (NBS1 in vertebrates) complex (Clerici et al., 2005; McKee and Kleckner, 1997; Prinz et al., 1997; Rattray et al., 2001). MRN^{MRX} recognizes DSBs very rapidly and recruits ATM^{Tel1} kinase. Several studies have shown that *sae2* mutants show a defect in checkpoint recovery, whereas overexpression of *SAE2* counteracts checkpoint activation (Clerici et al., 2006; Guenole et al., 2013; Kim et al., 2008a). Deletion of *SAE2* results in an increased level of MRX at DSBs, whereas overexpression of *SAE2* has the opposite effect, suggesting that Sae2 evicts MRX at the damage site and thereby limits Tel1 checkpoint signaling (Clerici et al., 2006; Kim et al., 2008a). This Sae2 function may facilitate switching from Tel1/ATM to Mec1/ATR signaling (see Section 5).

Recent studies in *S. cerevisiae* have shed light on yet another mechanism of the checkpoint attenuation that involves a scaffold complex called Slx4-Rtt107 (Figure 1.4C). The Mec1 activator Dpb11 binds Rad9 and up-regulates Rad53 activation (see Section 2.4) (Pfander and Diffley, 2011), and the Mec1/Tel1 phosphorylation of H2A at Ser129 (H2A-p; γ H2AX in mammals) recruits Rad9 to damage sites, also leading to the activation of Rad53 (Javaheri et al., 2006). Intriguingly, the DNA repair scaffold complex Slx4-Rtt107 can also bind Dpb11 in a Mec1-dependent manner (Ohouo et al., 2010), and the C-terminal tandem BRCT domain of Rtt107 interacts with H2A-P (Li et al., 2012). In a recent study, the Smolka group argues that the Slx4-Rtt107 complex negatively regulates Rad53 by competing with Rad9 for both Dpb11 and H2A-p, two positive checkpoint regulators (Ohouo et al., 2013).

Finally, a recent study suggests that both Isw2 and Ino80, confirmed targets of checkpoint kinases, interact with RPA and function to attenuate the checkpoint activity (Au et al., 2011). Molecular mechanisms of the remodeler function in checkpoint recovery are unclear, but a similar competition may exist where Ino80 and Isw2 exclude excess Mec1 from RPA binding.

7. SCOPE OF MY PROJECTS

7.1 YEAST PP4 INTERACTS WITH DDC2-MEC1 AND REGULATES CHECKPOINT SIGNALING

Checkpoint recovery through Rad53 dephosphorylation is well studied and several phosphatases have been implicated in this process (see Section 6.1), yet it is still unknown if and how the upstream checkpoint kinase Mec1 is regulated by phosphorylation/dephosphorylation cycles. Even though more ssDNA accumulates when replication forks stall, the structures that recruit Mec1 and its activators (ssDNA-dsDNA junctions; see Section 2.1) are also present during normal, discontinuous replication on the lagging strand (Sogo et al., 2002). However, normal replication does not lead to detectable checkpoint activation (Sanchez et al., 1996). Rather it has been described, that in S phase the threshold for checkpoint activation is even lower than in G2 phase and that a certain number of replication forks has to be generated in order to robustly sense and signal replication stress (Shimada et al., 2002; Tercero et al., 2003). One potential mechanism how this threshold could be generated is through cell cycle dependent modification and thus modulation of Rad53 activity (Schleker et al., 2010). Another hypothesis is that Mec1 might be regulated in a way that prevents aberrant checkpoint activation. Supporting this hypothesis, a recent study suggests that Mec1 is active during normal replication and phosphorylates proteins, especially chromatin modulating enzymes. Checkpoint activation may merely induce a switch that results in Mec1 phosphorylating a different set of targets (M. Smolka, unpublished data). However, the nature of this switch and how it is regulated remains unknown. The aim of this project was to identify novel factors involved in Mec1 checkpoint signaling. We were especially interested in potential negative regulators of Mec1. We reasoned that loss of function of a negative inhibitor might rescue HU sensitivity of replication checkpoint deficient *mec1-100* cells. Thus, we screened for suppressors of *mec1-100* HU sensitivity in two independent experiments and characterized the top hit, a conserved phosphatase complex, Psy2-Pph3 and its role in Mec1 signaling in this project.

7.2 CHARACTERIZATION OF *MEC1-100*, AN S PHASE DEFECTIVE ALLELE

The Longhese laboratory discovered a mutant allele of Mec1 that is specifically defective in activating the G1/S and replication checkpoint, but leaves the G2 checkpoint intact (Paciotti et al., 2001). It has two point mutations outside of the catalytic domain. F1179S resides in a helical region N-terminal of the conserved FAT domain, while N1700S is located within the FAT domain. Both residues are predicted to be in turns or loops between helices and therefore might be available for protein-protein contacts (see Chapter 3). A similar allele has been described in human ATR^{Mec1} with three mutations just N-terminal of the FAT domain (Figure 3.1) (Nam et al., 2011a). Therefore, we hypothesized that the mutated residues might reside in a regulatory region with a conserved function for the replication checkpoint. The aim of this project was to understand the mechanism by which these mutations cause a defect in replication checkpoint signaling. Several hypotheses, (e.g. mutations reduce kinase activity, impair oligomerization or disrupt a protein-protein interaction) were developed and tested during the course of this work. By studying intragenic suppressors that were identified in one of the genetic screens described in Chapter 2, we also hoped to better understand the mechanism of the *mec1-100* mutations.

7.3 AN ACIDIC DOMAIN IN *SGS1* INTERACTS WITH RPA AND RECRUITS RAD53

Sgs1 is the sole RecQ helicase in yeast and plays an important role in genome stability (Cobb et al., 2003). One of its functions is the resolution of homologous recombination intermediates (Ira et al., 2003). However, it is also involved in the stabilization of stalled replication forks (Cobb et al., 2003; Cobb et al., 2005). Both *sgs1*Δ and *mec1-100* mutations have been shown to be HU sensitive

and to lead to a partial loss of DNA polymerases from sites of stalled forks, as single mutants. The combination of both mutations is synthetic lethal on even low doses of HU and results in a complete loss of polymerase and RPA signals at replication forks stalled on HU (Cobb et al., 2005). Both Mec1 (through Ddc2) and Sgs1 interact with the single stranded binding protein RPA (Cobb et al., 2003; Zou and Elledge, 2003). We hypothesized that the Sgs1-RPA interaction might be key to understanding the role of Sgs1 in the response to replication stress. Although *sgs1* Δ is synergistic with *mec1-100* in regard to stabilization of stalled forks, suggesting that they act on two parallel pathways, it is also involved in Mec1-dependent Rad53 phosphorylation in a manner epistatic with the replication checkpoint mediator Mrc1 (Bjergbaek et al., 2005). In this context Sgs1 was shown to interact with Rad53 by co-immunoprecipitation and yeast two-hybrid assays (Bjergbaek et al., 2005). However, the mechanism through which Sgs1 contributes to replication checkpoint signaling and stabilizing polymerases at stalled forks remained unknown. By separating two of the Sgs1 functions, helicase activity and RPA binding, we aimed at dissecting and better understanding the role of Sgs1 in these processes.

REFERENCES

- Aguilera, A., and Gomez-Gonzalez, B. (2008). Genome instability: a mechanistic view of its causes and consequences. *Nat Rev Genet* 9, 204-217.
- Alabert, C., Bianco, J.N., and Pasero, P. (2009). Differential regulation of homologous recombination at DNA breaks and replication forks by the Mrc1 branch of the S-phase checkpoint. *EMBO J* 28, 1131-1141.
- Alani, E., Thresher, R., Griffith, J.D., and Kolodner, R.D. (1992). Characterization of DNA-binding and strand-exchange stimulation properties of γ -RPA, a yeast single-strand-DNA-binding protein. *J Mol Biol* 227, 54-71.
- Alcasabas, A.A., Osborn, A.J., Bachant, J., Hu, F., Werler, P.J., Bousset, K., Furuya, K., Diffley, J.F., Carr, A.M., and Elledge, S.J. (2001). Mrc1 transduces signals of DNA replication stress to activate Rad53. *Nat Cell Biol* 3, 958-965.
- Ali, A., Zhang, J., Bao, S., Liu, I., Otterness, D., Dean, N.M., Abraham, R.T., and Wang, X.F. (2004). Requirement of protein phosphatase 5 in DNA-damage-induced ATM activation. *Genes Dev* 18, 249-254.
- Allen, J.B., Zhou, Z., Siede, W., Friedberg, E.C., and Elledge, S.J. (1994). The SAD1/RAD53 protein kinase controls multiple checkpoints and DNA damage-induced transcription in yeast. *Genes Dev* 8, 2401-2415.
- Ammazzalorso, F., Pirzio, L.M., Bignami, M., Franchitto, A., and Pichierri, P. (2010). ATR and ATM differently regulate WRN to prevent DSBs at stalled replication forks and promote replication fork recovery. *EMBO J* 29, 3156-3169.
- Au, T.J., Rodriguez, J., Vincent, J.A., and Tsukiyama, T. (2011). ATP-dependent chromatin remodeling factors tune S phase checkpoint activity. *Mol Cell Biol* 31, 4454-4463.
- Aylon, Y., and Kupiec, M. (2003). The checkpoint protein Rad24 of *Saccharomyces cerevisiae* is involved in processing double-strand break ends and in recombination partner choice. *Mol Cell Biol* 23, 6585-6596.
- Azvolinsky, A., Giresi, P.G., Lieb, J.D., and Zakian, V.A. (2009). Highly transcribed RNA polymerase II genes are impediments to replication fork progression in *Saccharomyces cerevisiae*. *Mol Cell* 34, 722-734.
- Bailis, J.M., Luche, D.D., Hunter, T., and Forsburg, S.L. (2008). Minichromosome maintenance proteins interact with checkpoint and recombination proteins to promote s-phase genome stability. *Mol Cell Biol* 28, 1724-1738.
- Bakkenist, C.J., and Kastan, M.B. (2003). DNA damage activates ATM through intermolecular autophosphorylation and dimer dissociation. *Nature* 421, 499-506.
- Balakrishnan, L., Brandt, P.D., Lindsey-Boltz, L.A., Sancar, A., and Bambara, R.A. (2009). Long patch base excision repair proceeds via coordinated stimulation of the multienzyme DNA repair complex. *J Biol Chem* 284, 15158-15172.
- Baldo, V., Testoni, V., Lucchini, G., and Longhese, M.P. (2008). Dominant TEL1-hy mutations compensate for Mec1 lack of functions in the DNA damage response. *Mol Cell Biol* 28, 358-375.
- Ball, H.L., and Cortez, D. (2005). ATRIP oligomerization is required for ATR-dependent checkpoint signaling. *J Biol Chem* 280, 31390-31396.
- Ball, H.L., Ehrhardt, M.R., Mordes, D.A., Glick, G.G., Chazin, W.J., and Cortez, D. (2007). Function of a conserved checkpoint recruitment domain in ATRIP proteins. *Mol Cell Biol* 27, 3367-3377.
- Ball, H.L., Myers, J.S., and Cortez, D. (2005). ATRIP binding to replication protein A-single-stranded DNA promotes ATR-ATRIP localization but is dispensable for Chk1 phosphorylation. *Mol Biol Cell* 16, 2372-2381.
- Bando, M., Katou, Y., Komata, M., Tanaka, H., Itoh, T., Sutani, T., and Shirahige, K. (2009). Csm3, Tof1, and Mrc1 form a heterotrimeric mediator complex that associates with DNA replication forks. *J Biol Chem* 284, 34355-34365.
- Bandyopadhyay, S., Mehta, M., Kuo, D., Sung, M.K., Chuang, R., Jaehnig, E.J., Bodenmiller, B., Licon, K., Copeland, W., Shales, M., *et al.* (2010). Rewiring of genetic networks in response to DNA damage. *Science* 330, 1385-1389.

- Barberis, M., Spiesser, T.W., and Klipp, E. (2010). Replication origins and timing of temporal replication in budding yeast: how to solve the conundrum? *Current genomics* *11*, 199-211.
- Barlow, J.H., and Rothstein, R. (2009). Rad52 recruitment is DNA replication independent and regulated by Cdc28 and the Mec1 kinase. *EMBO J* *28*, 1121-1130.
- Bastos de Oliveira, F.M., Harris, M.R., Brazauskas, P., de Bruin, R.A., and Smolka, M.B. (2012). Linking DNA replication checkpoint to MBF cell-cycle transcription reveals a distinct class of G1/S genes. *EMBO J* *31*, 1798-1810.
- Bazzi, M., Mantiero, D., Trovesi, C., Lucchini, G., and Longhese, M.P. (2010). Dephosphorylation of gamma H2A by Glc7/protein phosphatase 1 promotes recovery from inhibition of DNA replication. *Mol Cell Biol* *30*, 131-145.
- Bean, J.M., Siggia, E.D., and Cross, F.R. (2005). High functional overlap between MluI cell-cycle box binding factor and Swi4/6 cell-cycle box binding factor in the G1/S transcriptional program in *Saccharomyces cerevisiae*. *Genetics* *171*, 49-61.
- Bennetzen, M.V., Larsen, D.H., Bunkenborg, J., Bartek, J., Lukas, J., and Andersen, J.S. (2010). Site-specific phosphorylation dynamics of the nuclear proteome during the DNA damage response. *Mol Cell Proteomics* *9*, 1314-1323.
- Benton, M.G., Somasundaram, S., Glasner, J.D., and Palecek, S.P. (2006). Analyzing the dose-dependence of the *Saccharomyces cerevisiae* global transcriptional response to methyl methanesulfonate and ionizing radiation. *BMC genomics* *7*, 305.
- Berens, T.J., and Toczyski, D.P. (2012). Colocalization of Mec1 and Mrc1 is sufficient for Rad53 phosphorylation in vivo. *Mol Biol Cell* *23*, 1058-1067.
- Bermejo, R., Capra, T., Jossen, R., Colosio, A., Frattini, C., Carotenuto, W., Cocito, A., Doksani, Y., Klein, H., Gomez-Gonzalez, B., *et al.* (2011). The replication checkpoint protects fork stability by releasing transcribed genes from nuclear pores. *Cell* *146*, 233-246.
- Bester, A.C., Roniger, M., Oren, Y.S., Im, M.M., Sarni, D., Chaoat, M., Bensimon, A., Zamir, G., Shewach, D.S., and Kerem, B. (2011). Nucleotide deficiency promotes genomic instability in early stages of cancer development. *Cell* *145*, 435-446.
- Bjergbaek, L., Cobb, J.A., Tsai-Pflugfelder, M., and Gasser, S.M. (2005). Mechanistically distinct roles for Sgs1p in checkpoint activation and replication fork maintenance. *EMBO J* *24*, 405-417.
- Blasius, M., Forment, J.V., Thakkar, N., Wagner, S.A., Choudhary, C., and Jackson, S.P. (2011). A phospho-proteomic screen identifies substrates of the checkpoint kinase Chk1. *Genome Biol* *12*, R78.
- Bonilla, C.Y., Melo, J.A., and Toczyski, D.P. (2008). Colocalization of sensors is sufficient to activate the DNA damage checkpoint in the absence of damage. *Mol Cell* *30*, 267-276.
- Bosotti, R., Isacchi, A., and Sonhammer, E.L. (2000). FAT: a novel domain in PIK-related kinases. *Trends Biochem Sci* *25*, 225-227.
- Brown, E.J., and Baltimore, D. (2000). ATR disruption leads to chromosomal fragmentation and early embryonic lethality. *Genes Dev* *14*, 397-402.
- Brush, G.S., and Kelly, T.J. (2000). Phosphorylation of the replication protein A large subunit in the *Saccharomyces cerevisiae* checkpoint response. *Nucleic Acids Res* *28*, 3725-3732.
- Brush, G.S., Morrow, D.M., Hieter, P., and Kelly, T.J. (1996). The ATM homologue MEC1 is required for phosphorylation of replication protein A in yeast. *Proc Natl Acad Sci U S A* *93*, 15075-15080.
- Busino, L., Donzelli, M., Chiesa, M., Guardavaccaro, D., Ganoth, D., Dorrello, N.V., Hershko, A., Pagano, M., and Draetta, G.F. (2003). Degradation of Cdc25A by beta-TrCP during S phase and in response to DNA damage. *Nature* *426*, 87-91.
- Byun, T.S., Pacek, M., Yee, M.C., Walter, J.C., and Cimprich, K.A. (2005). Functional uncoupling of MCM helicase and DNA polymerase activities activates the ATR-dependent checkpoint. *Genes Dev* *19*, 1040-1052.
- Casper, A.M., Nghiem, P., Arlt, M.F., and Glover, T.W. (2002). ATR regulates fragile site stability. *Cell* *111*, 779-789.
- Cayla, X., Goris, J., Hermann, J., Hendrix, P., Ozon, R., and Merlevede, W. (1990). Isolation and characterization of a tyrosyl phosphatase activator from rabbit skeletal muscle and *Xenopus laevis* oocytes. *Biochemistry* *29*, 658-667.

- Cejka, P., Cannavo, E., Polaczek, P., Masuda-Sasa, T., Pokharel, S., Campbell, J.L., and Kowalczykowski, S.C. (2010). DNA end resection by Dna2-Sgs1-RPA and its stimulation by Top3-Rmi1 and Mre11-Rad50-Xrs2. *Nature* *467*, 112-116.
- Cha, R.S., and Kleckner, N. (2002). ATR homolog Mec1 promotes fork progression, thus averting breaks in replication slow zones. *Science* *297*, 602-606.
- Chabes, A., Georgieva, B., Domkin, V., Zhao, X., Rothstein, R., and Thelander, L. (2003). Survival of DNA damage in yeast directly depends on increased dNTP levels allowed by relaxed feedback inhibition of ribonucleotide reductase. *Cell* *112*, 391-401.
- Chan, D.W., Ye, R., Veillette, C.J., and Lees-Miller, S.P. (1999). DNA-dependent protein kinase phosphorylation sites in Ku 70/80 heterodimer. *Biochemistry* *38*, 1819-1828.
- Chang, D.Y., and Lu, A.L. (2005). Interaction of checkpoint proteins Hus1/Rad1/Rad9 with DNA base excision repair enzyme MutY homolog in fission yeast, *Schizosaccharomyces pombe*. *J Biol Chem* *280*, 408-417.
- Chen, S.H., Albuquerque, C.P., Liang, J., Suhandynata, R.T., and Zhou, H. (2010). A proteome-wide analysis of kinase-substrate network in the DNA damage response. *J Biol Chem* *285*, 12803-12812.
- Chen, S.H., and Zhou, H. (2009). Reconstitution of Rad53 activation by Mec1 through adaptor protein Mrc1. *J Biol Chem* *284*, 18593-18604.
- Chen, X., Cui, D., Papusha, A., Zhang, X., Chu, C.D., Tang, J., Chen, K., Pan, X., and Ira, G. (2012). The Fun30 nucleosome remodeller promotes resection of DNA double-strand break ends. *Nature* *489*, 576-580.
- Cheung, H.C., San Lucas, F.A., Hicks, S., Chang, K., Bertuch, A.A., and Ribes-Zamora, A. (2012). An S/T-Q cluster domain census unveils new putative targets under Tel1/Mec1 control. *BMC genomics* *13*, 664.
- Chini, C.C., and Chen, J. (2003). Human claspin is required for replication checkpoint control. *J Biol Chem* *278*, 30057-30062.
- Chowdhury, D., Xu, X., Zhong, X., Ahmed, F., Zhong, J., Liao, J., Dykxhoorn, D.M., Weinstock, D.M., Pfeifer, G.P., and Lieberman, J. (2008). A PP4-phosphatase complex dephosphorylates gamma-H2AX generated during DNA replication. *Mol Cell* *31*, 33-46.
- Cimprich, K.A., and Cortez, D. (2008). ATR: an essential regulator of genome integrity. *Nat Rev Mol Cell Biol* *9*, 616-627.
- Clarke, D.J., Segal, M., Jensen, S., and Reed, S.I. (2001). Mec1p regulates Pds1p levels in S phase: complex coordination of DNA replication and mitosis. *Nat Cell Biol* *3*, 619-627.
- Clemenson, C., and Marsolier-Kergoat, M.C. (2009). DNA damage checkpoint inactivation: adaptation and recovery. *DNA Repair (Amst)* *8*, 1101-1109.
- Clerici, M., Mantiero, D., Lucchini, G., and Longhese, M.P. (2005). The *Saccharomyces cerevisiae* Sae2 protein promotes resection and bridging of double strand break ends. *J Biol Chem* *280*, 38631-38638.
- Clerici, M., Mantiero, D., Lucchini, G., and Longhese, M.P. (2006). The *Saccharomyces cerevisiae* Sae2 protein negatively regulates DNA damage checkpoint signalling. *EMBO Rep* *7*, 212-218.
- Cobb, J.A., Bjergbaek, L., Shimada, K., Frei, C., and Gasser, S.M. (2003). DNA polymerase stabilization at stalled replication forks requires Mec1 and the RecQ helicase Sgs1. *EMBO J* *22*, 4325-4336.
- Cobb, J.A., Schleker, T., Rojas, V., Bjergbaek, L., Tercero, J.A., and Gasser, S.M. (2005). Replisome instability, fork collapse, and gross chromosomal rearrangements arise synergistically from Mec1 kinase and RecQ helicase mutations. *Genes Dev* *19*, 3055-3069.
- Cortez, D., Glick, G., and Elledge, S.J. (2004). Minichromosome maintenance proteins are direct targets of the ATM and ATR checkpoint kinases. *Proc Natl Acad Sci U S A* *101*, 10078-10083.
- Cortez, D., Wang, Y., Qin, J., and Elledge, S.J. (1999). Requirement of ATM-dependent phosphorylation of brca1 in the DNA damage response to double-strand breaks. *Science* *286*, 1162-1166.
- Costanzo, V., Robertson, K., Bibikova, M., Kim, E., Grieco, D., Gottesman, M., Carroll, D., and Gautier, J. (2001). Mre11 protein complex prevents double-strand break accumulation during chromosomal DNA replication. *Mol Cell* *8*, 137-147.

- Costelloe, T., Louge, R., Tomimatsu, N., Mukherjee, B., Martini, E., Khadaroo, B., Dubois, K., Wiegant, W.W., Thierry, A., Burma, S., *et al.* (2012). The yeast Fun30 and human SMARCAD1 chromatin remodellers promote DNA end resection. *Nature* *489*, 581-584.
- Cotta-Ramusino, C., Fachinetti, D., Lucca, C., Dokhani, Y., Lopes, M., Sogo, J., and Foiani, M. (2005). Exo1 processes stalled replication forks and counteracts fork reversal in checkpoint-defective cells. *Mol Cell* *17*, 153-159.
- Crabbe, L., Thomas, A., Pantesco, V., De Vos, J., Pasero, P., and Lengronne, A. (2010). Analysis of replication profiles reveals key role of RFC-Ctf18 in yeast replication stress response. *Nat Struct Mol Biol* *17*, 1391-1397.
- D'Amours, D., and Jackson, S.P. (2001). The yeast Xrs2 complex functions in S phase checkpoint regulation. *Genes Dev* *15*, 2238-2249.
- Davies, S.L., North, P.S., Dart, A., Lakin, N.D., and Hickson, I.D. (2004). Phosphorylation of the Bloom's syndrome helicase and its role in recovery from S-phase arrest. *Mol Cell Biol* *24*, 1279-1291.
- Davies, S.L., North, P.S., and Hickson, I.D. (2007). Role for BLM in replication-fork restart and suppression of origin firing after replicative stress. *Nat Struct Mol Biol* *14*, 677-679.
- de Bruin, R.A., Kalashnikova, T.I., Aslanian, A., Wohlschlegel, J., Chahwan, C., Yates, J.R., 3rd, Russell, P., and Wittenberg, C. (2008). DNA replication checkpoint promotes G1-S transcription by inactivating the MBF repressor Nrm1. *Proc Natl Acad Sci U S A* *105*, 11230-11235.
- de Bruin, R.A., Kalashnikova, T.I., Chahwan, C., McDonald, W.H., Wohlschlegel, J., Yates, J., 3rd, Russell, P., and Wittenberg, C. (2006). Constraining G1-specific transcription to late G1 phase: the MBF-associated corepressor Nrm1 acts via negative feedback. *Mol Cell* *23*, 483-496.
- de Klein, A., Muijtjens, M., van Os, R., Verhoeven, Y., Smit, B., Carr, A.M., Lehmann, A.R., and Hoeijmakers, J.H. (2000). Targeted disruption of the cell-cycle checkpoint gene ATR leads to early embryonic lethality in mice. *Curr Biol* *10*, 479-482.
- de la Torre-Ruiz, M.A., Green, C.M., and Lowndes, N.F. (1998). RAD9 and RAD24 define two additive, interacting branches of the DNA damage checkpoint pathway in budding yeast normally required for Rad53 modification and activation. *EMBO J* *17*, 2687-2698.
- De Piccoli, G., Katou, Y., Itoh, T., Nakato, R., Shirahige, K., and Labib, K. (2012). Replisome stability at defective DNA replication forks is independent of S phase checkpoint kinases. *Mol Cell* *45*, 696-704.
- Delacroix, S., Wagner, J.M., Kobayashi, M., Yamamoto, K., and Karnitz, L.M. (2007). The Rad9-Hus1-Rad1 (9-1-1) clamp activates checkpoint signaling via TopBP1. *Genes Dev* *21*, 1472-1477.
- den Elzen, N.R., and O'Connell, M.J. (2004). Recovery from DNA damage checkpoint arrest by PP1-mediated inhibition of Chk1. *EMBO J* *23*, 908-918.
- Desany, B.A., Alcasabas, A.A., Bachant, J.B., and Elledge, S.J. (1998). Recovery from DNA replicational stress is the essential function of the S-phase checkpoint pathway. *Genes Dev* *12*, 2956-2970.
- Dokhani, Y., Bermejo, R., Fiorani, S., Haber, J.E., and Foiani, M. (2009). Replicon dynamics, dormant origin firing, and terminal fork integrity after double-strand break formation. *Cell* *137*, 247-258.
- Donnianni, R.A., Ferrari, M., Lazzaro, F., Clerici, M., Tamilselvan Nachimuthu, B., Plevani, P., Muzi-Falconi, M., and Pelliccioli, A. (2010). Elevated levels of the polo kinase Cdc5 override the Mec1/ATR checkpoint in budding yeast by acting at different steps of the signaling pathway. *PLoS Genet* *6*, e1000763.
- Downs, J.A., Lowndes, N.F., and Jackson, S.P. (2000). A role for *Saccharomyces cerevisiae* histone H2A in DNA repair. *Nature* *408*, 1001-1004.
- Dubrana, K., van Attikum, H., Hediger, F., and Gasser, S.M. (2007). The processing of double-strand breaks and binding of single-strand-binding proteins RPA and Rad51 modulate the formation of ATR-kinase foci in yeast. *J Cell Sci* *120*, 4209-4220.
- Durocher, D., and Jackson, S.P. (2002). The FHA domain. *FEBS Lett* *513*, 58-66.
- Duursma, A.M., Driscoll, R., Elias, J.E., and Cimprich, K.A. (2013). A Role for the MRN Complex in ATR Activation via TOPBP1 Recruitment. *Mol Cell* *50*, 116-122.

- Eapen, V.V., Sugawara, N., Tsabar, M., Wu, W.H., and Haber, J.E. (2012). The *Saccharomyces cerevisiae* chromatin remodeler Fun30 regulates DNA end resection and checkpoint deactivation. *Mol Cell Biol* 32, 4727-4740.
- Egloff, M.P., Cohen, P.T., Reinemer, P., and Barford, D. (1995). Crystal structure of the catalytic subunit of human protein phosphatase 1 and its complex with tungstate. *J Mol Biol* 254, 942-959.
- Eklund, H., Uhlin, U., Farnegardh, M., Logan, D.T., and Nordlund, P. (2001). Structure and function of the radical enzyme ribonucleotide reductase. *Progress in biophysics and molecular biology* 77, 177-268.
- El-Shemerly, M., Hess, D., Pyakurel, A.K., Moselhy, S., and Ferrari, S. (2008). ATR-dependent pathways control hEXO1 stability in response to stalled forks. *Nucleic Acids Res* 36, 511-519.
- Elledge, S.J. (1996). Cell cycle checkpoints: preventing an identity crisis. *Science* 274, 1664-1672.
- Emili, A. (1998). MEC1-dependent phosphorylation of Rad9p in response to DNA damage. *Mol Cell* 2, 183-189.
- Falbo, K.B., Alabert, C., Katou, Y., Wu, S., Han, J., Wehr, T., Xiao, J., He, X., Zhang, Z., Shi, Y., *et al.* (2009). Involvement of a chromatin remodeling complex in damage tolerance during DNA replication. *Nat Struct Mol Biol* 16, 1167-1172.
- Faustrop, H., Bekker-Jensen, S., Bartek, J., Lukas, J., and Mailand, N. (2009). USP7 counteracts SCFbetaTrCP- but not APCcdh1-mediated proteolysis of Claspin. *J Cell Biol* 184, 13-19.
- Fong, C.M., Arumugam, A., and Koepp, D.M. (2013). The *Saccharomyces cerevisiae* F-box protein Dia2 is a mediator of S-phase checkpoint recovery from DNA damage. *Genetics* 193, 483-499.
- Freeman, A.K., and Monteiro, A.N. (2010). Phosphatases in the cellular response to DNA damage. *Cell communication and signaling : CCS* 8, 27.
- Frei, C., and Gasser, S.M. (2000). The yeast Sgs1p helicase acts upstream of Rad53p in the DNA replication checkpoint and colocalizes with Rad53p in S-phase-specific foci. *Genes Dev* 14, 81-96.
- Friedel, A.M., Pike, B.L., and Gasser, S.M. (2009). ATR/Mec1: coordinating fork stability and repair. *Curr Opin Cell Biol* 21, 237-244.
- Fu, Y., Zhu, Y., Zhang, K., Yeung, M., Durocher, D., and Xiao, W. (2008). Rad6-Rad18 mediates a eukaryotic SOS response by ubiquitinating the 9-1-1 checkpoint clamp. *Cell* 133, 601-611.
- Fujimoto, H., Onishi, N., Kato, N., Takekawa, M., Xu, X.Z., Kosugi, A., Kondo, T., Imamura, M., Oishi, I., Yoda, A., *et al.* (2006). Regulation of the antioncogenic Chk2 kinase by the oncogenic Wip1 phosphatase. *Cell Death Differ* 13, 1170-1180.
- Furuya, K., Miyabe, I., Tsutsui, Y., Paderi, F., Kakusho, N., Masai, H., Niki, H., and Carr, A.M. (2010). DDK phosphorylates checkpoint clamp component Rad9 and promotes its release from damaged chromatin. *Mol Cell* 40, 606-618.
- Furuya, K., Poitelea, M., Guo, L., Caspari, T., and Carr, A.M. (2004). Chk1 activation requires Rad9 S/TQ-site phosphorylation to promote association with C-terminal BRCT domains of Rad4TOPBP1. *Genes Dev* 18, 1154-1164.
- Gardner, R., Putnam, C.W., and Weinert, T. (1999). RAD53, DUN1 and PDS1 define two parallel G2/M checkpoint pathways in budding yeast. *EMBO J* 18, 3173-3185.
- Gasch, A.P., Huang, M., Metzner, S., Botstein, D., Elledge, S.J., and Brown, P.O. (2001). Genomic expression responses to DNA-damaging agents and the regulatory role of the yeast ATR homolog Mec1p. *Mol Biol Cell* 12, 2987-3003.
- Gembka, A., Toueille, M., Smirnova, E., Poltz, R., Ferrari, E., Villani, G., and Hubscher, U. (2007). The checkpoint clamp, Rad9-Rad1-Hus1 complex, preferentially stimulates the activity of apurinic/apyrimidinic endonuclease 1 and DNA polymerase beta in long patch base excision repair. *Nucleic Acids Res* 35, 2596-2608.
- Giannattasio, M., Follonier, C., Tourriere, H., Puddu, F., Lazzaro, F., Pasero, P., Lopes, M., Plevani, P., and Muzi-Falconi, M. (2010). Exo1 competes with repair synthesis, converts NER intermediates to long ssDNA gaps, and promotes checkpoint activation. *Mol Cell* 40, 50-62.
- Giannattasio, M., Lazzaro, F., Plevani, P., and Muzi-Falconi, M. (2005). The DNA damage checkpoint response requires histone H2B ubiquitination by Rad6-Brel and H3 methylation by Dot1. *J Biol Chem* 280, 9879-9886.

- Gilbert, C.S., Green, C.M., and Lowndes, N.F. (2001). Budding yeast Rad9 is an ATP-dependent Rad53 activating machine. *Mol Cell* 8, 129-136.
- Gilbert, D.M., Takebayashi, S.I., Ryba, T., Lu, J., Pope, B.D., Wilson, K.A., and Hiratani, I. (2010). Space and time in the nucleus: developmental control of replication timing and chromosome architecture. *Cold Spring Harbor symposia on quantitative biology* 75, 143-153.
- Gingras, A.C., Caballero, M., Zarske, M., Sanchez, A., Hazbun, T.R., Fields, S., Sonenberg, N., Hafen, E., Raught, B., and Aebersold, R. (2005). A novel, evolutionarily conserved protein phosphatase complex involved in cisplatin sensitivity. *Mol Cell Proteomics* 4, 1725-1740.
- Goldberg, J., Huang, H.B., Kwon, Y.G., Greengard, P., Nairn, A.C., and Kuriyan, J. (1995). Three-dimensional structure of the catalytic subunit of protein serine/threonine phosphatase-1. *Nature* 376, 745-753.
- Goodarzi, A.A., Jonnalagadda, J.C., Douglas, P., Young, D., Ye, R., Moorhead, G.B., Lees-Miller, S.P., and Khanna, K.K. (2004). Autophosphorylation of ataxia-telangiectasia mutated is regulated by protein phosphatase 2A. *EMBO J* 23, 4451-4461.
- Grenon, M., Costelloe, T., Jimeno, S., O'Shaughnessy, A., Fitzgerald, J., Zgheib, O., Degerth, L., and Lowndes, N.F. (2007). Docking onto chromatin via the *Saccharomyces cerevisiae* Rad9 Tudor domain. *Yeast* 24, 105-119.
- Guan, X., Madabushi, A., Chang, D.Y., Fitzgerald, M.E., Shi, G., Drohat, A.C., and Lu, A.L. (2007). The human checkpoint sensor Rad9-Rad1-Hus1 interacts with and stimulates DNA repair enzyme TDG glycosylase. *Nucleic Acids Res* 35, 6207-6218.
- Guenole, A., Srivas, R., Vreeken, K., Wang, Z.Z., Wang, S., Krogan, N.J., Ideker, T., and van Attikum, H. (2013). Dissection of DNA damage responses using multiconditional genetic interaction maps. *Mol Cell* 49, 346-358.
- Guillemain, G., Ma, E., Mauger, S., Miron, S., Thai, R., Guerois, R., Ochsenbein, F., and Marsolier-Kergoat, M.C. (2007). Mechanisms of checkpoint kinase Rad53 inactivation after a double-strand break in *Saccharomyces cerevisiae*. *Mol Cell Biol* 27, 3378-3389.
- Guo, C.Y., Brautigam, D.L., and Lerner, J.M. (2002). ATM-dependent dissociation of B55 regulatory subunit from nuclear PP2A in response to ionizing radiation. *J Biol Chem* 277, 4839-4844.
- Haering, C.H., and Nasmyth, K. (2003). Building and breaking bridges between sister chromatids. *BioEssays : news and reviews in molecular, cellular and developmental biology* 25, 1178-1191.
- Halazonetis, T.D., Gorgoulis, V.G., and Bartek, J. (2008). An oncogene-induced DNA damage model for cancer development. *Science* 319, 1352-1355.
- Hammet, A., Magill, C., Heierhorst, J., and Jackson, S.P. (2007). Rad9 BRCT domain interaction with phosphorylated H2AX regulates the G1 checkpoint in budding yeast. *EMBO Rep* 8, 851-857.
- Harper, J.W., and Elledge, S.J. (2007). The DNA damage response: ten years after. *Mol Cell* 28, 739-745.
- Hartwell, L.H., and Weinert, T.A. (1989). Checkpoints: controls that ensure the order of cell cycle events. *Science* 246, 629-634.
- Hegnauer, A.M., Hustedt, N., Shimada, K., Pike, B.L., Vogel, M., Amsler, P., Rubin, S.M., van Leeuwen, F., Guenole, A., van Attikum, H., *et al.* (2012). An N-terminal acidic region of Sgs1 interacts with Rpa70 and recruits Rad53 kinase to stalled forks. *EMBO J* 31, 3768-3783.
- Heideker, J., Lis, E.T., and Romesberg, F.E. (2007). Phosphatases, DNA damage checkpoints and checkpoint deactivation. *Cell Cycle* 6, 3058-3064.
- Helt, C.E., Wang, W., Keng, P.C., and Bambara, R.A. (2005). Evidence that DNA damage detection machinery participates in DNA repair. *Cell Cycle* 4, 529-532.
- Hill, R., and Lee, P.W. (2010). The DNA-dependent protein kinase (DNA-PK): More than just a case of making ends meet? *Cell Cycle* 9, 3460-3469.
- Hiraga, S., Alvino, G.M., Chang, F., Lian, H.Y., Sridhar, A., Kubota, T., Brewer, B.J., Weinreich, M., Raghuraman, M.K., and Donaldson, A.D. (2014). Rif1 controls DNA replication by directing Protein Phosphatase 1 to reverse Cdc7-mediated phosphorylation of the MCM complex. *Genes Dev* 28, 372-383.
- Hishida, T., Kubota, Y., Carr, A.M., and Iwasaki, H. (2009). RAD6-RAD18-RAD5-pathway-dependent tolerance to chronic low-dose ultraviolet light. *Nature* 457, 612-615.

- Hombauer, H., Weismann, D., Mudrak, I., Stanzel, C., Fellner, T., Lackner, D.H., and Ogris, E. (2007). Generation of active protein phosphatase 2A is coupled to holoenzyme assembly. *PLoS Biol* 5, e155.
- Hsiang, Y.H., Hertzberg, R., Hecht, S., and Liu, L.F. (1985). Camptothecin induces protein-linked DNA breaks via mammalian DNA topoisomerase I. *J Biol Chem* 260, 14873-14878.
- Hsiang, Y.H., Lihou, M.G., and Liu, L.F. (1989). Arrest of replication forks by drug-stabilized topoisomerase I-DNA cleavable complexes as a mechanism of cell killing by camptothecin. *Cancer Res* 49, 5077-5082.
- Hu, F., Wang, Y., Liu, D., Li, Y., Qin, J., and Elledge, S.J. (2001). Regulation of the Bub2/Bfa1 GAP complex by Cdc5 and cell cycle checkpoints. *Cell* 107, 655-665.
- Hu, J., Sun, L., Shen, F., Chen, Y., Hua, Y., Liu, Y., Zhang, M., Hu, Y., Wang, Q., Xu, W., *et al.* (2012). The intra-S phase checkpoint targets Dna2 to prevent stalled replication forks from reversing. *Cell* 149, 1221-1232.
- Huang, D., Piening, B.D., and Paulovich, A.G. (2013). The Preference for Error-Free or Error-Prone Postreplication Repair in *Saccharomyces cerevisiae* Exposed to Low-Dose Methyl Methanesulfonate Is Cell Cycle Dependent. *Mol Cell Biol* 33, 1515-1527.
- Huang, J.C., Svoboda, D.L., Reardon, J.T., and Sancar, A. (1992). Human nucleotide excision nuclease removes thymine dimers from DNA by incising the 2'nd phosphodiester bond 5' and the 6th phosphodiester bond 3' to the photodimer. *Proc Natl Acad Sci U S A* 89, 3664-3668.
- Huang, M., Miao, Z.H., Zhu, H., Cai, Y.J., Lu, W., and Ding, J. (2008). Chk1 and Chk2 are differentially involved in homologous recombination repair and cell cycle arrest in response to DNA double-strand breaks induced by camptothecins. *Mol Cancer Ther* 7, 1440-1449.
- Huang, M., Zhou, Z., and Elledge, S.J. (1998). The DNA replication and damage checkpoint pathways induce transcription by inhibition of the Crt1 repressor. *Cell* 94, 595-605.
- Ikegami, S., Taguchi, T., Ohashi, M., Oguro, M., Nagano, H., and Mano, Y. (1978). Aphidicolin prevents mitotic cell division by interfering with the activity of DNA polymerase-alpha. *Nature* 275, 458-460.
- Ilves, I., Tamberg, N., and Botchan, M.R. (2012). Checkpoint kinase 2 (Chk2) inhibits the activity of the Cdc45/MCM2-7/GINS (CMG) replicative helicase complex. *Proc Natl Acad Sci U S A* 109, 13163-13170.
- Inagaki, A., Sleddens-Linkels, E., van Cappellen, W.A., Hibbert, R.G., Sixma, T.K., Hoeijmakers, J.H., Grootegoed, J.A., and Baarends, W.M. (2011). Human RAD18 interacts with ubiquitylated chromatin components and facilitates RAD9 recruitment to DNA double strand breaks. *PLoS One* 6, e23155.
- Ingebritsen, T.S., and Cohen, P. (1983). The protein phosphatases involved in cellular regulation. 1. Classification and substrate specificities. *European journal of biochemistry / FEBS* 132, 255-261.
- Ira, G., Malkova, A., Liberi, G., Foiani, M., and Haber, J.E. (2003). Srs2 and Sgs1-Top3 suppress crossovers during double-strand break repair in yeast. *Cell* 115, 401-411.
- Ishimi, Y., Komamura-Kohno, Y., Kwon, H.J., Yamada, K., and Nakanishi, M. (2003). Identification of MCM4 as a target of the DNA replication block checkpoint system. *J Biol Chem* 278, 24644-24650.
- Itakura, E., Sawada, I., and Matsuura, A. (2005). Dimerization of the ATRIP protein through the coiled-coil motif and its implication to the maintenance of stalled replication forks. *Mol Biol Cell* 16, 5551-5562.
- Iyer, V.R., Horak, C.E., Scafe, C.S., Botstein, D., Snyder, M., and Brown, P.O. (2001). Genomic binding sites of the yeast cell-cycle transcription factors SBF and MBF. *Nature* 409, 533-538.
- Jain, S., Sugawara, N., Lydeard, J., Vaze, M., Tanguy Le Gac, N., and Haber, J.E. (2009). A recombination execution checkpoint regulates the choice of homologous recombination pathway during DNA double-strand break repair. *Genes Dev* 23, 291-303.
- Javaheri, A., Wysocki, R., Jobin-Robitaille, O., Altaf, M., Cote, J., and Kron, S.J. (2006). Yeast G1 DNA damage checkpoint regulation by H2A phosphorylation is independent of chromatin remodeling. *Proc Natl Acad Sci U S A* 103, 13771-13776.
- Jazayeri, A., Falck, J., Lukas, C., Bartek, J., Smith, G.C., Lukas, J., and Jackson, S.P. (2006). ATM- and cell cycle-dependent regulation of ATR in response to DNA double-strand breaks. *Nat Cell Biol* 8, 37-45.

- Jelinsky, S.A., and Samson, L.D. (1999). Global response of *Saccharomyces cerevisiae* to an alkylating agent. *Proc Natl Acad Sci U S A* *96*, 1486-1491.
- Jin, J., Shirogane, T., Xu, L., Nalepa, G., Qin, J., Elledge, S.J., and Harper, J.W. (2003). SCFbeta-TRCP links Chk1 signaling to degradation of the Cdc25A protein phosphatase. *Genes Dev* *17*, 3062-3074.
- Jordens, J., Janssens, V., Longin, S., Stevens, I., Martens, E., Bultynck, G., Engelborghs, Y., Lescrinier, E., Waelkens, E., Goris, J., *et al.* (2006). The protein phosphatase 2A phosphatase activator is a novel peptidyl-prolyl cis/trans-isomerase. *J Biol Chem* *281*, 6349-6357.
- Kai, M., Boddy, M.N., Russell, P., and Wang, T.S. (2005). Replication checkpoint kinase Cds1 regulates Mus81 to preserve genome integrity during replication stress. *Genes Dev* *19*, 919-932.
- Kai, M., Furuya, K., Paderi, F., Carr, A.M., and Wang, T.S. (2007). Rad3-dependent phosphorylation of the checkpoint clamp regulates repair-pathway choice. *Nat Cell Biol* *9*, 691-697.
- Kai, M., and Wang, T.S. (2003). Checkpoint activation regulates mutagenic translesion synthesis. *Genes Dev* *17*, 64-76.
- Kanke, M., Kodama, Y., Takahashi, T.S., Nakagawa, T., and Masukata, H. (2012). Mcm10 plays an essential role in origin DNA unwinding after loading of the CMG components. *EMBO J* *31*, 2182-2194.
- Karlsson-Rosenthal, C., and Millar, J.B. (2006). Cdc25: mechanisms of checkpoint inhibition and recovery. *Trends in cell biology* *16*, 285-292.
- Karnani, N., and Dutta, A. (2011). The effect of the intra-S-phase checkpoint on origins of replication in human cells. *Genes Dev* *25*, 621-633.
- Karras, G.I., Fumasoni, M., Sienski, G., Vanoli, F., Branzei, D., and Jentsch, S. (2013). Noncanonical role of the 9-1-1 clamp in the error-free DNA damage tolerance pathway. *Mol Cell* *49*, 536-546.
- Katou, Y., Kanoh, Y., Bando, M., Noguchi, H., Tanaka, H., Ashikari, T., Sugimoto, K., and Shirahige, K. (2003). S-phase checkpoint proteins Tof1 and Mrc1 form a stable replication-pausing complex. *Nature* *424*, 1078-1083.
- Keogh, M.C., Kim, J.A., Downey, M., Fillingham, J., Chowdhury, D., Harrison, J.C., Onishi, M., Datta, N., Galicia, S., Emili, A., *et al.* (2006). A phosphatase complex that dephosphorylates gammaH2AX regulates DNA damage checkpoint recovery. *Nature* *439*, 497-501.
- Kim, H.S., and Brill, S.J. (2001). Rfc4 interacts with Rpa1 and is required for both DNA replication and DNA damage checkpoints in *Saccharomyces cerevisiae*. *Mol Cell Biol* *21*, 3725-3737.
- Kim, H.S., Vijayakumar, S., Reger, M., Harrison, J.C., Haber, J.E., Weil, C., and Petrini, J.H. (2008a). Functional interactions between Sae2 and the Mre11 complex. *Genetics* *178*, 711-723.
- Kim, J.A., Hicks, W.M., Li, J., Tay, S.Y., and Haber, J.E. (2011). Protein phosphatases pph3, ptc2, and ptc3 play redundant roles in DNA double-strand break repair by homologous recombination. *Mol Cell Biol* *31*, 507-516.
- Kim, J.M., Kakusho, N., Yamada, M., Kanoh, Y., Takemoto, N., and Masai, H. (2008b). Cdc7 kinase mediates Claspin phosphorylation in DNA replication checkpoint. *Oncogene* *27*, 3475-3482.
- Kim, S.M., Kumagai, A., Lee, J., and Dunphy, W.G. (2005). Phosphorylation of Chk1 by ATM- and Rad3-related (ATR) in *Xenopus* egg extracts requires binding of ATRIP to ATR but not the stable DNA-binding or coiled-coil domains of ATRIP. *J Biol Chem* *280*, 38355-38364.
- Kim, S.T., Lim, D.S., Canman, C.E., and Kastan, M.B. (1999). Substrate specificities and identification of putative substrates of ATM kinase family members. *J Biol Chem* *274*, 37538-37543.
- Komata, M., Bando, M., Araki, H., and Shirahige, K. (2009). The direct binding of Mrc1, a checkpoint mediator, to Mcm6, a replication helicase, is essential for the replication checkpoint against methyl methanesulfonate-induced stress. *Mol Cell Biol* *29*, 5008-5019.
- Krejci, L., Van Komen, S., Li, Y., Villemain, J., Reddy, M.S., Klein, H., Ellenberger, T., and Sung, P. (2003). DNA helicase Srs2 disrupts the Rad51 presynaptic filament. *Nature* *423*, 305-309.
- Krishnan, V., Nirantar, S., Crasta, K., Cheng, A.Y., and Surana, U. (2004). DNA replication checkpoint prevents precocious chromosome segregation by regulating spindle behavior. *Mol Cell* *16*, 687-700.
- Kumagai, A., and Dunphy, W.G. (2000). Claspin, a novel protein required for the activation of Chk1 during a DNA replication checkpoint response in *Xenopus* egg extracts. *Mol Cell* *6*, 839-849.

- Kumagai, A., Kim, S.M., and Dunphy, W.G. (2004). Claspin and the activated form of ATR-ATRIP collaborate in the activation of Chk1. *J Biol Chem* 279, 49599-49608.
- Kumagai, A., Lee, J., Yoo, H.Y., and Dunphy, W.G. (2006). TopBP1 activates the ATR-ATRIP complex. *Cell* 124, 943-955.
- Kumar, A., Mazzanti, M., Mistrik, M., Kosar, M., Beznoussenko, G.V., Mironov, A.A., Garre, M., Parazzoli, D., Shivashankar, G.V., Scita, G., *et al.* (2014). ATR Mediates a Checkpoint at the Nuclear Envelope in Response to Mechanical Stress. *Cell* 158, 633-646.
- Kumar, S., and Burgers, P.M. (2013). Lagging strand maturation factor Dna2 is a component of the replication checkpoint initiation machinery. *Genes Dev* 27, 313-321.
- Lambert, S., and Carr, A.M. (2005). Checkpoint responses to replication fork barriers. *Biochimie* 87, 591-602.
- Lambert, S., Mason, S.J., Barber, L.J., Hartley, J.A., Pearce, J.A., Carr, A.M., and McHugh, P.J. (2003). *Schizosaccharomyces pombe* checkpoint response to DNA interstrand cross-links. *Mol Cell Biol* 23, 4728-4737.
- Lee, D.H., Acharya, S.S., Kwon, M., Drane, P., Guan, Y., Adelmant, G., Kalev, P., Shah, J., Pellman, D., Marto, J.A., *et al.* (2014). Dephosphorylation enables the recruitment of 53BP1 to double-strand DNA breaks. *Mol Cell* 54, 512-525.
- Lee, D.H., Goodarzi, A.A., Adelmant, G.O., Pan, Y., Jeggo, P.A., Marto, J.A., and Chowdhury, D. (2012). Phosphoproteomic analysis reveals that PP4 dephosphorylates KAP-1 impacting the DNA damage response. *EMBO J* 31, 2403-2415.
- Lee, D.H., Pan, Y., Kanner, S., Sung, P., Borowiec, J.A., and Chowdhury, D. (2010). A PP4 phosphatase complex dephosphorylates RPA2 to facilitate DNA repair via homologous recombination. *Nat Struct Mol Biol* 17, 365-372.
- Lee, J., and Dunphy, W.G. (2013). The Mre11-Rad50-Nbs1 (MRN) complex has a specific role in the activation of Chk1 in response to stalled replication forks. *Mol Biol Cell* 24, 1343-1353.
- Lee, J., Kumagai, A., and Dunphy, W.G. (2007). The Rad9-Hus1-Rad1 checkpoint clamp regulates interaction of TopBP1 with ATR. *J Biol Chem* 282, 28036-28044.
- Lee, S.J., Duong, J.K., and Stern, D.F. (2004). A Ddc2-Rad53 fusion protein can bypass the requirements for RAD9 and MRC1 in Rad53 activation. *Mol Biol Cell* 15, 5443-5455.
- Lee, S.J., Schwartz, M.F., Duong, J.K., and Stern, D.F. (2003). Rad53 phosphorylation site clusters are important for Rad53 regulation and signaling. *Mol Cell Biol* 23, 6300-6314.
- Lee, Y.D., Wang, J., Stubbe, J., and Elledge, S.J. (2008). Dif1 is a DNA-damage-regulated facilitator of nuclear import for ribonucleotide reductase. *Mol Cell* 32, 70-80.
- Leroy, C., Lee, S.E., Vaze, M.B., Ochsenbein, F., Guerois, R., Haber, J.E., and Marsolier-Kergoat, M.C. (2003). PP2C phosphatases Ptc2 and Ptc3 are required for DNA checkpoint inactivation after a double-strand break. *Mol Cell* 11, 827-835.
- Leung-Pineda, V., Huh, J., and Piwnicka-Worms, H. (2009). DDB1 targets Chk1 to the Cul4 E3 ligase complex in normal cycling cells and in cells experiencing replication stress. *Cancer Res* 69, 2630-2637.
- Li, X., Liu, K., Li, F., Wang, J., Huang, H., Wu, J., and Shi, Y. (2012). Structure of C-terminal tandem BRCT repeats of Rtt107 protein reveals critical role in interaction with phosphorylated histone H2A during DNA damage repair. *J Biol Chem* 287, 9137-9146.
- Liang, X., Reed, E., and Yu, J.J. (2006). Protein phosphatase 2A interacts with Chk2 and regulates phosphorylation at Thr-68 after cisplatin treatment of human ovarian cancer cells. *International journal of molecular medicine* 17, 703-708.
- Lin, S.J., Wardlaw, C.P., Morishita, T., Miyabe, I., Chahwan, C., Caspari, T., Schmidt, U., Carr, A.M., and Garcia, V. (2012). The Rad4(TopBP1) ATR-activation domain functions in G1/S phase in a chromatin-dependent manner. *PLoS Genet* 8, e1002801.
- Lindahl, T. (1993). Instability and decay of the primary structure of DNA. *Nature* 362, 709-715.
- Lindsay, H.D., Griffiths, D.J., Edwards, R.J., Christensen, P.U., Murray, J.M., Osman, F., Walworth, N., and Carr, A.M. (1998). S-phase-specific activation of Cds1 kinase defines a subpathway of the checkpoint response in *Schizosaccharomyces pombe*. *Genes Dev* 12, 382-395.
- Liu, J., Xu, L., Zhong, J., Liao, J., Li, J., and Xu, X. (2012a). Protein phosphatase PP4 is involved in NHEJ-mediated repair of DNA double-strand breaks. *Cell Cycle* 11, 2643-2649.
- Liu, J.S., Kuo, S.R., and Melendy, T. (2003). Comparison of checkpoint responses triggered by DNA polymerase inhibition versus DNA damaging agents. *Mutat Res* 532, 215-226.

- Liu, Q., Guntuku, S., Cui, X.S., Matsuoka, S., Cortez, D., Tamai, K., Luo, G., Carattini-Rivera, S., DeMayo, F., Bradley, A., *et al.* (2000). Chk1 is an essential kinase that is regulated by Atr and required for the G(2)/M DNA damage checkpoint. *Genes Dev* *14*, 1448-1459.
- Liu, S., Ho, C.K., Ouyang, J., and Zou, L. (2013). Nek1 kinase associates with ATR-ATRIP and primes ATR for efficient DNA damage signaling. *Proc Natl Acad Sci U S A* *110*, 2175-2180.
- Liu, S., Opiyo, S.O., Manthey, K., Glanzer, J.G., Ashley, A.K., Amerin, C., Troksa, K., Shrivastav, M., Nickoloff, J.A., and Oakley, G.G. (2012b). Distinct roles for DNA-PK, ATM and ATR in RPA phosphorylation and checkpoint activation in response to replication stress. *Nucleic Acids Res* *40*, 10780-10794.
- Liu, S., Shiotani, B., Lahiri, M., Marechal, A., Tse, A., Leung, C.C., Glover, J.N., Yang, X.H., and Zou, L. (2011). ATR autophosphorylation as a molecular switch for checkpoint activation. *Mol Cell* *43*, 192-202.
- Liu, Y., Fang, Y., Shao, H., Lindsey-Boltz, L., Sancar, A., and Modrich, P. (2010). Interactions of human mismatch repair proteins MutSalpha and MutLalpha with proteins of the ATR-Chk1 pathway. *J Biol Chem* *285*, 5974-5982.
- Lopes, M., Cotta-Ramusino, C., Pelliccioli, A., Liberi, G., Plevani, P., Muzi-Falconi, M., Newlon, C.S., and Foiani, M. (2001). The DNA replication checkpoint response stabilizes stalled replication forks. *Nature* *412*, 557-561.
- Lopez-Mosqueda, J., Maas, N.L., Jonsson, Z.O., Defazio-Eli, L.G., Wohlschlegel, J., and Toczyski, D.P. (2010). Damage-induced phosphorylation of Sld3 is important to block late origin firing. *Nature* *467*, 479-483.
- Lou, H., Komata, M., Katou, Y., Guan, Z., Reis, C.C., Budd, M., Shirahige, K., and Campbell, J.L. (2008). Mrc1 and DNA polymerase epsilon function together in linking DNA replication and the S phase checkpoint. *Mol Cell* *32*, 106-117.
- Lu, X., Nannenga, B., and Donehower, L.A. (2005). PPM1D dephosphorylates Chk1 and p53 and abrogates cell cycle checkpoints. *Genes Dev* *19*, 1162-1174.
- Lucca, C., Vanoli, F., Cotta-Ramusino, C., Pelliccioli, A., Liberi, G., Haber, J., and Foiani, M. (2004). Checkpoint-mediated control of replisome-fork association and signalling in response to replication pausing. *Oncogene* *23*, 1206-1213.
- Lundin, C., North, M., Erixon, K., Walters, K., Jenssen, D., Goldman, A.S., and Helleday, T. (2005). Methyl methanesulfonate (MMS) produces heat-labile DNA damage but no detectable in vivo DNA double-strand breaks. *Nucleic Acids Res* *33*, 3799-3811.
- Ma, J.L., Lee, S.J., Duong, J.K., and Stern, D.F. (2006). Activation of the checkpoint kinase Rad53 by the phosphatidylinositol kinase-like kinase Mec1. *J Biol Chem* *281*, 3954-3963.
- MacDougall, C.A., Byun, T.S., Van, C., Yee, M.C., and Cimprich, K.A. (2007). The structural determinants of checkpoint activation. *Genes Dev* *21*, 898-903.
- Macurek, L., Benada, J., Mullers, E., Halim, V.A., Krejcikova, K., Burdova, K., Pechackova, S., Hodny, Z., Lindqvist, A., Medema, R.H., *et al.* (2013). Downregulation of Wip1 phosphatase modulates the cellular threshold of DNA damage signaling in mitosis. *Cell Cycle* *12*, 251-262.
- Macurek, L., Lindqvist, A., Lim, D., Lampson, M.A., Klompmaker, R., Freire, R., Clouin, C., Taylor, S.S., Yaffe, M.B., and Medema, R.H. (2008). Polo-like kinase-1 is activated by aurora A to promote checkpoint recovery. *Nature* *455*, 119-123.
- Mailand, N., Bekker-Jensen, S., Bartek, J., and Lukas, J. (2006). Destruction of Claspin by SCFbetaTrCP restrains Chk1 activation and facilitates recovery from genotoxic stress. *Mol Cell* *23*, 307-318.
- Majka, J., Binz, S.K., Wold, M.S., and Burgers, P.M. (2006a). Replication protein A directs loading of the DNA damage checkpoint clamp to 5'-DNA junctions. *J Biol Chem* *281*, 27855-27861.
- Majka, J., Niedziela-Majka, A., and Burgers, P.M. (2006b). The checkpoint clamp activates Mec1 kinase during initiation of the DNA damage checkpoint. *Mol Cell* *24*, 891-901.
- Mamely, I., van Vugt, M.A., Smits, V.A., Semple, J.I., Lemmens, B., Perrakis, A., Medema, R.H., and Freire, R. (2006). Polo-like kinase-1 controls proteasome-dependent degradation of Claspin during checkpoint recovery. *Curr Biol* *16*, 1950-1955.
- Manfrini, N., Gobbin, E., Baldo, V., Trovesi, C., Lucchini, G., and Longhese, M.P. (2012). G(1)/S and G(2)/M cyclin-dependent kinase activities commit cells to death in the absence of the S-phase checkpoint. *Mol Cell Biol* *32*, 4971-4985.

- Mantiero, D., Mackenzie, A., Donaldson, A., and Zegerman, P. (2011). Limiting replication initiation factors execute the temporal programme of origin firing in budding yeast. *EMBO J* *30*, 4805-4814.
- Marsolier, M.C., Roussel, P., Leroy, C., and Mann, C. (2000). Involvement of the PP2C-like phosphatase Ptc2p in the DNA checkpoint pathways of *Saccharomyces cerevisiae*. *Genetics* *154*, 1523-1532.
- Matsumoto, S., Shimmoto, M., Kakusho, N., Yokoyama, M., Kanoh, Y., Hayano, M., Russell, P., and Masai, H. (2010). Hsk1 kinase and Cdc45 regulate replication stress-induced checkpoint responses in fission yeast. *Cell Cycle* *9*, 4627-4637.
- Matsuoka, S., Ballif, B.A., Smogorzewska, A., McDonald, E.R., 3rd, Hurov, K.E., Luo, J., Bakalarski, C.E., Zhao, Z., Solimini, N., Lerenthal, Y., *et al.* (2007). ATM and ATR substrate analysis reveals extensive protein networks responsive to DNA damage. *Science* *316*, 1160-1166.
- Matsuoka, S., Rotman, G., Ogawa, A., Shiloh, Y., Tamai, K., and Elledge, S.J. (2000). Ataxia telangiectasia-mutated phosphorylates Chk2 in vivo and in vitro. *Proc Natl Acad Sci U S A* *97*, 10389-10394.
- McKee, A.H., and Kleckner, N. (1997). A general method for identifying recessive diploid-specific mutations in *Saccharomyces cerevisiae*, its application to the isolation of mutants blocked at intermediate stages of meiotic prophase and characterization of a new gene SAE2. *Genetics* *146*, 797-816.
- Meister, P., Taddei, A., Vernis, L., Poidevin, M., Gasser, S.M., and Baldacci, G. (2005). Temporal separation of replication and recombination requires the intra-S checkpoint. *J Cell Biol* *168*, 537-544.
- Michael, W.M., Ott, R., Fanning, E., and Newport, J. (2000). Activation of the DNA replication checkpoint through RNA synthesis by primase. *Science* *289*, 2133-2137.
- Mimitou, E.P., and Symington, L.S. (2011). DNA end resection--unraveling the tail. *DNA Repair (Amst)* *10*, 344-348.
- Moorhead, G.B., Trinkle-Mulcahy, L., and Ulke-Lemee, A. (2007). Emerging roles of nuclear protein phosphatases. *Nat Rev Mol Cell Biol* *8*, 234-244.
- Mordes, D.A., Glick, G.G., Zhao, R., and Cortez, D. (2008a). TopBP1 activates ATR through ATRIP and a PIKK regulatory domain. *Genes Dev* *22*, 1478-1489.
- Mordes, D.A., Nam, E.A., and Cortez, D. (2008b). Dpb11 activates the Mec1-Ddc2 complex. *Proc Natl Acad Sci U S A* *105*, 18730-18734.
- Morin, I., Ngo, H.P., Greenall, A., Zubko, M.K., Morrice, N., and Lydall, D. (2008). Checkpoint-dependent phosphorylation of Exo1 modulates the DNA damage response. *EMBO J* *27*, 2400-2410.
- Morrison, A.J., Kim, J.A., Person, M.D., Highland, J., Xiao, J., Wehr, T.S., Hensley, S., Bao, Y., Shen, J., Collins, S.R., *et al.* (2007). Mec1/Tel1 phosphorylation of the INO80 chromatin remodeling complex influences DNA damage checkpoint responses. *Cell* *130*, 499-511.
- Mu, J.J., Wang, Y., Luo, H., Leng, M., Zhang, J., Yang, T., Besusso, D., Jung, S.Y., and Qin, J. (2007). A proteomic analysis of ataxia telangiectasia-mutated (ATM)/ATM-Rad3-related (ATR) substrates identifies the ubiquitin-proteasome system as a regulator for DNA damage checkpoints. *J Biol Chem* *282*, 17330-17334.
- Myers, J.S., and Cortez, D. (2006). Rapid activation of ATR by ionizing radiation requires ATM and Mre11. *J Biol Chem* *281*, 9346-9350.
- Myung, K., Datta, A., and Kolodner, R.D. (2001). Suppression of spontaneous chromosomal rearrangements by S phase checkpoint functions in *Saccharomyces cerevisiae*. *Cell* *104*, 397-408.
- Nakada, D., Hirano, Y., Tanaka, Y., and Sugimoto, K. (2005). Role of the C terminus of Mec1 checkpoint kinase in its localization to sites of DNA damage. *Mol Biol Cell* *16*, 5227-5235.
- Nakada, S., Chen, G.I., Gingras, A.C., and Durocher, D. (2008). PP4 is a gamma H2AX phosphatase required for recovery from the DNA damage checkpoint. *EMBO Rep* *9*, 1019-1026.
- Nam, E.A., Zhao, R., and Cortez, D. (2011a). Analysis of mutations that dissociate G(2) and essential S phase functions of human ataxia telangiectasia-mutated and Rad3-related (ATR) protein kinase. *The Journal of biological chemistry* *286*, 37320-37327.

- Nam, E.A., Zhao, R., Glick, G.G., Bansbach, C.E., Friedman, D.B., and Cortez, D. (2011b). Thr-1989 phosphorylation is a marker of active ataxia telangiectasia-mutated and Rad3-related (ATR) kinase. *J Biol Chem* *286*, 28707-28714.
- Navadgi-Patil, V.M., and Burgers, P.M. (2009). The unstructured C-terminal tail of the 9-1-1 clamp subunit Ddc1 activates Mec1/ATR via two distinct mechanisms. *Mol Cell* *36*, 743-753.
- Navadgi-Patil, V.M., and Burgers, P.M. (2011). Cell-cycle-specific activators of the Mec1/ATR checkpoint kinase. *Biochem Soc Trans* *39*, 600-605.
- Navadgi-Patil, V.M., Kumar, S., and Burgers, P.M. (2011). The unstructured C-terminal tail of yeast Dpb11 (human TopBP1) protein is dispensable for DNA replication and the S phase checkpoint but required for the G2/M checkpoint. *J Biol Chem* *286*, 40999-41007.
- Navas, T.A., Sanchez, Y., and Elledge, S.J. (1996). RAD9 and DNA polymerase epsilon form parallel sensory branches for transducing the DNA damage checkpoint signal in *Saccharomyces cerevisiae*. *Genes Dev* *10*, 2632-2643.
- Naylor, M.L., Li, J.M., Osborn, A.J., and Elledge, S.J. (2009). Mrc1 phosphorylation in response to DNA replication stress is required for Mec1 accumulation at the stalled fork. *Proc Natl Acad Sci U S A* *106*, 12765-12770.
- Neecke, H., Lucchini, G., and Longhese, M.P. (1999). Cell cycle progression in the presence of irreparable DNA damage is controlled by a Mec1- and Rad53-dependent checkpoint in budding yeast. *EMBO J* *18*, 4485-4497.
- Nielsen, I., Bentsen, I.B., Lisby, M., Hansen, S., Mundbjerg, K., Andersen, A.H., and Bjergbaek, L. (2009). A Flp-nick system to study repair of a single protein-bound nick in vivo. *Nat Methods* *6*, 753-757.
- Nordlund, P., and Reichard, P. (2006). Ribonucleotide reductases. *Annual review of biochemistry* *75*, 681-706.
- O'Neill, B.M., Szyjka, S.J., Lis, E.T., Bailey, A.O., Yates, J.R., 3rd, Aparicio, O.M., and Romesberg, F.E. (2007). Pph3-Psy2 is a phosphatase complex required for Rad53 dephosphorylation and replication fork restart during recovery from DNA damage. *Proc Natl Acad Sci U S A* *104*, 9290-9295.
- Ohouo, P.Y., Bastos de Oliveira, F.M., Almeida, B.S., and Smolka, M.B. (2010). DNA damage signaling recruits the Rtt107-Slx4 scaffolds via Dpb11 to mediate replication stress response. *Mol Cell* *39*, 300-306.
- Ohouo, P.Y., Bastos de Oliveira, F.M., Liu, Y., Ma, C.J., and Smolka, M.B. (2013). DNA-repair scaffolds dampen checkpoint signalling by counteracting the adaptor Rad9. *Nature* *493*, 120-124.
- Oliva-Trastoy, M., Berthonaud, V., Chevalier, A., Ducrot, C., Marsolier-Kergoat, M.C., Mann, C., and Leteurtre, F. (2007). The Wip1 phosphatase (PPM1D) antagonizes activation of the Chk2 tumour suppressor kinase. *Oncogene* *26*, 1449-1458.
- Olson, E., Nievera, C.J., Lee, A.Y., Chen, L., and Wu, X. (2007). The Mre11-Rad50-Nbs1 complex acts both upstream and downstream of ataxia telangiectasia mutated and Rad3-related protein (ATR) to regulate the S-phase checkpoint following UV treatment. *J Biol Chem* *282*, 22939-22952.
- Osborn, A.J., and Elledge, S.J. (2003). Mrc1 is a replication fork component whose phosphorylation in response to DNA replication stress activates Rad53. *Genes Dev* *17*, 1755-1767.
- Pabla, N., Ma, Z., Mellhatton, M.A., Fishel, R., and Dong, Z. (2011). hMSH2 recruits ATR to DNA damage sites for activation during DNA damage-induced apoptosis. *J Biol Chem* *286*, 10411-10418.
- Pacek, M., and Walter, J.C. (2004). A requirement for MCM7 and Cdc45 in chromosome unwinding during eukaryotic DNA replication. *EMBO J* *23*, 3667-3676.
- Paciotti, V., Clerici, M., Scotti, M., Lucchini, G., and Longhese, M.P. (2001). Characterization of mec1 kinase-deficient mutants and of new hypomorphic mec1 alleles impairing subsets of the DNA damage response pathway. *Mol Cell Biol* *21*, 3913-3925.
- Paciotti, V., Lucchini, G., Plevani, P., and Longhese, M.P. (1998). Mec1p is essential for phosphorylation of the yeast DNA damage checkpoint protein Ddc1p, which physically interacts with Mec3p. *EMBO J* *17*, 4199-4209.

- Palancade, B., Liu, X., Garcia-Rubio, M., Aguilera, A., Zhao, X., and Doye, V. (2007). Nucleoporins prevent DNA damage accumulation by modulating Ulp1-dependent sumoylation processes. *Mol Biol Cell* *18*, 2912-2923.
- Papamichos-Chronakis, M., and Peterson, C.L. (2008). The Ino80 chromatin-remodeling enzyme regulates replisome function and stability. *Nat Struct Mol Biol* *15*, 338-345.
- Patro, B.S., Frohlich, R., Bohr, V.A., and Stevensner, T. (2011). WRN helicase regulates the ATR-CHK1-induced S-phase checkpoint pathway in response to topoisomerase-I-DNA covalent complexes. *J Cell Sci* *124*, 3967-3979.
- Paulovich, A.G., Armour, C.D., and Hartwell, L.H. (1998). The *Saccharomyces cerevisiae* RAD9, RAD17, RAD24 and MEC3 genes are required for tolerating irreparable, ultraviolet-induced DNA damage. *Genetics* *150*, 75-93.
- Paulovich, A.G., and Hartwell, L.H. (1995). A checkpoint regulates the rate of progression through S phase in *S. cerevisiae* in response to DNA damage. *Cell* *82*, 841-847.
- Pelliccioli, A., Lee, S.E., Lucca, C., Foiani, M., and Haber, J.E. (2001). Regulation of *Saccharomyces* Rad53 checkpoint kinase during adaptation from DNA damage-induced G2/M arrest. *Mol Cell* *7*, 293-300.
- Pelliccioli, A., Lucca, C., Liberi, G., Marini, F., Lopes, M., Plevani, P., Romano, A., Di Fiore, P.P., and Foiani, M. (1999). Activation of Rad53 kinase in response to DNA damage and its effect in modulating phosphorylation of the lagging strand DNA polymerase. *EMBO J* *18*, 6561-6572.
- Peng, A., Lewellyn, A.L., Schiemann, W.P., and Maller, J.L. (2010). Repo-man controls a protein phosphatase 1-dependent threshold for DNA damage checkpoint activation. *Curr Biol* *20*, 387-396.
- Peng, A., Wang, L., and Fisher, L.A. (2011). Greatwall and Polo-like kinase 1 coordinate to promote checkpoint recovery. *J Biol Chem* *286*, 28996-29004.
- Peng, C.Y., Graves, P.R., Thoma, R.S., Wu, Z., Shaw, A.S., and Piwnicka-Worms, H. (1997). Mitotic and G2 checkpoint control: regulation of 14-3-3 protein binding by phosphorylation of Cdc25C on serine-216. *Science* *277*, 1501-1505.
- Peschiaroli, A., Dorrello, N.V., Guardavaccaro, D., Venere, M., Halazonetis, T., Sherman, N.E., and Pagano, M. (2006). SCFbetaTrCP-mediated degradation of Claspin regulates recovery from the DNA replication checkpoint response. *Mol Cell* *23*, 319-329.
- Peterson, S.E., Li, Y., Chait, B.T., Gottesman, M.E., Baer, R., and Gautier, J. (2011). Cdk1 uncouples CtIP-dependent resection and Rad51 filament formation during M-phase double-strand break repair. *J Cell Biol* *194*, 705-720.
- Pfander, B., and Diffley, J.F. (2011). Dpb11 coordinates Mec1 kinase activation with cell cycle-regulated Rad9 recruitment. *EMBO J* *30*, 4897-4907.
- Pichierri, P., Rosselli, F., and Franchitto, A. (2003). Werner's syndrome protein is phosphorylated in an ATR/ATM-dependent manner following replication arrest and DNA damage induced during the S phase of the cell cycle. *Oncogene* *22*, 1491-1500.
- Pike, B.L., Yongkiettrakul, S., Tsai, M.D., and Heierhorst, J. (2003). Diverse but overlapping functions of the two forkhead-associated (FHA) domains in Rad53 checkpoint kinase activation. *The Journal of biological chemistry* *278*, 30421-30424.
- Poli, J., Tsaponina, O., Crabbe, L., Keszthelyi, A., Pantescio, V., Chabes, A., Lengronne, A., and Pasero, P. (2012). dNTP pools determine fork progression and origin usage under replication stress. *EMBO J* *31*, 883-894.
- Povirk, L.F. (1996). DNA damage and mutagenesis by radiomimetic DNA-cleaving agents: bleomycin, neocarzinostatin and other enediynes. *Mutat Res* *355*, 71-89.
- Prinz, S., Amon, A., and Klein, F. (1997). Isolation of COM1, a new gene required to complete meiotic double-strand break-induced recombination in *Saccharomyces cerevisiae*. *Genetics* *146*, 781-795.
- Puddu, F., Granata, M., Di Nola, L., Balestrini, A., Piergiovanni, G., Lazzaro, F., Giannattasio, M., Plevani, P., and Muzi-Falconi, M. (2008). Phosphorylation of the budding yeast 9-1-1 complex is required for Dpb11 function in the full activation of the UV-induced DNA damage checkpoint. *Mol Cell Biol* *28*, 4782-4793.
- Puddu, F., Piergiovanni, G., Plevani, P., and Muzi-Falconi, M. (2011). Sensing of replication stress and Mec1 activation act through two independent pathways involving the 9-1-1 complex and DNA polymerase epsilon. *PLoS Genet* *7*, e1002022.

- Randell, J.C., Fan, A., Chan, C., Francis, L.I., Heller, R.C., Galani, K., and Bell, S.P. (2010). Mec1 is one of multiple kinases that prime the Mcm2-7 helicase for phosphorylation by Cdc7. *Mol Cell* 40, 353-363.
- Raschle, M., Knipscheer, P., Enoiu, M., Angelov, T., Sun, J., Griffith, J.D., Ellenberger, T.E., Scharer, O.D., and Walter, J.C. (2008). Mechanism of replication-coupled DNA interstrand crosslink repair. *Cell* 134, 969-980.
- Rattray, A.J., McGill, C.B., Shafer, B.K., and Strathern, J.N. (2001). Fidelity of mitotic double-strand-break repair in *Saccharomyces cerevisiae*: a role for SAE2/COM1. *Genetics* 158, 109-122.
- Ray Chaudhuri, A., Hashimoto, Y., Herrador, R., Neelsen, K.J., Fachinetti, D., Bermejo, R., Cocito, A., Costanzo, V., and Lopes, M. (2012). Topoisomerase I poisoning results in PARP-mediated replication fork reversal. *Nat Struct Mol Biol* 19, 417-423.
- Redon, C., Pilch, D.R., Rogakou, E.P., Orr, A.H., Lowndes, N.F., and Bonner, W.M. (2003). Yeast histone 2A serine 129 is essential for the efficient repair of checkpoint-blind DNA damage. *EMBO Rep* 4, 678-684.
- Regairaz, M., Zhang, Y.W., Fu, H., Agama, K.K., Tata, N., Agrawal, S., Aladjem, M.I., and Pommier, Y. (2011). Mus81-mediated DNA cleavage resolves replication forks stalled by topoisomerase I-DNA complexes. *J Cell Biol* 195, 739-749.
- Rhind, N., and Russell, P. (1998). Tyrosine phosphorylation of cdc2 is required for the replication checkpoint in *Schizosaccharomyces pombe*. *Mol Cell Biol* 18, 3782-3787.
- Sanchez, Y., Bachant, J., Wang, H., Hu, F., Liu, D., Tetzlaff, M., and Elledge, S.J. (1999). Control of the DNA damage checkpoint by chk1 and rad53 protein kinases through distinct mechanisms. *Science* 286, 1166-1171.
- Sanchez, Y., Desany, B.A., Jones, W.J., Liu, Q., Wang, B., and Elledge, S.J. (1996). Regulation of RAD53 by the ATM-like kinases MEC1 and TEL1 in yeast cell cycle checkpoint pathways. *Science* 271, 357-360.
- Sanchez, Y., Wong, C., Thoma, R.S., Richman, R., Wu, Z., Piwnicka-Worms, H., and Elledge, S.J. (1997). Conservation of the Chk1 checkpoint pathway in mammals: linkage of DNA damage to Cdk regulation through Cdc25. *Science* 277, 1497-1501.
- Santocanale, C., and Diffley, J.F. (1998). A Mec1- and Rad53-dependent checkpoint controls late-firing origins of DNA replication. *Nature* 395, 615-618.
- Schleker, T., Shimada, K., Sack, R., Pike, B.L., and Gasser, S.M. (2010). Cell cycle-dependent phosphorylation of Rad53 kinase by Cdc5 and Cdc28 modulates checkpoint adaptation. *Cell Cycle* 9, 350-363.
- Schwartz, M.F., Duong, J.K., Sun, Z., Morrow, J.S., Pradhan, D., and Stern, D.F. (2002). Rad9 phosphorylation sites couple Rad53 to the *Saccharomyces cerevisiae* DNA damage checkpoint. *Mol Cell* 9, 1055-1065.
- Schwartz, M.F., Lee, S.J., Duong, J.K., Eminaga, S., and Stern, D.F. (2003). FHA domain-mediated DNA checkpoint regulation of Rad53. *Cell Cycle* 2, 384-396.
- Segurado, M., and Diffley, J.F. (2008). Separate roles for the DNA damage checkpoint protein kinases in stabilizing DNA replication forks. *Genes Dev* 22, 1816-1827.
- Shen, X., Mizuguchi, G., Hamiche, A., and Wu, C. (2000). A chromatin remodelling complex involved in transcription and DNA processing. *Nature* 406, 541-544.
- Sheu, Y.J., Kinney, J.B., Lengronne, A., Pasero, P., and Stillman, B. (2014). Domain within the helicase subunit Mcm4 integrates multiple kinase signals to control DNA replication initiation and fork progression. *Proc Natl Acad Sci U S A* 111, E1899-1908.
- Sheu, Y.J., and Stillman, B. (2006). Cdc7-Dbf4 phosphorylates MCM proteins via a docking site-mediated mechanism to promote S phase progression. *Mol Cell* 24, 101-113.
- Shi, Y. (2009). Serine/threonine phosphatases: mechanism through structure. *Cell* 139, 468-484.
- Shi, Y., Dodson, G.E., Mukhopadhyay, P.S., Shanware, N.P., Trinh, A.T., and Tibbetts, R.S. (2007). Identification of carboxyl-terminal MCM3 phosphorylation sites using polyreactive phosphospecific antibodies. *J Biol Chem* 282, 9236-9243.
- Shimada, K., Oma, Y., Schleker, T., Kugou, K., Ohta, K., Harata, M., and Gasser, S.M. (2008). Ino80 chromatin remodeling complex promotes recovery of stalled replication forks. *Curr Biol* 18, 566-575.
- Shimada, K., Pasero, P., and Gasser, S.M. (2002). ORC and the intra-S-phase checkpoint: a threshold regulates Rad53p activation in S phase. *Genes Dev* 16, 3236-3252.

- Shimada, M., and Nakanishi, M. (2013). Response to DNA damage: why do we need to focus on protein phosphatases? *Frontiers in oncology* 3, 8.
- Shiotani, B., and Zou, L. (2009). Single-stranded DNA orchestrates an ATM-to-ATR switch at DNA breaks. *Mol Cell* 33, 547-558.
- Shirahige, K., Hori, Y., Shiraishi, K., Yamashita, M., Takahashi, K., Obuse, C., Tsurimoto, T., and Yoshikawa, H. (1998). Regulation of DNA-replication origins during cell-cycle progression. *Nature* 395, 618-621.
- Shreeram, S., Demidov, O.N., Hee, W.K., Yamaguchi, H., Onishi, N., Kek, C., Timofeev, O.N., Dudgeon, C., Fornace, A.J., Anderson, C.W., *et al.* (2006). Wip1 phosphatase modulates ATM-dependent signaling pathways. *Mol Cell* 23, 757-764.
- Sievers, F., Wilm, A., Dineen, D., Gibson, T.J., Karplus, K., Li, W., Lopez, R., McWilliam, H., Remmert, M., Soding, J., *et al.* (2011). Fast, scalable generation of high-quality protein multiple sequence alignments using Clustal Omega. *Mol Syst Biol* 7, 539.
- Sirbu, B.M., Lachmayer, S.J., Wulfing, V., Marten, L.M., Clarkson, K.E., Lee, L.W., Gheorghiu, L., Zou, L., Powell, S.N., Dahm-Daphi, J., *et al.* (2011). ATR-p53 restricts homologous recombination in response to replicative stress but does not limit DNA interstrand crosslink repair in lung cancer cells. *PLoS One* 6, e23053.
- Smolka, M.B., Albuquerque, C.P., Chen, S.H., and Zhou, H. (2007). Proteome-wide identification of in vivo targets of DNA damage checkpoint kinases. *Proc Natl Acad Sci U S A* 104, 10364-10369.
- Sogo, J.M., Lopes, M., and Foiani, M. (2002). Fork reversal and ssDNA accumulation at stalled replication forks owing to checkpoint defects. *Science* 297, 599-602.
- Song, B., Liu, X.S., Davis, K., and Liu, X. (2011). Plk1 phosphorylation of Orc2 promotes DNA replication under conditions of stress. *Mol Cell Biol* 31, 4844-4856.
- Sorensen, C.S., Hansen, L.T., Dziegielewska, J., Syljuasen, R.G., Lundin, C., Bartek, J., and Helleday, T. (2005). The cell-cycle checkpoint kinase Chk1 is required for mammalian homologous recombination repair. *Nat Cell Biol* 7, 195-201.
- Sorensen, C.S., and Syljuasen, R.G. (2012). Safeguarding genome integrity: the checkpoint kinases ATR, CHK1 and WEE1 restrain CDK activity during normal DNA replication. *Nucleic Acids Res* 40, 477-486.
- Sorger, P.K., and Murray, A.W. (1992). S-phase feedback control in budding yeast independent of tyrosine phosphorylation of p34cdc28. *Nature* 355, 365-368.
- Stark, M.J. (1996). Yeast protein serine/threonine phosphatases: multiple roles and diverse regulation. *Yeast* 12, 1647-1675.
- Stiff, T., Walker, S.A., Cerosaletti, K., Goodarzi, A.A., Petermann, E., Concannon, P., O'Driscoll, M., and Jeggo, P.A. (2006). ATR-dependent phosphorylation and activation of ATM in response to UV treatment or replication fork stalling. *EMBO J* 25, 5775-5782.
- Stokes, M.P., Rush, J., Macneill, J., Ren, J.M., Sprott, K., Nardone, J., Yang, V., Beausoleil, S.A., Gygi, S.P., Livingstone, M., *et al.* (2007). Profiling of UV-induced ATM/ATR signaling pathways. *Proc Natl Acad Sci U S A* 104, 19855-19860.
- Strumberg, D., Pilon, A.A., Smith, M., Hickey, R., Malkas, L., and Pommier, Y. (2000). Conversion of topoisomerase I cleavage complexes on the leading strand of ribosomal DNA into 5'-phosphorylated DNA double-strand breaks by replication runoff. *Mol Cell Biol* 20, 3977-3987.
- Subramanian, L., and Nakamura, T.M. (2010). A kinase-independent role for the Rad3(ATR)-Rad26(ATRIP) complex in recruitment of Tel1(ATM) to telomeres in fission yeast. *PLoS Genet* 6, e1000839.
- Sun, Z., Fay, D.S., Marini, F., Foiani, M., and Stern, D.F. (1996). Spk1/Rad53 is regulated by Mec1-dependent protein phosphorylation in DNA replication and damage checkpoint pathways. *Genes Dev* 10, 395-406.
- Sun, Z., Hsiao, J., Fay, D.S., and Stern, D.F. (1998). Rad53 FHA domain associated with phosphorylated Rad9 in the DNA damage checkpoint. *Science* 281, 272-274.
- Sweeney, F.D., Yang, F., Chi, A., Shabanowitz, J., Hunt, D.F., and Durocher, D. (2005). *Saccharomyces cerevisiae* Rad9 acts as a Mec1 adaptor to allow Rad53 activation. *Curr Biol* 15, 1364-1375.

- Szyjka, S.J., Aparicio, J.G., Viggiani, C.J., Knott, S., Xu, W., Tavare, S., and Aparicio, O.M. (2008). Rad53 regulates replication fork restart after DNA damage in *Saccharomyces cerevisiae*. *Genes Dev* 22, 1906-1920.
- Szyjka, S.J., Viggiani, C.J., and Aparicio, O.M. (2005). Mrc1 is required for normal progression of replication forks throughout chromatin in *S. cerevisiae*. *Mol Cell* 19, 691-697.
- Takai, H., Tominaga, K., Motoyama, N., Minamishima, Y.A., Nagahama, H., Tsukiyama, T., Ikeda, K., Nakayama, K., Nakanishi, M., and Nakayama, K. (2000). Aberrant cell cycle checkpoint function and early embryonic death in Chk1(-/-) mice. *Genes Dev* 14, 1439-1447.
- Tanaka, K., Boddy, M.N., Chen, X.B., McGowan, C.H., and Russell, P. (2001). Threonine-11, phosphorylated by Rad3 and atm in vitro, is required for activation of fission yeast checkpoint kinase Cds1. *Mol Cell Biol* 21, 3398-3404.
- Tanaka, K., and Russell, P. (2001). Mrc1 channels the DNA replication arrest signal to checkpoint kinase Cds1. *Nat Cell Biol* 3, 966-972.
- Tanaka, S., and Araki, H. (2010). Regulation of the initiation step of DNA replication by cyclin-dependent kinases. *Chromosoma* 119, 565-574.
- Tanaka, S., Nakato, R., Katou, Y., Shirahige, K., and Araki, H. (2011). Origin association of Sld3, Sld7, and Cdc45 proteins is a key step for determination of origin-firing timing. *Curr Biol* 21, 2055-2063.
- Tenca, P., Brotherton, D., Montagnoli, A., Rainoldi, S., Albanese, C., and Santocanale, C. (2007). Cdc7 is an active kinase in human cancer cells undergoing replication stress. *J Biol Chem* 282, 208-215.
- Tercero, J.A., and Diffley, J.F. (2001). Regulation of DNA replication fork progression through damaged DNA by the Mec1/Rad53 checkpoint. *Nature* 412, 553-557.
- Tercero, J.A., Longhese, M.P., and Diffley, J.F. (2003). A central role for DNA replication forks in checkpoint activation and response. *Mol Cell* 11, 1323-1336.
- Terrak, M., Kerff, F., Langsetmo, K., Tao, T., and Dominguez, R. (2004). Structural basis of protein phosphatase 1 regulation. *Nature* 429, 780-784.
- Tittel-Elmer, M., Alabert, C., Pasero, P., and Cobb, J.A. (2009). The MRX complex stabilizes the replisome independently of the S phase checkpoint during replication stress. *EMBO J* 28, 1142-1156.
- Tittel-Elmer, M., Lengronne, A., Davidson, M.B., Bacal, J., Francois, P., Hohl, M., Petrini, J.H., Pasero, P., and Cobb, J.A. (2012). Cohesin association to replication sites depends on rad50 and promotes fork restart. *Mol Cell* 48, 98-108.
- Toczyski, D.P., Galgoczy, D.J., and Hartwell, L.H. (1997). CDC5 and CKII control adaptation to the yeast DNA damage checkpoint. *Cell* 90, 1097-1106.
- Toueille, M., El-Andaloussi, N., Frouin, I., Freire, R., Funk, D., Shevelev, I., Friedrich-Heineken, E., Villani, G., Hottiger, M.O., and Hubscher, U. (2004). The human Rad9/Rad1/Hus1 damage sensor clamp interacts with DNA polymerase beta and increases its DNA substrate utilisation efficiency: implications for DNA repair. *Nucleic Acids Res* 32, 3316-3324.
- Tourriere, H., Versini, G., Cordon-Preciado, V., Alabert, C., and Pasero, P. (2005). Mrc1 and Tof1 promote replication fork progression and recovery independently of Rad53. *Mol Cell* 19, 699-706.
- Traven, A., and Heierhorst, J. (2005). SQ/TQ cluster domains: concentrated ATM/ATR kinase phosphorylation site regions in DNA-damage-response proteins. *BioEssays : news and reviews in molecular, cellular and developmental biology* 27, 397-407.
- Travesa, A., Duch, A., and Quintana, D.G. (2008). Distinct phosphatases mediate the deactivation of the DNA damage checkpoint kinase Rad53. *J Biol Chem* 283, 17123-17130.
- Travesa, A., Kuo, D., de Bruin, R.A., Kalashnikova, T.I., Guaderrama, M., Thai, K., Aslanian, A., Smolka, M.B., Yates, J.R., 3rd, Ideker, T., et al. (2012). DNA replication stress differentially regulates G1/S genes via Rad53-dependent inactivation of Nrm1. *EMBO J* 31, 1811-1822.
- Trenz, K., Errico, A., and Costanzo, V. (2008). Plx1 is required for chromosomal DNA replication under stressful conditions. *EMBO J* 27, 876-885.
- Trenz, K., Smith, E., Smith, S., and Costanzo, V. (2006). ATM and ATR promote Mre11 dependent restart of collapsed replication forks and prevent accumulation of DNA breaks. *EMBO J* 25, 1764-1774.

- Tsuji, T., Lau, E., Chiang, G.G., and Jiang, W. (2008). The role of Dbf4/Drf1-dependent kinase Cdc7 in DNA-damage checkpoint control. *Mol Cell* 32, 862-869.
- Usui, T., Foster, S.S., and Petrini, J.H. (2009). Maintenance of the DNA-damage checkpoint requires DNA-damage-induced mediator protein oligomerization. *Mol Cell* 33, 147-159.
- van Attikum, H., Fritsch, O., Hohn, B., and Gasser, S.M. (2004). Recruitment of the INO80 complex by H2A phosphorylation links ATP-dependent chromatin remodeling with DNA double-strand break repair. *Cell* 119, 777-788.
- van Deursen, F., Sengupta, S., De Piccoli, G., Sanchez-Diaz, A., and Labib, K. (2012). Mcm10 associates with the loaded DNA helicase at replication origins and defines a novel step in its activation. *EMBO J* 31, 2195-2206.
- Van Hoof, C., Martens, E., Longin, S., Jordens, J., Stevens, I., Janssens, V., and Goris, J. (2005). Specific interactions of PP2A and PP2A-like phosphatases with the yeast PTPA homologues, Ypa1 and Ypa2. *Biochem J* 386, 93-102.
- van Leeuwen, F., Gafken, P.R., and Gottschling, D.E. (2002). Dot1p modulates silencing in yeast by methylation of the nucleosome core. *Cell* 109, 745-756.
- Vaze, M.B., Pellicoli, A., Lee, S.E., Ira, G., Liberi, G., Arbel-Eden, A., Foiani, M., and Haber, J.E. (2002). Recovery from checkpoint-mediated arrest after repair of a double-strand break requires Srs2 helicase. *Mol Cell* 10, 373-385.
- Vazquez, M.V., Rojas, V., and Tercero, J.A. (2008). Multiple pathways cooperate to facilitate DNA replication fork progression through alkylated DNA. *DNA Repair (Amst)* 7, 1693-1704.
- Veaute, X., Jeusset, J., Soustelle, C., Kowalczykowski, S.C., Le Cam, E., and Fabre, F. (2003). The Srs2 helicase prevents recombination by disrupting Rad51 nucleoprotein filaments. *Nature* 423, 309-312.
- Vidanes, G.M., Sweeney, F.D., Galicia, S., Cheung, S., Doyle, J.P., Durocher, D., and Toczyski, D.P. (2010). CDC5 inhibits the hyperphosphorylation of the checkpoint kinase Rad53, leading to checkpoint adaptation. *PLoS Biol* 8, e1000286.
- Vincent, J.A., Kwong, T.J., and Tsukiyama, T. (2008). ATP-dependent chromatin remodeling shapes the DNA replication landscape. *Nat Struct Mol Biol* 15, 477-484.
- Wang, H., and Elledge, S.J. (2002). Genetic and physical interactions between DPB11 and DDC1 in the yeast DNA damage response pathway. *Genetics* 160, 1295-1304.
- Wang, W., Brandt, P., Rossi, M.L., Lindsey-Boltz, L., Podust, V., Fanning, E., Sancar, A., and Bambara, R.A. (2004). The human Rad9-Rad1-Hus1 checkpoint complex stimulates flap endonuclease 1. *Proc Natl Acad Sci U S A* 101, 16762-16767.
- Wang, Y., and Qin, J. (2003). MSH2 and ATR form a signaling module and regulate two branches of the damage response to DNA methylation. *Proc Natl Acad Sci U S A* 100, 15387-15392.
- Watase, G., Takisawa, H., and Kanemaki, M.T. (2012). Mcm10 plays a role in functioning of the eukaryotic replicative DNA helicase, Cdc45-Mcm-GINS. *Curr Biol* 22, 343-349.
- Waterhouse, A.M., Procter, J.B., Martin, D.M., Clamp, M., and Barton, G.J. (2009). Jalview Version 2--a multiple sequence alignment editor and analysis workbench. *Bioinformatics* 25, 1189-1191.
- Watrif, E., and Peters, J.M. (2009). The cohesin complex is required for the DNA damage-induced G2/M checkpoint in mammalian cells. *EMBO J* 28, 2625-2635.
- Weinert, T.A., and Hartwell, L.H. (1988). The RAD9 gene controls the cell cycle response to DNA damage in *Saccharomyces cerevisiae*. *Science* 241, 317-322.
- Weinert, T.A., Kiser, G.L., and Hartwell, L.H. (1994). Mitotic checkpoint genes in budding yeast and the dependence of mitosis on DNA replication and repair. *Genes Dev* 8, 652-665.
- Weinreich, M., and Stillman, B. (1999). Cdc7p-Dbf4p kinase binds to chromatin during S phase and is regulated by both the APC and the RAD53 checkpoint pathway. *EMBO J* 18, 5334-5346.
- Wysocki, R., Javaheri, A., Allard, S., Sha, F., Cote, J., and Kron, S.J. (2005). Role of Dot1-dependent histone H3 methylation in G1 and S phase DNA damage checkpoint functions of Rad9. *Mol Cell Biol* 25, 8430-8443.
- Yeung, M., and Durocher, D. (2011). Srs2 enables checkpoint recovery by promoting disassembly of DNA damage foci from chromatin. *DNA Repair (Amst)* 10, 1213-1222.
- Yoo, H.Y., Shevchenko, A., Shevchenko, A., and Dunphy, W.G. (2004). Mcm2 is a direct substrate of ATM and ATR during DNA damage and DNA replication checkpoint responses. *J Biol Chem* 279, 53353-53364.

- Yue, M., Singh, A., Wang, Z., and Xu, Y.J. (2011). The phosphorylation network for efficient activation of the DNA replication checkpoint in fission yeast. *J Biol Chem* 286, 22864-22874.
- Zegerman, P., and Diffley, J.F. (2009). DNA replication as a target of the DNA damage checkpoint. *DNA Repair (Amst)* 8, 1077-1088.
- Zegerman, P., and Diffley, J.F. (2010). Checkpoint-dependent inhibition of DNA replication initiation by Sld3 and Dbf4 phosphorylation. *Nature* 467, 474-478.
- Zhang, J., Bao, S., Furumai, R., Kucera, K.S., Ali, A., Dean, N.M., and Wang, X.F. (2005). Protein phosphatase 5 is required for ATR-mediated checkpoint activation. *Mol Cell Biol* 25, 9910-9919.
- Zhang, W., and Durocher, D. (2010). De novo telomere formation is suppressed by the Mec1-dependent inhibition of Cdc13 accumulation at DNA breaks. *Genes Dev* 24, 502-515.
- Zhang, Y.W., Brognard, J., Coughlin, C., You, Z., Dolled-Filhart, M., Aslanian, A., Manning, G., Abraham, R.T., and Hunter, T. (2009). The F box protein Fbx6 regulates Chk1 stability and cellular sensitivity to replication stress. *Mol Cell* 35, 442-453.
- Zhao, S., and Lee, E.Y. (1997). A protein phosphatase-1-binding motif identified by the panning of a random peptide display library. *J Biol Chem* 272, 28368-28372.
- Zhao, X., Chabes, A., Domkin, V., Thelander, L., and Rothstein, R. (2001). The ribonucleotide reductase inhibitor Sml1 is a new target of the Mec1/Rad53 kinase cascade during growth and in response to DNA damage. *EMBO J* 20, 3544-3553.
- Zhao, X., Muller, E.G., and Rothstein, R. (1998). A suppressor of two essential checkpoint genes identifies a novel protein that negatively affects dNTP pools. *Mol Cell* 2, 329-340.
- Zhao, X., and Rothstein, R. (2002). The Dun1 checkpoint kinase phosphorylates and regulates the ribonucleotide reductase inhibitor Sml1. *Proc Natl Acad Sci U S A* 99, 3746-3751.
- Zou, L., and Elledge, S.J. (2003). Sensing DNA damage through ATRIP recognition of RPA-ssDNA complexes. *Science* 300, 1542-1548.

CHAPTER 2: YEAST PP4 INTERACTS WITH ATR HOMOLOGUE DDC2-MEC1 AND REGULATES CHECKPOINT SIGNALING

Nicole Hustedt^{1,2}, Andrew Seeber^{1,2}, Ragna Sack¹, Monika Tsai¹ Bhupinder Bhullar³, Hanneke Vlaming⁴, Fred van Leeuwen⁴, Aude Guénolé⁵, Haico van Attikum⁵, Rohith Srivas⁶, Trey Ideker⁶, Kenji Shimada¹ and Susan M. Gasser^{1,2}

1. Friedrich Miescher Institute for Biomedical Research, Maulbeerstrasse 66, CH-4058 Basel, Switzerland 2. University of Basel, Faculty of Sciences, CH-4056 Basel, Switzerland 3. Novartis Institutes for Biomedical Research, Novartis Pharma AG, Fabrikstrasse 22, CH-4056 Basel, Switzerland 4. Division of Gene Regulation, Netherlands Cancer Institute, Plesmanlaan 121, 1066 CX Amsterdam, The Netherlands 5. Department of Toxicogenetics, Leiden University Medical Center, Einthovenweg 20, 2333 ZC Leiden, The Netherlands 6. Departments of Bioengineering & Medicine, University of California, San Diego, La Jolla, CA 92093, USA

under revision for publication in *Molecular Cell*

AUTHOR CONTRIBUTIONS:

NH planned and performed most experiments, evaluated results, made all figures and wrote the paper. AS planned, performed and evaluated the FRET studies, KS supervised NH and assisted in spontaneous suppressor screen experiments, RS performed all mass spectroscopy analyses, MT performed β -galactosidase assays, BB performed genome-wide sequencing of yeast mutants, HV and FvL supervised and hosted NH for the EMAP analysis, AG and HvA provided strains and know-how for the EMAP analysis, TI and RS helped analyse the EMAP results and SMG supervised NH and KS; evaluated and planned experiments, and edited the paper.

SUMMARY

To study regulators of the central intra-S-phase checkpoint kinase, Mec1-Ddc2, we took advantage of a catalytically active yeast *mec1* mutant that compromises the intra-S-phase checkpoint, while retaining association with Ddc2 and stalled replication forks. A screen for spontaneous survivors of hydroxyurea (HU) in *mec1-100* cells yielded mutations that inactivate Pph3 or Psy2, both conserved PP4 phosphatase subunits. In a large-scale screen for synthetic growth effects, *pph3 Δ* and *psy2 Δ* were the strongest suppressors of *mec1-100* lethality on HU. Restored Rad53 phosphorylation accounts for part, but not all, of the *pph3 Δ* -mediated survival. Physical interaction between Pph3 and Mec1, mediated by cofactors Psy2 and Ddc2, is shown biochemically and through FRET in subnuclear foci in HU-treated cells. Phosphoproteomic analysis confirmed that 90% of the *mec1-100*-compromised targets are PP4-regulated, including a phosphoacceptor residue within Mec1 itself, mutation of which confers Zeocin-sensitivity. This establishes a physical and functional Mec1-PP4 unit for regulating the checkpoint response.

INTRODUCTION

Cells are constantly exposed to DNA damage. Lesions can arise either from exogenous agents (e.g. DNA damaging drugs) or endogenous events (e.g. replication forks encountering barriers) (Aguilera and Garcia-Muse, 2013). To preserve the genetic information cells have evolved DNA damage checkpoints to sense damage, stop the cell cycle and induce DNA repair events (Friedel et al., 2009). Key to those signaling cascades are the PI3K-like (PI3KK) kinases ATM and ATR, in budding yeast Tel1 and Mec1 (Cimprich and Cortez, 2008). ATR and Mec1 genes are essential for cell viability, although the absence of Mec1 in yeast can be tolerated by concomitantly up-regulating ribonucleotide reductase (i.e. by deleting the gene encoding the ribonucleotide reductase inhibitor, Sml1) (Zhao et al., 1998). PIKKs are generally large proteins, about 2,500 amino acids in length, with a C-terminal kinase domain which is flanked by a FAT (FRAP ATM TRAPP) and FATC (FAT C-terminal) domains (Cimprich and Cortez, 2008).

Whereas ATM is primarily activated in response to DNA double strand breaks (DSBs), ATR can sense a variety of lesions (Cimprich and Cortez, 2008). Most ATR activation, however, appears to involve single stranded (ss) DNA which is coated by the ssDNA binding protein replication protein A (RPA). ATR requires its cofactor ATRIP (ATR interacting protein, Ddc2 in yeast) to bind these structures (Zou and Elledge, 2003). Experiments in *Xenopus* egg extracts indicate an additional requirement of dsDNA adjacent to the ssDNA stretch for ATR dependent checkpoint activation (MacDougall et al., 2007). The Rad17-RFC2-5 clamp loading complex (Rad24-Rfc2-5 in yeast) recognizes these structures and loads the 9-1-1 clamp, consisting of Rad9, Rad1 and Hus1 in metazoans and Rad17, Mec3 and Ddc1 in *S. cerevisiae*. Phosphorylation of the Rad9 (*S.c.* Ddc1) subunit recruits TopBP1 (*S.c.* Dpb11), which can activate ATR-ATRIP *in vitro* (Mordes et al., 2008), yet the exact mechanism of TopBP1 mediated activation remains unclear. In budding yeast not only Dpb11, but also Ddc1 and Dna2 were shown to enhance Mec1 kinase activity *in vitro* through their N- or C-terminal unstructured tails (reviewed in (Hustedt et al., 2013).

In the checkpoint cascade Mec1 activation leads to phosphorylation of the downstream kinases Rad53 (functionally related to human CHK1) and Chk1 in yeast (Friedel et al., 2009). Activation of those effector kinases requires mediator proteins. In the case of Mec1 activation in response to DSB or DNA adducts (MMS treatment) in S phase, the checkpoint protein Rad9 (53BP1 in mammals) recruits Rad53 and prepares it for Mec1 phosphorylation (Hustedt et al., 2013). In response to hydroxyurea (HU)-induced replication stress the fork components Mrc1 and Sgs1 facilitate Rad53 phosphorylation instead (Alcasabas et al., 2001; Bjergbaek et al., 2005; Frei and Gasser, 2000). In S-phase cells higher levels of damage are required to activate the Mec1-dependent checkpoint, suggesting a threshold for intra-S checkpoint activation (Shimada et al., 2002). This threshold may ensure that the occurrence of ssDNA found at normal replication forks does not trigger the global checkpoint response (Shimada et al., 2002; Tercero et al., 2003).

While checkpoint activation has been extensively studied, how the replication checkpoint is downregulated and how aberrant checkpoint induction is prevented during a normal, unperturbed S phase, are not well understood. A number of phosphatases have been shown to dephosphorylate Rad53 and there seems to be some specificity among the phosphatases depending on the type of damage that led to Rad53 activation (Heideker et al., 2007). The PP1 phosphatase Glc7 was reported to promote Rad53 dephosphorylation after exposure to HU (Bazzi et al., 2010). Furthermore, while the PP2C phosphatases Ptc2 and Ptc3 have been implicated in dephosphorylating Rad53 after a DSB (Leroy et al., 2003), the PP4 phosphatase Pph3 was implicated instead in checkpoint recovery after MMS treatment (O'Neill et al., 2007; Szyjka et al., 2008), although Ptc2/3 may compensate for loss Pph3 and *vice versa* during DSB repair and recovery from MMS treatment (Kim et al., 2011; Travesa et al.,

2008). PP4 was also implicated in dephosphorylation of other Mec1 substrates Zip1 (Falk et al., 2010), Cdc13 (Zhang and Durocher, 2010) and Cbf1 (Bandyopadhyay et al., 2010). Similarly, dephosphorylation of histone H2A has been linked to the PP4 phosphatase Psy2-Pph3. However, this required a third subunit, Psy4 (Keogh et al., 2006).

In human cells the data on phosphatases and checkpoints is no less complicated: both downstream kinases CHK1 and CHK2 are counteracted by both the PP2C (Wip1) and PP2A phosphatase, and, as in yeast, PP4 was shown to dephosphorylate γ H2AX (phosphorylated H2AX) in human cells (Chowdhury et al., 2008; Freeman and Monteiro, 2010; Nakada et al., 2008). PP4 was also implicated in dephosphorylation of RPA2 in *C. albicans* and mammals (Lee et al., 2010; Wang et al., 2013), and mammalian 53BP1, KAP-1 and CHD4 (Lee et al., 2014; Lee et al., 2012). Other mechanisms that downregulate the checkpoint act by means of proteasome-mediated degradation of Mrc1 or human CLASPIN (Fong et al., 2013; Mailand et al., 2006; Peschiaroli et al., 2006) or by sequestration of Rad9 by Rtt107-Slx4 (Ohouo et al., 2013). However, there is no study examining whether Mec1-Ddc2 activity itself is under negative control through phosphorylation or other regulation.

Here we describe a novel interaction between the Ddc2-Mec1 checkpoint kinase and the yeast PP4 phosphatase Psy2-Pph3. A strong genetic relationship between mutants in both complexes was identified in two independent screens, involving both forward and reverse genetics. Furthermore, we found that Mec1-Ddc2 and PP4 co-regulate many Mec1-dependent phosphorylation targets in response to HU stress, including Rad53 and H2A, suggesting that this interaction maintains a balance of phosphorylation that is important for surviving fork-associated stress. We also identify a phosphoacceptor site within Mec1 itself that is regulated in a Pph3-dependent manner, and which contributes to survival of Zeocin-induced damage.

RESULTS

SPONTANEOUS *MEC1-100* SUPPRESSOR MUTATIONS MAP TO *PSY2* AND *PPH3* GENES

To study how the replication checkpoint is controlled we used a mutant allele of the checkpoint kinase Mec1, *mec1-100*, which shows a delayed activation of Rad53 in S-phase, but robust Rad53 phosphorylation in G2-phase cells (Paciotti et al., 2001). In this allele two residues outside of the catalytic domain are mutated, one (N1700S) within and one (F1179S) flanking the FAT domain (Paciotti et al., 2001). Despite these mutations, the mutant kinase activity is intact: the *mec1-100* kinase recovered from cell lysates by co-precipitation with Ddc2-GFP phosphorylates a well-characterized target peptide (Sgs1 aa404-604) (Hegnauer et al., 2012) as efficiently as wild-type Mec1 (Figure.S2.1A). Its recruitment to stalled forks is also equivalent to that of wild-type Mec1 (Cobb et al., 2005), yet on HU, *mec1-100* allows partial loss of engaged polymerases from stalled forks and fails to prevent late origin firing (Cobb et al., 2005). The mutation also leads to complete fork collapse on HU in the absence of the RecQ helicase Sgs1, which is not observed in *sgs1Δ rad53Δ* mutants (Cobb et al., 2005). This suggests that *mec1-100* fails to modify a select set of S-phase specific Mec1 targets that ensure survival of replicative stress.

While working with *mec1-100* cells, we realized that spontaneous suppressor mutations arise quite frequently, conferring HU resistance (Figure 2.1A). This is not seen for *mec1Δ* strains. Since suppression could stem from either loss of negative regulators or up-regulation of downstream Mec1 targets, we analysed 31 suppressor colonies by sequencing, after backcrossing 2-3 times with the parental wild-type strain. The suppressors fell into two classes: in the first, the suppressing mutation co-segregated with a marker integrated close to the *MEC1* locus (“intragenic”), and in the second, the suppressors segregated independently (“extragenic”). Consistently, all co-segregating suppressors had acquired one additional mutation in *mec1-100*, rendering them HU-resistant (Figures 2.1B; S2.1B). Remarkably, genome-wide sequencing showed that all twelve extragenic suppressors had mutations in one of two genes, *PSY2* or *PPH3*, which encode subunits of the PP4 phosphatase (Figures 2.1B, S2.1C). In case of *PPH3*, the mutations were found throughout the phosphatase domain, while in *PSY2*, we found premature STOP codons after either 39 or 182 aa (Figure 2.1B). HU sensitivity was restored to the *mec1-100 psy2* or *p-ph3* double mutants by transformation with wild-type *PSY2* or *PPH3* genes, respectively (data not shown). We conclude that loss of Psy2 or Pph3 function confers HU resistance to *mec1-100* cells.

EMAP PROFILING GROUPS *MEC1-100* WITH REPLICATION CHECKPOINT DEFICIENT MUTATIONS

To better characterize *mec1-100* effects, we performed a high-throughput genetic interaction screen based on the previously described Epistatic Miniarray profiling (EMAP) method (Collins et al., 2007; Collins et al., 2006; Schuldiner et al., 2006). We combined 35 query strains bearing mutations in 35 genes implicated in DNA replication fork or checkpoint function, with an array of 1525 deletions and a few DAmP (Decreased Abundance by mRNA Perturbation) mutants, all representing functions that are required for chromatin-based processes (Guenole et al., 2013). The resulting double mutants were scored for their growth in the presence of 0, 20 and 100 mM HU. Quantitative genetic interaction scores were calculated as previously described (Collins et al., 2006) (Figure 2.1C). A positive score indicates suppression (or potentially, epistasis), while a negative score shows additivity and synthetic sickness. Quality control of the data led to the exclusion of 214 mutants (see Supplementary Procedures), leaving 35x1311 scored double mutants (Tables S2.1).

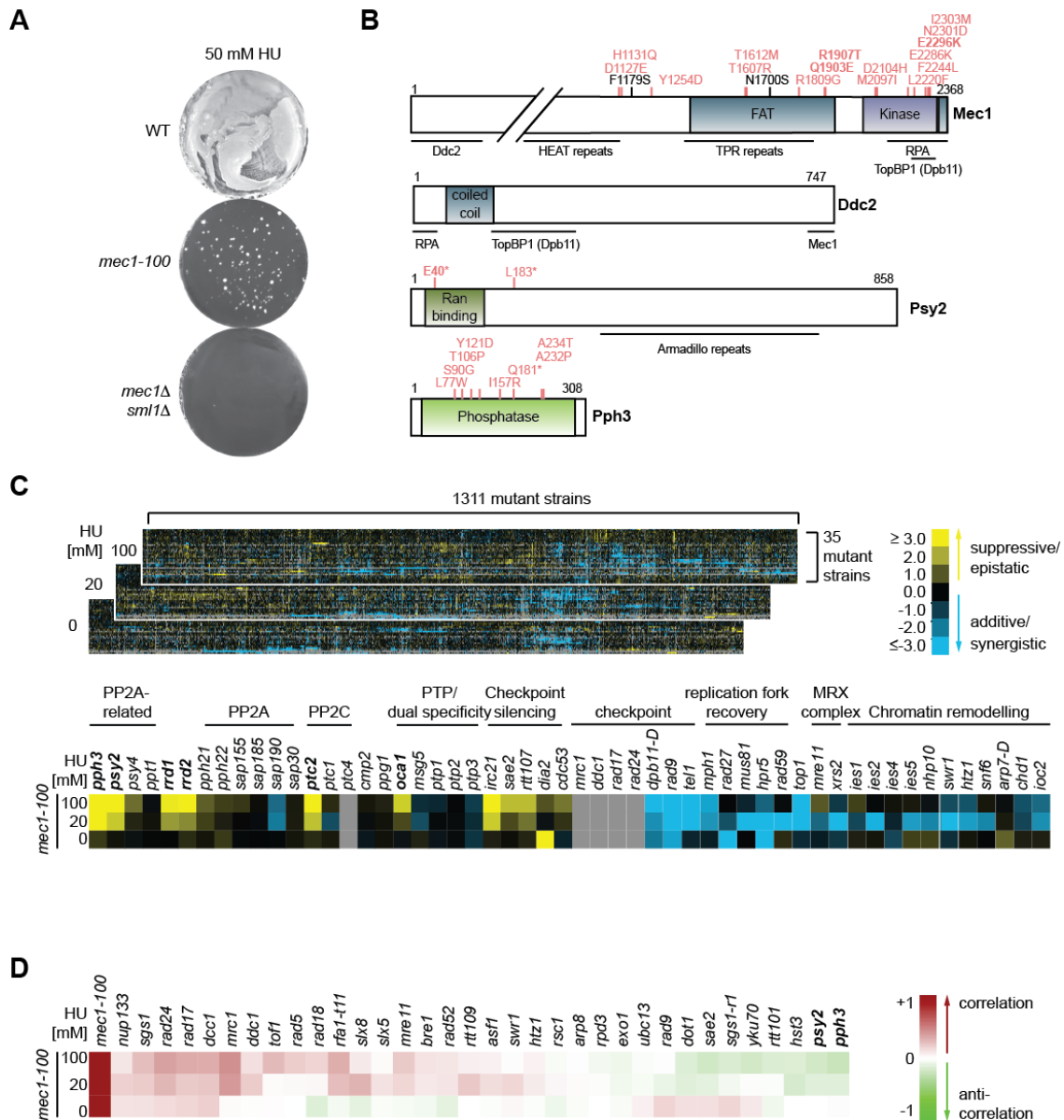


Figure 2.1: Mutations in *PSY2* and *PPH3* genes suppress *mec1-100* HU sensitivity. (A) WT (GA-1981), *mec1-100* (GA-4978) and *mec1Δ sml1Δ* (GA-2529) cells were plated on YPAD plates + 50 mM HU for 3 days at 30°C. Colonies appear white on dark background. (B) Mec1, Ddc2, Psy2 and Pph3 domain architecture with *mec1-100* mutations indicated in black and *mec1-100* suppressor mutations in red. Bold: mutations found more than once independently. Asterisks: STOP codon at indicated residue. Note that *PSY2-L183** (GA-6610) showed a deletion of a “G” generating a frameshift and stop codon at aa 183. (C) Upper panel: Overview of genetic interaction screen (EMAP): 35 mutant “query” strains were combined with 1525 (1311 after quality control) mutant strains. Growth of double mutants was scored in the presence of 0, 20 and 100 mM HU. Genetic interaction scores coding is at right. Lower panel: Selected *mec1-100* genetic interactions are shown, including mutants of other phosphatase classes and additional subunits of multisubunit complexes. Phosphatase mutants showing significant positive interaction with *mec1-100* are in bold. Complete *mec1-100* genetic interactions is in Figure S2.1. (D) Heat map showing Pearson correlation coefficients of *mec1-100* genetic interaction profile with the profiles of the other query strains on 0, 20 and 100 mM HU. Code for correlation coefficients at right.

We first compared the overall genetic interaction profile of *mec1-100* with the profiles of the other query mutants. Similar genetic interaction profiles of two mutants indicate related functions of the respective proteins (Collins et al., 2007). As expected, the *mec1-100* profile correlates best with other mutations that compromise the S-phase checkpoint (i.e. *sgs1Δ*, *rad24Δ*, *rad17Δ*, *ddc1Δ*, *mrc1Δ*

and *dcc1Δ*) (Figure 2.1D). In fact, *mrc1Δ*, which is the replication checkpoint mediator, shows the strongest correlation with *mecl-100* in the presence of HU, yet does not correlate in the absence of HU, arguing for cooperation on HU and distinct functions during an unperturbed S phase.

Interestingly, there are two groups of mutants whose genetic correlation patterns change dramatically upon HU treatment. The genetic interaction profiles of several genes implicated in either break-induced replication or translesion synthesis (notably, *rad18Δ*, *slx5Δ*, *slx8Δ*, *mre11Δ*, *rad52Δ* and *bre1Δ*) did not correlate with *mecl-100* in the absence of HU, but the profiles became quite similar on HU, indicating that they have common functions in replication fork stabilization and/or recovery. The opposite was observed for *rad9Δ*, *dot1Δ*, *sae2Δ*, *yku70Δ*, and *sgs1-r1Δ*, an internal deletion upstream of the Sgs1 helicase domain that confers sensitivity to Zeocin, but not HU (Hegnauer et al., 2012). This latter group of genes, which have genetic interaction profiles complementary to *mecl-100* on HU, identify activities involved at DSBs and not in stalled fork recovery. This reinforces the conclusion that *mecl-100* specifically compromises the replication checkpoint response.

If we look specifically at the mutants that interact with *mecl-100* (based on threshold scores of ≥ 2 for suppressive or epistatic and ≤ -2 for additive or synergistically negative interactions) the genetic interactions of *mecl-100* fall into several functional groups, which we discuss below (Figure 2.1C or S2.1D, for full list). However, of the 1311 array mutants scored, *psy2Δ* and *pph3Δ* showed the highest suppressive genetic interaction with *mecl-100*, and clearly promote survival on HU (Figure 2.1C, S2.1D, Table S2.1). This confirms with a comprehensive screen that the alleviating genetic interaction observed by the HU-suppressor screen is robust (Figure 2.1A).

PP4 SUBUNITS PSY2 AND PPH3 COUNTERACT *MECL-100* SENSITIVITIES

Psy2 and Pph3 form a conserved PP4 phosphatase complex with Pph3 being the catalytic subunit (Heideker et al., 2007). Psy4 has been reported to be a third subunit, but it is not required for dephosphorylation of all targets (Keogh et al., 2006; O'Neill et al., 2007). In our screen, *psy4Δ* showed no genetic interaction with *mecl-100* (Figure 2.1C). When profiles of mutant synergies were compared, we found that *psy2Δ* and *pph3Δ* were strongly anti-correlated with *mecl-100* on HU (Figure 2.1D), arguing that *PSY2* and *PPH3*, but not *PP4*, share a function that opposes that of *mecl-100*.

To see if this was simply a general feature of phosphatase mutants, we examined the impact of loss of *PSY2* and/or *PPH3* in comparison to other phosphatases. Loss of the PP5 phosphatase *ppt1Δ*, showed no genetic interaction with *mecl-100*, nor did deletions of the two PP2A catalytic subunits, *pph21Δ* and *pph22Δ*, or their regulatory subunits, *sap155Δ*, *sap185Δ*, *sap190Δ*, *sap33Δ* (Figure 2.1C). On the other hand, loss of Rrd2, which interacts with and regulates PP2A (Van Hoof et al., 2005), did provide some *mecl-100* suppression, like Rrd1, which interacts physically with the phosphatases Pph3 (PP4), Ppg1 (related to PP4 and PP6) and Sit4 (PP6) (Van Hoof et al., 2005) (Figure 2.1C; 2A). For PP2C we have contradictory results, given that *ptc2Δ* (one of seven genes encoding PP2C subunits) showed suppressive genetic interactions with *mecl-100* in the strain used for the EMAP assay, yet showed weak and variable suppression in a second background (W303; Figure 2.2B). Moreover, two other PP2C phosphatase subunits (*ptc1Δ* and *ptc4Δ*) either showed no genetic interaction or could not be scored in the EMAP assay. This latter can occur either because the double mutants form inefficiently, or because the resulting colonies are too small for accurate growth rate scoring. The only phosphotyrosyl phosphatase mutant interacting genetically with *mecl-100* was *oca1Δ*, yet its effect required 100 mM HU, was significantly less pronounced than *psy2Δ* or *pph3Δ*, and like *ptc2Δ*, was not reproducible in another background (Figure 2.2B). Besides the phosphatase mutants, *mecl-100* was

suppressed by mutations that dampen the checkpoint response such as deletions of *RTT107*, *SAE2*, *DIA2*, *CDC53* or *IRC21* (Clerici et al., 2006; Fong et al., 2013; Guenole et al., 2013; Ohouo et al., 2013) (Figure 2.1C). These factors may act in parallel with phosphatases in checkpoint downregulation.

Indeed, we find *pph3Δ* to be synthetic sick with *ptc2Δ* and *sae2Δ* (Figure S2.1D), which has been previously described (Guenole et al., 2013; Keogh et al., 2006; Kim et al., 2011; O'Neill et al., 2007; Szyjka et al., 2008). Moreover, we find a negative genetic interaction of *pph3Δ* with *dia2Δ*, indicating that *PTC2*, *SAE2* and *DIA2* act in parallel to *PPH3* to allow cell survival on HU, possibly through redundant targeting of Rad53 (Guillemain et al., 2007; Leroy et al., 2003; O'Neill et al., 2007; Travesa et al., 2008), limiting of Tel1 signaling (Clerici et al., 2006) or Mrc1 degradation (Fong et al., 2013).

MEC1-100 SHOWS SYNTHETIC LETHALITY WITH MUTANTS THAT PERTURB CHECKPOINT ACTIVATION OR REPLICATION FORK RECOVERY

Negative genetic interactions are scored when the loss of a gene renders cells more dependent on another gene for survival. That is, they identify factors acting on parallel pathways to achieve the same function, or in a redundant fashion on the same pathway. As expected, the replication checkpoint deficiency of *mecl-100* rendered cells highly dependent on other checkpoint proteins (i.e. Mrc1, Ddc1, Rad24, Rad17, Dpb11, Rad9 and Tel1) on HU (Figures 2.1C; S2.1D; S2.1E). These mutations also showed a strong correlation with *mecl-100* with respect to overall genetic interaction profiles (Figure 2.1D). Other synergistic genetic interactions included mutants involved in replication fork recovery and damage bypass, the MRX complex and chromatin remodelers, as well as a set of nuclear pore mutations (Figures 2.1D, S2.1D). In addition to the INO80 and SWR1 complexes, we recovered histone acetyltransferases (SAS and AHC) and histone methyltransferases that are closely associated with the transcription machinery (COMPASS) (Figure S2.1D). Interestingly, RNA Pol II subunits and certain translational regulators are far more sensitive to *mecl-100* mutation than to *mrc1* deletion. These may help prevent damage that pushes *mecl-100* cells towards lethality and thus work redundantly with *mecl-100* (Aguilera and Garcia-Muse, 2013).

DELETIONS OF THE PP4 SUBUNITS *PPH3* OR *PSY2* STRONGLY SUPPRESS *MEC1-100* SENSITIVITY

With two independent suppressor screens yielding mutations in *PPH3* and *PSY2*, we investigated this phosphatase complex further. Previous work suggested that Psy2-Pph3 (PP4) dephosphorylates the checkpoint effector kinase, Rad53, in a manner that is redundant with other phosphatases (Bazzi et al., 2010; Heideker et al., 2007). Specifically, Ptc2, Ptc3 (both PP2C-type phosphatases) and the PP1-type phosphatase Glc7 all appeared to dephosphorylate Rad53, depending on the type of damage used to activate the checkpoint (Bazzi et al., 2010; Leroy et al., 2003; O'Neill et al., 2007; Travesa et al., 2008)(Figure 2.2A). Indeed, it was reported that Pph3 was dispensable for Rad53 dephosphorylation after HU arrest, and that Glc7 might be responsible on HU instead (Bazzi et al., 2010; Travesa et al., 2008).

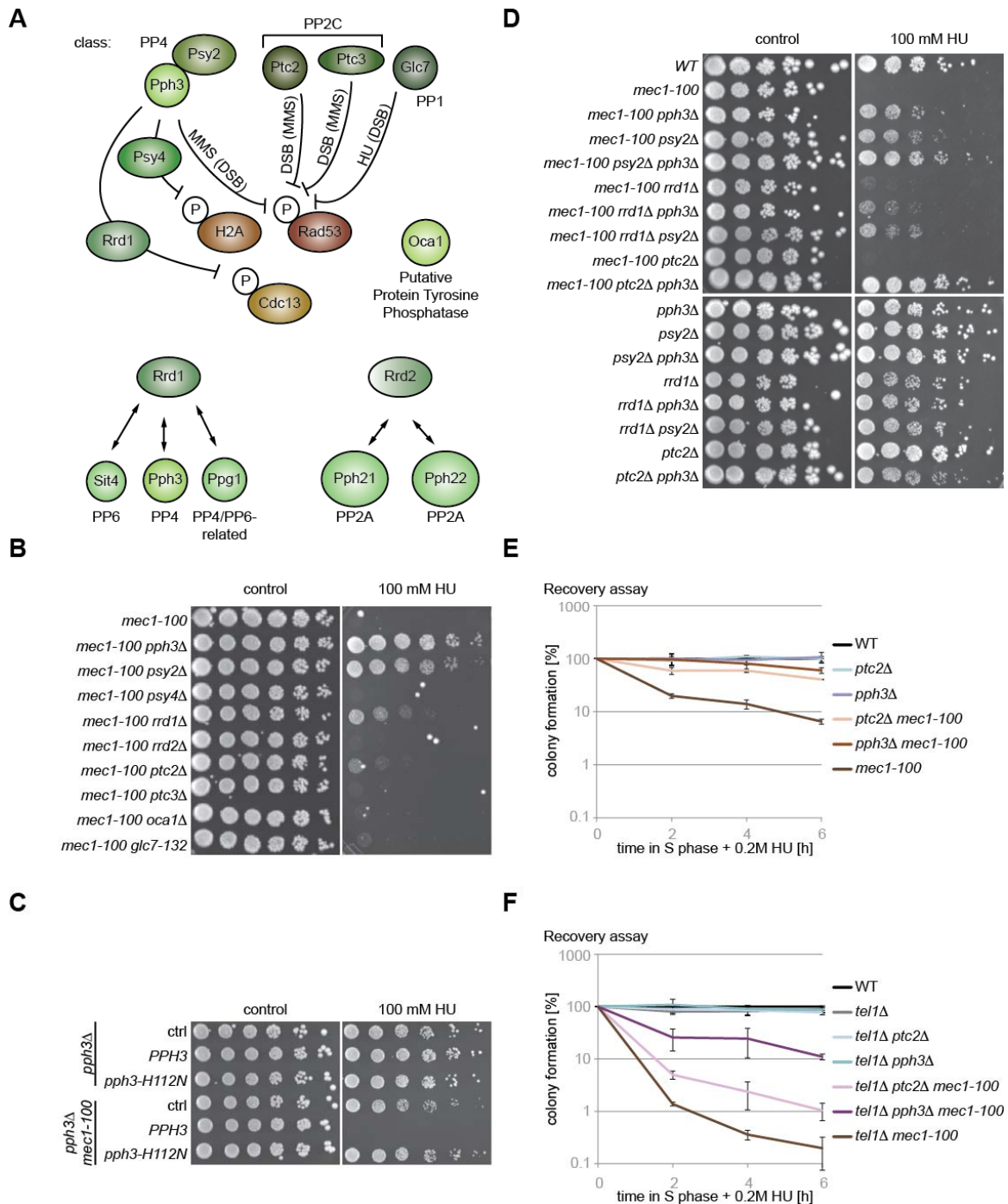


Figure 2.2: Validation of *psy2Δ* and *pph3Δ* as suppressors of *mec1-100* HU sensitivity. (A) Yeast phosphatases and their relationship showing those with substantial genetic interactions with *mec1-100* or those implicated in checkpoint down-regulation, see text. (B) Serial 5-fold dilutions of cultures were plated on YPAD \pm 100 mM HU. Relevant genotypes of isogenic strains are indicated in the figure. Strains used (Table S2.5) were: GA-6582, GA-7086, GA-7393, GA-7385, GA-7929, GA-7932, GA-7329, GA-7276, GA-7935, and GA-8079. (C) *pph3Δ* (GA-7049) or *pph3Δ mec1-100* (GA-7086) cells were transformed with *TRP1*-based control plasmid (#286) or plasmids expressing *PPH3* (#3367) or *pph3-H112N* (#3368) from *PPH3* promoter. Cells were grown in SC-TRP medium and serial 5-fold dilutions were plated on SC-TRP \pm 100 mM HU. (D) Cultures were treated as in (B). Relevant genotypes of isogenic strains are indicated in the figure. Isogenic strains (Table S5) used were: GA-1981, GA-6582, GA-7086, GA-7393, GA-7395, GA-7929, GA-7982, GA-8054, GA-7329, GA-7979, GA-7049, GA-7391, GA-7398, GA-7908, GA-7981, GA-8052, GA-7273 and GA-7977. (E) Recovery from replication fork stalling was monitored as colony outgrowth of cells after synchronization in G1 by α -factor arrest and release into S phase with 0.2M HU for the indicated times. Isogenic strains used were: GA-1981, GA-6582, GA-7086, GA-7329, GA-7049 and GA-7273. Error bars indicate standard deviation. (F) Cells were treated as in (E). Isogenic strains used were GA-1981, GA-6912, GA-6913, GA-7734, GA-7955, GA-7732 and GA-7953 (Table S2.5). See also Fig. S2.2.

To sort out these contradictions, we created single and double mutants with *mec1-100* in another budding yeast background (W303), and monitored growth on HU. Again, *psy2Δ* and *pph3Δ* were the strongest suppressors among the mutants tested (Figure 2.2B). Consistent with the EMAP result, loss of *RRD1* led to weak suppression, while *ptc2Δ* had almost no effect on the HU sensitivity of *mec1-100*. This latter was true for all other phosphatase mutants, including loss of the PP2A-associated factor Rrd2 (Van Hoof et al., 2005) (Figure 2.2B).

We confirmed that suppression of *mec1-100* by *pph3Δ* was due to loss of Pph3 phosphatase activity, because the catalytically inactive mutant (*pph3-H112N*) (O'Neill et al., 2007) supported *mec1-100* growth on HU to the same extent as *pph3Δ* (Figure 2.2C). Given previous work suggesting that Rrd1 and Pph3 act on the same pathway to dephosphorylate the Mec1 target Cdc13 at breaks (Zhang and Durocher, 2010), we tested whether *rrd1Δ* would be epistatic with *pph3Δ* by combining *rrd1Δ* and *mec1-100* with *psy2Δ*, *pph3Δ*, or both. Surprisingly, coupling *rrd1Δ* with *psy2Δ* or *pph3Δ* reduced the suppression of *mec1-100* sensitivity to HU (Figure 2.2D), arguing that *rrd1Δ* interferes with suppression by *psy2Δ* or *pph3Δ*. In contrast, both the *pph3Δ ptc2Δ* and *pph3Δ psy2Δ* double mutants were slightly additive for suppression. Furthermore, unlike loss of Psy2 or Pph3, loss of Rrd1 alone enhanced sensitivity to HU (Figure 2.2D), suggesting that Rrd1's suppression of *mec1-100* lethality on HU is distinct from that of PP4.

To examine if PP4-mediated suppression affects viability only (e.g. survival due to checkpoint function) or also helps maintain engaged and stalled replication forks, we tested single and double mutants for their ability to promote colony growth after having synchronously entered S phase and being held in high HU concentrations for 1 to 6 hours (Figure S2.2A). This assay is thought to measure restart of stalled forks, which enables colony outgrowth. In *mec1-100* cells ChIP signals of replicative polymerases are partially lost from sites of early replication by 1h of HU treatment and cells show recovery defects (Cobb et al., 2005). Importantly, the combination of *mec1-100* with *pph3Δ* rescued this defect, while *ptc2Δ* had a weaker effect (Figures 2.2E; S2.2B).

The loss of Tel1 kinase, the yeast ATM homologue, has no effect on fork stability or restart on its own, but it is possible that Tel1 might compensate checkpoint defects and promote cell survival on HU. Therefore we tested the ability of *ptc2Δ* and *pph3Δ* to rescue *mec1-100* in a *tel1Δ* background. Again, we found that *ptc2Δ* and *pph3Δ* rescued *mec1-100* recovery defects, independently of Tel1. Moreover, *pph3Δ* had a 10-fold stronger effect than *ptc2Δ* (Figures 2.2F; S2.2C). We conclude that loss of Pph3 efficiently suppresses both the HU sensitivity and fork recovery defects of *mec1-100*, with no recourse to Tel1/DSB checkpoint response.

RAD53 ACTIVATION CORRELATES WITH LEVEL OF SUPPRESSION

In the S-phase checkpoint cascade, Rad53 is activated by Mec1-mediated phosphorylation, which is compromised by the *mec1-100* mutation in S phase only (Paciotti et al., 2001). Previous work implicated our two suppressor phosphatases, Ptc2 and Pph3, in the dephosphorylation of Rad53 (Leroy et al., 2003; O'Neill et al., 2007; Travesa et al., 2008), although Pph3 was reportedly dispensable after exposure to HU (Travesa et al., 2008). We nonetheless tested the hypothesis that reduced Rad53 phosphorylation in *mec1-100* cells is balanced by loss of Pph3 or Ptc2, using Western blots to detect the hyper-phosphorylated form of Rad53. Cells bearing *mec1-100* in combination with *pph3Δ* or *ptc2Δ* were synchronized in G1 by α -factor, and released into S phase in the presence of HU. The Rad53 Western blot showed that the delayed upshift of Rad53 in the *mec1-100* background was compensated by *pph3Δ* or, albeit weaker, *ptc2Δ*: leading to more rapid Rad53 activation (Figure 2.3A). In *MEC1+* cells, *ptc2Δ* or *pph3Δ* had no effect on the kinetics of Rad53 activation (Figure

2.3A, S2.3A), possibly because the steady-state equilibrium between Rad53 phosphorylation and dephosphorylation is shifted towards dephosphorylation only in *mec1-100* cells. Thus, a compensatory effect by *pph3Δ* can be observed in *mec1-100*, but not in *Mec1+* cells.

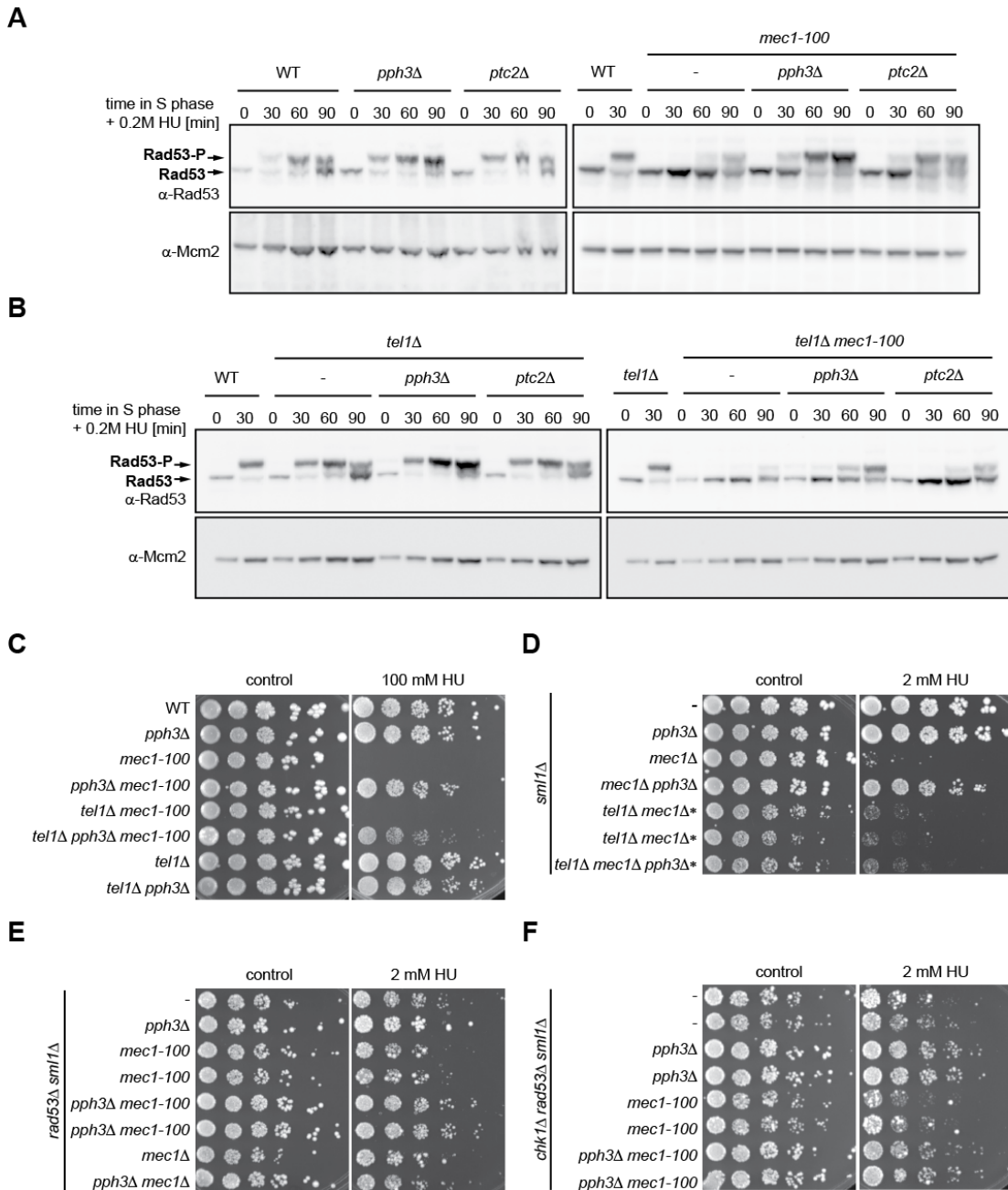


Figure 2.3: Suppression of *mec1-100* correlates with Rad53 activation. (A) Rad53 phosphorylation was monitored by synchronizing cells in G1 (α -factor) and releasing them for the indicated times into 0.2 M HU, before denatured extract preparation and Western blot analysis. Relevant genotypes are indicated in the figure for the following isogenic strains: GA-1981, GA-7049, GA-7273, GA-6582, GA-7086 and GA-7329. (B) Cells were treated as in (A). Isogenic strains were GA-1981, GA-6912, GA-6913, GA-7734, GA-7955, GA-7732 and GA-7953. (C) Serial 5-fold dilutions of cultures were plated on YPAD \pm 100 mM HU. Relevant genotypes are indicated in the figure. Isogenic strains were: GA-1981, GA-7049, GA-6582, GA-7086, GA-6913, GA-7734, GA-6912 and GA-7732. (D) Serial 5-fold dilutions of cultures were plated on YPAD \pm 2 mM HU. Relevant genotypes are indicated in the figure. Isogenic strains were: GA-4533, GA-7294, GA-5286, GA-7650, GA-7724, GA-7725, GA-7707 and GA-7708. Asterisk: 10x more cells plated (E) Cells were treated as in (D). Isogenic strains used were GA-7373, GA-7375, GA-7401, GA-7377 (two colonies of each) and GA-7709 and GA-7711. (F) Cells were treated as in (D). Isogenic strains were GA-7656, GA-7657, GA-7658, GA-7659, GA-7660, GA-7661, GA-7662 and GA-7663. Full genotypes of strains in Table S2.5 (see also Fig.S2.3).

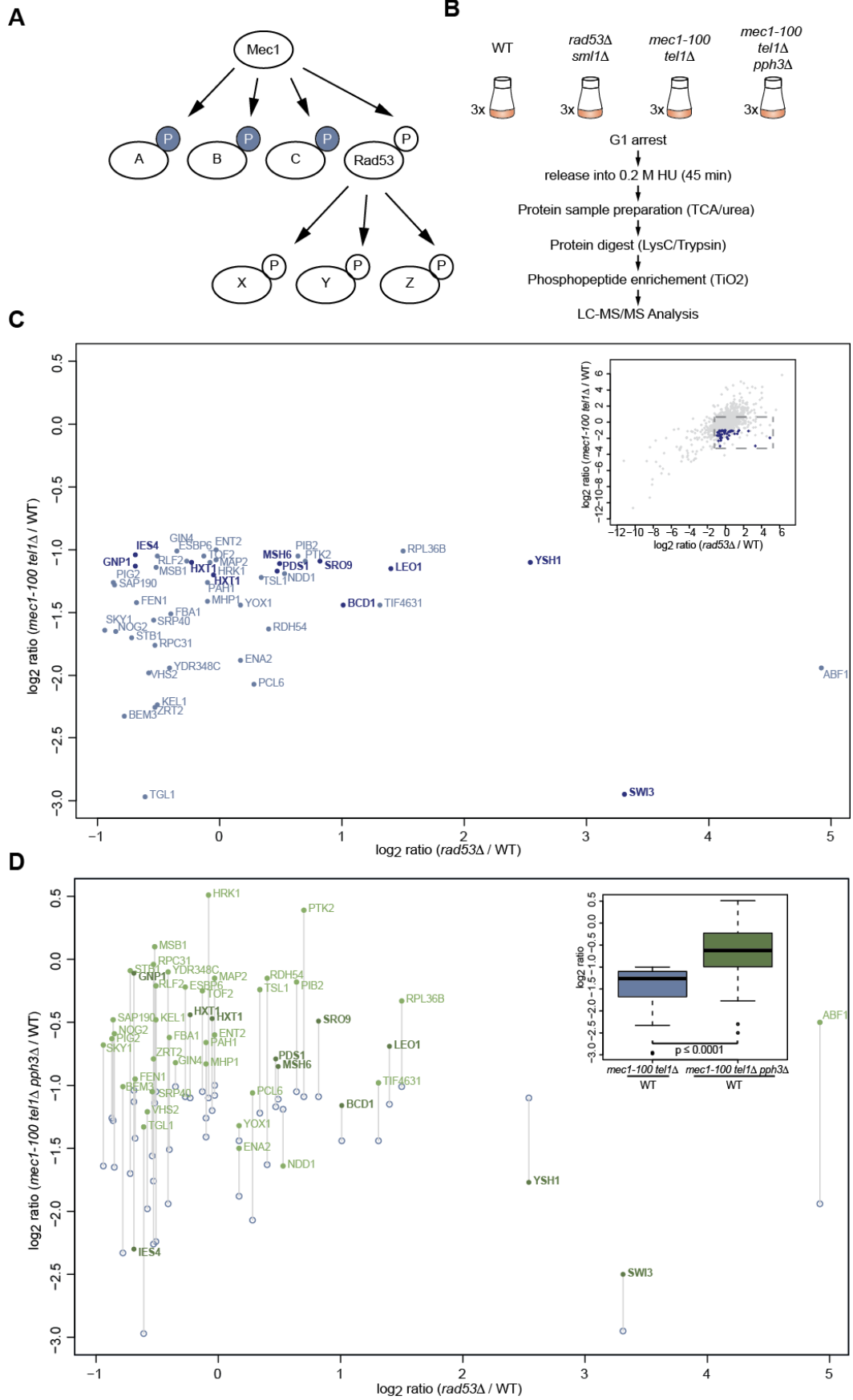
In order to exclude that the more rapid Rad53 phosphorylation observed in *mec1-100 pph3Δ* stems from compensation by Tel1, all assays were concurrently performed in a *tell1Δ* background (Figure 2.3B), but the effects of Pph3 or Psy2 on Rad53 activation were comparable in *tell1Δ* (Figures 2.3AB, S2.2A). Finally, we note that Rad53 remained more robustly phosphorylated at 90 min or after HU washout in *pph3Δ* cells, something only weakly affected by *ptc2Δ* (Figures 2.3AB, S2.3AB). This delay in Rad53 dephosphorylation during recovery from HU treatment did not correlate with survival defects, possibly because with sufficient time cells dephosphorylate Rad53 eventually (Figures 2.2EF; S2.2BC). In a complete *mec1* deletion, unlike *mec1-100, pph3Δ* only conferred HU-suppression in the presence of Tel1, indicating that specifically Mec1/Tel1 activity (no other kinases except those downstream of Mec1/Tel1) is needed for *pph3Δ* to exert its effect (Figure 2.3CD). We note that *ptc2Δ* had similar, but significantly less pronounced effects than *pph3Δ* in restoration of the Rad53 upshift on HU, consistent with its weaker responses in functional assays (Figures 2, 3). In sum, the correlation between Rad53 activation kinetics and the suppression of HU sensitivity argues that at least part of the mechanism through which *pph3Δ* and *psy2Δ* suppresses *mec1-100*, reflects Rad53 activation.

PP4 TARGETS RAD53 AND OTHER FACTORS TO MEDIATE *MEC1-100* SUPPRESSION

It is well established that *mec1-100* cells activate Rad53 weakly on HU (Figure 2.3A) and that Rad53 initiates many of the downstream checkpoint responses (e.g. cell cycle arrest and late origin firing). Nonetheless, there is extensive evidence that Mec1 has unique roles in the replication checkpoint that are independent of Rad53 (Cobb et al., 2005; Segurado and Diffley, 2008). Moreover, there are targets at the replication fork that are modified uniquely by Mec1 (Chen et al., 2010; Smolka et al., 2007) (M. Smolka, pers. communication). To see if the suppression of *mec1-100* phenotypes by *pph3Δ* involves targets other than Rad53, we checked whether *pph3Δ* can suppress *mec1-100* sensitivity to HU, in the absence of Rad53.

Because *RAD53* deletion is lethal, we coupled it with a bypass mutation (*sml1Δ*) (Zhao et al., 1998). The resulting *rad53Δ sml1Δ* strain is extremely sensitive to HU, yet the effect of *pph3Δ* on *mec1-100* coupled with *rad53Δ sml1Δ*, can be tested at low concentrations of this inhibitor. Serial dilution assays detected a mild, but highly reproducible suppression of *mec1-100* by *pph3Δ* even in the absence of Rad53 (Figure 2.3E). This suggests that while Rad53 is important, it is not the only target through which the phosphatase mutant rescues *mec1-100* defects. This residual suppression was not observed in *rad53Δ mec1Δ sml1Δ* cells, again suggesting that the residual kinase activity of *mec1-100* is required for the suppressive effect and that Tel1 coupled with *pph3Δ* is not sufficient to suppress the lethal effects of HU in the absence of Rad53 and Mec1. Again this underscores the crucial role of Mec1 in HU survival.

Interestingly, even in the absence of *mec1-100*, *PPH3* deletion suppressed the HU-sensitivity of *rad53Δ sml1Δ*, in contrast to a previous report that scored colony formation on MMS (O'Neill et al., 2007). Our result again suggests that the phosphorylation status of proteins other than Rad53 is beneficial for survival on HU. One candidate for this was the second checkpoint effector kinase, Chk1. However, deletion of *CHK1* had no effect on suppression by *pph3Δ* (Figure 2.3F). We conclude that activation of the downstream checkpoint kinase Rad53 is important, but is not the only Mec1-mediated phosphorylation event that is enhanced by loss of PP4, to ensure *mec1-100* survival on HU.



RESTORATION OF H2A PHOSPHORYLATION DOES NOT CORRELATE WITH SUPPRESSION

A further target of Pph3 (PP4) during the DNA damage response in both yeast and mammals is histone H2A (Chowdhury et al., 2008; Keogh et al., 2006; Nakada et al., 2008). Yeast H2A is phosphorylated on Serine 129 by Mec1 and/or Tel1 at DSBs and stalled replication forks, fulfilling the role of the mammalian γ H2AX (Cobb et al., 2005; Downs et al., 2000; van Attikum et al., 2004). We confirmed that H2A phosphorylation levels were increased by *PPH3* or *PSY2* deletion in both WT and *mec1-100* backgrounds after treating S-phase cells with HU (Figure S2.3D). However, unlike Rad53, phospho-H2A regulation is not only dependent on Pph3 and Psy2, but also on Psy4, a variable third subunit of the complex (Keogh et al., 2006; O'Neill et al., 2007). Consistently *psy4* Δ also led to increased H2A phosphorylation (Figure S2.3D). On the other hand, loss of Psy4 did not rescue *mec1-100* HU sensitivity in WT or *rad53* Δ *sml1* Δ backgrounds (Figures 2.2B, S2.3C). Thus, H2A phosphorylation does not strictly correlate with the rescue of *mec1-100* on HU.

PHOSPHOPEPTIDES DOWNREGULATED IN *MEC1-100* CELLS ARE UPREGULATED BY *PPH3* DELETION

Given that Rad53 activation correlates with the rescue of *mec1-100* HU-sensitivity, yet is not the only relevant target, we performed a quantitative phosphoproteomic study. Specifically, we screened for modifications that are downregulated in *mec1-100*, compensated by *pph3* Δ and left unaffected by *rad53* deletion (Figures 2.4A). Since Tel1 may compensate for *mec1-100* defects (Figures 2.2EF, 2.3B), we further used a *tell1* Δ *mec1-100* double mutant. Prior to extraction of proteins, the cultures were arrested in G1 by α -factor and released into S phase in the presence of HU (Figure 2.4B).

2396 phosphopeptides could be quantified (Table S2.2), of which 47 were specifically reduced in *mec1-100 tell1* Δ , but not in *rad53* Δ *sml1* Δ , cells (Figure 2.4C, Table S2.3). Among them were the repair factor Rdh54, chromatin remodeler INO80 subunit Ies4, the mismatch repair protein Msh6, and transcription regulators like Swi3 and Leo1, the latter being a component of the PAF1 complex (Figure 2.4C). Unexpectedly, we did not find any proteins that were involved directly in DNA replication. Remarkably, however, when the abundance of these phosphopeptides was scored after deletion of *PPH3*, almost all (94%) were upregulated (i.e. restored in *mec1-100 tell1* Δ *pph3* Δ vs *mec1-100 tell1* Δ ; Figure 2.4D).

Figure 2.4: Most *mec1-100*-regulated phosphopeptides are upregulated by loss of Pph3. (A) Scheme of Mec1-dependent, Rad53-independent phosphorylation sites. (B) Setup of phosphoproteomics experiment. Three cultures of wild-type (GA-1981), *rad53* Δ *sml1* Δ (GA-7373), *mec1-100 tell1* Δ (GA-6913) and *mec1-100 tell1* Δ *pph3* Δ (GA-7734) were synchronized in G1 and released into 0.2 M HU for 45 min. Samples were processed for phosphoproteomics analysis as described in supplemental material. (C) Phosphopeptide abundances (\log_2 ratio (mutant/WT)) in *mec1-100 tell1* Δ cells were plotted against abundances in *rad53* Δ *sml1* Δ . Shown are phosphopeptides which have a \log_2 ratio ≤ -1 for *mec1-100 tell1* Δ / WT ($p \leq 0.05$, Student's paired t-test over three replicates) and \log_2 ratio ≥ 1 for *rad53* Δ *sml1* Δ / WT. These were considered *mec1-100/tell1*-specific. Full list in Table S2.3. Phosphopeptides modified on [pS/pT]Q consensus are marked in dark blue and bold. Labels indicate names of proteins. Inlay: Indicated ratios of all quantified phosphopeptides (Table S2.2) were plotted. Phosphopeptides specific for the *mec1-100 tell1* strain in blue. (D) Phosphopeptide abundances (\log_2 ratio (mutant/WT)) in *mec1-100 tell1* Δ *pph3* Δ cells were plotted against phosphopeptide abundances in *rad53* Δ *sml1* Δ cells. Blue circles indicate position in previous plot of peptides selected in (C) to illustrate shift between *mec1-100 tell1* Δ and *mec1-100 tell1* Δ *pph3* Δ cells. Grey lines connect data points of the same phosphopeptides. Inlay: Boxplot showing indicated ratios of *mec1-100/tell1*-specific phosphopeptides. p-values calculated by one-tailed Wilcoxon signed rank test. See also Figure S2.4.

This increase was averaged over *mec1-100/tell1*-dependent peptides and is both highly significant (Figure 2.4D inlay) and specific, because it was not observed among the whole population of quantified phosphopeptides (Figure S2.4A). We conclude that the loss of Pph3 balances out most if not all of the phosphorylation defects that we detect in *mec1-100* cells on HU. This beautifully supports our genetic results which showed opposing functions for these two mutations (Figure 2.1).

S/TQ PHOSPHOPEPTIDES ARE UPREGULATED IN *RAD53*Δ BUT ARE UNAFFECTED BY *MEC1-100*

Among the 47 phosphopeptides that were specifically downregulated in the *mec1-100 tell1*Δ mutant, only a few (11 phosphopeptides) fit the generally assumed ATR/ATM consensus p[S/T]Q (Kim et al., 1999). This could mean either that S/TQ sites are also hit by Rad53, that we failed for technical reasons to recover S/TQ sites, or simply that S/TQ containing peptides did not match to the stringent criteria that we had applied to define *mec1-100 tell1*Δ-dependent phosphopeptides. We therefore scanned for phosphopeptides that were less abundant in *mec1-100 tell1*Δ cells as compared to *rad53*Δ *sml1*Δ cells (\log_2 ratio ≤ -1 , p-value ≤ 0.05), regardless of their abundance in WT cells, and screened independently for known Mec1/Tel1 targets (Chen et al., 2010). Using this approach we identified many p[S/T]Q phosphopeptides including known fork-associated Mec1/Tel1 targets such as Rfa2, (Brush et al., 1996) and H2A (Downs et al., 2000), in our phosphoproteomic dataset (Figure S2.4BC, Table S2.4). They did not appear in the first analysis because they were not downregulated in *mec1-100 tell1*Δ cells when compared to WT. This indicates that the mutant Mec1 kinase (*mec1-100*) is actually proficient for phosphorylating many S/TQ Mec1 targets on HU, consistent with its robust kinase activity in the pull-down assay (Figure S2.1A). Therefore we conclude that these targets are most likely not responsible for the lethality of *mec1-100* cells on HU.

Intriguingly, the majority of p[S/T]Q phosphopeptides that we recovered in the second analysis were more abundant in the *rad53*Δ *sml1*Δ mutant than in WT cells, and they were not further affected by loss of Pph3 (Figure S2.4CD). We confirmed that H2A phosphorylation is strongly elevated in *rad53*Δ *sml1*Δ cells compared to WT by Western blotting (Figure S2.4E). This may indicate that in *rad53*Δ *sml1*Δ cells on HU, Mec1 and/or Tel1 become hyperactivated, either because the cells accumulate additional DNA damage at the fork, or because there might be a negative feedback of Rad53 on Mec1 activity.

MEC1-DDC2 AND PSY2-PHP3 PHYSICALLY INTERACT IN A DNA DAMAGE INDEPENDENT MANNER

From our phosphoproteome analysis we conclude that almost every phosphopeptides that was uniquely reduced due to the *mec1-100 tell1*Δ mutations, was restored by elimination of Pph3. How could this robust coordination be guaranteed? We speculated that the kinase and phosphatase might bind each other, to ensure their coordinated action. To test this, we created yeast strains that expressed epitope-tagged versions of the kinase or phosphatase subunits from their native genomic loci. We confirmed that the tagging of Psy2 and Ddc2 did not render the cells sensitive to MMS or HU (Figure S2.5AD), whereas the same tags on Mec1 or Pph3 compromised their function (Figure S2.5BC). Since Ddc2 is known to form a stable complex with Mec1 (Paciotti et al., 2000), as does Psy2 with Pph3 (Gingras et al., 2005), we could use the functional tagged versions of Psy2 or Ddc2 in subsequent assays. For positive and negative controls, we tested Rfa1 and Ptc2 interactions (Figure S2.5EF).

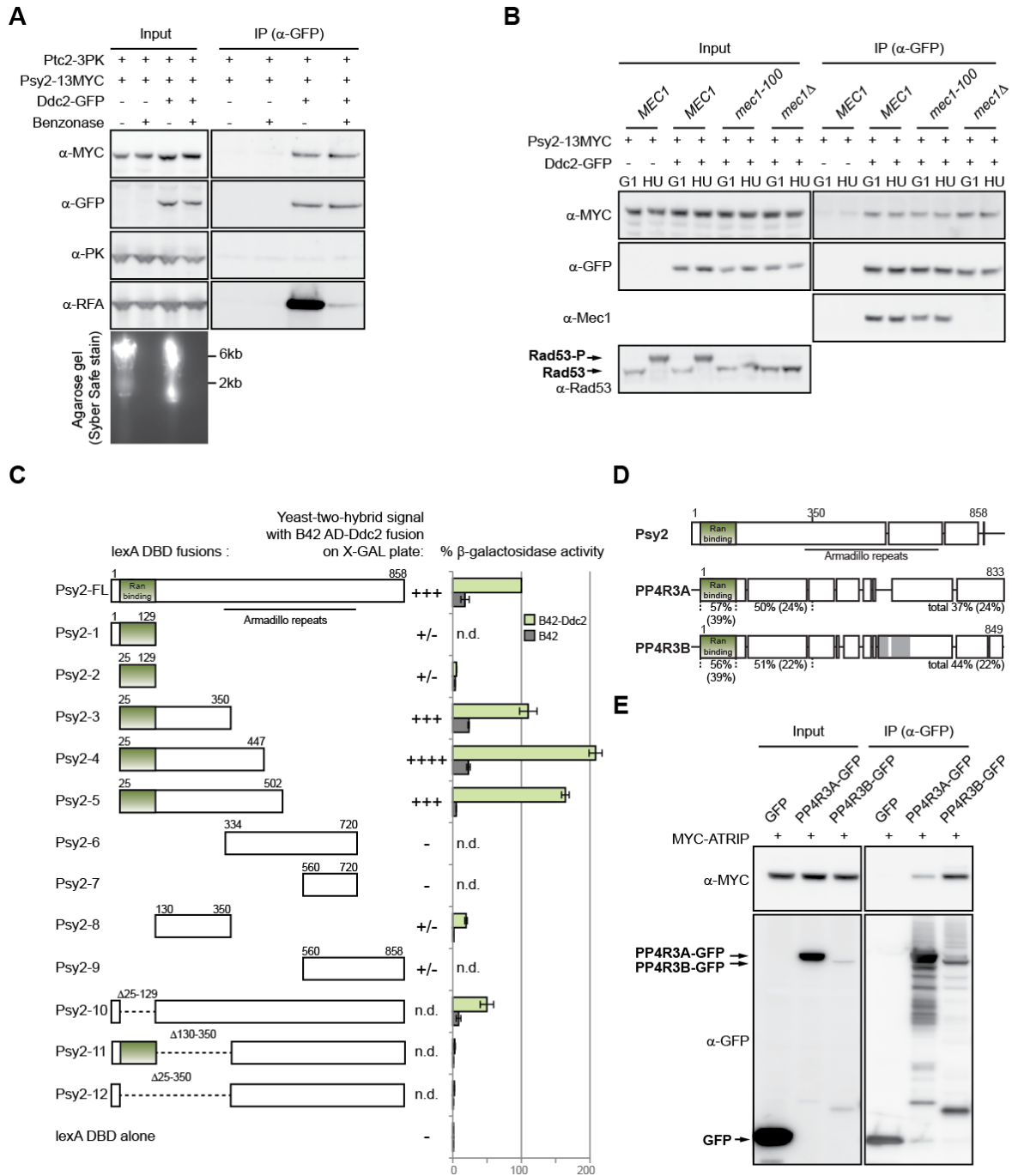


Figure 2.5: Ddc2 and Psy2 physically interact. (A) Native extracts from cycling *Psy2-13MYC Ptc2-3PK* (GA-7972) and *Psy2-13MYC Ptc2-3PK Ddc2-GFP* (GA-7975) cells were treated or not with RNaseA and benzonase. Ddc2-GFP was immunoprecipitated (IP) and analysed by Western blotting with indicated antibodies. DNA isolated from GFP-depleted extracts after IP was analysed by agarose gel to control for nucleic acid digestion. (B) *Psy2-13MYC* (GA-7799), *Psy2-13MYC Ddc2-GFP* (GA-7824), *Psy2-13MYC Ddc2-GFP mec1-100* (GA-7835) and *Psy2-13MYC Ddc2-GFP mec1 Δ smi1 Δ* (GA-7827) cells were arrested in G1 by α -factor and held or released into + 0.2 M HU for 30 min. Native and denatured extracts were subjected to α -GFP IP and Western blotting with indicated antibodies. Denatured extracts were blotted for Rad53 phosphorylation. (C) Y2H analysis of *DDC2* fused to B42-AD and *PSY2* fragments fused to *lexA*-DBD. Bars indicate β -galactosidase activity, symbols indicate color on X-GAL plate (raw data in Figure S2.5C). +/- indicates dubious interaction. n.d. not determined. (D) Schematic of Clustal Omega multiple sequence alignment of *Psy2* (P40164), *PP4R3A* (Q6IN85-1) and *PP4R3B* (Q5MIZ7-1). Vertical lines: Alignment gaps (≥ 5 amino acids); grey: region missing in Q5MIZ7-3, which was used in (E). % Sequence similarity (in brackets % sequence identity) was calculated based on *Psy2* sequence length or length of indicated *Psy2* fragments. (E) HEK293T cells were transfected with plasmids expressing MYC-ATRIP (#3525) and GFP (#3493), *PP4R3A*-GFP (#3518) or *PP4R3B*-GFP (#3588). Native extracts were prepared at 48h post transfection, and were subjected to IP with α -GFP. Samples were probed with indicated antibodies. See also Figs. S2.5, 2.6.

Immunoprecipitation experiments showed efficient recovery of Psy2-MYC with Ddc2-GFP, while Ptc2 (Ptc2-PK) did not co-precipitate (Figure 2.5A). The Psy2-Ddc2 interaction is unlikely to reflect nonspecific contact through nucleic acids, since combined DNA/RNA digestions using benzonase and RNaseA did not affect recovery. In contrast, most of the detected Ddc2-GFP-Rfa1 interaction that we detected was sensitive to this treatment (Figure 2.5A). The Ddc2-GFP Psy2-MYC interaction did not require HU-induced arrest, since it was detected in G1-phase cells, as well as in an HU-treated S-phase population (Figure 2.5B). Remarkably, the robust Ddc2-Psy2 interaction was independent of Mec1, being detected in *mec1*Δ as well as in the *mec1-100* mutant. Pph3 was also not required for the Psy2-Ddc2 interaction (Figure S2.6A). Finally, when precipitation occurred through Psy2-GFP, Ddc2-MYC could be specifically recovered (Figure S2.6B). The interaction was further mapped by yeast-two hybrid, through which we could define the minimal Psy2 domain that robustly binds Ddc2 (Psy2 amino acids 25-350) (Figures 2.5C, S2.6C). Although a smaller Psy2 fragment (amino acids 130-350) only weakly bound Ddc2, its deletion fully abolished the interaction. Another Psy2 fragment (amino acids 25-129), although robustly expressed (Figure S2.6D), failed to interact significantly and its deletion only reduced the interaction by about 50%. Expression of *psy2*Δ130-350 from its endogenous locus rendered cells as sensitive to MMS as *psy2*Δ cells (Figure 2.S6E), indicating that deletion of amino acids 130-350 impairs protein expression and/or function.

DDC2- PSY2 HOMOLOGUES INTERACT IN MAMMALIAN CELL EXTRACTS

Psy2 has two human homologs, PP4R3A and PP4R3B, which share an overall sequence similarity with Psy2 of 37% and 44% and an identity of 24% and 22%, respectively. Intriguingly, the interaction domain within Psy2 (aa 130-350) has 50% and 51% sequence similarity with PP4R3A and PP4R3B, respectively (Figure 2.5D). This high level of sequence conservation led us to test whether these regulatory phosphatase subunits bind ATRIP in human cells. Following transient transfection of HEK293T cells with plasmids encoding for MYC-tagged ATRIP and either PP4R3A-GFP, PP4R3B GFP or GFP alone, we performed immunoprecipitation with anti-GFP antibody and probed for MYC-tagged ATRIP. ATRIP precipitated efficiently with PP4R3B-GFP, but not with GFP alone and only weakly with PP4R3A-GFP (Figure 2.5E) even though PP4R3A expression levels were much higher. This suggests that the PP4R3B-ATRIP interaction is preferred. We conclude that in yeast the kinase subunit Ddc2 and the phosphatase subunit Psy2 interact in a HU-, Mec1- and Pph3-independent manner that involves a conserved region in Psy2. The ATRIP-PP4R3B interaction thus appears to be conserved in mammalian cells, suggesting a functional relevance of this interaction.

DDC2 AND PSY2 INTERACT AND COLOCALIZE IN NUCLEAR FOCI *IN VIVO*

Although the genetic and biochemical evidence for interaction was strong, it was unclear whether the Mec1/Ddc2 – Psy2/Pph3 interaction occurs at the right place and the right time; that is, at stalled replication forks or other sites of DNA damage. To localize the putative complex in living cells, we fused Psy2 and Ddc2 with distinct fluorescent proteins (RFP and GFP, respectively) and Rfa1 with ECFP. All fusions were expressed from their endogenous loci under the native promoter and were fully functional, as the cells behaved like WT cells when exposed to HU or MMS (Figure S2.5ADF). As expected, Rfa1-CFP has a punctate nuclear signal in S-phase cells, consistent with the existence of replication foci (Pasero et al., 1997)(Figure 2.6AB). The abundance of Rfa1 and the limited resolution of spinning disk (SD) confocal microscopy renders replication foci difficult to analyse in yeast. On the other hand, both Ddc2-GFP and Psy2-RFP foci were larger and less numerous, even in untreated S-phase cells (Figure 2.6B). Finally, consistent with previous reports, rare Rfa1/Ddc2 foci were detected in G1-phase cells (Figure S2.7A) (Lisby et al., 2004).

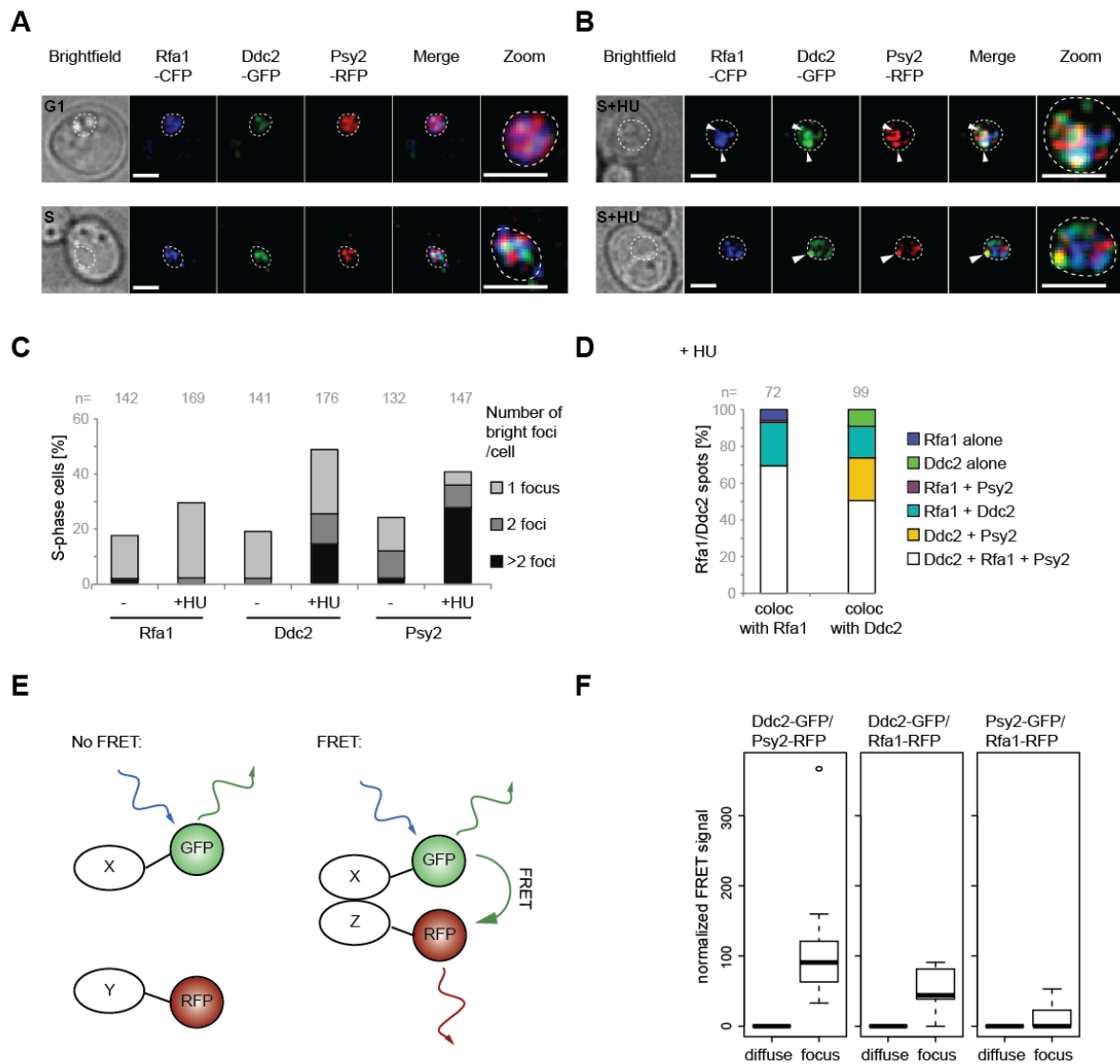


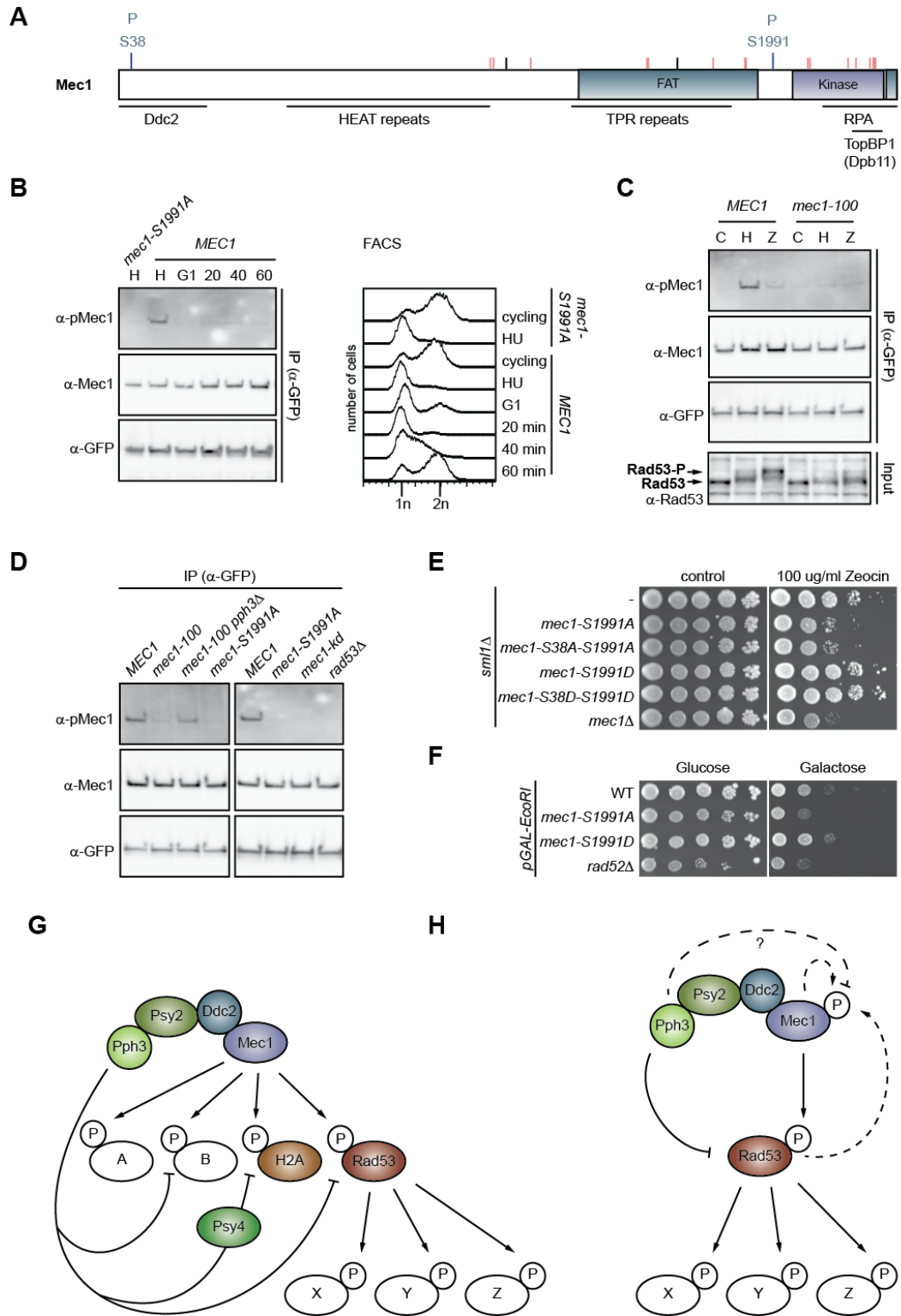
Figure 2.6: Ddc2-GFP and Psy2-RFP foci colocalize and show FRET signals. (A-D) *RFA1-RFP DDC2-GFP PSY2-RFP* (GA-8695) cells were incubated +/- 0.2M HU for 1h prior to fixation for microscopy. (A) Shown are images of untreated G1 and S phase cells, with indicated channels shown. Bar = 2 μ m. White dashed line: outline of cell nucleus. (B) Shown are examples of HU-treated cells. Upper panel: cell showing colocalization of all three proteins in two foci. Lower panel: Cell showing colocalization of Ddc2 and Psy2 only. Arrowheads indicate foci. (C) Quantification of bright foci number per S-phase cell. (D) Colocalization of Rfa1 and Ddc2 spots with other proteins was quantified after HU treatment. (E) Schematic of FRET principle: GFP and RFP must be within 10 nm for RFP emission. (F) *DDC2-GFP PSY2-RFP* (GA-8656), *DDC2-GFP RFA1-RFP* (GA-8705) and *PSY2-GFP RFA1-RFP* (GA-8702) cells were treated with 0.2 M HU for 1 h before fixation. Fixed samples were analyzed for FRET-induced RFP signals at either bright GFP foci (“focus”) or in the nucleus of cells that did not show a focus (“diffuse”). See also Fig. S2.7.

Following incubation with HU, all three tagged proteins, Rfa1, Ddc2 and Psy2, concentrated in intense nuclear foci (Figure 2.6B). We scored the number of bright foci in untreated and treated cells for each protein (Figures 2.6B, S2.7C). Approximately 15% of untreated cells in S phase contain single bright foci of Rfa1 and Ddc2, likely indicative of spontaneous damage, while a few cells contained more than one focus. These foci were not completely coextensive with Psy2-RFP foci, because 10% of cells had one Psy2-RFP focus, and another 10% had two or more bright spots (Figure 2.6C). After treatment with HU, however, the number of cells containing multiple foci of either Ddc2 or Psy2 increased strikingly (Figure 2.6C).

Since the test strain carries all three tagged proteins, we could monitor colocalization of the bright foci. On HU, 70% of the Rfa1 foci coincided with both Ddc2 and Psy2, while an additional 20% contained only Rfa1 and Ddc2 (Figure 2.6D). Almost no foci harbored only Rfa1 and Psy2. Importantly, by scoring colocalization with Ddc2 we found that over 70% of the Ddc2 foci also contained Psy2 (with or without Rfa1; Figure 2.6D). In cells treated with 400 $\mu\text{g/ml}$ Zeocin, a radiomimetic drug that induces both double- and single-stranded breaks, a small number of even larger Rfa1/Ddc2 foci were scored (Figure S2.7B-E), yet Psy2 colocalized with Rfa1 only when Ddc2 was present (roughly 50% of the bright foci, Figure S2.6F). We conclude that Psy2 and Ddc2 colocalize preferentially at HU-induced S-phase foci that contain Rfa1 (i.e. ssDNA at stalled forks), although they also bind coordinately at Zeocin-induced breaks.

Given the limited resolution of confocal microscopy we sought to confirm contact between these proteins by sensitized emission Förster resonance energy transfer (FRET). This method measures the energy transfer between a donor fluorescent protein (GFP) and an acceptor protein (RFP), and requires that the two are less than 10 nm apart (Figure 2.6E) (Piston and Kremers, 2007). Four FRET pairs were used in our study: Ddc2-GFP/Psy2-RFP; Ddc2-GFP/Rfa1-RFP; Psy2-GFP/Rfa1-RFP and Rfa1-GFP/Psy2-RFP. We find that there is no observable FRET between the non-focal nuclear fractions of any pairs. This does not rule out that they interact outside of foci, but rather suggests that any interaction outside of repair foci is below a detectable level (Piston and Kremers, 2007). Significant FRET signal was observed, however, at bright S-phase foci between Ddc2-GFP and Psy2-RFP after HU treatment, indicating that these proteins are in very close contact with each other (Figure 2.6F). The interaction between Ddc2 and Rfa1 is also substantial, while Psy2-Rfa1 contact is on average 10-fold lower than the other two pairs (Figure 2.6F). Thus we propose that Ddc2- Psy2 interact at stalled or collapsed fork foci, as does Ddc2-Rfa1.

Figure 2.7: Mec1 phosphoserine 1991 is regulated by Rad53 and Pph3. (A) Mec1 scheme: phosphosites in blue, vertical black lines = *mec1-100* mutations; vertical red lines = suppressor mutations (Fig.2.1). Interaction domains indicated below. (B) *Ddc2-GFP* (GA-7824) and *Ddc2-GFP mec1-S1991A* (GA-8232) cells were treated with 0.2 M HU for 1h or arrested in G1 and released into YPAD at 25 °C for indicated times. Fluorescence activated cell sorting (FACS) was performed on samples from which native extracts were prepared for IP with α -GFP. Western blotting used indicated antibodies, including α -pMec1 (Mec1 phosphoserine 1991). (C) Exponentially growing cultures of *Ddc2-GFP* (GA-7824) and *Ddc2-GFP mec1-100* (GA-7835) were untreated, or treated with 0.2 M HU or 400 $\mu\text{g/ml}$ Zeocin for 1h. Native extracts were subjected to IP by α -GFP and blots were probed with indicated antibodies. Input samples were probed with α -Rad53 to monitor Rad53 phosphorylation. (D) *Ddc2-GFP* (GA-7268), *Ddc2-GFP mec1-100* (GA-7327), *Ddc2-GFP mec1-100 pph3 Δ* (GA-7945) *Ddc2 mec1-S1991A* (GA-8232) *Ddc2-GFP mec1-kd sml1 Δ* (GA-8484) and *Ddc2-GFP rad53 Δ sml1 Δ* (GA-8486) cells + 0.2M HU for 1h prior to native extract preparation, α -GFP IP and Western blotting with indicated antibodies. (E) Serial 10-fold dilutions of cultures were plated on YPAD \pm 100 $\mu\text{g/ml}$ Zeocin. Relevant genotypes are indicated. Isogenic strains were GA-4533, GA-8242, GA-8246, GA-8243, GA-8247 and GA-5286. See Fig.S2.8, Table S2.5. (F) GA-1981, GA-8338, GA-8342 and GA-5975 (see Table S2.5) cells were transformed with pGAL-EcoRI (#2745) and grown in selective medium to ensure plasmid retention. Serial 10-fold dilutions were plated on selective medium containing 2% glucose or 2% galactose supplemented with 2% raffinose. (G) Model showing Ddc2-Psy2 interaction and coordinated action of Ddc2-Mec1 and Psy2-Pph3. Both target Rad53 and Histone H2A and other proteins. Histone H2A dephosphorylation alone requires Psy4. Most *mec1-100*/Tel1-specific phosphosites are also regulated by Psy2-Pph3 (“B”) while a few are not (“A”). (H) Mec1 phosphoserine 1991 requires Rad53 and Mec1 kinase activity. Reduced phosphorylation in *mec1-100* cells is rescued by Psy2-Pph3. Regulation of Mec1 may be indirect, potentially through Psy2-Pph3 regulation of Rad53. See also Fig. S2.8



We observed the same FRET result after treatment with Zeocin and by scoring spontaneous bright foci in untreated cells (Figure S2.7G). Because Rfa1-RFP cells showed a slight sensitivity to MMS (Figure S2.5F), we also confirmed the reduced Psy2-RPA interaction signal with a second FRET pair, Rfa2-GFP/Psy2-RFP. In agreement with the results for Rfa1-RFP, the Psy2-Rfa2 FRET signal is very low, while Psy2/Ddc2 and Ddc2/Rfa1 gave robust interactions (Figure S2.7G). Thus, the FRET data argue for tight interactions in living cells between the kinase cofactor Ddc2 and the phosphatase cofactor Psy2. We also confirm that Ddc2 contacts Rfa1 at stalled replication forks or collapsed fork foci. The scored colocalization at rare G1-phase foci may account for the cross recovery of Ddc2 and Psy2 in G1 phase extracts (Figure 2.5).

MEC1 PHOSPHORYLATION ON SERINE 1991 IS REGULATED IN A PPH3-DEPENDENT MANNER

Several Pph3/PP4 targets interact stably with the phosphatase (Keogh et al., 2006; Lee et al., 2010; Ma et al., 2014; O'Neill et al., 2007). Thus, we hypothesized that Pph3 might regulate Mec1, and not only counterbalance the enzyme by dephosphorylating its targets. To test this, we looked for phosphorylation sites in Ddc2 and Mec1 that are substrates for Psy2-Pph3. After 1h on HU, *mec1-100* or *MEC1+* cells expressing Ddc2-GFP were lysed, Mec1-Ddc2-GFP complexes were immunoprecipitated, and phosphopeptides analyzed by mass spectrometry. We identified two residues in Mec1 that were robustly phosphorylated in WT, but not in *mec1-100* strains, namely Mec1 Serine 38 and Mec1 Serine 1991 (Ser38, Ser1991, Figure 2.7A). While Ser38 has been described previously as a potential autophosphorylation site (Chen et al., 2010; Smolka et al., 2007), phosphorylation at Ser1991 has not been reported. Ser1991 sits between Mec1's conserved FAT and kinase domains and is well placed to be involved in Mec1 regulation. Indeed, a number of intragenic suppressor mutations in *mec1-100* map to this region (Figures 2.1, 2.7A). The mammalian ATR has an auto-phosphorylation site at the nearby residue Thr1989 (Liu et al., 2011; Nam et al., 2011).

We raised a specific antibody against the phosphorylated Ser1991; the antibody detected Mec1 after precipitation with Ddc2-GFP from HU treated cells, but did not react with a non-phosphorylatable *mec1-S1991A* form (Figure 2.7B). Using the antibody, we could show that Ser1991 phosphorylation is induced by HU, and is not detected in an unperturbed S phase (Figure 2.7B). Treatment with Zeocin induced Ser1991 phosphorylation to a weaker extent. In the *mec1-100* strain, Ser1991 phosphorylation was virtually absent in all conditions tested (Figure 2.7C). Thus loss of Ser1991 phosphorylation correlates with the *mec1-100* mutation. Importantly, Ser1991 phosphorylation could be restored in *mec1-100* cells by *pph3* Δ , indicating that Psy2-Pph3 indeed regulates Mec1 phosphorylation, compensating for the *mec1-100*-associated loss of Ser1991 modification (Figure 2.7D).

Using the phosphorylation specific antibody, we tested whether Mec1 Ser1991 is a site of autophosphorylation. Indeed, phospho-Ser1991 was absent in a catalytic-dead *mec1* mutant protein, yet we also failed to detect it in a *rad53* Δ mutant (Figure 2.7D). Ser1991 thus seems to require both Mec1 and Rad53 activity for its phosphorylation, although it remains unclear whether the *rad53* Δ effect is direct (Figure 2.7D). We attempted to demonstrate direct dephosphorylation of Ser1991 *in vitro* using Psy2-Pph3 isolated from cells expressing Psy2-Halo. Whereas the precipitated Psy2-Pph3 could dephosphorylate a control target, Cdc13 (Zhang and Durocher, 2010), it did not show reactivity with the phosphorylated Mec1 peptide (Figure S2.8A). In contrast, a nonspecific enzyme, calf intestinal alkaline phosphatase, could dephosphorylate both Cdc13 and Mec1 *in vitro* (Figure S2.8A). While we cannot exclude that our conditions were inappropriate for dephosphorylation it appears that Ser1991 is not a preferred substrate of Psy2-Pph3 *in vitro*.

To see whether loss of Mec1 Ser1991 phosphorylation leads to a phenotype, we scored the S1991A and S1991D mutants for growth in the presence HU, MMS, or Zeocin, and scored recovery after UV or γ -irradiation (IR) (Figures 2.7E, S2.8B). The acceptor-site mutant S1991A renders cells sensitive to the radiomimetic drug Zeocin (Figures 2.7E, S2.8B), independent of Ser38. We further confirmed that *mec1-S1991A* cells are strongly sensitive to induced DSBs by ectopically expressing *EcoRI* in all strains. Indeed, the *mec1-S1991A* mutant shows *EcoRI*-sensitivity (Figure 2.7F), while *mec1-S1991D* has a slight resistance.

DISCUSSION

Our key finding is that the central checkpoint kinase Mec1-Ddc2 (human ATR-ATRIP) forms a stable complex with the PP4 (Pph3-Psy2) phosphatase, and that they regulate, in an opposing manner, a large number of substrates. The modification of these latter targets is compromised in the S-phase-specific Mec1 mutant, *mec1-100*, which confers hypersensitivity to replication stress. We confirm this crosstalk genetically (by suppressor and EMAP analysis) and biochemically (by phosphoproteomics and a phosphospecific antibody for phospho-S1991). We further propose that the opposing action of Mec1 and PP4 and the direct interaction through Psy2-Ddc2 binding, are physiologically relevant, as they occur at sites of replication fork-induced damage in S phase cells and at induced DSBs (Figure 2.6) In an attempt to demonstrate the relevance of the interaction directly, we deleted the Ddc2 interaction domain in Psy2. The mutation showed the same sensitivity to MMS as a *psy2* Δ strain. This suggests either that the deletion inactivates the protein or destabilizes it.

Since about 70% of Ddc2 foci colocalize with Psy2, the majority of Mec1-Ddc2 appears to be associated with PP4, at least as judged by microscopy. IP/Western blot experiments, on the other hand, do not allow us to estimate the stoichiometry of the complex. Indeed, we cannot rule out that the Psy2-Ddc2 interaction also occurs outside of repair foci, given that they coimmunoprecipitate in the absence of damage.

Whereas the mechanisms that lead to checkpoint activation by Mec1-Ddc2 are well characterized, there is little information about what regulates or restricts the kinase complex. The *mec1-100* mutant was informative in this context. This mutant does not impair Mec1-Ddc2 recruitment to stalled forks (Cobb et al., 2005), nor does it attenuate kinase activity on a test peptide (Figure S2.1A). Rather, the mutation appears to alter the affinity of *mec1-100* towards a subset of targets that is particularly crucial for the survival of S-phase replication stress. Intriguingly, this same subset of targets is specifically upregulated by loss of Psy2 or Pph3 activity, which, importantly, suppresses the defects associated with the *mec1-100* mutation. The *mec1-100* deficiency also renders cells profoundly sensitive to HU, especially upon loss of the Sgs1 helicase or other S-phase checkpoint activating signals, as confirmed by our EMAP data.

This complex of phosphatase and kinase may allow the fine-tuning of ATR-ATRIP (Mec1-Ddc2) for different functions through the cell cycle. The fact that there seems to be a higher threshold for damage-induced checkpoint activation in S phase, as opposed to G2 phase, suggests that this may be an important regulatory event in the cell cycle (Shimada et al., 2002; Tercero et al., 2003). Finally, Mec1 not only has to react appropriately to ssDNA, but it must also switch off rapidly to allow efficient replication and cell cycle resumption. This may be a role for the closely associated Pph3-Psy2 complex. Indeed, Rad53 dephosphorylation during recovery from HU treatment is delayed in *pph3* Δ cells, although this did not result in detectable colony formation defects (Figures 2.2EF, S2.2BC, S2.3B). Presumably other phosphatases (Ptc2, Ptc3 or Glc7) eventually compensate for loss of Pph3 with time, as was reported for recovery from MMS treatment and repair of a double strand break (Kim et al., 2011; Szyjka et al., 2008). We note that *pph3* Δ shows synthetic sickness with loss of *dia2* Δ , *sae2* Δ and *ptc2* Δ on HU, which might contribute to recovery (Clerici et al., 2006; Fong et al., 2013; Kim et al., 2011; Leroy et al., 2003; Marsolier et al., 2000; Szyjka et al., 2008). However, in the presence of Pph3, a Ptc2 deletion showed significantly milder effects and did not physically interact with Mec1-Ddc2 (Figures 2.2; 2.3; 2.5)

The copurification of opposing enzymatic activities is not unique. We note that the human RAP80 complex contains both ubiquitin ligase and deubiquitinase enzymes (Sobhian et al., 2007) and histone acetyltransferases and deacetylases have been shown to not only create a dynamic balance of

acetylation of target proteins but also be physically associated with each other, sometimes even regulating each other's activity (Yamagoe et al., 2003). Relevant to this, we find that Pph3-Psy2 regulates a phosphorylation site within the Mec1 kinase, Ser1991, mutation of which compromises survival in face of DSBs. The Ser1991 modification is sensitive to loss of Mec1 activity, but also to *rad53* Δ (Figure 2.7). This suggests that it may be a target of Rad53, although we cannot rule out that it is an autophosphorylation site with an indirect dependence on Rad53 (Figure 2.7G,H). One might speculate that Ser1991 phosphorylation alters the specificity of Mec1 and/or triggers its downregulation, contributing to the attenuation of Mec1-Ddc2 activity during normal lagging strand DNA synthesis, or its inactivation at the end of a checkpoint response. Finally, based on our phosphoproteomic analysis one might speculate that Rad53 feeds back to downregulate Mec1-Ddc2, since we detected a large set of S/TQ phosphoacceptor peptides (Mec1 targets) that are upregulated in the *rad53* deletion strain (Figure S2.4CDE).

How does the checkpoint activation occur if an antagonizing activity is associated with the activating kinase? The phosphorylation of any given protein at any given time is always the result of competing kinase and phosphatase activities. Obviously, when checkpoint activation occurs, the catalytic rate of phosphorylation becomes stronger, because phosphorylated proteins accumulate. If it is stronger, it does not matter how much stronger it is (i.e. whether Pph3 is present or not). This may explain, why Pph3 does not affect phosphorylation in Mec1+ cells, but does in *mec1-100*, which may have a lower catalytic rate towards some substrates *in vivo*. The balance between the opposing activities can only be flipped by altering their specific activity. The recruitment of Rad53 by Sgs1 or Mrc1 (Alcasabas et al., 2001; Hegnauer et al., 2012) may induce a change in the specific activity of Mec1 towards Rad53, triggering checkpoint activation. Alternatively it is also possible that the kinase alters activity of the phosphatase, inhibiting it once a specific level of damage has occurred, and releasing it once damage is repaired. Although we did not detect phosphopeptides from either Psy2 or Pph3 in our *mec1-100* mass spectroscopic analysis of phosphorylation, we cannot exclude that PP4 is a target of Rad53 or Mec1.

The close association of Pph3-Psy2 with the checkpoint kinase may not only downregulate checkpoint by dephosphorylating Rad53, but also H2A-P. H2A dephosphorylation, however, requires a third factor, Psy4, which does not contribute to the suppression of *mec1-100* sensitivity to HU. Other phosphoproteomic studies have identified additional DNA damage-related PP4 targets, both in yeast and in mammals, among them RPA2, KAP-1, 53BP1, CHD4 and Cbfl, even though these studies were performed under non-damaging conditions (Bandyopadhyay et al., 2010; Lee et al., 2012; Lee et al., 2010). Those additional targets and the 47 targets hit by both Mec-Ddc2 and Psy2-Pph3 identified here, is most a likely non-exhaustive list, given that phosphopeptide coverage is rarely complete. We note that the Mec1/PP4 target Cbfl was not significantly downregulated in *mec1-100* cells after HU treatment (Figure S2.4C).

It is remarkable that 94% of the 47 phosphopeptides that show reduced phosphorylation levels in *mec1-100* responded to a deletion of *PPH3*. Combined with our genetic data, which showed suppression of *mec1-100* by *pph3* Δ and a strong anticorrelation of their genetic interaction profiles, we conclude that these two activities directly counteract each other. Among many other interesting genetic interactions scored for *mec1-100*, we found several subunits of the chromatin remodeling complexes INO80, SWI/SNF, ISW and Chd1, which show synthetic lethality with *mec1-100* (Figures 2.1C,S2.1D). Interestingly, subunits of these chromatin remodelers were also among the *mec1-100* downregulated phosphopeptides (e.g. Ies4 and Swi3). This reflects the close relationship of remodelers such as INO80 and fork recovery (Papamichos-Chronakis and Peterson, 2008; Shimada et al., 2008).

A parallel study indicated two different modes of Mec1 activity, one working during unchallenged DNA replication and one in response to damage (M. Smolka, personal communication). It is tempting to suggest that the association of Ddc2-Mec1 with Psy2-Pph3 might be involved in regulating the switch between these two functions. Further work will delineate the underlying molecular mechanisms of such a switch.

EXPERIMENTAL PROCEDURES

YEAST STRAINS, PLASMIDS, ANTIBODIES, MICROSCOPY, PHOSPHOPROTEOMICS, PHOSPHATASE ASSAY, AND EMAP

Yeast strains and plasmids are described in Table S2.5. If not stated otherwise cells were cultured at 30°C in YPAD medium using standard procedures. For Y2H analysis, fragments of *PSY2* were fused to the *lexA* DNA binding domain (#3616 - #3623, #3629,#3630) and *DDC2* was fused to the B42 transcription activation domain of pJG4-6 (#993), resulting in pJG4-6-DDC2 (#3308). WT cells (EGY48) containing the *lacZ* reporter pSH18-34 (#359), the bait and the prey were streaked on X-GAL plates (Golemis et al., 2011) and incubated 1-2 days at 30°C. β -galactosidase assays were performed as previously described (Hegnauer et al., 2012) using pGAL-*lexA* *Psy2* constructs (#3307, #3592-#3595, #3649-#3651, #3653). Details concerning antibodies, microscopy, phosphoproteomics, and the EMAP assay are found in Supplemental Methods.

MAMMALIAN CELL CULTURE

HEK293T cells were cultured in DMEM medium containing 10% fetal bovine serum. Transfections were carried out using jetPEI (Polyplus) transfection reagent according to manufacturer's instructions.

SPONTANEOUS SUPPRESSOR SCREENING

mec1-100 (GA-4978) and *mec1-100 exo1 Δ* (GA-6356) cells were plated on YPAD + 50 mM HU and incubated for 3 days. Colonies were picked and backcrossed 2-3 times with WT (GA-1982) cells. Strains yielding no HU sensitive *LEU+HIS+* (*mec1-100*) spores were considered to have intragenic suppressors and the *MEC1* locus was sequenced. Strains yielding both HU sensitive and insensitive *LEU+HIS+* (*mec1-100*) spores were deep sequenced to find extragenic mutations. Details are in Supplemental Methods.

KINASE AND PHOSPHATASE ASSAYS, RECOVERY AND DROP ASSAY, RAD53 AND H2A PHOSPHORYLATION, FACS

Mec1 kinase assay was performed as described (Hustedt and Shimada, 2014). A recombinant domain of Sgs1 (Sgs1 aa404-604) was used as substrate (Hegnauer et al., 2012). Recovery and drop assays, FACS analysis and Rad53 and H2A phosphorylation reactions were done as described previously (Hustedt and Shimada, 2014). Phosphatase assays are found in Supplemental Methods.

IMMUNOPRECIPITATION (IP)

Anti-GFP IP was carried out as described for kinase assays, except that the lysis buffer was supplemented with protease and phosphatase inhibitors (Complete protease inhibitors (Roche), 1mM phenylmethylsulfonyl fluoride, PhosSTOP phosphatase inhibitors (Roche), 0.1 mM Na₃VO₄, 1 mM NaF and 10 mM NaPP) and bead-bound protein complexes were washed three times with lysis buffer prior elution with 0.2 M glycine. Eluates were neutralized with Tris-HCl and analysed by Western blotting. Immunoprecipitation for mammalian cells was essentially performed the same, except that cells were harvested 48h post transfection by scraping off the plate into PBS, and washed once in PBS before snap-freezing pellets in liquid nitrogen. A modified lysis buffer (50 mM HEPES pH 8.0, 150 mM NaCl, 1 mM MgCl₂ and 0.5% NP-40) supplemented with protease and phosphatase inhibitors was used for nuclease treatment. Cleared lysates were incubated with 5 μ l RNaseA (Sigma) and 5 μ l benzonase (Invitrogen) for 30 min on ice prior to immunoprecipitation. After 1h incubation at 4°C

with antibody-coupled beads, lysates were recovered, DNA was isolated by phenol/chloroform extraction and analyzed by agarose gel electrophoresis and SYBR SAFE (Invitrogen) staining. Bead-bound protein complexes were analyzed as described above.

AUTHOR CONTRIBUTIONS

NH planned and performed most experiments, evaluated results, made all figures and wrote the paper, AS planned, performed and evaluated the FRET studies, KS supervised NH, performed experiments and helped in interpretations, RS performed all mass spectroscopy analyses, MT performed β -galactosidase assays, BB performed genome-wide sequencing of yeast mutants, HV and FvL supervised and hosted NH for the EMAP analysis, AG and HvA provided strains and know-how for the EMAP analysis, TI and RS helped analyse the EMAP results and SMG supervised NH and KS; evaluated and planned experiments, and helped write the paper.

ACKNOWLEDGEMENTS

NH thanks the EU ITN “Image DDR” for support, as well as the Swiss Cancer League. The Gasser laboratory is further supported by SNF, Novartis Research Foundation, HFSP, and the Frontiers in Genetics NCCR. FvL and HV were supported by The Dutch Cancer Society. HvA acknowledges support from NWO (TOP-GO grant). We thank M.P. Longhese for strains; F.E. Romesberg for plasmids; D. Durocher for reagents; D. Hoepfner (Novartis) for analysis of EMAP library, E. Oakeley, S. Schuierer for deep sequencing and analysis; T. Roloff, S. Dessus-Babus and M. Stadler for additional deep sequencing and analysis, H. Gut, I. Deshpande for assistance on construct design; Y. Murata, S. Nohara, M. Kawai and S. Ishikawa for assistance in cloning and generating strains.

REFERENCES

- Aguilera, A., and Garcia-Muse, T. (2013). Causes of genome instability. *Annu Rev Genet* 47, 1-32.
- Alcasabas, A.A., Osborn, A.J., Bachant, J., Hu, F., Werler, P.J., Bousset, K., Furuya, K., Diffley, J.F., Carr, A.M., and Elledge, S.J. (2001). Mrc1 transduces signals of DNA replication stress to activate Rad53. *Nat Cell Biol* 3, 958-965.
- Bandyopadhyay, S., Mehta, M., Kuo, D., Sung, M.K., Chuang, R., Jaehnig, E.J., Bodenmiller, B., Licon, K., Copeland, W., Shales, M., *et al.* (2010). Rewiring of genetic networks in response to DNA damage. *Science* 330, 1385-1389.
- Bazzi, M., Mantiero, D., Trovesi, C., Lucchini, G., and Longhese, M.P. (2010). Dephosphorylation of gamma H2A by Glc7/protein phosphatase 1 promotes recovery from inhibition of DNA replication. *Mol Cell Biol* 30, 131-145.
- Bjergbaek, L., Cobb, J.A., Tsai-Pflugfelder, M., and Gasser, S.M. (2005). Mechanistically distinct roles for Sgs1p in checkpoint activation and replication fork maintenance. *EMBO J* 24, 405-417.
- Brush, G.S., Morrow, D.M., Hieter, P., and Kelly, T.J. (1996). The ATM homologue MEC1 is required for phosphorylation of replication protein A in yeast. *Proc Natl Acad Sci U S A* 93, 15075-15080.
- Chen, S.H., Albuquerque, C.P., Liang, J., Suhandynata, R.T., and Zhou, H. (2010). A proteome-wide analysis of kinase-substrate network in the DNA damage response. *J Biol Chem* 285, 12803-12812.
- Chowdhury, D., Xu, X., Zhong, X., Ahmed, F., Zhong, J., Liao, J., Dykxhoorn, D.M., Weinstock, D.M., Pfeifer, G.P., and Lieberman, J. (2008). A PP4-phosphatase complex dephosphorylates gamma-H2AX generated during DNA replication. *Mol Cell* 31, 33-46.
- Cimprich, K.A., and Cortez, D. (2008). ATR: an essential regulator of genome integrity. *Nat Rev Mol Cell Biol* 9, 616-627.
- Clerici, M., Mantiero, D., Lucchini, G., and Longhese, M.P. (2006). The *Saccharomyces cerevisiae* Sae2 protein negatively regulates DNA damage checkpoint signalling. *EMBO Rep* 7, 212-218.
- Cobb, J.A., Schleker, T., Rojas, V., Bjergbaek, L., Tercero, J.A., and Gasser, S.M. (2005). Replisome instability, fork collapse, and gross chromosomal rearrangements arise synergistically from Mec1 kinase and RecQ helicase mutations. *Genes Dev* 19, 3055-3069.
- Collins, S.R., Miller, K.M., Maas, N.L., Roguev, A., Fillingham, J., Chu, C.S., Schuldiner, M., Gebbia, M., Recht, J., Shales, M., *et al.* (2007). Functional dissection of protein complexes involved in yeast chromosome biology using a genetic interaction map. *Nature* 446, 806-810.
- Collins, S.R., Schuldiner, M., Krogan, N.J., and Weissman, J.S. (2006). A strategy for extracting and analyzing large-scale quantitative epistatic interaction data. *Genome Biol* 7, R63.
- Downs, J.A., Lowndes, N.F., and Jackson, S.P. (2000). A role for *Saccharomyces cerevisiae* histone H2A in DNA repair. *Nature* 408, 1001-1004.
- Falk, J.E., Chan, A.C., Hoffmann, E., and Hochwagen, A. (2010). A Mec1- and PP4-dependent checkpoint couples centromere pairing to meiotic recombination. *Dev Cell* 19, 599-611.
- Fong, C.M., Arumugam, A., and Koepf, D.M. (2013). The *Saccharomyces cerevisiae* F-box protein Dia2 is a mediator of S-phase checkpoint recovery from DNA damage. *Genetics* 193, 483-499.
- Freeman, A.K., and Monteiro, A.N. (2010). Phosphatases in the cellular response to DNA damage. *Cell communication and signaling : CCS* 8, 27.
- Frei, C., and Gasser, S.M. (2000). The yeast Sgs1p helicase acts upstream of Rad53p in the DNA replication checkpoint and colocalizes with Rad53p in S-phase-specific foci. *Genes Dev* 14, 81-96.
- Friedel, A.M., Pike, B.L., and Gasser, S.M. (2009). ATR/Mec1: coordinating fork stability and repair. *Curr Opin Cell Biol* 21, 237-244.
- Gingras, A.C., Caballero, M., Zarske, M., Sanchez, A., Hazbun, T.R., Fields, S., Sonenberg, N., Hafen, E., Raught, B., and Aebersold, R. (2005). A novel, evolutionarily conserved protein phosphatase complex involved in cisplatin sensitivity. *Mol Cell Proteomics* 4, 1725-1740.
- Golemis, E.A., Serebriiskii, I., Finley, R.L., Jr., Kolonin, M.G., Gyuris, J., and Brent, R. (2011). Interaction trap/two-hybrid system to identify interacting proteins. *Current protocols in cell biology / editorial board, Juan S. Bonifacino ... [et al.] Chapter 17, Unit 17 13.*

- Guenole, A., Srivas, R., Vreeken, K., Wang, Z.Z., Wang, S., Krogan, N.J., Ideker, T., and van Attikum, H. (2013). Dissection of DNA damage responses using multiconditional genetic interaction maps. *Mol Cell* *49*, 346-358.
- Guillemain, G., Ma, E., Mauger, S., Miron, S., Thai, R., Guerois, R., Ochsenbein, F., and Marsolier-Kergoat, M.C. (2007). Mechanisms of checkpoint kinase Rad53 inactivation after a double-strand break in *Saccharomyces cerevisiae*. *Mol Cell Biol* *27*, 3378-3389.
- Hegnauer, A.M., Hustedt, N., Shimada, K., Pike, B.L., Vogel, M., Amsler, P., Rubin, S.M., van Leeuwen, F., Guenole, A., van Attikum, H., *et al.* (2012). An N-terminal acidic region of Sgs1 interacts with Rpa70 and recruits Rad53 kinase to stalled forks. *EMBO J* *31*, 3768-3783.
- Heideker, J., Lis, E.T., and Romesberg, F.E. (2007). Phosphatases, DNA damage checkpoints and checkpoint deactivation. *Cell Cycle* *6*, 3058-3064.
- Hustedt, N., Gasser, S.M., and Shimada, K. (2013). Replication checkpoint: tuning and coordination of replication forks in S phase. *Genes* *4*, 388-434.
- Hustedt, N., and Shimada, K. (2014). Analyzing DNA replication checkpoint in budding yeast. *Methods Mol Biol* *1170*, 321-341.
- Keogh, M.C., Kim, J.A., Downey, M., Fillingham, J., Chowdhury, D., Harrison, J.C., Onishi, M., Datta, N., Galicia, S., Emili, A., *et al.* (2006). A phosphatase complex that dephosphorylates gammaH2AX regulates DNA damage checkpoint recovery. *Nature* *439*, 497-501.
- Kim, J.A., Hicks, W.M., Li, J., Tay, S.Y., and Haber, J.E. (2011). Protein phosphatases pph3, ptc2, and ptc3 play redundant roles in DNA double-strand break repair by homologous recombination. *Mol Cell Biol* *31*, 507-516.
- Kim, S.T., Lim, D.S., Canman, C.E., and Kastan, M.B. (1999). Substrate specificities and identification of putative substrates of ATM kinase family members. *J Biol Chem* *274*, 37538-37543.
- Lee, D.H., Acharya, S.S., Kwon, M., Drane, P., Guan, Y., Adelmant, G., Kalev, P., Shah, J., Pellman, D., Marto, J.A., *et al.* (2014). Dephosphorylation enables the recruitment of 53BP1 to double-strand DNA breaks. *Mol Cell* *54*, 512-525.
- Lee, D.H., Goodarzi, A.A., Adelmant, G.O., Pan, Y., Jeggo, P.A., Marto, J.A., and Chowdhury, D. (2012). Phosphoproteomic analysis reveals that PP4 dephosphorylates KAP-1 impacting the DNA damage response. *EMBO J* *31*, 2403-2415.
- Lee, D.H., Pan, Y., Kanner, S., Sung, P., Borowiec, J.A., and Chowdhury, D. (2010). A PP4 phosphatase complex dephosphorylates RPA2 to facilitate DNA repair via homologous recombination. *Nat Struct Mol Biol* *17*, 365-372.
- Leroy, C., Lee, S.E., Vaze, M.B., Ochsenbein, F., Guerois, R., Haber, J.E., and Marsolier-Kergoat, M.C. (2003). PP2C phosphatases Ptc2 and Ptc3 are required for DNA checkpoint inactivation after a double-strand break. *Mol Cell* *11*, 827-835.
- Lisby, M., Barlow, J.H., Burgess, R.C., and Rothstein, R. (2004). Choreography of the DNA damage response: spatiotemporal relationships among checkpoint and repair proteins. *Cell* *118*, 699-713.
- Liu, S., Shiotani, B., Lahiri, M., Marechal, A., Tse, A., Leung, C.C., Glover, J.N., Yang, X.H., and Zou, L. (2011). ATR autophosphorylation as a molecular switch for checkpoint activation. *Mol Cell* *43*, 192-202.
- Ma, H., Han, B.K., Guaderrama, M., Aslanian, A., Yates, J.R., 3rd, Hunter, T., and Wittenberg, C. (2014). Psy2 targets the PP4 family phosphatase Pph3 to dephosphorylate Mth1 and repress glucose transporter gene expression. *Mol Cell Biol* *34*, 452-463.
- MacDougall, C.A., Byun, T.S., Van, C., Yee, M.C., and Cimprich, K.A. (2007). The structural determinants of checkpoint activation. *Genes Dev* *21*, 898-903.
- Mailand, N., Bekker-Jensen, S., Bartek, J., and Lukas, J. (2006). Destruction of Claspin by SCFbetaTrCP restrains Chk1 activation and facilitates recovery from genotoxic stress. *Mol Cell* *23*, 307-318.
- Marsolier, M.C., Roussel, P., Leroy, C., and Mann, C. (2000). Involvement of the PP2C-like phosphatase Ptc2p in the DNA checkpoint pathways of *Saccharomyces cerevisiae*. *Genetics* *154*, 1523-1532.
- Mordes, D.A., Glick, G.G., Zhao, R., and Cortez, D. (2008). TopBP1 activates ATR through ATRIP and a PIKK regulatory domain. *Genes Dev* *22*, 1478-1489.

- Nakada, S., Chen, G.I., Gingras, A.C., and Durocher, D. (2008). PP4 is a gamma H2AX phosphatase required for recovery from the DNA damage checkpoint. *EMBO Rep* *9*, 1019-1026.
- Nam, E.A., Zhao, R., Glick, G.G., Bansbach, C.E., Friedman, D.B., and Cortez, D. (2011). Thr-1989 phosphorylation is a marker of active ataxia telangiectasia-mutated and Rad3-related (ATR) kinase. *J Biol Chem* *286*, 28707-28714.
- O'Neill, B.M., Szyjka, S.J., Lis, E.T., Bailey, A.O., Yates, J.R., 3rd, Aparicio, O.M., and Romesberg, F.E. (2007). Pph3-Psy2 is a phosphatase complex required for Rad53 dephosphorylation and replication fork restart during recovery from DNA damage. *Proc Natl Acad Sci U S A* *104*, 9290-9295.
- Ohouo, P.Y., Bastos de Oliveira, F.M., Liu, Y., Ma, C.J., and Smolka, M.B. (2013). DNA-repair scaffolds dampen checkpoint signalling by counteracting the adaptor Rad9. *Nature* *493*, 120-124.
- Paciotti, V., Clerici, M., Lucchini, G., and Longhese, M.P. (2000). The checkpoint protein Ddc2, functionally related to *S. pombe* Rad26, interacts with Mec1 and is regulated by Mec1-dependent phosphorylation in budding yeast. *Genes Dev* *14*, 2046-2059.
- Paciotti, V., Clerici, M., Scotti, M., Lucchini, G., and Longhese, M.P. (2001). Characterization of mec1 kinase-deficient mutants and of new hypomorphic mec1 alleles impairing subsets of the DNA damage response pathway. *Mol Cell Biol* *21*, 3913-3925.
- Papamichos-Chronakis, M., and Peterson, C.L. (2008). The Ino80 chromatin-remodeling enzyme regulates replisome function and stability. *Nat Struct Mol Biol* *15*, 338-345.
- Pasero, P., Braguglia, D., and Gasser, S.M. (1997). ORC-dependent and origin-specific initiation of DNA replication at defined foci in isolated yeast nuclei. *Genes Dev* *11*, 1504-1518.
- Peschiaroli, A., Dorrello, N.V., Guardavaccaro, D., Venere, M., Halazonetis, T., Sherman, N.E., and Pagano, M. (2006). SCFbetaTrCP-mediated degradation of Claspin regulates recovery from the DNA replication checkpoint response. *Mol Cell* *23*, 319-329.
- Piston, D.W., and Kremers, G.J. (2007). Fluorescent protein FRET: the good, the bad and the ugly. *Trends Biochem Sci* *32*, 407-414.
- Schuldiner, M., Collins, S.R., Weissman, J.S., and Krogan, N.J. (2006). Quantitative genetic analysis in *Saccharomyces cerevisiae* using epistatic miniarray profiles (E-MAPs) and its application to chromatin functions. *Methods* *40*, 344-352.
- Segurado, M., and Diffley, J.F. (2008). Separate roles for the DNA damage checkpoint protein kinases in stabilizing DNA replication forks. *Genes Dev* *22*, 1816-1827.
- Shimada, K., Oma, Y., Schleker, T., Kugou, K., Ohta, K., Harata, M., and Gasser, S.M. (2008). Ino80 chromatin remodeling complex promotes recovery of stalled replication forks. *Curr Biol* *18*, 566-575.
- Shimada, K., Pasero, P., and Gasser, S.M. (2002). ORC and the intra-S-phase checkpoint: a threshold regulates Rad53p activation in S phase. *Genes Dev* *16*, 3236-3252.
- Smolka, M.B., Albuquerque, C.P., Chen, S.H., and Zhou, H. (2007). Proteome-wide identification of in vivo targets of DNA damage checkpoint kinases. *Proc Natl Acad Sci U S A* *104*, 10364-10369.
- Sobhian, B., Shao, G., Lilli, D.R., Culhane, A.C., Moreau, L.A., Xia, B., Livingston, D.M., and Greenberg, R.A. (2007). RAP80 targets BRCA1 to specific ubiquitin structures at DNA damage sites. *Science* *316*, 1198-1202.
- Szyjka, S.J., Aparicio, J.G., Viggiani, C.J., Knott, S., Xu, W., Tavare, S., and Aparicio, O.M. (2008). Rad53 regulates replication fork restart after DNA damage in *Saccharomyces cerevisiae*. *Genes Dev* *22*, 1906-1920.
- Tercero, J.A., Longhese, M.P., and Diffley, J.F. (2003). A central role for DNA replication forks in checkpoint activation and response. *Mol Cell* *11*, 1323-1336.
- Travesa, A., Duch, A., and Quintana, D.G. (2008). Distinct phosphatases mediate the deactivation of the DNA damage checkpoint kinase Rad53. *J Biol Chem* *283*, 17123-17130.
- van Attikum, H., Fritsch, O., Hohn, B., and Gasser, S.M. (2004). Recruitment of the INO80 complex by H2A phosphorylation links ATP-dependent chromatin remodeling with DNA double-strand break repair. *Cell* *119*, 777-788.
- Van Hoof, C., Martens, E., Longin, S., Jordens, J., Stevens, I., Janssens, V., and Goris, J. (2005). Specific interactions of PP2A and PP2A-like phosphatases with the yeast PTPA homologues, Ypa1 and Ypa2. *Biochem J* *386*, 93-102.

- Wang, H., Gao, J., Wong, A.H., Hu, K., Li, W., Wang, Y., and Sang, J. (2013). Rfa2 is specifically dephosphorylated by Pph3 in *Candida albicans*. *Biochem J* 449, 673-681.
- Yamagoe, S., Kanno, T., Kanno, Y., Sasaki, S., Siegel, R.M., Lenardo, M.J., Humphrey, G., Wang, Y., Nakatani, Y., Howard, B.H., *et al.* (2003). Interaction of histone acetylases and deacetylases in vivo. *Mol Cell Biol* 23, 1025-1033.
- Zhang, W., and Durocher, D. (2010). De novo telomere formation is suppressed by the Mec1-dependent inhibition of Cdc13 accumulation at DNA breaks. *Genes Dev* 24, 502-515.
- Zhao, X., Muller, E.G., and Rothstein, R. (1998). A suppressor of two essential checkpoint genes identifies a novel protein that negatively affects dNTP pools. *Mol Cell* 2, 329-340.
- Zou, L., and Elledge, S.J. (2003). Sensing DNA damage through ATRIP recognition of RPA-ssDNA complexes. *Science* 300, 1542-1548.

SUPPLEMENTAL MATERIAL TO CHAPTER 2

SUPPLEMENTAL EXPERIMENTAL PROCEDURES

Antibodies for Western blotting

Antibodies used were: Monoclonal α -Rad53 antibody (custom made by Genscript), goat α Mcm2 antibody (Santa Cruz) and rabbit α H2A phospho-serine 129 antibody (custom made by Sigma Genosys), mouse α -GFP (Roche), rabbit α -GFP, (Invitrogen), rabbit α -MYC (Santa Cruz), rabbit α -Rfa1 (Agrisera), rabbit α -PK (Novus Biologicals), rabbit α -Mec1 (custom made by SDIX), rabbit α Mec1 phospho-serine 1991 (custom made by Genscript), rat α -HA (Roche), rabbit α -lexA (Santa Cruz)

Sequencing of extragenic suppressors

Genomic DNA was isolated using Qiagen Genomic Tip100 (Qiagen) or phenol chloroform extraction and NucleoSpin PCR clean-up kit (Macherey-Nagel) in case of GA-6610 and quantified using a Nanodrop 3000 (Thermo Scientific) PicoGreen Assay. 50 ng of each individual sample were processed for library generation using Illumina's Nextera DNA sample preparation protocol, and barcoded as described for Illumina's TruSeq Dual Index Sequencing primers (Illumina). The samples were pooled at equimolar concentrations and sequenced using a single-end 75-base reads (50-base reads for GA-6610) on the Illumina's HiSeq2000 platform. The sequence data had >95% alignment, using BWA, to a reference S288C genome (genome build S288C_reference_genome_R62-1-1_20090218, obtained from Saccharomyces Genome Database, www.yeastgenome.org). A sequence of progenitor strains used in the experiment was done for *mec1-100* (GA-4978 and GA-6336) and *mec1-100 exo1 Δ* (GA-6356 and GA-6335). By comparison to the progenitor strain sequence, the SNP and indel calls were made in the sequence of the various derived sub-strains. In addition, large regions (>0.1 Megabase) of chromosome amplifications and deletions were assessed in each strain by comparison across all of the strains using read depth information.

High throughput genetic interaction screening

All query strains and the library are described in Table S6. For *mec1-100*, *sgs1-r1* and *rfa1-t11* query strains a NAT resistance cassette was integrated approximately 150 bp downstream of the gene. Subsequently, *mec1-100* and *sgs1-r1* mutations were introduced by pop-in/pop-out (Reid et al., 2002) with linear DNA fragments engineered by PCR using genomic DNA from already mutated strains (Hegnauer et al., 2012; Paciotti et al., 2001) as a template. *rfa1-t11* was created by transforming NheI-linearized plasmid #2221.

Double mutants of query strains and library strains were created as described (Hegnauer et al., 2012). Colony sizes were quantified using HT Colony Grid Analyzer (version 1.1) and genetic interaction scores were computed using the E-MAP toolkit (version 2.0) as previously described (Collins et al., 2006). A stringent QA/QC pipeline was employed to identify and remove (i) strains with a high error of measurement, and (ii) incorrectly deleted strains as identified through linkage analysis (Collins et al., 2010; Collins et al., 2006). In addition, all 1525 array mutants were pooled, genomic DNA extracted, and finally hybridized to a microarray containing probes covering tag sequences from the yeast deletion collection as described (Hegnauer et al., 2012). Strains with an intensity of <800 arbitrary fluorescent units were excluded from further analysis. In total, 214 array strains were dropped for further analysis. This included *ufo1 Δ* , for which a genetic interaction with *mec1-100* could not be confirmed despite recreating the mutation.

Mec1 phosphorylation

Immunoprecipitation to map phosphorylation sites in Ddc2-Mec1 was carried out starting from 1 liter cultures treated with 0.2M HU for 1h. Cells were harvested and washed once with PBS. Pellets were weighed, resuspended in 1ml /g PBS and dropped into liquid nitrogen. Droplets were subjected to three rounds of bead-milling using Mixer Mill MM 400 (Retsch). The frozen cell powder was resuspended in an equal volume of cold lysis buffer and IP was performed as described above in Experimental Procedures.

Eluted protein samples were treated with trypsin overnight at 37 °C after reduction and alkylation with tris(2-carboxyethyl)phosphine (TCEP) and iodoacetic acedic acid. The TFA acidified tryptic peptides (final concentration 0.1%) were separated on an Agilent 1100 nanoLC system (Agilent Technologies) coupled to an LTQ Orbitrap Velos hybrid mass spectrometer (Thermo Scientific). The LC system was equipped with a Peptide CapTrap column (Michrom BioResources, Inc.) and a capillary column with integrated nanospray tip (75 µm i.d. x 100 mm, Swiss BioAnalytics AG) filled with MagicC18 (5 µm, Michrom Bioresources, Inc.). Elution was performed with a gradient starting with 2% solvent B and continued with 2 to 10% solvent B in 3 min and 10 to 40% solvent B in 80 min at a flow rate of 400 nL/ min. Solvent A consisted of 0.1% formic acid/ 2% acetonitrile, solvent B was composed of 0.1% formic acid/ 80% acetonitrile. The mass spectrometer operated in positive mode using the top 15 DDA method. MS scans were acquired at a resolution of 60, 000 over a range of m/z 350 to 1200. Singly charged ions were rejected from MSMS fragmentation. Peptides were identified searching SwissProt (version 2011-08) using Mascot Distiller 2.3 and Mascot 2.3.0.2 (Matrix Science) considering acetylation at protein N-terms, deamidation at asparagine and glutamine, oxidation at methionine and phosphorylation at serine as well as at threonine. Two missed cleavage sites were allowed. Results were compiled in Scaffold 3.0 (Proteome Software).

Microscopy

Fluorescence microscopy used an Olympus IX81 microscope equipped with a Yokogawa CSU-X1 scan head, a Evolve 512 Delta EMCCD camera, a ASI MS-2000 Z-piezo stage and a PlanApo x1000 NA 1.45 total internal fluorescence microscope oil objective. Cells were grown from an overnight culture in synthetic complete media complemented with all amino acids until they reached approximately 5×10^6 cells/ml. They were treated for 1 hour + 400 µg/ml zeocin, + 0.2 M HU or left untreated. Cells were then fixed in 4% PFA for 30 seconds washed three times with PBS and finally resuspended in PBS. Images were acquired on 2% agarose pads. The lasers used to excite the different fluorophores are as follows: 445 nm for CFP (eCFP), 491 nm for GFP and 561 nm for RFP.

For foci number quantification 4 color Z-stacks were obtained taking 20 slices at 200 nm intervals. Exposure times were: 50 ms GFP, 100 ms CFP, 150 ms RFP, 10 ms brightfield. The EMCCD gain was set to approximately 600 in all cases except for the brightfield where it was set to 50. Images were deconvolved using Huygens Remote Manager v3.0.3. The deconvolution algorithm used was classic maximum likelihood estimate with a signal/noise ratio of 5, automatic background estimation and 30 iterations. “Bright foci” were counted and defined as foci that have clear borders. Thresholding was applied to help see foci over background nuclear signal and done with Fiji. We note that in the case of Ddc2 many smaller less bright foci were present.

For colocalization analysis single slice 4 channel images were acquired and processed as above except the exposure of CFP was increased to 150 ms and RFP to 250 ms. CFP, GFP and RFP were channel aligned using Huygens Pro software. Colocalization was scored when foci either completely overlapped or partially overlapped.

For FRET, the donor GFP was excited by light at 488 nm and the emission signals are collected using filters that allow selective detection of either donor or acceptor signals. Fluorescence bleed-through of the donor signal into the acceptor channel, or the reverse, is quantified by imaging strains that contain only donor or acceptor proteins. Automated subtraction of bleed-through signal, yields the significant FRET value.

Sensitized emission FRET images for each series were acquired on the same day. Four channel images were acquired: GFP channel, FRET channel, RFP channel as well as brightfield, even for donor only (GFP) and acceptor only strains. FRET was calculated using the PixFRET Fiji plugin (Feige et al., 2005). Spectral bleed through was calculated on using donor only (*DDC2-GFP* (GA-7268), *PSY2-GFP* (GA-8033), *RFA2-GFP* (GA-6022)) and acceptor only strains (*PSY2-RFP* (GA-8659), *RFA1-RFP* (GA-8687)). The PixFRET parameters used were 1.0 Gaussian blur, 1.0 Threshold and Output of FRET/sqrt(Donor*Acceptor). The donor only and acceptor only parameters for PixFRET are as follows and were acquired by a montage of 10 donor only or 10 acceptor only images: Ddc2-GFP, a = 2.328, b = 0.00047, linear; Psy2-RFP, a = 0.48385, -b = 0.00004 linear; rfa1-RFP, a = 1.27947, b = -0.00011, linear; Psy2-GFP, a = 0.03595, constant; Rfa2-GFP, a = 0.31318, constant. FRET values were calculated from the mean intensity of the NFRET image of each focus.

Phosphoproteomics

Cells were grown in synthetic medium. 50 ml cultures were grown to an $OD_{600}=0.75$, arrested in G1 using α -factor, and released into 75 ml synthetic medium containing 0.2M HU until the appearance of small buds (45 min). Proteins were extracted as previously described (Bodenmiller and Aebersold). In brief, proteins were denatured and precipitated by adding a final 6% trichloroacetic acid to the cultures and incubating on ice for 30 min. Precipitates were collected by centrifugation and washed three times with ice-cold acetone. Pellets were resuspended in 800 μ l urea buffer (8M Urea, 50 mM ammonium bicarbonate, 5 mM EDTA and PhosSTOP phosphatase inhibitors (Roche)) and a corresponding volume of silica beads was added. Extracts were prepared by five rounds of bead beating. Supernatant was collected, another 800 μ l urea buffer added to beads followed by five rounds of bead beating and pooling of supernatants.

Peptide generation and phosphopeptide enrichment

Extracts in 8 M urea, 50 mM ammonium bicarbonate, and 5 mM EDTA had a protein concentration of about 5.2 mg/ mL. 150 μ l 200 mM HEPES were added to 1.5 mL of each of the twelve extracts. Reduction and alkylation of cysteines were performed by adding of 160 μ l 45 mM DTT for 30 min followed by adding of 180 μ l 100 mM iodoacetamide for another 30 min (in the dark), both at room temperature. Before adding of 20 μ l 1 mg/ mL LysC (Wako, Japan) the extracts were twofold diluted to keep a final HEPES concentration of 20 mM. First digest was performed overnight at 25 °C. After further twofold diluting of the extracts 100 μ l of 0.5 mg/ mL trypsin were added and the second digest was performed at 37 °C overnight. Before phosphopeptide enrichment the digests were desalted using SepPak C18 columns (Waters). The eluates were dried down in a SpeedVac (Thermo Scientific).

The digests were reconstituted in 150 μ l 2.5% trifluoroacetic acid (TFA)/ 80% acetonitrile, saturated with phthalic acid and 30 min incubated with 1.5 mg TiO₂ beads (Inertsil Titansphere 5 μ m, GL Science, Japan) using Mobitec tubes (MoBiTec, Germany). The beads were thoroughly washed four times with 200 μ l 2.5% TFA/ 80% acetonitrile. Phospho-peptides were eluted with 100 μ l 0.3 M NH₄OH and 100 μ l 0.3 M NH₄OH/ 30% acetonitrile. The pH of the eluates was lowered to about 3 by adding 4 μ l TFA before drying down in a SpeedVac. The final desalting step was performed on Oligo R3 media (Life technologies) immobilized on C18 GELoader pipette tips (Proxeon).

LC/MS/MS analyses of enriched phosphopeptides

The LC/MS/MS analyses were performed on an Easy-nLC 1000 pump coupled to an LTQ Orbitrap Velos mass spectrometer (Thermo Scientific) using a Digital PicoView ion source (New Objective). The peptides were separated on a New Objective analytical column (75 μm x 25 cm, Reprosil, 3 μm) with a gradient from 2 to 30% solvent B in 110 min, 30 to 50% solvent B in 30 min and 50 to 80% solvent B in 5 min. Solvent A consisted of 0.1% formic acid in water, solvent B of 0.1% formic acid in acetonitrile. The flow rate was 200 nL/ min. The dried TiO₂ eluates were dissolved in 40 μL 0.1% TFA/ 2% acetonitrile and the peptide concentrations determined with a Qubit fluorometer and the Qubit protein assay kit (Life technologies). The injection volumes were adapted accordingly for 1 μg peptides on column.

Data were acquired in a Top25 data dependent analysis mode using three different charge (z) rejection settings: positive charged ions are considered for MSMS scans with either $z > 1$, $z = 2$ or with $z > 2$. A different charge selection mode was deployed for each of the replicates. MS scans were acquired at a resolution of 60, 000 over a range of m/z 350 to 1200.

Data evaluation with Progenesis-LC

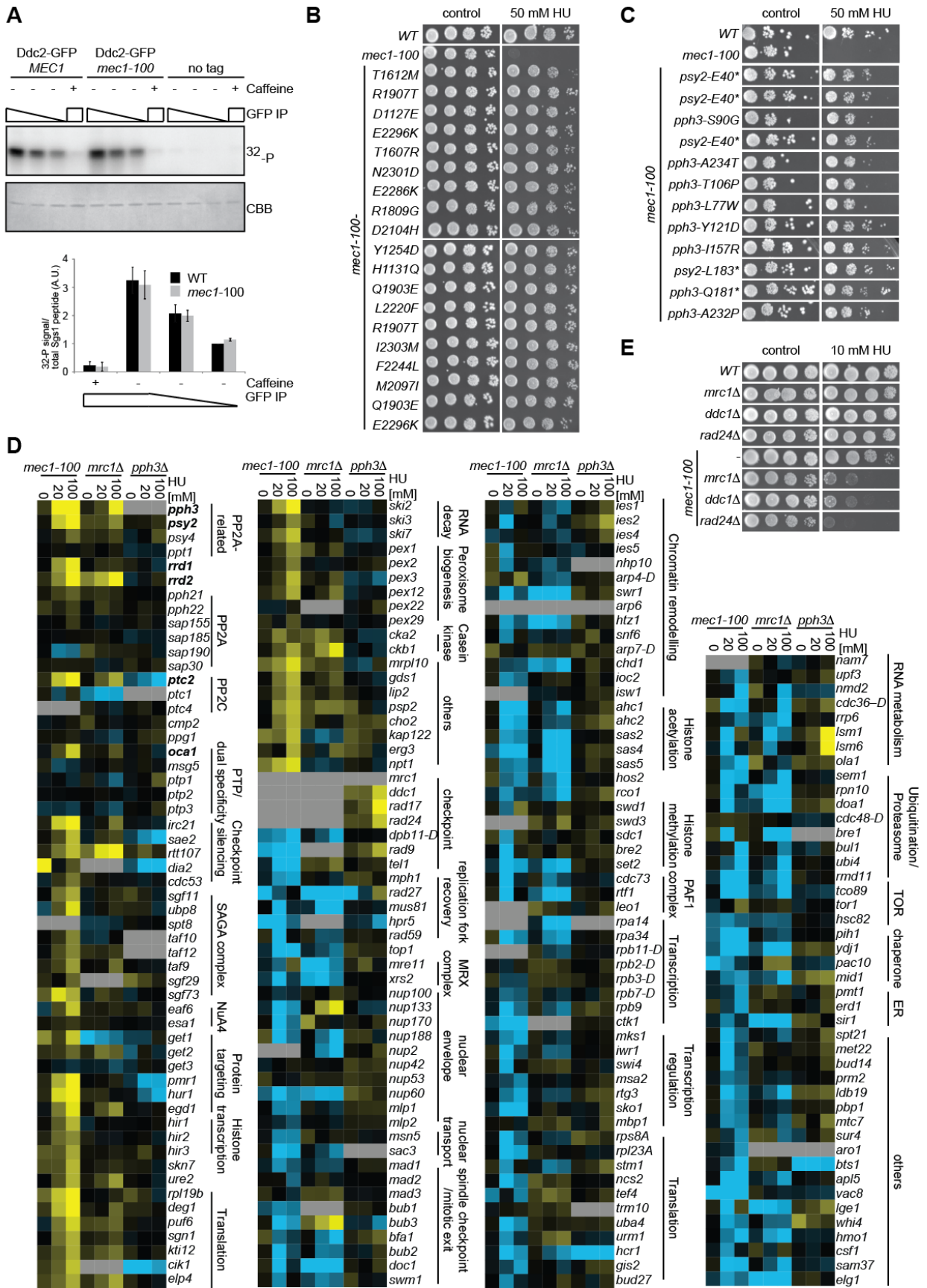
The twelve raw files were loaded into Progenesis-LC and automatically aligned. The alignments were manually corrected where needed. Finally, the alignment scores were 82.5% and better. Features with two charges and more than two isotopes, features with three to six charges having more than three isotopes and spectra with a limit fragment count of 150 were considered for a database search using MASCOT 2.3. Peptides were identified searching the Saccharomyces Genome Database (SGD), version Sept. 2011) considering the following settings: Carbamidomethylation at cysteines as fixed modification, deamidation at asparagine and glutamine, oxidation at methionine, acetylation at the protein N-terms and phosphorylation at serine as well as at threonine as variable modifications, two missed cleavage sites, a peptide mass tolerance of 7 ppm and a fragment mass tolerance of 0.6 Da, trypsin as enzyme, allowing the cleavage after arginine and lysine also if followed by a proline. Finally, in Progenesis-LC features were kept if they had a MASCOT ion score greater than 15 and were identified as phosphopeptides without any other modifications except acetylation at protein N-terminals. The normalization was performed considering only those phosphopeptides. The final feature data list was exported into Excel. Ratios “mutant versus wild type” were calculated from the average of the normalized abundances of the three replicates and the probability of a Student’s t-test was determined accordingly. Only phosphopeptides with a probability of 0.95 were considered for further evaluation. All SQ/ TQ containing peptides were checked for the phosphosite probability with MaxQuant (version 1.4.1.2, (Cox and Mann, 2008)) and Proteome Discoverer (version 1.4.1.14, Thermo Fisher Scientific) and kept only, if the site probability was higher than 75% in any of the two programs.

Phosphatase Assay

1L of late-log phase WT cells (GA-1981) or *PSY2-HALO* (GA-8179) cells were harvested and washed once with PBS. Pellets were weighed, resuspended in 1ml /g buffer 1 without NP-40 (50 mM Hepes pH7.5, 150 mM NaCl, 2mM EDTA) and dropped into liquid nitrogen. Droplets were subjected to three rounds of bead-milling using Mixer Mill MM 400 (Retsch). The frozen cell powder was resuspended in an equal volume of cold buffer 2 (50 mM Hepes pH7.5, 150 mM NaCl, 1mM DTT, 0.01% NP-40, and protease inhibitors: 1 mM PMSF, 300 $\mu\text{g}/\text{mL}$ benzamidine, 1 $\mu\text{g}/\text{mL}$ pepstatin, 0.5 $\mu\text{g}/\text{mL}$ leupeptin, 40 $\mu\text{g}/\text{mL}$ bestatin, 2 μM E64 and 50 $\mu\text{g}/\text{mL}$ TLCK), and cleared by centrifugation. HALO-link resin (Promega) was washed five times with buffer 2, 1ml resin was added to 7 mL cleared lysates and incubated at 4°C overnight. Resin-bound protein complexes were washed once

with buffer 3 (buffer 2 + 1mM EDTA), four times with buffer 3 lacking protease inhibitors and 2 times with phosphatase buffer (25mM Tris pH7.5, 100 mM NaCl, 0.1 mM EDTA, 1 mM DTT, 0.01% Brij-35). Resin-bound protein complexes were finally resuspended in 250 μ l Phosphatase buffer + TEV protease and incubated at 4°C overnight. Eluates were separated from resin by centrifuging through micro spin columns (Biorad). 35 μ L of eluates were incubated with 10 μ M of peptide (positive control: RRA(pT)VA (provided with Assay kit), Cdc13-p: Biotin-GGGKSYIQ(pS)QTPERK-amide, Cdc13: Biotin-GGGKSYIQSQTPERK-amide (both gifts from D. Durocher), Mec1-p: VK(pS)ITSRSGKSLEKC and Mec1: VKSITSRSGKSLEKC (both synthesized by Genscript)) in phosphatase buffer. Reactions also contained a final 5 mM manganese chloride. Release of phosphate was measured using a colorimetric Ser/Thr phosphatase assay kit (Promega). Phosphate leads to the proportional accumulation of a green dye, measured quantitatively as light absorption at 600 nm.

SUPPLEMENTAL FIGURES



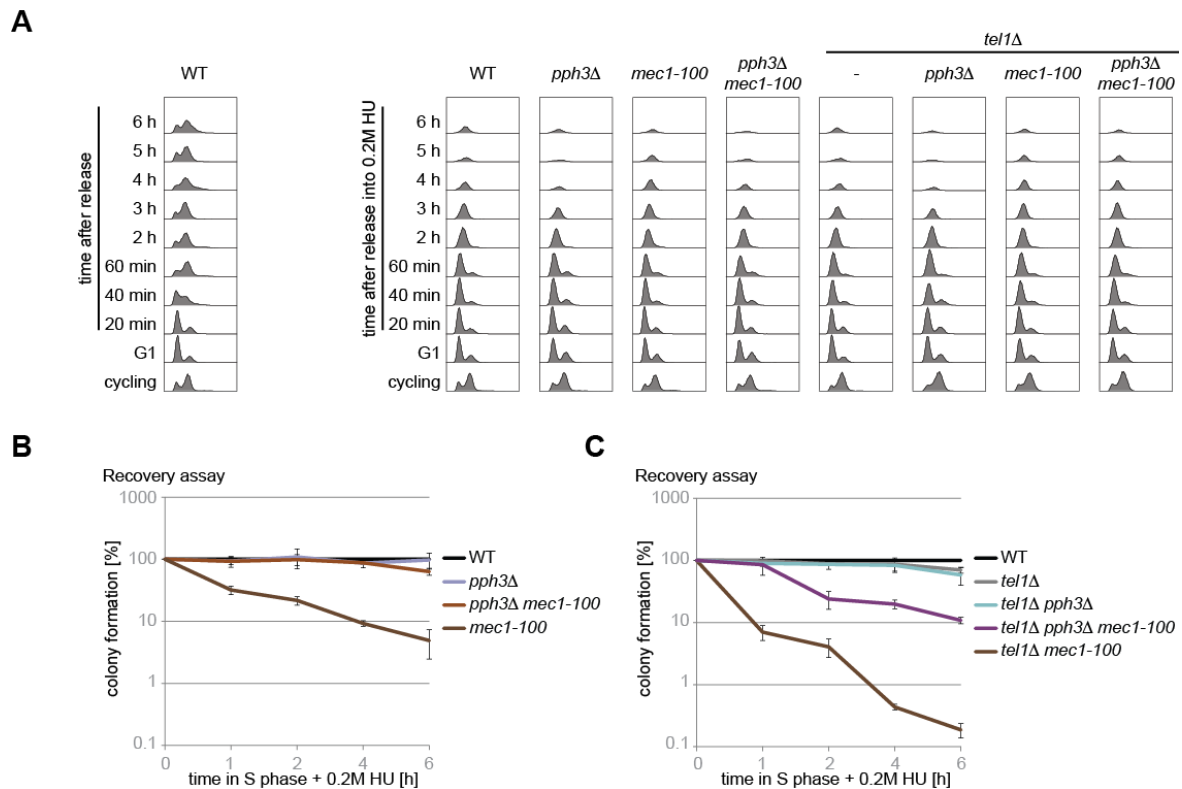


Figure S2.2: *pph3Δ* suppresses *mec1-100* recovery defects after HU treatment at early timepoints; related to Figure 2-2 (A) DNA content was monitored by FACS analysis after synchronization in G1 by α -factor arrest and release into S phase \pm 0.2 M HU for the indicated times. Isogenic strains used were: GA-1981, GA-6582, GA-7049, GA-7086, GA-6912, GA-6913, GA-7953 and GA-7955. **(B)** Recovery from replication fork stalling was monitored as colony outgrowth of cells after synchronization in G1 by α -factor arrest and release into S phase with 0.2 M HU for the indicated times. Isogenic strains used were GA-1981, GA-6582, GA-7049 and GA-7086. Error bars indicate standard deviation. **(C)** Cells were treated as in (B). Isogenic strains used were GA-1981, GA-6912, GA-6913, GA-7953 and GA-7955. Relevant genotypes are indicated in the figure and listed in Table S2.5.

Figure S2.1: The *mec1-100*/Ddc2 kinase shows robust activity, yet genetic interactions implicate its deficiency in replication checkpoint and fork recovery; related to Figure 2.1. (A) Kinase assay using α -GFP IP from *DDC2-GFP* (GA-7268), *DDC2-GFP mec1-100* (GA-7327) or WT (GA-1981) cell extracts. An Sgs1 peptide (aa 404–604, Hegnauer et al., 2010) was used as a substrate in the presence of γ -32P-ATP and was analysed by gel electrophoresis and autoradiography. Where indicated, 30mM caffeine was added to inhibit Mec1. 32 P autoradiography and Coomassie Brilliant Blue (CBB) staining are shown. Lower panel shows quantification of 32 P signal over CBB signal. Error bars indicate standard deviation of three independent experiments. **(B)** Drop assay of intragenic suppressors. Serial ten-fold dilutions of cultures were plated on YPAD \pm 50 mM HU. Relevant genotypes are indicated in the figure. Isogenic strains used were: GA-1981, GA-6583, GA-6769, GA-6410, GA-6412, GA-6416, GA-6418, GA-6422, GA-6466, GA-6468, GA-6470, GA-6472, GA-6480, GA-6510, GA-6514, GA-6518, GA-6522, GA-6529, GA-6533, GA-6537 and GA-6539. **(C)** Drop assay of extragenic suppressors. Cells were treated as in (B). Isogenic strains used were: GA-1981, GA-6583, GA-6575, GA-6596, GA-6577, GA-6598, GA-6600, GA-6601, GA-6603, GA-6605, GA-6606, GA-6610, GA-6608 and GA-6572. Genotypes indicated in figure and in Table S2.5. **(D)** Genetic interactions with *mec1-100* (genetic interaction score ≤ -2 or $\geq +2$) are shown. Interactions of *mec1-100* with mutants of other phosphatase classes. Mutations of additional subunits of multisubunit complexes were included. Interactions of *mrc1Δ* and *pph3Δ* with the same mutants are shown for comparison. **(E)** Serial ten-fold dilutions of cultures were plated on YPAD \pm 10 mM HU. Relevant genotypes are indicated in the figure and in Table S2.5. Isogenic strains used were: GA-1981, GA-6826, GA-7907, GA-5321, GA-6582, GA-7964 and GA-7209.

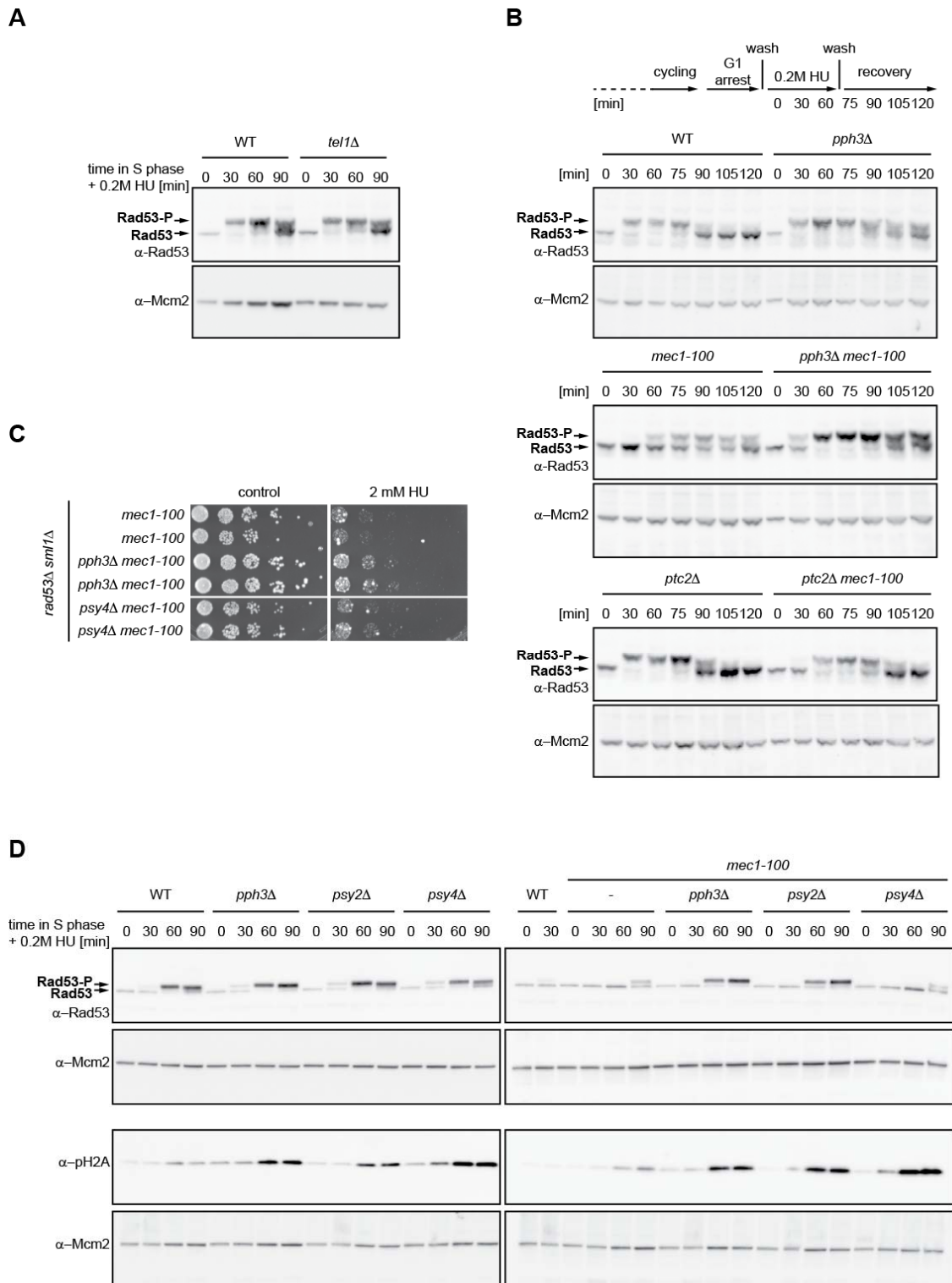


Figure S2.3: Psy4 dephosphorylates H2A, but does not suppress *mec1-100* HU sensitivity; related to Figure 2.3. (A) Rad53 activation was monitored in WT (GA-1981) and *tel1Δ* (GA-6912) cells. Cells were synchronized in G1 by α -factor arrest and released for indicated times into 0.2 M HU before denatured extract preparation and Western blot analysis. (B) Cells were treated as in (A) except that HU was washed out after 60 minutes. Samples were taken at indicated timepoints and analysed for Rad53 phosphorylation. (C) Serial five-fold dilutions of *rad53Δ sml1Δ mec1-100* (GA-7401), *rad53Δ, sml1Δ mec1-100 pph3Δ* (GA-7377), *rad53Δ sml1Δ mec1-100 psy4Δ* (GA-8581) cultures (2 colonies each) were plated on YPAD \pm 2 mM HU. (D) Rad53 and H2A serine 129 phosphorylation was monitored by treating cells as in (A) and blotting with indicated antibodies. Isogenic strains used GA-1981, GA-7049, GA-7391, GA-7383, GA-6582, GA-7086, GA-7393 and GA-7385 cells. Relevant genotypes are indicated in the figure and are listed in Table S2.5.

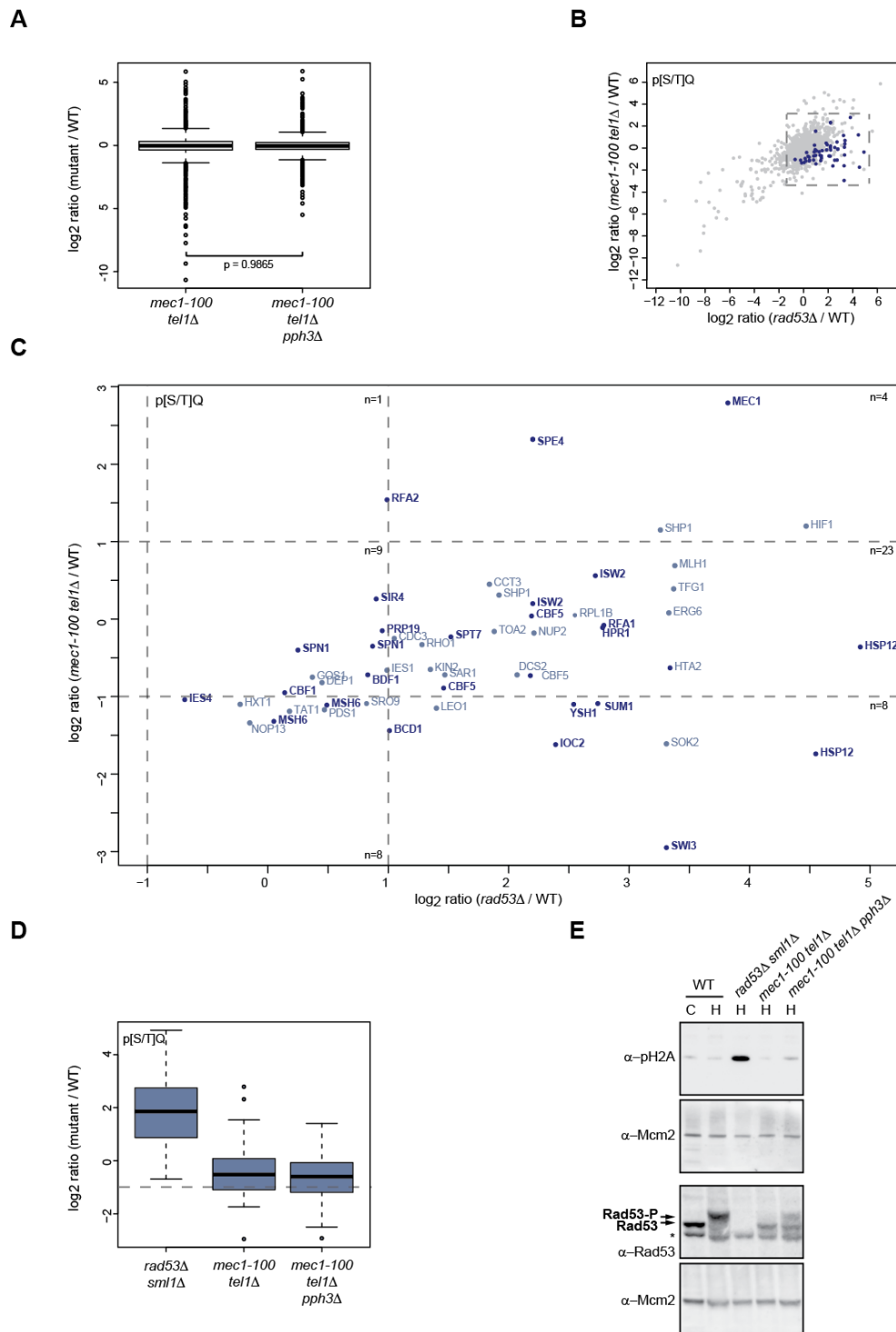


Figure S2.4: Most S/TQ phosphopeptides are not reduced in *mec1-100* cells on HU; related to Figure 2.4. (A) Boxplot of indicated abundance ratios of all quantified phosphopeptides. P-value was calculated by one-tailed Wilcoxon signed rank test. (B) Abundances (log₂ ratio (mutant/WT)) of all quantified phosphopeptides in *mec1-100 tel1Δ* cells were plotted against abundances in *rad53Δ sml1Δ*. Blue marked peptides are phosphorylated on [pS/pT]Q consensus and are (1) *mec1-100/tel1*-specific (see Figure 4) and/or (2) were at least two-fold more abundant in *rad53Δ* compared to *mec1-100 tel1Δ* samples (log₂ ratio ≥ 1, $p \leq 0.05$, Student's paired t-test) regardless of the levels in WT sample and/or (3) were previously described as Mec1/Tel1-dependent (Chen et al., 2010) (full list in Table S4). Dotted lines indicate area enlarged in (D). (C) Enlarged area of plot shown in (B). Displayed are selected phosphopeptides marked blue in (B). Labels indicated protein names. Bold: phosphopeptides previously described as Mec1/Tel1 specific (Chen et al., 2010). Dotted lines indicate thresholds for up/downregulation. n = number of phosphopeptides that fall between dotted lines. (D) Boxplot of indicated ratios of phosphopeptides that match the [pS/pT]Q consensus and were marked blue in (B). (E) Samples taken before synchronization (C) and prior protein extraction (H) (Fig. 2.4B) were analyzed by Western blotting with indicated antibodies

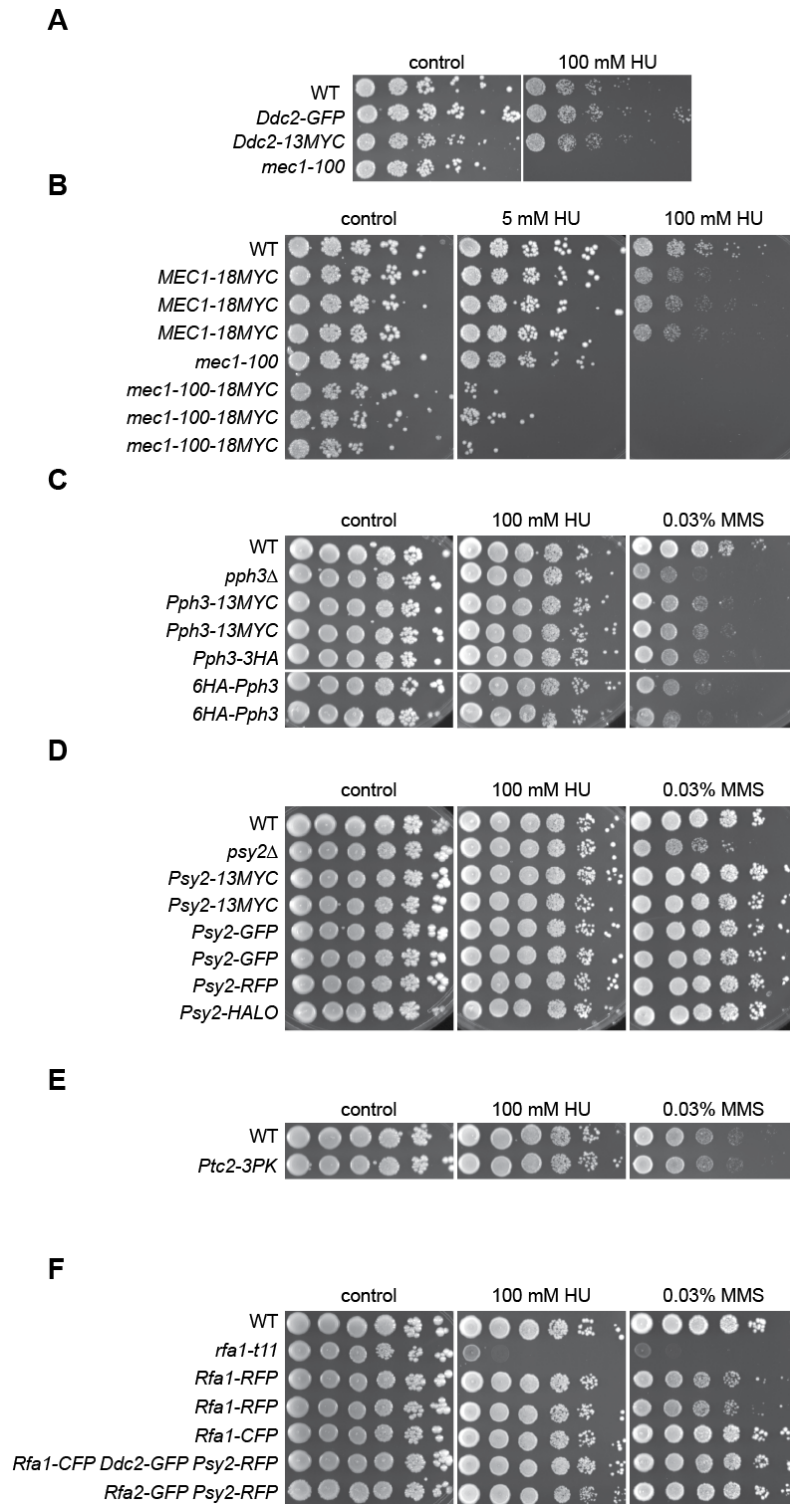


Figure S2.5. Functionality of tagged strains used in this study; Related to Figure 2.5. (A) Serial 5-fold dilutions of cultures were plated on YPAD ± 100 mM HU. Relevant genotypes are indicated in the figure. Strains used were GA-1981, GA-7268, GA-7337 and GA-6582. (B) Serial 5-fold dilutions of cultures were plated on YPAD, YPAD + 5 mM HU and YPAD + 100 mM HU. Strains used were GA-1981, GA-7353, GA-7354, GA-7355, GA-6582, GA-7366, GA-7367 and GA7368. (C) Serial ten-fold dilutions of cultures were plated on YPAD, YPAD + 100 mM HU and YPAD + 0.03% methyl methanesulfonate (MMS). Strains used were GA-1981, GA-7049, GA-7852, GA-7853, GA-7865, GA-7966 and GA-7967. (D) Cells were treated as in (C). Strains used were GA-1981, GA-7391, GA-7798, GA-7799, GA-8033, GA-8021, GA-8659 and GA-8179 (E) Cells were treated as in (C). Strains used were GA-1981 and GA-7923. (F) Cells were treated as in (C). Strains used were GA-1981, GA-8396, GA-8687, GA-8688, GA-8694, GA-8695 and GA-8676. Relevant genotypes are indicated and are listed in Table S2.5.

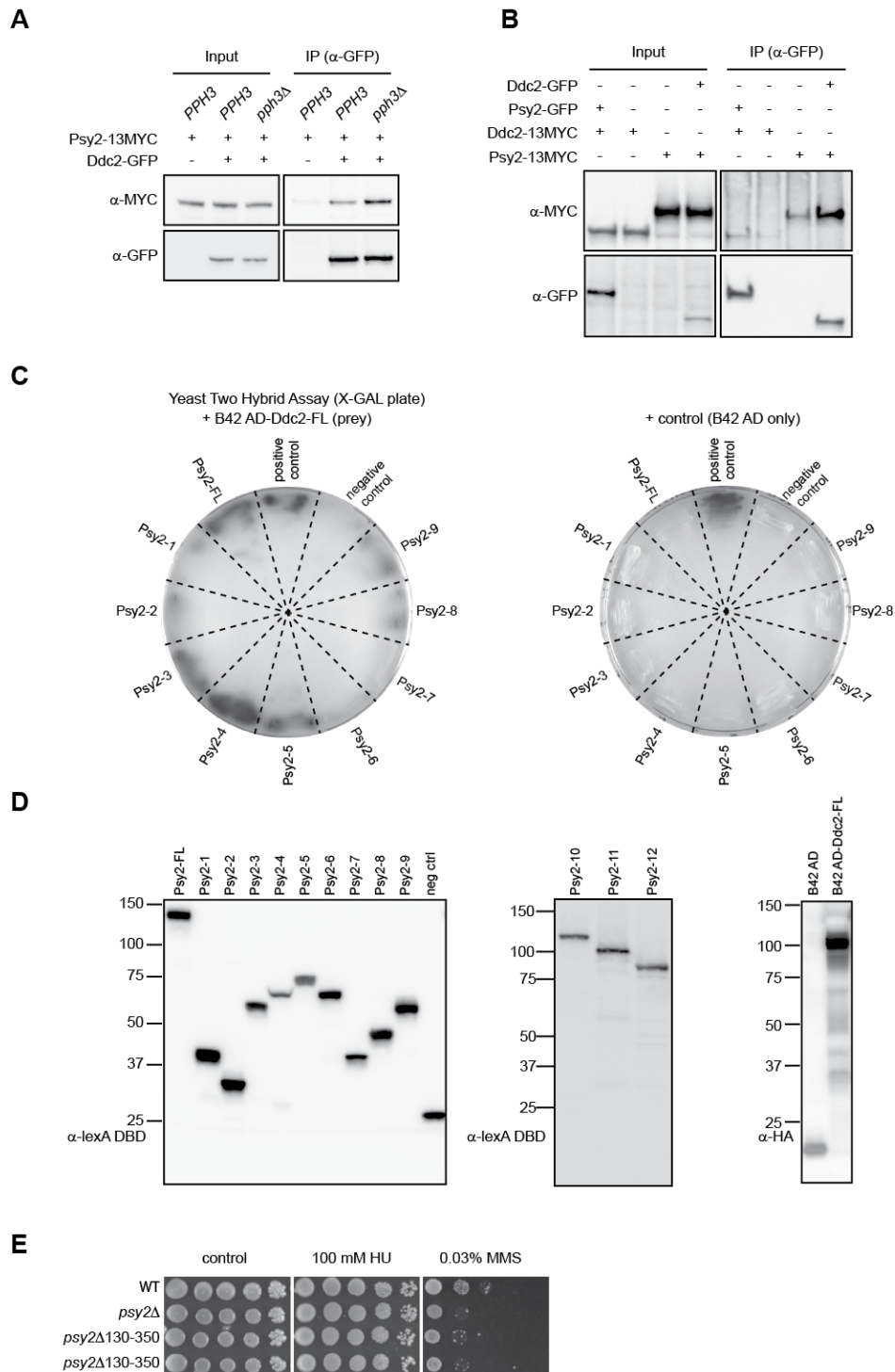


Figure S2.6. Ddc2-GFP and Psy2-MYC interaction does not require Pph3, and is detected when tags are swapped and in Y2H experiments; Related to Figure 2.5. (A) Native extracts were prepared from cycling *Psy2-13MYC* (GA-7798), *Psy2-13MYC DDC2-GFP* (GA-7824) and *Psy2-13MYC DDC2-GFP pph3 Δ* (GA-7939) cells, subjected to IP with anti-GFP and analysis by blotting with indicated antibodies. (B) Cells were treated as in (A). Strains used were *PSY2-13MYC* (GA-7972), *PSY2-13MYC DDC2-GFP* (GA-7975), *DDC2-13MYC* (GA-7337) and *DDC2-13MYC PSY2-GFP* (GA-8034). (C) Yeast two hybrid (Y2H) analysis between full length Ddc2 fused with the B42 transcription activation domain (B42 AD) and an HA-tag and Psy2 fragments fused with the lexA DNA binding domain (DBD) was performed by observing β -galactosidase expression on X-GAL plates. Negative control: empty lexA-DBD plasmid; positive control: LexA-DBD fused with B42-AD. (D) Yeast Two Hybrid construct expression. Cells were grown in 2% raffinose-containing selective medium to ensure plasmid retention and expression was induced with 2% galactose for 4h prior to denatured extract preparation and Western blot analysis with indicated antibodies. (E) Serial ten-fold dilution of cultures were plated on YPAD, YPAD + 100 mM HU and YPAD + 0.03% MMS. Isogenic strains used were GA-1981, GA-7391, GA-8821 and GA-8822. Relevant genotypes are indicated and listed in Table S2.5

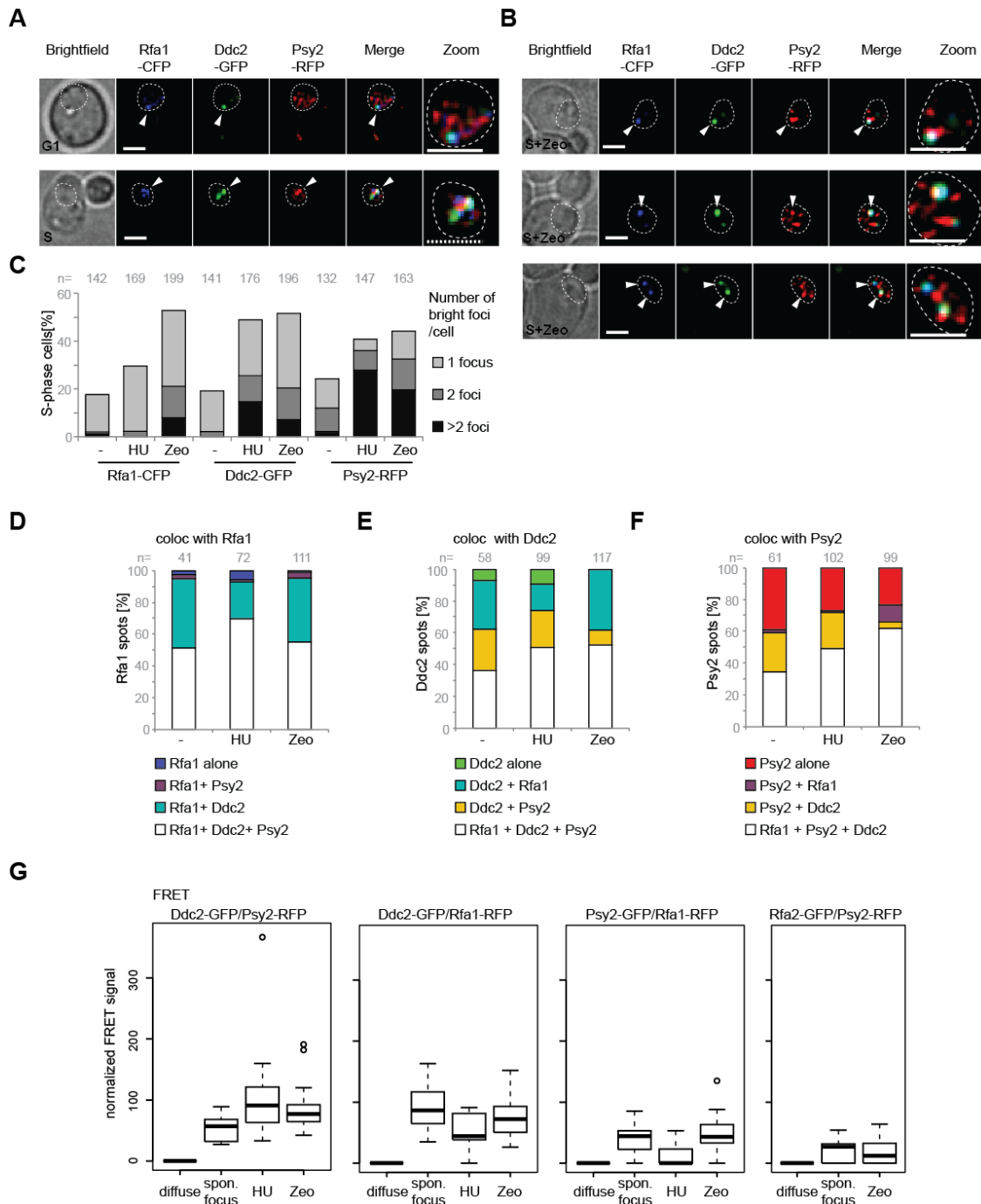


Figure S2.7. Ddc2 and Psy2 colocalize and show FRET at spontaneous and Zeocin induced foci; related to Figure 2.6. (A) Upper panel: Example of a G1-phase cell with a Ddc2/Rfa1 spot. Lower panel: Example of an S-phase cell with a spontaneous Rfa1/Ddc2/Psy2 focus. Strain used bears *RFA1-RFP DDC2-GFP PSY2-RFP* (GA-8695). Arrowheads indicate spots. Scale Bar = 2 μ m. White dashed line: outline of cell nucleus. (B) Example images of Zeocin-treated cells, which frequently leads to a few bright foci per cell. Upper and middle panel: example in which foci of all three fluorophores colocalize. Lower panel: Example of cell in which Ddc2 and Rfa1 colocalize, with partial colocalization of Rfa1/Ddc2/Psy2 in a second spot. The same strain was used as in (A). Arrowheads indicate foci. (C) Cells were treated +/- 0.2 M HU or 400 μ g/ml Zeocin for 1h prior to fixation. Bright spots per cell were quantified for S-phase cells. The same strain was used as in (A). (D) Cells were treated the same as in (C). Colocalization of Ddc2-GFP and/or Psy2-RFP spots with Rfa1-CFP spots was quantified. The same strain was used as in (A). (E) Colocalization of Rfa1-CFP and/or Psy2-RFP spots with Ddc2-GFP spots was quantified in the same experiment as (D). (F) Colocalization of Rfa1-CFP and/or Ddc2-GFP spots with Psy2-RFP spots was quantified in the same experiment as (D). (G) *DDC2-GFP PSY2-RFP* (GA-8656), *DDC2-GFP RFA1-RFP* (GA-8705), *PSY2-GFP RFA1-RFP* (GA-8702) and *RFA2-GFP PSY2-RFP* (GA-8676) cells were treated with 0.2M HU or 400 μ g/ml Zeocin or left untreated for 1 h before fixation. Fixed samples were analyzed for FRET-induced RFP signals at either bright GFP foci (“focus”, “HU”, “Zeo”) or in the nuclear background (“diffuse”).

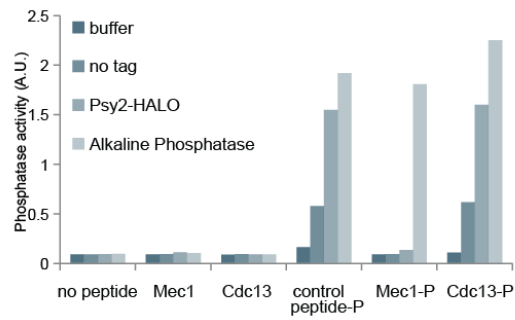
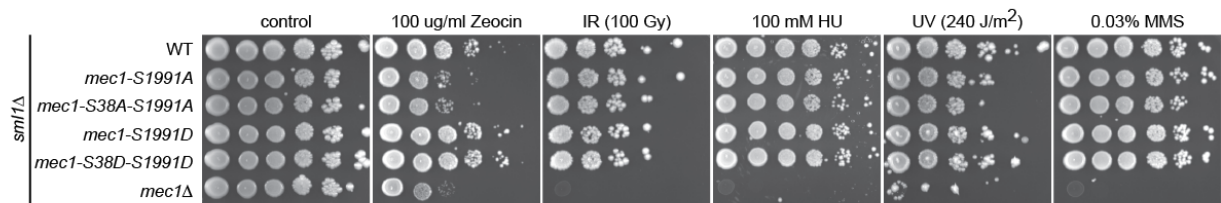
A**B**

Figure S2.8. Damage sensitivity of the non-phosphorylatable mutant *mec1-S1991A*; related to Figure 2.7. (A) Phosphatase Assay to test dephosphorylation of Mec1 serine 1991 and Cdc13 serine 306 by Psy2-Pph3. Psy2-Pph3 was purified from *PSY2-HALO* cells (GA-8179) and WT cells (GA-1981, “no tag”) served as a negative control. Purifications were incubated with indicated phosphopeptides for 60 min at 30 °C prior measurement of phosphatase activity by release of phosphate. Results are representative of two independent experiments. (B) Serial ten-fold dilutions of cultures were plated on YPAD, YPAD + 100 μ g/ml Zeocin, YPAD + 100 mM HU, YPAD + 0.03% MMS and on YPAD plates and subsequently treated with γ -irradiation (100 Gy) or UV light (240 J/m²). Relevant genotypes are indicated in the figure. Isogenic strains (see Table S2.5) used were: GA-4533, GA-8242, GA-8246, GA-8243, GA-8247 and GA-5286

SUPPLEMENTAL TABLES

Table S2.1: Genetic interaction data

see Appendix

Table S2.2: All quantified phosphopeptides

see Appendix

Table S2.3: Mec1-100 dependent phosphopeptides

see Appendix

Table S2.4: Selected SQ/TQ phosphopeptides

see Appendix

Table S2.6: Query strains and library used for EMAP

see Appendix

Table S2.5: Yeast strains and plasmids used in this study

<i>strain</i>	<i>genotype</i>	<i>source</i>
GA-181	<i>MATa, ade2-1, trp1-1, his3-11, -15, ura3-1, leu2-3, -112, can1-100 (W303)</i>	R. Rothstein
GA-338	<i>MATa, trp1, his3, ura3, leu2::(pLEU2-lexAop6)(EGY48)</i>	R. Brent
GA-1981	<i>MATa, ade2-1, trp1-1, his3-11, -15, ura3-1, leu2-3, -112, can1-100 (W303), RAD5+</i>	H.L. Klein
GA-1982	<i>MATa, ade2-1, trp1-1, his3-11, -15, ura3-1, leu2-3, -112, can1-100 (W303), RAD5+</i>	H.L. Klein
GA-2529	GA-181 with <i>mec1::HIS3, sml1::KanMX</i>	this study
GA-4533	GA-1981 with <i>sml1::HIS3</i>	this study
GA-4978	GA-1981 with <i>mec1-100::LEU2(HIS3)</i>	(Hegnauer et al., 2012)
GA-5286	GA-1981 with <i>mec1::TRP1, sml1::HIS3</i>	this study
GA-5321	GA-1981 with <i>rad24::TRP1</i>	(Hegnauer et al., 2012)
GA-5975	GA-1981 with <i>rad52::TRP1</i>	this study
GA-6022	<i>MATa, his3-D1, leu2D0, met15D0, ura3D0, rfa2::RFA2-GFP-HIS3 (BY4741)</i>	I.Filippuzzi
GA-6635	GA-1982 with <i>mec1-100::LEU2(HIS3) exo1::kanMX</i>	this study
GA-6636	GA-1982 with <i>mec1-100::LEU2(HIS3)</i>	this study
GA-6356	GA-1981 with <i>mec1-100::LEU2(HIS3) exo1::kanMX</i>	this study
GA-6410	GA-1981 with <i>mec1-100-R1907T::LEU2(HIS3)</i>	this study
GA-6412	GA-1981 with <i>mec1-100-D1127E::LEU2(HIS3)</i>	this study
GA-6416	GA-1981 with <i>mec1-100-E2296K::LEU2(HIS3)</i>	this study
GA-6418	GA-1981 with <i>mec1-100-T1607R::LEU2(HIS3)</i>	this study
GA-6422	GA-1981 with <i>mec1-100-N2301D::LEU2(HIS3)</i>	this study
GA-6466	GA-1981 with <i>mec1-100-E2286K::LEU2(HIS3)</i>	this study
GA-6468	GA-1981 with <i>mec1-100-R1809G::LEU2(HIS3)</i>	this study
GA-6470	GA-1981 with <i>mec1-100-D2104H::LEU2(HIS3)</i>	this study
GA-6472	GA-1981 with <i>mec1-100-Y1254D::LEU2(HIS3)</i>	this study
GA-6480	GA-1981 with <i>mec1-100-H1131Q::LEU2(HIS3)</i>	this study
GA-6510	GA-1981 with <i>mec1-100-Q1903E::LEU2(HIS3)</i>	this study
GA-6514	GA-1981 with <i>mec1-100-L2220F::LEU2(HIS3)</i>	this study
GA-6518	GA-1981 with <i>mec1-100-R1907T::LEU2(HIS3)</i>	this study
GA-6522	GA-1981 with <i>mec1-100-I2303M::LEU2(HIS3)</i>	this study
GA-6529	GA-1981 with <i>mec1-100-F2244L::LEU2(HIS3)</i>	this study
GA-6533	GA-1981 with <i>mec1-100-M2097I::LEU2(HIS3)</i>	this study
GA-6537	GA-1981 with <i>mec1-100-Q1903E::LEU2(HIS3)</i>	this study
GA-6539	GA-1981 with <i>mec1-100-E2296K::LEU2(HIS3)</i>	this study
GA-6572	GA-1981 with <i>mec1-100::LEU2(HIS3), pph3-A232P</i>	this study
GA-6575	GA-1981 with <i>mec1-100::LEU2(HIS3), psy2-E40*</i>	this study
GA-6577	GA-1981 with <i>mec1-100::LEU2(HIS3), psy2-E40*</i>	this study
GA-6582	GA-1981 with <i>mec1-100::natMX</i>	this study
GA-6583	GA-1982 with <i>mec1-100::natMX</i>	this study
GA-6596	GA-1981 with <i>mec1-100::LEU2(HIS3), psy2-E40*</i>	this study
GA-6598	GA-1981 with <i>mec1-100::LEU2(HIS3), pph3-S90G</i>	this study
GA-6600	GA-1981 with <i>mec1-100::LEU2(HIS3), pph3-A234T</i>	this study
GA-6601	GA-1981 with <i>mec1-100::LEU2(HIS3), pph3-T106P</i>	this study
GA-6603	GA-1981 with <i>mec1-100::LEU2(HIS3), pph3-L77W</i>	this study
GA-6605	GA-1981 with <i>mec1-100::LEU2(HIS3), pph3-Y121D</i>	this study
GA-6606	GA-1981 with <i>mec1-100::LEU2(HIS3), pph3-I157R</i>	this study
GA-6608	GA-1981 with <i>mec1-100::LEU2(HIS3), pph3-Q181*</i>	this study
GA-6610	GA-1981 with <i>mec1-100::LEU2(HIS3), psy2-L183*</i>	this study
GA-6769	GA-1981 with <i>mec1-100-T1612M::LEU2(HIS3)</i>	this study
GA-6826	GA-1981 with <i>mrc1::TRP1</i>	this study
GA-6828	GA-1981 with <i>mec1-100::natMX, mrc1::TRP1</i>	this study
GA-6912	GA-1981 with <i>tell1::URA3</i>	this study
GA-6913	GA-1981 with <i>tell1::URA3, mec1-100::natMX</i>	this study
GA-7049	GA-1981 with <i>pph3::HIS3</i>	this study
GA-7086	GA-1981 with <i>mec1-100::natMX, pph3::HIS3</i>	this study
GA-7209	GA-1981 with <i>mec1-100::natMX, rad24::TRP1</i>	this study
GA-7268	GA-1981 with <i>ddc2::DDC2-GFP-kanMX</i>	this study
GA-7273	GA-1981 with <i>ptc2::URA3</i>	this study
GA-7276	GA-1981 with <i>ptc3::HIS3, mec1-100::natMX</i>	this study
GA-7294	GA-1981 with <i>pph3::kanMX, sml1::HIS3</i>	this study
GA-7327	GA-1981 with <i>ddc2::DDC2-GFP-kanMX, mec1-100::natMX</i>	this study
GA-7329	GA-1981 with <i>ptc2::URA3, mec1-100::natMX</i>	this study
GA-7337	GA-1981 with <i>ddc2::DDC2-13MYC-URA3</i>	this study
GA-7353	GA-1981 with <i>mec1::LEU2-18MYC-MEC1</i>	this study

GA-7354	GA-1981 with <i>mec1::LEU2-18MYC-MEC1</i>	this study
GA-7355	GA-1981 with <i>mec1::LEU2-18MYC-MEC1</i>	this study
GA-7366	GA-1981 with <i>mec1::LEU2-18MYC-mec1-100::natMX</i>	this study
GA-7367	GA-1981 with <i>mec1::LEU2-18MYC-mec1-100::natMX</i>	this study
GA-7368	GA-1981 with <i>mec1::LEU2-18MYC-mec1-100::natMX</i>	this study
GA-7373	GA-1981 with <i>rad53::URA3, sml1::kanMX</i>	this study
GA-7375	GA-1981 with <i>rad53::URA3, sml1::kanMX, pph3::HIS3</i>	this study
GA-7377	GA-1981 with <i>rad53::URA3, sml1::kanMX, pph3::HIS3, mec1-100::natMX</i>	this study
GA-7383	GA-1981 with <i>psy4::hphMX</i>	this study
GA-7385	GA-1981 with <i>psy4::hphMX, mec1-100::natMX</i>	this study
GA-7391	GA-1981 with <i>psy2::URA3</i>	this study
GA-7393	GA-1981 with <i>psy2::URA3, mec1-100::natMX</i>	this study
GA-7395	GA-1981 with <i>psy2::URA3, mec1-100::natMX, pph3::HIS3</i>	this study
GA-7398	GA-1982 with <i>psy2::URA3, pph3::HIS3</i>	this study
GA-7401	GA-1981 with <i>rad53::URA3, sml1::kanMX, mec1-100::natMX</i>	this study
GA-7650	GA-1981 with <i>mec1::TRP1, sml1::HIS3, pph3::kanMX</i>	this study
GA-7656	GA-1981 with <i>rad53::URA3, sml1::kanMX, chk1::TRP1</i>	this study
GA-7657	GA-1982 with <i>rad53::URA3, sml1::kanMX, chk1::TRP1</i>	this study
GA-7658	GA-1981 with <i>rad53::URA3, sml1::kanMX, chk1::TRP1, pph3::HIS3</i>	this study
GA-7659	GA-1982 with <i>rad53::URA3, sml1::kanMX, chk1::TRP1, pph3::HIS3</i>	this study
GA-7660	GA-1981 with <i>rad53::URA3, sml1::kanMX, chk1::TRP1, mec1-100::natMX</i>	this study
GA-7661	GA-1982 with <i>rad53::URA3, sml1::kanMX, chk1::TRP1, mec1-100::natMX</i>	this study
GA-7662	GA-1981 with <i>rad53::URA3, sml1::kanMX, chk1::TRP1, mec1-100::natMX, pph3::HIS3</i>	this study
GA-7663	GA-1982 with <i>rad53::URA3, sml1::kanMX, chk1::TRP1, mec1-100::natMX, pph3::HIS3</i>	this study
GA-7707	GA-1981 with <i>mec1::TRP1, tel1::URA3, sml1::HIS3, pph3::kanMX</i>	this study
GA-7708	GA-1982 with <i>mec1::TRP1, tel1::URA3, sml1::HIS3, pph3::kanMX</i>	this study
GA-7709	GA-1981 with <i>mec1::TRP1, rad53::URA3, sml1::kanMX</i>	this study
GA-7711	GA-1981 with <i>mec1::TRP1, rad53::URA3, sml1::kanMX, pph3::HIS3</i>	this study
GA-7724	GA-1981 with <i>mec1::TRP1, tel1::URA3, sml1::HIS3</i>	this study
GA-7725	GA-1982 with <i>mec1::TRP1, tel1::URA3, sml1::HIS3</i>	this study
GA-7732	GA-1981 with <i>tel1::URA3, pph3::HIS3</i>	this study
GA-7734	GA-1981 with <i>tel1::URA3, pph3::HIS3, mec1-100::natMX</i>	this study
GA-7799	GA-1981 with <i>psy2::PSY2-13MYC-URA3</i>	this study
GA-7824	GA-1981 with <i>ddc2::DDC2-GFP-kanMX, psy2::PSY2-13MYC-URA3</i>	this study
GA-7827	GA-1981 with <i>ddc2::DDC2-GFP-kanMX, psy2::PSY2-13MYC-URA3, mec1::TRP1, sml1::HIS3</i>	this study
GA-7835	GA-1981 with <i>ddc2::DDC2-GFP-kanMX, psy2::PSY2-13MYC-URA3, mec1-100::natMX</i>	this study
GA-7852	GA-1981 with <i>pph3::PPH3-13MYC-URA3</i>	this study
GA-7853	GA-1981 with <i>pph3::PPH3-13MYC-URA3</i>	this study
GA-7865	GA-1981 with <i>pph3::PPH3-3HA-URA3</i>	this study
GA-7907	GA-1981 with <i>ddc1::URA3</i>	this study
GA-7908	GA-1981 with <i>rrd1::HIS3</i>	this study
GA-7923	GA-1981 with <i>ptc2::PTC2-3PK-LEU2</i>	this study
GA-7929	GA-1981 with <i>rrd1::HIS3, mec1-100::natMX</i>	this study
GA-7932	GA-1981 with <i>rrd2::kanMX, mec1-100::natMX</i>	this study
GA-7935	GA-1981 with <i>oca1::URA3, mec1-100::natMX</i>	this study
GA-7939	GA-1981 with <i>DDC2-GFP-kanMX, psy2::PSY2-13MYC-URA3, pph3::HIS3</i>	this study
GA-7945	GA-1981 with <i>DDC2-GFP-kanMX, mec1-100::natMX, pph3::HIS3</i>	this study
GA-7953	GA-1981 with <i>tel1::URA3, ptc2::HIS3</i>	this study
GA-7955	GA-1981 with <i>tel1::URA3, ptc2::HIS3, mec1-100::natMX</i>	this study
GA-7964	GA-1981 with <i>mec1-100::natMX, ddc1::URA3</i>	this study
GA-7966	GA-1981 with <i>pph3::6HA-PPH3</i>	this study
GA-7967	GA-1981 with <i>pph3::6HA-PPH3</i>	this study
GA-7972	GA-1981 with <i>psy2::PSY2-13MYC-URA3, ptc2::PTC2-3PK-LEU2</i>	this study
GA-7975	GA-1981 with <i>psy2::PSY2-13MYC-URA3, ptc2::PTC2-3PK-LEU2, ddc2::DDC2-GFP-kanMX</i>	this study
GA-7977	GA-1981 with <i>ptc2::URA3, pph3::HIS3</i>	this study
GA-7979	GA-1981 with <i>ptc2::URA3, pph3::HIS3, mec1-100::natMX</i>	this study
GA-7981	GA-1981 with <i>rrd1::HIS3, pph3::HIS3</i>	this study
GA-7982	GA-1981 with <i>rrd1::HIS3, pph3::HIS3, mec1-100::natMX</i>	this study
GA-8021	GA-1982 with <i>psy2::PSY2-GFP-kanMX</i>	this study
GA-8033	GA-1981 with <i>psy2::PSY2-GFP-kanMX</i>	this study
GA-8034	GA-1981 with <i>psy2::PSY2-GFP-kanMX, ddc2::DDC2-13MYC-URA3</i>	this study

GA-8052	GA-1981 with <i>rrd1::HIS3, psy2::URA3</i>	this study
GA-8054	GA-1981 with <i>rrd1::HIS3, psy2::URA3, mec1-100::natMX</i>	this study
GA-8079	GA-1981 with <i>glc7-132, mec1-100::natMX</i>	this study
GA-8179	GA-1981 with <i>psy2::PSY2-TEV-HALO-kanMX</i>	this study
GA-8232	GA-1981 with <i>DDC2-GFP-kanMX, psy2::PSY2-13MYC-URA3, mec1-S1991A::natMX</i>	this study
GA-8242	GA-1981 with <i>mec1-S38A::natMX, sml1::HIS3</i>	this study
GA-8243	GA-1981 with <i>mec1-S38D::natMX, sml1::HIS3</i>	this study
GA-8246	GA-1981 with <i>mec1-S38A-S1991A::natMX, sml1::HIS3</i>	this study
GA-8247	GA-1981 with <i>mec1-S38D-S1991D::natMX, sml1::HIS3</i>	this study
GA-8338	GA-1981 with <i>mec1-S1991A::natMX</i>	this study
GA-8342	GA-1981 with <i>mec1-S1991D::natMX</i>	this study
GA-8396	GA-1981 with <i>rfa1-t11</i>	this study
GA-8484	GA-1981 with <i>ddc2::DDC2-GFP-kanMX, mec1-D2243E(kd1), sml1::kanMX</i>	this study
GA-8486	GA-1981 with <i>ddc2::DDC2-GFP-kanMX, rad53::URA3, sml1::HIS3</i>	this study
GA-8659	GA-1981 with <i>psy2::PSY2-RFP-URA3</i>	this study
GA-8676	GA-1981 with <i>psy2::PSY2-RFP-URA3, rfa2::RFA2-GFP-HIS3</i>	this study
GA-8687	GA-1981 with <i>rfa1::RFA1-RFP-HIS3</i>	this study
GA-8688	GA-1981 with <i>rfa1::RFA1-RFP-HIS3</i>	this study
GA-8694	GA-1981 with <i>rfa1::RFA1-eCFP-hphMX</i>	this study
GA-8695	GA-1981 with <i>psy2::PSY2-RFP-URA3, ddc2-DDC2-GFP-kanMX, rfa1::RFA1-eCFP-hphMX</i>	this study
GA-8702	GA-1981 with <i>rfa1::RFA1-RFP-HIS3, psy2::PSY2-GFP-kanMX</i>	this study
GA-8705	GA-1981 with <i>rfa1::RFA1-RFP-HIS3, ddc2::DDC2-GFP-kanMX</i>	this study
GA-8821	GA-1981 with <i>psy2Δ130-350</i>	this study
GA-8822	GA-1982 with <i>psy2Δ130-350</i>	this study
plasmid No.	plasmid name	source
#286	<i>pRS416</i>	(Mumberg et al., 1995)
#359	<i>pSH18-34</i>	(Golemis et al., 2011)
#361	<i>pSH17-4</i>	(Golemis et al., 2011)
#965	<i>pGAL-lexA</i>	(Bjergbaek et al., 2005)
#993	<i>pJG4-6</i>	(Golemis et al., 2011)
#2221	<i>pKU2-rfa1-t11</i>	(Soustelle et al., 2002)
#2745	<i>pGAL-EcoRI</i>	(Schar et al., 2004)
#2842	<i>pEG203+NLS</i>	this study
#3307	<i>pGAL-lexA-PSY2</i>	this study
#3308	<i>pJG4-6-DDC2</i>	this study
#3367	<i>Yeplac195+PPH3</i>	(O'Neill et al., 2007)
#3368	<i>Yeplac195+pph3-H112N</i>	(O'Neill et al., 2007)
#3493	<i>pcDNA3.1-GFP</i>	Antoine Peters
#3518	<i>pcDNA3.1-PP4R3A-GFP</i>	this study
#3525	<i>pDEST12.2-MYC-ATRIP</i>	this study
#3588	<i>pcDNA3.1-PP4R3B-GFP</i>	this study
#3592	<i>pGAL-lexA-PSY2-2(aa25-129)</i>	this study
#3593	<i>pGAL-lexA-PSY2-3(aa25-350)</i>	this study
#3594	<i>pGAL-lexA-PSY2-4(aa25-447)</i>	this study
#3595	<i>pGAL-lexA-PSY2-5(aa25-502)</i>	this study
#3616	<i>pEG203+NLS+PSY2</i>	this study
#3617	<i>pEG203+NLS+PSY2-1(aa1-129)</i>	this study
#3618	<i>pEG203+NLS+PSY2-2(aa25-129)</i>	this study
#3619	<i>pEG203+NLS+PSY2-3(aa25-350)</i>	this study
#3620	<i>pEG203+NLS+PSY2-4(aa25-447)</i>	this study
#3621	<i>pEG203+NLS+PSY2-5(aa-25-502)</i>	this study
#3622	<i>pEG203+NLS+PSY2-6(aa-334-720)</i>	this study
#3623	<i>pEG203+NLS+PSY2-7(aa560-720)</i>	this study
#3629	<i>pEG203+NLS+PSY2-8(aa130-350)</i>	this study
#3630	<i>pEG203+NLS+PSY2-9(aa560-end)</i>	this study
#3649	<i>pGAL-lexA-PSY2-10(Δ aa25-129)</i>	this study
#3650	<i>pGAL-lexA-PSY2-11(Δ aa130-350)</i>	this study
#3651	<i>pGAL-lexA-PSY2-12(Δ aa25-350)</i>	this study
#3563	<i>pGAL-lexA-PSY2-8(aa130-350)</i>	this study

SUPPLEMENTAL REFERENCES

- Bjergbaek, L., Cobb, J.A., Tsai-Pflugfelder, M., and Gasser, S.M. (2005). Mechanistically distinct roles for Sgs1p in checkpoint activation and replication fork maintenance. *EMBO J* *24*, 405-417.
- Bodenmiller, B., and Aebersold, R. (2010). Quantitative analysis of protein phosphorylation on a system-wide scale by mass spectrometry-based proteomics. *Methods Enzymol* *470*, 317-334.
- Chen, S.H., Albuquerque, C.P., Liang, J., Suhandynata, R.T., and Zhou, H. (2010). A proteome-wide analysis of kinase-substrate network in the DNA damage response. *J Biol Chem* *285*, 12803-12812.
- Collins, S.R., Roguev, A., and Krogan, N.J. (2010). Quantitative genetic interaction mapping using the E-MAP approach. *Methods Enzymol* *470*, 205-231.
- Collins, S.R., Schuldiner, M., Krogan, N.J., and Weissman, J.S. (2006). A strategy for extracting and analyzing large-scale quantitative epistatic interaction data. *Genome Biol* *7*, R63.
- Cox, J., and Mann, M. (2008). MaxQuant enables high peptide identification rates, individualized p.p.b.-range mass accuracies and proteome-wide protein quantification. *Nature biotechnology* *26*, 1367-1372.
- Feige, J.N., Sage, D., Wahli, W., Desvergne, B., and Gelman, L. (2005). PixFRET, an ImageJ plug-in for FRET calculation that can accommodate variations in spectral bleed-throughs. *Microscopy research and technique* *68*, 51-58.
- Golemis, E.A., Serebriiskii, I., Finley, R.L., Jr., Kolonin, M.G., Gyuris, J., and Brent, R. (2011). Interaction trap/two-hybrid system to identify interacting proteins. *Current protocols in cell biology / editorial board, Juan S. Bonifacino ... [et al.] Chapter 17*, Unit 17 13.
- Hegnauer, A.M., Hustedt, N., Shimada, K., Pike, B.L., Vogel, M., Amsler, P., Rubin, S.M., van Leeuwen, F., Guenole, A., van Attikum, H., *et al.* (2012). An N-terminal acidic region of Sgs1 interacts with Rpa70 and recruits Rad53 kinase to stalled forks. *EMBO J* *31*, 3768-3783.
- Mumberg, D., Muller, R., and Funk, M. (1995). Yeast vectors for the controlled expression of heterologous proteins in different genetic backgrounds. *Gene* *156*, 119-122.
- O'Neill, B.M., Szyjka, S.J., Lis, E.T., Bailey, A.O., Yates, J.R., 3rd, Aparicio, O.M., and Romesberg, F.E. (2007). Pph3-Psy2 is a phosphatase complex required for Rad53 dephosphorylation and replication fork restart during recovery from DNA damage. *Proc Natl Acad Sci U S A* *104*, 9290-9295.
- Paciotti, V., Clerici, M., Scotti, M., Lucchini, G., and Longhese, M.P. (2001). Characterization of *mec1* kinase-deficient mutants and of new hypomorphic *mec1* alleles impairing subsets of the DNA damage response pathway. *Mol Cell Biol* *21*, 3913-3925.
- Reid, R.J., Lisby, M., and Rothstein, R. (2002). Cloning-free genome alterations in *Saccharomyces cerevisiae* using adaptamer-mediated PCR. *Methods Enzymol* *350*, 258-277.
- Schar, P., Fasi, M., and Jessberger, R. (2004). SMC1 coordinates DNA double-strand break repair pathways. *Nucleic Acids Res* *32*, 3921-3929.
- Soustelle, C., Vedel, M., Kolodner, R., and Nicolas, A. (2002). Replication protein A is required for meiotic recombination in *Saccharomyces cerevisiae*. *Genetics* *161*, 535-547.

CHAPTER 3: CHARACTERIZATION OF *MEC1-100*, AN S-PHASE DEFECTIVE ALLELE OF *MEC1*

This chapter provides additional data, which is unpublished.

Nicole Hustedt planned all and performed most experiments, evaluated results, made figures and wrote the chapter. Heinz Gut performed structure modeling and analysis, Ragna Sack performed mass spectroscopy analyses and Kenji Shimada performed cell fractionation.

SUMMARY

In an attempt to understand the causes for the S-phase specific defect in *mec1-100*, which carries two point mutations that result in N1700S and F1179S, we further characterized this mutant. We show that both mutations are required for full *mec1-100* HU sensitivity. Ddc2-Mec1 interaction, enzymatic activity, Ddc2-Ddc2-oligomerization and chromatin association are not altered compared to the wild-type protein complex. When testing genetic interactions with other checkpoint proteins we did not find clear epistasis between any of these mutants and *mec1-100*. Rather most of the double mutants were additive, indicating that *mec1-100* phenotypes cannot be explained by loss of interaction with any of these factors. In a screen for spontaneous suppressor mutations, in addition to extragenic suppressors in *PSY2* or *PPH3* (Chapter 2), we identified 16 additional mutations in *mec1-100*, each of which suppresses *mec1-100* HU sensitivity (Chapter 2). Here, we characterize some of those intragenic suppressors further and find that a subset of mutations are completely dependent on Rad24 for suppression of lethality on HU, while others act independently of Rad24. Those dependent on Rad24 are surface mutations that may alter protein-protein interactions while the others are buried in the catalytic domain of a modeled Mec1 structure. Once actual structural data of Ddc2-Mec1 together with its activators is available, these data may help dissect Rad24-dependent Mec1 activation on a molecular level.

INTRODUCTION

Ddc2-Mec1 is a central player in the replication and DNA damage checkpoint. While DNA damage leads to cell cycle arrest in G1 or G2 phases, the replication checkpoint senses and signals stalled replication forks in S phase. Once activated, it slows down replication by inhibiting late origin firing, induces transcription of DNA repair genes and stabilizes stalled forks to prevent their disengagement (Chapter 1). Several proteins promote Mec1 activation *in vitro*, i. e., Dpb11, Ddc1 (both are recruited in a Rad24 dependent manner), and Dna2, and it was suggested that they act in a cell-cycle dependent manner (Kumar and Burgers, 2013; Navadgi-Patil and Burgers, 2011) (Chapter 1). The Mec1 activating function of all three proteins relies on bulky hydrophobic residues embedded in the unstructured N- or C-terminal tails. Point mutants of the critical residues were shown to impair Rad53 activation *in vivo*. The mediator proteins Rad9, Mrc1 and Sgs1 also facilitate Rad53 activation, but rather act downstream of Mec1 (Alcasabas et al., 2001; Bjergbaek et al., 2005; Sweeney et al., 2005) (Chapter 4), although Sgs1, through its helicase function, could also act upstream by providing single stranded DNA. Rad9 and Sgs1 were both shown to bind and recruit Rad53 after their phosphorylation by Mec1 (Sun et al., 1998; Sweeney et al., 2005) (Chapter 4). Similarly, *in vitro* experiments showed that Mrc1 stimulates Mec1-enzyme-Rad53-substrate interaction rather than enhancing Mec1 catalytic activity (Chen and Zhou, 2009). While Rad9 is important for the response to DNA damage which results in a cell cycle arrest in G1 or G2, before mitosis, Mrc1 and Sgs1 are localized at stalled replication forks and promote Rad53 activation in response to HU (Chapter 1). Interestingly, *mec1-100* shows strong synergistic lethality with a deletion of *SGS1* on HU (Cobb et al., 2003; Cobb et al., 2005), but not with a *sgs1-r1* mutant lacking the Rad53-recruiting domain (Chapter 4). It could be that lack of Mec1 activity in S phase might create structures at forks that need the Sgs1 helicase activity, rather than its checkpoint function, for their resolution.

Paciotti and colleagues reported the discovery of an S phase defective allele of Mec1, *mec1-100* (Paciotti et al., 2001). *mec1-100* cells show delayed Rad53 phosphorylation in S phase. In contrast, the DNA damage G2 checkpoint is intact and Rad53 phosphorylation in G2 phase shows similar kinetics in WT and *mec1-100* cells. *mec1-100* consists of two point mutations, one in the conserved FAT domain (N1700S) (Bosotti et al., 2000) and one N-terminal of the FAT domain (F1179S) (Figure 3.1). Both are located outside of the catalytic domain and in Chapter 2 we show that *mec1-100* catalytic activity measured in an *in vitro* assay in complex with Ddc2, is comparable to the wild-type Mec1-Ddc2 complex. Therefore the mechanism of how the two *mec1-100* mutations impair Mec1 function is unclear.

Here, we aimed at understanding the causes for the S phase specific defect of *mec1-100*. *MEC1+* and mutant cells were compared for several known features of Ddc1-Mec1 such as its oligomerization and association with chromatin and other proteins. Also, we analyzed some of the intragenic *mec1-100* suppressor mutations identified in Chapter 2 further and found that a subset of presumably surface exposed suppressors require Rad24 for the *mec1-100* survival on HU.

RESULTS AND DISCUSSION

BOTH F1179S AND N1700S MUTATIONS ARE REQUIRED FOR FULL *MEC1-100* PHENOTYPE

mecl-100 has two point mutations, F1179S, which is located at the end of a HEAT (Huntingtin, EF3, PP2A, TOR1) repeat stretch, and N1700S, which is located in the TPR (tetratricopeptide) repeat-forming FAT (FRAP, ATM, TRRAP) domain (Figure 3.1). Since no separation of these mutations had been reported, we created each mutation independently to ask whether either of the two mutations is dispensable for the *mecl-100* phenotype. Single *mecl-F1179S* and *mecl-N1700S* mutants were integrated in the *MEC1* locus under the native promoter. We found that *mecl-N1700S* cells did not show sensitivity to HU in this assay (Figure 3.2A). Cells expressing *mecl-F1179S* were HU sensitive, although less so than *mecl-100* cells. This shows that both mutations act in an additive manner and neither of the single mutation is sufficient for the full *mecl-100* phenotype. Both *mecl-100*-mutated residues are conserved among yeast species, but not in higher eucaryotes (Figure 3.1). However, in human ATR a mutant (3A-ATR) has been described, which also shows S phase but not G2 checkpoint defects (Nam et al., 2011). The responsible mutations mapped to a region immediately N-terminal of the FAT domain and thus are located in between F1179 and N1700 in Mec1 (Figure 3.1). This suggests that this region mediates an important and possibly conserved function of ATR/Mec1 for the replication checkpoint.

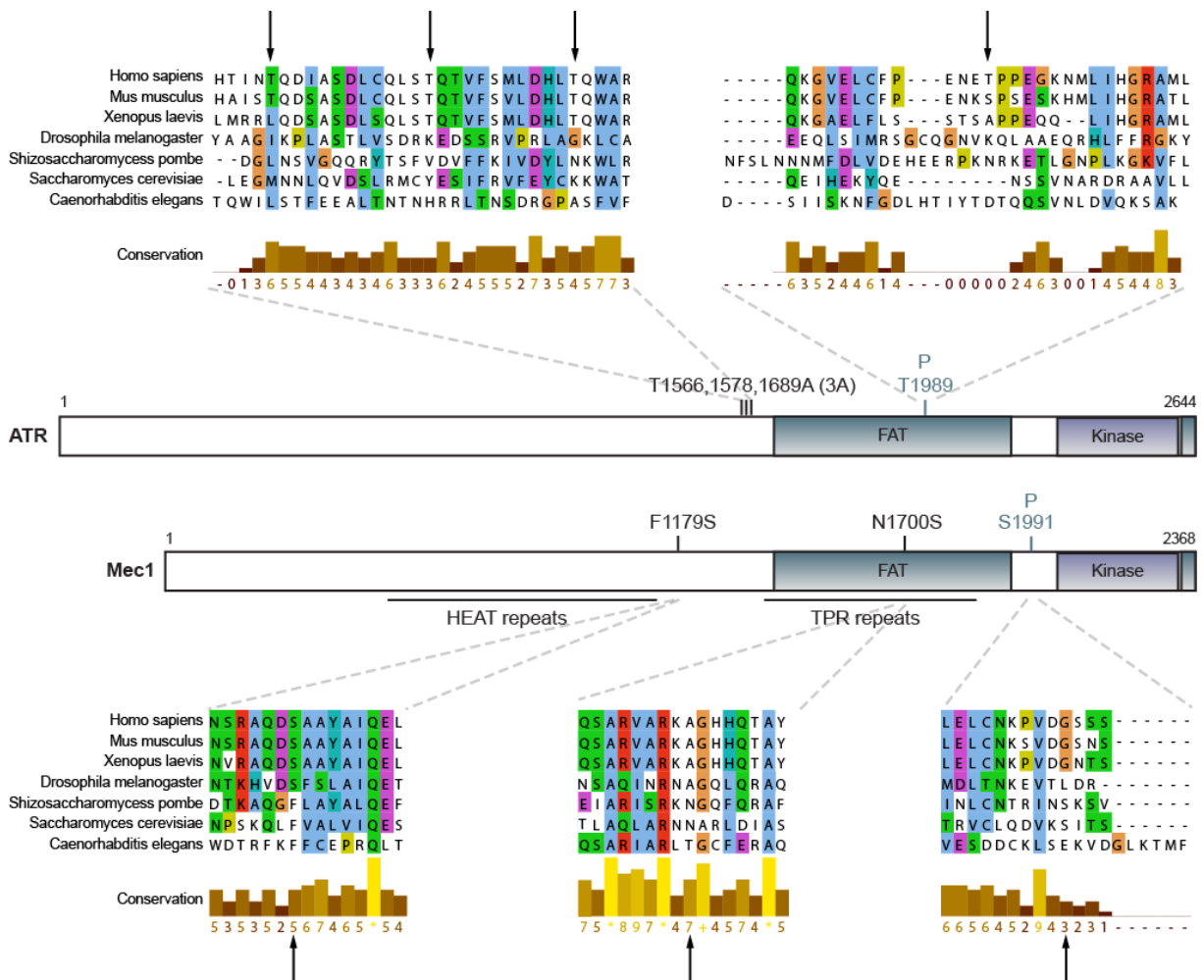


Figure 3.1: *Mec1-100* mutations are in conserved regions. Mec1 protein sequence was aligned with ATR sequences from indicated species using ClustalW and Jalview to visualize the alignment. Residues were colored according to ClustalX standard. Shown are alignment sections around *mecl-100* mutations, 3A-ATR mutations and phosphorylated residues (ATR T1989 and Mec1 S1991; see Chapter 2). Relevant residues are marked with arrows.

DDC2-MEC1 OLIGOMERIZATION IS NOT IMPAIRED IN *MEC1-100* CELLS

TPR and HEAT repeats are often involved in protein-protein interactions or oligomerization (Andrade et al., 2001). Indeed, Mec1-Ddc2 and ATR-ATRIP were shown to oligomerize, although the size of the resulting oligomer, as well as the function of oligomerization is still unclear (Chapter 1). Ddc2 contains a predicted coiled coil domain (Figure 2.1B), that could also oligomerize. Consistently, it has been shown that both ATRIP and ATR contribute to oligomerization (Ball and Cortez, 2005). To test whether oligomerization of Mec1-Ddc2 is impaired in *mec1-100* cells, we created diploid yeast strains that had one allele of *DDC2* fused with a GFP and the second fused with a triple HA tag. Immunoprecipitation (IP) with anti-GFP antibody following HU treatment showed efficient recovery of Ddc2-HA from both WT and *mec1-100* cells to the same extent (Figure 3.2D). Thus, *mec1-100* is proficient for oligomerization in this assay. We note, however, that much less Ddc2-HA was recovered when the IP was performed from *mec1Δ* cells, indicating that Mec1 contributes to oligomerization in agreement with previous studies on ATR-ATRIP (Ball and Cortez, 2005). Even though the mutated residues of *mec1-100* are not located in the kinase domain, they might nonetheless reduce enzymatic activity of Mec1. In Chapter 2 we show that Mec1⁺ and *mec1-100* have comparable enzymatic activity on an Sgs1 target peptide *in vitro*, when recovered in an immunoprecipitate with Ddc2 (Figure S2.1A). Moreover, The Mec1-Ddc2 interaction was not affected by the mutation (Figure. 2.5B) and previous studies reported that both Mec1-Ddc2 and *mec1-100*-Ddc2 localize to stalled replication forks in a similar manner as revealed by chromatin immunoprecipitation and Ddc2 focus formation (Cobb et al., 2005; Tercero et al., 2003). Thus, we did not find any evidence that *mec1-100* defects are caused by reduced enzymatic activity, Ddc2 interaction, oligomerization or defective localization.

MEC1-100 IS ADDITIVE WITH OTHER CHECKPOINT MUTANTS

We then hypothesized that the mutated region might constitute a binding platform for another factor important for Mec1 *in vivo* activity. We first addressed this question using a genetic approach. If the *mec1-100* mutations disrupted a specific protein-protein interaction that is crucial for *mec1-100 in vivo* activity, mutation of this factor should be epistatic with *mec1-100*. Therefore we tested genetic interactions of *mec1-100* with several candidates that are known to either activate Mec1 or mediate Rad53 activation just downstream of Mec1 in the checkpoint pathway and thus might be Mec1 binding partners. Dpb11, Ddc1 and Dna2 were shown to enhance Mec1 catalytic activity *in vitro* through critical residues in their N- or C-terminal unstructured tails (Kumar and Burgers, 2013; Navadgi-Patil and Burgers, 2009; Navadgi-Patil et al., 2011). Mutation of these residues also affected Mec1 activation *in vivo*. Thus, we considered Dpb11, Ddc1 and Dna2 as good candidates for upstream activators that might directly bind to Ddc2-Mec1. Dpb11 and Ddc1 are both recruited in a Rad24-dependent manner; therefore *rad24Δ* affects Mec1 activation through both proteins. Other than kinase activation, a protein-protein interaction could serve to bridge between Mec1 and one or several of its substrates. Mrc1, Sgs1 and Rad9 can recruit Rad53 for phosphorylation by Mec1 (Chapter 1). Thus, loss of a potential protein-protein interaction between Mec1 and Rad9, Sgs1 or Mrc1 could result in Rad53 activation defects. Additional checkpoint mutants that rather act in parallel to the Mec1-Rad53 checkpoint branch (i.e. *tell1Δ* and *chk1Δ*) were also included, although we did not expect an epistatic genetic relationship between *tell1Δ* or *chk1Δ* and *mec1-100*.

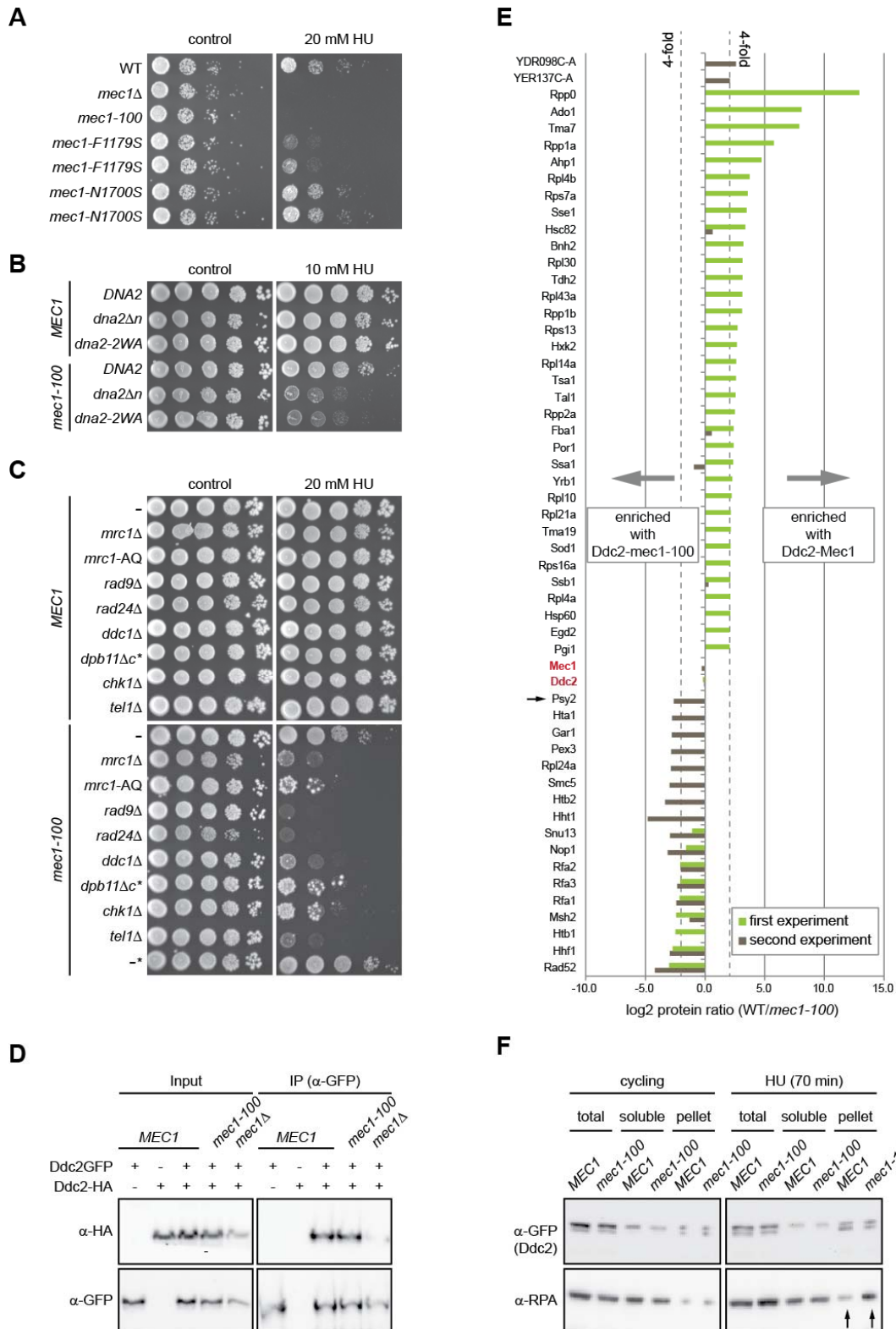
We created checkpoint protein double mutants with *mec1-100* and compared HU sensitivity of both single and double mutants (Figures 3.2B, C). As expected, mutations of checkpoint proteins that act in parallel to Mec1-Rad53 signaling (*chk1Δ* and *tell1Δ*) were found to be additive with *mec1-100* on HU. To assess the genetic interaction of *mec1-100* with the upstream activator Dna2, two mutants of *dna2* were used. A deletion of the N-terminus (*dna2Δn*) that contains two residues important for its function in Mec1 activation, as well as point mutations of the respective residues (*dna2-2WA*) (Kumar and Burgers, 2013), were additive with *mec1-100* rather than epistatic (Figure 3.1B). Similarly, *ddc1Δ* and a deletion of the C-terminal Mec1 activation domain in Dpb11, as well as *rad24Δ* were additive with *mec1-100*, rather than epistatic. Regarding the downstream factors, Mrc1 is not only involved in the replication checkpoint but also in normal replication. A separation of function mutant, *mrc1-AQ*, that is impaired for checkpoint signaling, but shows normal S phase progression and replication (Osborn and Elledge, 2003), was used in addition to *mrc1Δ*. However, both *mrc1* mutants were found additive with *mec1-100* rather than epistatic (Figure 3.2C). The same was observed when we combined *mec1-100* with *rad9Δ*. An Sgs1 mutant that disrupts Rad53 binding, did not show detectable HU sensitivity on its own, arguing that it is redundant with other factors (Chapter 4). Thus, it might be necessary to assess a genetic interaction between *sgs1-r1* and *mec1-100* in a sensitizing background, e.g. *rad24Δ* which was previously shown to be on a parallel pathway with Sgs1 for checkpoint activation (Bjergbaek et al., 2005)

This additive sensitivity of *mec1-100* with checkpoint mutants indicates that *mec1-100* and any of the checkpoint mutants are not epistatic. Thus, *mec1-100* defects cannot simply be explained by impaired interaction with one of these factors. Besides the canonical checkpoint proteins tested here there are other factors (e.g. the alternative clamp loader containing Ctf18, Ctf8 and Dcc1) involved in replication checkpoint activation or maintenance, although their exact role remains enigmatic (Crabbe et al., 2010). Further experiments would be needed to test whether *mec1-100* behaves epistatic with and consequently might impair checkpoint function of any of these factors.

ANALYSIS OF MEC1/MEC1-100 DIFFERENTIALLY INTERACTING PROTEINS IDENTIFIED EXCLUSIVELY FACTORS WITH INCREASED BINDING TO MEC1-100

None of the canonical checkpoint proteins was epistatic with *mec1-100*. Thus, we reasoned that an unknown factor might bind the regulatory region spanning F1179 and N1700 and that this interaction would be impaired when the two residues were mutated. To identify this unrevealed factor we first tried a proteomics approach. We immunoprecipitated Mec1-Ddc2 and *mec1-100*-Ddc2 complexes after HU treatment and identified co-precipitating proteins by mass spectrometry. Protein abundance ratios (Mec1/*mec1-100*) were calculated. Figure 3.2E shows protein abundance ratios for all differentially interacting proteins that were at least four times enriched with either WT Mec1-Ddc2 or *mec1-100*-Ddc2 ($\log_2 \geq 2$ or $\log_2 \leq -2$, respectively). Table 3.3 shows a full list of all co-precipitating proteins. We did not detect any proteins that were reproducibly enriched in WT Mec1-Ddc2 pull-down in two independent experiments. However, we found several proteins reproducibly enriched with mutant *mec1-100*-Ddc2. Among them were all three RPA subunits (Rfa1, Rfa2, Rfa3), Rad52 and Histone H4. All of these bind to DNA, and since we did not digest DNA with nucleases prior IP we cannot rule out that proteins were co-precipitated due to unspecific DNA binding. In fact, in Figure 2.5A we show that most of the Ddc2-RPA interaction is lost when extracts are pretreated with benzonase/RNaseA. Impaired replication fork stabilization in *mec1-100* cells could result in a higher level of ssDNA, thus leading to elevated RPA accumulation on DNA, which might be nonspecifically pulled down together with *mec1-100*-Ddc2.

Importantly, in one of the two experiments we identified Psy2 (Figure 3.2E, arrow), confirming the interaction described in Chapter 2. Here, Psy2 was found enriched with *mec1-100*-Ddc2 compared to *Mec1*⁺-Ddc2. This enrichment with *mec1-100*, however, was not reproduced by IP and subsequent Western blotting (Chapter 2).



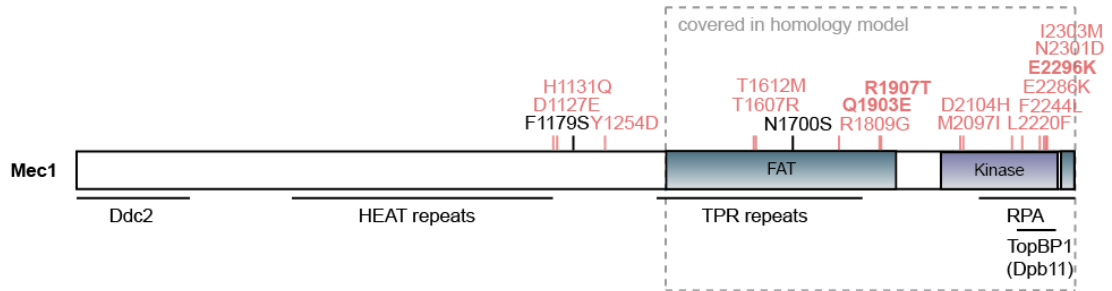
To test whether *mec1-100* cells generally showed higher levels of RPA accumulation on DNA, we isolated chromatin fractions from HU-treated WT and *mec1-100* cells and analyzed them by

western blotting. While Ddc2 association with Chromatin was comparable in WT and mutant cells, RPA was more enriched in chromatin fractions of mutant cells compared to WT after HU treatment (Figure 3.2F, arrows). We note that in this experiment we detected two Ddc2-GFP species by Western blot, with the faster migrating form being absent from non-chromatin bound fractions. These two species were not detected in other extracts of Ddc2-GFP expressing cells (Figure 2.5). It is unclear whether one of them is a degradation product due to the spheroplast preparation or the result of a posttranslational modification. Indeed, Ddc2 was shown to be phosphorylated in a Mec1-dependent manner after MMS or UV treatment but also in an unperturbed S phase (Paciotti et al., 2000). In our Ddc2 IP combined with mass spectrometry experiments (Figure 3.2E) we found multiple phosphorylation sites in Ddc2 (serine 10, serine 11, threonine 159, serine 162, serine 163, and serine 182), although we did not detect any Ddc2 phosphopeptide in our phosphoproteomics experiment (Chapter 2).

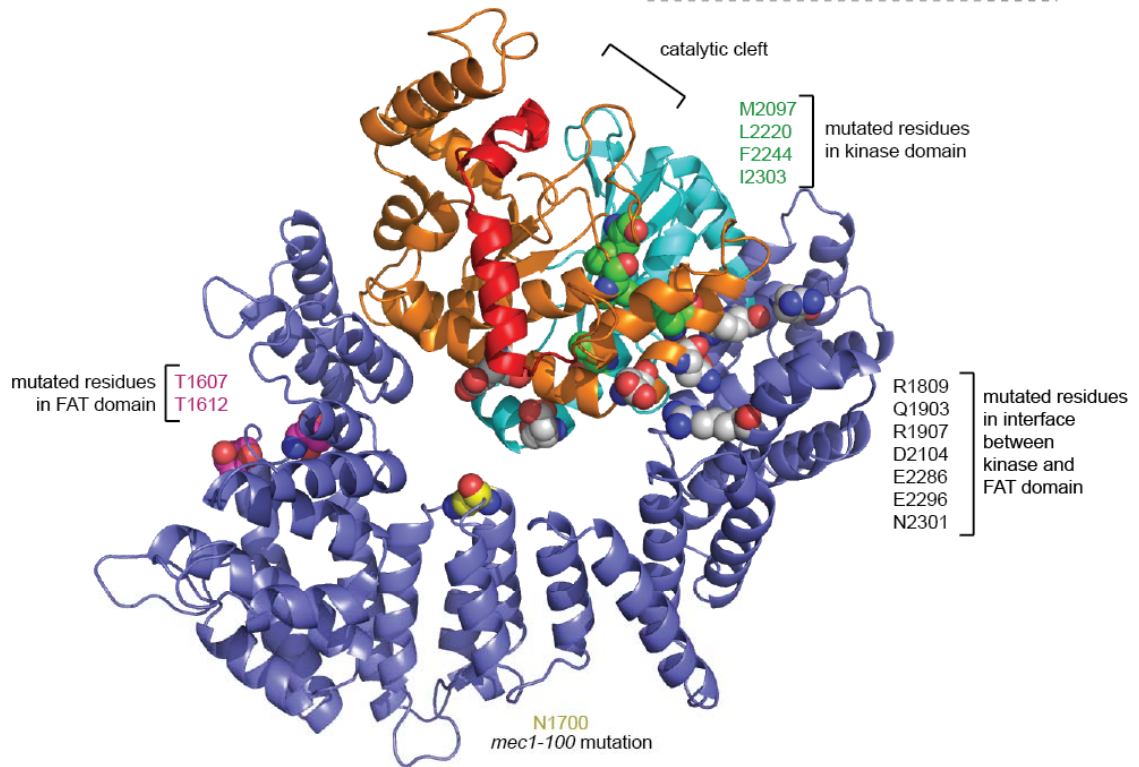
From these experiments we cannot absolutely rule out that *mec1-100*-Ddc2 indeed binds more RPA than WT Mec1-Ddc2 directly, which might somehow impair *mec1-100* S-phase function. Yet, this seems unlikely, since the major site of RPA interaction in Mec1-Ddc2 was mapped to the N-terminus of Ddc2 (Ball et al., 2005), rather than the mutated domain of *mec1-100*. Although the C-terminus of Mec1 might contribute to RPA interaction (Nakada et al., 2005), *mec1-100* mutations are far from the C-terminus. Instead, it is more conceivable that *mec1-100* cells accumulate more ssDNA after HU treatment, reflecting an inability of *mec1-100* to preserve replication fork structures. This would result in enhanced RPA binding to chromatin and elevated RPA levels in *mec1-100*-Ddc2 IPs due to co-precipitation of chromatin. Thus, we hypothesize that the elevated coprecipitation of RPA with *mec1-100*-Ddc2 is a consequence rather than a cause of the *mec1-100* defects. Similarly, elevated Rad52 coprecipitation could reflect a stronger association of Rad52 with chromatin broken forks in *mec1-100* cells. It is currently unclear why more histones were pulled down with *mec1-100*-Ddc2, even though Ddc2 association with chromatin was not altered in WT compared to mutant cells (Figure 3.2F). This result could, however, reflect a different chromatin structure. Indeed, several chromatin remodeling complexes were shown to be phosphorylated by Mec1 (Chapter 2). Further experiments, especially IPs combined with prior treatment of extracts with benzonase/RNase would be needed to differentiate between protein-protein interactions and co-precipitation due to protein-DNA interactions.

Figure 3.2: Characterization of *mec1-100* (A) Serial 10-fold dilutions of cultures were plated on YPAD \pm 20 mM HU. Relevant genotypes are indicated in the figure. Strains used were GA-1981, GA-2529, GA-4978, GA-6330, GA-6331, GA-6332 and GA-6333. (B) Cells were treated as in (A). Strains used were GA-8605, GA-8606, GA-8607, GA-8608, GA-8609 and GA-8610. (C) Serial 10-fold dilutions of cultures were plated on YPAD \pm 10 mM HU. Relevant genotypes are indicated in the figure. Asterisk indicates *rad5-535* background. Strains used were GA-1981, GA-6826, GA-6574, GA-6625, GA-5321, GA-7907, GA-7795, GA-7062, GA-6912, GA-6582, GA-6828, GA-6663, GA-6624, GA-7209, GA-7964, GA-7764, 7064, GA-7064, GA-6913 and GA-2474. (D) Exponentially growing cultures were treated with 0.2 M HU for 1h. Native extracts were subjected to IP by α -GFP and blots were probed with indicated antibodies. Diploid strains used were GA-7760, GA-7668, GA-7761, GA-7762 and GA-7763. (E) Exponentially growing cultures of Ddc2-GFP (GA-7268) and Ddc2-GFP *mec1-100* (GA-7327) were treated with 0.2 M HU for 1h. Native extracts were subjected to IP by α -GFP and isolated protein complexes were digested with Trypsin for LC-MS/MS analysis. Shown are protein abundance ratios (WT/*mec1-100*) of differentially ($\log_2 \leq -2$ or $\log_2 \geq 2$) interacting proteins, in addition to ratios for Ddc2 and Mec1 as controls (red). Arrow indicates Psy2, which was found as an interactor with *mec1-100* in one of the two experiments. (F) Ddc2-GFP (GA-7268) and Ddc2-GFP *mec1-100* (GA-7327) cells were untreated or treated with 0.2 M HU for 70 min prior cell fractionation. Samples of cells fractions were subjected to western blot analysis using indicated antibodies. total: total protein extracts; pellet: Chromatin - bound fraction; soluble: non-Chromatin bound, soluble fraction. Arrows indicate Rfa1 bands to compare (see text).

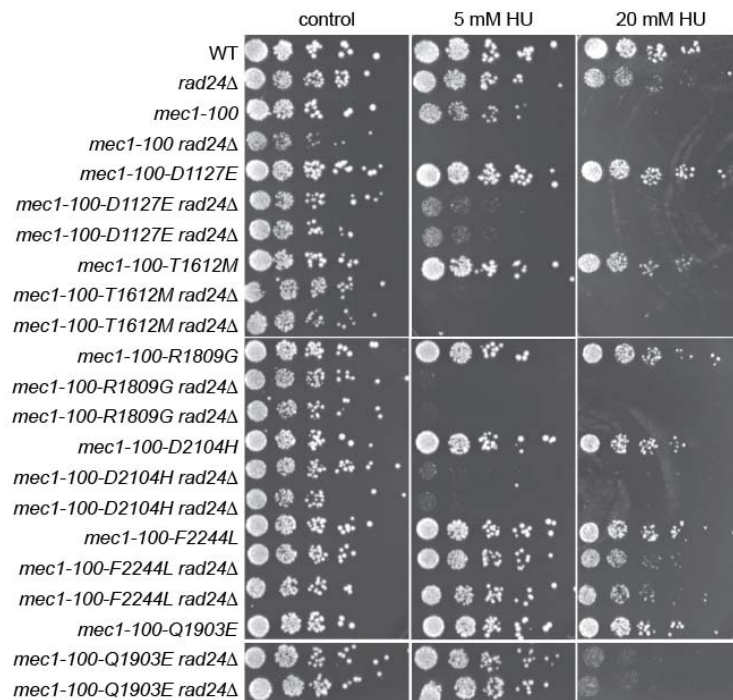
A



B



C



SOME, BUT NOT ALL MEC1-100 INTRAGENIC SUPPRESSORS REQUIRE RAD24 FOR SUPPRESSION OF HU SENSITIVITY

To identify novel, potentially regulating, factors in the Mec1 checkpoint pathway we conducted a screen in the *mec1-100* background for spontaneous suppressors of HU sensitivity (Figure 2.1AB). We found both additional mutations in *mec1-100* (intragenic suppressors) and mutations in Psy2-Pph3 (extragenic suppressors). For intragenic suppressor mutations outside the catalytic domain we used secondary structure prediction to locate the mutated residues relative to the alpha helices of HEAT and TPR repeats or non-repeat helices. Both D1127 and H1131 reside in loop regions between helices and should not affect the overall protein fold. In contrast, Y1254 is at the beginning of a helix and the impact of its mutation is unclear. For mutations in FAT and kinase domains a homology model was built based on the resolved structure of the PI3K-like kinase mTOR (Yang et al., 2013). T1612 and T1607 were located in turns between helices of TPR repeats in the FAT domain, and therefore unlikely disturb the fold, similar to N1700. Rather, these residues could be involved in protein-protein interactions. The FAT domain wraps around the kinase domain and although N1700 is located far away from the kinase domain in this model, small differences in the actual Mec1 structure could result in a different curvature of the FAT domain. Thus, we cannot absolutely exclude that N1700 might be involved in intra-molecular interactions with residues in the kinase domain. M2097, L2220 and I2303 residues were found to be buried in the helical core that attaches N-terminal and C-terminal kinase lobe and therefore might impact folding or protein stability (Figure 3.3A). It is noteworthy that F2244, which is highly conserved, resides at the beginning of the activation loop and could position both catalytic and activation loops, thereby influencing kinase activity. Importantly, the neighboring residue, D2243, is mutated in an activity-dead allele of Mec1 (Paciotti et al., 2001). Another group of mutated residues (R1809G, Q1903, R1907, D2104, E2286, E2296 and N2301) is located at the interface between kinase and FAT domain, either on kinase or FAT domain. Some of them seem surface exposed (R1809, D2104), while the others might stabilize the position of the FAT relative to the kinase domain and therefore could influence enzymatic activity.

Figure 3.3: Some intragenic suppressors require RAD24 for HU sensitivity suppression. (A) Mec1 domain architecture with *mec1-100* mutations indicated in black and *mec1-100* suppressor mutations in red. Bold: mutations found twice independently. Box indicates region that is covered by homology model in (B). (B) Homology model of Mec1 kinase domain based on crystal structure of mTOR. dark blue: FAT domain, light blue: N-terminal kinase lobe; orange: C-terminal kinase lobe; red: FATC domain, pink: mutated residues located within FAT domain, yellow: *mec1-100* –mutated residue N1700, grey: mutated residues located in interface between kinase and FAT domain, green: mutated residues in kinase lobes. (C) Serial 5-fold dilutions of cultures were plated on YPAD, YPAD + 5 mM HU and YPAD + 20 mM HU. Relevant genotypes are indicated in the figure. Strains used were GA-1981, GA-5321, GA-6582, GA-7209, GA-6412, GA-7220, GA-7221, GA-6341, GA-7218, GA-7219, GA-6468, GA-7201, GA-7202, GA-6470, GA-7193, GA-7194, GA-6529, GA-7191, GA-7192, GA-6510, GA-7199 and GA-7200.

To see if the suppressors act through specific cofactors of Mec1-Ddc2, we further studied a subset of these intragenic suppressor mutations by genetic interactions. Mutations that are predicted to influence kinase activity (i.e. Q1903E and F2244L) and others that seem surface exposed and might be involved in protein-protein interactions (i.e. D1127E, T1612M, R1809G and D2104H) were used. We asked whether the suppression required Mec1 activation through the Rad24 pathway. Interestingly, in the absence of Rad24 some intragenic suppressors (T1612M, R1809G and D2104H) became as HU sensitive as the *mec1-100 rad24Δ* double mutant, indicating that Rad24 was absolutely required for their mechanism of suppression (Figure 3.3C). Others (D1127E and Q1903E) showed some residual suppression of *mec1-100* HU sensitivity in a *rad24Δ* background. Interestingly, F2244L was found to act independently of Rad24. It is reasonable to speculate that this residue would enhance Mec1 kinase activity independent of Rad24, thereby balancing *mec1-100* S phase defects. Further experiments, e.g. *in vitro* kinase assays with a *mec1-F2244L* single mutant would be required to test this hypothesis. Interestingly, several attempts to generate a *mec1-F2244L* single mutant failed, indicating that this mutation might result in cell lethality.

Table 3.1: Growth of *mec1-100* intragenic suppressors in combination with checkpoint mutants on HU.

	<i>rad24Δ</i>	<i>dpb11Δc</i>	<i>mrc1Δ</i>	<i>rad9Δ</i>	<i>tell1Δ</i>	<i>chk1Δ</i>	position of suppressor mutation
-	++++	++++	++++	++++	++++	++++	
<i>mec1-100</i>	-	++	-	-	-	++	
<i>mec1-100-D1127E</i>	++	+++	++	+++	++++	++++	unclear
<i>mec1-100-T1612M</i>	-	++	+	+	++++	++++	surface
<i>mec1-100-R1809G</i>	-	+++	++	++	++++	++++	surface
<i>mec1-100-Q1903E</i>	+++	++++	++	++++	++++	++++	buried
<i>mec1-100-D2104H</i>	-	+++	++	++	++++	++++	surface
<i>mec1-100-F2244L</i>	++++	++++	++	++++	++++	++++	buried

We further combined the selected subset of intragenic suppressors with other checkpoint mutants (i.e. *mrc1Δ*, *rad9Δ*, *dpb11Δc*, *tell1Δ*, *chk1Δ*) and tested their growth on HU by Drop Assays. The results are summarized in Table 3.1. Combination of the intragenic suppressors with *rad9Δ* or *dpb11Δc* showed a similar tendency as with *rad24Δ*, but the effects on HU sensitivity were not as strong. On the other hand, neither Tel1 nor Chk1 were required for the suppression of HU sensitivity, indicating that the mutations do not rely on signaling through Tel1 or Chk1. Interestingly, deletion of *Mrc1* rendered all suppressors slightly HU sensitive again, thus all of the suppressors require *Mrc1* for the full suppression. The strong dependency of some intragenic suppressors on Rad24 might indicate that they enhance Mec1 activation through Ddc1 and/or Dpb11 which are recruited in a Rad24-dependent manner (Chapter 1). Again, further *in vitro* assays are necessary to address this hypothesis. However, once there is actual structural data of the Ddc2-Mec1 complex available, possibly together with Mec1 activators Dna2, Ddc1 or Dpb11, these data on Mec1 mutations could help to elucidate the molecular mechanism of Mec1 activation.

EXPERIMENTAL PROCEDURES

YEAST STRAINS, DROP ASSAYS AND IMMUNOPRECIPITATION

Yeast strains used in this chapter are described in Table 3.2. Cells were cultured at 30°C in YPAD medium using standard procedures. Drop assays were performed as previously described (Hustedt and Shimada, 2014). IP experiments, mass spectrometry sample preparation and analysis were performed as described in Chapter 2. The identification and relative quantification of proteins was performed with Progenesis-LC (Nonlinear Dynamics Ltd) using Mascot 2.3.0.2 (Matrix Science) for databases search. Protein abundances were normalized to Ddc2 and Mec1 within Progenesis-LC. Finally data were exported to Excel and protein ratios were calculated from the normalized abundances.

CELL FRACTIONATION

Cells were centrifuged and resuspended in YPAD containing 1 M sorbitol, 0.05M EDTA-KOH, 10mM DTT, 20mM K-phosphate pH7.0. 0.2 M HU was further supplemented to the buffer for HU-treated cells. Cells were spheroplasted with zymolyase (0.4 mg/ml) and lyticase (50 U/ml) for 15 min at 30°C. Spheroplasts were recovered by centrifugation and washed once in wash buffer (50mM HEPES-KOH pH7.5, 20mM KCl, 2mM K-EDTA, 0.125 mM spermidine, 0.05 mM spermine, 0.4 M sorbitol, 1% Trasyolol, and 0.5 mM PMSF). A total of 100 µl of the cell pellet was resuspended in 500 µl of EB buffer (100 mM KCl, 50 mM HEPES-KOH pH7.5, 2.5 mM MgCl₂, 1% Trasyolol and COMPLETE protease inhibitors (Roche)) and cells were lysed on ice by adding a final concentration of 0.25% TritonX-100. An aliquot was kept as total protein extract. The remaining cells were sedimented through 30% sucrose in EB buffer. Supernatant was kept as non-chromatin bound fraction. The cell pellet (chromatin bound fraction) was resuspended in EB buffer with 0.25% Triton X-100. Total protein extracts, non-chromatin bound and chromatin bound fractions were analyzed by western blotting.

HOMOLOGY MODELING OF MEC1

The amino acid sequence of *S. cerevisiae* Mec1 (Uniprot P38111, residues 1400-2368) was submitted to the HHPRED server for homology detection and structure prediction (Hildebrand et al., 2009). The structure of *H. sapiens* mTOR (PDB 4JSN) (Yang et al., 2013) was the top hit resulting in very high scores (Score=1498, E-value=1.9e-145, 23% sequence identity). The HHPRED Mec1 mTOR sequence alignment was sent to the HHPRED MODELLER pipeline for homology modeling. Structural figures were prepared using PyMOL (www.pymol.org).

Table 3.2: Yeast strain used in this chapter

strain	genotype	source
GA-181	<i>MATa, ade2-1, trp1-1, his3-11, -15, ura3-1, leu2-3, -112, can1-100 (W303)</i>	R. Rothstein
GA-1981	<i>MATa, ade2-1, trp1-1, his3-11, -15, ura3-1, leu2-3, -112, can1-100 (W303), RAD5+</i>	H.L. Klein
GA-1982	<i>MATα, ade2-1, trp1-1, his3-11, -15, ura3-1, leu2-3, -112, can1-100 (W303), RAD5+</i>	H.L. Klein
GA-2474	GA-181 with <i>mec1-100::LEU2(HIS3)</i>	(Cobb et al., 2005)
GA-2529	GA-181 with <i>mec1::HIS3, sml1::KanMX</i>	this study
GA-4978	GA-1981 with <i>mec1-100::LEU2(HIS3)</i>	(Hegnauer et al., 2012)
GA-5321	GA-1981 with <i>rad24::TRP1</i>	(Hegnauer et al., 2012)
GA-6330	GA-1981 with <i>mec1-F1179S sml1::HIS3</i>	this study
GA-6331	GA-1981 with <i>mec1-F1179S sml1::HIS3</i>	this study
GA-6332	GA-1981 with <i>mec1-N1700S sml1::HIS3</i>	this study
GA-6333	GA-1981 with <i>mec1-F1179S sml1::HIS3</i>	this study
GA-6341	GA-1982 with <i>mec1-100-T1612M::LEU2(HIS3)</i>	this study
GA-6412	GA-1981 with <i>mec1-100-D1127E::LEU2(HIS3)</i>	this study
GA-6468	GA-1981 with <i>mec1-100-R1809G::LEU2(HIS3)</i>	this study
GA-6470	GA-1981 with <i>mec1-100-D2104H::LEU2(HIS3)</i>	this study
GA-6510	GA-1981 with <i>mec1-100-Q1903E::LEU2(HIS3)</i>	this study
GA-6529	GA-1981 with <i>mec1-100-F2244L::LEU2(HIS3)</i>	this study
GA-6574	GA-1981 with <i>mrc1::HIS3, pRS405-mrc1-AQ (LEU2) URA3::GPD-TK (PP676)</i>	P. Pasero
GA-6582	GA-1981 with <i>mec1-100::natMX</i>	this study
GA-6624	GA-1981 with <i>mec1-100::natMX, rad9::TRP1</i>	this study
GA-6625	GA-1981 with <i>rad9::TRP1</i>	this study
GA-6663	GA-1981 with <i>mec1-100::natMX, mrc1::HIS3, pRS405-mrc1-AQ (LEU2) URA3::GPD-TK</i>	this study
GA-6723	GA-1981 with <i>mec1-100-D1127E::LEU2(HIS3), rad9::TRP1</i>	this study
GA-6725	GA-1981 with <i>mec1-100-T1612M::LEU2(HIS3), rad9::TRP1</i>	this study
GA-6727	GA-1981 with <i>mec1-100-R1809G::LEU2(HIS3), rad9::TRP1</i>	this study
GA-6730	GA-1981 with <i>mec1-100-F2244L::LEU2(HIS3), rad9::TRP1</i>	this study
GA-6732	GA-1981 with <i>mec1-100-D2104H::LEU2(HIS3), rad9::TRP1</i>	this study
GA-6815	GA-1981 with <i>mec1-100-D1127E::LEU2(HIS3), mrc1::TRP</i>	this study
GA-6817	GA-1981 with <i>mec1-100-T1612M::LEU2(HIS3), mrc1::TRP</i>	this study
GA-6819	GA-1981 with <i>mec1-100-D2104H::LEU2(HIS3), mrc1::TRP</i>	this study
GA-6821	GA-1981 with <i>mec1-100-R1809G::LEU2(HIS3), mrc1::TRP</i>	this study
GA-6823	GA-1981 with <i>mec1-100-F2244L::LEU2(HIS3), mrc1::TRP</i>	this study
GA-6826	GA-1981 with <i>mrc1::TRP</i>	this study
GA-6828	GA-1981 with <i>mec1-100::natMX, mrc1::TRP</i>	this study
GA-6912	GA-1981 with <i>tel1::URA</i>	this study
GA-6913	GA-1981 with <i>mec1-100::natMX, tel1::URA</i>	this study
GA-6920	GA-1981 with <i>mec1-100-D1127E::LEU2(HIS3), tel1::URA</i>	this study
GA-6922	GA-1981 with <i>mec1-100-T1612M::LEU2(HIS3), tel1::URA</i>	this study
GA-6924	GA-1981 with <i>mec1-100-R1809G::LEU2(HIS3), tel1::URA</i>	this study
GA-6926	GA-1981 with <i>mec1-100-D2104H::LEU2(HIS3), tel1::URA</i>	this study
GA-6928	GA-1981 with <i>mec1-100-F2244L::LEU2(HIS3), tel1::URA</i>	this study
GA-7062	GA-1981 with <i>chk1::TRP1</i>	this study
GA-7064	GA-1981 with <i>mec1-100::natMX, chk1::TRP1</i>	this study
GA-7069	GA-1981 with <i>mec1-100-D1127E::LEU2(HIS3), chk1::TRP1</i>	this study
GA-7071	GA-1981 with <i>mec1-100-T1612M::LEU2(HIS3), chk1::TRP1</i>	this study
GA-7073	GA-1981 with <i>mec1-100-R1809G::LEU2(HIS3), chk1::TRP1</i>	this study
GA-7075	GA-1981 with <i>mec1-100-D2104H::LEU2(HIS3), chk1::TRP1</i>	this study
GA-7077	GA-1981 with <i>mec1-100-F2244L::LEU2(HIS3), chk1::TRP1</i>	this study
GA-7183	GA-1981 with <i>mec1-100-Q1903E::LEU2(HIS3), mrc1::TRP</i>	this study
GA-7185	GA-1981 with <i>mec1-100-Q1903E::LEU2(HIS3), rad9::TRP1</i>	this study
GA-7187	GA-1981 with <i>mec1-100-Q1903E::LEU2(HIS3), chk1::TRP1</i>	this study
GA-7189	GA-1981 with <i>mec1-100-Q1903E::LEU2(HIS3), tel1::URA</i>	this study
GA-7191	GA-1981 with <i>mec1-100-F2244L::LEU2(HIS3), rad24::TRP1</i>	this study
GA-7192	GA-1982 with <i>mec1-100-F2244L::LEU2(HIS3), rad24::TRP1</i>	this study
GA-7193	GA-1981 with <i>mec1-100-D2104H::LEU2(HIS3), rad24::TRP1</i>	this study
GA-7194	GA-1982 with <i>mec1-100-D2104H::LEU2(HIS3), rad24::TRP1</i>	this study
GA-7199	GA-1981 with <i>mec1-100-Q1903E::LEU2(HIS3), rad24::TRP1</i>	this study
GA-7200	GA-1982 with <i>mec1-100-Q1903E::LEU2(HIS3), rad24::TRP1</i>	this study
GA-7201	GA-1981 with <i>mec1-100-R1809G::LEU2(HIS3), rad24::TRP1</i>	this study
GA-7202	GA-1982 with <i>mec1-100-R1809G::LEU2(HIS3), rad24::TRP1</i>	this study
GA-7209	GA-1981 with <i>mec1-100::natMX, rad24::TRP1</i>	this study
GA-7218	GA-1981 with <i>mec1-100-T1612M::LEU2(HIS3), rad24::TRP1</i>	this study
GA-7219	GA-1982 with <i>mec1-100-T1612M::LEU2(HIS3), rad24::TRP1</i>	this study
GA-7220	GA-1981 with <i>mec1-100-D1127E::LEU2(HIS3), rad24::TRP1</i>	this study
GA-7221	GA-1982 with <i>mec1-100-D1127E::LEU2(HIS3), rad24::TRP1</i>	this study
GA-7268	GA-1981 with <i>ddc2::DDC2-GFP-kanMX</i>	this study
GA-7327	GA-1981 with <i>ddc2::DDC2-GFP-kanMX, mec1-100::natMX</i>	this study
W303 diploid	<i>MATa/MATα, ade2-1/ade2-1, trp1-1/trp1-1, his3-11/his3-11, his3-15/his3-15, ura3-1/ura3-1, leu2-3/leu2-3, leu2-112/leu2-112, can1-100/can1-100</i>	

GA-7668	W303 diploid with <i>ddc2::DDC2-3HA-URA3/DDC2, sml1::HIS3/SML1, RAD5/rad5-535</i>	this study
GA-7760	W303 diploid with <i>ddc2::DDC2-GFP-KanMX/DDC2, sml1::HIS3/SML1, RAD5+/RAD5+</i>	this study
GA-7761	W303 diploid with <i>ddc2::DDC2-3HA-URA3/ddc2::DDC2-GFP-KanMX, RAD5+/rad5-535</i>	this study
GA-7762	W303 diploid with <i>ddc2::DDC2-3HA-URA3/ddc2::DDC2-GFP-KanMX, mec1-100::LEU2(HIS3)/mec1-100::natMX, sml1::KanMX/SML1, RAD5+/rad5-535</i>	this study
GA-7763	W303 diploid with <i>ddc2::DDC2-3HA-URA3/ddc2::DDC2-GFP-KanMX, mec1::HIS3/mec1::TRP1, sml1::KanMX4/sml1::His3 RAD5+/rad5-535</i>	this study
GA-7764	GA-1981 with <i>mec1-100::natMX, dpb11Δc::hphMX</i>	this study
GA-7767	GA-1982 with <i>mec1-100-D2104H::LEU2(HIS3), dpb11Δc::hphMX</i>	this study
GA-7768	GA-181 with <i>mec1-100-D1127E::LEU2(HIS3), dpb11Δc::hphMX</i>	this study
GA-7770	GA-1981 with <i>mec1-100-T1612M::LEU2(HIS3), dpb11Δc::hphMX</i>	this study
GA-7774	GA-1981 with <i>mec1-100-F2244L::LEU2(HIS3), dpb11Δc::hphMX</i>	this study
GA-7776	GA-1981 with <i>mec1-100-R1809G::LEU2(HIS3), dpb11Δc::hphMX</i>	this study
GA-7795	GA-181 with <i>dpb11Δc::hphMX</i>	this study
GA-7797	GA-1981 with <i>mec1-100-Q1903E::LEU2(HIS3), dpb11Δc::hphMX</i>	this study
GA-7907	GA-1981 with <i>ddc1::URA3</i>	this study
GA-7964	GA-1981 with <i>mec1-100::natMX, ddc1::URA3</i>	this study
GA-8605	GA-1981 with <i>dna2::Hyg, pBL584-DNA2(TRP1)</i>	this study
GA-8606	GA-1981 with <i>dna2::Hyg, pBL584-dna2-ΔN (TRP1)</i>	this study
GA-8607	GA-1981 with <i>dna2::Hyg, pBL584-dna2-2WA(TRP1)</i>	this study
GA-8608	GA-1981 with <i>mec1-100::natMX, dna2::Hyg, pBL584-DNA2(TRP1)</i>	this study
GA-8609	GA-1981 with <i>mec1-100::natMX, dna2::Hyg, pBL584-dna2-ΔN (TRP1)</i>	this study
GA-8610	GA-1981 with <i>mec1-100::natMX, dna2::Hyg, pBL584-dna2-2WA(TRP1)</i>	this study

Table 3.3: Mec1-Ddc2 co-precipitating proteins

Accession (UNIPROT/SGD)	log ₂ protein ratio (wt/ mec100)		Description
	first experiment	second experiment	
RAD52_YEAST/Rad52	-3.00	-4.22	DNA repair and recombination protein RAD52
H4_YEAST/Hhf1	-2.71	-2.97	Histone H4
H2B1_YEAST/Htb1	-2.48		Histone H2B.1
MSH2_YEAST/Msh2	-2.43	-1.30	DNA mismatch repair protein MSH2
RFA1_YEAST/Rfa1	-2.15	-2.40	Replication factor A protein 1
RFA3_YEAST/Rfa3	-2.09	-2.33	Replication factor A protein 3
RFA2_YEAST/Rfa2	-2.08	-2.04	Replication factor A protein 2
YO086_YEAST/YOL086W-A	-1.68	-1.38	Uncharacterized protein YOL086W-A
FBRL_YEAST/Nop1	-1.60	-3.14	rRNA 2'-O-methyltransferase fibrillar
YG1T_YEAST/YGR042W	-1.46	-1.22	Uncharacterized protein YGR042W
ABF2_YEAST/Abf2	-1.15		ARS-binding factor 2, mitochondrial
SNU13_YEAST/Snu13	-1.08	-2.93	13 kDa ribonucleoprotein-associated protein
RL28_YEAST/Rpl28	-0.76		60S ribosomal protein L28
ACS2_YEAST/Acs2	-0.43	0.44	Acetyl-coenzyme A synthetase 2
LCD1_YEAST/Ddc2	-0.17	-0.08	DNA damage checkpoint protein LCD1
RL39_YEAST/Rpl39	-0.08	0.06	60S ribosomal protein L39
ATR_YEAST/Mec1	0.01	-0.27	Serine/threonine-protein kinase MEC1
RL9A_YEAST/Rpl9a	0.07	0.01	60S ribosomal protein L9-A
PMA1_YEAST/Pma1	0.19		Plasma membrane ATPase 1
RS7B_YEAST/Rpl26a	0.33		40S ribosomal protein S7-B
RL26A_YEAST/Rps7b	0.44	0.31	60S ribosomal protein L26-A
RL38_YEAST/Rpl38	0.46	0.29	60S ribosomal protein L38
HSP72_YEAST/Ssa2	0.47	-0.36	Heat shock protein SSA2
RL9B_YEAST/Rpl9b	0.51	0.09	60S ribosomal protein L9-B
RL2A_YEAST/Rpl2a	0.59		60S ribosomal protein L2-A
RS11A_YEAST/Rps11a	0.61	0.26	40S ribosomal protein S11-A
RS28A_YEAST/Rps28a	0.63		40S ribosomal protein S28-A
RL34A_YEAST/Rpl34a	0.73	-0.15	60S ribosomal protein L34-A
RS19A_YEAST/Rps19a	0.81		40S ribosomal protein S19-A
RL23A_YEAST/Rpl23a	0.82	-0.01	60S ribosomal protein L23-A
RS20_YEAST/Rps20	0.88	0.18	40S ribosomal protein S20
RS17A_YEAST/Rps17a	0.93	-1.62	40S ribosomal protein S17-A
RL36A_YEAST/Rpl36a	0.93		60S ribosomal protein L36-A
KPYK1_YEAST/Cdc19	1.05	0.53	Pyruvate kinase 1
RS29A_YEAST/Rps29a	1.05	0.79	40S ribosomal protein S29-A
RL13A_YEAST/Rpl13a	1.07	-0.02	60S ribosomal protein L13-A
G3P3_YEAST/Tdh3	1.08	0.15	Glyceraldehyde-3-phosphate dehydrogenase 3
RS14A_YEAST/Rps14a	1.08	-0.02	40S ribosomal protein S14-A
RS15_YEAST/Rps15	1.13	-0.12	40S ribosomal protein S15
PMG1_YEAST/Gpm1	1.14	0.22	Phosphoglycerate mutase 1
RS9B_YEAST/Rps9b	1.20	-0.03	40S ribosomal protein S9-B
RS25A_YEAST/Rps25a	1.21		40S ribosomal protein S25-A
RS3_YEAST/Rps3	1.25	0.40	40S ribosomal protein S3
RL19A_YEAST/Rpl19a	1.25		60S ribosomal protein L19-A
RL32_YEAST/Rpl32	1.25	-0.01	60S ribosomal protein L32
HSP77_YEAST/Ssc1	1.28		Heat shock protein SSC1, mitochondrial
RL17A_YEAST/Rpl17a	1.29	-0.41	60S ribosomal protein L17-A
ATPA_YEAST/Atp1	1.30		ATP synthase subunit alpha, mitochondrial
EF1A_YEAST/Tef1	1.32	0.09	Elongation factor 1-alpha
RS5_YEAST/Rps5	1.37		40S ribosomal protein S5
RL31A_YEAST/Rpl31a	1.38		60S ribosomal protein L31-A

ENO2_YEAST/Eno2	1.44	0.00	Enolase 2
RS12_YEAST/Rps12	1.45	-0.30	40S ribosomal protein S12
RS2_YEAST/Rps2	1.48	-0.18	40S ribosomal protein S2
FHP_YEAST/Yhb1	1.50		Flavohepotein
RS21A_YEAST/Rps21a	1.56	0.42	40S ribosomal protein S21-A
IF5A1_YEAST/Hyp2	1.60		Eukaryotic translation initiation factor 5A-1
RL12A_YEAST/Rpl12a	1.64	-0.33	60S ribosomal protein L12-A
RS26A_YEAST/Rps26a	1.66		40S ribosomal protein S26-A
RS27B_YEAST/Rps27b	1.66	0.04	40S ribosomal protein S27-B
RS18A_YEAST/Rps18a	1.66	0.17	40S ribosomal protein S18-A
ENO1_YEAST/Eno1	1.72		Enolase 1
EF3A_YEAST/Yef3	1.73	0.25	Elongation factor 3A
RL22A_YEAST/Rpl22a	1.74		60S ribosomal protein L22-A
ADH1_YEAST/Adh1	1.80	0.56	Alcohol dehydrogenase 1
PGK_YEAST/Pgk1	1.82	-0.25	Phosphoglycerate kinase
EF1B_YEAST/Efb1	1.82		Elongation factor 1-beta
CYS3_YEAST/Cys3	1.83		Cystathionine gamma-lyase
RL8A_YEAST/Rpl8a	1.83		60S ribosomal protein L8-A
CYPH_YEAST/Cpr1	1.84		Peptidyl-prolyl cis-trans isomerase
PDC1_YEAST/Pdc1	1.86	-1.29	Pyruvate decarboxylase isozyme 1
TPIS_YEAST/Tpi1	1.88		Triosephosphate isomerase
RL35A_YEAST/Rpl35a	1.91	-0.02	60S ribosomal protein L35-A
RL1A_YEAST/Rpl1a	1.94		60S ribosomal protein L1-A
RS24A_YEAST/Rps24a	1.97		40S ribosomal protein S24-A
STM1_YEAST/Stm1	1.97		Suppressor protein STM1
G6PI_YEAST/Pgi1	2.05		Glucose-6-phosphate isomerase
NACA_YEAST/Egd2	2.06		Nascent polypeptide-associated complex subunit alpha
HSP60_YEAST/Hsp60	2.10		Heat shock protein 60, mitochondrial
RL4A_YEAST/Rpl4a	2.11		60S ribosomal protein L4-A
HSP75_YEAST/Ssb1	2.11	0.29	Heat shock protein SSB1
RS16A_YEAST/Rps16a	2.12	0.07	40S ribosomal protein S16-A
SODC_YEAST/Sod1	2.14		Superoxide dismutase [Cu-Zn]
TCTP_YEAST/Tma19	2.14		Translationally-controlled tumor protein homolog
RL21A_YEAST/Rpl21a	2.15		60S ribosomal protein L21-A
RL10_YEAST/Rpl10	2.23		60S ribosomal protein L10
YRB1_YEAST/Yrb1	2.29		Ran-specific GTPase-activating protein 1
HSP71_YEAST/Hsp71	2.35	-0.93	Heat shock protein SSA1
VDAC1_YEAST/Por1	2.39		Mitochondrial outer membrane protein porin 1
ALF_YEAST/Fba1	2.39	0.55	Fructose-bisphosphate aldolase
RLA2_YEAST/Rpp2a	2.50		60S acidic ribosomal protein P2-alpha
TAL1_YEAST/Tal1	2.55		Transaldolase
TSA1_YEAST/Tsa1	2.58		Peroxiredoxin TSA1
RL14A_YEAST/Rpl14a	2.61		60S ribosomal protein L14-A
HXKB_YEAST/Hxk2	2.65		Hexokinase-2
RS13_YEAST/Rpl43a	2.72		40S ribosomal protein S13
RLA3_YEAST/Tdh2	3.10		60S acidic ribosomal protein P1-beta
RL43A_YEAST/Rpl43a	3.11		60S ribosomal protein L43-A
G3P2_YEAST/Tdh2	3.13	0.01	Glyceraldehyde-3-phosphate dehydrogenase 2
RL30_YEAST/Rpl30	3.13		60S ribosomal protein L30
BMH2_YEAST/Bmh2	3.21		Protein BMH2
HSC82_YEAST/Hsc82	3.37	0.62	ATP-dependent molecular chaperone HSC82
HSP7F_YEAST/Sse1	3.49		Heat shock protein homolog SSE1
RS7A_YEAST/Rps7a	3.57		40S ribosomal protein S7-A
RL4B_YEAST/Rpl4b	3.72		60S ribosomal protein L4-B
AHP1_YEAST/Ahp1	4.73		Peroxiredoxin type-2
RLA1_YEAST/Rpp1a	5.77		60S acidic ribosomal protein P1-alpha

TMA7_YEAST/Tma7	7.89		Translation machinery-associated protein 7
ADK_YEAST/Ado1	8.08		Adenosine kinase
RLA0_YEAST/Rpp0	12.92		60S acidic ribosomal protein P0
CAF17_YEAST/Iba57		0.47	Putative transferase CAF17, mitochondrial
EF2_YEAST/Eft1		0.32	Elongation factor 2
GAR1_YEAST/Gar1		-2.80	H/ACA ribonucleoprotein complex subunit 1
GAT1_YEAST/Gat1		0.97	Transcriptional regulatory protein GAT1
GDE_YEAST/Gdb1		0.75	Glycogen debranching enzyme
H2A1_YEAST/Hta1		-2.77	Histone H2A.1
H2B2_YEAST/Thb2		-3.36	Histone H2B.2
H3_YEAST/Hht1		-4.80	Histone H3
MAL31_YEAST/Mal31		1.00	Maltose permease MAL31
MSB1_YEAST/Msb1		1.10	Morphogenesis-related protein MSB1
MSH6_YEAST/Msh6		-0.84	DNA mismatch repair protein MSH6
NOP56_YEAST/Nop56		-0.85	(Q12460) Nucleolar protein 56
PEX3_YEAST/Pex3		-2.84	Peroxisomal biogenesis factor 3
PP4R3_YEAST/Psy2		-2.63	Serine/threonine-protein phosphatase 4 regulatory subunit 3
RIM1_YEAST/Rim1		-1.24	Single-stranded DNA-binding protein RIM1, mitochondrial
RL24A_YEAST/Rpl24a		-2.86	60S ribosomal protein L24-A
RL3_YEAST/Rpl3		0.38	60S ribosomal protein L3
RL8B_YEAST/Rpl8b		-0.07	60S ribosomal protein L8-B
RTF1_YEAST/Rtf1		0.02	RNA polymerase-associated protein RTF1
SGS1_YEAST/Sgs1		-1.30	ATP-dependent helicase SGS1
SMC5_YEAST/Smc5		-2.97	Structural maintenance of chromosomes protein 5
SMY2_YEAST/Smy2		0.29	Protein SMY2
SPO13_YEAST/Spo13		0.17	Meiosis-specific protein SPO13
SPT5_YEAST/Spt5		-0.17	Transcription elongation factor SPT5
SWR1_YEAST/Swr1		0.26	Helicase SWR1
UAP1_YEAST/Qri1		0.23	UDP-N-acetylglucosamine pyrophosphorylase
YB21A_YEAST/Ty2a-b		1.82	Transposon Ty2-B Gag polyprotein
YD11A_YEAST/YDL160C-A		2.58	Transposon Ty1-DR1 Gag polyprotein
YD160_YEAST/YDL160C-A		-0.89	Uncharacterized protein YDL160C-A
YE11A_YEAST/Ty1a-ER1		2.08	Transposon Ty1-ER1 Gag polyprotein

ACKNOWLEDGEMENTS

We thank J. Diffley, P. Pasero, M. Longhese and P. Burgers for strains and constructs. Furthermore we thank Y. Hirata, K. Maeguchi and S. Ishikawa for assistance in generating strains.

REFERENCES

- Alcasabas, A.A., Osborn, A.J., Bachant, J., Hu, F., Werler, P.J., Bousset, K., Furuya, K., Diffley, J.F., Carr, A.M., and Elledge, S.J. (2001). Mrc1 transduces signals of DNA replication stress to activate Rad53. *Nat Cell Biol* 3, 958-965.
- Andrade, M.A., Perez-Iratxeta, C., and Ponting, C.P. (2001). Protein repeats: structures, functions, and evolution. *J Struct Biol* 134, 117-131.
- Ball, H.L., and Cortez, D. (2005). ATRIP oligomerization is required for ATR-dependent checkpoint signaling. *J Biol Chem* 280, 31390-31396.
- Ball, H.L., Myers, J.S., and Cortez, D. (2005). ATRIP binding to replication protein A-single-stranded DNA promotes ATR-ATRIP localization but is dispensable for Chk1 phosphorylation. *Mol Biol Cell* 16, 2372-2381.
- Bjergbaek, L., Cobb, J.A., Tsai-Pflugfelder, M., and Gasser, S.M. (2005). Mechanistically distinct roles for Sgs1p in checkpoint activation and replication fork maintenance. *EMBO J* 24, 405-417.
- Bosotti, R., Isacchi, A., and Sonnhammer, E.L. (2000). FAT: a novel domain in PIK-related kinases. *Trends Biochem Sci* 25, 225-227.
- Chen, S.H., and Zhou, H. (2009). Reconstitution of Rad53 activation by Mec1 through adaptor protein Mrc1. *J Biol Chem* 284, 18593-18604.
- Cobb, J.A., Bjergbaek, L., Shimada, K., Frei, C., and Gasser, S.M. (2003). DNA polymerase stabilization at stalled replication forks requires Mec1 and the RecQ helicase Sgs1. *EMBO J* 22, 4325-4336.
- Cobb, J.A., Schleker, T., Rojas, V., Bjergbaek, L., Tercero, J.A., and Gasser, S.M. (2005). Replisome instability, fork collapse, and gross chromosomal rearrangements arise synergistically from Mec1 kinase and RecQ helicase mutations. *Genes Dev* 19, 3055-3069.
- Crabbe, L., Thomas, A., Pantesco, V., De Vos, J., Pasero, P., and Lengronne, A. (2010). Analysis of replication profiles reveals key role of RFC-Ctf18 in yeast replication stress response. *Nat Struct Mol Biol* 17, 1391-1397.
- Hegnauer, A.M., Hustedt, N., Shimada, K., Pike, B.L., Vogel, M., Amsler, P., Rubin, S.M., van Leeuwen, F., Guenole, A., van Attikum, H., *et al.* (2012). An N-terminal acidic region of Sgs1 interacts with Rpa70 and recruits Rad53 kinase to stalled forks. *EMBO J* 31, 3768-3783.
- Hildebrand, A., Remmert, M., Biegert, A., and Soding, J. (2009). Fast and accurate automatic structure prediction with HHpred. *Proteins* 77 Suppl 9, 128-132.
- Hustedt, N., and Shimada, K. (2014). Analyzing DNA replication checkpoint in budding yeast. *Methods Mol Biol* 1170, 321-341.
- Kumar, S., and Burgers, P.M. (2013). Lagging strand maturation factor Dna2 is a component of the replication checkpoint initiation machinery. *Genes Dev* 27, 313-321.
- Nakada, D., Hirano, Y., Tanaka, Y., and Sugimoto, K. (2005). Role of the C terminus of Mec1 checkpoint kinase in its localization to sites of DNA damage. *Mol Biol Cell* 16, 5227-5235.
- Nam, E.A., Zhao, R., and Cortez, D. (2011). Analysis of mutations that dissociate G(2) and essential S phase functions of human ataxia telangiectasia-mutated and Rad3-related (ATR) protein kinase. *The Journal of biological chemistry* 286, 37320-37327.
- Navadgi-Patil, V.M., and Burgers, P.M. (2009). The unstructured C-terminal tail of the 9-1-1 clamp subunit Ddc1 activates Mec1/ATR via two distinct mechanisms. *Mol Cell* 36, 743-753.
- Navadgi-Patil, V.M., and Burgers, P.M. (2011). Cell-cycle-specific activators of the Mec1/ATR checkpoint kinase. *Biochem Soc Trans* 39, 600-605.
- Navadgi-Patil, V.M., Kumar, S., and Burgers, P.M. (2011). The unstructured C-terminal tail of yeast Dpb11 (human TopBP1) protein is dispensable for DNA replication and the S phase checkpoint but required for the G2/M checkpoint. *J Biol Chem* 286, 40999-41007.

- Osborn, A.J., and Elledge, S.J. (2003). Mrc1 is a replication fork component whose phosphorylation in response to DNA replication stress activates Rad53. *Genes Dev* *17*, 1755-1767.
- Paciotti, V., Clerici, M., Lucchini, G., and Longhese, M.P. (2000). The checkpoint protein Ddc2, functionally related to *S. pombe* Rad26, interacts with Mec1 and is regulated by Mec1-dependent phosphorylation in budding yeast. *Genes Dev* *14*, 2046-2059.
- Paciotti, V., Clerici, M., Scotti, M., Lucchini, G., and Longhese, M.P. (2001). Characterization of mec1 kinase-deficient mutants and of new hypomorphic mec1 alleles impairing subsets of the DNA damage response pathway. *Mol Cell Biol* *21*, 3913-3925.
- Sun, Z., Hsiao, J., Fay, D.S., and Stern, D.F. (1998). Rad53 FHA domain associated with phosphorylated Rad9 in the DNA damage checkpoint. *Science* *281*, 272-274.
- Sweeney, F.D., Yang, F., Chi, A., Shabanowitz, J., Hunt, D.F., and Durocher, D. (2005). *Saccharomyces cerevisiae* Rad9 acts as a Mec1 adaptor to allow Rad53 activation. *Curr Biol* *15*, 1364-1375.
- Tercero, J.A., Longhese, M.P., and Diffley, J.F. (2003). A central role for DNA replication forks in checkpoint activation and response. *Mol Cell* *11*, 1323-1336.
- Yang, H., Rudge, D.G., Koos, J.D., Vaidialingam, B., Yang, H.J., and Pavletich, N.P. (2013). mTOR kinase structure, mechanism and regulation. *Nature* *497*, 217-223.

CHAPTER 4: AN N-TERMINAL ACIDIC REGION OF SGS1 INTERACTS WITH RPA70 AND RECRUITS RAD53 KINASE TO STALLED FORKS

Anna Maria Hegnauer^{1,2,6}, Nicole Hustedt^{1,2,6}, Kenji Shimada¹, Brietta L Pike¹, Markus Vogel¹, Philipp Amsler^{1,2}, Seth M Rubin³, Fred van Leeuwen⁴, Aude Guéolé⁵, Haico van Attikum⁵, Nicolas H Thomä¹ and Susan M Gasser^{1,2,*}

1. Friedrich Miescher Institute for Biomedical Research, Basel, Switzerland, 2. Faculty of Sciences, University of Basel, Basel, Switzerland, 3. Department of Chemistry and Biochemistry, University of California, Santa Cruz, CA, USA, 4. Division of Gene Regulation, Netherlands Cancer Institute, Amsterdam, The Netherlands, 5. Department of Toxicogenetics, Leiden University Medical Center, Leiden, The Netherlands, 6. These authors contributed equally to this work

published in *EMBO J*, 2012. 31(18): p. 3768-83.

AUTHOR CONTRIBUTIONS:

AMH performed yeast two hybrid, ChIP, recovery assay and Sgs1-RPA co-IP experiments, contributed to writing and assembled figures; NH performed E-MAP screen, western blots (Sgs1 *in vivo* phosphorylation, Rad53 phosphorylation and Sgs1 expression), Sgs1-Rad53 Co-IP and additional ChIP and recovery assay experiments, contributed to writing and assembled figures; KS advised, performed *in vitro* kinase assay experiments, contributed to writing and figures; BLP advised and contributed to writing; PA and MV purified proteins and cooperated on biochemical analyses; SMR performed and analysed ITC experiments; NHT advised MV, PA, and contributed to writing; HvA advised AG who generated strains used in the E-MAP analysis, and FvL hosted NH for same; SMG advised, interpreted results, planned experiments, contributed to writing, figures and funding of the project.

SUMMARY

DNA replication fork stalling poses a major threat to genome stability. This is counteracted in part by the intra-S phase checkpoint, which stabilizes arrested replication machinery, prevents cell-cycle progression and promotes DNA repair. The checkpoint kinase Mec1/ATR and RecQ helicase Sgs1/BLM contribute synergistically to fork maintenance on hydroxyurea (HU). Both enzymes interact with replication protein A (RPA). We identified and deleted the major interaction sites on Sgs1 for Rpa70, generating a mutant called *sgs1-r1*. In contrast to a helicase-dead mutant of Sgs1, *sgs1-r1* did not significantly reduce recovery of DNA polymerase alpha at HU-arrested replication forks. However, the Sgs1 R1 domain is a target of Mec1 kinase, deletion of which compromises Rad53 activation on HU. Full activation of Rad53 is achieved through phosphorylation of the Sgs1 R1 domain by Mec1, which promotes Sgs1 binding to the FHA1 domain of Rad53 with high affinity. We propose that the recruitment of Rad53 by phosphorylated Sgs1 promotes the replication checkpoint response on HU. Loss of the R1 domain increases lethality selectively in cells lacking Mus81, Slx4, Slx5 or Slx8.

An N-terminal acidic region of Sgs1 interacts with Rpa70 and recruits Rad53 kinase to stalled forks

Anna Maria Hegnauer^{1,2,6},
Nicole Hustedt^{1,2,6}, Kenji Shimada¹,
Brietta L Pike¹, Markus Vogel¹,
Philipp Amsler^{1,2}, Seth M Rubin³,
Fred van Leeuwen⁴, Aude Guénolé⁵,
Haico van Attikum⁵, Nicolas H Thomä¹
and Susan M Gasser^{1,2,*}

¹Friedrich Miescher Institute for Biomedical Research, Basel, Switzerland, ²Faculty of Sciences, University of Basel, Basel, Switzerland, ³Department of Chemistry and Biochemistry, University of California, Santa Cruz, CA, USA, ⁴Division of Gene Regulation, Netherlands Cancer Institute, Amsterdam, The Netherlands and ⁵Department of Toxicogenetics, Leiden University Medical Center, Leiden, The Netherlands

DNA replication fork stalling poses a major threat to genome stability. This is counteracted in part by the intra-S phase checkpoint, which stabilizes arrested replication machinery, prevents cell-cycle progression and promotes DNA repair. The checkpoint kinase Mec1/ATR and RecQ helicase Sgs1/BLM contribute synergistically to fork maintenance on hydroxyurea (HU). Both enzymes interact with replication protein A (RPA). We identified and deleted the major interaction sites on Sgs1 for Rpa70, generating a mutant called *sgs1-r1*. In contrast to a helicase-dead mutant of Sgs1, *sgs1-r1* did not significantly reduce recovery of DNA polymerase α at HU-arrested replication forks. However, the Sgs1 R1 domain is a target of Mec1 kinase, deletion of which compromises Rad53 activation on HU. Full activation of Rad53 is achieved through phosphorylation of the Sgs1 R1 domain by Mec1, which promotes Sgs1 binding to the FHA1 domain of Rad53 with high affinity. We propose that the recruitment of Rad53 by phosphorylated Sgs1 promotes the replication checkpoint response on HU. Loss of the R1 domain increases lethality selectively in cells lacking Mus81, Slx4, Slx5 or Slx8.

The EMBO Journal (2012) 31, 3768–3783. doi:10.1038/emboj.2012.195; Published online 20 July 2012

Subject Categories: genome stability & dynamics

Keywords: intra-S checkpoint; RPA; replication stress; Rad53; Sgs1

Introduction

The accurate replication of DNA and its segregation into daughter cells is aided by the intra-S checkpoint, which is

*Corresponding author. Friedrich Miescher Institute for Biomedical Research, Maulbeerstrasse 66, Basel 4058, Switzerland.

Tel.: +41 61 697 7255; Fax: +41 61 697 3976;

E-mail: susan.gasser@fmi.ch

⁶These authors contributed equally to this work

Received: 9 January 2012; accepted: 28 June 2012; published online: 20 July 2012

triggered by the single-stranded DNA (ssDNA) that accumulates when DNA polymerases pause, either due to reduced nucleotide concentration or due to the presence of adducts that impair fork progression. Avoidance of fork collapse is mediated both by the Mec1/ATR kinase and by the action of a RecQ helicase, which reverses fold-back structures and resolves strand exchange to suppress inappropriate recombination events. Resumption of replication generally requires that engaged DNA polymerases remain associated with paused forks, which in wild-type yeast cells can persist for many hours (reviewed in Cobb and Bjergbaek, 2006; Tourriere and Pasero, 2007 and Aguilera and Gomez-Gonzalez, 2008).

The checkpoint kinase Mec1-Ddc2 in *S. cerevisiae* (ATR-ATRIP in humans) plays two critical roles in this event (reviewed in Cimprich and Cortez, 2008 and Friedel *et al.*, 2009). First, Mec1-Ddc2 regulates replisome function and enables the stable retention of replicative polymerases at very early origins like ARS607 (Cobb *et al.*, 2003, 2005; De Piccoli *et al.*, 2012). Second, it modifies and activates Rad53, the downstream checkpoint kinase that in turn retards cell-cycle progression, regulates levels of dNTPs and repair enzymes, represses the firing of late origins, and prevents fork collapse through poorly identified pathways (reviewed in Tourriere and Pasero, 2007; Segurado and Diffley, 2008).

The activation of Mec1/Ddc2 kinase under restricted nucleotide conditions (0.2 M hydroxyurea, HU) most likely stems from the stalling of leading and/or lagging strand DNA polymerases, which generates stretches of ssDNA. These become coated by replication protein A (RPA; Aparicio *et al.*, 1999), which signals the recruitment and activation of Mec1-Ddc2 checkpoint kinase (Zou and Elledge, 2003), not unlike the situation at resected double-strand breaks (Dubrana *et al.*, 2007). In both budding yeast and mammals, RPA contributes to the recruitment of Mec1/ATR to stalled or damaged replication forks, through its cofactor, Ddc2/ATRIP (Melo *et al.*, 2001; Rouse and Jackson, 2002). Intriguingly, RPA is itself a target of Mec1/ATR phosphorylation (Brush *et al.*, 1996; Zou and Elledge, 2003).

Besides RPA, fork-associated activators of the intra-S phase checkpoint include the 9-1-1 checkpoint clamp and Dbp11/TOPBP1 (Majka *et al.*, 2006; Mordes *et al.*, 2008; Navadgi-Patil and Burgers, 2008), while additional, unidentified co-activators are postulated to exist (Navadgi-Patil and Burgers, 2011). Once recruited Mec1/ATR phosphorylates Mrc1/Claspin, which helps activate the downstream effector kinases Rad53/CHK2, or CHK1 in mammalian cells (reviewed in Tourriere and Pasero, 2007), possibly by facilitating the contact between Mec1 and its target Rad53 (Chen and Zhou, 2009). In mammals, the RecQ helicase BLM was also reported to be a target of ATR/ATM phosphorylation, and to contribute to recovery from replicative stress (Davies *et al.*, 2004; Rao *et al.*, 2005).

Whereas the Rad53 kinase mediates crucial downstream events in the yeast checkpoint response, Mec1/ATR has a distinct role in stabilizing replicative polymerases, particu-

larly at early firing origins, such as the budding yeast ARS607 or ARS305. This was demonstrated by chromatin immunoprecipitation (ChIP) from cells synchronously arrested in S phase: the recovery of DNA polymerases α and ϵ bound to the replication fork dropped rapidly in cells lacking Mec1, but not in cells lacking Rad53 (Cobb *et al*, 2003, 2005). Similar separation of function was demonstrated in a study of *exo1* deletion effects on viability in *rad53* versus *mec1* mutants (Segurado and Diffley, 2008). Nonetheless, a loss of Rad53 triggers an accumulation of both ssDNA (Sogo *et al*, 2002; Tourriere and Pasero, 2007) and recombination intermediates (Lucca *et al*, 2004). Surprisingly, and in contrast to the situation at early firing origins, it was recently reported that the replisome can be recovered largely intact and associated with later firing origins upon replication stress, in cells lacking either Mec1 or Rad53 (De Piccoli *et al*, 2012). These checkpoint kinases were proposed to regulate replication fork progression through multiple targets, including Psf1, a component of the replicative Cdc45-MCM-GINS helicase (De Piccoli *et al*, 2012).

RecQ helicases have also been shown to be important for the stable binding of DNA polymerases at stalled replication forks and for efficient fork restart after exposure to HU or aphidicolin (Cobb *et al*, 2005; Davies *et al*, 2007; Bachrati and Hickson, 2008; Pirzio *et al*, 2008). Loss of Sgs1, the unique RecQ helicase in budding yeast, leads to a reduced recovery of DNA polymerases at early firing origins, a lower survival rate after exposure to HU (Cobb *et al*, 2003, 2005), and the accumulation of aberrant recombination structures after exposure to MMS (Liberi *et al*, 2005). Indeed, *sgs1* deficient cells display abnormally high levels of recombination (Watt *et al*, 1996) and spontaneous gross chromosomal rearrangements (GCRs), particularly on HU (Myung and Kolodner, 2002; Schmidt and Kolodner, 2006). The role of RecQ helicases in resistance to replicative stress is conserved: mutations in three human RecQ helicases (BLM, Bloom's; WRN; Werner's, and RECQ4) cause syndromes associated with a predisposition to cancer and/or genome instability (reviewed by Bachrati and Hickson, 2008 and Ashton and Hickson, 2010).

Genetic studies argue that Sgs1 acts both in complex with Top3 and Rmi1 (Gangloff *et al*, 1994; Chang *et al*, 2005; Mullen *et al*, 2005) and alone (reviewed in Bernstein *et al*, 2010). Sgs1 requires Top3 for dissolution of Holliday junctions and for enhancing DNA polymerase at stalled forks (Liberi *et al*, 2005; Mankouri *et al*, 2011), while it acts independently of Top3 to activate Rad53 in the presence of HU (Bjergbaek *et al*, 2005). Sgs1, like BLM and WRN, also binds Rad51 and RPA, and acts both upstream and downstream of Rad51-mediated strand invasion, to prevent and to resolve recombination intermediates. Finally, synthetic lethal screens link Sgs1 not only to recombination enzymes, but also to enzymes and proteins essential for lagging strand synthesis, such as Pol32, RNase H2 and FEN1/Rad27 (Ooi *et al*, 2003; Tong *et al*, 2004; Ii and Brill, 2005).

Here, we focus on the role of Sgs1 at replication forks stalled by HU, which seems to mimic the situation that ensues when forks encounter tight DNA-protein complexes (reviewed in Aguilera and Gomez-Gonzalez, 2008). Double mutants in budding yeast have been particularly helpful in elucidating this pathway. Whereas the effects of *sgs1 Δ are relatively mild (Cobb *et al*, 2003), its combination with *mec1*-*

100, an S phase-specific mutation in Mec1, causes extensive fork collapse and a failure of nucleotide incorporation after recovery from acute exposure to HU (Cobb *et al*, 2005). The *mec1*-100 mutation compromises the intra-S phase checkpoint response, but is able to modify and activate Rad53, triggering the G2/M checkpoint (Paciotti *et al*, 2001). Importantly, and in contrast to the effects of *mec1*-100, deletion of *rad53* is not additive with *sgs1 Δ in GCR or polymerase stability assays. Indeed, neither the loss of checkpoint activity in the *rad53*-11 mutant nor *rad53* deletion coupled with *sml1 Δ affects polymerase recovery by ChIP at early firing origins (Cobb *et al*, 2003, 2005).**

The fact that Sgs1, Mec1-Ddc2 and DNA pol α all bind RPA, led us to test the hypothesis that Sgs1 influences the association of lagging strand polymerases at stalled forks through its interaction with the ssDNA binding complex. To this end, we mapped the region of Sgs1 that binds RPA and generated a mutant lacking the interaction domain, which we call *sgs1*-r1. We monitored the status of DNA pol α at stalled forks in mutants lacking the main RPA-interaction domain, with and without Sgs1 helicase activity. We found that the Sgs1 helicase activity and not its RPA interacting domain contributes to the stabilization of engaged DNA pol α /primase at the HU-stalled replication fork. Moreover, we show that Mec1-Ddc2 modifies Sgs1 within the RPA-interaction domain, and that once phosphorylated, Sgs1 has a significant affinity for the FHA1 phospho-threonine binding module of the downstream checkpoint kinase Rad53. We propose that the interaction of Sgs1 and Rad53 contributes to checkpoint kinase activation during replicative stress, independent of the role of Sgs1 helicase activity in stabilizing polymerases at the fork.

Results

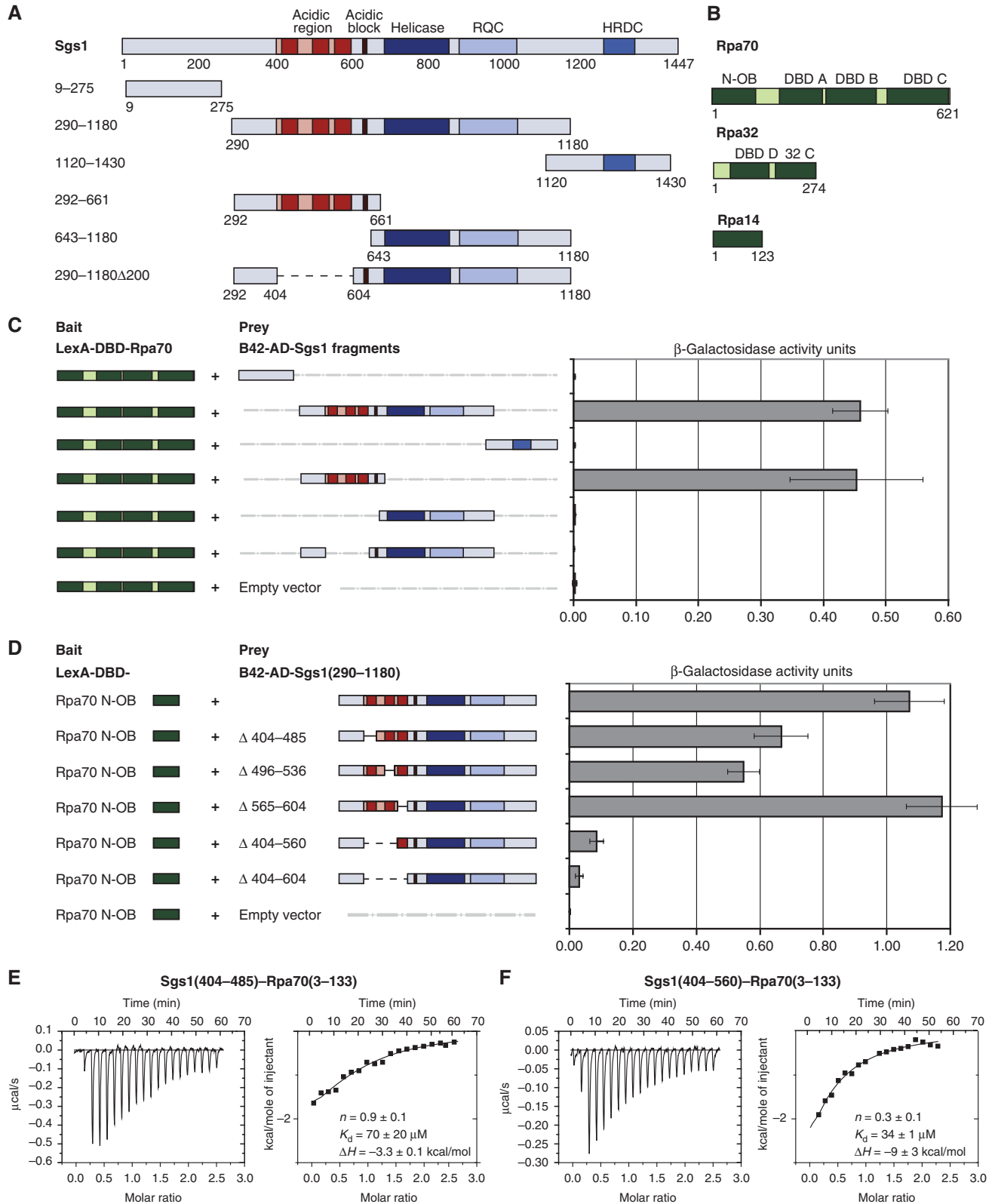
Sgs1 interacts with Rpa70 through an acidic region N-terminal of the helicase domain

To analyse the role of Sgs1 in stabilizing lagging strand polymerases at stalled forks, we first mapped the Sgs1-RPA interaction site. Sgs1 contains three conserved domains that are characteristic of RecQ helicases: an SF2-type helicase domain, an RQC (RecQ C-terminal) motif and an HRDC (helicase and RNase D C-terminal) domain (Figure 1A). In addition, a region of unknown structure in the N-terminus of Sgs1 (first 158 aa) has been shown to interact with Top3/Rmi1 (Bennett *et al*, 2000; Fricke *et al*, 2001; Chen and Brill, 2007; Weinstein and Rothstein, 2008). There is both an acidic block at aa 664 and a larger acidic region located N-terminal of the helicase domain. Although structure prediction suggests that this region is intrinsically disordered in solution, it has been proposed to help prevent or resolve aberrant recombination structures at MMS-treated forks (Bernstein *et al*, 2009). To see which domain is responsible for binding to RPA, we fused fragments containing the functional domains of Sgs1 to a B42 transactivation domain (B42-AD) and performed yeast two-hybrid (Y2H) analysis with RPA (Figure 1A).

RPA is an evolutionarily conserved heterotrimeric protein, consisting of Rpa70, Rpa32 and Rpa14 (names based on molecular weight, or Rpa1, Rpa2 and Rpa3, based on gene names). The smallest subunit, Rpa14, is believed to mediate protein-protein interaction only within the RPA complex, while Rpa70 and Rpa32 were shown to bind other proteins

(Binz *et al*, 2004; Zou *et al*, 2006). We therefore expressed full-length Rpa70 and Rpa32 fused to the LexA-DNA binding domain (LexA-DBD) under control of a galactose inducible promoter, as bait in the Y2H assay (Figure 1B). Strong interactions were scored between the largest subunit Rpa70 and the large core of the Sgs1 enzyme (aa 290–1180;

Figure 1C; Supplementary Figure S1A), while Rpa32 showed a very weak β -galactosidase signal in the Y2H assay with Sgs1 (Supplementary Figure S1B). A 400-aa fragment containing only the acidic region N-terminal of the Sgs1 helicase domain bound Rpa70 as efficiently as a larger fragment (Figure 1C). Within this region, we identified three sequences of 35–41 aa



by BLAST and Quick2D analysis, which are conserved among close homologues of the *S. cerevisiae* enzyme (dark red boxes, Figure 1; aa 404–485, aa 496–536 and aa 565–604). To test the importance of these conserved sequences for the Sgs1–Rpa70 interaction, we removed them by deleting aa 404–604 in the Sgs1-B42-AD construct. Consistently, this deletion abolished Y2H interaction between Rpa70 and Sgs1 (Figure 1C). Similarly, we mapped the interaction site on Rpa70 by fusing Rpa70 subdomains to the LexA-DBD and monitoring their interaction with the Sgs1(290–1180)-B42-AD fusion. The highest β -galactosidase activity was measured for the N-terminal oligonucleotide binding fold (N-OB) of Rpa70 without the linker region (Supplementary Figure S1A).

Sgs1 bears multiple interaction sites for the Rpa70 N-OB fold

To see if each conserved repeat within the Sgs1 acidic domain contributed equally to the interaction, we created three Sgs1-B42-AD deletion constructs each lacking only one of the three conserved sequences (Sgs1(290–1180, Δ 404–485), Sgs1(290–1180, Δ 496–536) and Sgs1(290–1180, Δ 565–604)). These constructs were tested for interaction with the Rpa70 N-OB fold (Rpa70(1–133)) by Y2H analysis (Figure 1D). Deletion of the first or second conserved sequence (Sgs1(290–1180, Δ 404–485) or Sgs1(290–1180, Δ 496–536)) cut the β -galactosidase signal in half, while deletion of the third conserved sequence (Sgs1(290–1180, Δ 565–604)) had no effect. This suggests that Sgs1 binds the RPA70 N-OB fold through two sites, aa 404–485 and aa 496–536. Indeed, deletion of the first two of the three motifs (aa 404–560 in Sgs1-B42-AD), abolished the interaction with the N-OB fold of Rpa70 almost as efficiently as deleting the entire 200 aa region, arguing that two related motifs spanning from aa 404 to 485 and aa 496 to 536, mediate the interaction with Rpa70.

We confirmed that these regions of Sgs1 and Rpa70 interact directly by performing an isothermal titration calorimetry (ITC) assay with purified recombinant proteins (Figure 1E and F). We found that both Sgs1(404–485) and Sgs1(404–560) bound RPA70(3–133) with similar affinity ($K_d = 70 \pm 20 \mu\text{M}$ and $K_d = 34 \pm 1 \mu\text{M}$, respectively). The ITC data suggested differences in the complex stoichiometry (n) and molar enthalpy (ΔH) between the two Sgs1 fragments: it appears that the more N-terminal motif of Sgs1 (aa 404–485) binds one molecule of the RPA70 N-OB fold, while the larger domain (aa 404–560) is able to bind two. This suggests that Sgs1 might be able to bind multiple RPA complexes, possibly leading to RPA delivery and/or removal as Sgs1 unwinds duplex DNA.

The Sgs1–RPA interaction site is structurally isolated from the helicase domain and its deletion does not affect protein stability

To determine whether this region of Sgs1 is also important for interaction with RPA *in vivo*, we deleted amino acids 404–604 within the *SGS1* chromosomal locus using a PCR-based allele-replacement technique. The resulting allele (*sgs1-r1*; Figure 2A), C-terminally tagged by 13Myc, is expressed when tested by western blot analysis on whole cell extracts (Figure 2B and C, inputs). The signal for *sgs1-r1*-13Myc is slightly stronger than for wild-type Sgs1–13Myc, which may either reflect a better blotting efficiency or slightly improved stability. This deletion leaves intact the aa 664 shown to be important for resolving recombination intermediates, and is distinct from the previously published AR2 deletion, which reduced Sgs1 levels (Bernstein *et al*, 2009).

To monitor the interaction of the *sgs1-r1* mutant protein with RPA *in vivo*, we performed co-immunoprecipitation (co-IP) experiments with appropriately tagged proteins. Strains expressing Rpa70–3HA and either 13Myc-tagged Sgs1 or *sgs1-r1* were released from G1 phase for 20 min to allow cells to accumulate in S phase. Rpa70–3HA and Sgs1–13Myc were efficiently precipitated as a complex using either anti-Myc antibody (Figure 2C) or anti-HA (Supplementary Figure S2). In the *sgs1-r1*-13Myc precipitation, the efficiency of Rpa70 recovery was reduced roughly two-fold (Figure 2C), as was the reciprocal recovery (*sgs1-r1* by Rpa70, Supplementary Figure S2). This suggests that the deleted domain indeed mediates Sgs1–RPA interaction *in vivo*, although other contacts may support interactions in the context of the holo-RPA complex. Indeed, residual binding could be explained by the interaction detected between Sgs1 and Rpa32 (Supplementary Figure S1B), through a site unaffected by the *sgs1-r1* mutation, or by an indirect interaction of *sgs1-r1*-13Myc and Rpa70–3HA to DNA.

To ensure that the *sgs1-r1* protein retained helicase activity, despite the reduced interaction with RPA, we tested the ability of *sgs1-r1* to support growth in a *srs2* null background. Rothstein and colleagues have shown that the helicase activity of Sgs1 is essential for growth in the absence of the Srs2 helicase (Weinstein and Rothstein, 2008). Tetrad analysis confirms that spores containing helicase-dead Sgs1 (K706R or *sgs1-hd*) in combination with *srs2* Δ showed almost no growth, while the *sgs1-r1 srs2* Δ double mutant spores grew normally (Figure 2D). We conclude that *sgs1-r1* retains helicase activity, consistent with its weak suppression of *top3* Δ slow growth (Supplementary Figure S3).

We next tested whether the *sgs1-r1* allele yields the same levels of sensitivity to DNA damage as *sgs1* Δ in drop assays. This assay monitors the capacity of cells to repair DNA

Figure 1 Mapping the interaction site between Sgs1 and Rpa70. (A) Schematic representation of Sgs1 and its functional domains. Dark and light red—largely disordered acidic region, dark red—sequences that are conserved in close homologues of *S. cerevisiae*; other domains labelled in figure. RQC = RecQ C-terminal motif, HRDC = helicase and RNase D C-terminal. Below are the Sgs1 domains used in Y2H experiments, which were fused to the B42 activation domain (B42-AD) in pJG46 and expressed under a galactose-inducible promoter. Numbers indicate the boundaries of the Sgs1 domains in aa. (B) Scheme of the RPA subunits with their functional domains. Rpa70 and Rpa32 were fused to the LexA-DNA binding domain (LexA-DBD) in pGAL-LexA, expressed under a galactose-inducible promoter and subjected to Y2H analysis. N-OB = N-terminal OB fold, DBD = DNA binding domain, 32 C = Rpa32 C-terminus. (C) Y2H analysis between Rpa70 fused to LexA-DBD and Sgs1 fragments fused to B42-AD was performed using a quantitative β -galactosidase assay as described in Materials and Methods. Error bars indicate standard error of four or more independent transformants. (D) Y2H analysis between Rpa70 N-OB fused to LexA-DBD and Sgs1 fragments fused to B42-AD with different deletions of the three conserved regions within the RPA binding site. (E, F) Isothermal titration calorimetry (ITC) experiment of Rpa70(3–133) with Sgs1(aa 404–485) and Sgs1(aa 404–560). The dissociation constant (K_d), stoichiometry (n) and molar enthalpy (ΔH) are indicated within the figure.

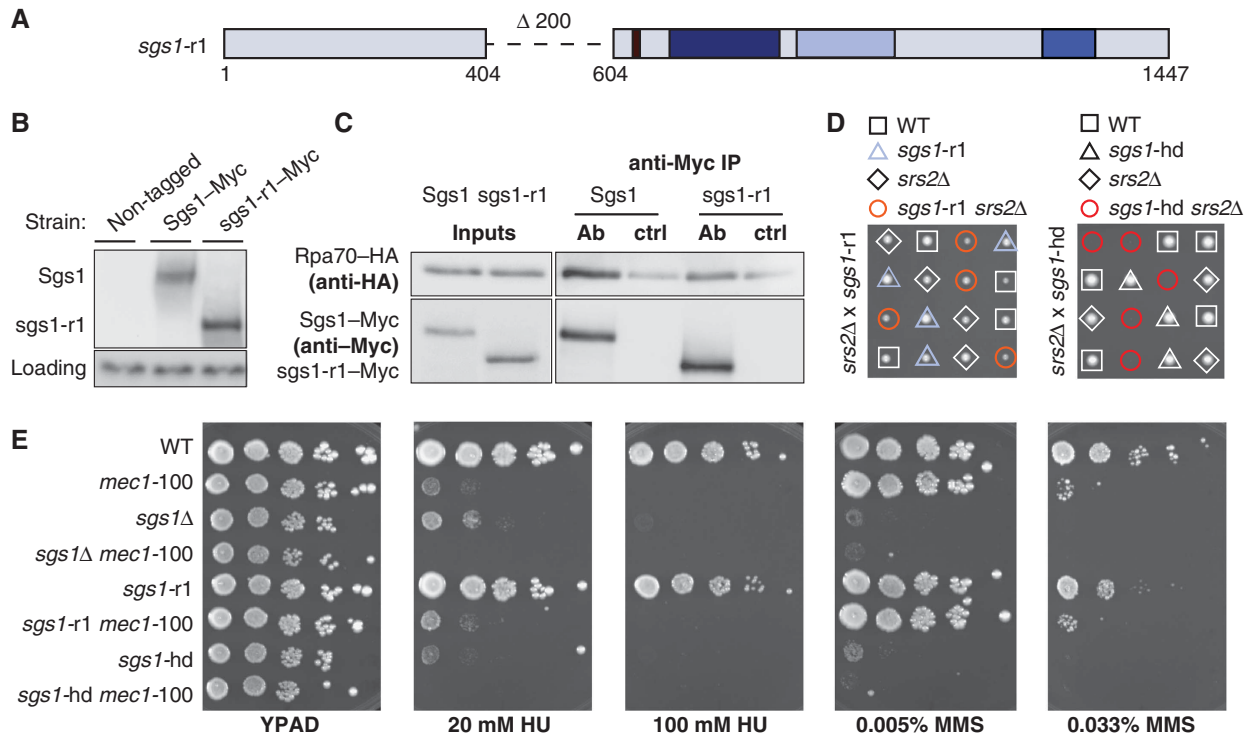


Figure 2 Loss of the acidic region in Sgs1 impairs Sgs1-RPA interaction *in vivo*. (A) Schematic representation of *sgs1-r1*: a new allele generated by deleting the acidic region (aa 404–604) at the endogenous *SGS1* locus. The deleted region is indicated by a dashed line. Black = acidic block, dark blue = helicase domain, light blue = RQC domain, blue = HRDC domain. (B) Wild type and *sgs1-r1* were C-terminally fused to 13Myc epitopes at the endogenous *SGS1* locus (Sgs1-13Myc; GA-5311, *sgs1-r1*-13Myc; GA-5313) and expression levels were analysed by western blot with anti-Myc antibody. Non-tagged strain (GA-7249) was used as a negative control. Anti-actin was used to detect Act1 as a loading control. (C) Co-IP of exponentially growing 13Myc-tagged Sgs1 (GA-1759) or *sgs1-r1* (GA-5316) with 3HA-tagged Rpa70. Exponentially growing cells were collected for IP using Dynabeads either coupled to monoclonal anti-Myc (AB) or not (ctrl). Western blots were probed with anti-Myc (9E10) for Sgs1 or *sgs1-r1* and anti-HA (F-7) for Rpa70. (D) *sgs1-r1* (GA-4848) and *srs2Δ* (GA-1805), as well as *sgs1-hd* (GA-5445) and *srs2Δ* (GA-5334) mutants were crossed and sporulated and tetrad analysis was performed. (E) Ten-fold serial dilutions of the following strains were plated onto YPAD, ± 20 mM or 100 mM HU, 0.005% or 0.033% MMS: GA-1981 (WT), GA-4978 (*mec1-100*), GA-5457 (*sgs1Δ*), GA-4967 (*sgs1Δ mec1-100*), GA-5076 (*sgs1-r1*), GA-5077 (*sgs1-r1 mec1-100*), GA-5445 (*sgs1-hd*) and GA-5447 (*sgs1-hd mec1-100*).

damage induced by different genotoxic drugs. Previous work has shown that *sgs1Δ* is sensitive to low concentrations of the replication fork inhibitor HU and the alkylating agent MMS, and that this phenotype is dramatically enhanced when *sgs1Δ* is coupled to the S phase-specific Mec1 mutant, *mec1-100* (Cobb *et al*, 2005). As described previously, we observed that both *sgs1Δ* and the helicase-dead mutant *sgs1-hd* are sensitive to HU and MMS, and show synthetic sensitivity when combined with the *mec1-100* allele (Figure 2E). This was not observed for the *sgs1-r1* mutant, although it did show a mild sensitivity to high concentrations of MMS (0.033% MMS, Figure 2E). Surprisingly, no additive effects were seen when *sgs1-r1 mec1-100* cells were compared with the single *mec1-100* mutant, suggesting that either *sgs1-r1* acts on the same pathway as *mec1-100* or it simply does not affect survival during persistent replicative stress (Figure 2E).

The Sgs1 helicase function, but not its R1 domain, stabilizes DNA pol α on HU

Given that fork restart after prolonged exposure to HU requires different activities than does growth under persistent damage, we next arrested S-phase cells in 0.2 M HU for 2–6 h, and quantitatively measured cell survival after plating on HU-free YPAD (Figure 3A). Similar to the lack of sensitivity observed on HU-containing plates, we found that *sgs1-r1* did not confer sensitivity to this acute HU treatment. Unlike

the *sgs1Δ mec1-100* or *sgs1-hd mec1-100* double mutants (Figure 3A), the *sgs1-r1 mec1-100* combination showed no additive or synergistic effects. This suggested that strong RPA-Sgs1 binding is not crucial for fork recovery after HU-induced replication fork arrest.

We next tested the effects of *sgs1-r1* on DNA pol α association at replication forks arrested on HU. We performed ChIP for DNA pol α after synchronizing single and double mutants in G1 and releasing them into S phase in the presence of 0.2 M HU. Over 1 h, the abundance of DNA-bound DNA pol α was quantified by real-time PCR analysis of the recovered DNA, using primers that amplify the early firing origin ARS607 and the late firing origin ARS522 (formerly ARS501; Figure 3E). As a negative control, a primer set placed 14 kb away from ARS607 was analysed and used to normalize the absolute enrichment at ARS607 or ARS522. As previously reported (Cobb *et al*, 2005), *sgs1Δ* or *mec1-100* cells yield lower recoveries of DNA pol α at HU-arrested replication forks (Figure 3B, black solid and stippled lines). This effect is additive when both mutations are combined, resulting in complete loss of DNA pol α from the stalled fork (Figure 3B, blue stippled line). The *sgs1-r1* mutant showed a much weaker displacement of DNA pol α than *sgs1Δ*, and was not additive when combined with the *mec1-100* mutation (Figure 3B, second panel). Similar results were obtained, when we scored DNA pol α association at two other early

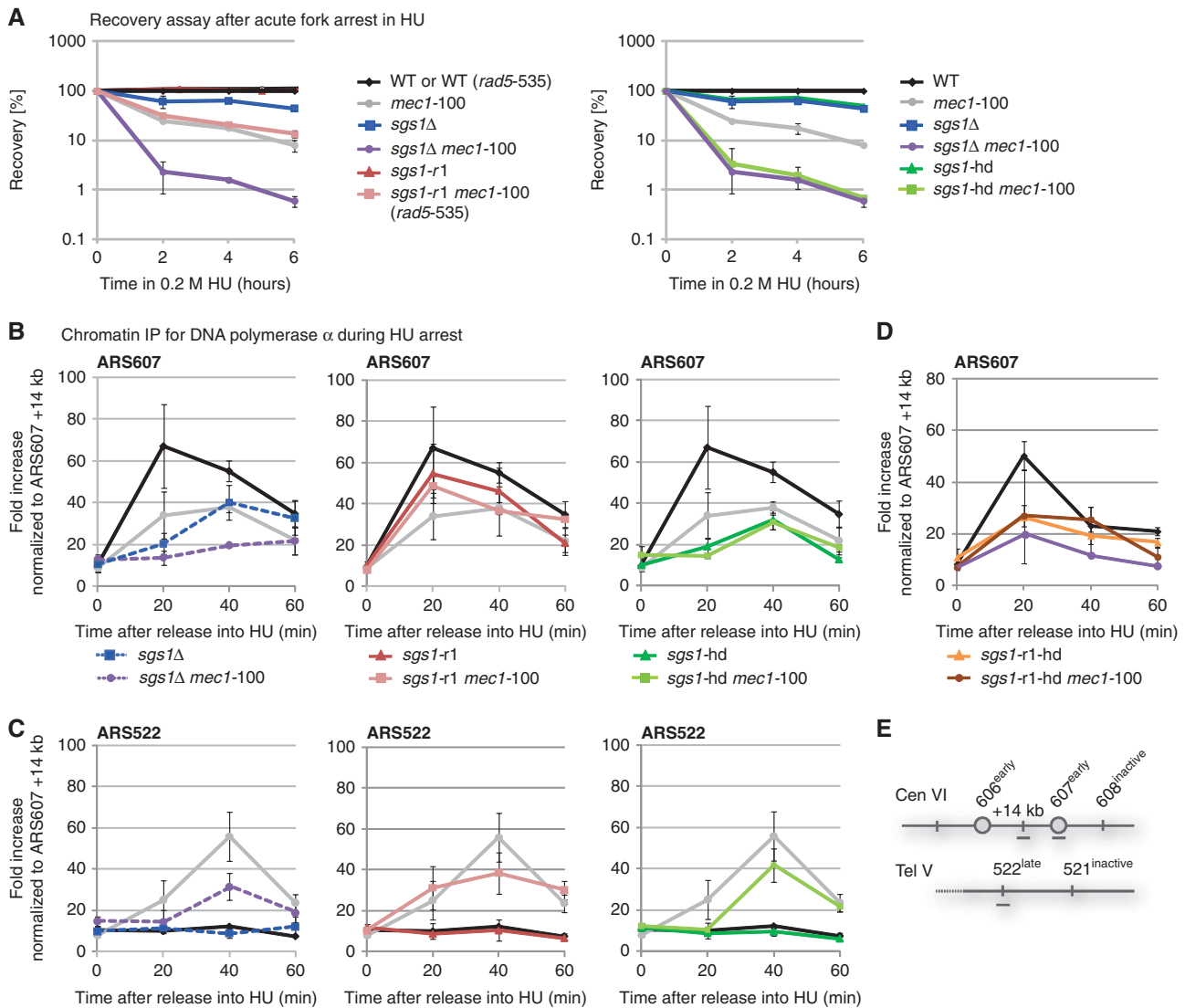


Figure 3 *sgs1-r1* does not destabilize DNA pol α from HU-stalled replication forks in contrast to a helicase-deficient *sgs1* mutant. **(A)** Recovery from replication fork stalling was monitored as colony outgrowth of cells which were synchronized in G1 by α -factor arrest and released into S phase in the presence of 0.2 M HU for the indicated times. Strains used were GA-1981 (WT), GA-180 (WT *rad5-535*), GA-5457 (*sgs1Δ*), GA-4978 (*mec1-100*), GA-4967 (*sgs1Δ mec1-100*), GA-5076 (*sgs1-r1*), GA-4504 (*sgs1-r1 mec1-100 rad5-535*), GA-5445 (*sgs1-hd*) and GA-5447 (*sgs1-hd mec1-100*). 0 min after release indicates G1 phase. **(B, C)** ChIP was performed on synchronized cultures released into S phase in the presence of 0.2 M HU. 3HA-tagged DNA pol α was precipitated with monoclonal anti-HA antibody (F-7) coupled to Dynabeads. Strains used were GA-4973 (WT), GA-4974 (*mec1-100*), GA-5055 (*sgs1-r1*), GA-5075 (*sgs1-r1 mec1-100*), GA-5449 (*sgs1-hd*) and GA-5451 (*sgs1-hd mec1-100*). The ChIP data for *sgs1Δ* and *sgs1Δ mec1-100* from Cobb et al (2005) are shown for comparison (indicated by the dashed lines). The relative enrichment for ARS607 or ARS522 was obtained by normalizing the absolute enrichment at ARS607 or ARS522 for each time point to the absolute enrichment at a locus 14 kb away from ARS607. Mutant strains are indicated using the same colour code as in **(A)**. **(D)** ChIP was performed as described above using strains GA-4973 (WT), GA-6266 (*sgs1-r1-hd*), GA-6260 (*sgs1-r1-hd mec1-100*) and GA-4975 (*sgs1Δ mec1-100*). **(E)** Primers (grey bars) used for ChIP that amplify the genomic regions corresponding to the early firing origin ARS607, a region 14 kb away from ARS607 (+14 kb) and the late firing origin ARS522 are shown.

firing origins, ARS306 and ARS606, while ARS603.5, which fires in mid-S phase, displayed a pattern similar to the late origin ARS522 (Supplementary Figure S4).

Because HU treatment activates the intra-S phase checkpoint response, late firing origins like ARS522 are repressed, and show no DNA pol α in wild-type cells (Figure 3C, black line). However, due to the compromised intra-S-phase checkpoint in *mec1-100* cells, DNA pol α is detected at the late firing origin ARS522, by 40 min on HU (Figure 3C, grey line). Interestingly, loss of Sgs1 combined with *mec1-100* reduces polymerase recovery at this late origin firing, or else partially maintains repression. However, the *sgs1-r1* mutation alone

did not promote late origin firing, and was largely epistatic with *mec1-100* for late origin activation (Figure 3C, second panel). Similar effects were observed at the mid-to-late firing origin ARS603.5 (Supplementary Figure S4). We conclude that deletion of a major Sgs1-RPA interaction domain has little or no effect on DNA pol α binding at HU-arrested forks, consistent with the colony outgrowth assay in Figure 3A.

Given that the R1 deletion did not affect polymerase binding, nor act synergistically with *mec1-100* like *sgs1Δ*, we examined if Sgs1 helicase activity is responsible for these functions. By performing ChIP in the *sgs1-hd* (K706R) and the *sgs1-hd mec1-100* double mutant (Figure 3B and C,

third panel), we scored a significant destabilization of DNA pol α at the HU-stalled fork, comparable to *sgs1 Δ* . This shows that the enzymatic activity of Sgs1 helicase is indeed critical for DNA pol α stabilization. However, the *sgs1*-hd mutation was not additive with *mec1*-100; the double mutant showed the same level of residual DNA pol α recovery as *sgs1*-hd alone (Figure 3B). Thus, whereas *sgs1*-hd and *mec1*-100 are synergistic in the recovery assay (Figure 3A), they are not with respect to polymerase stability. The *sgs1 Δ* and *mec1*-100 defects, on the other hand, are additive in both assays (Cobb *et al*, 2005).

To see if a strain that carries both the R1 deletion and helicase deficiency in Sgs1 (*sgs1*-r1-hd) shows even stronger polymerase destabilization, we tested this strain alone and in combination with *mec1*-100. However, *sgs1*-r1-hd *mec1*-100 cells resemble *sgs1*-r1-hd for polymerase ChIP, with neither completely displacing DNA pol α from ARS607 (Figure 3D). We conclude that the helicase function of Sgs1, and not its interaction with RPA, is crucial for stabilizing DNA pol α at stalled replication forks. We note that other Sgs1 functions may contribute to lagging strand replisome retention, given that *sgs1*-r1-hd *mec1*-100 cells still retain low levels of polymerase on HU-stalled forks. Consistently, *sgs1*-r1-hd mutants grew better than *sgs1 Δ* cells on 10 mM HU, although both display synergistic lethality with *mec1*-100 (Supplementary Figure S5).

The *sgs1*-r1 mutant is a separation-of-function mutant that does not cause synthetic defects with replication mutants

To shed light on the function of the R1 domain within Sgs1, we next compared the behaviour of *sgs1 Δ* and *sgs1*-r1 in a synthetic lethal screen against a sublibrary of yeast deletion strains. Previously, Collins *et al* (2007) had sorted 743 *S. cerevisiae* genes using hierarchical clustering according to the similarity of their genetic interaction profiles, which allowed them to distinguish functionally multi-protein complexes and to group different protein complexes into pathways. We performed a similar epistasis analysis (epistasis miniarray profile, E-MAP), comparing the interaction profiles of *sgs1 Δ* and *sgs1*-r1 cells with 1536 genes involved in various chromatin functions (Guénole *et al*, under review). For this, we created four sets of double mutants in two independent experiments using a high-throughput setup (Schuldiner *et al*, 2006). Genetic interactions were quantified by calculating scores based on colony sizes of double mutants (Collins *et al*, 2006). Threshold levels of genetic interaction scores equal or lower than -2 and equal or higher than $+2$ were used to define negative (synthetically sick, blue) or positive (epistatic or suppressive, yellow) genetic interactors. In Figure 4A, we list genes showing genetic interaction with either *sgs1 Δ* or *sgs1*-r1 in two independent experiments (bold), and genes that were previously shown to be synthetically lethal with *sgs1 Δ* (in red; Ooi *et al*, 2003; Tong *et al*, 2004), along with other genes falling within the relevant functional clusters (Collins *et al*, 2007).

In the E-MAP, the *sgs1*-r1 mutant displayed a distinct interaction profile from either that of *sgs1 Δ* or wild-type cells (Figure 4A). There are a few clear conclusions from this analysis. Importantly, *sgs1*-r1 did not display negative interaction with replication mutants. In particular, *sgs1*-r1 shows mildly improved growth with strains that lack en-

zymes involved in lagging strand synthesis, such as Rad27, Pol32 and RNaseH2 (Qiu *et al*, 1999; Arudchandran *et al*, 2000; Li and Brill, 2005), whereas the *sgs1 Δ* mutant showed synthetic sickness with these strains, even under non-damaging conditions. Neither query strain scored negatively with genes involved in homologous recombination, perhaps because the screen was performed under non-damaging conditions. Nonetheless, several interactions stand out as having negative synthetic effects with *sgs1*-r1, namely *mus81 Δ* and *wss1 Δ* . Mus81 works together with Mms4 as a Holliday junction resolvase that is thought to work together with Sgs1-Top3-Rmi1 to process homologous recombination repair (HRR) intermediates that occur behind replication forks (for review, Hickson and Mankouri, 2011). Wss1 is a SUMO peptidase associated with Slx5/Slx8, the SUMO-dependent Ubiquitin ligase required for telomere-telomere recombination and recovery from fork collapse (Mullen *et al*, 2010; Nagai *et al*, 2011).

We confirmed the strongly negative interaction of *sgs1*-r1 with *mus81 Δ* by generating the double mutant independently. The slow growth phenotype persisted and cells were hypersensitive to HU (Figure 4B), while the *mus81 Δ* *sgs1 Δ* strain was synthetic lethal (data not shown and Tong *et al*, 2001). This implicates the R1 domain of Sgs1 in the resolution of, or recovery from, recombination events at the fork, particularly those that might form in the absence of Mus81-Mms4. We note, however, that *sgs1*-r1 does not aggravate the HRR pathway *per se* (Figure 4A, including *rad51 Δ* , Supplementary Figure S6B). Based on the E-MAP data, we suspected that *slx4 Δ* , *slx5 Δ* , *slx8 Δ* and *mre11 Δ* might also be synthetic lethal with *sgs1*-r1, since they failed to yield E-MAP results. We crossed strains bearing these null alleles with *sgs1*-r1 and again tested synthetic lethality. We confirmed that *slx4 Δ* , *slx5 Δ* and *slx8 Δ* are synthetic lethal with *sgs1*-r1, whereas *mre11 Δ* is not (Figure 4A; data not shown). This result suggests that the R1 domain of Sgs1 confers an essential function when cells lack the activity for Slx5/Slx8 SUMO-dependent ubiquitin ligase or the Slx4-Slx1 structure-specific endonuclease. These results are fully consistent with the synthetic lethality observed in the absence of Wss1, which forms a complex with Slx5/Slx8, or of Mus81, which together with Mms4 helps resolve strand-exchange events, in parallel to the Slx4-Slx1 complex (Muñoz-Galván *et al*, 2012). In contrast, even though the loss of topoisomerase I should enhance torsional stress and promote strand exchange, we saw only a minor negative interaction between *sgs1*-r1 and *top1 Δ* , by E-MAP or in drop assays on HU (Supplementary Figure S6A).

We extended the E-MAP observations to conditions of replicative stress by testing different mutant combinations with *sgs1*-r1 or *sgs1 Δ* on plates containing HU (Figure 4B). Consistently, we saw that combinations of *sgs1*-r1 with genes that function in lagging strand synthesis (*pol32 Δ* , *rad27 Δ*) do not show negative interactions even on HU, while the corresponding double mutants with *sgs1 Δ* showed either synthetic lethality or synthetic slow growth (Figure 4A and B). Similarly, there was no synthetic defect when *sgs1*-r1 was combined with the deletion mutant of the origin and replication fork associated F-box protein Dia2 (Mimura *et al*, 2009; Morohashi *et al*, 2009), either with or without HU (Figure 4A and B). Consistent with the ChIP data, we conclude that the *sgs1*-r1 mutation does not destabilize the stalled replication

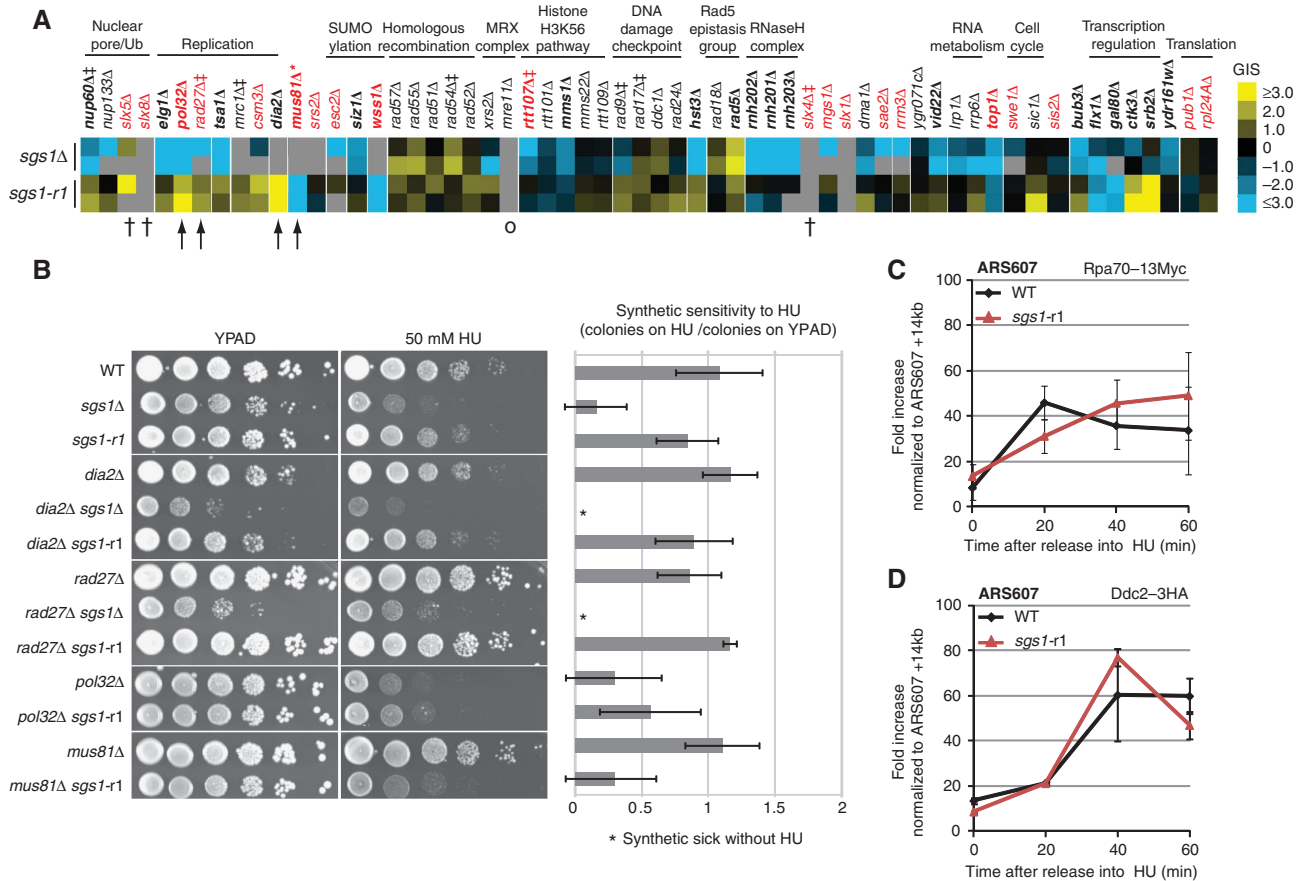


Figure 4 *sgs1-r1* does not interact genetically with lagging strand replication machinery. **(A)** Genetic interaction profiles of *sgs1Δ* and *sgs1-r1* were determined by crossing with a strain library comprising 1536 knockout alleles (Guénole *et al*, under review) and measuring growth of resulting double mutants as described in Materials and Methods. Genetic interaction scores (GIS) of selected double mutants obtained from two independent experiments are depicted by colour (positive (yellow) = epistatic/suppressive, negative (blue) = synthetically sick). Genes were sorted into functional groups as performed earlier (Collins *et al*, 2007). Bold represents the mutant genes with GIS above threshold (-2 for negative or $+2$ for positive interactions) for double mutants with *sgs1Δ* and/or *sgs1-r1* in two independent screens. Red represents gene deletions previously reported as synthetically lethal with *sgs1Δ* (Tong *et al*, 2001). Genes marked with ‡ were previously reported to be a target of checkpoint kinases (Chen *et al*, 2010). Mus81 (*) was reported to be a target of *S. pombe* Cds1 (*S. cerevisiae* Rad53) (Kai *et al*, 2005). The † indicates genes that showed synthetic lethality with *sgs1-r1*, while o indicates no synthetic lethal interaction. Arrows indicated mutants further analysed in **(B)**. **(B)** Left: a representative picture of 10-fold serial dilutions of the following strains plated onto YPAD and YPAD with 50 mM HU: WT, GA-1981 (*WT*), GA-5457 (*sgs1Δ*), GA-5076 (*sgs1-r1*), GA-7549 (*dia2Δ*), GA-7540 (*dia2Δ sgs1Δ*), GA-7542 (*dia2Δ sgs1-r1*), GA-7548 (*rad27Δ*), GA-7530 (*rad27Δ sgs1Δ*), GA-7532 (*rad27Δ sgs1-r1*), GA-7498 (*pol32Δ*), GA-7499 (*pol32Δ sgs1-r1*), GA-7494 (*mus81Δ*) and GA-6326 (*mus81Δ sgs1-r1*). Right: the number of colonies scored on 50 mM HU plates normalized by colony number on YPAD plates. Error bars indicate standard deviation of three independent experiments. **(C, D)** ChIP of 13Myc-tagged RPA or 3HA-tagged Ddc2 using strains GA-5525 (WT) and GA-5365 (*sgs1-r1*) as described in Figure 3.

fork. However, *sgs1-r1* is important when cells are deficient for functional complexes that promote replication fork recovery through exchange or invasion of the sister chromatid.

Given that the R1 domain of Sgs1 binds RPA, we asked whether the RPA levels at the stalled replication fork might be altered in the *sgs1-r1* mutant. However, levels of Myc-tagged RPA at the early origin ARS607 were not changed in *sgs1-r1* cells synchronously arrested in S phase by 0.2M HU (Figure 4C). RPA was undetectable at the late firing origin ARS522 (Supplementary Figure S7A). This argues that although RPA-Sgs1 interaction is diminished in *sgs1-r1* cells, it neither affects RPA deposition at stalled replication forks, nor the amount of ssDNA generated. Synthetic lethality might also arise through an inability to recruit or activate Mec1-Ddc2. To test this, we performed ChIP for the essential Mec1 cofactor, Ddc2, in both wild-type and *sgs1-r1* cells (Figure 4D; Supplementary Figure S7B). Again, we detected no change in the level of Mec1-Ddc2 recruitment in the

R1 mutant. We conclude that the R1 domain functions, but on a pathway that is essential in the absence of Mus81, Slx4/Slx1 or the Slx5/Slx8/Wss1 ubiquitin conjugating complex.

The Sgs1 R1 domain is phosphorylated by Mec1 in vitro and in vivo

Earlier work had implicated a function of Sgs1 in intra-S phase checkpoint activation, independent of its enzymatic activity (Frei and Gasser, 2000; Bjergbaek *et al*, 2005). We therefore investigated whether the R1 domain of Sgs1 might be implicated in checkpoint activation, or be a target of Mec1-Ddc2 phosphorylation. Activation of the intra-S phase checkpoint by Mec1 occurs through the phosphorylation of numerous targets containing SQ/TQ motifs. Previous studies report that Mec1 substrates often contain several closely spaced motifs, which are also referred to as SQ/TQ cluster domains (SCDs; Traven and Heierhorst, 2005). Such SCDs are

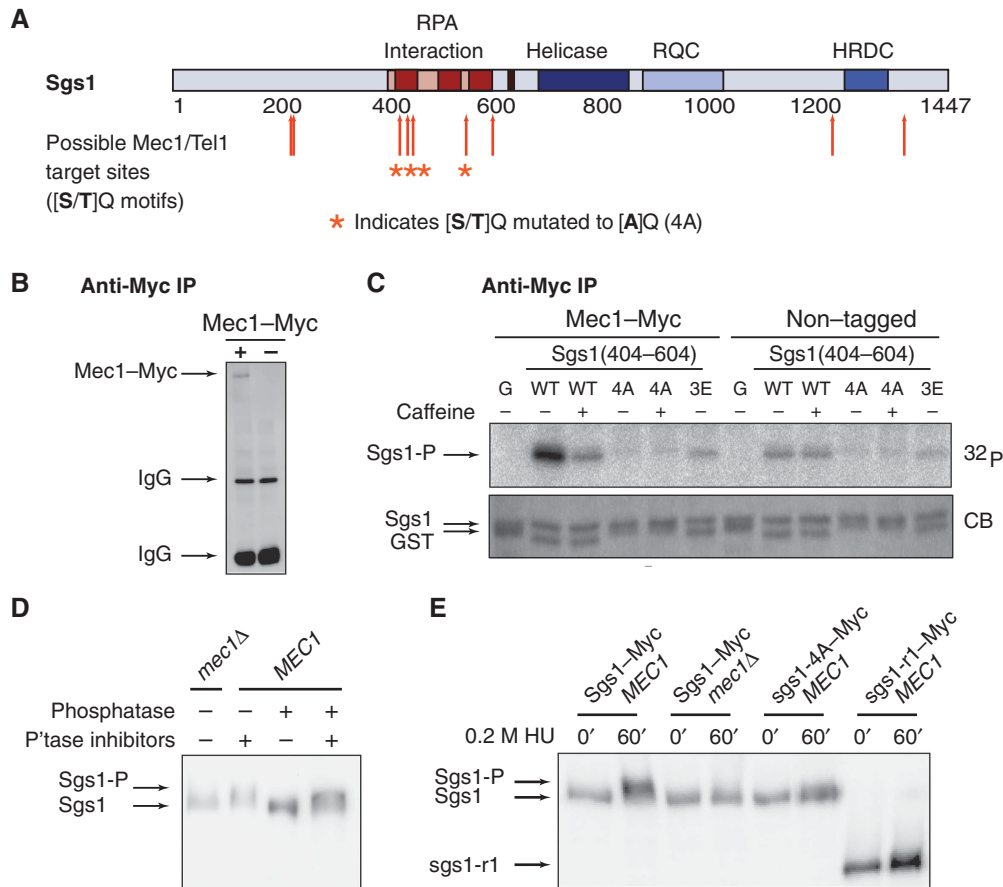


Figure 5 Mec1 targets the RPA-interacting site on Sgs1 *in vitro* and *in vivo*. (A) Schematic representation of Sgs1 with its functional domains. Mec1/Tel1 consensus target sites are indicated by red arrows, while asterisks tag phospho-acceptor sites mutated to A or E. (B) Exponentially growing GA-1456 (Mec1-18Myc) and GA-426 (non-tagged) cells were exposed for 1 h to 0.1% MMS. After cell lysis, Mec1-18Myc was precipitated using anti-Myc coupled Sepharose beads and analysed by western blot. (C) Kinase assay using Mec1-18Myc or control immunoprecipitates (non-tagged lysates). Sgs1 peptides (aa 404–604) were used as substrates in the presence of γ - 32 P-ATP and analysed by gel electrophoresis and autoradiography. Where indicated, 30 mM caffeine was added to the reaction to inhibit Mec1. Mutant Sgs1 peptides were as follows: 4A = Sgs1(404–604-T451A-S470A-S482A-T585A) or 3E = Sgs1(404–604-T451E-S470E-S482E). 32 P autoradiography and Coomassie Brilliant Blue (CB) staining are shown. (D) Exponentially growing GA-6402 (Sgs1-13Myc) cells were exposed for 2 h to 0.2 M HU. Native extracts were treated with phosphatase and/or phosphatase inhibitors as described in Materials and methods and subjected to western blot analysis using anti-Myc antibody. A denatured extract of GA-6403 (Sgs1-13Myc *mec1* Δ) cells treated as described in (E) was loaded as a control. (E) Cells were synchronized in G1 by α -factor arrest and released into S phase in the presence of 0.2 M HU for 60 min. Protein extracts were analysed by western blot using anti-Myc antibody. Strains used were GA-6402 (Sgs1-13Myc), GA-6403 (Sgs1-13Myc *mec1* Δ), GA-7485 (sgs1-4A-13Myc) and GA-5313 (sgs1-r1-13Myc).

defined by at least three SQ/TQ motifs within 100 aa with additional sites within another 100 aa. The human Sgs1 homologues BLM and WRN contain such clusters and are phosphorylated by ATR/ATRIP (Pichierrri *et al*, 2003; Davies *et al*, 2004; Rao *et al*, 2005), the human homologue of Mec1-Ddc2.

Sequence analysis revealed nine SQ or TQ sites within Sgs1, of which four are clustered in the R1 region (T₄₅₁Q₄₅₂, S₄₇₀Q₄₇₁, S₄₈₂Q₄₈₃, T₅₈₅Q₅₈₆) with a fifth nearby (S₆₂₈Q₆₂₉; Figure 5A). To test if this domain of Sgs1 was indeed a target for Mec1 *in vitro*, we expressed Sgs1 aa 404–604 in bacteria and challenged it with kinase immunoprecipitated from a yeast strain expressing an epitope-tagged Mec1. A parallel precipitate from a yeast strain lacking the 18Myc tag was used as a control (Figure 5B and C). The Sgs1(404–604) domain is a robust substrate for Mec1-Myc phosphorylation (Figure 5C). We could significantly reduce the phosphate incorporation into the domain by adding the Mec1/Tel1 inhibitor caffeine to the *in-vitro* reaction, while the

background phosphorylation in a non-tagged strain was not caffeine sensitive.

We next mutated the SQ/TQ motifs in this region and purified substrates with either alanine or glutamate substitutions at the relevant phospho-acceptor sites, generating *sgs1-4A* (Sgs1(404–604-T451A-S470A-S482A-T585A)) and *sgs1-3E* (Sgs1(404–604-T451E-S470E-S482E)). These mutations efficiently abolished the modification of Sgs1 by precipitated Mec1-18Myc (Figure 5C). As the *sgs1-3E* mutant was also sufficient to abrogate Sgs1 phosphorylation *in vitro*, it is likely that Mec1-Ddc2 targets T₄₅₁, S₄₇₀ and/or S₄₈₂.

To investigate whether Sgs1 is phosphorylated *in vivo*, we examined extracts from both wild-type and *mec1* Δ *sml1* Δ strains expressing Sgs1-13Myc, after growth for 2 h in 0.2 M HU. Indeed, in wild-type cells a diffuse and more slowly migrating form of Sgs1-13Myc was observed, that was not detected in cells lacking Mec1 (Figure 5D), or in wild-type cells not treated with HU (data not shown). Treatment of the cell lysate with phosphatase eliminated the presence of the

slower migrating band, while the addition of both phosphatase and phosphatase inhibitors restored the signal. We conclude that the slower migrating band of Sgs1 reflects a phosphorylated form, generation of which requires Mec1 kinase.

We next asked whether Mec1 indeed targets the R1 region of Sgs1, by expressing Myc-tagged versions of wild-type Sgs1, and mutant forms bearing either the four S/T mutations (sgs1-4A-13Myc) or a deletion of the entire R1 domain (sgs1-r1-13Myc). We examined the shift in mobility in cells that were first synchronized in G1 and released into medium containing 0.2 M HU. A strain lacking Mec1 kinase (*mec1Δ sml1Δ*) was used as a control (Figure 5E). Sgs1-13Myc did not show a shift in G1-arrested *MEC1* cells, while the slower migrating, phosphorylated form was evident in cells exposed to HU (Figure 5E). The phosphorylation of Sgs1 was lost in *mec1Δ sml1Δ* cells exposed to HU, and importantly, also greatly diminished in both the *sgs1-4A-13Myc* and *sgs1-r1-13Myc* mutants (Figure 5E). We detected a residual shift in the *sgs1-4A-13Myc* and *sgs1-r1-13Myc*, which may be explained by phosphorylation outside of the R1 domain. Indeed, our own LC-MS/MS data and data of (Bodenmiller *et al*, 2008, 2010) indicate that Sgs1 may be phosphorylated either on residue 1221/1222/1223 (Supplementary Table S2) or on residues 348, 1268 or in peptide aa 605–619. These Sgs1 phospho-acceptor sites are not typical Mec1 target sites as they lack the SQ/TQ consensus, and they may reflect phosphorylation by a kinase downstream of Mec1. Important to note is that the confirmed *in-vitro* Mec1 target sites within the R1 domain (T₄₅₁ and/or S₄₇₀) are found within a large tryptic cleavage fragment that could not be detected in our MS analysis (47 aa; see Supplementary Table S2), even when combined chymotryptic and tryptic digestions were used (data not shown). In contrast, S₄₈₂ is in a smaller peptide that is not phosphorylated *in vivo*.

Earlier work from our laboratory showed that Sgs1 interacts directly with the FHA1 domain of the major Mec1 target and checkpoint kinase, Rad53 (Bjergbaek *et al*, 2005). The FHA1 domain of Rad53 is a phosphopeptide binding module that has a key role for both intra-S checkpoint activation and late origin control (Pike *et al*, 2004a). To determine whether the Mec1-modified R1 domain of Sgs1 is the site of Rad53 interaction, we first employed Y2H assays. We detect a strong interaction between the core Sgs1 fragment (290–1180) and the FHA1 domain of Rad53, which is entirely lost upon deletion of aa 404–604 (*sgs1-r1*; Figure 6A). The Sgs1 sub-domain aa 292–661 was sufficient to mediate binding to the Rad53 FHA1 domain, and again, deletion of aa 404–604 ablated interaction with Rad53 FHA1 (Figure 6A). We also tested a non-phosphorylatable *sgs1-4A* substitution within the smaller Sgs1 fragment, which gave a 50% drop in β -galactosidase signal, suggesting that phosphorylation is important for high binding affinity, although contacts to flanking residues may contribute to the interaction (Figure 6A). Given that Y2H assays can detect indirect interactions, we decided to turn to a more quantitative binding assay to evaluate the importance of the Mec1 phosphorylation sites on the Sgs1-Rad53 interaction.

Using ITC with the FHA1 domain and short Sgs1 peptides that encompass phosphorylated T₄₅₁, S₄₇₀ or S₄₈₂ (Sgs1 (446–456), Sgs1(466–475) and Sgs1(478–487) respectively), we analysed the interaction between these peptides and the

minimal FHA1 domain (aa 22–162) comparing phosphorylated and non-phosphorylated acceptor sites. Remarkably, only the Sgs1(446–456) peptide carrying a phosphorylated T₄₅₁Q₄₅₂, and not its unphosphorylated counterpart, bound the FHA1 domain of Rad53 (Rad53(22–162) significantly (Figure 6B). The phosphorylated Sgs1(446–456) peptide had a dissociation constant $K_D = 21 \pm 0.2 \mu\text{M}$ for the FHA1 domain, a value that is similar to that observed between Rpa70(3–133) and Sgs1(404–560) (Figure 1F). Two other peptides bearing phospho-serine (S₄₇₀ in Sgs1(466–475) and S₄₈₂ in Sgs1(478–487)) did not show significant binding to the Rad53 FHA1 domain by ITC (Supplementary Figure S8), consistent with the demonstrated preference of FHA1 for p-Thr over p-Ser (Durocher *et al*, 2000; Pennell *et al*, 2010).

To determine if the phosphorylation of Sgs1 by Mec1 on these residues also mediates Rad53 interaction *in vivo*, we performed co-IP experiments with strains expressing Rad53-9PK and either Sgs1-13Myc or *sgs1-4A-13Myc*. A strain lacking the Sgs1-Myc tag was used as a control. Cells were synchronized in G1 and released into 0.2 M HU for 60 min, prior to lysis in buffer with phosphatase inhibitors. Precipitation by anti-Myc antibody, and subsequent western blotting with anti-PK or anti-Myc antibodies, showed that Rad53-9PK and Sgs1-13Myc precipitate efficiently as a complex (Figure 6C and D). The amount of Rad53-9PK recovered with *sgs1-4A-13Myc* was >2-fold less than with wild-type Sgs1 (Figure 6C and D). We conclude that Sgs1 interacts with Rad53 in a phosphorylation-dependent manner, requiring modification on SQ/TQ acceptor sites within its R1 domain. The RPA-interaction site on Sgs1 would thus be targeted by Mec1 after HU-induced replication fork stalling, enabling phospho-T₄₅₁ interaction with Rad53.

***sgs1-r1* cells display a defect in Rad53 activation in a rad24 background**

Previous studies have shown that Sgs1 and Rad24 act on parallel pathways to activate Rad53 when cells are exposed to HU during S phase (Frei and Gasser, 2000; Bjergbaek *et al*, 2005), yet how Sgs1 leads to Rad53 activation is unclear. Since both the helicase activity of Sgs1 and its interaction with Top3 are dispensable for Rad53 activation (Bjergbaek *et al*, 2005), we next examined whether the *sgs1-r1* and/or *sgs1-4A* mutations, which lack the Mec1-dependent phosphorylation sites and show reduced binding to Rad53 in Y2H, ITC and *in-vivo* assays, have an effect on checkpoint activation.

We released G1-synchronized cells into HU-containing media for 30 or 60 min and monitored Rad53 activation on SDS-PAGE. The hyper-phosphorylated, activated form of Rad53 was visualized on western blots as a band with delayed migration (Figure 6E). We tested the impact of either *sgs1-r1* or *sgs1-4A* in both wild-type and *rad24* mutant backgrounds, since Rad24/9-1-1 contributes to checkpoint activation through an alternative pathway in response to fork stalling (Frei and Gasser, 2000). Upon release from α factor arrest into HU, Rad53 became phosphorylated, not only in wild-type cells, but also in *rad24Δ*, *sgs1-r1* or *sgs1-4A* single mutant cells, as well (Figure 6E). In the *sgs1-r1 rad24Δ* double mutant, however, the upshift of Rad53 was significantly reduced, as observed in the *sgs1Δ rad24Δ* mutant. Similarly, the *sgs1-4A* in combination with *rad24Δ* showed a

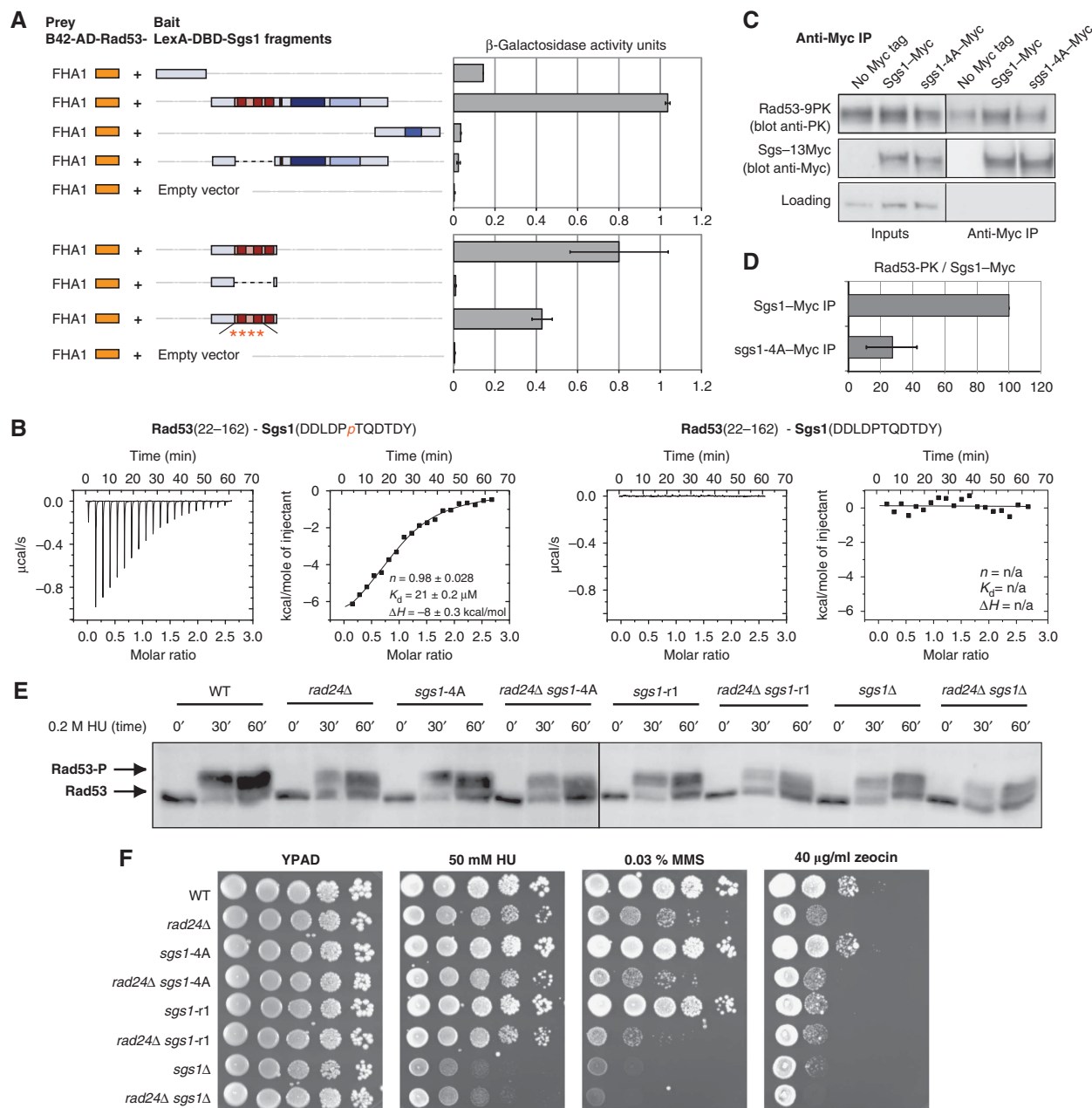


Figure 6 Sgs1 phosphorylation promotes Sgs1-Rad53 interaction. (A) Y2H analysis of Rad53-FHA1 fused to the B42-AD and Sgs1 fragments fused to LexA-DBD, as in Figure 1. Asterisks indicate phospho-acceptor sites mutated to alanine. (B) ITC assay of the FHA1 domain of Rad53, Rad53(22–162), and two Sgs1(446–456) peptides, Sgs1 (DDLDP_pTQDTDY), encompassing either phosphorylated T₄₅₁Q₄₅₂ (left panel) or non-phosphorylated T₄₅₁Q₄₅₂ (right panel). Parameters as in Figure 1E. (C) Co-IP of 13Myc-tagged Sgs1 (GA-7487), sgs1-4A (GA-7483) or sgs1-4A-Myc (GA-7467) with 9PK-tagged Rad53. Cells were released from G1 (α -factor arrest) for 60 min in the presence of 0.2 M HU and lysed for Dynabead-IP using monoclonal anti-Myc. Western blots were probed with anti-Myc for Sgs1 or sgs1-r1 and anti-PK for Rad53. An anti-PK-cross-reacting 250 kDa protein served as loading control. (D) Quantification of three independent Sgs1-Rad53 co-IP experiments. The unspecific binding (no tag control) signal was subtracted from Rad53-9PK signals in Sgs1- and sgs1-4A IPs, and normalized to Sgs1-13Myc or sgs1-4A-13Myc signals in the IP fractions. Error bars indicate standard deviation. (E) Rad53 activation in GA-1981 (WT), GA-5321 (*rad24Δ*), GA-5932 (*sgs1-4A*), GA-5934 (*sgs1-4A rad24Δ*), GA-5076 (*sgs1-r1*), GA-5324 (*sgs1-r1 rad24Δ*), GA-1761 (*sgs1Δ*) and GA-2056 (*sgs1Δ rad24Δ*). Cells were synchronized in G1 by α -factor arrest and released for 60 min into 0.2 M HU before denatured extract preparation as done previously (Pike *et al*, 2003). Rad53 phosphorylation (Rad53-P) was monitored by western blot with anti-Rad53. (F) Ten-fold serial dilutions of (WT), GA-5321 (*rad24Δ*), GA-5932 (*sgs1-4A*), GA-5934 (*sgs1-4A rad24Δ*), GA-5076 (*sgs1-r1*), GA-5324 (*sgs1-r1 rad24Δ*), GA-5457 (*sgs1Δ*) and GA-2056 (*sgs1Δ rad24Δ*) on YPAD \pm 50 mM HU, 0.03% MMS, or 40 μ g/ml Zeocin.

strongly impaired upshift of Rad53. Since Mec1-Ddc2 recruitment is not altered in *sgs1-r1* cells (Figure 4D), we conclude that the drop in Rad53 activation likely stems from impaired Rad53 recruitment by Sgs1.

Finally, we checked the effect of the Mec1 target sites in Sgs1 by combining the *sgs1-4A* mutant with *mec1-100* or

rad24Δ. In a drop assay on media containing HU, cells expressing a non-phosphorylatable *sgs1-4A* protein, behaved like *sgs1-r1* cells: both showed wild-type sensitivity to HU and both were epistatic with *mec1-100* (Figure 2E; Supplementary Figure S9A). Indeed, when we scored recovery from HU-induced arrest in S phase, the *sgs1-4A* mutant cells behaved

like wild-type cells, even though the synergy of *sgs1Δ* with *mec1-100* was readily reproducible (Supplementary Figure S9B). This was also true, when we combined *sgs1-r1* and *sgs1-4A* mutant cells with *rad24Δ* cells in survival assays on HU (Figure 6F). However, when double mutants were scored on MMS, we found that *sgs1-r1* is slightly additive with *rad24Δ*, and, both alone and in combination with *rad24Δ*, *sgs1-r1* was as sensitive as either *rad24Δ* or *sgs1Δ* to Zeocin (Figure 6F). Surprisingly, *sgs1-4A* was not, suggesting that the R1 domain contributes more than just assisting checkpoint activation, which was reduced identically in *sgs1-r1* and *sgs1-4A* mutants (Figure 6E). This is consistent with the E-MAP data which implicated the R1 domain in the resolution of strand-exchange intermediates that might arise as a result of double-strand breaks. The sensitivity of the *sgs1-r1* mutation to Zeocin may reflect both Rad53 recruitment and a downstream function that is partially redundant with Mus81-Mms4 or Slx4-Slx1 (Figure 4A and B).

Discussion

RecQ helicases have been implicated in the maintenance of genome stability in multiple pathways, some of which involve the double cross-over resolving activity of Top3, while others do not (Cobb and Bjergbaek, 2006). Here, we show that the role of Sgs1 in preserving DNA pol α on the lagging strand at stalled replication forks is largely due to its helicase activity (Figure 3). Despite the strong affinity shown by Sgs1 for RPA, deletion of a major interaction site within Sgs1 for Rpa70 did not destabilize DNA pol α during HU arrest. On the other hand, we found that the Rpa70-binding domain also mediates interaction with the downstream checkpoint kinase Rad53 (Figure 5). Given that both *in vitro* and *in vivo* this interaction requires the phosphorylation of Sgs1 by the ATR homologue, Mec1, we propose that the Sgs1 phospho-R1-Rad53 interaction occurs only under conditions that activate Mec1-Ddc2, for example, at stalled replication forks.

Functional studies confirm the relevance of the interaction between the phosphorylated Sgs1 R1 domain with Rad53 FHA1, a domain of demonstrated importance for intra-S phase checkpoint activation (Boddy *et al*, 2000; Pike *et al*, 2004b; Smolka *et al*, 2006). Using appropriate mutants, we show that the R1 domain and the Mec1 phosphorylation sites within this domain contribute to Rad53 activation during fork arrest. This is most obvious in a *rad24Δ* background. Whether loss of Rad24 leads to a particular type of damage that requires Sgs1-mediated Rad53 recruitment, or whether it simply unmasks the dependence of the event on Sgs1, is unknown. However, our results suggest that the *sgs1-r1* mutation neither impairs the generation of ssDNA nor Mec1-Ddc2 recruitment (Figure 4C and D); nonetheless, it affects Rad53 activation during fork arrest on HU (Figure 6E). We therefore suggest that the R1 domain of Sgs1, once modified by Mec1, recruits Rad53 to the complex of ssDNA, RPA, Ddc2-Mec1, to facilitate its activation. This demonstrates a non-enzymatic role of Sgs1 in the DNA damage response at stalled forks (Figure 7). Sgs1 clearly plays other roles in the pathways leading to replication fork recovery, namely, the helicase-dependent reversal of fold-back structures and the resolution of unproductive strand exchange events behind the fork (reviewed in Bernstein *et al*, 2010).

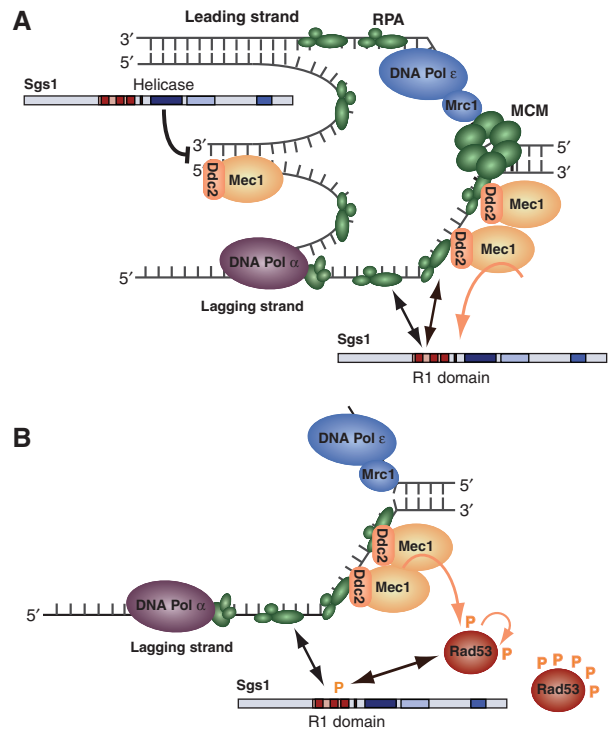


Figure 7 Multiple roles for Sgs1 helicase at stalled replication forks: reversal of fold-back structures, polymerase stabilization and Rad53 recruitment. (A) Sgs1 helicase activity contributes to the retention of DNA polymerases at stalled replication forks possibly by reversal of fold-back or strand invasion structures between nascent or template strands. The checkpoint kinase Mec1-Ddc2 is recruited to ssDNA coated by RPA and phosphorylates Sgs1 in the R1 domain. The green hexameric ring is the MCM helicase. (B) Sgs1 phosphorylation may shift Sgs1 binding preference from RPA to the Rad53 FHA1 domain. This could recruit Rad53 into close proximity of Mec1-Ddc2 which is associated with stalled forks. Mec1-Ddc2 then phosphorylates Rad53, to activate it and initiate the intra-S phase checkpoint response.

Multiple binding sites in a domain upstream of the Sgs1 helicase domain

The domain we identify here in Sgs1 as both an RPA and Rad53 binding site is upstream of the helicase domain and overlaps partially with an acidic domain (aa 502–648) implicated in replication fork stability on MMS (Bernstein *et al*, 2009). We define both an RPA-binding region (aa 404–560) and a Rad53-binding motif (aa 446–456), and show by ITC, Y2H interaction and co-IP that the latter interaction is phosphorylation dependent, while the former is not.

Both the interaction sites and the Mec1 acceptor sites that we have mapped are distinct from the *sgs1-D664Δ* point mutant studied by Bernstein *et al* (2009), which partially mimics the larger deletion. Their AR2 deletion does not eliminate the Sgs1-FHA1 interaction site, but may have indirect effects, given that the mutant protein appeared to be unstable. Both the RPA and Rad53 binding activities of Sgs1 are also independent of the Siz1/Siz2 sumoylation site K621 in Sgs1, which remains intact in our mutants, but was removed by the AR2 deletion (SC Teng, personal communication). Nonetheless, the *sgs1-r1* mutant shows similar phenotypes as *sgs1-AR2Δ* or *sgs1-D664Δ* with respect to HU and MMS sensitivity during continuous growth on plates. Both sets of mutations suppress *top3Δ* slow growth (Supplementary Figure S3), and thus retain Sgs1 helicase activity (Bernstein *et al*, 2009).

sgs1-hd mutants fail to stabilize the replisome at stalled forks

In our attempt to explore the importance of Sgs1–RPA interaction on lagging strand polymerases, we found instead that Sgs1 helicase activity is essential for the maintenance of DNA pol α at ARS607 (Figure 3). Additional removal of the R1 domain in the *sgs1-r1-hd* mutant did not aggravate this effect. This result supports earlier findings from our laboratory suggesting that *sgs1-hd* expression cannot complement *sgs1 Δ* for DNA pol ϵ stability on HU (Cobb *et al*, 2003). We show by epistasis analysis that *sgs1-r1* is a separation of function mutant, because *sgs1-r1*, unlike *sgs1 Δ* , does not exhibit negative synthetic interaction when combined with replication mutants. Nonetheless, the R1 domain contributes to Rad53 activation on HU, and shows strong synergistic lethality with deletions of *mus81*, *slx4*, or with *slx5* and/or *slx8* (Figure 4).

These results argue that Sgs1 probably contributes to replication polymerase stability by a dissolution of fold-back structures (i.e., upstream of Mec1 activation) and/or resolution of strand exchange behind the fork (Bennett *et al*, 1999; Bjergbaek *et al*, 2005; Ashton and Hickson, 2010). Holliday junction dissolution is especially important for restart of a collapsed fork after DNA damage, which occurs after persistent exposure with MMS or HU in drop assays. Consistently, both Sgs1 helicase activity and its Top3 interaction contribute to DNA repair and survival during prolonged exposure to HU or MMS. This may explain the synthetic lethality observed between *sgs1-r1* and *mus81 Δ* and *slx4 Δ* in the E-MAP analysis, since strand exchange is thought to enable the fork restart that is necessary when lesions block leading or lagging strand elongation (Lambert *et al*, 2010; Muñoz-Galván *et al*, 2012). Given that these pathways may be controlled by Slx5–Slx8 ubiquitination and subsequent degradation of a factor blocking strand exchange, all E-MAP results are consistent with a contribution of the R1 domain of Sgs1 to this pathway.

What, then, is the importance of the Sgs1–RPA interaction? Whereas RPA has been shown to stimulate RecQ helicase activity in human cells (Shen *et al*, 2003; Machwe *et al*, 2006; Sowd *et al*, 2009; Yodh *et al*, 2009), it is not clear that RPA truly promotes unwinding. Direct interaction of RPA with RecQ helicases may alter enzymatic activity through a conformational change or switch in the oligomeric state of the RecQ helicase. It is noteworthy that RPA also counteracts the annealing activity of the RecQ helicase by stabilizing the ssDNA that occurs from unwinding (Bachrati and Hickson, 2008). Different Sgs1–RPA disruption mutants or further analysis of the relevant Rpa70 OB fold will be necessary to identify the exact role of Sgs1–RPA interaction for helicase activity and replication fork integrity.

Sgs1 R1 domain phosphorylation by Mec1-Ddc2 aids Rad53 activation

The most novel aspect of our study is to show how Sgs1 contributes to Rad53 activation during conditions that arrest replication forks. We propose that phosphorylated Sgs1 interacts with the FHA1 domain of Rad53 to promote Rad53 recruitment to sites of damage. We found that Sgs1 is a target of Mec1 *in vitro* and *in vivo* and we map the phosphorylation sites to the Rad53-interaction domain. Importantly, ITC stu-

dies show that the binding of Sgs1(446–456) to Rad53 FHA1 is phospho-threonine dependent, while Sgs1 binding to RPA through the same domain is not. We confirm that mutation of the key Mec1 acceptor sites alters Rad53 activation, Sgs1–Rad53 interaction, and deletion of the domain confers sensitivity to Zeocin. We do not know if phosphorylation of the Sgs1 R1 domain also facilitates Rad53 recruitment to DSBs, but we consider it likely.

An additional fork-associated adaptor protein, Mrc1, has been implicated as a bridge between Mec1–Ddc2 and Rad53 activation at stalled replication forks (Alcasabas *et al*, 2001; Osborn and Elledge, 2003; Crabbé *et al*, 2010). Indeed, *in-vitro* checkpoint reconstitution assays have shown that Mrc1 can facilitate the phosphorylation and activation of Rad53 probably by promoting Mec1–Rad53 interaction (Chen and Zhou, 2009). A recent study demonstrated that Mec1- but not Rad53-dependent phosphorylation of Mrc1 is necessary for the establishment of a positive feedback loop that leads to Mec1 stabilization at stalled replication forks (Naylor *et al*, 2009). Thus, Mrc1 may act prior to Sgs1 function ensuring Mec1–Ddc2 recruitment to stalled replication forks, which in turn is necessary for Sgs1 phosphorylation (Naylor *et al*, 2009). While Mrc1 and Sgs1 are epistatic for Rad53 activation on HU, they nonetheless show strong synergistic defects for stalled fork recovery and DNA polymerase stability on HU (Bjergbaek *et al*, 2005). This argues that Mrc1, like Sgs1, serves multiple roles at stalled forks. One possible scenario for the synergy observed between Sgs1 and Mrc1 would be that they act preferentially on different strands (the leading versus the lagging strand). Indeed, Mrc1 has been shown to function together with leading strand polymerase pol ϵ (Lou *et al*, 2008).

As in yeast, the human RecQ helicase BLM has been shown to be a target of ATR in a region N-terminal of its helicase domain (Davies *et al*, 2004; Rao *et al*, 2005). Interestingly, the N-terminal region of BLM (aa 1–477) including the ATR-target sites (T₉₉Q₁₀₀, T₁₂₂Q₁₂₃) binds hRPA *in vitro* (Davies *et al*, 2004, 2007). In contrast to Sgs1, BLM is not a constitutive component of the replisome, but is recruited from PML bodies to sites of stalled replication forks in response to HU (Sengupta *et al*, 2003). This re-localization requires ATR-dependent phosphorylation of BLM (Davalos *et al*, 2004). It has been suggested that ATR phosphorylation of BLM is required for recovery from HU-mediated replication fork stalling, but not for the recruitment of BLM to damaged forks nor for the suppression of sister chromatid exchanges with hTOPO III α –hRMI1–hRMI2 (Davies *et al*, 2004; Wu, 2007). Davies *et al* (2007) demonstrated that ATR-dependent phosphorylation of BLM is required for efficient replication fork resumption and repression of new origin firing after aphidicolin treatment. Furthermore, and similar to our findings, the presence of BLM at stalled replication forks is required for robust intra-S phase checkpoint activation in human cells (Franchitto and Pichierri, 2002; Davalos and Campisi, 2003). Nonetheless, the mechanisms through which mammalian ATR and BLM work together to maintain replisomes at stalled replication forks and activate the intra-S phase checkpoint are unknown. A conserved, damage-specific assembly of a RecQ homologue (BLM and/or WRN) with a downstream checkpoint kinase is an attractive hypothesis.

Materials and methods

Yeast strains and plasmids

S. cerevisiae strains (Supplementary Table S1) were derived from W303-1A (*MATa ade2-1 ura3-1 his3-11,15 trp1-1 leu2-3,112 can1-100*). If not stated otherwise, all strains were cultured at 30°C in YPAD media. The *sgs1-r1* allele was generated using pop-in/pop-out mutagenesis as previously described (Tam *et al*, 2007). For Y2H analyses, fragments of Sgs1, Rpa70 and Rpa32 were fused in frame to the B42 activator domain in the pJG46 or the *lexA* DNA binding domain in the pGAL-*lexA* vector (Bjergbaek *et al*, 2005). Y2H was performed as described (Bjergbaek *et al*, 2005), except that both bait and prey were under *GAL_{UAS}* control. EGY191 cells (GA-1211) containing the *lacZ* reporter pSH18-34, the bait and the prey were glucose depleted, then 2% galactose added to the exponentially growing culture to induce expression of the fusion proteins. The quantitative β -galactosidase assay for permeabilized cells (Adams *et al*, 1997) was performed on four independent transformants in at least two independent experiments for each data point. Expression of the fusion proteins was confirmed by western blot analysis (data not shown). β -Galactosidase units are defined as $OD_{420}/(OD_{600} \times \text{dilution} \times \text{time}(\text{min}))$.

Survival and drop assays

For liquid survival assays, overnight cultures were diluted to $OD_{600} = 0.15$ and grown for 3 h, then synchronized with α -factor in G1 and released into YPAD containing 0.2 M HU. At the indicated time points, relevant dilutions were plated onto fresh YPAD plates and colonies were counted after 3–4 days. Survival is defined as the fraction of colonies compared to the untreated control (0 h) normalized to the survival of WT cells for each time point. Drop tests used overnight cultures diluted to $OD_{600} = 0.5$ with 2 μ l drops of 10-fold dilutions plated on YPAD or the appropriate selective medium with indicated concentrations of damaging agents.

ChIP analysis, co-IP and kinase assays

ChIP experiments were performed as described (Cobb *et al*, 2005) using monoclonal anti-HA (F-7, Santa Cruz) to precipitate HA-tagged DNA pol α or Ddc2, and anti-Myc (9E10) to precipitate Myc-tagged Rpa70. Details are in Supplementary Methods. For each time point, the relative enrichment for ARS607 or ARS522 was obtained by normalizing the absolute enrichment at ARS607 or ARS522 to the absolute enrichment 14 kb away from ARS607.

Co-IP was performed essentially as described in Bjergbaek *et al* (2005), except that two additional rounds of washing with 100 mM Tris pH 8.0, 500 mM NaCl, 1 mM EDTA, 0.5% NP-40 and 0.5% sodium deoxycholate were performed. Note that the use of more stringent washing conditions most probably explains why the Sgs1-Rad53 interaction was not dependent on checkpoint induction in the previous study (Bjergbaek *et al*, 2005). Mec1 immunoprecipitation and kinase assays are described in Supplementary Methods.

Rad53 and Sgs1 phosphorylation and mass spectroscopic analysis

Conditions used to monitor Rad53 or Sgs1 phosphorylation by western blot and by semi-quantitative mass spectroscopy are described in Supplementary Methods. In brief, peptides were separated by nano-HPLC (Agilent 1100 nanoLC system, Agilent Technologies) coupled to an LTQ Orbitrap Velos hybrid mass spectrometer (Thermo Scientific) using a top 15 DDA method and an LC-MSMS method containing *m/z* values of predicted phosphopeptides. Peptides were identified by searching SwissProt database (version 2010-09) with Mascot 2.3.0 (Matrix Science). Data were

References

- Adams A, Gottschling DE, Kaiser CA, Stearns T (1997) *Methods in Yeast Genetics*. New York: Cold Spring Harbor Laboratory Press
- Aguilera A, Gomez-Gonzalez B (2008) Genome instability: a mechanistic view of its causes and consequences. *Nat Rev Genet* 9: 204–217
- Alcasabas AA, Osborn AJ, Bachant J, Hu F, Werler PJ, Bousset K, Furuya K, Diffley JF, Carr AM, Elledge SJ (2001) Mrc1 transduces signals of DNA replication stress to activate Rad53. *Nat Cell Biol* 3: 958–965

compiled and evaluated with Scaffold 3.4.3 and Scaffold PTM 1.1.3 (Proteome Software).

Protein purification and ITC

The Rad53(22–162) and Rpa70(1–133) and Rpa70(3–133) constructs inserted into a pET15 derived vector, containing a TEV protease cleavable His₆-tag, and Sgs1 constructs (404–485, 404–560) were amplified and inserted into a pET15 derived vector, containing a thrombin protease cleavable His₆ tag. All were expressed in *E. coli* BL21 cells and purified by metal chelate affinity (His-Select Nickel Affinity Gel, Sigma-Aldrich), anion-exchange (Resource 15 Q, GE Healthcare), and gel-filtration chromatography (Superdex S-200, GE Healthcare). ITC experiments were conducted with a MicroCal VP-ITC calorimeter as described in Supplementary Methods.

Genetic interactions and sequence analysis

GA-6998 (*sgs1-r1*) and yHA429 (*sgs1 Δ*) cells together with 33 other query strains (data to be published elsewhere) were crossed with a library of 1536 mutants (Guénole *et al*, under review) as described (Schuldiner *et al*, 2006), except that four sets of double mutants were created in two independent experiments. Results and the analysis of the library by pooled TAG amplification are described in Supplementary Methods. Genetic interaction scores (S scores) were calculated using the E-MAP toolbox (Collins *et al*, 2006). The analysis of sequence motifs in Sgs1 is described in Supplementary Methods.

Supplementary data

Supplementary data are available at *The EMBO Journal* Online (<http://www.embojournal.org>).

Acknowledgements

The Gasser laboratory acknowledges the help from T Aust, J Eichenberger, S Schuierer and D Hoepfner of the Novartis Institutes for Biomedical Research (Basel, Switzerland); H Vlaming from the van Leeuwen laboratory; and M Rebhan, D Gaidatzis and R Sack (FMI). Experimental assistance and discussion were contributed by Y Moriyama (Kyoto University), P Maillard (U of Geneva), S Kueng and other Gasser laboratory members. The mutant *sgs1-hd* was a gift from R Rothstein (Columbia U, NY). Funding from the Swiss Cancer League, the Novartis Research Foundation, the Swiss National Science Foundation and the EU ITR Image DDR is gratefully acknowledged.

Author contributions: AMH performed experiments, contributed to writing and assembled figures; NH performed experiments, contributed to writing and assembled figures; KS advised, performed experiments, contributed to writing and figures; BLP advised, performed experiments and contributed to writing; PA and MV purified proteins and cooperated on biochemical analyses; SMR performed and analysed ITC experiments; NHT advised MV, PA, and contributed to writing; HvA advised AG who generated strains used in the E-MAP analysis, and FvL hosted NH for same; SMG advised, interpreted results, planned experiments, contributed to writing, figures and funding of the project.

Conflict of interest

The authors declare that they have no conflict of interest.

- Ashton TM, Hickson ID (2010) Yeast as a model system to study RecQ helicase function. *DNA Repair* **9**: 303–314
- Bachrati CZ, Hickson ID (2008) RecQ helicases: guardian angels of the DNA replication fork. *Chromosoma* **117**: 219–233
- Bennett RJ, Keck JL, Wang JC (1999) Binding specificity determines polarity of DNA unwinding by the Sgs1 protein of *S. cerevisiae*. *J Mol Biol* **289**: 235–248
- Bennett RJ, Noirot-Gros MF, Wang JC (2000) Interaction between yeast sgs1 helicase and DNA topoisomerase III. *J Biol Chem* **275**: 26898–26905
- Bernstein KA, Gangloff S, Rothstein R (2010) The RecQ DNA helicases in DNA repair. *Annu Rev Genet* **44**: 393–417
- Bernstein KA, Shor E, Sunjevaric I, Fumasoni M, Burgess RC, Foiani M, Branzei D, Rothstein R (2009) Sgs1 function in the repair of DNA replication intermediates is separable from its role in homologous recombinational repair. *EMBO J* **28**: 915–925
- Binz SK, Sheehan AM, Wold MS (2004) Replication protein A phosphorylation and the cellular response to DNA damage. *DNA Repair (Amst)* **3**: 1015–1024
- Bjergbaek L, Cobb JA, Tsai-Pflugfelder M, Gasser SM (2005) Mechanistically distinct roles for Sgs1p in checkpoint activation and replication fork maintenance. *EMBO J* **24**: 405–417
- Boddy MN, Lopez-Girona A, Shanahan P, Interthal H, Heyer WD, Russell P (2000) Damage tolerance protein Mus81 associates with the FHA1 domain of checkpoint kinase Cds1. *Mol Cell Biol* **20**: 8758–8766
- Bodenmiller B, Campbell D, Gerrits B, Lam H, Jovanovic M, Picotti P, Schlapbach R, Aebersold R (2008) PhosphoPep—a database of protein phosphorylation sites in model organisms. *Nat Biotechnol* **26**: 1339–1340
- Bodenmiller B, Wanka S, Kraft C, Urban J, Campbell D, Pedrioli PG, Gerrits B, Picotti P, Lam H, Vitek O, Brusniak MY, Roschitzki B, Zhang C, Shokat KM, Schlapbach R, Colman-Lerner A, Nolan GP, Nesvizhskii AI, Peter M, Loewith R *et al* (2010) Phosphoproteomic analysis reveals interconnected system-wide responses to perturbations of kinases and phosphatases in yeast. *Sci Signal* **3**: rs4
- Brush GS, Morrow DM, Hieter P, Kelly TJ (1996) The ATM homolog MEK1 is required for phosphorylation of replication protein A in yeast. *Proc Natl Acad Sci USA* **93**: 15075–15080
- Chang M, Bellaoui M, Zhang C, Desai R, Morozov P, Delgado-Cruzata L, Rothstein R, Freyer GA, Boone C, Brown GW (2005) RMI1/NCE4, a suppressor of genome instability, encodes a member of the RecQ helicase/Topo III complex. *EMBO J* **24**: 2024–2033
- Chen CF, Brill SJ (2007) Binding and activation of DNA topoisomerase III by the Rmi1 subunit. *J Biol Chem* **282**: 28971–28979
- Chen SH, Albuquerque CP, Liang J, Suhandynata RT, Zhou H (2010) A proteome-wide analysis of kinase-substrate network in the DNA damage response. *J Biol Chem* **285**: 12803–12812
- Chen SH, Zhou H (2009) Reconstitution of Rad53 activation by Mec1 through adaptor protein Mrc1. *J Biol Chem* **284**: 18593–18604
- Cimprich KA, Cortez D (2008) ATR: an essential regulator of genome integrity. *Nat Rev Mol Cell Biol* **9**: 616–627
- Cobb JA, Bjergbaek L (2006) RecQ helicases: lessons from model organisms. *Nucleic Acids Res* **34**: 4106–4114
- Cobb JA, Bjergbaek L, Shimada K, Frei C, Gasser SM (2003) DNA polymerase stabilization at stalled replication forks requires Mec1 and the RecQ helicase Sgs1. *EMBO J* **22**: 4325–4336
- Cobb JA, Schleker T, Rojas V, Bjergbaek L, Tercero JA, Gasser SM (2005) Replisome instability, fork collapse, and gross chromosomal rearrangements arise synergistically from Mec1 kinase and RecQ helicase mutations. *Genes Dev* **19**: 3055–3069
- Collins SR, Miller KM, Maas NL, Roguev A, Fillingham J, Chu CS, Schuldiner M, Gebbia M, Recht J, Shales M, Ding H, Xu H, Han J, Ingvarsdottir K, Cheng B, Andrews B, Boone C, Berger SL, Hieter P, Zhang Z *et al* (2007) Functional dissection of protein complexes involved in yeast chromosome biology using a genetic interaction map. *Nature* **446**: 806–810
- Collins SR, Schuldiner M, Krogan NJ, Weissman JS (2006) A strategy for extracting and analyzing large-scale quantitative epistatic interaction data. *Genome Biol* **7**: R63
- Crabbé L, Thomas A, Pantescio V, De Vos J, Pasero P, Lengronne A (2010) Analysis of replication profiles reveals key role of RFC-Ctf18 in yeast replication stress response. *Nat Struct Mol Biol* **17**: 1391–1397
- Devalos AR, Campisi J (2003) Bloom syndrome cells undergo p53-dependent apoptosis and delayed assembly of BRCA1 and NBS1 repair complexes at stalled replication forks. *J Cell Biol* **162**: 1197–1209
- Devalos AR, Kaminker P, Hansen RK, Campisi J (2004) ATR and ATM-dependent movement of BLM helicase during replication stress ensures optimal ATM activation and 53BP1 focus formation. *Cell Cycle* **3**: 1579–1586
- Davies SL, North PS, Dart A, Lakin ND, Hickson ID (2004) Phosphorylation of the Bloom's syndrome helicase and its role in recovery from S-phase arrest. *Mol Cell Biol* **24**: 1279–1291
- Davies SL, North PS, Hickson ID (2007) Role for BLM in replication-fork restart and suppression of origin firing after replicative stress. *Nat Struct Mol Biol* **14**: 677–679
- De Piccoli G, Katou Y, Itoh T, Nakato R, Shirahige K, Labib K (2012) Replisome stability at defective DNA replication forks is independent of S phase checkpoint kinases. *Mol Cell* **45**: 696–704
- Dubrana K, van Attikum H, Hediger F, Gasser SM (2007) The processing of double-strand breaks and binding of single-strand-binding proteins RPA and Rad51 modulate the formation of ATR-kinase foci in yeast. *J Cell Sci* **120**: 4209–4220
- Durocher D, Taylor IA, Sarbasova D, Haire LF, Westcott SL, Jackson SP, Smerdon SJ, Yaffe MB (2000) The molecular basis of FHA domain:phosphopeptide binding specificity and implications for phospho-dependent signaling mechanisms. *Mol Cell* **6**: 1169–1182
- Franchitto A, Pichierri P (2002) Bloom's syndrome protein is required for correct relocalization of RAD50/MRE11/NBS1 complex after replication fork arrest. *J Cell Biol* **157**: 19–30
- Frei C, Gasser SM (2000) The yeast Sgs1p helicase acts upstream of Rad53p in the DNA replication checkpoint and colocalizes with Rad53p in S-phase-specific foci. *Genes Dev* **14**: 81–96
- Fricke WM, Kaliraman V, Brill SJ (2001) Mapping the DNA topoisomerase III binding domain of the Sgs1 DNA helicase. *J Biol Chem* **276**: 8848–8855
- Friedel AM, Pike BL, Gasser SM (2009) ATR/Mec1: coordinating fork stability and repair. *Curr Opin Cell Biol* **21**: 237–244
- Gangloff S, McDonald JP, Bendixen C, Arthur L, Rothstein R (1994) The yeast type I topoisomerase Top3 interacts with Sgs1, a DNA helicase homolog: a potential eukaryotic reverse gyrase. *Mol Cell Biol* **14**: 8391–8398
- Guénole A, Srivas R, Vreeken K, Wang S, Krogan NJ, Ideker T, Van Attikum H. Dissection of DNA damage response pathways using a multi-conditional genetic interaction map. (Submitted).
- Hickson ID, Mankouri HW (2011) Processing of homologous recombination repair intermediates by the Sgs1-Top3-Rmi1 and Mus81-Mms4 complexes. *Cell Cycle* **10**: 3078–3085
- Ii M, Brill SJ (2005) Roles of SGS1, MUS81, and RAD51 in the repair of lagging-strand replication defects in *Saccharomyces cerevisiae*. *Curr Genet* **48**: 213–225
- Kai M, Boddy MN, Russell P, Wang TS (2005) Replication checkpoint kinase Cds1 regulates Mus81 to preserve genome integrity during replication stress. *Genes Dev* **19**: 919–932
- Lambert S, Mizuno K, Blaisonneau J, Martineau S, Chanet R, Freon K, Murray JM, Carr AM, Baldacci G (2010) Homologous recombination restarts blocked replication forks at the expense of genome rearrangements by template exchange. *Mol Cell* **39**: 346–359
- Liberi G, Maffioletti G, Lucca C, Chiolo I, Baryshnikova A, Cotta-Ramusino C, Lopes M, Pelliccioli A, Haber JE, Foiani M (2005) Rad51-dependent DNA structures accumulate at damaged replication forks in sgs1 mutants defective in the yeast ortholog of BLM RecQ helicase. *Genes Dev* **19**: 339–350
- Lou H, Komata M, Katou Y, Guan Z, Reis CC, Budd M, Shirahige K, Campbell JL (2008) Mrc1 and DNA polymerase epsilon function together in linking DNA replication and the S phase checkpoint. *Mol Cell* **32**: 106–117
- Lucca C, Vanoli F, Cotta-Ramusino C, Pelliccioli A, Liberi G, Haber J, Foiani M (2004) Checkpoint-mediated control of replisome-fork association and signalling in response to replication pausing. *Oncogene* **23**: 1206–1213
- Machwe A, Lozada EM, Xiao L, Orren DK (2006) Competition between the DNA unwinding and strand pairing activities of the Werner and Bloom syndrome proteins. *BMC Mol Biol* **7**: 1
- Majka J, Niedziela-Majka A, Burgers PM (2006) The checkpoint clamp activates Mec1 kinase during initiation of the DNA damage checkpoint. *Mol Cell* **24**: 891–901

- Mankouri HW, Ashton TM, Hickson ID (2011) Holliday junction-containing DNA structures persist in cells lacking Sgs1 or Top3 following exposure to DNA damage. *Proc Natl Acad Sci USA* **108**: 4944–4949
- Melo JA, Cohen J, Toczyski DP (2001) Two checkpoint complexes are independently recruited to sites of DNA damage in vivo. *Genes Dev* **15**: 2809–2821
- Mimura S, Komata M, Kishi T, Shirahige K, Kamura T (2009) SCF(Dia2) regulates DNA replication forks during S-phase in budding yeast. *EMBO J* **28**: 3693–3705
- Mordes DA, Nam EA, Cortez D (2008) Dpb11 activates the Mec1-Ddc2 complex. *Proc Natl Acad Sci USA* **105**: 18730–18734
- Morohashi H, Maculins T, Labib K (2009) The amino-terminal TPR domain of Dia2 tethers SCF(Dia2) to the replisome progression complex. *Curr Biol* **19**: 1943–1949
- Mullen JR, Chen CF, Brill SJ (2010) Wss1 is a SUMO-dependent isopeptidase that interacts genetically with the Slx5-Slx8 SUMO-targeted ubiquitin ligase. *Mol Cell Biol* **30**: 3737–3748
- Mullen JR, Nallaseth FS, Lan YQ, Slagle CE, Brill SJ (2005) Yeast Rm1/Nce4 controls genome stability as a subunit of the Sgs1-Top3 complex. *Mol Cell Biol* **25**: 4476–4487
- Muñoz-Galván S, Tous C, Blanco MG, Schwartz EK, Ehmsen KT, West SC, Heyer WD, Aguilera A (2012) Distinct roles of Mus81, Yen1, Slx1-Slx4, and Rad1 nucleases in the repair of replication-born double-strand breaks by sister chromatid exchange. *Mol Cell Biol* **32**: 1592–1603
- Myung K, Kolodner RD (2002) Suppression of genome instability by redundant S-phase checkpoint pathways in *Saccharomyces cerevisiae*. *Proc Natl Acad Sci USA* **99**: 4500–4507
- Nagai S, Davoodi N, Gasser SM (2011) Nuclear organization in genome stability: SUMO connections. *Cell Res* **21**: 474–485
- Navadgi-Patil VM, Burgers PM (2008) Yeast DNA replication protein Dpb11 activates the Mec1/ATR checkpoint kinase. *J Biol Chem* **283**: 35853–35859
- Navadgi-Patil VM, Burgers PM (2011) Cell-cycle-specific activators of the Mec1/ATR checkpoint kinase. *Biochem Soc Trans* **39**: 600–605
- Naylor ML, Li JM, Osborn AJ, Elledge SJ (2009) Mrc1 phosphorylation in response to DNA replication stress is required for Mec1 accumulation at the stalled fork. *Proc Natl Acad Sci USA* **106**: 12765–12770
- Ooi SL, Shoemaker DD, Boeke JD (2003) DNA helicase gene interaction network defined using synthetic lethality analyzed by microarray. *Nat Genet* **35**: 277–286
- Osborn AJ, Elledge SJ (2003) Mrc1 is a replication fork component whose phosphorylation in response to DNA replication stress activates Rad53. *Genes Dev* **17**: 1755–1767
- Paciotti V, Clerici M, Scotti M, Lucchini G, Longhese MP (2001) Characterization of mec1 kinase-deficient mutants and of new hypomorphic mec1 alleles impairing subsets of the DNA damage response pathway. *Mol Cell Biol* **21**: 3913–3925
- Pennell S, Westcott S, Ortiz-Lombardia M, Patel D, Li J, Nott TJ, Mohammed D, Buxton RS, Yaffe MB, Verma C, Smerdon SJ (2010) Structural and functional analysis of phosphothreonine-dependent FHA domain interactions. *Structure* **18**: 1587–1595
- Pichierrì P, Rosselli F, Franchitto A (2003) Werner's syndrome protein is phosphorylated in an ATR/ATM-dependent manner following replication arrest and DNA damage induced during the S phase of the cell cycle. *Oncogene* **22**: 1491–1500
- Pike BL, Tenis N, Heierhorst J (2004a) Rad53 kinase activation-independent replication checkpoint function of the N-terminal forkhead-associated (FHA1) domain. *J Biol Chem* **279**: 39636–39644
- Pike BL, Yongkiettrakul S, Tsai MD, Heierhorst J (2003) Diverse but overlapping functions of the two forkhead-associated (FHA) domains in Rad53 checkpoint kinase activation. *J Biol Chem* **278**: 30421–30424
- Pike BL, Yongkiettrakul S, Tsai MD, Heierhorst J (2004b) Mdt1, a novel Rad53 FHA1 domain-interacting protein, modulates DNA damage tolerance and G(2)/M cell cycle progression in *Saccharomyces cerevisiae*. *Mol Cell Biol* **24**: 2779–2788
- Pirzio LM, Pichierrì P, Bignami M, Franchitto A (2008) Werner syndrome helicase activity is essential in maintaining fragile site stability. *J Cell Biol* **180**: 305–314
- Qiu J, Qian Y, Frank P, Wintersberger U, Shen B (1999) *Saccharomyces cerevisiae* RNase H(35) functions in RNA primer removal during lagging-strand DNA synthesis, most efficiently in cooperation with Rad27 nuclease. *Mol Cell Biol* **19**: 8361–8371
- Rao VA, Fan AM, Meng L, Doe CF, North PS, Hickson ID, Pommier Y (2005) Phosphorylation of BLM, dissociation from topoisomerase IIIalpha, and colocalization with gamma-H2AX after topoisomerase I-induced replication damage. *Mol Cell Biol* **25**: 8925–8937
- Rouse J, Jackson SP (2002) Lcd1p recruits Mec1p to DNA lesions in vitro and in vivo. *Mol Cell* **9**: 857–869
- Schmidt KH, Kolodner RD (2006) Suppression of spontaneous genome rearrangements in yeast DNA helicase mutants. *Proc Natl Acad Sci USA* **103**: 18196–18201
- Schuldiner M, Collins SR, Weissman JS, Krogan NJ (2006) Quantitative genetic analysis in *Saccharomyces cerevisiae* using epistatic miniarray profiles (E-MAPs) and its application to chromatin functions. *Methods* **40**: 344–352
- Segurado M, Diffley JF (2008) Separate roles for the DNA damage checkpoint protein kinases in stabilizing DNA replication forks. *Genes Dev* **22**: 1816–1827
- Sengupta S, Linke SP, Pedoux R, Yang Q, Farnsworth J, Garfield SH, Valerie K, Shay JW, Ellis NA, Wasyluk B, Harris CC (2003) BLM helicase-dependent transport of p53 to sites of stalled DNA replication forks modulates homologous recombination. *EMBO J* **22**: 1210–1222
- Shen JC, Lao Y, Kamath-Loeb A, Wold MS, Loeb LA (2003) The N-terminal domain of the large subunit of human replication protein A binds to Werner syndrome protein and stimulates helicase activity. *Mech Ageing Dev* **124**: 921–930
- Smolka MB, Chen SH, Maddox PS, Enserink JM, Albuquerque CP, Wei XX, Desai A, Kolodner RD, Zhou H (2006) An FHA domain-mediated protein interaction network of Rad53 reveals its role in polarized cell growth. *J Cell Biol* **175**: 743–753
- Sogo JM, Lopes M, Foiani M (2002) Fork reversal and ssDNA accumulation at stalled replication forks owing to checkpoint defects. *Science* **297**: 599–602
- Sowd G, Wang H, Pretto D, Chazin WJ, Opresko PL (2009) Replication protein A stimulates the werner syndrome protein branch migration activity. *J Biol Chem* **284**: 34682–34691
- Tam AT, Pike BL, Hammet A, Heierhorst J (2007) Telomere-related functions of yeast KU in the repair of bleomycin-induced DNA damage. *Biochem Biophys Res Commun* **357**: 800–803
- Tong AH, Evangelista M, Parsons AB, Xu H, Bader GD, Page N, Robinson M, Raghibizadeh S, Hogue CW, Bussey H, Andrews B, Tyers M, Boone C (2001) Systematic genetic analysis with ordered arrays of yeast deletion mutants. *Science* **294**: 2364–2368
- Tong AH, Lesage G, Bader GD, Ding H, Xu H, Xin X, Young J, Berriz GF, Brost RL, Chang M, Chen Y, Cheng X, Chua G, Friesen H, Goldberg DS, Haynes J, Humphries C, He G, Hussein S, Ke L *et al* (2004) Global mapping of the yeast genetic interaction network. *Science* **303**: 808–813
- Tourriere H, Pasero P (2007) Maintenance of fork integrity at damaged DNA and natural pause sites. *DNA Repair (Amst)* **6**: 900–913
- Traven A, Heierhorst J (2005) SQ/TQ cluster domains: concentrated ATM/ATR kinase phosphorylation site regions in DNA-damage-response proteins. *Bioessays* **27**: 397–407
- Watt PM, Hickson ID, Borts RH, Louis EJ (1996) SGS1, a homologue of the Bloom's and Werner's syndrome genes, is required for maintenance of genome stability in *Saccharomyces cerevisiae*. *Genetics* **144**: 935–945
- Weinstein J, Rothstein R (2008) The genetic consequences of ablating helicase activity and the Top3 interaction domain of Sgs1. *DNA Repair (Amst)* **7**: 558–571
- Wu L (2007) Role of the BLM helicase in replication fork management. *DNA Repair (Amst)* **6**: 936–944
- Yodh JG, Stevens BC, Kanagaraj R, Janscak P, Ha T (2009) BLM helicase measures DNA unwound before switching strands and hRPA promotes unwinding reinitiation. *EMBO J* **28**: 405–416
- Zou L, Elledge SJ (2003) Sensing DNA damage through ATRIP recognition of RPA-ssDNA complexes. *Science* **300**: 1542–1548
- Zou Y, Liu Y, Wu X, Shell SM (2006) Functions of human replication protein A (RPA): from DNA replication to DNA damage and stress responses. *J Cell Physiol* **208**: 267–273

CHAPTER 5: CONCLUDING REMARKS AND FUTURE PROSPECTS

This work contributes to our understanding of Mec1 signaling. Specifically, in Chapter 2, I have revealed an intimate and unexpected relationship between the checkpoint kinase complex Mec1-Ddc2 and the PP4 phosphatase Pph3-Psy2. We identify PP4 as a major regulator of Mec1 signaling. In two independent genetic screens we found that mutants lacking *PPH3* or its regulatory subunit *PSY2* suppress *mec1-100* defects on HU. We further show that both complexes physically interact and co-regulate many phosphorylation sites including a previously unidentified acceptor site in Mec1, S1991. In the mutant *mec1-100* the replication checkpoint is compromised, but the G2 DNA damage checkpoint remains intact (Paciotti et al., 2001). In Chapter 3, I extended my analysis of *mec1-100* by characterizing intragenic suppressors and I further investigate the molecular nature of the *mec1-100* defects. In a third project, I studied the role of the RecQ helicase Sgs1 in checkpoint signaling and replication fork stabilization in collaboration with a previous graduate student. The main conclusions drawn from these three projects are summarized and areas of potential future research are discussed here.

MEC1-DDC2 AND PSY2-PPH3 PHYSICALLY INTERACT

In Chapter 2 we show that Ddc2 and Psy2 subunits physically interact by yeast two-hybrid assays, IP combined with western blotting and FRET. We also provide evidence that the Ddc2-Psy2 interaction may be conserved. Two different, but not mutually exclusive scenarios regarding the function of such a complex can be envisioned.

First, the two opposing enzymes might interact to regulate steady-state phosphorylation of overlapping targets. Even though at first glance this seems to be a waste of energy, other examples of association of antagonizing enzymes exist in nature: The deubiquitinating enzyme BRCC3 associates with the ubiquitin ligase BRCA1 within the RAP80 complex (Sobhian et al., 2007) Also, histone acetyltransferases and deacetylases have been reported to bind each other and are often found in single transcription-regulatory complexes (Yamagoe et al., 2003). Finally, histone methylating and demethylating enzymes are also found linked together, notably in conserved versions of the Trithorax and Polycomb group complexes, originally described in flies. The Trx complex contains both the H3K4me3 methyltransferase MLL/KMT2 and the H3K27 demethylase UTX/KDM6A, while the PcG complex PRC2, contains the H3K27 methyltransferase subcomplex PRC2/KMT6 and the H3K4me3 demethylase RBP2/KDM5A (reviewed in (Nottke et al., 2009)).

Systems biology studies revealed that antagonizing enzymatic functions in the same complex can confer robustness to enzyme or substrate perturbations in order to preserve steady-state levels (Russo and Silhavy, 1993). However, it was argued that this can only be achieved if the antagonizing functions are found exclusively together in one complex and share the same targets (reviewed in (Hart and Alon, 2013)). Psy2 is about ten times more abundant in cells (about 7000 molecules/cell on average) than Ddc2 (about 600 molecules/cell on average) (Ghaemmaghami et al., 2003). Although we do not know the stoichiometry of the complex, we observed by microscopy that a fraction of Psy2 foci did not colocalize with Ddc2 foci (Figure 2.6). Both observations suggest that a population of Psy2-Pph3 exists in yeast cells that does not bind Ddc2. Thus it seems unlikely that the function of this complex is to provide robustness, although we cannot exclude that the non-Ddc2 bound fraction might be inactive or otherwise sequestered. On the other hand, our microscopy data suggests that most of Ddc2 colocalizes with Psy2 (Chapter 2). Thus, it is tempting to speculate that the association of the kinase with the counteracting phosphatase could serve to keep target phosphorylation levels low until kinase activation overcomes phosphatase activity.

We sought to study the function of the Psy2-Ddc2 interaction by mapping and disrupting the interaction domain on Psy2. We found that a region within amino acids 25 – 350 of Psy2 interacted

with Ddc2 by yeast two hybrid and deleting amino acids 130-350 within Psy2 disrupted the interaction (Chapter 2). However, cells expressing *psy2Δ130-350* from the endogenous promoter were as MMS sensitive as *psy2Δ* cells, indicating that deleting amino acids 130-350 turned Psy2 dysfunctional. It is unclear at present whether this renders Psy2 unstable, interferes with its binding to Pph3, or whether the Psy2-Ddc2 interaction is essential for survival on MMS. Future research will aim at better defining the interaction domain and possibly generating point mutants that disrupt the Psy2-Ddc2 interaction, rather than deleting a large domain. Alternatively, the interaction site within Ddc2 could be mapped and mutated. Unfortunately, initial yeast two hybrid experiments to map the interaction on the Ddc2 side were inconclusive, although it should be possible to map the interaction site by GST pull-down experiments.

A second scenario for the function of the Mec1-Ddc2/Psy2-Pph3 complex is that the two might not only regulate overlapping targets, but also may regulate the other's activity. In this context other regulatory interactions between checkpoint kinases and phosphatases have been described previously: ATM has been shown to associate with and be regulated by PP1, PP2A and the PP2C phosphatase Wip1. Similarly, CHK1 and CHK2 interact with and are regulated by PP2A and Wip1 (reviewed by (Shimada and Nakanishi, 2013)). ATR is reported to associate with PP5, although PP5 rather seems to positively influence ATR signaling (Zhang et al., 2005). In all other cases, the phosphatase negatively regulates kinase function, thereby preventing untimely activation and/or promoting checkpoint recovery. Often the phosphatase was shown to achieve this through targeting of a phosphorylation site within the kinase that is crucial for kinase activity (e.g. PP2A dephosphorylates ATM serine 1981 and CHK1 serine 317 and 345) (Goodarzi et al., 2004; Leung-Pineda et al., 2006). Relevant to this, we also find a phosphorylation site in Mec1 that is regulated by Pph3, although this regulation may be indirect. Important to this scenario of cross-control is that the association between checkpoint kinase and phosphatase in mammalian cells often seems to be disrupted in response to DNA damage (Freeman et al., 2010; Goodarzi et al., 2004). Dissociation relieves the inhibition of the kinase by the phosphatase, allowing kinase activation.

In our study, we did not observe a detectable difference in the interaction of Ddc2 with Psy2 before or after HU treatment, following IP or western blot analysis. Interestingly, a similar, constitutive interaction was reported for the PP2C phosphatase Wip1 and ATM (Shreeram et al., 2006). A second study showed, however, that Wip1 protein levels are regulated in a cell-cycle and DNA damage-dependent manner (Macurek et al., 2013), thereby providing an explanation how Wip1-mediated ATM inhibition might be relieved upon DNA damage. Currently, it remains unclear whether or not Mec1 is directly inhibited by Psy2-Pph3. Nor do we know how the potential inhibition of Mec1 is overcome during the process of checkpoint activation. Psy2 or Pph3 mRNAs do not show cell-cycle or damage-induced variations in levels (Benton et al., 2006; Cho et al., 1998; Lee et al., 2000; Pramila et al., 2006; Spellman et al., 1998; van Attikum et al., 2004). Similarly, protein abundance is not reported to change upon HU or MMS treatment, nor is protein localization (Mazumder et al., 2013; Tkach et al., 2012). Accordingly, genome-wide studies did not report any posttranslational modifications (i.e. acetylation, ubiquitination, sumoylation or phosphorylation) on either Psy2 or Pph3 (Bodenmiller et al., 2008; Henriksen et al., 2012; Peng et al., 2003; Wohlschlegel et al., 2004) Thus, we have no evidence for cell-cycle and/or damage-induced regulation of Psy2-Pph3. Another possibility is that the association between Psy2 and Pph3 is regulated. Unfortunately, several attempts to fuse Pph3 to epitope tags have resulted in dysfunctional proteins and MMS-sensitive cells (Figure S2.4), and thus we have not been able to address directly whether Psy2-Pph3 interaction is regulated. Raising an antibody against Pph3 would allow us to address this question.

PPH3 TARGETS PHOSPHOPEPTIDES THAT ARE DOWNREGULATED IN *MEC1-100* CELLS

In support of the hypothesis that Pph3 might negatively regulate Mec1 function, I was able to show that most of the phosphopeptides that are downregulated in the *mec1-100* mutant are restored to their wild-type levels by the deletion of *PPH3* (Chapter 2). Interestingly, only few of the *mec1-100* dependent downregulated phosphotarget sites match the reported S/TQ consensus sequence (Kim et al., 1999). Several explanations for this phenomenon are plausible. First, the original consensus was determined by using peptides in ATM *in vitro* kinase assays (Kim et al., 1999). Regarding *in vivo* targets, one yeast phosphoproteomics study found that only 51% of all Mec1/Tell1-dependent (and Rad53-independent) targets matched to the consensus (Chen et al., 2010). A rather prominent example for non-consensus targeting is ATR autophosphorylation at threonine 1989, which is followed by a proline (Liu et al., 2011; Nam et al., 2011b). Similarly, the S1991 phosphoacceptor site in Mec1 is also not an S/TQ consensus site (Figure 3.1). Thus, the S/TQ consensus might be not as strict as generally assumed.

Alternatively, non-S/TQ phosphorylation sites might represent targets that are indirectly regulated by Mec1, that is, be targets of another kinase that is activated by Mec1. Rad53 can be ruled out, since we specifically filtered our data for Rad53-independent phosphorylation sites. Chk1 could be a candidate for this pathway. On the other hand our genetic data shows that Chk1 is not involved in suppression of *mec1-100* HU sensitivity by loss of Pph3. This does not rule out, however, that Chk1 might be regulated by Pph3, without functional significance for survival on HU.

Besides the two checkpoint signaling kinases, other kinase candidates were found in the list of *mec1-100* targets. Namely, Hrk1, Vhs2, Gin4, Sky1, Ptk2, Pcl6 are all kinases that showed reduced phosphorylation in *mec1-100* cells after HU treatment in our phosphoproteomics dataset. Pcl6, a kinase mainly involved in glycogen metabolism (Wang et al., 2001) shows partial nuclear localization, while all others are exclusively cytoplasmic. Interestingly, it has been reported that a small fraction of Ddc2 is also localized in the cytoplasm, providing an explanation how phosphorylation of these cytoplasmic kinases could be targeted by Mec1-Ddc2 (Huh et al., 2003). The sole link of these kinases to the replication checkpoint or to replication stress signaling is Hrk1, which regulates trans-membrane transport (Goossens et al., 2000). Its protein level was found affected after replication stress (Tkach et al., 2012), although the functional significance of this remains unclear. While we cannot exclude that another kinase might be responsible for non-S/TQ consensus site modification that shows *mec1-100* sensitivity, there is no obvious mediator for this modification other than Mec1.

To confirm that the detected phosphoacceptor sites are indeed direct Mec1 phosphorylation sites, we must perform *in vitro* kinase assays, even though this is often inconclusive, as kinases can show promiscuous phosphorylation *in vitro*. Nonetheless, our work shows strikingly that most Mec1-100-dependent phosphorylation sites are also targeted by Psy2-Pph3, whether directly or indirectly. This confirms the intimate functional relationship between both kinase and phosphatase as found in our two independent genetic screens (Figure 2.1).

MEC1 IS PHOSPHORYLATED AT SERINE 1991

Not only does this work show that the kinase Mec1-Ddc2 and the PP4 phosphatase Psy2-Pph3 interact and balance each other's functions, we also report a phosphorylation site in Mec1, serine 1991, that is regulated in a Pph3-dependent manner. Similarly, human ATR autophosphorylates at a site in its FAT domain (T1989, Figure 3.1), (Liu et al., 2011; Nam et al., 2011b). and phosphorylation correlates with ATR activation. We show that Mec1 kinase activity but also the Rad53 protein is required for serine 1991 phosphorylation (Figure 2.7). At this stage we do not know whether Rad53 regulates Mec1 phosphorylation directly or indirectly. Even though it is unlikely, we cannot rule out

that Rad53 presence contributes in a manner independent of its kinase activity. It is intriguing that although Rad53 is required for Mec1 phosphorylation, S1991 modification does not strictly correlate with Rad53 phosphorylation, which is often taken as a measure for Rad53 activity. Specifically, Mec1 S1991 phosphorylation after Zeocin treatment is barely detectable compared to after HU treatment, yet Rad53 phosphorylation due to Zeocin is much stronger than on HU (Figure 2.7). Thus, additional unknown mechanisms seem to influence the Mec1 phosphorylation status. HU treatment leads to accumulation in S phase due to replication checkpoint activation, while the radiomimetic drug Zeocin rather triggers G1 or G2 checkpoints. Thus, the cell cycle stage might somehow influence Mec1 phosphorylation. Finally, it remains possible that Mec1 autophosphorylates in a manner dependent on Rad53.

Phosphorylation can regulate proteins on different levels. It can affect protein stability, enzymatic activity or association with binding partners, or it can occur without any detectable function. We were unable to directly measure protein levels of a non-phosphorylatable *mec1-S1991A* or phosphomimicking *mec1-S1991D* mutant, because all Mec1 antibodies that we tested so far, were too weak to detect Mec1 in extract samples by western blot. However, the amount of *mec1-S1991A* that is pulled down with Ddc2 is comparable to *Mec1⁺* (Figure 2.7). This indicates that expression and Mec1-Ddc2 interaction are not affected due to S1991 mutation, although we have not ruled out that the phosphomimicking *mec1-S1991D* mutant might be impaired for Ddc2 binding. We further find that mutating S1991A renders cells sensitive to double strand breaks, indicating that S1991 phosphorylation does have a function in survival of DNA damage. Since S1991 is localized close to the catalytic domain, in a helical area that might fold back onto the kinase domain (Figure 3.3), it is reasonable to speculate that it might regulate enzymatic activity. Similarly, we identified *mec1-100* intragenic suppressor mutations around that same area (e.g. Q1903E, R1907T, D2104H). Further genetic analysis showed that a surface exposed subset of mutations required Rad24 for *mec1-100* suppression while others act independently of Rad24 (Chapter 3). We speculate that these may enhance Mec1 enzymatic activity possibly through a similar mechanism as Mec1 S1991 phosphorylation.

The phosphorylation of S1991 after HU treatment is reduced in *mec1-100* cells, due to the reduced activity of the *mec1-100* protein *in vivo* after HU treatment. Phosphorylation is rescued by loss of Pph3, which also rescues the majority of *mec1-100* targets. By this criteria, S1991 phosphorylation correlates with Mec1 activity. However, even though Mec1 is activated and Mec1 S1991 phosphorylation is strongly induced after HU treatment, cells expressing the non-phosphorylatable *mec1-S1991A* mutant are not as HU sensitive as *mec1-100* or *mec1Δ* cells by drop assay, although we have not analyzed *mec1-S1991A* in other assays (e.g. replication fork restart). Thus, S1991 phosphorylation might contribute to, but cannot be crucial for, Mec1 activity. Alternatively, S1991 modification might induce or disrupt binding of an unknown factor or interaction with a subset of substrates, and thus may be important for the survival of double strand breaks. Analysis of genetic interactions of *mec1-S1991A* with mutants defective in specific repair pathways (e.g. *rad9Δ* for DNA damage checkpoint, *mrc1-AQ* for replication checkpoint, *rad52Δ* for homologous recombination or *dnl4Δ* for non-homologous end joining) could result in testable hypotheses regarding the function of this modification. Additionally, *in vitro* kinase assays would contribute to dissect a potential role of S1991 phosphorylation in Mec1 activation.

To study Mec1 function in the replication checkpoint we make use of an S-phase defective allele of Mec1, *mec1-100* (Paciotti et al., 2001). A similar mutant allele of human ATR has been described, with three mutations just N-terminal of the FAT domain (Figure 3.1) (Nam et al., 2011a). Therefore, this region seems to be a conserved regulatory domain important for replication checkpoint function. One part of my work aimed to identify the cause for this S phase defect. In Chapter 3 several hypotheses were developed and tested. Neither kinase activity (Figure S2.1), dimerization, Ddc2 interaction (Figure 2.5) nor localization (Cobb et al., 2005; Tercero et al., 2003) seem to be impaired to a measurable extent in the mutant. Genetic interaction analysis showed that *mec1-100* likely acts on a different pathway than other known canonical checkpoint mutants (Figure 3.2). We could not identify binding partners by IP and mass spectrometry that were lost due to *mec1-100* mutations (Figure 3.2). However, in order to identify binding partners by IP and mass spectrometry, an interaction must be strong and stable enough to be maintained throughout the procedure. Weak and transient interactions may be undetectable by this method, unless crosslinking agents are used.

Some of the other features tested, e.g. oligomerization, could be studied further *in vitro* using purified proteins and more sensitive methods, like size exclusion chromatography. Mec1-Ddc2 is a very large protein complex (Ddc2: 86 kDa, Mec1: 273 kDa) and not very abundant in cells (Ddc2 abundance: about 600 molecules per cell) (Ghaemmaghami et al., 2003). Together with the fact that fusing Mec1 with an epitope tag, even an internal one, impairs its function (Figure S2.4), turns large scale Mec1-Ddc2 complex purification into a great challenge. In order to perform *in vitro* assays, Galactose-inducible overexpression and 500g of yeast for Mec1-Ddc2 purification were used (Majka et al., 2006). On the other hand, resolution of the partial structure of another PI3K-like kinase, mammalian target of Rapamycin (mTOR), covering its FAT, kinase and FATC domain was recently reported (Yang et al., 2013). Thus it seems reasonable to expect that the Mec1-Ddc2 structure could be resolved in the near future as well. Structural data would certainly help to understand the mechanism of Mec1 activation, the function of residues mutated in *mec1-100* and the mechanism of intragenic *mec1-100* suppressor mutations described and modeled in Chapter 3.

SGS1 IS A MEC1 TARGET AND BINDS RAD53 IN A MEC1-DEPENDENT MANNER *IN VIVO*

In a third project I contributed to understanding the role of the yeast RecQ helicase Sgs1 in checkpoint signaling and replication fork stabilization. Genetically, *sgs1Δ* shows synthetic lethality with *mec1-100* on HU and the two mutations destabilize replication forks in a synergistic manner (Cobb et al., 2005). The rate of spontaneous gross chromosomal rearrangements in yeast increases 80-fold in *sgs1Δ* cells, 500-fold when *sgs1Δ* is combined with *mec1-100* and then 160 thousand-fold when the double mutant is exposed to HU (Cobb et al., 2005). The ability of Sgs1 to preserve or stabilize replication forks on HU requires its helicase activity, but not its ability to bind Rad53 (Chapter 4). Finally, it was shown that Sgs1 or other RecQ homologs such as BLM or WRN can unwind some simple double-stranded DNA substrates, although they prefer more complex structures like G4 quartets, three-way junctions, fold-back structures or Holliday junctions *in vitro* (Cejka and Kowalczykowski, 2010; Huber et al., 2002; Mohaghegh et al., 2001; Sun et al., 1998).

The contribution of Sgs1 and BLM to preserve genome stability during DNA double strand break (DSB) repair has been intensively studied: Sgs1 promotes resection together with Dna2 (Cejka et al., 2010; Nimonkar et al., 2011; Zhu et al., 2008), regulates Rad51 filament and D-loop formation (Bachrati et al., 2006; Bugreev et al., 2007; van Brabant et al., 2000). Furthermore, together with Top3 and Rmi1, Sgs1 can resolve double Holliday junctions such that exclusively non-crossover products are generated (Ira et al., 2003; Wu and Hickson, 2003).

On the other hand, Bloom Syndrome cells progress slowly through S phase, accumulate replication intermediates and are sensitive to replication fork stalling agents such as HU (reviewed by (Manthei and Keck, 2013)), indicating an additional role in replication fork stabilization and restart. Indeed, *sgs1* mutants are more sensitive to perturbed replication than to the induction of DSBs. Furthermore, BLM and Sgs1 protein levels peak in S phase (Dutertre et al., 2000; Frei and Gasser, 2000), and BLM was recently shown to be stabilized through an interaction with TopBP1 in S phase, independent of TopBP1 functions in ATR activation and DNA replication (Wang et al., 2013). In budding yeast the stabilization of replicative polymerases at forks stalled on HU, and recovery from HU treatment, depends on Sgs1 helicase activity. Given the preference of Sgs1 and BLM to unwind unusual folded DNA structures, one likely function of the helicase at stalled replication forks is the reversal or elimination of fold-back or reversed forks, which accumulate when forks stall and excessive ssDNA accumulates. This would explain the ability of Sgs1 to promote RPA and Pol α binding at stalled forks. Thus, in addition to well-known functions in DSB repair, multiple lines of evidence point to an important role of BLM/Sgs1 in the survival of stalled replication forks.

It has been suggested that BLM/Sgs1 can promote lesion bypass through driving fork regression by its branch migration activity followed by template switching. Subsequently, BLM/Sgs1 could reverse the regressed fork by branch migration. Alternatively, BLM/Sgs1 might regulate recombination events, either to prevent aberrant recombination or in contrast to promote homologous recombination-mediated restart (reviewed by (Manthei and Keck, 2013)). BLM sumoylation was recently proposed to facilitate RPA/Rad51 exchange and Rad51 accumulation after prolonged replication fork stalling (Eladad et al., 2005; Ouyang et al., 2009; Ouyang et al., 2013). WRN and Sgs1 are sumoylated as well (Branzei et al., 2006; Kawabe et al., 2000), but Sgs1 sumoylation seems to be important for telomere recombination only (Lu et al., 2010). Although the exact role of BLM/Sgs1 in restart of stalled replication forks remains to be determined, BLM directly interacts and collaborates with several components of the Fanconi anemia pathway both in intra-strand crosslink repair and replication fork restart (Chaudhury et al., 2013; Deans and West, 2009; Suhasini and Brosh, 2012). The Fanconi anemia pathway is thought not to be conserved as such in yeast, although putative FancM, FancJ and FancP homologs exist (reviewed by (McHugh et al., 2012)). Interestingly, the putative FancM homolog Mph1 is also implicated in limiting crossover formations, similar to Sgs1 (Prakash et al., 2009). Further delineating the crosstalk between Fanconi anemia pathway proteins and Sgs1/BLM is an area of ongoing research.

RPA, which is essential for DNA repair and replication, interacts with all RecQ helicases (Croteau et al., 2014). In Chapter 4 we show that an acidic region distinct from the helicase domain in Sgs1 binds RPA. Impaired RPA binding in the *sgs1-rl* mutant, however, did not result in replication fork stabilization defects, unlike disrupting Sgs1 helicase function. Previously, RPA was found to stimulate Sgs1 and other RecQ helicases *in vitro* (Cejka and Kowalczykowski, 2010; Croteau et al., 2014). It was suggested, however, that RPA might stabilize a single stranded reaction intermediate (Cejka and Kowalczykowski, 2010), rather than enhancing catalytic activity through a direct interaction with Sgs1. This is in agreement with our genetic results that show that *sgs1-rl* retains helicase activity *in vivo* (Chapter 4). BLM and WRN were shown to bind RPA through a similar acidic domain as Sgs1 (Doherty et al., 2005). In contrast, a recent study mapped the RPA interaction within the BLM-TopIII α -RMI1-RMI2 complex to a region in RMI1 (Xue et al., 2013). The discrepancy between both studies remains unresolved, but the respective RMI domain is not conserved in *S. cerevisiae* Rmi1. Thus, the acidic domain in Sgs1 remains the strongest interaction domain for the large subunit of RPA in the yeast Sgs1-Top3-Rmi1 complex.

Apart from its function in resolving complex DNA templates Sgs1 was shown to act in checkpoint signaling independent of its helicase activity (Bjergbaek et al., 2005). It associates with

Rad53 and promotes Mec1-dependent Rad53 phosphorylation (Bjergbaek et al., 2005; Frei and Gasser, 2000). In Chapter 4 we show that the acidic region bound by RPA is also phosphorylated by Mec1. The phosphorylation of Sgs1 allows it to bind Rad53 through the same acidic region both *in vitro* and *in vivo*. Similar to Sgs1, WRN and BLM are phosphorylated by ATM/ATR (Ammazzalorso et al., 2010; Davies et al., 2004; Pichierri et al., 2003). On the other hand, BLM and WRN phosphorylation seems to be important for their recruitment or stable association with stalled replication forks, while Sgs1 is permanently associated with replication forks, also during an unperturbed S phase (Cobb et al., 2003). Recently, it was shown that BLM knockdown did not affect CHK1 phosphorylation, although WRN knockdown does in response to CPT, but not to HU (Patro et al., 2011; Wang et al., 2013) This may indicate that redundant pathways recruit the downstream kinase. Even in yeast, multiple pathways for Rad53 recruitment to stalled or damaged forks exist (Chapter 1).

Whether RPA and Rad53 binding to Sgs1 can occur at the same time or is mutually exclusive remains to be investigated. Sgs1 associates with replication forks and can be recovered from cell lysates tightly bound to RPA even in the absence of DNA damage (Cobb et al., 2003). However, Sgs1 phosphorylation is only detected after HU treatment (Chapter 4). Thus, Sgs1 would only acquire Rad53 binding activity after Mec1 activation. Given that the RPA-Sgs1 interaction seems to be constitutive and is not disrupted by Sgs1 phosphorylation, a trimeric RPA-Sgs1-Rad53 complex is possible. On the other hand, given the size of the acidic stretch (200 aa) it may be unlikely that both bind concurrently. Interestingly, Sgs1 is epistatic with the replication checkpoint mediator Mrc1 with respect to Rad53 activation, but not with respect to fork stabilization (Alcasabas et al., 2001; Bjergbaek et al., 2005). Mrc1 has been suggested to promote Mec1-Rad53 interaction (Chen and Zhou, 2009), but may also play a role in stabilizing recruited Mec1-Ddc2 (Naylor et al., 2009). It could therefore act upstream of Sgs1 in the signaling pathway to Rad53. The broad range of contributions made by Sgs1 at replication forks, renders it difficult to determine the exact interplay of partially redundant pathways, that enable fork restart, checkpoint activation or translesion synthesis.

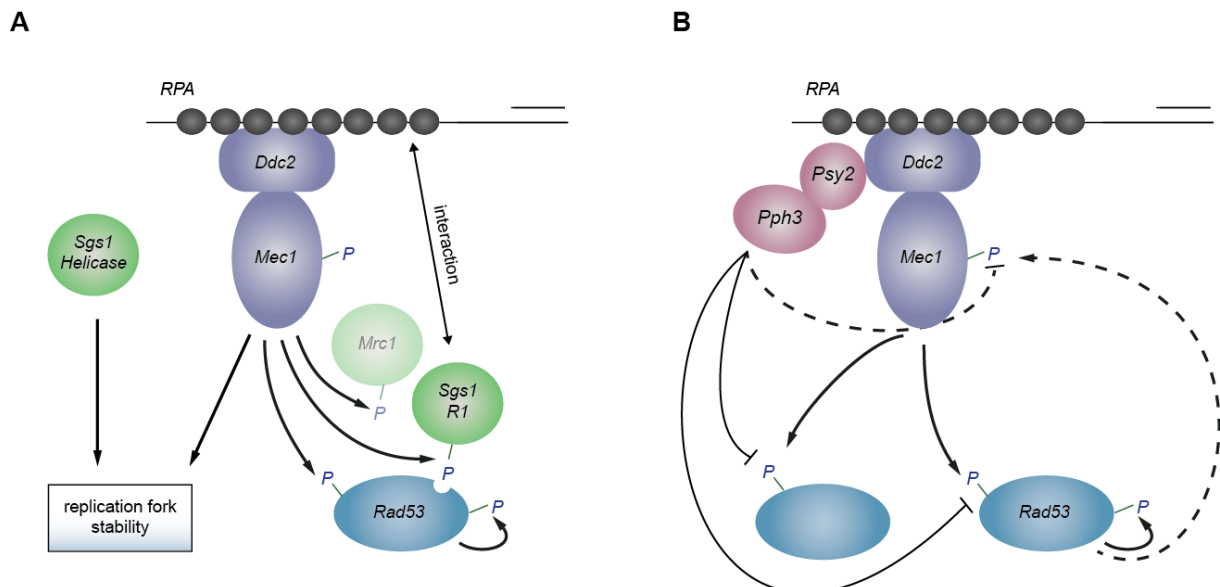


Figure 5.1: Conclusions from this work. (A) While Mec1 and the Sgs1 helicase activity synergistically contribute to replication fork stabilization, the Sgs1 R1 region contributes to checkpoint signaling. R1 both interacts with RPA and binds Rad53, the latter being dependent on phosphorylation by Mec1. Regarding checkpoint signaling Sgs1 is epistatic with the replication checkpoint mediator Mrc1. (B) Psy2-Pph3 physically interact with Mec1-Ddc2 and regulates phosphorylation of both Rad53 and other Mec1 targets that were found downregulated in *mec1-100* cells. Pph3 further regulates Mec1 S1991 phosphorylation, although likely indirectly through Rad53.

The relationship between the study of Sgs1 and our insights into the regulation of Mec1-Ddc2 requires comment. Sgs1 is a target of Mec1, both are found at stalled or damage replication forks, and mutation of each leads to a profound sensitivity to replication fork stalling on HU. The combination of *sgs1*Δ with loss of the S-phase function of Mec1 (*mec1-100*) leads to full fork collapse and cell death on even low doses of HU. Such synergism is not observed when *sgs1*Δ is combined with *rad53*Δ, and it places *mec1-100* on a distinct pathway from that of *sgs1*Δ with respect to fork stability (Cobb et al., 2005). This reinforces earlier conclusions that the roles of Mec1 and Rad53 are not equivalent at stalled replication forks: Indeed, whereas *rad53* mutation can be suppressed by *exo1* deletion, *mec1* mutants are not (Segurado and Diffley, 2008). Unlike the synergism observed between *mec1-100* and the loss of Sgs1 helicase activity, there was no synergy with the *sgs1-r1* mutation which deleted the Rad53 binding site. In fact, this mutant was not hypersensitive to HU, although it showed Zeocin sensitivity, indicating that it acts redundantly with other factors in the checkpoint response to HU. My main goal was to understand Mec1 function and regulation by characterizing a specific Mec1 mutant, *mec1-100*, which shows a selective, S-phase specific loss of Rad53 activation ((Paciotti et al., 2001) (Chapter 3). Consistently, in the main part of my work I found that the PP4 phosphatase regulates Mec1 signaling, both by targeting Rad53, but also by regulating a majority (94%) of Rad53-independent targets, and a phosphoacceptor site within Mec1 (Chapter 2). In summary, I found both a new factor acting in the Rad53 branch (the R1 region in Sgs1, Chapter 4) and a major regulatory factor of overall Mec1 signaling (Psy2-Pph3, Chapter 2), that fine-tune Mec1 activity to ensure precise timing and level of target protein phosphorylation (Figure 5.1). These insights significantly expand our knowledge of this central kinase of the DNA damage checkpoint and its impact on genome stability.

REFERENCES

- Alcasabas, A.A., Osborn, A.J., Bachant, J., Hu, F., Werler, P.J., Bousset, K., Furuya, K., Diffley, J.F., Carr, A.M., and Elledge, S.J. (2001). Mrc1 transduces signals of DNA replication stress to activate Rad53. *Nat Cell Biol* 3, 958-965.
- Ammazzalorso, F., Pirzio, L.M., Bignami, M., Franchitto, A., and Pichierri, P. (2010). ATR and ATM differently regulate WRN to prevent DSBs at stalled replication forks and promote replication fork recovery. *EMBO J* 29, 3156-3169.
- Bachrati, C.Z., Borts, R.H., and Hickson, I.D. (2006). Mobile D-loops are a preferred substrate for the Bloom's syndrome helicase. *Nucleic Acids Res* 34, 2269-2279.
- Benton, M.G., Somasundaram, S., Glasner, J.D., and Palecek, S.P. (2006). Analyzing the dose-dependence of the *Saccharomyces cerevisiae* global transcriptional response to methyl methanesulfonate and ionizing radiation. *BMC genomics* 7, 305.
- Bjergbaek, L., Cobb, J.A., Tsai-Pflugfelder, M., and Gasser, S.M. (2005). Mechanistically distinct roles for Sgs1p in checkpoint activation and replication fork maintenance. *EMBO J* 24, 405-417.
- Bodenmiller, B., Campbell, D., Gerrits, B., Lam, H., Jovanovic, M., Picotti, P., Schlapbach, R., and Aebersold, R. (2008). PhosphoPep--a database of protein phosphorylation sites in model organisms. *Nature biotechnology* 26, 1339-1340.
- Branzei, D., Sollier, J., Liberi, G., Zhao, X., Maeda, D., Seki, M., Enomoto, T., Ohta, K., and Foiani, M. (2006). Ubc9- and mms21-mediated sumoylation counteracts recombinogenic events at damaged replication forks. *Cell* 127, 509-522.
- Bugreev, D.V., Yu, X., Egelman, E.H., and Mazin, A.V. (2007). Novel pro- and anti-recombination activities of the Bloom's syndrome helicase. *Gene Dev* 21, 3085-3094.
- Cejka, P., Cannavo, E., Polaczek, P., Masuda-Sasa, T., Pokharel, S., Campbell, J.L., and Kowalczykowski, S.C. (2010). DNA end resection by Dna2-Sgs1-RPA and its stimulation by Top3-Rmi1 and Mre11-Rad50-Xrs2. *Nature* 467, 112-116.
- Cejka, P., and Kowalczykowski, S.C. (2010). The full-length *Saccharomyces cerevisiae* Sgs1 protein is a vigorous DNA helicase that preferentially unwinds holliday junctions. *J Biol Chem* 285, 8290-8301.
- Chaudhury, I., Sareen, A., Raghunandan, M., and Sobeck, A. (2013). FANCD2 regulates BLM complex functions independently of FANCI to promote replication fork recovery. *Nucleic Acids Res* 41, 6444-6459.
- Chen, S.H., Albuquerque, C.P., Liang, J., Suhandynata, R.T., and Zhou, H. (2010). A proteome-wide analysis of kinase-substrate network in the DNA damage response. *J Biol Chem* 285, 12803-12812.
- Chen, S.H., and Zhou, H. (2009). Reconstitution of Rad53 activation by Mec1 through adaptor protein Mrc1. *J Biol Chem* 284, 18593-18604.
- Cho, R.J., Campbell, M.J., Winzler, E.A., Steinmetz, L., Conway, A., Wodicka, L., Wolfsberg, T.G., Gabrielian, A.E., Landsman, D., Lockhart, D.J., *et al.* (1998). A genome-wide transcriptional analysis of the mitotic cell cycle. *Mol Cell* 2, 65-73.
- Cobb, J.A., Bjergbaek, L., Shimada, K., Frei, C., and Gasser, S.M. (2003). DNA polymerase stabilization at stalled replication forks requires Mec1 and the RecQ helicase Sgs1. *EMBO J* 22, 4325-4336.
- Cobb, J.A., Schleker, T., Rojas, V., Bjergbaek, L., Tercero, J.A., and Gasser, S.M. (2005). Replisome instability, fork collapse, and gross chromosomal rearrangements arise synergistically from Mec1 kinase and RecQ helicase mutations. *Genes Dev* 19, 3055-3069.
- Croteau, D.L., Popuri, V., Opresko, P.L., and Bohr, V.A. (2014). Human RecQ helicases in DNA repair, recombination, and replication. *Annual review of biochemistry* 83, 519-552.

- Davies, S.L., North, P.S., Dart, A., Lakin, N.D., and Hickson, I.D. (2004). Phosphorylation of the Bloom's syndrome helicase and its role in recovery from S-phase arrest. *Mol Cell Biol* *24*, 1279-1291.
- Deans, A.J., and West, S.C. (2009). FANCM connects the genome instability disorders Bloom's Syndrome and Fanconi Anemia. *Mol Cell* *36*, 943-953.
- Doherty, K.M., Sommers, J.A., Gray, M.D., Lee, J.W., von Kobbe, C., Thoma, N.H., Kureekattil, R.P., Kenny, M.K., and Brosh, R.M., Jr. (2005). Physical and functional mapping of the replication protein a interaction domain of the werner and bloom syndrome helicases. *J Biol Chem* *280*, 29494-29505.
- Dutertre, S., Ababou, M., Onclercq, R., Delic, J., Chatton, B., Jaulin, C., and Amor-Gueret, M. (2000). Cell cycle regulation of the endogenous wild type Bloom's syndrome DNA helicase. *Oncogene* *19*, 2731-2738.
- Eladad, S., Ye, T.Z., Hu, P., Leversha, M., Beresten, S., Matunis, M.J., and Ellis, N.A. (2005). Intra-nuclear trafficking of the BLM helicase to DNA damage-induced foci is regulated by SUMO modification. *Hum Mol Genet* *14*, 1351-1365.
- Freeman, A.K., Dapic, V., and Monteiro, A.N. (2010). Negative regulation of CHK2 activity by protein phosphatase 2A is modulated by DNA damage. *Cell Cycle* *9*, 736-747.
- Frei, C., and Gasser, S.M. (2000). The yeast Sgs1p helicase acts upstream of Rad53p in the DNA replication checkpoint and colocalizes with Rad53p in S-phase-specific foci. *Genes Dev* *14*, 81-96.
- Ghaemmaghami, S., Huh, W.K., Bower, K., Howson, R.W., Belle, A., Dephoure, N., O'Shea, E.K., and Weissman, J.S. (2003). Global analysis of protein expression in yeast. *Nature* *425*, 737-741.
- Goodarzi, A.A., Jonnalagadda, J.C., Douglas, P., Young, D., Ye, R., Moorhead, G.B., Lees-Miller, S.P., and Khanna, K.K. (2004). Autophosphorylation of ataxia-telangiectasia mutated is regulated by protein phosphatase 2A. *EMBO J* *23*, 4451-4461.
- Goossens, A., de La Fuente, N., Forment, J., Serrano, R., and Portillo, F. (2000). Regulation of yeast H(+)-ATPase by protein kinases belonging to a family dedicated to activation of plasma membrane transporters. *Mol Cell Biol* *20*, 7654-7661.
- Hart, Y., and Alon, U. (2013). The utility of paradoxical components in biological circuits. *Mol Cell* *49*, 213-221.
- Henriksen, P., Wagner, S.A., Weinert, B.T., Sharma, S., Bacinskaja, G., Rehman, M., Juffer, A.H., Walther, T.C., Lisby, M., and Choudhary, C. (2012). Proteome-wide analysis of lysine acetylation suggests its broad regulatory scope in *Saccharomyces cerevisiae*. *Mol Cell Proteomics* *11*, 1510-1522.
- Huber, M.D., Lee, D.C., and Maizels, N. (2002). G4 DNA unwinding by BLM and Sgs1p: substrate specificity and substrate-specific inhibition. *Nucleic Acids Res* *30*, 3954-3961.
- Huh, W.K., Falvo, J.V., Gerke, L.C., Carroll, A.S., Howson, R.W., Weissman, J.S., and O'Shea, E.K. (2003). Global analysis of protein localization in budding yeast. *Nature* *425*, 686-691.
- Ira, G., Malkova, A., Liberi, G., Foiani, M., and Haber, J.E. (2003). Srs2 and Sgs1-Top3 suppress crossovers during double-strand break repair in yeast. *Cell* *115*, 401-411.
- Kawabe, Y., Seki, M., Seki, T., Wang, W.S., Imamura, O., Furuichi, Y., Saitoh, H., and Enomoto, T. (2000). Covalent modification of the Werner's syndrome gene product with the ubiquitin-related protein, SUMO-1. *J Biol Chem* *275*, 20963-20966.
- Kim, S.T., Lim, D.S., Canman, C.E., and Kastan, M.B. (1999). Substrate specificities and identification of putative substrates of ATM kinase family members. *J Biol Chem* *274*, 37538-37543.
- Lee, S.E., Pelliccioli, A., Demeter, J., Vaze, M.P., Gasch, A.P., Malkova, A., Brown, P.O., Botstein, D., Stearns, T., Foiani, M., *et al.* (2000). Arrest, adaptation, and recovery following a

- chromosome double-strand break in *Saccharomyces cerevisiae*. Cold Spring Harbor symposia on quantitative biology 65, 303-314.
- Leung-Pineda, V., Ryan, C.E., and Piwnicka-Worms, H. (2006). Phosphorylation of Chk1 by ATR is antagonized by a Chk1-regulated protein phosphatase 2A circuit. *Mol Cell Biol* 26, 7529-7538.
- Liu, S., Shiotani, B., Lahiri, M., Marechal, A., Tse, A., Leung, C.C., Glover, J.N., Yang, X.H., and Zou, L. (2011). ATR autophosphorylation as a molecular switch for checkpoint activation. *Mol Cell* 43, 192-202.
- Lu, C.Y., Tsai, C.H., Brill, S.J., and Teng, S.C. (2010). Sumoylation of the BLM ortholog, Sgs1, promotes telomere-telomere recombination in budding yeast. *Nucleic Acids Res* 38, 488-498.
- Macurek, L., Benada, J., Mullers, E., Halim, V.A., Krejcikova, K., Burdova, K., Pechackova, S., Hodny, Z., Lindqvist, A., Medema, R.H., *et al.* (2013). Downregulation of Wip1 phosphatase modulates the cellular threshold of DNA damage signaling in mitosis. *Cell Cycle* 12, 251-262.
- Majka, J., Niedziela-Majka, A., and Burgers, P.M. (2006). The checkpoint clamp activates Mec1 kinase during initiation of the DNA damage checkpoint. *Mol Cell* 24, 891-901.
- Manthei, K.A., and Keck, J.L. (2013). The BLM dissolvosome in DNA replication and repair. *Cellular and Molecular Life Sciences* 70, 4067-4084.
- Mazumder, A., Pesudo, L.Q., McRee, S., Bathe, M., and Samson, L.D. (2013). Genome-wide single-cell-level screen for protein abundance and localization changes in response to DNA damage in *S. cerevisiae*. *Nucleic Acids Res* 41, 9310-9324.
- McHugh, P.J., Ward, T.A., and Chovanec, M. (2012). A prototypical Fanconi anemia pathway in lower eukaryotes? *Cell Cycle* 11, 3739-3744.
- Mohaghegh, P., Karow, J.K., Brosh, R.M., Jr., Bohr, V.A., and Hickson, I.D. (2001). The Bloom's and Werner's syndrome proteins are DNA structure-specific helicases. *Nucleic Acids Res* 29, 2843-2849.
- Nam, E.A., Zhao, R., and Cortez, D. (2011a). Analysis of mutations that dissociate G(2) and essential S phase functions of human ataxia telangiectasia-mutated and Rad3-related (ATR) protein kinase. *The Journal of biological chemistry* 286, 37320-37327.
- Nam, E.A., Zhao, R., Glick, G.G., Bansbach, C.E., Friedman, D.B., and Cortez, D. (2011b). Thr-1989 phosphorylation is a marker of active ataxia telangiectasia-mutated and Rad3-related (ATR) kinase. *J Biol Chem* 286, 28707-28714.
- Naylor, M.L., Li, J.M., Osborn, A.J., and Elledge, S.J. (2009). Mrc1 phosphorylation in response to DNA replication stress is required for Mec1 accumulation at the stalled fork. *Proc Natl Acad Sci U S A* 106, 12765-12770.
- Nimonkar, A.V., Genschel, J., Kinoshita, E., Polaczek, P., Campbell, J.L., Wyman, C., Modrich, P., and Kowalczykowski, S.C. (2011). BLM-DNA2-RPA-MRN and EXO1-BLM-RPA-MRN constitute two DNA end resection machineries for human DNA break repair. *Genes Dev* 25, 350-362.
- Nottke, A., Colaiacovo, M.P., and Shi, Y. (2009). Developmental roles of the histone lysine demethylases. *Development* 136, 879-889.
- Ouyang, K.J., Woo, L.L., Zhu, J.M., Huo, D.Z., Matunis, M.J., and Ellis, N.A. (2009). SUMO Modification Regulates BLM and RAD51 Interaction at Damaged Replication Forks. *PLoS Biol* 7.
- Ouyang, K.J., Yagle, M.K., Matunis, M.J., and Ellis, N.A. (2013). BLM SUMOylation regulates ssDNA accumulation at stalled replication forks. *Frontiers in genetics* 4, 167.
- Paciotti, V., Clerici, M., Scotti, M., Lucchini, G., and Longhese, M.P. (2001). Characterization of mec1 kinase-deficient mutants and of new hypomorphic mec1 alleles impairing subsets of the DNA damage response pathway. *Mol Cell Biol* 21, 3913-3925.

- Patro, B.S., Frohlich, R., Bohr, V.A., and Stevnsner, T. (2011). WRN helicase regulates the ATR-CHK1-induced S-phase checkpoint pathway in response to topoisomerase-I-DNA covalent complexes. *J Cell Sci* 124, 3967-3979.
- Peng, J., Schwartz, D., Elias, J.E., Thoreen, C.C., Cheng, D., Marsischky, G., Roelofs, J., Finley, D., and Gygi, S.P. (2003). A proteomics approach to understanding protein ubiquitination. *Nature biotechnology* 21, 921-926.
- Pichierri, P., Rosselli, F., and Franchitto, A. (2003). Werner's syndrome protein is phosphorylated in an ATR/ATM-dependent manner following replication arrest and DNA damage induced during the S phase of the cell cycle. *Oncogene* 22, 1491-1500.
- Prakash, R., Satory, D., Dray, E., Papusha, A., Scheller, J., Kramer, W., Krejci, L., Klein, H., Haber, J.E., Sung, P., *et al.* (2009). Yeast Mph1 helicase dissociates Rad51-made D-loops: implications for crossover control in mitotic recombination. *Genes Dev* 23, 67-79.
- Pramila, T., Wu, W., Miles, S., Noble, W.S., and Breeden, L.L. (2006). The Forkhead transcription factor Hcm1 regulates chromosome segregation genes and fills the S-phase gap in the transcriptional circuitry of the cell cycle. *Genes Dev* 20, 2266-2278.
- Russo, F.D., and Silhavy, T.J. (1993). The essential tension: opposed reactions in bacterial two-component regulatory systems. *Trends in microbiology* 1, 306-310.
- Segurado, M., and Diffley, J.F. (2008). Separate roles for the DNA damage checkpoint protein kinases in stabilizing DNA replication forks. *Genes Dev* 22, 1816-1827.
- Shimada, M., and Nakanishi, M. (2013). Response to DNA damage: why do we need to focus on protein phosphatases? *Frontiers in oncology* 3, 8.
- Shreeram, S., Demidov, O.N., Hee, W.K., Yamaguchi, H., Onishi, N., Kek, C., Timofeev, O.N., Dudgeon, C., Fornace, A.J., Anderson, C.W., *et al.* (2006). Wip1 phosphatase modulates ATM-dependent signaling pathways. *Mol Cell* 23, 757-764.
- Sobhian, B., Shao, G., Lilli, D.R., Culhane, A.C., Moreau, L.A., Xia, B., Livingston, D.M., and Greenberg, R.A. (2007). RAP80 targets BRCA1 to specific ubiquitin structures at DNA damage sites. *Science* 316, 1198-1202.
- Spellman, P.T., Sherlock, G., Zhang, M.Q., Iyer, V.R., Anders, K., Eisen, M.B., Brown, P.O., Botstein, D., and Futcher, B. (1998). Comprehensive identification of cell cycle-regulated genes of the yeast *Saccharomyces cerevisiae* by microarray hybridization. *Mol Biol Cell* 9, 3273-3297.
- Suhasini, A.N., and Brosh, R.M., Jr. (2012). Fanconi anemia and Bloom's syndrome crosstalk through FANCD1-BLM helicase interaction. *Trends Genet* 28, 7-13.
- Sun, H., Karow, J.K., Hickson, I.D., and Maizels, N. (1998). The Bloom's syndrome helicase unwinds G4 DNA. *J Biol Chem* 273, 27587-27592.
- Tercero, J.A., Longhese, M.P., and Diffley, J.F. (2003). A central role for DNA replication forks in checkpoint activation and response. *Mol Cell* 11, 1323-1336.
- Tkach, J.M., Yimit, A., Lee, A.Y., Riffle, M., Costanzo, M., Jaschob, D., Hendry, J.A., Ou, J., Moffat, J., Boone, C., *et al.* (2012). Dissecting DNA damage response pathways by analysing protein localization and abundance changes during DNA replication stress. *Nat Cell Biol* 14, 966-976.
- van Attikum, H., Fritsch, O., Hohn, B., and Gasser, S.M. (2004). Recruitment of the INO80 complex by H2A phosphorylation links ATP-dependent chromatin remodeling with DNA double-strand break repair. *Cell* 119, 777-788.
- van Brabant, A.J., Ye, T., Sanz, M., German, I.J., Ellis, N.A., and Holloman, W.K. (2000). Binding and melting of D-loops by the Bloom syndrome helicase. *Biochemistry* 39, 14617-14625.
- Wang, J.D., Chen, J.J., and Gong, Z.H. (2013). TopBP1 Controls BLM Protein Level to Maintain Genome Stability. *Molecular Cell* 52, 667-678.

- Wang, Z., Wilson, W.A., Fujino, M.A., and Roach, P.J. (2001). The yeast cyclins Pc16p and Pc17p are involved in the control of glycogen storage by the cyclin-dependent protein kinase Pho85p. *FEBS Lett* 506, 277-280.
- Wohlschlegel, J.A., Johnson, E.S., Reed, S.I., and Yates, J.R., 3rd (2004). Global analysis of protein sumoylation in *Saccharomyces cerevisiae*. *J Biol Chem* 279, 45662-45668.
- Wu, L., and Hickson, I.D. (2003). The Bloom's syndrome helicase suppresses crossing over during homologous recombination. *Nature* 426, 870-874.
- Xue, X., Raynard, S., Busygina, V., Singh, A.K., and Sung, P. (2013). Role of replication protein A in double holliday junction dissolution mediated by the BLM-Topo IIIalpha-RMI1-RMI2 protein complex. *J Biol Chem* 288, 14221-14227.
- Yamagoe, S., Kanno, T., Kanno, Y., Sasaki, S., Siegel, R.M., Lenardo, M.J., Humphrey, G., Wang, Y., Nakatani, Y., Howard, B.H., *et al.* (2003). Interaction of histone acetylases and deacetylases in vivo. *Mol Cell Biol* 23, 1025-1033.
- Yang, H., Rudge, D.G., Koos, J.D., Vaidialingam, B., Yang, H.J., and Pavletich, N.P. (2013). mTOR kinase structure, mechanism and regulation. *Nature* 497, 217-223.
- Zhang, J., Bao, S., Furumai, R., Kucera, K.S., Ali, A., Dean, N.M., and Wang, X.F. (2005). Protein phosphatase 5 is required for ATR-mediated checkpoint activation. *Mol Cell Biol* 25, 9910-9919.
- Zhu, Z., Chung, W.H., Shim, E.Y., Lee, S.E., and Ira, G. (2008). Sgs1 helicase and two nucleases Dna2 and Exo1 resect DNA double-strand break ends. *Cell* 134, 981-994.

CHAPTER 6: APPENDIX

LIST OF ABBREVIATIONS

4-NQO	<u>4-nitroquinoline 1-oxide</u>
53BP1	<u>p53-binding protein 1</u>
9-1-1	<u>Rad9-Hus1-Rad1</u>
A	<u>alanine</u>
AAD	<u>ATR activation domain</u>
AD	<u>transcription activation domain</u>
AHC	<u>ADA histone acetyltransferase complex</u>
ATM	<u>Ataxia telangiectasia mutated</u>
ATP	<u>adenosine triphosphate</u>
ATR	<u>Ataxia telangiectasia and Rad3 related</u>
ATRIP	<u>ATR interacting protein</u>
BER	<u>base excision repair</u>
Bfa1	<u>Byr-four-alike 1</u>
BLAST	<u>basic local alignment search tool</u>
BLM	<u>Bloom's syndrome protein</u>
BRCA1	<u>Breast cancer type 1 susceptibility protein</u>
BRCT	<u>BRCA1 C-terminal domain</u>
Bre1	<u>brefeldin A sensitivity 1</u>
Bub2*	<u>budding uninhibited by benzimidazole 2</u>
C	<u>cytosine</u>
CAF-1B	<u>chromatin assembly factor 1 subunit B</u>
CCT	<u>chaperonin containing TCP1</u>
Cdc6*	<u>cell division cycle 6</u>
CDK	<u>cyclin dependent kinase</u>
Cds1	<u>checking DNA synthesis 1</u>
Cdt1	<u>Cdc10 dependent transcript 1</u>
Chd1	<u>chromatin organization modifier, helicase, and DNA-binding domains</u>
ChIP	<u>chromatin immunoprecipitation</u>
Chk1*	<u>checkpoint kinase 1</u>
Cin8	<u>chromosome instability 8</u>
CMG	<u>Cdc45, MCM, GINS</u>
Cmp2	<u>calmodulin binding protein 2</u>
Cna1	<u>calcineurin A 1</u>
co-IP	<u>co-immunoprecipitation</u>
COMPASS	<u>complex proteins associated with Set1p</u>
CPT	<u>camptothecin</u>
Crb2	<u>Cut5-repeat binding 2</u>
Crt1	<u>constitutive RNR transcription 1</u>
Csm3	<u>chromosome segregation in meiosis</u>
CTD	<u>C-terminal domain</u>
Ctf4*	<u>chromosome transmission fidelity</u>
CtIP	<u>CtBP-interacting protein</u>
CUL1*	<u>Cullin-1</u>
Cut5	<u>cell untimely torn 5</u>
D	<u>aspartate</u>

DAmP	<u>d</u> e <u>cre</u> ased <u>a</u> bundance by <u>m</u> RNA <u>p</u> erturbation
DBD	<u>D</u> NA <u>b</u> inding <u>d</u> omain
Dbf4	<u>d</u> umb <u>b</u> ell <u>f</u> ormer 4
Dcc1	<u>d</u> efective in sister <u>c</u> hromatid <u>c</u> ohesion 1
Ddc1*	DNA damage checkpoint 1
DDK	Dbf4-dependent kinase
Dia2	<u>d</u> igs <u>i</u> nto <u>a</u> gar
Dis2	<u>d</u> efective <u>i</u> n sister chromatid disjoining
DMEM	<u>D</u> ulbecco's <u>m</u> odified <u>E</u> agle's <u>m</u> edium
DNA	<u>d</u> eoxyribo <u>n</u> ucleic <u>a</u> cid
Dna2	<u>D</u> NA synthesis defective 2
dNTP	deoxynucleotide
Dot1	<u>d</u> isruptor of telomeric silencing 1
Dpb11*	<u>D</u> NA polymerase <u>B</u> 11
DSB	<u>d</u> ouble <u>s</u> trand <u>b</u> reak
dsDNA	<u>d</u> ouble <u>s</u> tranded <u>D</u> NA
DTT	<u>d</u> ithio <u>t</u> hreit <u>o</u> l
Dun1	<u>D</u> NA-damage <u>u</u> ninducible 1
E	glutamate
ECFP	<u>e</u> nhanced <u>c</u> yan <u>f</u> luorescent <u>p</u> rotein
EDTA	<u>e</u> thylenediaminetetra <u>a</u> cetic acid
EMAP	epistatic <u>m</u> iniarray profiling
Eme1	<u>e</u> ssential <u>m</u> eiotic <u>e</u> ndonuclease 1
Exo1	<u>e</u> xonuclease 1
F	phenylalanine
FAT	<u>F</u> RAP, <u>A</u> TM, <u>T</u> RRAP
FATC	<u>F</u> AT <u>C</u> -terminal domain
FCP	TFIIF-associating component of <u>C</u> TD phosphatase
Fen1	<u>F</u> lap <u>e</u> ndonuclease 1
FHA	<u>f</u> ork <u>h</u> ead- <u>a</u> ssociated domain
Flp	<u>f</u> lippase
Fob1	<u>f</u> ork <u>b</u> locking less
FRET	Förster resonance energy transfer
Fun30	<u>f</u> unction <u>u</u> nknown <u>n</u> ow 30
G	glycine
G1 phase	<u>g</u> ap <u>1</u> phase
G2 phase	<u>g</u> ap <u>2</u> phase
GAP	<u>G</u> TPase- <u>a</u> ctivating protein
GCR	<u>g</u> ross <u>c</u> hromosomal <u>r</u> earrangement
GFP	<u>g</u> reen <u>f</u> luorescent <u>p</u> rotein
GINS	go-ichi-ni-san
Glc7	<u>g</u> ly <u>c</u> ogen 7
H	histidine
H2A	histone H2A
H2AX	histone variant H2A.X
H3	histone H3
HAD	haloacid dehalogenase
HEAT	<u>H</u> untingtin, <u>E</u> F3, <u>P</u> P2 <u>A</u> , <u>T</u> OR1
HEK	human embryonic kidney

HELB	DNA <u>h</u> elicase <u>B</u>
HEPES	4-(2-hydroxyethyl)-1-piperazineethanesulfonic acid
HIR	<u>h</u> istone <u>r</u> egulation
<i>HIS</i>	<i><u>HIS3</u></i> gene
HPLC	<u>h</u> igh- <u>p</u> erformance <u>l</u> iquid <u>c</u> hromatography
HR	<u>h</u> omologous <u>r</u> ecombination
HRDC	<u>h</u> elicase and <u>R</u> Nase <u>D</u> <u>C</u> -terminal
HU	<u>h</u> ydroxy <u>u</u> rea
HUS1	<u>h</u> ydroxy <u>u</u> rea <u>s</u> ensitive 1
I	isoleucine
IC	Interstrand crosslink
Ies4*	<u>i</u> no <u>e</u> ighty <u>s</u> ubunit 4
Ino80	<u>i</u> nositol requiring 80
IP	<u>i</u> mmunoprecipitation
IR	irradiation
Irc21	<u>i</u> ncreased <u>r</u> ecombination <u>c</u> enters 21
Isw2*	<u>i</u> mitation <u>s</u> witch subfamily 2
ITC	<u>i</u> sothermal <u>c</u> alibration
K	lysine
KAP1	KRAB-domain-associated protein 1
kD	<u>k</u> ilo <u>d</u> alton
L	leucine
lacZ	β -Galactosidase gen
LC	liquid chromatography
Leo1	<u>l</u> eft <u>o</u> pen reading frame 1
<i>LEU</i>	<i><u>LEU2</u></i> gene
M phase	mitosis
M	methionine
MBF	MluI cell-cycle box (<u>M</u> CB) <u>b</u> inding <u>f</u> actor
MCM	<u>m</u> ini- <u>c</u> hromosome <u>m</u> aintenance
Mcm4*	<u>m</u> ini- <u>c</u> hromosome <u>m</u> aintenance 4
MDC1	<u>m</u> ediator of <u>D</u> NA damage <u>c</u> heckpoint protein 1
Mec1*	<u>m</u> itosis <u>e</u> nter <u>c</u> heckpoint 1
Mih1	<u>m</u> itotic <u>i</u> nducer <u>h</u> omolog 1
Mlp1	<u>m</u> ysin- <u>l</u> ike <u>p</u> rotein 1
MMS	<u>m</u> ethyl <u>m</u> ethanesulfonate
Mrc1	<u>m</u> ediator of the <u>r</u> eplication <u>c</u> heckpoint 1
Mre11	<u>m</u> eiotic <u>r</u> ecombination 1
MRN	<u>M</u> re11, <u>R</u> ad50, <u>N</u> bs1
MRX	<u>M</u> re11, <u>R</u> ad50, <u>X</u> rs2
MS	<u>m</u> ass <u>s</u> pectrometry
Mus81	<u>M</u> MS and <u>U</u> V <u>s</u> ensitive 81
MYH	<u>M</u> ut <u>Y</u> <u>h</u> omolog
N	asparagine
NaPP	sodium pyrophosphate
Nbs1	<u>N</u> ijmegen <u>b</u> reakage <u>s</u> yndrome 1
Nek1	<u>N</u> ever in mitosis <u>A</u> - <u>r</u> elated <u>k</u> inase 1
N-OB	<u>N</u> -terminal <u>O</u> B fold
NP-40	4- <u>N</u> onylphenyl-polyethylene glycol

Nrm1	<u>n</u> egative <u>r</u> egulator of <u>M</u> BF targets 1
Nup84*	<u>n</u> uclear <u>p</u> ore 84
OB	<u>o</u> ligonucleotide <u>b</u> inding
Oca1	<u>o</u> xidant-induced <u>c</u> ell-cycle <u>a</u> rrest 1
ORC	<u>o</u> rig <u>i</u> n <u>r</u> ecognition <u>c</u> omplex
p	phosphorylated
P	proline
PAF1	RNA polymerase II <u>a</u> ssociated <u>f</u> actor 1
PBS	<u>p</u> hosphate <u>b</u> uffered <u>s</u> aline
PCR	<u>p</u> olymerase <u>c</u> hain <u>r</u> eaction
Pds1	<u>p</u> recocious <u>d</u> issociation of <u>s</u> isters 1
PI3K	<u>p</u> hosphoinositide <u>3</u> - <u>k</u> inase
PIKK	<u>P</u> I3 <u>K</u> -related <u>k</u> inase
Plk1	<u>P</u> olo- <u>l</u> ike <u>k</u> inase 1
Plx1	<u>X</u> enopus <u>P</u> olo- <u>l</u> ike kinase 1
PMSF	<u>p</u> henyl <u>m</u> ethyl <u>s</u> ulfonyl <u>f</u> luoride,
Pol1*	<u>p</u> olymerase 1
PP	<u>p</u> rotein <u>p</u> hosphatase
PP4C	<u>PP</u> 4 catalytic subunit
PP4R3*	<u>PP</u> 4 regulatory subunit 3
Ppg1	<u>p</u> rotein <u>p</u> hosphatase involved in glycogen accumulation 1
Pph3*	<u>p</u> rotein <u>p</u> hosphatase 3
PPM	<u>p</u> hosphatase, <u>m</u> etal dependent
PPP	<u>p</u> hosphoprotein <u>p</u> hosphatase
Ppq1	<u>p</u> rotein <u>p</u> hosphatase <u>Q</u> 1
Ppt1	<u>p</u> rotein <u>p</u> hosphatase <u>T</u> 1
Ppz1*	<u>p</u> rotein <u>p</u> hosphatase <u>Z</u> 1
pre-RC	<u>p</u> re- <u>r</u> eplicative <u>c</u> omplex
Psf1*	<u>p</u> artner of <u>S</u> ld <u>f</u> ive
Psy2*	<u>p</u> latinum <u>s</u> ensitivity
Ptc2*	<u>p</u> hosphatase <u>t</u> wo <u>C</u> 2
PTP	<u>p</u> rotein <u>t</u> yrosine <u>p</u> hosphatase
PTPA	<u>p</u> hosphotyrosyl <u>p</u> hosphatase <u>a</u> ctivator
Q	glutamine
R	arginine
Rad53*	<u>r</u> adiation sensitive 53
RAP80	<u>R</u> eceptor- <u>a</u> ssociated protein 80
rDNA	<u>r</u> ibosomal <u>D</u> NA
Rfa1*	<u>r</u> eplication <u>f</u> actor <u>A</u> 1
RFC	<u>r</u> eplication <u>f</u> actor <u>C</u>
RFP	<u>r</u> ed <u>f</u> luorescent protein
Rif1	<u>R</u> AP1- <u>i</u> nteracting <u>f</u> actor 1
Rmi1	<u>R</u> ecQ <u>m</u> ediated genome <u>i</u> nstability
RNA	<u>r</u> ibonucleic acid
RNR	<u>r</u> ibonucleotide <u>r</u> eductase
RPA	<u>r</u> eplication protein <u>A</u>
RQC	<u>R</u> ecQ <u>C</u> -terminal motif
Rqh1	<u>R</u> ecQ-type DNA <u>h</u> elicase 1
Rrd1*	resistant to rapamycin <u>d</u> eletion 1

Rts1*	rox three suppressor 1
Rtt107	regulator of Ty1 transposition 107
Rvb1*	RuvB-like 1
S phase	synthesis phase
S	serine
S. c.	<i>Saccharomyces cerevisiae</i>
<i>S. cerevisiae</i>	<i>Saccharomyces cerevisiae</i>
<i>S. pombe</i>	<i>Shizosaccharomyces pombe</i>
Sae2	sporulation in the absence of spo eleven 2
SAGA	Spt-Ada-Gcn5 acetyltransferase
SAP	Sit4 associated protein
Sap155*	Sit4 associated protein 155
SAS	something about silencing
SBF	Swi4-Swi6 cell-cycle box (SCB) binding factor
SC	synthetic complete medium
SCD	SQ/TQ cluster domain
SCF	Skp, Cullin, F-box containing complex
SCP	small CTD phosphatase
SD	spinning disc
Ser	serine
SGD	Saccharomyces genome database
Sgs1	slow growth suppressor 1
Sit4	suppressor of initiation of transcription 4
Siz1*	SAP and MIZ-finger domain
Sld2*	synthetically lethal with <i>dpb11-1</i>
Slx4*	synthetic lethal of unknown (X) function 4
SMARCAD1	SWI/SNF-related matrix-associated actin-dependent regulator of chromatin subfamily A containing DEAD/H box 1
Sml1	suppressor of <i>mec1</i> lethality
SNF	sucrose non fermenting
Srs2	suppressor of rad six
ssDNA	single stranded DNA
Ssn6	suppressor of <i>snf1</i> 6
SUMO	small ubiquitin-like modifier
SWI	switching defective
Swi3	switching defective 3
T	threonine
Tap42	two A phosphatase associated protein 42
TDG	thymine DNA glycosylase
Tel1	telomere maintenance 1
TFA	trifluoroacetic acid
THO	suppressor of the transcriptional defect of <i>hpr1</i> by overexpression
Thr	threonine
THREX-2	transcription/export-2
Tip41	Tap42 interacting protein 41
TIPIN	TIMELESS-interacting protein
TLCK	N-alpha-tosyl-L-lysiny-chloromethylketone
Tof1	topoisomerase I-interacting factor 1
Top1*	topoisomerase 1

TopBP1	DNA <u>topoisomerase 2-binding</u> protein 1
TOR	<u>target of rapamycin</u>
Tpd3	<u>tRNA processing deficient</u> 3
TPR	<u>tetratricopeptide repeat</u>
Tris	2-amino-2-hydroxymethyl-propane-1,3-diol
tRNA	<u>transfer RNA</u>
TRP	tryptophane
Tup1	d <u>TMP-uptake</u> 1
Ubc13	<u>ubiquitin-conjugating</u> 13
Ubi	<u>ubiquitin</u>
Ulp1	<u>UbL-specific protease</u> 1
USP7*	<u>ubiquitin-specific-processing protease</u> 7
UV	<u>ultraviolet</u> light
V	valine
W	tryptophane
WDHD1	<u>WD repeat and HMG-box DNA-binding</u> protein 1
Wip1	<u>wild-type p53-induced phosphatase</u> 1
WRN	<u>Werner syndrome ATP-dependent</u> helicase
Wss1	<u>weak suppressor of smt3</u> 1
WT	<u>wild type</u>
X-GAL	5-bromo-4-chloro-3-indolyl- β -D-galactopyranoside
Xrs2	X-ray sensitive 2
Y	tyrosine
Y2H	<u>yeast two hybrid</u>
Yku70*	yeast KU protein 70 kD
YPAD	Yeast extract-peptone-dextrose medium + adenine
α	anti
γ H2AX	Ser 139 phosphorylated mammalian histone H2AX

*= alternative numbers may be possible

TABLES 2.1-2.4 AND 2.6 (RELATED TO CHAPTER 2)

SWR2	NA	0.220133	-0.268802	2.56857	-1.137392	0.030477	1.254332	-0.724865	0.66691	-0.025112	0.01021	NA	0.92842	0.58884	0.08374	-0.37457	-0.30459	-1.110939	0.704116	0.21038	1.475009	NA	0.973991	-1.164779	0.530966	0.210248	0.040305	1.073446	0.107747	-0.888157	0.079006	0.070404		
SWR1	NA	-1.010489	0.518389	0.937346	0.568242	0.040435	-1.02446	0.620294	-1.244114	0.100441	0.01694	NA	0.76556	0.017624	0.01832	0.271362	0.01832	0.271362	0.01832	0.271362	0.01832	0.271362	NA	0.481356	-0.32445	0.332216	-0.066388	0.234438	-0.092189	0.056044	0.107747	-0.888157	0.079006	0.070404
SWR0	NA	0.151105	NA	0.03928	0.02930	0.123481	0.01694	0.01694	0.01694	0.01694	0.01694	NA	0.01694	0.01694	0.01694	0.01694	0.01694	0.01694	0.01694	0.01694	0.01694	NA	0.01694	0.01694	0.01694	0.01694	0.01694	0.01694	0.01694	0.01694	0.01694	0.01694	0.01694	0.01694
SWR3	NA	0.132726	0.135693	0.130359	0.130359	0.130359	0.130359	0.130359	0.130359	0.130359	0.130359	NA	0.130359	0.130359	0.130359	0.130359	0.130359	0.130359	0.130359	0.130359	0.130359	NA	0.130359	0.130359	0.130359	0.130359	0.130359	0.130359	0.130359	0.130359	0.130359	0.130359	0.130359	0.130359
SW4	NA	0.848843	-0.132848	-0.211591	0.252411	-0.214843	0.166894	0.176885	-0.267076	-0.166894	0.032071	NA	0.127441	-0.202949	0.232714	0.028151	0.208451	0.06092	0.492106	0.373807	0.3182	0.030477	NA	0.084153	0.298025	0.140243	-0.044576	0.094443	0.44133	-0.832619	-0.865339	-0.386156	0.112209	
SW5	NA	0.099315	0.932884	0.08814	0.08814	0.08814	0.08814	0.08814	0.08814	0.08814	0.08814	NA	0.08814	0.08814	0.08814	0.08814	0.08814	0.08814	0.08814	0.08814	0.08814	NA	0.08814	0.08814	0.08814	0.08814	0.08814	0.08814	0.08814	0.08814	0.08814	0.08814	0.08814	0.08814
SW6	NA	-1.06145	-0.541251	0.992864	0.08814	0.08814	0.08814	0.08814	0.08814	0.08814	0.08814	NA	0.08814	0.08814	0.08814	0.08814	0.08814	0.08814	0.08814	0.08814	0.08814	NA	0.08814	0.08814	0.08814	0.08814	0.08814	0.08814	0.08814	0.08814	0.08814	0.08814	0.08814	0.08814
SW7	NA	0.073744	-0.5109	0.073744	0.073744	0.073744	0.073744	0.073744	0.073744	0.073744	0.073744	NA	0.073744	0.073744	0.073744	0.073744	0.073744	0.073744	0.073744	0.073744	0.073744	NA	0.073744	0.073744	0.073744	0.073744	0.073744	0.073744	0.073744	0.073744	0.073744	0.073744	0.073744	0.073744
SW8	NA	-2.568148	NA	0.023304	0.712209	0.023304	0.712209	0.023304	0.712209	0.023304	0.712209	NA	0.023304	0.712209	0.023304	0.712209	0.023304	0.712209	0.023304	0.712209	0.023304	NA	0.023304	0.712209	0.023304	0.712209	0.023304	0.712209	0.023304	0.712209	0.023304	0.712209	0.023304	0.712209
SW9	NA	-0.843899	-0.110513	0.810066	0.787457	0.23521	0.839085	0.843899	0.184332	-0.028977	0.42471	NA	0.467212	0.832929	0.1708	-0.807661	0.01694	0.092911	0.092911	0.092911	0.092911	NA	0.092911	0.092911	0.092911	0.092911	0.092911	0.092911	0.092911	0.092911	0.092911	0.092911	0.092911	0.092911
SW10	NA	-0.179003	-0.337956	-0.371577	0.458842	0.184132	-0.028977	0.42471	0.467212	0.832929	0.1708	NA	0.092911	0.092911	0.092911	0.092911	0.092911	0.092911	0.092911	0.092911	0.092911	NA	0.092911	0.092911	0.092911	0.092911	0.092911	0.092911	0.092911	0.092911	0.092911	0.092911	0.092911	0.092911
SW11	NA	0.413849	0.587665	0.718866	0.413849	0.587665	0.718866	0.413849	0.587665	0.718866	0.413849	NA	0.587665	0.718866	0.413849	0.587665	0.718866	0.413849	0.587665	0.718866	0.413849	NA	0.587665	0.718866	0.413849	0.587665	0.718866	0.413849	0.587665	0.718866	0.413849	0.587665	0.718866	0.413849
SW12	NA	0.189198	NA	0.06863	-0.051024	-0.265808	0.382672	-0.70351	-0.175529	0.119002	0.243442	NA	0.119002	0.243442	0.119002	0.243442	0.119002	0.243442	0.119002	0.243442	0.119002	NA	0.119002	0.243442	0.119002	0.243442	0.119002	0.243442	0.119002	0.243442	0.119002	0.243442	0.119002	0.243442
SW13	NA	-1.198096	-0.089916	NA	0.45441	0.831614	0.296743	-0.21871	-0.21794	0.87636	NA	0.21871	-0.21794	0.87636	NA	0.21871	-0.21794	0.87636	NA	0.21871	-0.21794	NA	0.21871	-0.21794	0.87636	NA	0.21871	-0.21794	0.87636	NA	0.21871	-0.21794	0.87636	NA
SW14	NA	0.021574	NA	0.148332	0.021574	0.148332	0.021574	0.148332	0.021574	0.148332	0.021574	NA	0.021574	0.148332	0.021574	0.148332	0.021574	0.148332	0.021574	0.148332	0.021574	NA	0.021574	0.148332	0.021574	0.148332	0.021574	0.148332	0.021574	0.148332	0.021574	0.148332	0.021574	0.148332
SW15	NA	-1.467473	0.175253	-0.088564	1.01029	0.71873	-0.184858	0.471039	0.648857	-0.5867	0.10276	NA	0.648857	-0.5867	0.10276	0.10276	0.10276	0.10276	0.10276	0.10276	0.10276	NA	0.10276	0.10276	0.10276	0.10276	0.10276	0.10276	0.10276	0.10276	0.10276	0.10276	0.10276	0.10276
SW16	NA	0.168839	NA	-0.448265	NA	-0.448265	NA	-0.448265	NA	-0.448265	NA	NA	-0.448265	NA	-0.448265	NA	-0.448265	NA	-0.448265	NA	-0.448265	NA	NA	-0.448265	NA	-0.448265	NA	-0.448265	NA	-0.448265	NA	-0.448265	NA	-0.448265
SW17	NA	-0.441709	-0.369745	-1.14003	0.31869	0.31869	0.31869	0.31869	0.31869	0.31869	0.31869	NA	0.31869	0.31869	0.31869	0.31869	0.31869	0.31869	0.31869	0.31869	0.31869	NA	0.31869	0.31869	0.31869	0.31869	0.31869	0.31869	0.31869	0.31869	0.31869	0.31869	0.31869	0.31869
SW18	NA	-1.39194	-0.584875	NA	-0.25326	0.30162	0.3713	0.669489	0.520133	0.180743	0.669489	NA	0.520133	0.180743	0.669489	0.520133	0.180743	0.669489	0.520133	0.180743	0.669489	NA	0.520133	0.180743	0.669489	0.520133	0.180743	0.669489	0.520133	0.180743	0.669489	0.520133	0.180743	0.669489
SW19	NA	-0.360646	-0.068444	-0.429065	0.562759	0.14774	0.69309	-0.368643	-0.181693	-0.085603	NA	0.14774	0.69309	-0.368643	-0.181693	-0.085603	NA	0.14774	0.69309	-0.368643	-0.181693	NA	0.14774	0.69309	-0.368643	-0.181693	-0.085603	NA	0.14774	0.69309	-0.368643	-0.181693	-0.085603	NA
SW20	NA	0.169658	-0.286213	0.71344	0.783075	0.340278	0.484642	0.58822	0.95688	-0.96381	0.58824	NA	0.58824	0.95688	-0.96381	0.58824	0.95688	-0.96381	0.58824	0.95688	-0.96381	NA	0.58824	0.95688	-0.96381	0.58824	0.95688	-0.96381	0.58824	0.95688	-0.96381	0.58824	0.95688	-0.96381
SW21	NA	0.021574	NA	0.148332	0.021574	0.148332	0.021574	0.148332	0.021574	0.148332	0.021574	NA	0.021574	0.148332	0.021574	0.148332	0.021574	0.148332	0.021574	0.148332	0.021574	NA	0.021574	0.148332	0.021574	0.148332	0.021574	0.148332	0.021574	0.148332	0.021574	0.148332	0.021574	0.148332
SW22	NA	-1.467473	0.175253	-0.088564	1.01029	0.71873	-0.184858	0.471039	0.648857	-0.5867	0.10276	NA	0.648857	-0.5867	0.10276	0.10276	0.10276	0.10276	0.10276	0.10276	0.10276	NA	0.10276	0.10276	0.10276	0.10276	0.10276	0.10276	0.10276	0.10276	0.10276	0.10276	0.10276	0.10276
SW23	NA	0.168839	NA	-0.448265	NA	-0.448265	NA	-0.448265	NA	-0.448265	NA	NA	-0.448265	NA	-0.448265	NA	-0.448265	NA	-0.448265	NA	-0.448265	NA	NA	-0.448265	NA	-0.448265	NA	-0.448265	NA	-0.448265	NA	-0.448265	NA	-0.448265
SW24	NA	-0.441709	-0.369745	-1.14003	0.31869	0.31869	0.31869	0.31869	0.31869	0.31869	0.31869	NA	0.31869	0.31869	0.31869	0.31869	0.31869	0.31869	0.31869	0.31869	0.31869	NA	0.31869	0.31869	0.31869	0.31869	0.31869	0.31869	0.31869	0.31869	0.31869	0.31869	0.31869	0.31869
SW25	NA	-1.39194	-0.584875	NA	-0.25326	0.30162	0.3713	0.669489	0.520133	0.180743	0.669489	NA	0.520133	0.180743	0.669489	0.520133	0.180743	0.669489	0.520133	0.180743	0.669489	NA	0.520133	0.180743	0.669489	0.520133	0.180743	0.669489	0.520133	0.180743	0.669489	0.520133	0.180743	0.669489
SW26	NA	-0.360646	-0.068444	-0.429065	0.562759	0.14774	0.69309	-0.368643	-0.181693	-0.085603	NA	0.14774	0.69309	-0.368643	-0.181693	-0.085603	NA	0.14774	0.69309	-0.368643	-0.181693	NA	0.14774	0.69309	-0.368643	-0.181693	-0.085603	NA	0.14774	0.69309	-0.368643	-0.181693	-0.085603	NA
SW27	NA	0.169658	-0.286213	0.71344	0.783075	0.340278	0.484642	0.58822	0.95688	-0.96381	0.58824	NA	0.58824	0.95688	-0.96381	0.58824	0.95688	-0.96381	0.58824	0.95688	-0.96381	NA	0.58824	0.95688	-0.96381	0.58824	0.95688	-0.96381	0.58824	0.95688	-0.96381	0.58824	0.95688	-0.96381
SW28	NA	0.021574	NA	0.148332	0.021574	0.148332	0.021574	0.148332	0.021574	0.148332	0.021574	NA	0.021574	0.148332	0.021574	0.148332	0.021574	0.148332	0.021574	0.148332	0.021574	NA	0.021574	0.148332	0.021574	0.148332	0.021574	0.148332	0.021574	0.148332	0.021574	0.148332	0.021574	0.148332
SW29	NA	-1.467473	0.175253	-0.088564	1.01029	0.71873	-0.184858	0.471039	0.648857	-0.5867	0.10276	NA	0.648857	-0.5867	0.10276	0.10276	0.10276	0.10276	0.10276	0.10276	0.10276	NA	0.10276	0.10276	0.10276	0.10276	0.10276	0.10276	0.10276	0.10276	0.10276	0.10276	0.10276	0.10276
SW30	NA	0.168839	NA	-0.448265	NA	-0.448265	NA	-0.44826																										

CT4	-4.33713	2377806	-3.568313	-0.99278	NA	NA	1.87344	0.84377	NA	NA	NA	0.615783	0.63442	0.79836	-0.844938	-0.31976	0.564203	-0.23417	1.157813	2.78284	NA	1.21871	0.60735	0.62276	NA	-0.838635	1.17255	-0.72166	0.900652	
CT5	-0.274018	-1.78439	-4.62316	-0.191568	0.75714	0.274828	NA	-0.24058	0.00555	-1.46215	0.18648	0.04565	-2.3124	-1.64723	1.06527	-1.44758	NA	0.795638	0.82038	0.25231	0.400368	-1.48394	-0.460188	0.13231	0.400368	-1.48394	-0.460188	0.13231	0.400368	
CT6	-0.96059	0.73105	-1.95359	-0.65862	-0.12863	-0.302507	0.282824	NA	-0.80063	-0.00441	-8.17102	0.187607	0.05201	0.33114	-0.92897	-0.49234	NA	-1.53429	-0.11443	NA	NA	-0.15077	-0.11443	NA	-0.15077	-0.11443	NA	-0.15077	-0.11443	
CT7	0.68359	0.73762	-1.04018	-1.42118	0.06631	-0.04779	0.150088	0.295207	0.88354	0.139211	-0.19388	-0.06757	-0.728249	0.78413	0.02959	0.682524	0.120001	0.626211	-0.692714	-0.244891	-0.905283	0.640047	0.451887	0.451887	0.640047	0.451887	0.451887	0.640047	0.451887	
CT8	-1.84561	2.12565	-0.53693	0.00812	1.96693	-0.65889	-0.71028	NA	0.47178	0.568975	0.945094	0.23537	0.15219	0.32362	-0.40088	0.48259	0.846888	0.324075	0.314035	0.314035	0.314035	0.314035	0.314035	0.314035	0.314035	0.314035	0.314035	0.314035	0.314035	
CT9	0.35065	0.35065	0.88687	0.35065	0.88687	0.35065	0.88687	0.35065	0.88687	0.35065	0.88687	0.35065	0.88687	0.35065	0.88687	0.35065	0.88687	0.35065	0.88687	0.35065	0.88687	0.35065	0.88687	0.35065	0.88687	0.35065	0.88687	0.35065	0.88687	
CT10	0.35065	0.35065	0.88687	0.35065	0.88687	0.35065	0.88687	0.35065	0.88687	0.35065	0.88687	0.35065	0.88687	0.35065	0.88687	0.35065	0.88687	0.35065	0.88687	0.35065	0.88687	0.35065	0.88687	0.35065	0.88687	0.35065	0.88687	0.35065	0.88687	
CT11	0.620686	-0.21696	-0.130117	0.68408	NA	-0.38682	0.14939	0.14777	0.73789	NA	0.0251149	0.78453	0.14485	0.25782	0.29652	0.07076	0.27344	0.35274	NA	0.66188	0.18818	-1.31773	NA	0.18818	0.18818	0.18818	0.18818	0.18818	0.18818	
CT12	-1.40519	0.25264	-0.40459	-0.03661	0.68408	NA	-0.38682	0.14939	0.14777	0.73789	NA	0.0251149	0.78453	0.14485	0.25782	0.29652	0.07076	0.27344	0.35274	NA	0.66188	0.18818	-1.31773	NA	0.18818	0.18818	0.18818	0.18818	0.18818	
CT13	-3.49489	0.21392	-1.38137	0.04699	0.04213	0.12567	0.23063	0.01458	-3.40648	0.15132	-0.89892	0.150219	-0.89892	0.15132	-0.89892	0.150219	-0.89892	0.15132	-0.89892	0.150219	-0.89892	0.15132	-0.89892	0.150219	-0.89892	0.15132	-0.89892	0.150219	-0.89892	
CT14	0.09725	1.23246	0.30238	0.04213	0.09845	-0.95883	1.93342	0.69294	NA	0.167584	0.08621	1.50071	-0.31706	0.07485	1.10074	0.22529	1.20544	0.31328	0.11248	0.20515	0.15274	0.15274	0.15274	0.15274	0.15274	0.15274	0.15274	0.15274	0.15274	
CT15	0.87458	0.249026	0.249026	0.249026	0.249026	0.249026	0.249026	0.249026	0.249026	0.249026	0.249026	0.249026	0.249026	0.249026	0.249026	0.249026	0.249026	0.249026	0.249026	0.249026	0.249026	0.249026	0.249026	0.249026	0.249026	0.249026	0.249026	0.249026	0.249026	
CT16	-1.76927	0.15745	0.88376	0.02321	0.27258	NA	0.08924	0.09614	0.09614	0.09614	0.09614	0.09614	0.09614	0.09614	0.09614	0.09614	0.09614	0.09614	0.09614	0.09614	0.09614	0.09614	0.09614	0.09614	0.09614	0.09614	0.09614	0.09614	0.09614	
CT17	0.55261	0.39762	0.31696	0.68424	-0.130117	0.68408	NA	-0.38682	0.14939	0.14777	0.73789	NA	0.0251149	0.78453	0.14485	0.25782	0.29652	0.07076	0.27344	0.35274	NA	0.66188	0.18818	-1.31773	NA	0.18818	0.18818	0.18818	0.18818	
CT18	-0.17159	NA	-0.37305	0.64050	0.91084	-0.021	0.61183	0.072114	0.75252	1.23874	0.502119	-0.89892	0.150219	-0.89892	0.15132	-0.89892	0.150219	-0.89892	0.15132	-0.89892	0.150219	-0.89892	0.15132	-0.89892	0.150219	-0.89892	0.15132	-0.89892	0.150219	
CT19	0.09725	1.23246	0.30238	0.04213	0.09845	-0.95883	1.93342	0.69294	NA	0.167584	0.08621	1.50071	-0.31706	0.07485	1.10074	0.22529	1.20544	0.31328	0.11248	0.20515	0.15274	0.15274	0.15274	0.15274	0.15274	0.15274	0.15274	0.15274	0.15274	
CT20	0.16256	-0.99528	0.06584	NA	0.06584	0.06584	0.06584	0.06584	0.06584	0.06584	0.06584	0.06584	0.06584	0.06584	0.06584	0.06584	0.06584	0.06584	0.06584	0.06584	0.06584	0.06584	0.06584	0.06584	0.06584	0.06584	0.06584	0.06584	0.06584	
CT21	0.87458	0.249026	0.249026	0.249026	0.249026	0.249026	0.249026	0.249026	0.249026	0.249026	0.249026	0.249026	0.249026	0.249026	0.249026	0.249026	0.249026	0.249026	0.249026	0.249026	0.249026	0.249026	0.249026	0.249026	0.249026	0.249026	0.249026	0.249026	0.249026	
CT22	0.10902	-6.26451	-0.139896	-0.14423	0.169218	0.46855	-2.61637	0.126469	0.126469	0.126469	0.126469	0.126469	0.126469	0.126469	0.126469	0.126469	0.126469	0.126469	0.126469	0.126469	0.126469	0.126469	0.126469	0.126469	0.126469	0.126469	0.126469	0.126469	0.126469	
CT23	-2.26669	NA	0.795638	0.82038	0.25231	0.400368	-1.48394	-0.460188	0.13231	0.400368	-1.48394	-0.460188	0.13231	0.400368	-1.48394	-0.460188	0.13231	0.400368	-1.48394	-0.460188	0.13231	0.400368	-1.48394	-0.460188	0.13231	0.400368	-1.48394	-0.460188	0.13231	0.400368
CT24	-0.07402	1.32594	-0.66139	0.47959	0.78138	-0.99895	-0.74373	1.82511	-0.65291	-1.446106	0.58972	0.159172	1.762024	0.61739	0.17426	0.67279	0.17426	0.67279	0.17426	0.67279	0.17426	0.67279	0.17426	0.67279	0.17426	0.67279	0.17426	0.67279	0.17426	0.67279
CT25	0.02189	0.42488	0.85912	0.06862	-0.11245	0.70226	0.26628	1.03797	0.00116	-0.70709	0.33440	0.23252	-1.35331	0.35851	-0.28899	0.02271	-0.18501	0.78755	0.04508	0.04508	0.04508	0.04508	0.04508	0.04508	0.04508	0.04508	0.04508	0.04508	0.04508	0.04508
CT26	0.33924	-0.82055	-0.41866	-1.72510	0.06873	0.12603	-0.11543	0.76232	0.92714	0.69076	0.8654	0.70957	0.37658	0.64036	0.61468	0.53146	0.10365	0.62714	0.20416	0.04276	0.04276	0.04276	0.04276	0.04276	0.04276	0.04276	0.04276	0.04276	0.04276	
CT27	0.67857	-5.50816	-0.16445	0.19107	0.19015	0.37692	-0.87957	0.00732	0.56915	-0.10484	0.28259	1.77001	0.17403	-0.92654	-0.10305	-0.22124	0.26658	0.27861	0.48728	-0.12949	0.04514	0.04514	0.04514	0.04514	0.04514	0.04514	0.04514	0.04514	0.04514	
CT28	0.85844	1.31738	-0.82950	0.18851	0.23471	0.44881	-0.18851	0.91697	0.29216	0.08813	-0.35129	0.26397	0.13808	0.26658	0.55717	0.10473	-0.20628	0.37978	NA	-0.20628	0.37978	NA	-0.20628	0.37978	NA	-0.20628	0.37978	NA	-0.20628	0.37978
CT29	0.53794	-0.02391	0.62646	0.24281	0.04213	0.09845	-0.95883	1.93342	0.69294	NA	0.167584	0.08621	1.50071	-0.31706	0.07485	1.10074	0.22529	1.20544	0.31328	0.11248	0.20515	0.15274	0.15274	0.15274	0.15274	0.15274	0.15274	0.15274	0.15274	
CT30	-1.39746	-0.0542	0.76573	-0.06013	0.89518	0.11786	0.12411	0.02167	0.54446	NA	-0.05971	0.21932	1.26022	-1.04048	-0.46721	-0.42713	-0.28272	0.16763	0.21268	0.21268	0.21268	0.21268	0.21268	0.21268	0.21268	0.21268	0.21268	0.21268	0.21268	
CT31	0.46262	0.56123	-0.169015	0.10097	0.82038	-0.23286	-0.02611	0.61451	0.96806	-0.18238	0.69004	0.01323	-1.28539	0.12695	-0.10256	-0.54055	-0.19631	-0.23066	0.18268	0.12882	0.12882	0.12882	0.12882	0.12882	0.12882	0.12882	0.12882	0.12882	0.12882	
CT32	0.15420	0.13407	0.33989	-0.48091	NA	0.75848	0.18317	0.86071	0.27449	0.20106	-0.08612	0.02851	-0.29519	-0.10652	0.08091	0.15148	-0.99048	0.76486	0.98956	-0.45561	0.45561	0.45561	0.45561	0.45561	0.45561	0.45561	0.45561	0.45561	0.45561	
CT33	-4.92627	NA	0.03824	-0.17249	0.02509	-0.52942	0.18274	1.50552	-1.80981	-0.61207	0.12164	0.18044	0.09772	0.38547	-0.13897	-0.337516	0.80118	0.78992	0.34327	0.52001	-0.54706	0.16329	0.84429	0.38408	1.00088	0.11579	-0.32706	NA	0.130517	
CT34	-2.46261	-2.12120	0.34348	-0.97347	0.02509	-0.52942	0.18274	1.50552	-1.80981	-0.61207	0.12164	0.18044	0.09772	0.38547	-0.13897	-0.337516	0.80118	0.78992	0.34327	0.52001	-0.54706	0.16329	0.84429	0.38408	1.00088	0.11579	-0.32706	NA	0.130517	
CT35	0.00575	0.94432	0.41439	0.71467	0.16163	-0.15892	-0.71372	-0.54669	NA	-1.85948	-0.17912	-0.54669	NA	0.71633	0.75835	0.23163	NA	0.71633	0.75835	0.23163	NA	0.71633	0.75835	0.23163	NA	0.71633	0.75835	0.23163	NA	
CT36	0.12793	0.15188	0.8652	-0.24143	0.0282	0.13019	-0.54283	0.23119	2.95888	0.61057	0.112108	1.31843	0.65725	0.09324	-0.06536	0.20378	0.14263	0.04864	0.49285	0.64834	0.15739	-0.32706	NA	0.130517	0.30517	0.12008	NA	0.160071	0.08225	
CT37	-0.43121	-0.20287	0.44578	0.84576	0.00052	0.93679	-1.33267	0.930168	-0.00054	-0.12878	0.70425	-0.52731	0.80118	0.78992	0.34327	0.52001	-0.54706	0.16329	0.84429	0.38408	1.00088	0.11579	-0.32706	NA	0.130517	0.30517	0.12008	NA	0.160071	
CT38	0.56181	1.91599	0.01006	0.86217	-0.119556	-0.331	0.181653	1.07862	0.86641	NA	0.186741	0.19599	0.00076	-0.14261	0.053															

PT11	1.34598 NA	1.08549 -0.77686	-0.27108 -0.06604	0.11084	1.62847	0.01328	-0.15707	-0.72365	0.39934 NA	0.97884 NA	-0.75458 -0.07378	0.03779	0.68814 NA	-0.34605	0.60358 NA	0.86939	0.72397	-0.87284	0.58719	-0.33583	-0.44736	-0.33805	-0.46424		
PT12	1.59475 NA	0.14191	-0.70618	-0.13789	-0.67954	-0.21378	-0.55916 NA	-0.06629 NA	0.39934 NA	0.97884 NA	-0.75458 -0.07378	0.03779	0.68814 NA	-0.34605	0.60358 NA	0.86939	0.72397	-0.87284	0.58719	-0.33583	-0.44736	-0.33805	-0.46424		
PT13	0.576675	-0.35224	-0.80270	-0.03189	-0.44264	-0.39378	-0.60360 NA	0.23189	0.04883	0.62244	-0.25304	0.15556 NA	-0.80878	-0.72722	0.54102	-0.10936	0.86939	0.72397	-0.87284	0.58719	-0.33583	-0.44736	-0.33805	-0.46424	
PT14	NA	0.274	0.2928	0.07269	0.48105	0.14685	0.51389 NA	0.23189	0.04883	0.62244	-0.25304	0.15556 NA	-0.80878	-0.72722	0.54102	-0.10936	0.86939	0.72397	-0.87284	0.58719	-0.33583	-0.44736	-0.33805	-0.46424	
PT15	NA	-1.0423	0.42061	-0.79451	0.78015	-0.60264	-0.24781	0.15703	0.15703	0.15703	0.15703	0.15703	0.15703	0.15703	0.15703	0.15703	0.15703	0.15703	0.15703	0.15703	0.15703	0.15703	0.15703	0.15703	
PT16	NA	-1.83357	-0.88146	-0.39682 NA	-0.09149	0.73081	-0.73628	0.73731	0.84169	-0.27507	0.65674 NA	0.13868	0.27507	0.13868	0.27507	0.13868	0.27507	0.13868	0.27507	0.13868	0.27507	0.13868	0.27507	0.13868	
PT17	-2.20589	0.60793	-1.02079	0.78274	-1.76523	0.82601	-1.37897 NA	-0.40272	0.75458	-0.79089	-1.06862	0.42373	0.05182	0.13342	0.33582	0.61404	0.81894 NA	0.86441	0.20245	0.10208	0.13342	0.33582	0.61404	0.81894	
PT18	NA	0.78855	0.93839	1.03544 NA	0.99862	0.64916 NA	0.55605	0.24066	1.03848	-0.77272	1.78644	-1.94513	0.24778 NA	0.26239	0.64154	0.68339 NA	0.86441	0.20245	0.10208	0.13342	0.33582	0.61404	0.81894		
PT19	NA	-4.72479	0.20217	0.13261	0.15752	0.18426	0.25549	0.71932 NA	0.16889	0.52877 NA	0.33770	0.19204	-0.16037 NA	0.25342	0.274375	-1.57652	0.19204	0.16037 NA	0.25342	0.274375	-1.57652	0.19204	0.16037 NA	0.25342	
PT20	NA	0.16175	-0.54504	0.27812	0.66478	0.88276	-0.98392	-0.42871	0.42871	0.42871	0.42871	0.42871	0.42871	0.42871	0.42871	0.42871	0.42871	0.42871	0.42871	0.42871	0.42871	0.42871	0.42871	0.42871	
QK1	0.40712	0.92828 NA	0.27812	0.66478	0.88276	-0.98392	-0.42871	0.42871	0.42871	0.42871	0.42871	0.42871	0.42871	0.42871	0.42871	0.42871	0.42871	0.42871	0.42871	0.42871	0.42871	0.42871	0.42871	0.42871	
QK2	-1.28156	-0.45756	0.50737	-0.98001	-0.85841	0.24263	-1.63817	0.31624 NA	0.15177	0.20746	0.05536	0.79501	0.68313	-0.34105	0.78382	-1.80639	0.41239	-0.75226	0.24927 NA	0.71654	0.14983	0.153971	0.40712	0.92828	
QK3	-0.26241	-1.91526	0.50737	-0.98001	-0.85841	0.24263	-1.63817	0.31624 NA	0.15177	0.20746	0.05536	0.79501	0.68313	-0.34105	0.78382	-1.80639	0.41239	-0.75226	0.24927 NA	0.71654	0.14983	0.153971	0.40712	0.92828	
QK4	-0.18989 NA	NA	NA	NA	NA	NA	NA	0.0591	0.61887 NA	0.39178 NA	0.58619 NA	0.31239	0.59318 NA	0.14767	0.29232	0.68249	0.26345	0.13378	0.72782 NA	0.11018 NA	0.14983	0.153971	0.40712	0.92828	
QK5	NA	0.49473	-2.14820	0.34027	-0.7001	-0.45015	0.47951	-2.51457	0.02148 NA	0.15177	0.20746	0.05536	0.79501	0.68313	-0.34105	0.78382	-1.80639	0.41239	-0.75226	0.24927 NA	0.71654	0.14983	0.153971	0.40712	0.92828
QK6	NA	0.92785 NA	0.78855	0.93839	1.03544 NA	0.99862	0.64916 NA	0.55605	0.24066	1.03848	-0.77272	1.78644	-1.94513	0.24778 NA	0.26239	0.64154	0.68339 NA	0.86441	0.20245	0.10208	0.13342	0.33582	0.61404	0.81894	
QK7	1.18366	-0.82415	-0.04545	-0.84847	2.84719	0.28109	-0.05154	0.40144	1.31815	-1.31224	0.35854	-0.15175	0.34361	0.15175	0.34361	0.15175	0.34361	0.15175	0.34361	0.15175	0.34361	0.15175	0.34361	0.15175	0.34361
QK8	-0.32202	-0.18273	-1.0439	-1.07008 NA	1.53282	0.27555	0.38613 NA	0.23657	1.07145 NA	0.65881	-1.41233	0.15906 NA	0.14651	0.16465	0.16465	0.16465	0.16465	0.16465	0.16465	0.16465	0.16465	0.16465	0.16465	0.16465	0.16465
QK9	0.05637	-0.56783	0.18428	-0.34068	0.18428	-0.34068	0.18428	-0.34068	0.18428	-0.34068	0.18428	-0.34068	0.18428	-0.34068	0.18428	-0.34068	0.18428	-0.34068	0.18428	-0.34068	0.18428	-0.34068	0.18428	-0.34068	0.18428
QK10	0.70615	-0.93489	-2.34815	1.93956	-1.08437	0.80212	0.38949 NA	0.15703	0.15703	0.15703	0.15703	0.15703	0.15703	0.15703	0.15703	0.15703	0.15703	0.15703	0.15703	0.15703	0.15703	0.15703	0.15703	0.15703	
QK11	-0.7159	-1.09349	-2.34815	1.93956	-1.08437	0.80212	0.38949 NA	0.15703	0.15703	0.15703	0.15703	0.15703	0.15703	0.15703	0.15703	0.15703	0.15703	0.15703	0.15703	0.15703	0.15703	0.15703	0.15703	0.15703	
QK12	-1.74571	-1.04274 NA	0.90010 NA	0.90010 NA	0.90010 NA	0.90010 NA	0.90010 NA	0.90010 NA	0.90010 NA	0.90010 NA	0.90010 NA	0.90010 NA	0.90010 NA	0.90010 NA	0.90010 NA	0.90010 NA	0.90010 NA	0.90010 NA	0.90010 NA	0.90010 NA	0.90010 NA	0.90010 NA	0.90010 NA	0.90010 NA	
QK13	NA	0.05746 NA	0.13261	0.15752	0.18426	0.25549	0.71932 NA	0.16889	0.52877 NA	0.33770	0.19204	-0.16037 NA	0.25342	0.274375	-1.57652	0.19204	0.16037 NA	0.25342	0.274375	-1.57652	0.19204	0.16037 NA	0.25342	0.274375	
QK14	NA	-1.71305 NA	0.13261	0.15752	0.18426	0.25549	0.71932 NA	0.16889	0.52877 NA	0.33770	0.19204	-0.16037 NA	0.25342	0.274375	-1.57652	0.19204	0.16037 NA	0.25342	0.274375	-1.57652	0.19204	0.16037 NA	0.25342	0.274375	
QK15	NA	1.40942	0.41265	-0.25163	0.30836	0.41728	0.63094	-2.10961	-0.56843	0.95222	0.14323	0.59318 NA	0.14767	0.29232	0.68249	0.26345	0.13378	0.72782 NA	0.11018 NA	0.14983	0.153971	0.40712	0.92828	0.15177	
QK16	NA	0.88729	0.311028 NA	0.15177	0.20746	0.05536	0.79501	0.68313	-0.34105	0.78382	-1.80639	0.41239	-0.75226	0.24927 NA	0.71654	0.14983	0.153971	0.40712	0.92828	0.15177	0.20746	0.05536	0.79501	0.68313	-0.34105
QK17	NA	0.92785 NA	0.78855	0.93839	1.03544 NA	0.99862	0.64916 NA	0.55605	0.24066	1.03848	-0.77272	1.78644	-1.94513	0.24778 NA	0.26239	0.64154	0.68339 NA	0.86441	0.20245	0.10208	0.13342	0.33582	0.61404	0.81894	
QK18	NA	1.18366	-0.82415	-0.04545	-0.84847	2.84719	0.28109	-0.05154	0.40144	1.31815	-1.31224	0.35854	-0.15175	0.34361	0.15175	0.34361	0.15175	0.34361	0.15175	0.34361	0.15175	0.34361	0.15175	0.34361	0.15175
QK19	-0.32202	-0.18273	-1.0439	-1.07008 NA	1.53282	0.27555	0.38613 NA	0.23657	1.07145 NA	0.65881	-1.41233	0.15906 NA	0.14651	0.16465	0.16465	0.16465	0.16465	0.16465	0.16465	0.16465	0.16465	0.16465	0.16465	0.16465	0.16465
QK20	0.05637	-0.56783	0.18428	-0.34068	0.18428	-0.34068	0.18428	-0.34068	0.18428	-0.34068	0.18428	-0.34068	0.18428	-0.34068	0.18428	-0.34068	0.18428	-0.34068	0.18428	-0.34068	0.18428	-0.34068	0.18428	-0.34068	0.18428
QK21	0.70615	-0.93489	-2.34815	1.93956	-1.08437	0.80212	0.38949 NA	0.15703	0.15703	0.15703	0.15703	0.15703	0.15703	0.15703	0.15703	0.15703	0.15703	0.15703	0.15703	0.15703	0.15703	0.15703	0.15703	0.15703	
QK22	-0.7159	-1.09349	-2.34815	1.93956	-1.08437	0.80212	0.38949 NA	0.15703	0.15703	0.15703	0.15703	0.15703	0.15703	0.15703	0.15703	0.15703	0.15703	0.15703	0.15703	0.15703	0.15703	0.15703	0.15703	0.15703	
QK23	-1.74571	-1.04274 NA	0.90010 NA	0.90010 NA	0.90010 NA	0.90010 NA	0.90010 NA	0.90010 NA	0.90010 NA	0.90010 NA	0.90010 NA	0.90010 NA	0.90010 NA	0.90010 NA	0.90010 NA	0.90010 NA	0.90010 NA	0.90010 NA	0.90010 NA	0.90010 NA	0.90010 NA	0.90010 NA	0.90010 NA	0.90010 NA	
QK24	NA	0.05746 NA	0.13261	0.15752	0.18426	0.25549	0.71932 NA	0.16889	0.52877 NA	0.33770	0.19204	-0.16037 NA	0.25342	0.274375	-1.57652	0.19204	0.16037 NA	0.25342	0.274375	-1.57652	0.19204	0.16037 NA	0.25342	0.274375	
QK25	NA	-1.71305 NA	0.13261	0.15752	0.18426	0.25549	0.71932 NA	0.16889	0.52877 NA	0.33770	0.19204	-0.16037 NA	0.25342	0.274375	-1.57652	0.19204	0.16037 NA	0.25342	0.274375	-1.57652	0.19204	0.16037 NA	0.25342	0.274375	
QK26	NA	1.40942	0.41265	-0.25163	0.30836	0.41728	0.63094	-2.10961	-0.56843	0.95222	0.14323	0.59318 NA	0.14767	0.29232	0.68249	0.26345	0.13378	0.72782 NA	0.11018 NA	0.14983	0.153971	0.40712	0.92828	0.15177	
QK27	NA	0.88729	0.311028 NA	0.15177	0.20746	0.05536	0.79501	0.68313	-0.34105	0.78382	-1.80639	0.41239	-0.75226	0.24927 NA	0.71654	0.14983	0.153971	0.40712	0.92828	0.15177	0.20746	0.05536	0.79501	0.68313	-0.34105
QK28	NA	0.92785 NA	0.78855	0.93839	1.03544 NA	0.99862	0.64916 NA	0.55605	0.24066	1.03848	-0.77272	1.78644	-1.94513	0.24778 NA	0.26239	0.64154	0.68339 NA	0.86441	0.20245	0.10208	0.13342	0.33582	0.61404	0.81894	
QK29	NA	1.18366	-0.82415	-0.04545	-0.84847	2.84719	0.28109	-0.05154	0.40144	1.31815	-1.31224	0.35854	-0.15175	0.34361	0.15175	0.34361	0.15175	0.34361	0.15175	0.34361	0.15175	0.34361	0.15175	0.34361	0.15175
QK30	-0.32202	-0.18273	-1.0439	-1.07008 NA	1.53282	0.27555	0.38613 NA	0.23657	1.07145 NA	0.65881	-1.41233	0.15906 NA	0.14651	0.16465	0.16465	0.16465	0.16465	0.16465	0.16465	0.16465	0.16465	0.16465	0.16465	0.16465	0.16465
QK31	0.05637	-0.56783	0.18428	-0.34068	0.18428	-0.34068	0.18428	-0.34068	0.18428	-0.34068	0.18428	-0.3													

100 mM HU

Table with columns: Gene, AF1, AF2, AF3, AF4, AF5, AF6, AF7, AF8, AF9, AF10, AF11, AF12, AF13, AF14, AF15, AF16, AF17, AF18, AF19, AF20, AF21, AF22, AF23, AF24, AF25, AF26, AF27, AF28, AF29, AF30, AF31, AF32, AF33, AF34, AF35, AF36, AF37, AF38, AF39, AF40, AF41, AF42, AF43, AF44, AF45, AF46, AF47, AF48, AF49, AF50, AF51, AF52, AF53, AF54, AF55, AF56, AF57, AF58, AF59, AF60, AF61, AF62, AF63, AF64, AF65, AF66, AF67, AF68, AF69, AF70, AF71, AF72, AF73, AF74, AF75, AF76, AF77, AF78, AF79, AF80, AF81, AF82, AF83, AF84, AF85, AF86, AF87, AF88, AF89, AF90, AF91, AF92, AF93, AF94, AF95, AF96, AF97, AF98, AF99, AF100. Each row contains a gene symbol and a long list of numerical values.

BCR1	YL02C	TAVVDHNSQNTVNVLSQPTK	0.77	-0.11	-0.16	0.351	0.337	0.276	0.23	1.11E-06	9.22E-05	8.27E-05	1.11E-06	8.07E-05	7.80E-05	9.64E-05	1.14E-06	9.07E-05	1.01E-06	7.99E-05	8.52E-05	1016.995	3	48.31	
BP1	YL02Z	RSVVAFLK	-0.11	-0.34	0.23	0.168	0.266	0.412	0.08	3.58E-05	1.40E-05	1.75E-05	2.04E-05	1.85E-05	2.38E-05	2.38E-05	1.64E-05	1.77E-05	2.92E-05	1.01E-06	1.97E-05	1.53E-05	967.982	3	43.24
GP1	YL03C	WVAFPEKGTSGKSTAMVNRK	-0.25	-0.40	0.14	0.188	0.347	0.394	0.12	1.41E-06	8.81E-05	1.34E-06	1.48E-06	1.22E-06	1.62E-06	1.62E-06	9.13E-05	1.02E-06	1.71E-06	1.35E-06	1.97E-05	1.59E-05	967.984	3	20.06
GP2	YL03H	SDGVAFLK	-0.45	-0.92	-0.55	0.07	0.004	0.017	0.050	5.11E-05	5.30E-05	5.05E-05	3.86E-05	4.27E-05	3.37E-05	3.37E-05	2.62E-05	4.13E-05	4.31E-05	4.11E-05	2.00E-05	1.31E-05	698.2826	2	66.49
NP12	YL05H	LDGVPKATLTKSEK	0.33	0.17	0.10	0.150	0.122	0.136	0.160	1.21E-06	1.30E-06	1.01E-06	1.21E-06	1.67E-06	1.14E-06	1.22E-06	1.12E-06	1.16E-06	1.71E-06	1.17E-06	1.26E-06	998.4208	2	38.59	
MD1	YL05W	WVNTAMNAGSVPFK	0.27	0.03	0.06	0.069	0.001	0.05	0.205	3.20E-05	2.94E-05	2.24E-05	3.82E-05	3.28E-05	4.21E-05	4.21E-05	4.18E-05	5.07E-05	4.33E-05	4.30E-05	4.65E-05	898.8963	2	74.4	
STLZ	YL05K	RSLSGDHPH	-0.10	-0.02	0.00	0.172	0.069	0.493	0.35	3.91E-05	2.86E-05	2.36E-05	2.10E-05	2.18E-05	2.10E-05	2.56E-05	1.84E-05	2.19E-05	2.10E-05	2.40E-05	2.89E-05	478.5578	3	44.4	
YL05W-B	YL05W	HSYSDNEMTHVPISTGTTNK	-0.85	-0.06	-0.1	0.00	0.00	0.343	0.110	7.53E-05	5.44E-05	6.77E-05	4.58E-05	3.06E-05	5.94E-05	5.94E-05	6.14E-05	6.79E-05	2.92E-05	3.24E-05	4.86E-05	952.881	3	58.32	
SC16	YL02Z	WVPSVYQDK	-0.35	-0.08	-0.14	0.20	0.188	0.336	0.28	3.15E-05	3.70E-05	4.23E-05	2.77E-05	2.45E-05	3.77E-05	3.77E-05	3.79E-05	3.84E-05	2.88E-05	3.01E-05	4.11E-05	689.3286	3	38.13	
CAF20	YL02Z	GGDDEEITTPYVATAGTK	0.39	0.12	0.20	0.188	0.336	0.28	0.31	3.10E-06	1.21E-06	4.83E-05	1.68E-06	2.31E-06	1.20E-06	1.61E-06	1.61E-06	1.71E-06	1.21E-06	1.30E-06	1.16E-06	1089.1285	3	50.4	
YF3	YL05H	EGDVAFLK	0.43	1.11	-0.08	-0.68	0.403	0.182	0.463	0.11	5.04E-05	4.65E-05	1.68E-06	4.82E-05	3.64E-05	3.64E-05	4.08E-06	1.21E-06	7.84E-05	8.44E-05	1.33E-06	867.7922	2	16.85	
HKL1	YL05K	NFSDNHSLEQVAVFPNTK	-0.93	-0.73	-0.21	0.00	0.00	0.002	0.12	7.17E-05	6.98E-05	7.35E-05	4.15E-05	3.40E-05	3.75E-05	3.75E-05	4.86E-05	4.49E-05	4.33E-05	5.20E-05	5.53E-05	1090.8001	3	27.29	
YK2	YL03Z	WVNSDQVDEK	-0.49	-0.33	-0.26	0.005	0.041	0.220	0.01	1.00E-06	1.39E-06	8.83E-05	7.28E-05	8.99E-05	7.60E-05	1.18E-06	1.18E-06	9.65E-05	7.89E-05	9.17E-05	1.00E-06	807.3338	3	82.59	
AMZ1	YL03W	SKQIEEDVDSK	0.06	0.13	-0.07	0.452	0.418	0.394	0.65	7.78E-05	2.41E-05	6.17E-05	7.14E-05	6.86E-05	3.88E-05	3.88E-05	2.98E-06	9.93E-05	6.92E-05	6.70E-05	870.3007	2	47.1		
RPS3	YL03W	NSQIEEDVDSK	-0.15	0.08	-0.13	-0.21	0.48	0.386	0.249	2.98E-05	2.48E-05	3.16E-05	2.45E-05	3.04E-05	3.16E-05	3.16E-05	2.57E-05	2.80E-05	2.44E-05	4.29E-05	674.3953	3	25.82		
VTZ2	YL03W	IEPQVDSK	-0.25	-0.13	-0.30	0.097	0.241	0.084	0.26	5.71E-05	7.95E-05	6.34E-05	5.08E-05	5.89E-05	5.74E-05	5.74E-05	5.13E-05	5.80E-05	4.77E-05	4.77E-05	6.63E-05	963.5224	2	31.86	
YF5	YL03W	GGDDEEITTPYVATAGTK	-0.68	-0.31	-0.27	0.042	0.203	0.283	0.12	1.50E-06	8.39E-05	1.93E-06	7.07E-05	7.07E-05	7.07E-05	6.94E-05	1.18E-06	1.01E-06	1.23E-06	1.07E-06	1.07E-06	972.0881	3	39.96	
YF6	YL03W	NFSDNHSLEQVAVFPNTK	0.51	0.08	0.19	0.059	0.048	0.111	0.04	1.42E-05	1.31E-05	2.09E-05	1.57E-05	1.57E-05	1.57E-05	1.57E-05	1.38E-05	1.98E-05	1.98E-05	1.98E-05	1.98E-05	968.5897	3	36.31	
YF7	YL03W	NFSDNHSLEQVAVFPNTK	0.51	0.08	0.19	0.059	0.048	0.111	0.04	1.42E-05	1.31E-05	2.09E-05	1.57E-05	1.57E-05	1.57E-05	1.57E-05	1.38E-05	1.98E-05	1.98E-05	1.98E-05	1.98E-05	968.5897	3	36.31	
YF8	YL03W	NFSDNHSLEQVAVFPNTK	0.51	0.08	0.19	0.059	0.048	0.111	0.04	1.42E-05	1.31E-05	2.09E-05	1.57E-05	1.57E-05	1.57E-05	1.57E-05	1.38E-05	1.98E-05	1.98E-05	1.98E-05	1.98E-05	968.5897	3	36.31	
YF9	YL03W	NFSDNHSLEQVAVFPNTK	0.51	0.08	0.19	0.059	0.048	0.111	0.04	1.42E-05	1.31E-05	2.09E-05	1.57E-05	1.57E-05	1.57E-05	1.57E-05	1.38E-05	1.98E-05	1.98E-05	1.98E-05	1.98E-05	968.5897	3	36.31	
YF10	YL03W	NFSDNHSLEQVAVFPNTK	0.51	0.08	0.19	0.059	0.048	0.111	0.04	1.42E-05	1.31E-05	2.09E-05	1.57E-05	1.57E-05	1.57E-05	1.57E-05	1.38E-05	1.98E-05	1.98E-05	1.98E-05	1.98E-05	968.5897	3	36.31	
YF11	YL03W	NFSDNHSLEQVAVFPNTK	0.51	0.08	0.19	0.059	0.048	0.111	0.04	1.42E-05	1.31E-05	2.09E-05	1.57E-05	1.57E-05	1.57E-05	1.57E-05	1.38E-05	1.98E-05	1.98E-05	1.98E-05	1.98E-05	968.5897	3	36.31	
YF12	YL03W	NFSDNHSLEQVAVFPNTK	0.51	0.08	0.19	0.059	0.048	0.111	0.04	1.42E-05	1.31E-05	2.09E-05	1.57E-05	1.57E-05	1.57E-05	1.57E-05	1.38E-05	1.98E-05	1.98E-05	1.98E-05	1.98E-05	968.5897	3	36.31	
YF13	YL03W	NFSDNHSLEQVAVFPNTK	0.51	0.08	0.19	0.059	0.048	0.111	0.04	1.42E-05	1.31E-05	2.09E-05	1.57E-05	1.57E-05	1.57E-05	1.57E-05	1.38E-05	1.98E-05	1.98E-05	1.98E-05	1.98E-05	968.5897	3	36.31	
YF14	YL03W	NFSDNHSLEQVAVFPNTK	0.51	0.08	0.19	0.059	0.048	0.111	0.04	1.42E-05	1.31E-05	2.09E-05	1.57E-05	1.57E-05	1.57E-05	1.57E-05	1.38E-05	1.98E-05	1.98E-05	1.98E-05	1.98E-05	968.5897	3	36.31	
YF15	YL03W	NFSDNHSLEQVAVFPNTK	0.51	0.08	0.19	0.059	0.048	0.111	0.04	1.42E-05	1.31E-05	2.09E-05	1.57E-05	1.57E-05	1.57E-05	1.57E-05	1.38E-05	1.98E-05	1.98E-05	1.98E-05	1.98E-05	968.5897	3	36.31	
YF16	YL03W	NFSDNHSLEQVAVFPNTK	0.51	0.08	0.19	0.059	0.048	0.111	0.04	1.42E-05	1.31E-05	2.09E-05	1.57E-05	1.57E-05	1.57E-05	1.57E-05	1.38E-05	1.98E-05	1.98E-05	1.98E-05	1.98E-05	968.5897	3	36.31	
YF17	YL03W	NFSDNHSLEQVAVFPNTK	0.51	0.08	0.19	0.059	0.048	0.111	0.04	1.42E-05	1.31E-05	2.09E-05	1.57E-05	1.57E-05	1.57E-05	1.57E-05	1.38E-05	1.98E-05	1.98E-05	1.98E-05	1.98E-05	968.5897	3	36.31	
YF18	YL03W	NFSDNHSLEQVAVFPNTK	0.51	0.08	0.19	0.059	0.048	0.111	0.04	1.42E-05	1.31E-05	2.09E-05	1.57E-05	1.57E-05	1.57E-05	1.57E-05	1.38E-05	1.98E-05	1.98E-05	1.98E-05	1.98E-05	968.5897	3	36.31	
YF19	YL03W	NFSDNHSLEQVAVFPNTK	0.51	0.08	0.19	0.059	0.048	0.111	0.04	1.42E-05	1.31E-05	2.09E-05	1.57E-05	1.57E-05	1.57E-05	1.57E-05	1.38E-05	1.98E-05	1.98E-05	1.98E-05	1.98E-05	968.5897	3	36.31	
YF20	YL03W	NFSDNHSLEQVAVFPNTK	0.51	0.08	0.19	0.059	0.048	0.111	0.04	1.42E-05	1.31E-05	2.09E-05	1.57E-05	1.57E-05	1.57E-05	1.57E-05	1.38E-05	1.98E-05	1.98E-05	1.98E-05	1.98E-05	968.5897	3	36.31	
YF21	YL03W	NFSDNHSLEQVAVFPNTK	0.51	0.08	0.19	0.059	0.048	0.111	0.04	1.42E-05	1.31E-05	2.09E-05	1.57E-05	1.57E-05	1.57E-05	1.57E-05	1.38E-05	1.98E-05	1.98E-05	1.98E-05	1.98E-05	968.5897	3	36.31	
YF22	YL03W	NFSDNHSLEQVAVFPNTK	0.51	0.08	0.19	0.059	0.048	0.111	0.04	1.42E-05	1.31E-05	2.09E-05	1.57E-05	1.57E-05	1.57E-05	1.57E-05	1.38E-05	1.98E-05	1.98E-05	1.98E-05	1.98E-05	968.5897	3	36.31	
YF23	YL03W	NFSDNHSLEQVAVFPNTK	0.51	0.08	0.19	0.059	0.048	0.111	0.04	1.42E-05	1.31E-05	2.09E-05	1.57E-05	1.57E-05	1.57E-05	1.57E-05	1.38E-05	1.98E-05	1.98E-05	1.98E-05	1.98E-05	968.5897	3	36.31	
YF24	YL03W	NFSDNHSLEQVAVFPNTK	0.51	0.08	0.19	0.059	0.048	0.111	0.04	1.42E-05	1.31E-05	2.09E-05	1.57E-05	1.57E-05	1.57E-05	1.57E-05	1.38E-05	1.98E-05	1.98E-05	1.98E-05	1.98E-05	968.5897	3	36.31	
YF25	YL03W	NFSDNHSLEQVAVFPNTK	0.51	0.08	0.19	0.059	0.048	0.111	0.04	1.42E-05	1.31E-05	2.09E-05	1.57E-05	1.57E-05	1.57E-05	1.57E-05	1.38E-05	1.98E-05	1.98E-05	1.98E-05	1.98E-05	968.5897	3	36.31	
YF26	YL03W	NFSDNHSLEQVAVFPNTK	0.51	0.08	0.19	0.059	0.048	0.111	0.04	1.42E-05	1.31E-05	2.09E-05	1.57E-05	1.57E-05	1.57E-05	1.57E-05	1.38E-05	1.98E-05	1.98E-05	1.98E-05	1.98E-05	968.5897	3	36.31	
YF27	YL03W	NFSDNHSLEQVAVFPNTK	0.51	0.08	0.19	0.059	0.048	0.111	0.04	1.42E-05	1.31E-05	2.09E-05	1.57E-05	1.57E-05	1.57E-05	1.57E-05	1.38E-05	1.98E-05	1.98E-05	1.98E-05	1.98E-05	968.5897	3	36.31	
YF28	YL03W	NFSDNHSLEQVAVFPNTK	0.5																						

GH01	YRQZGQ	RASISNWTTPAPNADIK	10] Phospho (S)	0.80	0.400	0.441	0.05	5.0E-05	4.7E-05	3.16E-05	3.11E-05	3.70E-05	2.82E-05	4.74E-05	4.15E-05	3.94E-05	3.28E-05	5.54E-05	3.70E-05	844.42779	3	16.85
GH02	RLZ3WA	ASDAFTFSR	[N-term] Acetyl [Protein N-term][1] Phospho	0.89	0.324	0.369	0.37	1.30E-05	7.7E-04	1.29E-05	1.2E-05	9.26E-04	1.26E-05	8.87E-04	1.32E-05	1.81E-05	1.47E-05	2.01E-05	3.70E-05	607.78008	2	20.74
GH03	YRQZGQ	YRQZGQ	[Phospho (S)]	0.82	0.242	0.281	0.00	1.10E-04	5.62E-03	1.99E-05	1.4E-05	1.60E-05	2.85E-05	7.01E-03	3.90E-03	6.51E-03	3.85E-03	1.18E-03	2.19E-03	607.78014	2	42.09
GH04	YRQZGQ	ALLELDLDDVPGCTRWAYGVASK	[12] Phospho (S)	0.42	0.324	0.369	0.14	2.64E-05	3.78E-05	1.82E-05	6.75E-05	4.62E-05	5.03E-05	3.08E-05	2.98E-05	2.46E-05	1.79E-05	6.18E-05	9.86E-05	996.40971	3	48.3
GH05	YRQZGQ	YRQZGQ	[Phospho (S)]	0.05	0.42	0.463	0.15	4.23E-04	3.24E-04	9.42E-04	6.52E-04	5.15E-04	3.06E-04	9.75E-04	7.88E-04	2.01E-05	1.16E-05	3.21E-05	7.81E-05	586.26935	3	62.22
GH06	YRQZGQ	KPFGQLDQSDVNR	[3] Phospho (S)	0.28	0.03	0.048	0.031	2.22E-05	4.25E-05	1.39E-05	3.27E-05	3.32E-05	3.32E-05	3.03E-05	3.48E-05	2.05E-05	1.64E-05	3.09E-05	500.61418	3	47.97	
GH07	YRQZGQ	EAAMSDSDHNDHAR	[2] Phospho (S)	0.29	0.136	0.186	0.029	2.28E-05	1.73E-05	2.43E-05	1.48E-05	1.95E-05	1.37E-05	1.43E-05	2.19E-05	2.07E-05	1.64E-05	1.70E-05	715.93813	3	27.27	
GH08	YRQZGQ	YRQZGQ	[Phospho (S)]	0.42	0.42	0.463	0.34	6.58E-04	4.98E-04	5.64E-04	5.91E-04	5.30E-04	8.34E-04	8.34E-04	6.86E-04	6.86E-04	4.16E-04	1.07E-05	546.27003	3	16.29	
GH09	YRQZGQ	YRQZGQ	[Phospho (S)]	0.40	0.432	0.473	0.49	2.35E-05	2.48E-05	2.61E-05	2.30E-05	2.61E-05	1.93E-05	2.23E-05	2.12E-05	2.12E-05	2.14E-05	1.07E-05	729.32812	3	16.29	
GH10	YRQZGQ	KYDSSVYGVATLPTFTFK	[3] Phospho (S)	0.10	0.385	0.430	0.19	1.44E-06	1.79E-06	9.17E-06	9.85E-05	7.32E-06	1.18E-06	1.18E-06	1.42E-06	1.42E-06	1.39E-06	8.25E-06	153.02616	2	57.26	
GH11	YRQZGQ	KYDSSVYGVATLPTFTFK	[Phospho (S)]	0.07	0.385	0.430	0.09	1.35E-05	1.11E-05	1.22E-05	1.66E-05	1.46E-05	1.68E-05	1.68E-05	1.44E-05	1.04E-05	1.39E-05	9.74E-04	647.78807	2	71.95	
GH12	YRQZGQ	YRQZGQ	[Phospho (S)]	0.33	0.077	0.105	0.27	9.67E-04	1.31E-05	1.53E-05	1.66E-05	1.46E-05	1.68E-05	1.68E-05	1.44E-05	1.04E-05	1.39E-05	9.74E-04	647.78807	2	71.95	
GH13	YRQZGQ	YRQZGQ	[Phospho (S)]	0.31	0.077	0.105	0.31	3.89E-05	9.73E-05	4.08E-05	5.27E-05	8.91E-05	5.15E-05	7.65E-05	8.04E-05	5.29E-05	4.92E-05	1.09E-05	65.30039	3	81.66	
GH14	YRQZGQ	YRQZGQ	[Phospho (S)]	0.11	0.509	0.548	0.11	4.12E-05	3.98E-05	2.69E-05	3.07E-05	3.13E-05	2.16E-05	3.16E-05	3.16E-05	2.95E-05	3.17E-05	4.05E-05	947.78334	3	81.66	
GH15	YRQZGQ	NFTAFDQVKEEENADGVSK	[13] Phospho (S)	0.85	0.509	0.548	0.85	4.82E-05	6.05E-05	3.70E-05	4.47E-05	3.84E-05	4.21E-05	4.55E-05	4.48E-05	3.88E-05	3.96E-05	4.05E-05	892.06834	3	49.71	
GH16	YRQZGQ	NFTAFDQVKEEENADGVSK	[2] Phospho (S)	0.08	0.444	0.483	0.46	4.82E-05	6.05E-05	3.70E-05	4.47E-05	3.84E-05	4.21E-05	4.55E-05	4.48E-05	3.88E-05	3.96E-05	4.05E-05	892.06834	3	49.71	
GH17	YRQZGQ	YRQZGQ	[Phospho (S)]	0.31	0.227	0.266	0.30	3.84E-04	1.08E-05	6.80E-04	5.86E-04	7.92E-04	5.28E-04	1.40E-05	7.00E-04	1.31E-04	4.94E-04	9.32E-05	462.92967	4	16.14	
GH18	YRQZGQ	YRQZGQ	[Phospho (S)]	0.47	0.531	0.570	0.44	3.48E-05	1.25E-05	3.96E-05	1.18E-05	1.49E-05	1.25E-05	1.49E-05	1.25E-05	1.09E-05	1.25E-05	1.49E-05	478.94291	2	71.77	
GH19	YRQZGQ	YRQZGQ	[Phospho (S)]	0.36	0.31	0.349	0.37	2.81E-05	6.86E-04	3.24E-04	3.56E-04	3.52E-04	7.46E-04	7.46E-04	6.14E-04	6.14E-04	3.98E-04	4.51E-04	486.52731	3	41.91	
GH20	YRQZGQ	YRQZGQ	[Phospho (S)]	0.43	0.28	0.319	0.43	8.98E-04	8.31E-04	1.18E-05	1.06E-05	1.58E-05	1.58E-05	1.07E-05	8.08E-04	1.08E-05	3.40E-04	8.98E-04	486.52731	3	41.91	
GH21	YRQZGQ	YRQZGQ	[Phospho (S)]	0.75	0.28	0.319	0.49	3.81E-04	3.88E-04	4.86E-04	6.44E-04	5.76E-04	6.06E-04	3.99E-04	4.56E-04	4.88E-04	3.40E-04	3.81E-04	541.2556	2	76.32	
GH22	YRQZGQ	YRQZGQ	[Phospho (S)]	0.07	0.12	0.14	0.19	0.405	0.384	0.419	0.405	0.384	0.419	0.405	0.384	0.419	0.405	0.384	541.2556	2	76.32	
GH23	YRQZGQ	YRQZGQ	[Phospho (S)]	0.15	0.46	0.42	0.31	1.94	0.043	0.008	0.12	2.22E-05	1.63E-05	1.62E-05	1.11E-05	1.25E-05	1.52E-05	1.07E-05	462.89832	3	21.48	
GH24	YRQZGQ	YRQZGQ	[Phospho (S)]	1.04	0.68	0.729	1.04	0.68	0.729	1.04	0.68	0.729	1.04	0.68	0.729	1.04	0.68	0.729	462.89832	3	21.48	
GH25	YRQZGQ	YRQZGQ	[Phospho (S)]	0.54	0.63	0.676	0.54	0.63	0.676	0.54	0.63	0.676	0.54	0.63	0.676	0.54	0.63	0.676	700.29025	3	63.61	
GH26	YRQZGQ	YRQZGQ	[Phospho (S)]	2.15	0.05	-0.20	2.50	0.03	0.461	0.388	0.40	0.39	1.92E-04	5.40E-04	1.38E-05	2.06E-05	1.99E-05	2.64E-05	850.3935	3	63.61	
GH27	YRQZGQ	YRQZGQ	[Phospho (S)]	0.35	0.03	-0.04	0.32	0.182	0.043	0.045	0.18	5.98E-04	7.85E-04	1.31E-05	1.04E-04	1.18E-04	1.68E-04	7.98E-03	436.70754	2	29.38	
GH28	YRQZGQ	YRQZGQ	[Phospho (S)]	0.24	0.90	0.85	-0.05	0.142	0.006	0.025	0.42	4.98E-04	4.62E-04	6.76E-04	8.27E-04	6.17E-04	8.58E-04	7.47E-04	497.24214	2	34.38	
GH29	YRQZGQ	YRQZGQ	[Phospho (S)]	-0.40	-0.35	-0.44	-0.40	-0.35	-0.44	-0.40	-0.35	-0.44	-0.40	-0.35	-0.44	-0.40	-0.35	-0.44	561.2633	2	17.86	
GH30	YRQZGQ	YRQZGQ	[Phospho (S)]	2.79	-0.08	1.41	2.87	0.010	0.468	0.049	0.01	4.03E-04	9.94E-03	1.33E-05	1.20E-04	1.20E-04	7.20E-04	3.01E-04	6.43E-04	1073.052	3	36.01
GH31	YRQZGQ	YRQZGQ	[Phospho (S)]	0.18	-0.49	0.00	0.68	0.20	0.116	0.498	0.01	1.37E-05	1.22E-04	1.02E-05	6.09E-04	6.65E-04	1.27E-04	8.43E-04	8.28.3732	2	25.38	
GH32	YRQZGQ	YRQZGQ	[Phospho (S)]	-0.02	-0.28	-0.36	0.26	0.429	0.156	0.023	0.19	2.78E-05	2.42E-05	2.95E-05	3.12E-05	2.16E-05	2.44E-05	1.86E-05	866.36882	2	20.97	
GH33	YRQZGQ	YRQZGQ	[Phospho (S)]	0.11	-0.78	-0.24	0.87	0.362	0.200	0.209	0.21	2.91E-05	1.04E-05	1.40E-05	8.17E-04	8.74E-04	1.19E-05	1.11E-05	1094.9222	2	49.63	
GH34	YRQZGQ	YRQZGQ	[Phospho (S)]	0.21	0.08	0.44	0.13	0.31	0.382	0.058	0.22	5.56E-04	1.94E-05	1.04E-05	8.86E-04	8.74E-04	7.86E-04	1.05E-05	861.36884	2	47.21	
GH35	YRQZGQ	YRQZGQ	[Phospho (S)]	0.29	0.15	0.14	0.14	0.165	0.044	0.174	0.30	3.27E-04	9.95E-04	1.34E-05	8.24E-04	1.02E-05	2.44E-04	1.04E-05	811.36884	2	47.21	
GH36	YRQZGQ	YRQZGQ	[Phospho (S)]	0.34	0.36	0.32	0.34	0.474	0.040	0.263	0.37	3.51E-04	4.27E-04	9.98E-04	2.78E-04	2.20E-04	2.44E-04	9.23E-04	5.43E-04	471.78977	2	27.98
GH37	YRQZGQ	YRQZGQ	[Phospho (S)]	0.34	0.36	0.32	0.34	0.474	0.040	0.263	0.37	3.51E-04	4.27E-04	9.98E-04	2.78E-04	2.20E-04	2.44E-04	9.23E-04	5.43E-04	471.78977	2	27.98
GH38	YRQZGQ	YRQZGQ	[Phospho (S)]	0.09	0.327	0.32	0.38	0.025	0.240	0.257	0.03	1.18E-04	3.93E-04	1.15E-05	1.02E-05	8.29E-04	1.14E-05	4.30E-04	492.29888	3	30.84	
GH39	YRQZGQ	YRQZGQ	[Phospho (S)]	0.09	0.327	0.32	0.38	0.025	0.240	0.257	0.03	1.18E-04	3.93E-04	1.15E-05	1.02E-05	8.29E-04	1.14E-05	4.30E-04	492.29888	3	30.84	
GH40	YRQZGQ	YRQZGQ	[Phospho (S)]	0.12	0.57	0.04	-0.08	0.222	0.040	0.438	0.01	5.90E-04	6.64E-04	8.04E-04	8.26E-04	6.16E-04	2.77E-04	3.95E-04	526.55778	3	26.56	
GH41	YRQZGQ	YRQZGQ	[Phospho (S)]	-0.03	-0.07	0.12	0.04	0.332	0.255	0.123	0.35	1.28E-05	1.41E-05	1.44E-05	1.46E-05	1.31E-05	1.61E-05	4.58E-04	505.73911	3	36.1	
GH42	YRQZGQ	YRQZGQ	[Phospho (S)]	-0.32	-0.23	0.07	-0.08	0.300	0.235	0.305	0.19	1.60E-05	1.64E-05	1.55E-05	1.37E-05	1.24E-05	1.84E-05	1.98E-05	660.9771	3	47.27	
GH43	YRQZGQ	YRQZGQ	[N-term] Acetyl [Protein N-term][1] Phospho	-0.13	0.08	0.04	-0.21	0.030	0.436	0.403	0.38	6.05E-05	5.72E-05	5.00E-05	4.00E-05	9.75E-05	6.41E-05	4.92E-05	880.2971	3	60.46	
GH44	YRQZGQ	YRQZGQ	[17] Phospho (S)	-0.88	0.72	-0.37	-1.61	0.082	0.170	0.233	0.10	3.07E-04	3.31E-04	1.20E-04	1.75E-04	6.02E-04	3.68E-04	2.58E-04	466.20004	2	21.17	
GH45	YRQZGQ	YRQZGQ	[17] Phospho (S)	-0.13	0.73	0.70	-0.29	0.055	0.138	0.051	0.15	1.10E-05	1.10E-05	1.49E-05	1.39E-05	1.39E-05	1.74E-05	2.21E-05	768.28994	3	40.05	
GH46	YRQZGQ	YRQZGQ	[Phospho (S)]	-0.17	0.09	0.12	-0.28	0.153	0.033	0.232	0.23	3.18E-05	3.59E-05	4.26E-05	3.92E-05	4.26E-05	8.31E-05	7.45E-05	436.88683	2	32.66	
GH47	YRQZGQ	YRQZGQ	[Phospho (S)]	0.44	0.09	0.03	0.38	0.027	0.198	0.05	0.02	1.48E-05	1.71E-05	1.48E-05	1.48E-05	1.48E-05	1.07E-05	6.82E-05	103.23017	2	46.96	
GH48	YRQZGQ	YRQZGQ	[Phospho (S)]	0.17	0.17	0.17	0.17	0.17	0.17	0.17	0.17	0.17	0.17	0.17	0.17	0.17	0.17	0.17	466.52731	2	46.96	
GH49	YRQZGQ	YRQZGQ	[Phospho (S)]	-0.62	-0.14	-0.19	-0.46	0.022	0.188	0.020	0.64	3.76E-04	6.68E-05	6.73E-05	6.38E-05	6.38E-05	5.15E-05	6.19E-05	871.6231	4	62.84	
GH50	YRQZGQ	YRQZGQ	[Phospho (S)]	0.15	0.16	0.467	0.13	0.10	0.214	0.140	0.10	8.21E-04	4.38E-04	7.87E-04	8.98E-0							

FLCZ	VAL033W	MANDELELEIK	0.60	0.16	0.73	0.44	0.007	0.222	0.012	0.06	5.021E-04	6.31E-04	7.71E-04	9.76E-04	9.61E-04	9.78E-04	9.62E-04	6.43E-04	5.41E-04	1.14E-05	8.87E-04	1.18E-05	5.2493891	3	30.05
FLCZ	VAL033W	SATRSAPANO	0.43	-0.66	-0.07	1.10	0.156	0.106	0.433	0.01	4.321E-04	5.00E-04	5.91E-04	7.33E-04	4.59E-04	5.95E-04	2.86E-04	2.66E-04	3.12E-04	4.47E-04	3.87E-04	4.35E-04	6.87287	3	27.26
FLCZ	VAL033W	KEGSEDEDELETPTTYPVAVTAQELK	0.28	0.31	-0.05	-0.03	0.182	0.170	0.434	0.46	3.97E-05	5.08E-05	3.07E-05	4.28E-05	6.68E-05	4.24E-05	4.82E-05	3.86E-05	4.95E-05	4.84E-05	3.71E-05	4.37E-05	1.514825	3	39.64
FLCZ	VAL033W	RSNYSIHGANNASVYK	-0.18	-0.09	-0.60	0.18	0.367	0.382	0.37	1.02E-05	8.39E-06	7.02E-06	8.16E-06	4.12E-06	6.93E-06	7.72E-06	1.04E-06	1.04E-06	7.06E-06	9.57E-06	6.08E-06	8.14E-06	6.8639847	3	31.24
FLCZ	VAL033W	RSNYSIBTK	-0.11	-2.63	-0.60	2.52	0.451	0.097	0.255	0.05	1.30E-05	3.39E-05	4.48E-05	1.18E-05	4.12E-05	3.83E-05	1.47E-05	1.21E-05	1.61E-05	3.79E-05	3.08E-05	3.07E-05	5.762985	3	42.42
FLCZ	VAL033W	NASUAWANDSDGTR	0.15	0.09	-0.02	0.07	0.093	0.284	0.427	0.31	2.74E-05	2.59E-05	1.04E-05	2.88E-05	3.33E-05	2.35E-05	2.35E-05	3.35E-05	3.02E-05	2.64E-05	2.78E-05	3.80E-05	6.903805	3	32.91
FLCZ	VAL033W	SMSISTPTVPDHEK	0.13	0.15	-0.04	0.01	0.305	0.384	0.447	0.26	2.69E-04	1.20E-04	3.73E-04	1.22E-05	1.67E-05	1.16E-05	1.46E-05	1.44E-05	1.13E-05	3.14E-05	6.04E-05	8.51E-05	6.4438039	3	32.96
FLCZ	VAL033W	ATGELMHPK	0.21	0.50	-0.14	0.37	0.137	0.016	0.26	0.26	1.28E-04	1.02E-04	1.78E-04	2.00E-04	2.00E-04	3.96E-04	7.96E-04	7.96E-04	3.81E-04	8.57E-04	6.28E-04	7.83E-04	5.6828872	3	44.1
FLCZ	VAL033W	DODGSPAVPVSICK	-2.57	-0.94	-0.32	0.16	0.356	0.441	0.158	0.10	2.98E-05	1.02E-05	1.48E-05	2.74E-05	2.19E-05	2.80E-05	2.80E-05	1.94E-05	2.56E-05	4.65E-05	2.92E-05	1.0033611	3	33.18	
FLCZ	VAL033W	DODGSPAVPVSICK	0.11	-0.07	0.32	0.16	0.273	0.198	0.123	0.17	3.79E-05	4.34E-05	4.87E-05	3.99E-05	4.56E-05	5.33E-05	5.84E-05	4.45E-05	4.35E-05	3.40E-05	4.62E-05	1.37481	3	31.2	
FLCZ	VAL033W	DODGSPAVPVSICK	0.16	0.02	0.35	0.18	0.291	0.427	0.190	0.24	1.50E-05	3.22E-05	1.28E-05	1.72E-05	1.19E-05	1.30E-05	1.03E-05	1.68E-05	1.50E-05	1.38E-05	1.38E-05	6.024422	3	36.73	
FLCZ	VAL033W	RFSYGSGTGNNDVTHPK	-0.28	0.22	0.05	-0.51	0.167	0.233	0.428	0.24	1.42E-05	1.92E-05	1.02E-05	1.11E-05	1.31E-05	1.06E-05	1.36E-05	1.18E-05	1.29E-05	1.14E-05	1.55E-05	6.97557	4	22.46	
FLCZ	VAL033W	VALD055DOLAK	-0.16	0.08	0.23	-0.24	0.135	0.202	0.07	1.17E-05	1.27E-05	1.41E-05	1.02E-05	1.11E-05	1.11E-05	1.34E-05	1.41E-05	1.22E-05	1.05E-05	1.47E-05	1.56E-05	7.9338835	2	60.55	
FLCZ	VAL033W	VALD055DOLAK	-0.40	-0.30	-0.41	-0.30	0.048	0.288	0.211	0.43	6.11E-04	7.88E-04	5.42E-04	4.52E-04	4.54E-04	4.65E-04	8.73E-04	2.77E-04	3.99E-04	2.86E-04	6.88E-04	5.84E-04	5.84227	2	21.46
FLCZ	VAL033W	ADDELDNDMPK	0.18	-0.20	-0.27	0.10	0.253	0.240	0.111	0.47	1.13E-05	1.25E-05	1.39E-05	1.18E-05	1.31E-05	1.26E-05	1.26E-05	2.01E-05	1.41E-05	1.02E-05	1.42E-05	6.893562	2	30.35	
FLCZ	VAL033W	SFNYSFPAUSK	-0.55	-0.03	-0.14	-0.33	0.005	0.270	0.134	0.03	1.51E-05	1.93E-05	1.07E-05	1.08E-05	1.02E-05	1.32E-05	1.32E-05	6.98E-05	6.22E-05	1.68E-05	1.31E-05	1.45E-05	8.023543	2	48.29
FLCZ	VAL033W	PROGSEKURK	0.33	0.14	0.39	0.51	0.025	0.128	0.099	0.03	1.80E-05	8.87E-06	1.02E-05	3.80E-05	1.02E-05	9.31E-06	9.31E-06	9.31E-06	9.31E-06	1.69E-05	1.22E-05	1.42E-05	6.3033	2	45.09
FLCZ	VAL033W	VALD055DOLAK	-0.36	-0.03	0.29	0.16	0.289	0.411	0.158	0.07	6.85E-06	8.21E-06	6.51E-06	5.34E-06	6.20E-06	5.34E-06	7.52E-06	1.04E-06	6.65E-06	7.01E-06	1.24E-06	1.16E-06	1.056311	4	52.89
FLCZ	VAL033W	VALD055DOLAK	-0.56	-0.03	0.42	0.22	0.099	0.464	0.243	0.22	6.85E-06	8.21E-06	6.51E-06	5.34E-06	6.20E-06	5.34E-06	7.52E-06	1.04E-06	6.65E-06	7.01E-06	1.24E-06	1.16E-06	1.056311	4	52.89
FLCZ	VAL033W	RUSVATSPK	0.42	-0.03	-0.43	0.38	0.055	0.449	0.448	0.12	6.47E-06	7.21E-06	6.64E-06	7.58E-06	8.98E-06	9.38E-06	9.38E-06	4.04E-06	6.55E-06	5.16E-06	8.28E-06	4.863884	2	53.26	
FLCZ	VAL033W	RUSVATSPK	-0.49	-0.15	-0.40	-0.34	0.129	0.361	0.072	0.25	2.53E-05	1.63E-05	1.65E-05	1.82E-05	1.52E-05	7.99E-06	1.59E-05	2.52E-05	1.13E-05	2.86E-05	2.31E-05	7.613291	3	72.46	
FLCZ	VAL033W	IGSGLSK	2.39	2.45	0.75	-0.16	0.001	0.040	0.01	0.40	1.29E-04	2.83E-04	2.01E-04	8.92E-04	1.30E-05	1.30E-05	1.30E-05	9.65E-04	1.08E-05	2.77E-04	3.39E-04	7.032963	3	25.36	
FLCZ	VAL033W	ANVSYSANSDINSEK	-0.28	-0.45	-0.12	0.17	0.180	0.009	0.340	0.22	1.53E-05	4.69E-05	2.41E-05	2.81E-05	3.10E-05	3.63E-05	3.63E-05	7.00E-05	3.16E-05	3.47E-05	1.68E-05	7.032963	3	25.36	
FLCZ	VAL033W	SESVYDSAGATAFACK	-0.41	0.14	-0.08	-0.35	0.141	0.346	0.422	0.06	3.37E-05	4.69E-05	2.41E-05	6.2E-05	3.10E-05	6.65E-05	6.65E-05	1.02E-05	3.16E-05	3.47E-05	1.68E-05	7.032963	3	25.36	
FLCZ	VAL033W	KEPVYDPAWAK	1.50	1.92	0.78	-0.42	0.000	0.011	0.018	0.02	2.69E-04	1.79E-04	2.29E-04	6.2E-04	3.10E-04	3.10E-04	3.10E-04	5.00E-04	3.16E-04	4.70E-04	3.15E-04	5.0259785	3	20.1	
FLCZ	VAL033W	EDDVSAPALDTEPVLEK	0.85	0.62	0.54	0.24	0.012	0.328	0.078	0.14	4.65E-04	7.92E-04	5.31E-04	8.99E-04	1.22E-05	1.14E-05	1.14E-05	1.84E-04	7.82E-04	6.37E-04	1.04E-05	9.30E-04	6.007938	4	17.85
FLCZ	VAL033W	EDDVSAPALDTEPVLEK	0.04	-0.10	-0.14	0.14	0.429	0.032	0.234	0.28	1.85E-05	1.77E-05	1.25E-05	1.80E-05	1.88E-05	1.54E-05	1.54E-05	1.84E-04	7.82E-04	6.37E-04	1.04E-05	9.30E-04	6.007938	4	17.85
FLCZ	VAL033W	ICPVQVEADLDNJDSEIPTNDVQDSEK	-0.77	-0.71	-0.41	-0.05	0.048	0.063	0.132	0.41	4.98E-05	3.98E-05	2.55E-05	1.80E-05	2.28E-05	2.54E-05	2.54E-05	2.54E-05	2.54E-05	1.81E-05	2.63E-05	3.31E-05	1.024854	4	39.58
FLCZ	VAL033W	VHSKZDANASITFK	-0.29	-0.04	0.03	-0.25	0.164	0.455	0.466	0.18	6.72E-04	6.93E-04	9.64E-04	6.07E-04	5.23E-04	7.01E-04	7.73E-04	5.13E-04	8.80E-04	6.89E-04	6.39E-04	9.51E-04	8.763932	2	86.88
FLCZ	VAL033W	NDSVDEJEGVQHR	-0.48	-0.05	-0.27	-0.43	0.043	0.407	0.108	0.03	2.27E-05	3.17E-05	2.42E-05	1.80E-05	2.20E-05	2.38E-05	2.38E-05	1.79E-05	2.31E-05	1.96E-05	2.39E-05	2.16E-05	1.093489	3	47.48
FLCZ	VAL033W	GESYQAEDHTAPEK	0.87	0.34	0.54	0.34	0.043	0.025	0.007	0.01	1.38E-05	1.51E-05	1.25E-05	2.32E-05	2.37E-05	2.37E-05	2.37E-05	1.87E-05	1.52E-05	1.82E-05	1.90E-05	2.28E-05	5.984914	3	24.71
FLCZ	VAL033W	KEPVYDPAWAK	-0.14	-0.14	-0.14	-0.14	0.278	0.443	0.313	0.19	3.82E-04	5.86E-04	4.48E-04	4.36E-04	4.84E-04	5.05E-04	6.26E-04	4.32E-04	5.49E-04	3.98E-04	4.74E-04	5.89E-04	4.913087	3	41.53
FLCZ	VAL033W	LFTSMAAQDQPP	0.57	0.24	-0.40	-0.80	0.018	0.120	0.383	0.20	2.37E-05	3.17E-05	2.42E-05	1.80E-05	2.20E-05	2.38E-05	2.38E-05	1.79E-05	2.31E-05	1.96E-05	2.39E-05	2.16E-05	1.093489	3	47.48
FLCZ	VAL033W	KEPVYDPAWAK	-0.44	-0.44	-0.44	-0.44	0.278	0.443	0.313	0.19	3.82E-04	5.86E-04	4.48E-04	4.36E-04	4.84E-04	5.05E-04	6.26E-04	4.32E-04	5.49E-04	3.98E-04	4.74E-04	5.89E-04	4.913087	3	41.53
FLCZ	VAL033W	KEPVYDPAWAK	-0.44	-0.44	-0.44	-0.44	0.278	0.443	0.313	0.19	3.82E-04	5.86E-04	4.48E-04	4.36E-04	4.84E-04	5.05E-04	6.26E-04	4.32E-04	5.49E-04	3.98E-04	4.74E-04	5.89E-04	4.913087	3	41.53
FLCZ	VAL033W	RUSVATSPK	0.38	0.17	-0.43	0.21	0.201	0.370	0.188	0.14	1.11E-05	1.79E-05	1.16E-05	1.18E-05	1.16E-05	1.40E-05	1.40E-05	1.45E-05	1.19E-05	1.02E-05	1.20E-05	2.80E-05	8.720881	3	66.63
FLCZ	VAL033W	SANSISDHQLOFQLEK	-0.38	-0.13	-0.45	-0.25	0.125	0.320	0.088	0.14	1.11E-05	1.79E-05	1.16E-05	1.18E-05	1.16E-05	1.40E-05	1.40E-05	1.45E-05	1.19E-05	1.02E-05	1.20E-05	2.80E-05	8.720881	3	66.63
FLCZ	VAL033W	RANVYSAPYK	-1.05	-0.97	-0.62	-0.80	0.056	0.066	0.127	0.34	1.20E-05	7.93E-06	1.41E-05	3.10E-05	3.72E-05	4.34E-05	5.02E-05	3.49E-05	3.81E-05	5.67E-05	9.49E-05	9.72E-05	4.952354	3	18.87
FLCZ	VAL033W	DNVSDQVSDSTELEK	-0.38	-0.12	-0.44	-0.26	0.175	0.376	0.054	0.32	2.51E-05	2.13E-05	2.43E-05	1.67E-05	2.34E-05	1.43E-05	1.43E-05	1.85E-05	2.87E-05	1.39E-05	1.49E-05	1.69E-05	4.952354	3	17.09
FLCZ	VAL033W	VHSKZDANASITFK	-0.25	-0.09	-0.10	-0.16	0.214	0.400	0.382	0.24	3.98E-04	2.82E-04	2.06E-04	3.68E-04	3.70E-04	3.41E-04	3.41E-04	3.06E-04	4.25E-04	3.76E-04	3.14E-04	4.34E-04	5.8439088	3	26.6
FLCZ	VAL033W	NPFSNGVSGEHLVEEDSDSK	0.01	0.01	-0.40	0.00	0.468	0.476	0.045	0.50	1.98E-05	1.84E-05	2.05E-05	2.05E-05	1.71E-05	1.71E-05	1.49E-05	1.82E-05	2.91E-05	1.56E-05	1.24E-05	93.32754	3	67	
FLCZ	VAL033W	SEPHTEADAGSATPMSKALR	-0.47	0.54	0.71	-1.01	0.389	0.079	0.074	0.03	2.32E-05	2.51E-05	1.97E-05	1.40E-05	2.33E-05	1.94E-05	1.94E-05	4.05E-05	2.17E-05	1.19E-05	5.91E-05	2.69E-05	9.8106667	3	48.08
FLCZ	VAL033W	SPSTVNEFH	0.29	0.45	0.27	-1.16	0.350	0.067	0.255	0.															

YMR124W	YMR124W	TLS1NGR	0.11	0.14	0.02	-0.25	0.13	0.236	0.470	0.03	2.90E+04	3.40E+04	3.27E+04	4.02E+04	3.97E+04	4.26E+04	4.50E+04	4.40E+04	3.74E+04	3.54E+04	5.075288	2	4485
WHB	WHB	LNPS5NWK	-1.09	-1.68	-2.11	0.59	0.255	0.187	0.170	0.28	2.48E+05	3.78E+04	1.87E+04	3.75E+04	1.01E+04	2.35E+04	6.03E+04	2.77E+04	1.28E+04	1.58E+04	5.907731	3	5041
YMR132C	YMR132C	SFE5SDPSNLSQDQ3Q0Q0CQP0CQ0T0K	-0.23	-0.01	-0.22	-0.20	0.300	0.483	0.057	0.17	5.78E+05	5.71E+05	5.20E+05	5.50E+05	5.50E+05	5.74E+05	5.14E+05	4.83E+05	3.66E+05	3.66E+05	1.099562	4	3596
YMR133W	YMR133W	KDPS5DSEADBEK	-0.21	-0.08	-0.26	-0.13	0.072	0.130	0.069	0.16	6.18E+04	7.70E+04	5.84E+04	6.17E+04	6.61E+04	7.65E+04	6.00E+04	6.62E+04	5.90E+04	5.80E+04	741.32746	7	7319
YMR134W	YMR134W	YMR134W	0.62	0.21	-0.07	0.41	0.025	0.133	0.045	0.19	1.41E+05	8.22E+04	1.27E+05	1.60E+05	1.60E+05	1.76E+05	1.41E+05	1.36E+05	9.00E+04	9.00E+04	841.31643	3	3509
YMR135W	YMR135W	R555E5H5P5M5AL5V5G5P5D5R	0.34	0.39	0.46	-0.05	0.159	0.238	0.183	0.44	2.53E+05	1.17E+05	4.23E+05	3.43E+05	5.13E+05	3.50E+05	2.39E+05	3.09E+05	5.27E+05	5.27E+05	1083.4672	3	4493
YMR136W	YMR136W	YMR136W	0.01	0.08	0.10	-0.07	0.473	0.096	0.337	0.40	2.60E+04	2.38E+04	3.20E+04	2.50E+04	3.97E+04	1.88E+04	3.27E+04	2.46E+04	3.97E+04	3.57E+04	556.78802	2	3076
YMR137W	YMR137W	YMR137W	0.53	0.62	0.45	-0.08	0.025	0.088	0.041	0.31	3.23E+04	2.85E+04	4.05E+04	4.59E+04	3.81E+04	4.69E+04	4.69E+04	4.45E+04	3.18E+04	3.66E+04	6.82.76699	3	2215
YMR138W	YMR138W	YMR138W	-0.55	-0.30	-0.53	-0.26	0.038	0.029	0.085	0.29	7.69E+04	1.12E+05	5.24E+04	7.55E+04	1.09E+05	4.18E+04	1.16E+05	3.10E+04	5.76E+04	5.76E+04	521.92974	3	2326
YMR139W	YMR139W	YMR139W	0.73	0.38	0.27	0.33	0.086	0.175	0.220	0.11	1.87E+04	1.31E+04	3.70E+04	3.70E+04	1.93E+04	2.15E+04	3.31E+04	4.29E+04	8.82E+04	8.82E+04	898.92782	2	3648
YMR140W	YMR140W	YMR140W	-0.30	-0.31	-0.50	-0.18	0.018	0.117	0.041	0.01	8.52E+04	1.03E+05	1.75E+05	1.75E+05	1.28E+05	1.24E+05	1.04E+05	2.05E+04	8.00E+04	8.00E+04	738.93955	2	4126
YMR141W	YMR141W	YMR141W	0.13	0.18	0.20	0.31	0.349	0.181	0.167	0.09	1.69E+05	1.32E+05	1.54E+05	1.57E+05	1.28E+05	1.28E+05	1.64E+05	2.01E+04	6.85E+04	6.85E+04	1027.419	2	6572
YMR142W	YMR142W	YMR142W	0.88	1.32	0.48	-0.44	0.048	0.051	0.236	0.10	3.20E+04	3.93E+04	1.17E+05	8.96E+04	1.89E+05	7.69E+04	1.20E+05	4.07E+04	6.95E+04	6.95E+04	691.3661	1	3849
YMR143W	YMR143W	YMR143W	-0.38	0.03	-0.40	-0.41	0.104	0.076	0.135	0.20	7.94E+04	6.85E+04	7.22E+04	6.15E+04	1.25E+05	8.00E+04	8.20E+04	4.58E+04	1.08E+05	1.08E+05	686.98973	3	3816
YMR144W	YMR144W	YMR144W	0.72	0.42	0.26	0.29	0.007	0.082	0.038	0.11	1.88E+04	1.38E+04	2.04E+04	3.24E+04	2.89E+04	1.91E+04	2.54E+04	2.11E+04	2.13E+04	2.13E+04	452.1212	2	183
YMR145W	YMR145W	YMR145W	-0.21	0.18	0.02	-0.38	0.337	0.049	0.081	0.07	6.17E+04	1.55E+05	8.38E+04	7.96E+04	1.37E+05	1.08E+05	1.01E+05	7.07E+04	1.39E+05	1.39E+05	849.92929	2	6938
YMR146W	YMR146W	YMR146W	0.65	0.42	0.21	0.21	0.009	0.061	0.073	0.34	2.48E+04	3.48E+04	4.94E+04	6.82E+04	6.82E+04	6.82E+04	6.82E+04	3.07E+04	6.82E+04	6.82E+04	753.28077	3	2088
YMR147W	YMR147W	YMR147W	0.82	0.78	0.72	0.28	0.005	0.022	0.042	0.01	3.78E+04	5.95E+04	5.84E+04	6.86E+04	6.86E+04	6.86E+04	6.86E+04	3.21E+04	6.86E+04	6.86E+04	818.28077	2	6438
YMR148W	YMR148W	YMR148W	-0.55	-0.38	-0.37	-0.28	0.005	0.053	0.023	0.02	4.79E+04	5.84E+04	6.66E+04	8.86E+04	8.86E+04	4.08E+04	4.61E+04	8.23E+04	5.16E+04	5.28E+04	666.8272	2	6438
YMR149W	YMR149W	YMR149W	0.89	1.25	0.61	0.84	0.000	0.002	0.001	0.00	3.95E+04	4.86E+04	3.75E+04	1.77E+05	1.08E+05	1.15E+05	8.64E+04	5.57E+04	6.23E+04	5.94E+04	866.8862	2	613
YMR150W	YMR150W	YMR150W	2.09	1.15	0.69	-0.31	0.134	0.091	0.158	0.25	1.64E+05	8.68E+04	8.17E+04	1.14E+05	1.33E+05	1.84E+04	3.00E+04	1.81E+04	1.53E+04	1.53E+04	380.17852	2	633
YMR151W	YMR151W	YMR151W	-0.42	-0.46	-0.44	-0.52	0.044	0.108	0.061	0.27	3.22E+04	4.92E+04	2.97E+04	3.33E+04	3.93E+04	2.08E+04	2.97E+04	2.43E+04	2.66E+04	3.64E+04	535.9845	3	3827
YMR152W	YMR152W	YMR152W	-0.54	0.03	0.40	-0.57	0.203	0.078	0.256	0.13	8.59E+04	5.84E+04	8.36E+04	8.66E+04	4.00E+05	6.82E+05	2.90E+05	4.93E+05	2.76E+05	3.75E+05	906.02006	3	5545
YMR153W	YMR153W	YMR153W	0.30	-0.07	0.20	0.37	0.085	0.049	0.191	0.01	8.98E+04	8.84E+04	7.67E+04	9.17E+04	9.17E+04	7.06E+04	7.19E+04	9.81E+04	1.01E+05	8.75E+04	690.77136	4	3744
YMR154W	YMR154W	YMR154W	-0.13	0.36	0.22	-0.49	0.175	0.034	0.274	0.38	2.45E+04	3.91E+04	3.91E+04	2.92E+04	3.49E+04	8.62E+04	9.90E+04	5.55E+04	1.01E+05	8.45E+04	634.28666	4	3744
YMR155W	YMR155W	YMR155W	-0.23	-0.15	-0.19	-0.08	0.175	0.034	0.274	0.38	2.45E+04	3.91E+04	3.91E+04	2.92E+04	3.49E+04	8.62E+04	9.90E+04	5.55E+04	1.01E+05	8.45E+04	504.70979	2	2638
YMR156W	YMR156W	YMR156W	0.24	0.21	-0.08	0.03	0.201	0.246	0.403	0.54	2.62E+04	3.76E+04	4.09E+04	4.72E+04	4.72E+04	2.00E+04	4.81E+04	2.09E+04	3.11E+04	3.05E+04	400.19118	2	3814
YMR157W	YMR157W	YMR157W	-0.35	0.20	-0.07	-0.55	0.212	0.309	0.434	0.88	1.63E+05	8.32E+05	4.72E+05	4.52E+05	8.96E+05	1.12E+06	6.55E+05	7.70E+05	6.74E+05	5.36E+05	1.089.917	3	61
YMR158W	YMR158W	YMR158W	0.10	-0.13	0.18	0.23	0.12	0.245	0.238	0.05	6.83E+04	7.30E+04	9.32E+04	8.65E+04	7.67E+04	6.19E+04	7.59E+04	9.37E+04	9.01E+04	1.05E+05	564.9296	3	2819
YMR159W	YMR159W	YMR159W	0.28	0.26	0.50	0.02	0.139	0.158	0.027	0.46	1.98E+04	3.91E+04	2.80E+04	3.67E+04	3.67E+04	3.08E+04	2.98E+04	3.91E+04	3.89E+04	3.89E+04	538.20937	3	2453
YMR160W	YMR160W	YMR160W	-0.42	-0.22	-0.16	-0.20	0.003	0.031	0.203	0.01	1.38E+05	1.37E+05	1.13E+05	1.08E+05	1.28E+05	1.37E+05	1.21E+05	1.05E+05	1.31E+05	1.55E+05	611.9879	3	4664
YMR161W	YMR161W	YMR161W	-1.17	-0.97	-0.38	-0.19	0.066	0.082	0.137	0.36	2.07E+05	9.88E+04	1.57E+05	1.42E+05	4.40E+04	1.28E+05	1.31E+05	1.17E+05	1.41E+05	8.99E+04	796.28047	2	3751
YMR162W	YMR162W	YMR162W	0.45	-0.46	-0.11	0.91	0.300	0.486	0.833	0.01	5.79E+04	5.47E+04	6.27E+04	8.13E+04	4.24E+04	3.93E+04	4.88E+04	6.18E+04	4.64E+04	7.30E+04	460.68842	3	7873
YMR163W	YMR163W	YMR163W	-0.04	-0.28	-0.21	0.30	0.468	0.249	0.332	0.11	2.52E+04	2.09E+04	2.50E+04	3.34E+04	3.34E+04	1.84E+04	2.82E+04	1.46E+04	2.08E+04	3.05E+04	548.24027	2	2166
YMR164W	YMR164W	YMR164W	-0.05	-0.10	-0.25	0.05	0.395	0.372	0.288	0.44	6.17E+04	4.56E+04	5.47E+04	4.60E+04	3.91E+04	1.59E+04	6.21E+04	1.00E+05	4.30E+04	4.21E+04	604.23292	3	3456
YMR165W	YMR165W	YMR165W	-0.20	-0.11	-0.49	0.19	0.130	0.094	0.046	0.33	5.78E+04	8.01E+04	5.91E+04	6.96E+04	4.97E+04	5.06E+04	5.83E+04	6.28E+04	3.90E+04	6.11E+04	508.23292	3	3838
YMR166W	YMR166W	YMR166W	0.03	-0.11	-0.14	0.14	0.462	0.348	0.343	0.26	6.73E+04	4.24E+04	7.08E+04	6.96E+04	4.40E+04	6.29E+04	6.00E+04	6.38E+04	4.70E+04	4.63E+04	643.28088	3	3838
YMR167W	YMR167W	YMR167W	-0.42	-0.40	-0.37	-0.02	0.076	0.076	0.100	0.46	1.57E+05	1.48E+05	1.38E+05	1.16E+05	1.07E+05	1.10E+05	1.13E+05	1.01E+05	8.24E+04	5.63E+04	1.093.9882	2	9135
YMR168W	YMR168W	YMR168W	0.59	-0.20	0.17	0.79	0.000	0.129	0.115	0.00	3.59E+04	3.44E+04	3.71E+04	5.31E+04	3.98E+04	2.45E+04	3.51E+04	4.62E+04	3.79E+04	3.65E+04	663.3252	2	4768
YMR169W	YMR169W	YMR169W	0.07	-0.10	0.58	0.17	0.437	0.313	0.002	0.36	3.01E+05	2.44E+05	3.74E+05	1.30E+05	2.96E+05	2.46E+05	2.00E+05	4.18E+05	3.08E+05	1.085.9355	3	6262	
YMR170W	YMR170W	YMR170W	-0.65	-0.68	-0.41	0.05	0.005	0.059	0.104	0.48	1.34E+05	1.14E+05	1.47E+05	2.09E+05	8.46E+04	1.26E+05	1.26E+05	1.36E+05	6.98E+04	8.64E+04	1024.6319	3	1576
YMR171W	YMR171W	YMR171W	-2.33	-0.72	-0.23	-1.60	0.002	0.043	0.256	0.02	5.48E+05	3.70E+05	1.35E+05	3.87E+04	3.07E+05	3.42E+05	1.57E+05	2.52E+05	6.98E+04	6.98E+04	604.3016	3	6302
YMR172W	YMR172W	YMR172W	0.27	-0.43	0.02	-0.19	0.322	0.257	0.090	0.00	7.83E+04	2.86E+04	3.92E+04	6.98E+04	3.46E+04	3.38E+04	3.61E+04	7.91E+04	3.22E+04	3.98E+04	481.979	2	2522
YMR173W	YMR173W	YMR173W	-0.05	0.08	0.53	-0.13	0.436	0.400	0.059	0.00	5.21E+04	4.86E+04	3.92E+04	4.91E+04	6.44E+04	4.74E+04	5.08E+04	7.91E+04	1.08E+05	1.39E+05	546.29714	2	3077
YMR174W	YMR174W	YMR174W	-0.27	-0.09	-0.08	-0.38	0.086	0.257	0.382	0.14	1.04E+05	1.16E+05	1.10E+05	7.61E+04	8.34E+04	8.92E+04	9.07E+04	8.09E+04	8.19E+04	1.31E+05	783.8861	3	283
YMR175W	YMR175W	YMR175W	-0.04	0.11	-0.37	-0.35	0.426	0.288	0.079	0.10	4.84												

MUK1	YLVDYD	ILVGTSP/SPNK	0.14	1.34	1.06	-1.20	0.181	0.001	0.002	0.000	0.000	5.85E+04	6.51E+04	6.14E+04	1.36E+05	1.65E+05	1.31E+05	1.11E+05	1.36E+05	1.09E+05	697.8857	2	58.07
SWH1	YBQ4ZL	SQ3SLETGHPKSR	-0.12	0.00	-0.12	0.245	0.020	0.033	0.17	5.51E+04	7.27E+04	6.25E+04	6.32E+04	6.14E+04	6.36E+04	6.28E+04	6.48E+04	6.30E+04	6.30E+04	7.38E+04	786.3829	3	82.1
YBQ4ZL	YBQ4ZL	SNSHETGHPKSR	-0.75	-0.58	-0.36	-0.17	0.012	0.027	0.069	1.47E+05	1.31E+05	1.31E+05	1.01E+05	1.01E+05	9.77E+04	9.77E+04	9.77E+04	9.77E+04	1.04E+05	1.04E+05	666.9891	3	36.79
YBQ4ZL	YBQ4ZL	RVNFSQWQK	-0.42	-0.27	-0.16	0.030	0.084	0.341	0.08	5.16E+04	3.97E+04	7.05E+04	4.88E+04	4.88E+04	4.88E+04	4.88E+04	4.88E+04	4.88E+04	4.88E+04	6.75E+04	688.7859	2	26.4
YBQ4ZL	YBQ4ZL	RVNFSQWQK	-0.70	-0.06	-0.22	-0.65	0.008	0.381	0.01	3.28E+04	1.81E+04	4.18E+04	2.28E+04	2.28E+04	2.28E+04	2.28E+04	2.28E+04	2.28E+04	2.28E+04	3.31E+04	567.7555	2	22.2
YBQ4ZL	YBQ4ZL	RVNFSQWQK	-0.42	-0.26	-0.16	-0.46	0.269	0.31	0.42	1.09E+05	1.45E+05	3.95E+05	1.59E+05	1.59E+05	1.59E+05	1.59E+05	1.59E+05	1.59E+05	1.59E+05	2.00E+05	1150.8686	2	65.97
YBQ4ZL	YBQ4ZL	RVNFSQWQK	-0.18	0.23	0.14	0.35	0.358	0.291	0.48	2.08E+05	2.66E+05	1.80E+05	1.80E+05	1.80E+05	1.80E+05	1.80E+05	1.80E+05	1.80E+05	1.80E+05	2.40E+05	986.0278	3	34.91
YBQ4ZL	YBQ4ZL	RVNFSQWQK	0.07	-0.29	-0.04	0.35	0.042	0.446	0.04	7.84E+04	7.31E+04	3.89E+04	7.86E+04	7.86E+04	6.38E+04	6.38E+04	6.38E+04	6.38E+04	6.38E+04	6.99E+04	798.3442	2	39.77
YBQ4ZL	YBQ4ZL	RVNFSQWQK	-0.76	-0.50	-0.37	-0.06	0.012	0.057	0.090	0.19	6.97E+04	4.86E+04	3.01E+04	3.01E+04	3.01E+04	3.01E+04	3.01E+04	3.01E+04	3.01E+04	4.79E+04	528.2881	2	47.47
YBQ4ZL	YBQ4ZL	RVNFSQWQK	1.35	0.92	0.84	0.43	0.022	0.078	0.072	0.04	7.04E+03	1.88E+04	1.88E+04	1.88E+04	1.88E+04	1.88E+04	1.88E+04	1.88E+04	1.88E+04	2.49E+04	404.5948	3	30.73
YBQ4ZL	YBQ4ZL	RVNFSQWQK	-0.21	-0.24	0.23	0.04	0.126	0.151	0.210	0.41	4.20E+04	3.95E+04	4.94E+04	3.10E+04	3.10E+04	3.10E+04	3.10E+04	3.10E+04	3.10E+04	4.02E+04	636.7988	2	35.15
YBQ4ZL	YBQ4ZL	RVNFSQWQK	-0.03	0.05	0.00	-0.38	0.40	0.459	0.500	0.42	1.82E+04	2.18E+04	3.45E+04	3.27E+04	3.27E+04	3.27E+04	3.27E+04	3.27E+04	3.27E+04	4.95E+04	639.2902	2	34.69
YBQ4ZL	YBQ4ZL	RVNFSQWQK	-0.24	-0.10	-0.14	-0.13	0.008	0.237	0.279	0.23	3.89E+04	5.12E+04	4.54E+04	4.22E+04	4.22E+04	4.22E+04	4.22E+04	4.22E+04	4.22E+04	4.95E+04	480.2289	3	20.07
YBQ4ZL	YBQ4ZL	RVNFSQWQK	-0.62	-0.28	0.38	0.05	0.012	0.131	0.02	2.94E+05	2.21E+05	2.08E+05	1.24E+05	1.24E+05	1.24E+05	1.24E+05	1.24E+05	1.24E+05	1.24E+05	1.57E+05	664.6255	3	49.89
YBQ4ZL	YBQ4ZL	RVNFSQWQK	-0.01	0.14	0.33	-0.25	0.464	0.425	0.020	0.21	4.98E+04	4.08E+04	4.44E+04	3.98E+04	3.98E+04	3.98E+04	3.98E+04	3.98E+04	3.98E+04	4.95E+04	743.2367	2	38.19
YBQ4ZL	YBQ4ZL	RVNFSQWQK	-0.63	-0.67	-0.55	0.04	0.055	0.089	0.085	0.45	1.31E+05	7.99E+04	1.37E+05	7.28E+04	7.28E+04	7.28E+04	7.28E+04	7.28E+04	7.28E+04	8.30E+04	743.2368	2	38.19
YBQ4ZL	YBQ4ZL	RVNFSQWQK	-0.15	-0.15	-0.18	0.04	0.022	0.028	0.030	0.46	6.82E+04	9.46E+04	9.46E+04	9.46E+04	9.46E+04	9.46E+04	9.46E+04	9.46E+04	9.46E+04	1.07E+05	849.4255	2	66.57
YBQ4ZL	YBQ4ZL	RVNFSQWQK	-0.35	-0.13	-0.44	-0.32	0.175	0.049	0.104	0.36	3.28E+04	1.37E+05	2.31E+05	1.68E+05	1.68E+05	1.68E+05	1.68E+05	1.68E+05	1.68E+05	1.73E+05	836.7823	2	61.83
YBQ4ZL	YBQ4ZL	RVNFSQWQK	-0.05	-0.2	-0.45	-0.06	0.394	0.464	0.046	0.05	7.24E+04	9.94E+04	1.14E+05	9.94E+04	9.94E+04	9.94E+04	9.94E+04	9.94E+04	9.94E+04	1.23E+05	596.7823	2	62.03
YBQ4ZL	YBQ4ZL	RVNFSQWQK	-0.11	0.02	-0.19	-0.13	0.348	0.482	0.298	0.36	2.54E+04	4.30E+04	4.30E+04	3.26E+04	3.26E+04	3.26E+04	3.26E+04	3.26E+04	3.26E+04	4.09E+04	487.2809	2	55.73
YBQ4ZL	YBQ4ZL	RVNFSQWQK	-0.24	-0.17	-0.22	-0.4	0.135	0.234	0.151	0.03	4.85E+04	6.54E+04	6.14E+04	4.76E+04	4.76E+04	4.76E+04	4.76E+04	4.76E+04	4.76E+04	5.18E+04	629.2979	2	55.28
YBQ4ZL	YBQ4ZL	RVNFSQWQK	-0.26	-0.48	-0.20	-0.46	0.001	0.002	0.01	5.10E+04	7.32E+04	7.55E+04	6.00E+04	6.00E+04	6.00E+04	6.00E+04	6.00E+04	6.00E+04	6.00E+04	1.90E+04	480.2812	2	21.18
YBQ4ZL	YBQ4ZL	RVNFSQWQK	-0.04	-0.37	-0.07	0.41	0.485	0.102	0.413	0.12	3.54E+04	3.29E+04	2.22E+04	2.14E+04	2.14E+04	2.14E+04	2.14E+04	2.14E+04	2.14E+04	2.66E+04	407.2812	2	33.91
YBQ4ZL	YBQ4ZL	RVNFSQWQK	-0.21	0.17	-0.16	0.38	0.336	0.048	0.370	0.12	3.54E+04	3.29E+04	2.22E+04	2.14E+04	2.14E+04	2.14E+04	2.14E+04	2.14E+04	2.14E+04	2.66E+04	407.2812	2	33.91
YBQ4ZL	YBQ4ZL	RVNFSQWQK	-0.09	0.12	0.40	-0.79	0.130	0.221	0.160	0.42	2.41E+04	5.17E+04	4.30E+04	3.06E+04	3.06E+04	3.06E+04	3.06E+04	3.06E+04	3.06E+04	3.78E+04	862.3518	3	66.55
YBQ4ZL	YBQ4ZL	RVNFSQWQK	-0.46	-0.33	-0.40	-0.39	0.164	0.039	0.233	0.02	3.80E+04	4.95E+04	4.35E+04	4.18E+04	4.18E+04	4.18E+04	4.18E+04	4.18E+04	4.18E+04	4.72E+04	509.2424	2	48.23
YBQ4ZL	YBQ4ZL	RVNFSQWQK	0.26	-0.30	-0.09	0.56	0.079	0.037	0.233	0.02	3.80E+04	4.95E+04	4.35E+04	4.18E+04	4.18E+04	4.18E+04	4.18E+04	4.18E+04	4.18E+04	4.72E+04	509.2424	2	48.23
YBQ4ZL	YBQ4ZL	RVNFSQWQK	0.43	-0.89	0.01	1.13	0.044	0.102	0.488	0.22	1.02E+05	2.87E+04	1.04E+05	1.28E+05	1.28E+05	1.28E+05	1.28E+05	1.28E+05	1.28E+05	1.51E+05	998.9312	2	38.36
YBQ4ZL	YBQ4ZL	RVNFSQWQK	0.17	0.29	0.22	-0.12	0.201	0.105	0.180	0.01	4.10E+04	3.97E+04	4.39E+04	4.56E+04	4.56E+04	4.56E+04	4.56E+04	4.56E+04	4.56E+04	5.29E+04	598.9312	2	38.36
YBQ4ZL	YBQ4ZL	RVNFSQWQK	0.43	-0.89	0.01	1.13	0.044	0.102	0.488	0.22	1.02E+05	2.87E+04	1.04E+05	1.28E+05	1.28E+05	1.28E+05	1.28E+05	1.28E+05	1.28E+05	1.51E+05	998.9312	2	38.36
YBQ4ZL	YBQ4ZL	RVNFSQWQK	0.88	0.88	0.25	0.80	0.002	0.389	0.314	0.04	4.39E+04	5.00E+04	5.95E+04	1.06E+05	1.06E+05	1.06E+05	1.06E+05	1.06E+05	1.06E+05	1.21E+05	616.9401	3	39.1
YBQ4ZL	YBQ4ZL	RVNFSQWQK	0.10	0.37	0.27	-0.41	0.464	0.078	0.314	0.04	4.39E+04	5.00E+04	5.95E+04	1.06E+05	1.06E+05	1.06E+05	1.06E+05	1.06E+05	1.06E+05	1.21E+05	616.9401	3	39.1
YBQ4ZL	YBQ4ZL	RVNFSQWQK	-0.03	0.54	0.34	-0.57	0.464	0.078	0.314	0.04	4.39E+04	5.00E+04	5.95E+04	1.06E+05	1.06E+05	1.06E+05	1.06E+05	1.06E+05	1.06E+05	1.21E+05	616.9401	3	39.1
YBQ4ZL	YBQ4ZL	RVNFSQWQK	-0.15	-0.81	0.00	0.66	0.291	0.333	0.498	0.00	4.31E+04	2.48E+04	3.81E+04	3.50E+04	3.50E+04	3.50E+04	3.50E+04	3.50E+04	3.50E+04	4.39E+04	710.8078	2	40.69
YBQ4ZL	YBQ4ZL	RVNFSQWQK	-0.33	-0.42	-0.17	0.25	0.275	0.408	0.368	0.02	9.03E+04	9.19E+04	9.19E+04	1.07E+05	1.07E+05	1.07E+05	1.07E+05	1.07E+05	1.07E+05	1.48E+05	694.8006	2	20.88
YBQ4ZL	YBQ4ZL	RVNFSQWQK	-0.37	-0.29	-0.36	-0.08	0.013	0.115	0.027	0.38	7.94E+04	6.99E+04	6.80E+04	6.00E+04	6.00E+04	6.00E+04	6.00E+04	6.00E+04	6.00E+04	6.82E+04	694.8006	2	20.88
YBQ4ZL	YBQ4ZL	RVNFSQWQK	-2.02	-0.61	-0.32	-1.41	0.029	0.154	0.196	0.00	6.62E+04	1.55E+05	1.55E+05	1.99E+04	1.99E+04	1.99E+04	1.99E+04	1.99E+04	1.99E+04	2.40E+04	694.8006	2	54.25
YBQ4ZL	YBQ4ZL	RVNFSQWQK	-0.92	-0.32	-0.72	-0.60	0.000	0.076	0.001	0.03	1.40E+05	1.61E+05	1.61E+05	1.80E+05	1.80E+05	1.80E+05	1.80E+05	1.80E+05	1.80E+05	2.12E+05	694.8006	2	54.25
YBQ4ZL	YBQ4ZL	RVNFSQWQK	-0.35	-0.45	-0.33	0.10	0.009	0.028	0.093	0.30	1.19E+05	9.65E+04	1.29E+05	7.15E+04	7.15E+04	7.15E+04	7.15E+04	7.15E+04	7.15E+04	8.91E+04	487.7017	3	60.39
YBQ4ZL	YBQ4ZL	RVNFSQWQK	1.50	-1.01	-0.33	2.50	0.002	0.016	0.132	0.00	9.30E+03	1.44E+04	1.12E+04	3.77E+04	3.77E+04	3.77E+04	3.77E+04	3.77E+04	3.77E+04	4.82E+04	487.7017	3	60.39
YBQ4ZL	YBQ4ZL	RVNFSQWQK	-0.17	0.76	0.01	-0.59	0.24	0.065	0.481	0.00	2.88E+04	3.77E+04	2.88E+04	2.88E+04	2.88E+04	2.88E+04	2.88E+04	2.88E+04	2.88E+04	3.88E+04	606.9847	2	23.3
YBQ4ZL	YBQ4ZL	RVNFSQWQK	-0.03	0.10	0.06	-0.13	0.465	0.355	0.447	0.02	5.28E+04	8.42E+04	6.05E+04	6.48E+04	6.48E+04	6.48E+04	6.48E+04	6.48E+04	6.48E+04	7.86E+04	786.9847	2	25.28
YBQ4ZL	YBQ4ZL	RVNFSQWQK	0.11	-0.03	0.35	0.14	0.332	0.264	0.116	0.14	1.78E+04	2.89E+04	3.08E+04	3.08E+04	3.08E+04	3.08E+04	3.08E+04	3.08E+04	3.08E+04	4.24E+04	487.7017	2	23.3
YBQ4ZL	YBQ4ZL	RVNFSQWQK	-0.27	-0.47	-0.46	0.20	0.053	0.050	0.005	0.25	1.61E+05	1.88E+05	1.88E+05	2.08E+05	2.08E+05	2.08E+05	2.08E+05	2.08E+05	2.08E+05	2.40E+05	487.7017	2	25.28
YBQ4ZL	YBQ4ZL	RVNFSQWQK	0.29	0.59	0.47	-0.38	0.000	0.024	0.083	0.00	2.02E+04	2.07E+04	2.76E+04	2.76E+04	2.76E+04	2.76E+04	2.76E+04	2.76E+04	2.76E+04	3.96E+04	682.2598	2	39.17
YBQ4ZL	YBQ4ZL	RVNFSQWQK	0.30	0.23																			

V0R3BC	NFLVDQVATVRSIPVPRK	0.11	0.14	0.01	7.74E+04	9.27E+04	7.29E+04	5.48E+04	7.51E+04	6.04E+04	8.88E+04	1.08E+05	8.91E+04	6.75E+04	8.14E+04	6.27E+04	6.5779639	4	15.66
SECT7	VHLT3C	-0.30	0.06	0.43	1.44E+04	1.86E+04	1.81E+04	1.75E+04	1.11E+04	1.29E+04	1.88E+04	1.09E+04	1.31E+04	2.28E+04	1.81E+04	1.57E+04	1.47E+04	4	18.82
TR1107	VANV5E5SR	-0.40	0.09	0.35	1.23E+05	1.22E+05	1.05E+04	1.32E+04	7.52E+04	6.28E+04	8.70E+04	8.8E+04	8.7E+04	1.91E+04	1.36E+04	1.49E+04	1.71E+04	3	36.62
SPM2	F5HUGLESDHNDHDK	-0.74	-0.40	0.03	1.23E+05	1.22E+05	1.05E+04	1.32E+04	7.52E+04	6.28E+04	8.70E+04	8.8E+04	8.7E+04	1.91E+04	1.36E+04	1.49E+04	1.71E+04	3	36.62
FR4	VY5HK	-0.29	0.23	0.03	2.20E+03	1.16E+04	1.85E+04	1.06E+04	1.23E+04	1.52E+04	3.32E+04	1.76E+04	2.08E+04	6.67E+04	7.00E+04	2.14E+04	2.14E+04	2	20.14
PH13	SSNLSL5K	-0.38	-0.26	0.59	9.35E+04	1.17E+05	1.85E+04	7.66E+04	7.28E+04	7.30E+04	7.54E+04	1.05E+05	6.01E+04	1.36E+04	5.08E+04	6.98E0336	6.98E0336	2	44.15
BD1	VH939C	-0.29	0.24	0.38	3.93E+04	2.99E+04	3.62E+04	4.13E+04	2.96E+04	4.32E+04	3.68E+04	5.61E+04	3.13E+04	3.80E+04	2.50E+04	3.12E+04	7.2232775	2	32.36
MD1	VGL197W	-0.20	0.28	-0.19	4.01E+04	4.99E+04	4.99E+04	6.36E+04	4.59E+04	5.41E+04	6.61E+04	2.61E+04	6.29E+04	7.26E+04	7.13E+04	6.98E02922	6.98E02922	3	18.34
GR1	VNSD10YK	-0.71	-0.09	0.84	4.89E+04	1.16E+05	1.05E+04	4.18E+04	2.93E+04	3.92E+04	2.43E+04	4.12E+04	4.12E+04	3.21E+04	1.87E+04	4.27E+04	680.7746	2	18.34
OP1	SVY0YAR	-0.18	0.08	0.64	1.47E+04	2.18E+04	1.98E+04	3.82E+04	1.94E+04	3.92E+04	1.96E+04	4.60E+04	2.60E+04	2.90E+04	1.94E+04	1.87E+04	585.77489	2	42.15
DC17	ELD029DVPVHWK	-0.21	0.37	-0.25	7.48E+04	7.83E+04	9.27E+04	4.05E+04	1.05E+05	6.69E+04	7.98E+04	1.36E+05	1.01E+05	7.89E+04	8.56E+04	7.32E+04	699.94866	3	36.37
YR1	SEDSIGNK	-0.28	-0.18	-0.20	8.63E+03	9.66E+03	8.20E+03	5.25E+04	2.93E+04	2.50E+04	4.99E+04	7.04E+04	5.85E+04	4.84E+04	5.75E+04	3.58E+04	578.26922	3	61.84
SE3	VNSMAALP5K	-0.09	0.02	0.09	5.97E+04	4.94E+04	6.70E+04	5.11E+04	4.44E+04	5.36E+04	4.87E+04	4.86E+04	5.23E+04	5.34E+04	4.65E+04	5.70E+04	746.67067	3	58.14
SE2	VH939C	-0.15	0.27	0.17	4.79E+04	4.08E+04	5.45E+04	5.14E+05	3.14E+05	4.19E+05	3.65E+05	5.18E+05	4.28E+05	5.07E+05	4.64E+05	4.24E+05	185.2002	3	36.04
AL1	VH939C	-0.15	0.27	0.17	4.79E+04	4.08E+04	5.45E+04	5.14E+05	3.14E+05	4.19E+05	3.65E+05	5.18E+05	4.28E+05	5.07E+05	4.64E+05	4.24E+05	185.2002	3	36.04
AL2	VH939C	-0.15	0.27	0.17	4.79E+04	4.08E+04	5.45E+04	5.14E+05	3.14E+05	4.19E+05	3.65E+05	5.18E+05	4.28E+05	5.07E+05	4.64E+05	4.24E+05	185.2002	3	36.04
YCK1	VH939C	-0.15	0.27	0.17	4.79E+04	4.08E+04	5.45E+04	5.14E+05	3.14E+05	4.19E+05	3.65E+05	5.18E+05	4.28E+05	5.07E+05	4.64E+05	4.24E+05	185.2002	3	36.04
SE5	VH939C	-0.15	0.27	0.17	4.79E+04	4.08E+04	5.45E+04	5.14E+05	3.14E+05	4.19E+05	3.65E+05	5.18E+05	4.28E+05	5.07E+05	4.64E+05	4.24E+05	185.2002	3	36.04
PH1	VH939C	-0.15	0.27	0.17	4.79E+04	4.08E+04	5.45E+04	5.14E+05	3.14E+05	4.19E+05	3.65E+05	5.18E+05	4.28E+05	5.07E+05	4.64E+05	4.24E+05	185.2002	3	36.04
PH2	VH939C	-0.15	0.27	0.17	4.79E+04	4.08E+04	5.45E+04	5.14E+05	3.14E+05	4.19E+05	3.65E+05	5.18E+05	4.28E+05	5.07E+05	4.64E+05	4.24E+05	185.2002	3	36.04
SP6	VH939C	-0.15	0.27	0.17	4.79E+04	4.08E+04	5.45E+04	5.14E+05	3.14E+05	4.19E+05	3.65E+05	5.18E+05	4.28E+05	5.07E+05	4.64E+05	4.24E+05	185.2002	3	36.04
SE7	VH939C	-0.15	0.27	0.17	4.79E+04	4.08E+04	5.45E+04	5.14E+05	3.14E+05	4.19E+05	3.65E+05	5.18E+05	4.28E+05	5.07E+05	4.64E+05	4.24E+05	185.2002	3	36.04
SE8	VH939C	-0.15	0.27	0.17	4.79E+04	4.08E+04	5.45E+04	5.14E+05	3.14E+05	4.19E+05	3.65E+05	5.18E+05	4.28E+05	5.07E+05	4.64E+05	4.24E+05	185.2002	3	36.04
SE9	VH939C	-0.15	0.27	0.17	4.79E+04	4.08E+04	5.45E+04	5.14E+05	3.14E+05	4.19E+05	3.65E+05	5.18E+05	4.28E+05	5.07E+05	4.64E+05	4.24E+05	185.2002	3	36.04
SE10	VH939C	-0.15	0.27	0.17	4.79E+04	4.08E+04	5.45E+04	5.14E+05	3.14E+05	4.19E+05	3.65E+05	5.18E+05	4.28E+05	5.07E+05	4.64E+05	4.24E+05	185.2002	3	36.04
SE11	VH939C	-0.15	0.27	0.17	4.79E+04	4.08E+04	5.45E+04	5.14E+05	3.14E+05	4.19E+05	3.65E+05	5.18E+05	4.28E+05	5.07E+05	4.64E+05	4.24E+05	185.2002	3	36.04
SE12	VH939C	-0.15	0.27	0.17	4.79E+04	4.08E+04	5.45E+04	5.14E+05	3.14E+05	4.19E+05	3.65E+05	5.18E+05	4.28E+05	5.07E+05	4.64E+05	4.24E+05	185.2002	3	36.04
SE13	VH939C	-0.15	0.27	0.17	4.79E+04	4.08E+04	5.45E+04	5.14E+05	3.14E+05	4.19E+05	3.65E+05	5.18E+05	4.28E+05	5.07E+05	4.64E+05	4.24E+05	185.2002	3	36.04
SE14	VH939C	-0.15	0.27	0.17	4.79E+04	4.08E+04	5.45E+04	5.14E+05	3.14E+05	4.19E+05	3.65E+05	5.18E+05	4.28E+05	5.07E+05	4.64E+05	4.24E+05	185.2002	3	36.04
SE15	VH939C	-0.15	0.27	0.17	4.79E+04	4.08E+04	5.45E+04	5.14E+05	3.14E+05	4.19E+05	3.65E+05	5.18E+05	4.28E+05	5.07E+05	4.64E+05	4.24E+05	185.2002	3	36.04
SE16	VH939C	-0.15	0.27	0.17	4.79E+04	4.08E+04	5.45E+04	5.14E+05	3.14E+05	4.19E+05	3.65E+05	5.18E+05	4.28E+05	5.07E+05	4.64E+05	4.24E+05	185.2002	3	36.04
SE17	VH939C	-0.15	0.27	0.17	4.79E+04	4.08E+04	5.45E+04	5.14E+05	3.14E+05	4.19E+05	3.65E+05	5.18E+05	4.28E+05	5.07E+05	4.64E+05	4.24E+05	185.2002	3	36.04
SE18	VH939C	-0.15	0.27	0.17	4.79E+04	4.08E+04	5.45E+04	5.14E+05	3.14E+05	4.19E+05	3.65E+05	5.18E+05	4.28E+05	5.07E+05	4.64E+05	4.24E+05	185.2002	3	36.04
SE19	VH939C	-0.15	0.27	0.17	4.79E+04	4.08E+04	5.45E+04	5.14E+05	3.14E+05	4.19E+05	3.65E+05	5.18E+05	4.28E+05	5.07E+05	4.64E+05	4.24E+05	185.2002	3	36.04
SE20	VH939C	-0.15	0.27	0.17	4.79E+04	4.08E+04	5.45E+04	5.14E+05	3.14E+05	4.19E+05	3.65E+05	5.18E+05	4.28E+05	5.07E+05	4.64E+05	4.24E+05	185.2002	3	36.04
SE21	VH939C	-0.15	0.27	0.17	4.79E+04	4.08E+04	5.45E+04	5.14E+05	3.14E+05	4.19E+05	3.65E+05	5.18E+05	4.28E+05	5.07E+05	4.64E+05	4.24E+05	185.2002	3	36.04
SE22	VH939C	-0.15	0.27	0.17	4.79E+04	4.08E+04	5.45E+04	5.14E+05	3.14E+05	4.19E+05	3.65E+05	5.18E+05	4.28E+05	5.07E+05	4.64E+05	4.24E+05	185.2002	3	36.04
SE23	VH939C	-0.15	0.27	0.17	4.79E+04	4.08E+04	5.45E+04	5.14E+05	3.14E+05	4.19E+05	3.65E+05	5.18E+05	4.28E+05	5.07E+05	4.64E+05	4.24E+05	185.2002	3	36.04
SE24	VH939C	-0.15	0.27	0.17	4.79E+04	4.08E+04	5.45E+04	5.14E+05	3.14E+05	4.19E+05	3.65E+05	5.18E+05	4.28E+05	5.07E+05	4.64E+05	4.24E+05	185.2002	3	36.04
SE25	VH939C	-0.15	0.27	0.17	4.79E+04	4.08E+04	5.45E+04	5.14E+05	3.14E+05	4.19E+05	3.65E+05	5.18E+05	4.28E+05	5.07E+05	4.64E+05	4.24E+05	185.2002	3	36.04
SE26	VH939C	-0.15	0.27	0.17	4.79E+04	4.08E+04	5.45E+04	5.14E+05	3.14E+05	4.19E+05	3.65E+05	5.18E+05	4.28E+05	5.07E+05	4.64E+05	4.24E+05	185.2002	3	36.04
SE27	VH939C	-0.15	0.27	0.17	4.79E+04	4.08E+04	5.45E+04	5.14E+05	3.14E+05	4.19E+05	3.65E+05	5.18E+05	4.28E+05	5.07E+05	4.64E+05	4.24E+05	185.2002	3	36.04
SE28	VH939C	-0.15	0.27	0.17	4.79E+04	4.08E+04	5.45E+04	5.14E+05	3.14E+05	4.19E+05	3.65E+05	5.18E+05	4.28E+05	5.07E+05	4.64E+05	4.24E+05	185.2002	3	36.04
SE29	VH939C	-0.15	0.27	0.17	4.79E+04	4.08E+04	5.45E+04	5.14E+05	3.14E+05	4.19E+05	3.65E+05	5.18E+05	4.28E+05	5.07E+05	4.64E+05	4.24E+05	185.2002	3	36.04
SE30	VH939C	-0.15	0.27	0.17	4.79E+04	4.08E+04	5.45E+04	5.14E+05	3.14E+05	4.19E+05	3.65E+05	5.18E+05	4.28E+05	5.07E+05	4.64E+05	4.24E+05	185.2002	3	36.04
SE31	VH939C	-0.15	0.27	0.17	4.79E+04	4.08E+04	5.45E+04	5.14E+05	3.14E+05	4.19E+05	3.65E+05	5.18E+05	4.28E+05	5.07E+05	4.64E+05	4.24E+05	185.2002	3	36.04
SE32	VH939C	-0.15	0.27	0.17	4.79E+04	4.08E+04	5.45E+04	5.14E+05	3.14E+05	4.19E+05	3.65E+05	5.18E+05	4.28E+05	5.07E+05	4.64E+05	4.24E+05	185.2002	3	36.04
SE33	VH939C	-0.15	0.27	0.17	4.79E+04	4.08E+04	5.45E+04	5.14E+05	3.14E+05	4.19E+05	3.65E+05	5.18E+05	4.28E+05	5.07E+05	4.64E+05	4.24E+05	185.2002	3	36.04

GT13	YEL07W	ATKEDKPKQSDQSDATK	0.45	-0.19	-0.28	0.64	0.050	0.236	0.177	0.022	3.30E+04	2.83E+04	4.22E+04	5.28E+04	3.88E+04	4.96E+04	2.79E+04	2.54E+04	3.71E+04	3.17E+04	2.04E+04	3.17E+04	7.86E+04	3.13E+04	868.0126	3	47.46
GT14	YEL04W	SNEFASPLASAK	-0.59	0.29	0.24	-0.37	0.388	0.151	0.106	0.088	4.80E+04	6.70E+04	6.78E+04	6.15E+04	5.03E+04	6.05E+04	8.97E+04	7.18E+04	5.79E+04	7.86E+04	2.04E+04	3.17E+04	7.86E+04	7.18E+04	868.3266	3	43.62
SR40	YK092C	AETPMASNTSPASSSANK	-0.54	-1.56	-1.05	1.02	0.119	0.031	0.032	0.022	8.91E+04	4.61E+04	3.73E+04	5.96E+04	3.73E+04	3.73E+04	2.04E+04	2.04E+04	2.82E+04	3.73E+04	2.04E+04	3.17E+04	2.82E+04	2.04E+04	768.3478	3	22.17
GT15	YEL03W	YGGASQADPTTR	0.20	-0.66	0.23	0.86	0.429	0.042	0.242	0.237	1.78E+04	5.82E+04	2.86E+04	2.42E+04	1.24E+05	1.35E+04	2.83E+04	3.64E+04	2.46E+04	2.86E+04	1.94E+04	3.17E+04	2.86E+04	1.94E+04	868.81352	3	41.11
GNP1	YK058C	DSSSLDMLNRK	0.01	-0.10	0.06	0.11	0.471	0.310	0.420	0.179	4.31E+04	2.03E+04	2.46E+04	2.19E+04	2.08E+04	1.99E+04	1.71E+04	1.71E+04	2.22E+04	2.86E+04	1.94E+04	3.17E+04	2.86E+04	1.94E+04	529.2382	3	17.69
NMT1	YK120W	MATYGLQYLSVGSK	-0.27	-0.66	-0.11	0.59	0.268	0.031	0.389	0.145	2.45E+05	1.56E+05	2.33E+05	3.58E+05	1.06E+05	1.62E+05	6.87E+04	1.34E+05	1.46E+05	2.87E+04	3.17E+04	2.86E+04	1.94E+04	1.074.0307	2	16.94	
NMT2	YK120W	KATYGLQYLSVGSK	-0.34	-0.58	0.08	0.23	0.283	0.206	0.449	0.333	4.13E+04	1.28E+04	1.41E+04	3.58E+04	1.06E+05	1.84E+04	9.51E+03	1.35E+04	2.30E+04	2.87E+04	3.17E+04	2.86E+04	1.94E+04	694.7824	2	17.79	
MOR1	YK118W	YSQNHFGQDTR	0.28	1.48	0.03	-1.20	0.235	0.021	0.041	0.030	5.20E+04	9.02E+04	4.28E+04	6.82E+04	9.47E+04	6.54E+04	1.97E+05	1.79E+05	1.57E+05	1.02E+05	1.76E+04	3.17E+04	2.86E+04	1.94E+04	935.9881	2	65.81
ATG3	YK118W	YSQNHFGQDTR	0.10	0.24	0.09	-0.14	0.330	0.169	0.301	0.255	1.34E+04	2.02E+04	1.62E+04	1.63E+04	1.81E+04	2.08E+04	2.18E+04	1.72E+04	2.13E+04	1.76E+04	4.06E+04	3.17E+04	2.86E+04	1.94E+04	587.8668	2	32.74
MU1	YK120C	PHSDGSDNSK	-0.44	-0.43	0.09	-0.01	0.149	0.161	0.377	0.417	4.78E+04	2.37E+04	4.97E+04	3.58E+04	2.77E+04	2.19E+04	1.95E+04	7.36E+04	3.48E+04	4.06E+04	4.06E+04	3.17E+04	2.86E+04	1.94E+04	662.2626	2	42.16
FU1	YK120C	PHSDGSDNSK	-0.12	-0.27	0.05	0.16	0.314	0.171	0.403	0.177	1.23E+05	7.95E+04	8.69E+04	6.73E+04	9.75E+04	8.26E+04	1.75E+04	7.36E+04	3.48E+04	4.06E+04	4.06E+04	3.17E+04	2.86E+04	1.94E+04	852.3864	2	47.14
MU2	YK120C	PHSDGSDNSK	-0.49	0.33	0.58	0.04	0.075	0.066	0.061	0.441	4.31E+04	7.90E+04	4.69E+04	7.38E+04	3.35E+04	2.78E+04	8.90E+04	6.13E+04	6.69E+04	7.15E+04	1.02E+05	3.17E+04	2.86E+04	1.94E+04	772.3608	2	36.53
SPI1	YK042C	DNGSSTGLNNHK	-0.33	-0.37	-0.09	0.04	0.163	0.040	0.031	0.433	6.01E+04	8.12E+04	4.12E+04	7.30E+04	4.92E+04	5.50E+04	4.90E+04	6.13E+04	6.69E+04	7.15E+04	1.02E+05	3.17E+04	2.86E+04	1.94E+04	652.3939	3	24.94
SEC1B	YK085W	TSYQNPNNSPSPSR	-0.89	-0.83	-0.39	-0.06	0.022	0.041	0.036	0.433	1.75E+05	1.97E+05	1.54E+05	1.06E+05	5.34E+04	9.38E+04	7.65E+04	1.38E+05	8.40E+04	1.54E+05	1.16E+05	3.17E+04	2.86E+04	1.94E+04	129.2807	2	28.65
CEK2B	YK085W	TSYQNPNNSPSPSR	-0.28	0.13	-0.28	-0.41	0.383	0.039	0.275	0.223	4.95E+05	4.72E+05	2.01E+05	1.82E+05	4.54E+05	1.88E+05	4.92E+04	5.97E+05	3.80E+05	2.45E+05	1.82E+05	3.17E+04	2.86E+04	1.94E+04	79.2944	3	50.25
CDK2B	YK085W	TSYQNPNNSPSPSR	0.43	0.54	0.07	-0.11	0.124	0.082	0.352	0.377	2.68E+04	3.98E+04	3.98E+04	3.98E+04	3.98E+04	3.98E+04	3.98E+04	3.98E+04	3.98E+04	3.98E+04	3.98E+04	3.17E+04	2.86E+04	1.94E+04	682.2944	2	30.05
YK118W	YK118W	YK118W	-0.06	0.19	0.13	-0.42	0.138	0.036	0.233	0.024	1.72E+04	2.16E+04	2.94E+04	2.95E+04	3.09E+04	3.58E+04	4.12E+04	2.28E+04	2.95E+04	3.58E+04	1.94E+04	3.17E+04	2.86E+04	1.94E+04	126.9853	4	29.89
YK118W	YK118W	YK118W	-0.06	0.19	0.13	-0.42	0.138	0.036	0.233	0.024	1.72E+04	2.16E+04	2.94E+04	2.95E+04	3.09E+04	3.58E+04	4.12E+04	2.28E+04	2.95E+04	3.58E+04	1.94E+04	3.17E+04	2.86E+04	1.94E+04	126.9853	4	29.89
YK118W	YK118W	YK118W	-0.06	0.19	0.13	-0.42	0.138	0.036	0.233	0.024	1.72E+04	2.16E+04	2.94E+04	2.95E+04	3.09E+04	3.58E+04	4.12E+04	2.28E+04	2.95E+04	3.58E+04	1.94E+04	3.17E+04	2.86E+04	1.94E+04	126.9853	4	29.89
YK118W	YK118W	YK118W	-0.06	0.19	0.13	-0.42	0.138	0.036	0.233	0.024	1.72E+04	2.16E+04	2.94E+04	2.95E+04	3.09E+04	3.58E+04	4.12E+04	2.28E+04	2.95E+04	3.58E+04	1.94E+04	3.17E+04	2.86E+04	1.94E+04	126.9853	4	29.89
YK118W	YK118W	YK118W	-0.06	0.19	0.13	-0.42	0.138	0.036	0.233	0.024	1.72E+04	2.16E+04	2.94E+04	2.95E+04	3.09E+04	3.58E+04	4.12E+04	2.28E+04	2.95E+04	3.58E+04	1.94E+04	3.17E+04	2.86E+04	1.94E+04	126.9853	4	29.89
YK118W	YK118W	YK118W	-0.06	0.19	0.13	-0.42	0.138	0.036	0.233	0.024	1.72E+04	2.16E+04	2.94E+04	2.95E+04	3.09E+04	3.58E+04	4.12E+04	2.28E+04	2.95E+04	3.58E+04	1.94E+04	3.17E+04	2.86E+04	1.94E+04	126.9853	4	29.89
YK118W	YK118W	YK118W	-0.06	0.19	0.13	-0.42	0.138	0.036	0.233	0.024	1.72E+04	2.16E+04	2.94E+04	2.95E+04	3.09E+04	3.58E+04	4.12E+04	2.28E+04	2.95E+04	3.58E+04	1.94E+04	3.17E+04	2.86E+04	1.94E+04	126.9853	4	29.89
YK118W	YK118W	YK118W	-0.06	0.19	0.13	-0.42	0.138	0.036	0.233	0.024	1.72E+04	2.16E+04	2.94E+04	2.95E+04	3.09E+04	3.58E+04	4.12E+04	2.28E+04	2.95E+04	3.58E+04	1.94E+04	3.17E+04	2.86E+04	1.94E+04	126.9853	4	29.89
YK118W	YK118W	YK118W	-0.06	0.19	0.13	-0.42	0.138	0.036	0.233	0.024	1.72E+04	2.16E+04	2.94E+04	2.95E+04	3.09E+04	3.58E+04	4.12E+04	2.28E+04	2.95E+04	3.58E+04	1.94E+04	3.17E+04	2.86E+04	1.94E+04	126.9853	4	29.89
YK118W	YK118W	YK118W	-0.06	0.19	0.13	-0.42	0.138	0.036	0.233	0.024	1.72E+04	2.16E+04	2.94E+04	2.95E+04	3.09E+04	3.58E+04	4.12E+04	2.28E+04	2.95E+04	3.58E+04	1.94E+04	3.17E+04	2.86E+04	1.94E+04	126.9853	4	29.89
YK118W	YK118W	YK118W	-0.06	0.19	0.13	-0.42	0.138	0.036	0.233	0.024	1.72E+04	2.16E+04	2.94E+04	2.95E+04	3.09E+04	3.58E+04	4.12E+04	2.28E+04	2.95E+04	3.58E+04	1.94E+04	3.17E+04	2.86E+04	1.94E+04	126.9853	4	29.89
YK118W	YK118W	YK118W	-0.06	0.19	0.13	-0.42	0.138	0.036	0.233	0.024	1.72E+04	2.16E+04	2.94E+04	2.95E+04	3.09E+04	3.58E+04	4.12E+04	2.28E+04	2.95E+04	3.58E+04	1.94E+04	3.17E+04	2.86E+04	1.94E+04	126.9853	4	29.89
YK118W	YK118W	YK118W	-0.06	0.19	0.13	-0.42	0.138	0.036	0.233	0.024	1.72E+04	2.16E+04	2.94E+04	2.95E+04	3.09E+04	3.58E+04	4.12E+04	2.28E+04	2.95E+04	3.58E+04	1.94E+04	3.17E+04	2.86E+04	1.94E+04	126.9853	4	29.89
YK118W	YK118W	YK118W	-0.06	0.19	0.13	-0.42	0.138	0.036	0.233	0.024	1.72E+04	2.16E+04	2.94E+04	2.95E+04	3.09E+04	3.58E+04	4.12E+04	2.28E+04	2.95E+04	3.58E+04	1.94E+04	3.17E+04	2.86E+04	1.94E+04	126.9853	4	29.89
YK118W	YK118W	YK118W	-0.06	0.19	0.13	-0.42	0.138	0.036	0.233	0.024	1.72E+04	2.16E+04	2.94E+04	2.95E+04	3.09E+04	3.58E+04	4.12E+04	2.28E+04	2.95E+04	3.58E+04	1.94E+04	3.17E+04	2.86E+04	1.94E+04	126.9853	4	29.89
YK118W	YK118W	YK118W	-0.06	0.19	0.13	-0.42	0.138	0.036	0.233	0.024	1.72E+04	2.16E+04	2.94E+04	2.95E+04	3.09E+04	3.58E+04	4.12E+04	2.28E+04	2.95E+04	3.58E+04	1.94E+04	3.17E+04	2.86E+04	1.94E+04	126.9853	4	29.89
YK118W	YK118W	YK118W	-0.06	0.19	0.13	-0.42	0.138	0.036	0.233	0.024	1.72E+04	2.16E+04	2.94E+04	2.95E+04	3.09E+04	3.58E+04	4.12E+04	2.28E+04	2.95E+04	3.58E+04	1.94E+04	3.17E+04	2.86E+04	1.94E+04	126.9853	4	29.89
YK118W	YK118W	YK118W	-0.06	0.19	0.13	-0.42	0.138	0.036	0.233	0.024	1.72E+04	2.16E+04	2.94E+04	2.95E+04	3.09E+04	3.58E+04	4.12E+04	2.28E+04	2.95E+04	3.58E+04	1.94E+04	3.17E+04	2.86E+04	1.94E+04	126.9853	4	29.89
YK118W	YK118W	YK118W	-0.06	0.19	0.13	-0.42	0.138	0.036	0.233	0.024	1.72E+04	2.16E+04	2.94E+04	2.95E+04	3.09E+04	3.58E+04	4.12E+04	2.28E+04	2.95E+04	3.58E+04	1.94E+04	3.17E+04	2.86E+04	1.94E+04	126.9853	4	29.89
YK118W	YK118W	YK118W	-0.06	0.19	0.13	-0.42	0.138	0.036	0.233	0.024	1.72E+04	2.16E+04	2.94E+04	2.95E+04	3.09E+04	3.58E+04	4.12E+04	2.28E+04	2.95E+04	3.58E+04	1.94E+04	3.17E+04	2.86E+04	1.94E+04	126.9853	4	29.89
YK118W	YK118W	YK118W	-0.06	0.19	0.13	-0.42	0.138	0.036	0.233	0.024	1.72E+04	2.16E+04	2.94E+04	2.95E+04	3.09E+04	3.58E+04	4.12E+04	2.28E+04	2.95E+04	3.58E+04	1.94E+04	3.17E+04	2.86E+04	1.94E+04	126.9853	4	29.89
YK118W	YK118W	YK118W	-0.06	0.19	0.13	-0.42	0.138	0.036	0.233	0.024	1.72E+04	2.16E+04	2.94E+04	2.95E+04	3.09E+04	3.58E+04	4.12E+04	2.28E+04	2.95E+04	3.58E+04	1.94E+04	3.17E+04	2.86E+04	1.94E+04	126.9853	4	29.89
YK118W	YK118W	YK118W	-0.06	0.19																							

VF31	YB01C	SEDVGVYDVLK	0.25	0.53	-0.59	-0.77	0.32	0.45	0.22	0.14	1.0E+04	2.41E+04	5.94E+03	9.87E+03	1.72E+04	7.36E+03	2.43E+04	2.64E+04	8.22E+03	6.83E+03	1.22E+04	8.13E+03	9.18E6692	2	2394
HDS1	YB03C	SSIR	6.26	5.85	1.88	0.41	0.000	0.001	0.000	0.06	0.00E+00	4.43E+01	0.000E+00	2.01E+03	1.64E+03	2.44E+03	1.20E+03	1.78E+03	1.80E+03	1.37E+03	1.48E+03	1.67E+03	9.18E6692	2	1502
HTD1	YB04C	RAVSPK	1.10	1.80	1.23	0.00	0.01	0.00	0.01	0.16	1.15E+03	1.83E+03	1.39E+03	3.25E+03	1.24E+03	2.44E+03	7.38E+03	2.42E+03	4.39E+03	3.55E+03	3.47E+03	3.48E+03	46.23802	2	2019
TAH1	YB06C	YUJSSK	0.35	0.37	-0.02	0.26	0.16	0.31	0.40	0.40	1.34E+03	1.34E+03	1.29E+03	7.58E+03	1.34E+03	1.64E+03	1.23E+03	2.68E+03	2.13E+03	2.61E+03	2.04E+03	1.15E+03	908.88817	2	1936
IMH1	YB02C	KNDYDTHASGSD	0.08	-0.16	-0.39	0.24	0.40	0.49	0.34	0.37	5.82E+02	1.01E+04	2.75E+03	7.58E+03	6.24E+03	3.60E+03	7.65E+03	6.68E+03	3.81E+02	2.87E+03	6.06E+03	4.59E+03	932.78542	3	2813
BMH1	YB13C	GQSTGQDER	0.10	-0.66	-0.26	0.77	0.49	0.18	0.355	0.09	5.07E+03	7.90E+03	3.44E+03	1.05E+04	1.72E+03	1.72E+03	1.21E+04	1.18E+04	1.09E+04	2.40E+03	4.58E+03	1.55E+03	54.23522	2	1735
DC2	YB05C	RFPQRETPFR	2.07	0.39	0.81	-0.32	0.425	0.206	0.013	0.25	1.02E+01	2.16E+03	3.97E+03	1.85E+03	1.69E+03	2.65E+03	3.43E+03	3.43E+03	2.82E+02	3.45E+03	2.77E+03	3.60E+03	78.31189	4	1721
ETS1	YB07C	SPQSDPTPHR	0.04	0.58	-0.26	-0.54	0.44	0.49	0.230	0.21	0.00E+00	2.40E+03	3.67E+03	1.18E+04	7.60E+03	6.64E+03	2.63E+03	5.14E+03	1.28E+03	1.00E+03	3.48E+03	1.91E+03	48.97916	2	1597
STH1	YB12C	TSVVAEK	1.74	1.15	0.59	0.66	0.00	0.038	0.256	0.01	2.38E+03	1.65E+03	1.73E+03	1.53E+03	1.88E+03	1.57E+03	8.38E+03	3.84E+03	2.23E+03	3.23E+03	1.98E+03	58.79886	2	2046	
MTB4	YB10C	AVPVSQSPK	1.81	1.15	0.59	0.66	0.00	0.038	0.256	0.01	2.38E+03	1.65E+03	1.73E+03	1.53E+03	1.88E+03	1.57E+03	8.38E+03	3.84E+03	2.23E+03	3.23E+03	1.98E+03	68.79236	2	2046	
MTB3	YB10C	VYVVAQDFGQR	1.58	-1.50	-0.94	3.48	0.06	0.016	0.137	0.03	1.69E+03	1.20E+04	5.08E+03	1.60E+04	2.35E+04	1.66E+04	1.27E+04	2.08E+03	1.85E+03	4.49E+03	1.39E+03	93.44227	2	4047	
BMH3	YB09C	RFPEUQV	0.63	0.08	0.11	0.64	0.342	0.332	0.466	0.42	1.32E+03	6.92E+03	3.21E+03	2.07E+03	2.65E+03	7.64E+03	7.67E+03	1.70E+02	8.63E+01	3.23E+03	2.64E+03	3.66E+03	64.88283	2	2171
MC0G	YB09C	VNDQNSQSPK	-0.11	-0.64	0.08	0.33	0.378	0.089	0.407	0.10	1.39E+03	3.33E+03	3.80E+03	2.48E+03	2.28E+03	3.64E+03	3.80E+03	2.24E+03	4.18E+03	3.50E+02	6.71E+03	4.67E+03	59.28881	2	2171
TH42	YB02C	ETLQR	0.83	0.34	0.55	0.34	0.049	0.277	0.140	0.23	5.88E+02	3.91E+02	1.88E+03	1.42E+03	1.11E+03	1.12E+03	1.48E+03	1.82E+03	2.71E+03	1.28E+03	9.71E+02	3.52E+02	70.83311	2	2611
PH43	YB06C	STPSPQSPK	1.62	0.59	0.14	0.04	0.056	0.059	0.088	0.10	2.10E+03	1.70E+03	1.84E+03	1.72E+03	3.84E+03	3.84E+03	1.79E+03	3.26E+03	2.85E+03	1.80E+03	1.60E+03	48.73997	2	1967	
PH44	YB06C	STPSPQSPK	1.62	0.59	0.14	0.04	0.056	0.059	0.088	0.10	2.10E+03	1.70E+03	1.84E+03	1.72E+03	3.84E+03	3.84E+03	1.79E+03	3.26E+03	2.85E+03	1.80E+03	1.60E+03	48.73997	2	1967	
PH45	YB06C	STPSPQSPK	1.62	0.59	0.14	0.04	0.056	0.059	0.088	0.10	2.10E+03	1.70E+03	1.84E+03	1.72E+03	3.84E+03	3.84E+03	1.79E+03	3.26E+03	2.85E+03	1.80E+03	1.60E+03	48.73997	2	1967	
PH46	YB06C	STPSPQSPK	1.62	0.59	0.14	0.04	0.056	0.059	0.088	0.10	2.10E+03	1.70E+03	1.84E+03	1.72E+03	3.84E+03	3.84E+03	1.79E+03	3.26E+03	2.85E+03	1.80E+03	1.60E+03	48.73997	2	1967	
PH47	YB06C	STPSPQSPK	1.62	0.59	0.14	0.04	0.056	0.059	0.088	0.10	2.10E+03	1.70E+03	1.84E+03	1.72E+03	3.84E+03	3.84E+03	1.79E+03	3.26E+03	2.85E+03	1.80E+03	1.60E+03	48.73997	2	1967	
PH48	YB06C	STPSPQSPK	1.62	0.59	0.14	0.04	0.056	0.059	0.088	0.10	2.10E+03	1.70E+03	1.84E+03	1.72E+03	3.84E+03	3.84E+03	1.79E+03	3.26E+03	2.85E+03	1.80E+03	1.60E+03	48.73997	2	1967	
PH49	YB06C	STPSPQSPK	1.62	0.59	0.14	0.04	0.056	0.059	0.088	0.10	2.10E+03	1.70E+03	1.84E+03	1.72E+03	3.84E+03	3.84E+03	1.79E+03	3.26E+03	2.85E+03	1.80E+03	1.60E+03	48.73997	2	1967	
PH50	YB06C	STPSPQSPK	1.62	0.59	0.14	0.04	0.056	0.059	0.088	0.10	2.10E+03	1.70E+03	1.84E+03	1.72E+03	3.84E+03	3.84E+03	1.79E+03	3.26E+03	2.85E+03	1.80E+03	1.60E+03	48.73997	2	1967	
PH51	YB06C	STPSPQSPK	1.62	0.59	0.14	0.04	0.056	0.059	0.088	0.10	2.10E+03	1.70E+03	1.84E+03	1.72E+03	3.84E+03	3.84E+03	1.79E+03	3.26E+03	2.85E+03	1.80E+03	1.60E+03	48.73997	2	1967	
PH52	YB06C	STPSPQSPK	1.62	0.59	0.14	0.04	0.056	0.059	0.088	0.10	2.10E+03	1.70E+03	1.84E+03	1.72E+03	3.84E+03	3.84E+03	1.79E+03	3.26E+03	2.85E+03	1.80E+03	1.60E+03	48.73997	2	1967	
PH53	YB06C	STPSPQSPK	1.62	0.59	0.14	0.04	0.056	0.059	0.088	0.10	2.10E+03	1.70E+03	1.84E+03	1.72E+03	3.84E+03	3.84E+03	1.79E+03	3.26E+03	2.85E+03	1.80E+03	1.60E+03	48.73997	2	1967	
PH54	YB06C	STPSPQSPK	1.62	0.59	0.14	0.04	0.056	0.059	0.088	0.10	2.10E+03	1.70E+03	1.84E+03	1.72E+03	3.84E+03	3.84E+03	1.79E+03	3.26E+03	2.85E+03	1.80E+03	1.60E+03	48.73997	2	1967	
PH55	YB06C	STPSPQSPK	1.62	0.59	0.14	0.04	0.056	0.059	0.088	0.10	2.10E+03	1.70E+03	1.84E+03	1.72E+03	3.84E+03	3.84E+03	1.79E+03	3.26E+03	2.85E+03	1.80E+03	1.60E+03	48.73997	2	1967	
PH56	YB06C	STPSPQSPK	1.62	0.59	0.14	0.04	0.056	0.059	0.088	0.10	2.10E+03	1.70E+03	1.84E+03	1.72E+03	3.84E+03	3.84E+03	1.79E+03	3.26E+03	2.85E+03	1.80E+03	1.60E+03	48.73997	2	1967	
PH57	YB06C	STPSPQSPK	1.62	0.59	0.14	0.04	0.056	0.059	0.088	0.10	2.10E+03	1.70E+03	1.84E+03	1.72E+03	3.84E+03	3.84E+03	1.79E+03	3.26E+03	2.85E+03	1.80E+03	1.60E+03	48.73997	2	1967	
PH58	YB06C	STPSPQSPK	1.62	0.59	0.14	0.04	0.056	0.059	0.088	0.10	2.10E+03	1.70E+03	1.84E+03	1.72E+03	3.84E+03	3.84E+03	1.79E+03	3.26E+03	2.85E+03	1.80E+03	1.60E+03	48.73997	2	1967	
PH59	YB06C	STPSPQSPK	1.62	0.59	0.14	0.04	0.056	0.059	0.088	0.10	2.10E+03	1.70E+03	1.84E+03	1.72E+03	3.84E+03	3.84E+03	1.79E+03	3.26E+03	2.85E+03	1.80E+03	1.60E+03	48.73997	2	1967	
PH60	YB06C	STPSPQSPK	1.62	0.59	0.14	0.04	0.056	0.059	0.088	0.10	2.10E+03	1.70E+03	1.84E+03	1.72E+03	3.84E+03	3.84E+03	1.79E+03	3.26E+03	2.85E+03	1.80E+03	1.60E+03	48.73997	2	1967	
PH61	YB06C	STPSPQSPK	1.62	0.59	0.14	0.04	0.056	0.059	0.088	0.10	2.10E+03	1.70E+03	1.84E+03	1.72E+03	3.84E+03	3.84E+03	1.79E+03	3.26E+03	2.85E+03	1.80E+03	1.60E+03	48.73997	2	1967	
PH62	YB06C	STPSPQSPK	1.62	0.59	0.14	0.04	0.056	0.059	0.088	0.10	2.10E+03	1.70E+03	1.84E+03	1.72E+03	3.84E+03	3.84E+03	1.79E+03	3.26E+03	2.85E+03	1.80E+03	1.60E+03	48.73997	2	1967	
PH63	YB06C	STPSPQSPK	1.62	0.59	0.14	0.04	0.056	0.059	0.088	0.10	2.10E+03	1.70E+03	1.84E+03	1.72E+03	3.84E+03	3.84E+03	1.79E+03	3.26E+03	2.85E+03	1.80E+03	1.60E+03	48.73997	2	1967	
PH64	YB06C	STPSPQSPK	1.62	0.59	0.14	0.04	0.056	0.059	0.088	0.10	2.10E+03	1.70E+03	1.84E+03	1.72E+03	3.84E+03	3.84E+03	1.79E+03	3.26E+03	2.85E+03	1.80E+03	1.60E+03	48.73997	2	1967	
PH65	YB06C	STPSPQSPK	1.62	0.59	0.14	0.04	0.056	0.059	0.088	0.10	2.10E+03	1.70E+03	1.84E+03	1.72E+03	3.84E+03	3.84E+03	1.79E+03	3.26E+03	2.85E+03	1.80E+03	1.60E+03	48.73997	2	1967	
PH66	YB06C	STPSPQSPK	1.62	0.59	0.14	0.04	0.056	0.059	0.088	0.10	2.10E+03	1.70E+03	1.84E+03	1.72E+03	3.84E+03	3.84E+03	1.79E+03	3.26E+03	2.85E+03	1.80E+03	1.60E+03	48.73997	2	1967	
PH67	YB06C	STPSPQSPK	1.62	0.59	0.14	0.04	0.056	0.059	0.088	0.10	2.10E+03	1.70E+03	1.84E+03	1.72E+03	3.84E+03	3.84E+03	1.79E+03	3.26E+03	2.85E+03	1.80E+03	1.60E+03	48.73997	2	1967	
PH68	YB06C	STPSPQSPK	1.62	0.59	0.14	0.04	0.056	0.059	0.088	0.10	2.10E+03	1.70E+03	1.84E+03	1.72E+03	3.84E+03	3.84E+03	1.79E+03	3.26E+03	2.85E+03						

CC1	VH052W	KTPWTRSK	2.03	1.53	1.22	0.50	0.62	0.18	0.08	0.29	3.41E+02	1.76E+03	5.20E+02	4.71E+03	9.50E+02	5.12E+03	4.74E+03	1.25E+03	1.63E+03	1.78E+03	1.71E+03	2.64E+03	5.6E+2314	2	23.39	
	VH053W	SEFQCEQEPQQR	0.35	-0.22	-1.63	0.57	0.169	0.370	0.022	0.15	5.93E+03	2.46E+03	8.84E+02	4.78E+03	5.95E+03	6.12E+03	1.56E+03	3.21E+03	6.55E+03	1.49E+03	1.71E+03	2.41E+03	964.4827	2	17.77	
	VH054W	SDFSFR	0.32	-0.69	-0.34	0.37	0.35	0.238	0.376	0.27	1.73E+03	2.02E+02	3.96E+02	1.03E+03	1.71E+02	4.50E+02	3.95E+02	8.62E+02	3.58E+02	1.53E+03	1.78E+03	4.74E+02	1.41E+02	4.40.1676	2	18.1
	VH055W	RSLOQTYTK	1.80	0.93	0.77	0.80	0.91	0.52	0.092	0.16	9.64E+02	7.62E+02	7.59E+02	4.18E+03	1.48E+03	4.77E+03	2.76E+03	1.34E+03	1.43E+03	2.10E+03	1.30E+03	1.60E+03	5.97.75669	2	17.32	
	VH056W	RSQSTESTER	1.92	0.66	0.73	1.27	0.017	0.122	0.051	0.04	2.73E+02	1.12E+03	3.39E+02	2.48E+03	1.87E+03	3.34E+03	1.87E+03	1.56E+02	1.63E+02	1.81E+03	1.07E+03	1.30E+03	8.10E+02	2	19.67	
	VH057W	VVDVA5YFK	-1.54	-1.60	-0.30	0.05	0.03	0.043	0.190	0.41	2.28E+02	3.17E+03	2.27E+03	1.98E+02	9.14E+02	6.99E+02	1.07E+03	1.08E+02	7.66E+02	2.40E+03	2.58E+03	5.78E+02	5.8E.78899	2	18.72	
	VH058W	VW5V5YFK	0.79	-0.06	-0.29	0.85	0.105	0.073	0.248	0.08	1.88E+02	1.47E+03	1.27E+02	1.98E+02	1.34E+03	1.27E+02	2.72E+02	1.43E+03	1.83E+02	8.47E+02	1.00E+03	1.41E+03	9.34.1957	2	21.21	
	VH059W	STDPGDFEYVAMK	3.09	-0.66	-0.22	3.74	0.096	0.221	0.402	0.09	5.22E+02	1.13E+03	4.89E+02	2.24E+02	1.16E+04	6.34E+03	7.07E+02	8.05E+02	4.37E+02	6.62E+02	1.00E+03	4.78E+02	5.20.28859	2	64.02	
	VH060W	SA5S9YFK	-1.06	0.90	-0.11	-1.97	0.216	0.190	0.456	0.06	2.18E+02	2.20E+03	3.03E+02	2.00E+02	5.89E+02	1.44E+03	1.44E+03	3.19E+02	1.39E+03	1.31E+03	1.16E+03	4.78E+02	4.62.72959	2	15.3	
	VH061W	KS5LKK	-0.32	-1.05	-0.25	0.92	0.348	0.438	0.037	0.03	1.73E+03	9.12E+02	1.49E+03	1.46E+03	1.24E+03	1.04E+03	1.04E+03	5.17E+02	1.84E+03	9.14E+02	1.27E+03	8.94E+02	4.92.2041	2	19.19	
	VH062W	SP5S9YFK	-3.86	0.48	0.07	-3.86	0.48	0.07	0.233	0.01	0.00E+00	4.10E+01	1.52E+02	1.12E+02	1.21E+02	2.09E+02	1.62E+03	3.24E+02	1.84E+03	1.50E+03	1.50E+03	1.50E+03	6.44.2854	2	17.97	
	VH063W	RT5S9YFK	1.42	-0.69	1.12	2.10	0.056	0.287	0.033	0.06	5.31E+03	9.41E+02	6.26E+02	4.76E+03	1.31E+03	2.52E+03	2.52E+03	2.69E+03	1.88E+03	2.92E+03	1.71E+03	7.84E+02	9.84.8216	2	23.87	
	VH064W	VW5S9YFK	0.01	-0.96	-0.40	0.98	0.40	0.114	0.322	0.08	1.09E+03	2.25E+02	2.42E+02	1.48E+03	1.07E+03	7.02E+02	1.34E+03	1.91E+02	1.81E+03	2.04E+02	9.64E+02	6.27E+02	7.83.3322	2	15.82	
	VH065W	RP5S9YFK	-0.34	-0.97	-0.21	0.83	0.38	0.249	0.121	0.28	3.88E+03	1.29E+03	2.85E+02	1.45E+03	1.74E+03	1.37E+03	1.37E+03	2.78E+02	2.63E+03	2.34E+02	4.37E+02	1.33E+03	9.86.9596	2	23.23	
	VH066W	NP5S9YFK	0.82	-1.09	-0.49	1.51	0.093	0.044	0.125	0.02	4.28E+03	2.89E+03	2.24E+02	5.35E+03	3.05E+03	3.05E+03	3.05E+03	7.31E+02	1.33E+03	2.42E+02	1.54E+03	2.65E+03	9.85.3551	3	30.51	
	VH067W	DS5S9YFK	1.46	-0.18	-0.14	1.64	0.034	0.384	0.352	0.02	2.77E+03	3.97E+03	1.89E+03	8.10E+03	4.82E+03	8.79E+03	1.88E+02	1.16E+03	3.96E+03	1.92E+02	2.87E+03	4.94E+02	8.89.5242	2	16.94	
	VH068W	AP5S9YFK	1.54	0.72	0.54	0.92	0.038	0.088	0.338	0.08	1.57E+03	2.96E+02	7.04E+02	1.30E+03	1.97E+03	3.28E+03	3.28E+03	1.82E+03	2.71E+03	1.92E+02	1.92E+02	1.92E+02	4.92.21554	2	16.94	
	VH069W	SP5S9YFK	1.18	0.18	0.18	0.60	0.134	0.134	0.134	0.08	1.18E+03	1.18E+03	1.18E+03	1.18E+03	1.18E+03	1.18E+03	1.18E+03	1.18E+03	1.18E+03	1.18E+03	1.18E+03	1.18E+03	8.89.5242	2	16.94	
	VH070W	SS5S9YFK	-1.18	-1.68	-1.68	0.60	0.134	0.134	0.134	0.08	7.31E+02	3.97E+03	7.04E+02	1.30E+03	1.97E+03	3.28E+03	3.28E+03	1.82E+03	2.71E+03	1.92E+02	1.92E+02	1.92E+02	4.92.21554	2	16.94	
	VH071W	NS5S9YFK	-0.63	0.62	0.43	-1.25	0.132	0.132	0.132	0.08	1.53E+03	5.97E+02	1.07E+03	6.82E+02	4.72E+02	7.26E+02	1.18E+03	1.18E+03	1.56E+03	2.22E+02	1.43E+03	6.59E+02	7.86.2874	2	25.43	
	VH072W	AH5S9YFK	1.40	0.42	-0.14	0.92	0.138	0.028	0.245	0.16	6.72E+02	9.18E+02	1.74E+02	5.96E+02	1.09E+03	1.09E+03	1.09E+03	9.19E+02	1.22E+02	1.64E+02	1.64E+02	6.29E+02	4.86.2314	2	24.43	
	VH073W	SE5S9YFK	1.68	0.09	0.51	1.60	0.067	0.160	0.040	0.07	1.56E+03	1.53E+03	1.24E+02	1.99E+03	1.47E+03	4.55E+03	2.65E+03	1.98E+03	1.37E+03	4.44E+02	1.58E+03	9.62.3961	2	30.93		
	VH074W	NG5S9YFK	1.17	-0.87	-2.82	-0.76	0.435	0.307	0.173	0.27	1.10E+04	1.24E+03	8.35E+02	3.48E+03	1.47E+03	1.51E+02	1.51E+02	1.51E+02	1.37E+03	1.23E+03	1.42E+03	5.62.2372	2	15.4		
	VH075W	NO5S9YFK	-1.63	-0.97	-0.64	0.32	0.233	0.34	0.197	0.40	1.91E+03	2.60E+03	8.38E+02	3.00E+03	4.67E+02	2.31E+02	2.31E+02	1.18E+03	2.09E+03	4.45E+03	4.58E+02	7.16E+01	1.05.8918	2	25.68	
	VH076W	NS5S9YFK	0.09	0.26	0.61	0.76	0.455	0.304	0.137	0.26	4.44E+02	1.69E+02	8.31E+02	6.09E+02	4.23E+02	4.50E+02	6.47E+02	1.72E+02	7.04E+02	0.05E+00	3.91E+02	5.24E+02	9.62.4098	2	38.02	
	VH077W	GS5S9YFK	1.98	1.17	1.12	0.80	0.090	0.014	0.107	0.21	1.11E+03	7.77E+02	6.01E+02	5.29E+03	3.25E+02	4.27E+02	2.29E+02	1.36E+02	2.01E+02	3.05E+02	1.51E+02	8.58E+02	6.48.3214	2	40.77	
	VH078W	NS5S9YFK	2.00	1.15	0.34	0.85	0.301	0.119	0.238	0.13	5.21E+02	1.12E+03	3.79E+02	2.81E+03	1.37E+03	4.03E+02	2.57E+02	6.50E+02	1.33E+02	9.59E+02	3.95E+02	3.95E+02	5.82.78935	2	38.36	
	VH079W	SV5S9YFK	-0.28	-0.21	-2.73	-0.08	0.39	0.421	0.114	0.44	4.80E+02	1.74E+03	1.81E+02	8.94E+02	6.63E+02	4.09E+02	1.04E+03	5.91E+02	4.38E+02	0.00E+00	2.56E+02	5.71E+02	4.78E+02	9.91.7237	2	22.55
	VH080W	KNS5S9YFK	1.51	0.09	0.04	1.41	0.010	0.407	0.452	0.01	7.98E+02	4.94E+02	6.23E+02	1.60E+03	1.46E+03	2.45E+03	9.25E+02	4.02E+02	7.19E+02	8.68E+02	6.84E+02	4.64E+02	7.86.8248	2	25.41	
	VH081W	EL5S9YFK	2.55	1.14	1.21	1.41	0.018	0.065	0.118	0.05	3.51E+02	2.79E+02	1.75E+02	3.13E+03	2.78E+02	3.33E+02	3.86E+02	2.58E+02	3.51E+02	6.55E+01	1.14E+02	6.28E+01	7.04.8077	2	21.95	
	VH082W	VTV5S9YFK	3.38	0.69	-1.19	2.68	0.029	0.033	0.033	0.13	3.31E+02	2.79E+02	4.25E+02	3.64E+02	2.15E+02	3.16E+02	4.59E+02	2.36E+02	3.51E+02	1.79E+02	1.90E+02	7.77E+02	8.96.33386	2	28.57	
	VH083W	VTV5S9YFK	-0.33	-0.32	-0.30	-0.01	0.206	0.202	0.152	0.49	5.56E+02	1.83E+03	1.13E+03	3.63E+03	6.34E+02	3.06E+02	2.03E+02	2.78E+02	1.58E+02	1.79E+02	1.30E+02	4.53E+02	4.65.1509	2	25.35	
	VH084W	NS5S9YFK	-0.11	-1.40	-1.13	3.98	0.451	0.132	0.392	0.17	1.48E+03	1.91E+02	1.78E+02	1.05E+04	3.53E+00	0.00E+00	2.88E+02	3.32E+02	5.08E+02	1.00E+00	1.58E+02	4.01E+02	7.86.80943	2	28.89	
	VH085W	NS5S9YFK	1.55	0.38	0.12	1.16	0.138	0.024	0.172	0.17	4.72E+02	2.76E+02	3.24E+02	4.88E+03	6.94E+02	1.82E+02	1.82E+02	1.67E+02	1.34E+02	3.18E+03	1.08E+03	8.51E+02	7.86.80943	2	20.32	
	VH086W	KP5S9YFK	1.27	0.68	0.58	0.58	0.028	0.047	0.070	0.12	5.78E+02	5.23E+02	9.82E+02	1.56E+03	1.23E+02	1.22E+02	8.36E+02	3.78E+02	6.66E+02	8.57E+02	4.21E+02	4.19E+02	5.64.28447	2	25.17	
	VH087W	NS5S9YFK	2.46	-0.58	-2.06	2.59	0.076	0.350	0.180	0.06	0.00E+00	8.81E+02	1.21E+02	4.74E+02	3.60E+02	2.97E+01	3.66E+00	4.39E+01	3.16E+01	1.27E+03	0.00E+00	2.43E+00	515.2819	2	15.35	
	VH088W	NS5S9YFK	2.51	-1.08	1.49	0.72	0.001	0.019	0.007	0.03	5.29E+02	8.80E+01	1.63E+02	2.00E+03	2.56E+02	2.31E+02	1.87E+02	8.66E+01	1.44E+01	1.76E+02	1.11E+03	9.95E+02	1.095.9065	2	18.15	
	VH089W	NS5S9YFK	2.02	0.76	1.01	1.26	0.031	0.036	0.106	0.06	4.73E+02	6.76E+02	3.55E+02	2.58E+03	8.78E+02	2.79E+02	1.03E+03	8.93E+02	6.48E+02	1.70E+02	6.18E+02	7.58E+02	1.007.8811	2	28.21	
	VH090W	KP5S9YFK	2.30	1.44	1.43	1.46	0.036	0.141	0.024	0.09	8.33E+01	4.19E+02	1.79E+02	2.48E+03	5.81E+02	2.35E+02	1.26E+02	2.99E+02	3.50E+0							

Table 2.4: Selected SQ/TQ phosphopeptides

Protein	log2 Ratio mutant vs WT		T-test		mutant vs WT		WT		Normalized abundance		mecl-100-letl-pphs		Best peptide m/z
	rad53 vs. mutant vs WT	let1 mect-1 100 vs WT	rad53 vs. 100 vs WT	let1 mect-1 100 vs WT	rad53 vs. 100 vs WT	let1 mect-1 100 vs WT	mecl3	mecl3 vs. 100 vs WT	mecl-100-letl-pphs	mecl-100-letl-pphs	mecl-100-letl-pphs	mecl-100-letl-pphs	
BOD1	1.01	-1.44	0.001	0.004	0.00	0.006	13114_198	13114_198	13114_198	13114_198	13114_198	13114_198	962.407596
BDF1	0.83	-0.72	0.159	0.107	0.025	0.09	13114_198	13114_198	13114_198	13114_198	13114_198	13114_198	564.26118
CBF1	0.14	-0.95	0.179	0.037	0.067	0.03	13114_198	13114_198	13114_198	13114_198	13114_198	13114_198	945.75941
CB5	2.19	0.04	0.001	0.43	0.003	0.00	13114_198	13114_198	13114_198	13114_198	13114_198	13114_198	1086.9627
CB8	1.46	-0.89	0.002	0.009	0.000	0.00	13114_198	13114_198	13114_198	13114_198	13114_198	13114_198	1056.13869
CBT3	2.18	-0.73	0.001	0.009	0.000	0.00	13114_198	13114_198	13114_198	13114_198	13114_198	13114_198	1012.45808
CC3	1.84	0.6	0.015	0.071	0.084	0.01	13114_198	13114_198	13114_198	13114_198	13114_198	13114_198	1128.43866
CC5	1.05	-0.25	0.015	0.025	0.108	0.01	13114_198	13114_198	13114_198	13114_198	13114_198	13114_198	483.97357
CCS2	2.07	-0.72	0.015	0.025	0.108	0.01	13114_198	13114_198	13114_198	13114_198	13114_198	13114_198	863.45673
DE6	3.33	0.82	0.001	0.167	0.011	0.03	13114_198	13114_198	13114_198	13114_198	13114_198	13114_198	934.61924
EP6	0.47	-0.75	0.001	0.167	0.011	0.03	13114_198	13114_198	13114_198	13114_198	13114_198	13114_198	763.36979
HFL1	4.47	1.20	0.000	0.024	0.132	0.25	13114_198	13114_198	13114_198	13114_198	13114_198	13114_198	823.02402
HPL1	2.78	-0.11	0.000	0.332	0.002	0.00	13114_198	13114_198	13114_198	13114_198	13114_198	13114_198	786.31909
HP12	4.35	-1.74	0.000	0.000	0.373	0.87	13114_198	13114_198	13114_198	13114_198	13114_198	13114_198	699.63024
HT2	3.34	-0.63	0.000	0.002	0.224	0.01	13114_198	13114_198	13114_198	13114_198	13114_198	13114_198	464.21201
HT1	0.99	-0.66	0.000	0.009	0.039	0.04	13114_198	13114_198	13114_198	13114_198	13114_198	13114_198	662.30324
IB1	0.29	-0.66	0.000	0.009	0.039	0.04	13114_198	13114_198	13114_198	13114_198	13114_198	13114_198	1086.98867
IB4	2.29	-1.62	0.000	0.004	0.120	0.07	13114_198	13114_198	13114_198	13114_198	13114_198	13114_198	658.29707
IBW2	2.20	0.30	0.000	0.003	0.129	0.18	13114_198	13114_198	13114_198	13114_198	13114_198	13114_198	728.80209
LC01	2.72	0.56	0.001	0.116	0.001	0.16	13114_198	13114_198	13114_198	13114_198	13114_198	13114_198	781.36549
LC02	1.35	-0.65	0.000	0.075	0.310	0.68	13114_198	13114_198	13114_198	13114_198	13114_198	13114_198	704.8087
LC03	1.40	-1.15	0.000	0.075	0.310	0.68	13114_198	13114_198	13114_198	13114_198	13114_198	13114_198	808.86315
LC04	3.38	2.79	0.000	0.001	0.014	0.12	13114_198	13114_198	13114_198	13114_198	13114_198	13114_198	875.36821
LC05	0.49	-1.11	0.000	0.045	0.066	0.64	13114_198	13114_198	13114_198	13114_198	13114_198	13114_198	797.31856
LC06	-0.15	-1.34	0.000	0.127	0.152	0.23	13114_198	13114_198	13114_198	13114_198	13114_198	13114_198	456.33846
LC07	0.05	-1.32	0.000	0.375	0.305	0.12	13114_198	13114_198	13114_198	13114_198	13114_198	13114_198	604.75219
LC08	2.21	-0.18	0.000	0.280	0.086	0.09	13114_198	13114_198	13114_198	13114_198	13114_198	13114_198	955.93802
LC09	0.95	-0.15	0.000	0.488	0.009	0.05	13114_198	13114_198	13114_198	13114_198	13114_198	13114_198	555.75929
LC10	2.79	-0.08	0.000	0.237	0.060	0.38	13114_198	13114_198	13114_198	13114_198	13114_198	13114_198	616.7043
LC11	0.99	1.54	0.000	0.056	0.087	0.29	13114_198	13114_198	13114_198	13114_198	13114_198	13114_198	435.70543
LC12	2.55	0.05	0.000	0.481	0.003	0.83	13114_198	13114_198	13114_198	13114_198	13114_198	13114_198	699.34988
LC13	1.97	-0.72	0.000	0.279	0.163	0.02	13114_198	13114_198	13114_198	13114_198	13114_198	13114_198	935.07989
LC14	3.26	1.15	0.000	0.069	0.342	0.01	13114_198	13114_198	13114_198	13114_198	13114_198	13114_198	91.70175
LC15	0.90	0.26	0.000	0.069	0.342	0.01	13114_198	13114_198	13114_198	13114_198	13114_198	13114_198	1086.9627
LC16	3.31	-1.61	0.000	0.079	0.088	0.00	13114_198	13114_198	13114_198	13114_198	13114_198	13114_198	640.29585
LC17	1.52	-0.23	0.000	0.124	0.019	0.84	13114_198	13114_198	13114_198	13114_198	13114_198	13114_198	960.74911
LC18	0.25	-0.40	0.000	0.168	0.087	0.84	13114_198	13114_198	13114_198	13114_198	13114_198	13114_198	799.85184
LC19	1.87	-0.35	0.000	0.124	0.019	0.84	13114_198	13114_198	13114_198	13114_198	13114_198	13114_198	860.23982
LC20	0.82	-1.09	0.000	0.305	0.125	0.02	13114_198	13114_198	13114_198	13114_198	13114_198	13114_198	785.31909
LC21	2.74	-1.11	0.000	0.080	0.040	0.00	13114_198	13114_198	13114_198	13114_198	13114_198	13114_198	910.70542
LC22	3.31	-3.85	0.000	0.086	0.040	0.00	13114_198	13114_198	13114_198	13114_198	13114_198	13114_198	572.23396
LC23	0.18	-1.19	0.000	0.160	0.027	0.07	13114_198	13114_198	13114_198	13114_198	13114_198	13114_198	703.6886
LC24	3.37	0.39	0.000	0.097	0.307	0.00	13114_198	13114_198	13114_198	13114_198	13114_198	13114_198	435.70543
LC25	1.88	-0.16	0.000	0.389	0.331	0.00	13114_198	13114_198	13114_198	13114_198	13114_198	13114_198	837.34465
LC26	2.24	-1.10	0.000	0.086	0.083	0.00	13114_198	13114_198	13114_198	13114_198	13114_198	13114_198	1086.9627

ref: S/TQ phosphopeptides

Table 2.5: Query strains and library used for EMAP

NOTE: Gene description taken from the SGD Database (March 17th, 2007). Essentiality status taken from Saccharomyces Genome Deletion Project

NOTE: The Primary Functional category was defined by the the top ranked GO term in the list of the 25 most frequently found GO slim terms (taken from SGD) for all array and query genes.

Gene	ORF	Essential?	Description	Primary Functional Category
PEX22	YAL055W	No	Putative Peroxisomal Membrane Protein	Signaling
CBP4	YGR174C	No	Mitochondrial Protein Required For Assembly Of Cytochrome Bc1 Complex	Protein Complex Biogenesis
ERG2	YMR202W	No	C-8 Sterol Isomerase	Lipid Metabolic Process
	YLR224W	No	F-Box Protein And Component Of Scf Ubiquitin Ligase Complexes	Response To Chemical
FLC2	YAL053W	No	Putative Fad Transporter	Miscellaneous
PBP1	YGR178C	No	Component Of Glucose Deprivation Induced Stress Granules	Miscellaneous
PFK2	YMR205C	No	Beta Subunit Of Heterooctameric Phosphofructokinase	Carbohydrate Metabolic Process
CAP1	YKL007W	No	Alpha Subunit Of The Capping Protein Heterodimer (Cap1P And Cap2P)	Protein Complex Biogenesis
GEM1	YAL048C	No	Outer Mitochondrial Membrane Gtpase, Subunit Of The Ermes Complex	Regulation Of Organelle Organization
UBR1	YGR184C	No	E3 Ubiquitin Ligase (N-Recognin)	Response To Chemical
SKY1	YMR216C	No	Sr Protein Kinase (Srpk)	Response To Chemical
SPT23	YKL020C	No	Er Membrane Protein Involved In Regulation Of Ole1 Transcription	Transcription From Rna Polymerase Ii Promoter
SAW1	YAL027W	No	5'- And 3'-Flap DNA Binding Protein	Cellular Response To DNA Damage Stimulus
ELP2	YGR200C	No	Subunit Of Elongator Complex	Transcription From Rna Polymerase Ii Promoter
MRE11	YMR224C	No	Nuclease Subunit Of The Mrx Complex With Rad50P And Xrs2P	Cellular Response To DNA Damage Stimulus
IXR1	YKL032C	No	Transcriptional Repressor That Regulates Hypoxic Genes During Normoxia	Transcription From Rna Polymerase Ii Promoter
CCR4	YAL021C	No	Component Of The Ccr4-Not Transcriptional Complex	Transcription From Rna Polymerase Ii Promoter
RPS0A	YGR214W	No	Ribosomal 40S Subunit Protein S0A	Miscellaneous
GFD1	YMR255W	No	Coiled-Coiled Protein Of Unknown Function	Miscellaneous
TMA19	YKL056C	No	Protein That Associates With Ribosomes	Response To Chemical
MDM10	YAL010C	No	Subunit Of Both The Ermes And The Sam Complex	Protein Complex Biogenesis
WSC4	YHL028W	No	Endoplasmic Reticulum (Er) Membrane Protein	Protein Targeting
RCE1	YMR274C	No	Type Ii Caax Prenyl Protease	Miscellaneous
TEF4	YKL081W	No	Gamma Subunit Of Translational Elongation Factor Eef1B	Miscellaneous
KIN3	YAR018C	No	Nonessential Serine/Threonine Protein Kinase	Protein Phosphorylation
VPS29	YHR012W	No	Subunit Of The Membrane-Associated Retromer Complex	Miscellaneous
NGL2	YMR285C	No	Protein Involved In 5.8S Rrna Processing	Miscellaneous
RAD27	YKL113C	No	5' To 3' Exonuclease, 5' Flap Endonuclease	Cellular Response To DNA Damage Stimulus
UBI4	YLL039C	No	Ubiquitin	Meiotic Cell Cycle
	YHR078W	No	High Osmolarity-Regulated Gene Of Unknown Function	Biological_Process
PEX6	YNL329C	No	Aaa-Peroxin	Signaling
LST4	YKL176C	No	Protein Possibly Involved In A Post-Golgi Secretory Pathway	Golgi Vesicle Transport
SPT8	YLR055C	No	Subunit Of The Saga Transcriptional Regulatory Complex	Transcription From Rna Polymerase Ii Promoter
DMA1	YHR115C	No	Ubiquitin-Protein Ligase (E3)	Mitotic Cell Cycle
TRF5	YNL299W	No	Non-Canonical Poly(A) Polymerase	Miscellaneous
ENV11	YGR071C	No	Protein Proposed To Be Involved In Vacuolar Functions	Miscellaneous
GEP5	YLR091W	No	Protein Of Unknown Function	Miscellaneous
REC104	YHR157W	No	Protein Involved In Early Stages Of Meiotic Recombination	Organelle Fission
TOF1	YNL273W	No	Subunit Of A Replication-Pausing Checkpoint Complex	Mitotic Cell Cycle
UFO1	YML088W	No	F-Box Receptor Protein	Cellular Response To DNA Damage Stimulus
MNL1	YHR204W	No	Alpha-1,2-Specific Exomannosidase Of The Endoplasmic Reticulum	Proteolysis Involved In Cellular Protein Catabolic Process
TSR3	YOR006C	No	Protein Required For 20S Pre-Rrna Processing	Miscellaneous
VAM3	YOR106W	No	Syntaxin-Like Vacuolar T-Snare	Miscellaneous
GSF2	YML048W	No	Endoplasmic Reticulum (Er) Localized Integral Membrane Protein	Miscellaneous
BIK1	YCL029C	No	Microtubule-Associated Protein	Mitotic Cell Cycle
DFG16	YOR030W	No	Probable Multiple Transmembrane Protein	Miscellaneous
VPS17	YOR132W	No	Subunit Of The Membrane-Associated Retromer Complex	Miscellaneous
MAD1	YGL086W	No	Coiled-Coil Protein Involved In Spindle-Assembly Checkpoint	Mitotic Cell Cycle
DMA2	YNL116W	No	Ubiquitin-Protein Ligase (E3)	Mitotic Cell Cycle
RP0A1	YFL036W	No	Mitochondrial Rna Polymerase	Miscellaneous
DAL81	YIR023W	No	Positive Regulator Of Genes In Multiple Nitrogen Degradation Pathways	Transcription From Rna Polymerase Ii Promoter
MMS2	YGL087C	No	Ubiquitin-Conjugating Enzyme Variant	Cellular Response To DNA Damage Stimulus
RAS2	YNL098C	No	Gtp-Binding Protein	Response To Chemical
SWP82	YFL049W	No	Member Of The Swi/Snf Chromatin Remodeling Complex	Transcription From Rna Polymerase Ii Promoter
MDM35	YKL053C-A	No	Mitochondrial Intermembrane Space Protein	Protein Complex Biogenesis
KEX2	YNL238W	No	Subtilisin-Like Protease (Proprotein Convertase)	Miscellaneous
YD1	YNL064C	No	Type I Hsp40 Co-Chaperone	Protein Targeting
UBP6	YFR010W	No	Ubiquitin-Specific Protease	Protein Modification By Small Protein Conjugation Or Removal
RBL2	YOR265W	No	Protein Involved In Microtubule Morphogenesis	Protein Complex Biogenesis
PDR16	YNL231C	No	Phosphatidylinositol Transfer Protein (Pitp)	Response To Chemical
HPM1	YIL110W	No	Adomet-Dependent Methyltransferase	Miscellaneous
YTA7	YGR270W	No	Protein That Localizes To Chromatin	Transcription From Rna Polymerase Ii Promoter
RIM20	YOR275C	No	Protein Involved In Proteolytic Activation Of Rim101P	Miscellaneous
SQS1	YNL224C	No	Protein That Stimulates The Atpase And Helicase Activities Of Prp43P	Miscellaneous
MET18	YIL128W	No	Component Of Cytosolic Iron-Sulfur Protein Assembly (Cia) Machinery	Miscellaneous
MGA2	YIR033W	No	Er Membrane Protein Involved In Regulation Of Ole1 Transcription	Transcription From Rna Polymerase Ii Promoter
IWR1	YDL115C	No	Rna Polymerase Ii Transport Factor, Conserved From Yeast To Humans	Miscellaneous
RTT106	YNL206C	No	Histone Chaperone	Transcription From Rna Polymerase Ii Promoter
MLP2	YIL149C	No	Myosin-Like Protein Associated With The Nuclear Envelope	Mitotic Cell Cycle
NUP133	YKR082W	No	Subunit Of Nup84P Subcomplex Of Nuclear Pore Complex (Npc)	Transcription From Rna Polymerase Ii Promoter
ESL2	YKR096W	No	Protein Of Unknown Function	Biological_Process
SKO1	YNL167C	No	Basic Leucine Zipper Transcription Factor Of The Atf/Creb Family	Transcription From Rna Polymerase Ii Promoter
MPH1	YIR002C	No	3'-5' DNA Helicase Involved In Error-Free Bypass Of DNA Lesions	Cellular Response To DNA Damage Stimulus
RCO1	YMR075W	No	Essential Component Of The Rpd3S Histone Deacetylase Complex	Transcription From Rna Polymerase Ii Promoter
EAF3	YPR023C	No	Component Of The Rpd3S Histone Deacetylase Complex	Transcription From Rna Polymerase Ii Promoter
CBT1	YKL208W	No	Protein Involved In 5' Rna End Processing	Protein Complex Biogenesis
FKH2	YNL068C	No	Forkhead Family Transcription Factor	Transcription From Rna Polymerase Ii Promoter
INO4	YOL108C	No	Transcription Factor Involved In Phospholipid Synthesis	Transcription From Rna Polymerase Ii Promoter
PBY1	YBR094W	No	Putative Tubulin Tyrosine Ligase Associated With P-Bodies	Biological_Process
GMH1	YKR030W	No	Golgi Membrane Protein Of Unknown Function	Miscellaneous
TCB2	YNL087W	No	Er Protein Involved In Er-Plasma Membrane Tethering	Lipid Metabolic Process
IES5	YER092W	No	Protein That Associates With The Ino80 Chromatin Remodeling Complex	Biological_Process
TPS1	YBR126C	No	Synthase Subunit Of Trehalose-6-P Synthase/Phosphatase Complex	Response To Chemical
PAM17	YKR065C	No	Constituent Of The Tim23 Complex	Protein Targeting
RAV2	YDR202C	No	Subunit Of Rave Complex (Rav1P, Rav2P, Skp1P)	Protein Complex Biogenesis
	YMR209C	No	Putative S-Adenosylmethionine-Dependent Methyltransferase	Biological_Process
TYR1	YBR166C	No	Prephenate Dehydrogenase Involved In Tyrosine Biosynthesis	Miscellaneous
PMP3	YDR276C	No	Small Plasma Membrane Protein	Response To Chemical
CTK1	YKL139W	No	Catalytic (Alpha) Subunit Of C-Terminal Domain Kinase I (Ctdk-I)	Transcription From Rna Polymerase Ii Promoter
CAC2	YML102W	No	Subunit Of Chromatin Assembly Factor I (Caf-1), With Rif2P And Msi1P	Chromatin Organization
SLM3	YDL033C	No	Trna-Specific 2-Thiouridylase	Miscellaneous
SUM1	YDR310C	No	Transcriptional Repressor That Regulates Middle-Sporulation Genes	Transcription From Rna Polymerase Ii Promoter
BIT2	YBR270C	No	Subunit Of Torc2 Membrane-Associated Complex	Biological_Process
TUB3	YML124C	No	Alpha-Tubulin	Mitotic Cell Cycle
BDF2	YDL070W	No	Protein Involved In Transcription Initiation	Chromatin Organization
	YOR342C	No	Protein Of Unknown Function	Biological_Process
FAR1	YJL157C	No	Cdk Inhibitor And Nuclear Anchor	Response To Chemical
SWC5	YBR231C	No	Component Of The Swr1 Complex	Chromatin Organization

UGA1	YGR019W	No	Gamma-Aminobutyrate (Gaba) Transaminase	Miscellaneous
TYE7	YOR344C	No	Serine-Rich Protein That Contains A Bhlh DNA Binding Motif	Carbohydrate Metabolic Process
VPS35	YJL154C	No	Endosomal Subunit Of Membrane-Associated Retromer Complex	Miscellaneous
	YBR238C	No	Mitochondrial Membrane Protein	Miscellaneous
RPS6A	YPL090C	No	Protein Component Of The Small (40S) Ribosomal Subunit	Miscellaneous
CIN1	YOR349W	No	Tubulin Folding Factor D Involved In Beta-Tubulin (Tub2P) Folding	Protein Complex Biogenesis
RPA34	YJL148W	No	Rna Polymerase I Subunit A34.5	Miscellaneous
MTC4	YBR255W	No	Protein Of Unknown Function	Biological_Process
ELP3	YPL086C	No	Subunit Of Elongator Complex	Transcription From Rna Polymerase Ii Promoter
PDE2	YOR360C	No	High-Affinity Cyclic Amp Phosphodiesterase	Signaling
TIF2	YJL138C	No	Translation Initiation Factor Eif4A	Miscellaneous
VMS1	YDR049W	No	Component Of A Cdc48P-Complex Involved In Protein Quality Control	Response To Chemical
BTS1	YPL069C	No	Geranylgeranyl Diphosphate Synthase	Lipid Metabolic Process
PFA4	YOL003C	No	Palmitoyltransferase With Autoacylation Activity	Miscellaneous
NUP2	YLR335W	No	Nucleoporin Involved In Nucleocytoplasmic Transport	Protein Targeting
DOA4	YDR069C	No	Ubiquitin Hydrolase That Deubiquitinates Iiv Cargo Proteins	Proteolysis Involved In Cellular Protein Catabolic Process
ARL3	YPL051W	No	Arf-Like Small Gtpase Of The Ras Superfamily	Golgi Vesicle Transport
HTZ1	YOL012C	No	Histone Variant H2Az	Transcription From Rna Polymerase Ii Promoter
VPS38	YLR360W	No	Part Of A Vps34P Phosphatidylinositol 3-Kinase Complex	Miscellaneous
VPS41	YDR080W	No	Vacuolar Membrane Protein That Is A Subunit Of The Hops Complex	Protein Complex Biogenesis
EGD1	YPL037C	No	Subunit Beta1 Of The Nascent Polypeptide-Associated Complex (Nac)	Protein Targeting
SIL1	YOL031C	No	Nucleotide Exchange Factor For The Er Lumenal Hsp70 Chaperone Kar2F	Protein Targeting
PSY3	YLR376C	No	Component Of The Shu Complex, Which Promotes Error-Free DNA Repair	Cellular Response To DNA Damage Stimulus
ARL1	YDR101C	No	Nuclear Export Factor For The Ribosomal Pre-60S Subunit	Miscellaneous
CLB2	YPR119W	No	B-Type Cyclin Involved In Cell Cycle Progression	Mitotic Cell Cycle
PSH1	YOL054W	No	E3 Ubiquitin Ligase Targeting Centromere-Binding Protein Cse4P	Protein Modification By Small Protein Conjugation Or Removal
DUS3	YLR401C	No	Dihydrouridine Synthase	Miscellaneous
ARO1	YDR127W	No	Pentafunctional Arom Protein	Miscellaneous
URN1	YPR152C	No	Putative Protein Of Unknown Function Containing Ww And Ff Domains	Biological_Process
IRA2	YOL081W	No	Gtpase-Activating Protein	Response To Chemical
LIP2	YLR239C	No	Lipoyl Ligase	Miscellaneous
XRS2	YDR369C	No	Protein Required For DNA Repair	Cellular Response To DNA Damage Stimulus
CDC26	YFR036W	No	Subunit Of The Anaphase-Promoting Complex/Cyclosome (Apc/C)	Chromatin Organization
YAR1	YPL239W	No	Ankyrin-Repeat Containing, Nucleocytoplasmic Shuttling Chaperone	Response To Chemical
PIG1	YLR273C	No	Putative Targeting Subunit For Type-1 Protein Phosphatase Glc7P	Carbohydrate Metabolic Process
SAC7	YDR389W	No	Gtpase Activating Protein (Gap) For Rho1P	Regulation Of Organelle Organization
	YGR237C	No	Putative Protein Of Unknown Function	Biological_Process
DDC1	YPL194W	No	DNA Damage Checkpoint Protein	Mitotic Cell Cycle
NKP2	YLR315W	No	Central Kinetochores Protein And Subunit Of The Ctf19 Complex	Miscellaneous
SIP1	YDR422C	No	Alternate Beta-Subunit Of The Snf1P Kinase Complex	Protein Complex Biogenesis
RPL19B	YBL027W	No	Ribosomal 60S Subunit Protein L19B	Miscellaneous
NIP100	YPL174C	No	Large Subunit Of The Dynactin Complex	Mitotic Cell Cycle
SAC3	YDR159W	No	Nuclear Pore-Associated Protein	Mitotic Cell Cycle
MT7	YEL033W	No	Protein Of Unknown Function	Biological_Process
SKT5	YBL061C	No	Activator Of Chs3P (Chitin Synthase Iii) During Vegetative Growth	Carbohydrate Metabolic Process
PHO86	YJL117W	No	Endoplasmic Reticulum (Er) Resident Protein	Golgi Vesicle Transport
ITC1	YGL133W	No	Subunit Of Atp-Dependent Isw2P-Itc1P Chromatin Remodeling Complex	Transcription From Rna Polymerase Ii Promoter
APE3	YBR286W	No	Vacuolar Aminopeptidase Y	Miscellaneous
VAM6	YDL077C	No	Vacuolar Protein Involved In Vacuolar Membrane Fusion Tethering	Protein Complex Biogenesis
ASF1	YJL115W	No	Nucleosome Assembly Factor	Transcription From Rna Polymerase Ii Promoter
MRM2	YGL136C	No	Mitochondrial 2' O-Ribose Methyltransferase	Miscellaneous
BSD2	YBR290W	No	Heavy Metal Ion Homeostasis Protein	Protein Targeting
VPS72	YDR485C	No	Htz1P-Binding Component Of The Swr1 Complex	Chromatin Organization
SAP185	YJL098W	No	Protein That Forms A Complex With The Sit4P Protein Phosphatase	Mitotic Cell Cycle
RPL9A	YGL147C	No	Ribosomal 60S Subunit Protein L9A	Miscellaneous
PCA1	YBR295W	No	Cadmium Transporting P-Type Atpase	Miscellaneous
HAP2	YGL237C	No	Subunit Of The Hap2P/3P/4P/5P Ccaat-Binding Complex	Transcription From Rna Polymerase Ii Promoter
IML2	YJL082W	No	Protein Of Unknown Function	Biological_Process
YIP5	YGL161C	No	Protein That Interacts With Rab Gtpases	Biological_Process
PMP1	YCR024C-A	No	Regulatory Subunit For The Plasma Membrane H(+)-Atpase Pma1P	Miscellaneous
CCW12	YLR110C	No	Cell Wall Mannoprotein	Response To Chemical
UBX6	YJL048C	No	Ubx (Ubiquitin Regulatory X) Domain-Containing Protein	Proteolysis Involved In Cellular Protein Catabolic Process
XRN1	YGL173C	No	Evolutionarily-Conserved 5'-3' Exonuclease	Transcription From Rna Polymerase Ii Promoter
ELO2	YCR034W	No	Fatty Acid Elongase, Involved In Sphingolipid Biosynthesis	Lipid Metabolic Process
	YJL029C	No	Putative Protein Of Unknown Function	Biological_Process
UBC8	YEL012W	No	Ubiquitin-Conjugating Enzyme That Regulates Gluconeogenesis	Protein Modification By Small Protein Conjugation Or Removal
SLX8	YER116C	No	Subunit Of Slx5-Slx8 Sumo-Targeted Ubiquitin Ligase (Stubl) Complex	Cellular Response To DNA Damage Stimulus
RAD18	YCR066W	No	E3 Ubiquitin Ligase	Cellular Response To DNA Damage Stimulus
CDC53	YDL132W	Yes	Cullin	Mitotic Cell Cycle
TDA3	YHR009C	No	Putative Oxidoreductase Involved In Late Endosome To Golgi Transport	Miscellaneous
UBP3	YER151C	No	Ubiquitin-Specific Protease Involved In Transport And Osmotic Response	Protein Modification By Small Protein Conjugation Or Removal
	YCR087C-A	No	Putative Protein Of Unknown Function	Biological_Process
UBC1	YDR177W	Yes	Ubiquitin-Conjugating Enzyme	Protein Modification By Small Protein Conjugation Or Removal
OPI3	YJR073C	No	Methylene-Fatty-Acyl-Phospholipid Synthase	Lipid Metabolic Process
BCK2	YER167W	No	Serine/Threonine-Rich Protein Involved In Pkc1 Signaling Pathway	Mitotic Cell Cycle
RAD26	YJR035W	No	Protein Involved In Transcription-Coupled Nucleotide Excision Repair	Chromatin Organization
POL3	YDL102W	Yes	Catalytic Subunit Of DNA Polymerase Delta	Miscellaneous
BAS1	YKR099W	No	Myb-Related Transcription Factor	Transcription From Rna Polymerase Ii Promoter
FET3	YMR058W	No	Ferro-O2-Oxidoreductase	Response To Chemical
BUG1	YDL099W	No	Cis-Golgi Localized Protein Involved In Er To Golgi Transport	Golgi Vesicle Transport
RPB5	YBR154C	Yes	Rna Polymerase Subunit Abc27	Transcription From Rna Polymerase Ii Promoter
TSR2	YLR435W	No	Protein With A Potential Role In Pre-Rrna Processing	Miscellaneous
BIM1	YER016W	No	Microtubule Plus End-Tracking Protein	Mitotic Cell Cycle
RPL35B	YDL136W	No	Ribosomal 60S Subunit Protein L35B	Miscellaneous
APC2	YLR127C	Yes	Subunit Of The Anaphase-Promoting Complex/Cyclosome (Apc/C)	Mitotic Cell Cycle
	YNR065C	No	Protein Of Unknown Function	Biological_Process
SPT20	YOL148C	No	Subunit Of The Saga Transcriptional Regulatory Complex	Chromatin Organization
DOM34	YNL001W	No	Protein That Facilitates Ribosomal Subunit Dissociation	Miscellaneous
SMT3	YDR510W	Yes	Ubiquitin-Like Protein Of The Sumo Family	Protein Modification By Small Protein Conjugation Or Removal
JHD2	YJR119C	No	JmjC Domain Family Histone Demethylase	Chromatin Organization
RRN10	YDL025W	No	Protein Involved In Promoting High Level Transcription Of RDNA	Miscellaneous
SIW14	YNL032W	No	Tyrosine Phosphatase Involved In Actin Organization And Endocytosis	Cytoskeleton Organization
RSC4	YKR008W	Yes	Component Of The Rsc Chromatin Remodeling Complex	Transcription From Rna Polymerase Ii Promoter
OAF1	YAL051W	No	Oleate-Activated Transcription Factor	Transcription From Rna Polymerase Ii Promoter
TIM13	YGR181W	No	Mitochondrial Intermembrane Space Protein	Protein Targeting
SCI1	YMR214W	No	One Of Several Homologs Of Bacterial Chaperone DnaJ	Response To Chemical
MRT4	YKL009W	No	Protein Involved In Mrna Turnover And Ribosome Assembly	Miscellaneous
ERV46	YAL042W	No	Protein Localized To Copii-Coated Vesicles	Golgi Vesicle Transport
FYV8	YGR196C	No	Protein Of Unknown Function	Biological_Process
ESC1	YMR219W	No	Protein Localized To The Nuclear Periphery	Miscellaneous
	YKL023W	No	Putative Protein Of Unknown Function	Biological_Process
DRS2	YAL026C	No	Trans-Golgi Network Aminophospholipid Translocase (Flippase)	Golgi Vesicle Transport
PCT1	YGR202C	No	Cholinephosphate Cytidylyltransferase	Lipid Metabolic Process
RPS10B	YMR230W	No	Protein Component Of The Small (40S) Ribosomal Subunit	Miscellaneous
AIM26	YKL037W	No	Putative Protein Of Unknown Function	Miscellaneous

ATS1	YAL020C	No	Protein Required For Modification Of Wobble Nucleosides In Trna	Cytoskeleton Organization
CCH1	YGR217W	No	Voltage-Gated High-Affinity Calcium Channel	Miscellaneous
CUE1	YMR264W	No	Ubiquitin-Binding Protein	Proteolysis Involved In Cellular Protein Catabolic Process
NUP100	YKL068W	No	Fg-Nucleoporin Component Of Central Core Of The Nuclear Pore Complex	Protein Targeting
ERP2	YAL007C	No	Member Of The P24 Family Involved In Er To Golgi Transport	Golgi Vesicle Transport
RIM101	YHL027W	No	Cys2His2 Zinc-Finger Transcriptional Repressor	Transcription From Rna Polymerase Ii Promoter
BUL1	YMR275C	No	Ubiquitin-Binding Component Of The Rsp5 E3-Ubiquitin Ligase Complex	Protein Modification By Small Protein Conjugation Or Removal
CUE2	YKL090W	No	Protein Of Unknown Function	Biological_Process
DNM1	YLL001W	No	Dynamidin-Related Gtpase Involved In Mitochondrial Organization	Organelle Fission
SLT2	YHR030C	No	Serine/Threonine Map Kinase	Response To Chemical
GOT1	YMR292W	No	Homodimeric Protein That Is Packaged Into Copii Vesicles	Golgi Vesicle Transport
OAC1	YKL120W	No	Mitochondrial Inner Membrane Transporter	Miscellaneous
VPS13	YLL040C	No	Protein Of Unknown Function	Meiotic Cell Cycle
IRE1	YHR079C	No	Serine-Threonine Kinase And Endoribonuclease	Response To Chemical
FIG4	YNL325C	No	Phosphatidylinositol 3,5-Bisphosphate (Ptdins[3,5]P) Phosphatase	Lipid Metabolic Process
COY1	YKL179C	No	Golgi Membrane Protein With Similarity To Mammalian Casp	Golgi Vesicle Transport
ERG3	YLR056W	No	C-5 Sterol Desaturase	Lipid Metabolic Process
ARP1	YHR129C	No	Actin-Related Protein Of The Dynactin Complex	Mitotic Cell Cycle
CLA4	YNL298W	No	Cdc42P-Activated Signal Transducing Kinase	Mitotic Cell Cycle
UPF3	YGR072W	No	Component Of The Nonsense-Mediated Mrna Decay (Nmd) Pathway	Protein Modification By Small Protein Conjugation Or Removal
IOC2	YLR095C	No	Subunit Of The Isw1B Complex	Chromatin Organization
KEL1	YHR158C	No	Protein Required For Proper Cell Fusion And Cell Morphology	Mitotic Cell Cycle
BN1	YNL271C	No	Formin	Mitotic Cell Cycle
SRB5	YGR104C	No	Subunit Of The Rna Polymerase Ii Mediator Complex	Transcription From Rna Polymerase Ii Promoter
RPS18	YML063W	No	Ribosomal Protein 10 (Rp10) Of The Small (40S) Subunit	Miscellaneous
SKN7	YHR206W	No	Nuclear Response Regulator And Transcription Factor	Transcription From Rna Polymerase Ii Promoter
SLG1	YOR008C	No	Sensor-Transducer Of The Stress-Activated Pkc1-Mpk1 Kinase Pathway	Signaling
INP53	YOR109W	No	Polyphosphatidylinositol Phosphatase	Lipid Metabolic Process
AMD1	YML035C	No	Amp Deaminase	Miscellaneous
STE50	YCL032W	No	Protein Involved In Mating Response	Response To Chemical
EXO1	YOR033C	No	5'-3' Exonuclease And Flap-Endonuclease	Cellular Response To DNA Damage Stimulus
SFL1	YOR140W	No	Transcriptional Repressor And Activator	Transcription From Rna Polymerase Ii Promoter
PP21	YML016C	No	Serine/Threonine Protein Phosphatase Z, Isoform Of Ppz2P	Miscellaneous
MRC1	YCL061C	No	S-Phase Checkpoint Protein Required For DNA Replication	Mitotic Cell Cycle
STD1	YOR047C	No	Protein Involved In Control Of Glucose-Regulated Gene Expression	Transcription From Rna Polymerase Ii Promoter
GAC1	YOR178C	No	Regulatory Subunit For Glc7P Type-1 Protein Phosphatase (Pp1)	Transcription From Rna Polymerase Ii Promoter
LIF1	YGL090W	No	Component Of The Dna Ligase Iv Complex	Cellular Response To DNA Damage Stimulus
RPL16B	YNL069C	No	Ribosomal 60S Subunit Protein L16B	Miscellaneous
GCN20	YFR009W	No	Positive Regulator Of The Gcn2P Kinase Activity	Miscellaneous
ATP11	YNL315C	No	Molecular Chaperone	Protein Complex Biogenesis
SIN4	YNL236W	No	Subunit Of The Rna Polymerase Ii Mediator Complex	Transcription From Rna Polymerase Ii Promoter
VAC7	YNL054W	No	Integral Vacuolar Membrane Protein	Lipid Metabolic Process
RPL2A	YFR031C-A	No	Ribosomal 60S Subunit Protein L2A	Miscellaneous
PNT1	YOR266W	No	Mitochondrial Integral Inner Membrane Protein	Miscellaneous
ELA1	YNL230C	No	Elongin A	Protein Modification By Small Protein Conjugation Or Removal
HOS4	YIL112W	No	Subunit Of The Set3 Complex	Chromatin Organization
RTT102	YGR275W	No	Component Of Both The Swi/Snf And Rsc Chromatin Remodeling Complexes	Transcription From Rna Polymerase Ii Promoter
IRC15	YPL017C	No	Microtubule Associated Protein	Mitotic Cell Cycle
ALG9	YNL219C	No	Mannosyltransferase, Involved In N-Linked Glycosylation	Carbohydrate Metabolic Process
RPL16A	YIL133C	No	Ribosomal 60S Subunit Protein L16A	Miscellaneous
GPT2	YKR067W	No	Glycerol-3-Phosphate/Dihydroxyacetone Phosphate Sn-1 Acyltransferase	Lipid Metabolic Process
FAB1	YFR019W	No	1-Phosphatidylinositol-3-Phosphate 5-Kinase	Lipid Metabolic Process
PSY2	YNL201C	No	Subunit Of Protein Phosphatase Pp4 Complex	Cellular Response To DNA Damage Stimulus
RRD1	YIL153W	No	Peptidyl-Prolyl Cis/Trans-Isomerase	Transcription From Rna Polymerase Ii Promoter
KAR5	YMR065W	No	Protein Required For Nuclear Membrane Fusion During Karyogamy	Miscellaneous
BN15	YNL166C	No	Protein Involved In Organization Of Septins At The Mother-Bud Neck	Protein Complex Biogenesis
AIM21	YIR003W	No	Protein Of Unknown Function	Miscellaneous
CTF18	YMR078C	No	Subunit Of A Complex With Ctf8P	Mitotic Cell Cycle
YME1	YPR024W	No	Catalytic Subunit Of The I-Aaa Protease Complex	Protein Targeting
TRP3	YKL211C	No	Indole-3-Glycerol-Phosphate Synthase	Miscellaneous
TOM7	YNL070W	No	Component Of The Tom (Translocase Of Outer Membrane) Complex	Protein Targeting
MDY2	YOL111C	No	Protein Involved In Inserting Tail-Anchored Proteins Into Er Membranes	Response To Chemical
RXT2	YBR095C	No	Component Of The Histone Deacetylase Rpd3L Complex	Transcription From Rna Polymerase Ii Promoter
UTH1	YKR042W	No	Mitochondrial Inner Membrane Protein	Chromatin Organization
PHO23	YNL097C	No	Component Of The Rpd3L Histone Deacetylase Complex	Transcription From Rna Polymerase Ii Promoter
RAD51	YER095W	No	Strand Exchange Protein	Organelle Fission
AGP2	YBR132C	No	Plasma Membrane Regulator Of Polyamine And Carnitine Transport	Miscellaneous
PEX5	YDR244W	No	Peroxisomal Membrane Signal Receptor For Peroxisomal Matrix Proteins	Protein Complex Biogenesis
MDM34	YGL219C	No	Mitochondrial Component Of The Erms Complex	Miscellaneous
ELP6	YMR312W	No	Subunit Of Hexameric Reca-Like Atpase Elp456 Elongator Subcomplex	Transcription From Rna Polymerase Ii Promoter
NPL4	YBR170C	No	Substrate-Recruiting Cofactor Of The Cdc48P-Npl4P-Ufd1P Segregase	Mitotic Cell Cycle
RNH202	YDR279W	No	Ribonuclease H2 Subunit	Miscellaneous
MNN4	YKL201C	No	Putative Positive Regulator Of Mannosylphosphate Transferase Mnn6P	Carbohydrate Metabolic Process
NUP188	YML103C	No	Subunit Of The Inner Ring Of The Nuclear Pore Complex (Npc)	Protein Targeting
STP4	YDL048C	No	Protein Containing A Kruppel-Type Zinc-Finger Domain	Biological_Process
SF2	YDR312W	No	Protein Required For Ribosomal Large Subunit Maturation	Miscellaneous
RPL19A	YBR084C-A	No	Ribosomal 60S Subunit Protein L19A	Miscellaneous
MSC1	YML128C	No	Protein Of Unknown Function	Organelle Fission
RXT3	YDL076C	No	Component Of The Rpd3L Histone Deacetylase Complex	Miscellaneous
IRC3	YDR332W	No	Putative Rna Helicase Of The Deah/D-Box Family	Biological_Process
HSM3	YBR272C	No	Proteasome-Interacting Protein	Cellular Response To DNA Damage Stimulus
ASC1	YMR116C	No	G-Protein Beta Subunit And Guanine Dissociation Inhibitor For Gpa2P	Response To Chemical
PMT5	YDL093W	No	Protein O-Mannosyltransferase	Carbohydrate Metabolic Process
REV1	YOR346W	No	Deoxycytidyl Transferase	Cellular Response To DNA Damage Stimulus
DAS1	YIL149W	No	Putative Scf Ubiquitin Ligase F-Box Protein	Proteolysis Involved In Cellular Protein Catabolic Process
ISW1	YBR245C	No	Atpase Subunit Of Imitation-Switch (Iswi) Class Chromatin Remodelers	Transcription From Rna Polymerase Ii Promoter
RLM1	YPL089C	No	Mads-Box Transcription Factor	Transcription From Rna Polymerase Ii Promoter
GDS1	YOR355W	No	Protein Of Unknown Function	Miscellaneous
RPB4	YJL140W	No	Rna Polymerase Ii Subunit B32	Transcription From Rna Polymerase Ii Promoter
RGD1	YBR260C	No	Gtpase-Activating Protein (Rhogap) For Rho3P And Rho4P	Response To Chemical
RPL21B	YPL079W	No	Ribosomal 60S Subunit Protein L21B	Miscellaneous
RAD17	YOR368W	No	Checkpoint Protein	Cellular Response To DNA Damage Stimulus
LCB3	YJL134W	No	Long-Chain Base-1-Phosphate Phosphatase	Signaling
YOS9	YDR057W	No	Er Quality-Control Lectin	Response To Chemical
	YPL068C	No	Protein Of Unknown Function	Biological_Process
SIN3	YOL004W	No	Component Of Both The Rpd3S And Rpd3L Histone Deacetylase Complexes	Transcription From Rna Polymerase Ii Promoter
FK51	YLR342W	No	Catalytic Subunit Of 1,3-Beta-D-Glucan Synthase	Carbohydrate Metabolic Process
IPT1	YDR072C	No	Inositolphosphotransferase	Lipid Metabolic Process
SGF11	YPL047W	No	Integral Subunit Of Saga Histone Acetyltransferase Complex	Transcription From Rna Polymerase Ii Promoter
HRD1	YOL013C	No	Ubiquitin-Protein Ligase	Response To Chemical
NMD4	YLR363C	No	Protein That May Be Involved In Nonsense-Mediated Mrna Decay	Miscellaneous
RRP8	YDR083W	No	Nucleolar S-Adenosylmethionine-Dependent Rna Methyltransferase	Miscellaneous
RAD1	YPL022W	No	Single-Stranded Dna Endonuclease (With Rad10P)	Cellular Response To DNA Damage Stimulus
OPI10	YOL032W	No	Protein With A Possible Role In Phospholipid Biosynthesis	Carbohydrate Metabolic Process
CTF3	YLR381W	No	Outer Kinetochore Protein That Forms A Complex With Mcm16P And Mcm22F Mitotic Cell Cycle	

TRS85	YDR108W	No	Subunit Of Trappiii (Transport Protein Particle)	Organelle Fission
CLB5	YPR120C	No	B-Type Cyclin Involved In DNA Replication During S Phase	Mitotic Cell Cycle
PRS5	YOL061W	No	5-Phospho-Ribosyl-1(Alpha)-Pyrophosphate Synthetase	Miscellaneous
VIP1	YLR410W	No	Inositol Hexakisphosphate And Inositol Heptakisphosphate Kinase	Miscellaneous
MTCS	YDR128W	No	Subunit Of The Sea (Seh1-Associated) Complex	Biological_Process
MMS1	YPR164W	No	Subunit Of E3 Ubiquitin Ligase Complex Involved In Replication Repair	Cellular Response To DNA Damage Stimulus
KAR9	YPL269W	No	Karyogamy Protein	Cytoskeleton Organization
ARV1	YLR242C	No	Cortical Er Protein	Lipid Metabolic Process
VP574	YDR372C	No	Golgi Phosphatidylinositol-4-Kinase Effector And Ptdins4P Sensor	Response To Chemical
SAP155	YFR040W	No	Protein Required For Function Of The Sit4P Protein Phosphatase	Mitotic Cell Cycle
ALG5	YPL227C	No	Udp-Glucose:Dolichyl-Phosphate Glucosyltransferase	Carbohydrate Metabolic Process
	YLR278C	No	Zinc-Cluster Protein	Biological_Process
SPT3	YDR392W	No	Subunit Of The Saga And Saga-Like Transcriptional Regulatory Complexes	Transcription From Rna Polymerase Ii Promoter
SLA1	YBL007C	No	Cytoskeletal Protein Binding Protein	Protein Complex Biogenesis
PRM3	YPL192C	No	Protein Required For Nuclear Envelope Fusion During Karyogamy	Miscellaneous
EST2	YLR318W	No	Reverse Transcriptase Subunit Of The Telomerase Holoenzyme	Miscellaneous
CAD1	YDR423C	No	Ap-1-Like Basic Leucine Zipper (bzp) Transcriptional Activator	Transcription From Rna Polymerase Ii Promoter
HEK2	YBL032W	No	Rna Binding Protein Involved In Asymmetric Localization Of Ash1 Mrna	Miscellaneous
COX10	YPL172C	No	Heme A:Farnesyltransferase	Miscellaneous
	YDR161W	No	Putative Protein Of Unknown Function	Proteolysis Involved In Cellular Protein Catabolic Process
RAD23	YEL037C	No	Protein With Ubiquitin-Like N Terminus	Proteolysis Involved In Cellular Protein Catabolic Process
SEF1	YBL066C	No	Putative Transcription Factor	Biological_Process
	YPL150W	No	Protein Kinase Of Unknown Cellular Role	Protein Phosphorylation
PLP1	YDR183W	No	Protein That Interacts With Cct (Chaperonin Containing Tcp-1) Complex	Transcription From Rna Polymerase Ii Promoter
HAT2	YEL056W	No	Subunit Of The Hat1P-Hat2P Histone Acetyltransferase Complex	Chromatin Organization
ALG3	YBL082C	No	Dolichol-P-Man Dependent Alpha(1-3) Mannosyltransferase	Lipid Metabolic Process
CH56	YJL099W	No	Member Of The Chaps (Chs5P-Arf1P-Binding Proteins) Family	Carbohydrate Metabolic Process
HUL5	YGL141W	No	Multiubiquitin Chain Assembly Factor (E4)	Protein Complex Biogenesis
CTP1	YBR291C	No	Mitochondrial Inner Membrane Citrate Transporter	Miscellaneous
NCS6	YGL211W	No	Protein Required For Uridine Thiolation Of Gln, Lys, And Glu Trnas	Protein Modification By Small Protein Conjugation Or Removal
BCK1	YJL095W	No	Mapkkk Acting In The Protein Kinase C Signaling Pathway	Response To Chemical
NUT1	YGL151W	No	Component Of The Rna Polymerase Ii Mediator Complex	Transcription From Rna Polymerase Ii Promoter
MAL31	YBR298C	No	Maltose Permease	Miscellaneous
YNG2	YHR090C	No	Subunit Of Nua4, An Essential Histone Acetyltransferase Complex	Chromatin Organization
JEM1	YJL073W	No	DNAJ-Like Chaperone Required For Nuclear Membrane Fusion During Mating	Proteolysis Involved In Cellular Protein Catabolic Process
RAD54	YGL163C	No	DNA-Dependent Atpase That Stimulates Strand Exchange	Chromatin Organization
NPP1	YCR026C	No	Nucleotide Pyrophosphatase/Phosphodiesterase	Miscellaneous
SPP1	YPL138C	No	Subunit Of Compass (Set1C)	Chromatin Organization
RTT101	YJL047C	No	Cullin Subunit Of A Roc1P-Dependent E3 Ubiquitin Ligase Complex	Mitotic Cell Cycle
BUD13	YGL174W	No	Subunit Of The Res Complex	Mitotic Cell Cycle
RBK1	YCR036W	No	Putative Ribokinase	Carbohydrate Metabolic Process
PEX2	YJL210W	No	Ring-Finger Peroxin And E3 Ubiquitin Ligase	Protein Targeting
YPT31	YER031C	No	Rab Family Gtpase	Golgi Vesicle Transport
SC52	YER120W	No	Integral Er Membrane Protein, Regulates Phospholipid Metabolism	Protein Targeting
IMG2	YCR071C	No	Mitochondrial Ribosomal Protein Of The Large Subunit	Miscellaneous
RP021	YDL140C	Yes	Rna Polymerase Ii Largest Subunit B220	Transcription From Rna Polymerase Ii Promoter
THR1	YHR025W	No	Homoserine Kinase	Miscellaneous
BEM2	YER155C	No	Rho Gtpase Activating Protein (Rhogap)	Signaling
BBC1	YJL020C	No	Protein Possibly Involved In Assembly Of Actin Patches	Cytoskeleton Organization
ABF1	YKL112W	Yes	DNA Binding Protein With Possible Chromatin-Reorganizing Activity	Transcription From Rna Polymerase Ii Promoter
HOC1	YJR075W	No	Alpha-1,6-Mannosyltransferase	Carbohydrate Metabolic Process
RAD24	YER173W	No	Checkpoint Protein	Cellular Response To DNA Damage Stimulus
HUL4	YJR036C	No	Protein With Similarity To Hect Domain E3 Ubiquitin-Protein Ligases	Protein Modification By Small Protein Conjugation Or Removal
TFA2	YKR062W	Yes	Tfiie Small Subunit	Transcription From Rna Polymerase Ii Promoter
SKG1	YKR100C	No	Transmembrane Protein With A Role In Cell Wall Polymer Composition	Miscellaneous
TOR1	YJR066W	No	Pik-Related Protein Kinase And Rapamycin Target	Cellular Response To DNA Damage Stimulus
GET3	YDL100C	No	Guanine Nucleotide Exchange Factor For Gpa1P	Response To Chemical
CDC28	YBR160W	Yes	Cyclin-Dependent Kinase (Cdk) Catalytic Subunit	Transcription From Rna Polymerase Ii Promoter
ECM30	YLR436C	No	Putative Protein Of Unknown Function	Biological_Process
LTE1	YAL024C	No	Protein Similar To Gdp/Gtp Exchange Factors	Mitotic Cell Cycle
CRD1	YDL142C	No	Cardiolipin Synthase	Lipid Metabolic Process
TAF11	YML015C	Yes	Tfiid Subunit (40 Kda)	Transcription From Rna Polymerase Ii Promoter
HAM1	YJR069C	No	Nucleoside Triphosphate Pyrophosphohydrolase	Miscellaneous
GSM1	YJL103C	No	Putative Zinc Cluster Protein Of Unknown Function	Transcription From Rna Polymerase Ii Promoter
AS13	YNL008C	No	Putative Integral Membrane E3 Ubiquitin Ligase	Proteolysis Involved In Cellular Protein Catabolic Process
RBAS0	YDR527W	Yes	Protein Involved In Transcription	Transcription From Rna Polymerase Ii Promoter
ENT3	YJR125C	No	Protein Containing An N-Terminal Epsin-Like Domain	Cytoskeleton Organization
GET1	YGL020C	No	Subunit Of The Get Complex	Golgi Vesicle Transport
IDH1	YNL037C	No	Subunit Of Mitochondrial Nad(+)-Dependent Isocitrate Dehydrogenase	Miscellaneous
RSP5	YER125W	Yes	E3 Ubiquitin Ligase Of The Nedd4 Family	Transcription From Rna Polymerase Ii Promoter
RP54A	YJR145C	No	Protein Component Of The Small (40S) Ribosomal Subunit	Miscellaneous
GR1	YJR090C	No	F-Box Protein Component Of An Scf Ubiquitin-Ligase Complex	Mitotic Cell Cycle
ATP23	YNR020C	No	Putative Metalloprotease Of The Mitochondrial Inner Membrane	Protein Complex Biogenesis
CDC36	YDL165W	Yes	Component Of The Kinetochore-Associated Ndc80 Complex	Transcription From Rna Polymerase Ii Promoter
CLN3	YAL040C	No	G1 Cyclin Involved In Cell Cycle Progression	Transcription From Rna Polymerase Ii Promoter
SNG1	YGR197C	No	Protein Involved In Resistance To Nitrosguanidine And 6-Azauracil	Miscellaneous
UBP8	YMR223W	No	Ubiquitin-Specific Protease Component Of The Saga Acetylation Complex	Chromatin Organization
PAN3	YKL025C	No	Essential Subunit Of The Pan2P-Pan3P Poly(A)-Ribonuclease Complex	Cellular Response To DNA Damage Stimulus
YCH1	YGR203W	No	Phosphatase With Sequence Similarity To Cdc25P	Miscellaneous
PEP5	YMR231W	No	Histone E3 Ligase, Component Of Corvet Tethering Complex	Chromatin Organization
VP524	YKL041W	No	One Of Four Subunits Of The Escrt-Iii Complex	Proteolysis Involved In Cellular Protein Catabolic Process
FUN30	YAL019W	No	Snf2P Family Member With Atp-Dependent Chromatin Remodeling Activity	Chromatin Organization
RPL8A	YHL033C	No	Ribosomal 60S Subunit Protein L8A	Miscellaneous
RSN1	YMR266W	No	Membrane Protein Of Unknown Function	Golgi Vesicle Transport
LHS1	YKL073W	No	Molecular Chaperone Of The Endoplasmic Reticulum Lumen	Response To Chemical
VP58	YAL002W	No	Membrane-Binding Component Of The Corvet Complex	Protein Targeting
NPR3	YHL023C	No	Subunit Of Sea (Seh1-Associated), Npr2/3, And Iml1P Complexes	Organelle Fission
CAT8	YMR280C	No	Zinc Cluster Transcriptional Activator	Transcription From Rna Polymerase Ii Promoter
BUD2	YKL092C	No	Gtpase Activating Factor For Rsr1P/Bud1P	Mitotic Cell Cycle
RTT109	YLL002W	No	Histone Acetyltransferase	Transcription From Rna Polymerase Ii Promoter
RRM3	YHR031C	No	DNA Helicase Involved In RDNA Replication And Ty1 Transposition	Miscellaneous
JNM1	YMR294W	No	Component Of The Yeast Dynactin Complex	Mitotic Cell Cycle
DGR2	YKL121W	No	Protein Of Unknown Function	Biological_Process
FP51	YLL043W	No	Aquaglyceroporin, Plasma Membrane Channel	Response To Chemical
LRP1	YHR081W	No	Nuclear Exosome-Associated Nucleic Acid Binding Protein	Miscellaneous
LEM3	YNL323W	No	Membrane Protein Of The Plasma Membrane And Er	Signaling
ASH1	YKL185W	No	Component Of The Rpd3L Histone Deacetylase Complex	Transcription From Rna Polymerase Ii Promoter
SIC1	YLR079W	No	Cyclin-Dependent Kinase Inhibitor (Cki)	Mitotic Cell Cycle
WSS1	YHR134W	No	Sumoylated Protein Localizing To The Nuclear Periphery Of Mother Cells	Cellular Response To DNA Damage Stimulus
SNN1	YNL086W	No	Subunit Of The Bloc-1 Complex Involved In Endosomal Maturation	Miscellaneous
PEX8	YGR077C	No	Intra-peroxisomal Organizer Of The Peroxisomal Import Machinery	Protein Targeting
KIN2	YLR096W	No	Serine/Threonine Protein Kinase Involved In Regulation Of Exocytosis	Protein Phosphorylation
THP2	YHR167W	No	Subunit Of The Tho And Trex Complexes	Transcription From Rna Polymerase Ii Promoter
ALP1	YNL270C	No	Arginine Transporter	Miscellaneous
VMA21	YGR105W	No	Integral Membrane Protein Required For V-Atpase Function	Protein Complex Biogenesis

MFT1	YML062C	No	Subunit Of The Tho Complex	Transcription From Rna Polymerase Ii Promoter
SET5	YHR207C	No	Methyltransferase Involved In Methylation Of Histone H4 Lys5, -8, -12	Chromatin Organization
RTS1	YOR014W	No	B-Type Regulatory Subunit Of Protein Phosphatase 2A (Pp2A)	Mitotic Cell Cycle
CEX1	YOR112W	No	Component Of The Nuclear Aminoacylation-Dependent Trna Export Pathway	Miscellaneous
SRC1	YML034W	No	Inner Nuclear Membrane Protein	Mitotic Cell Cycle
MXR2	YCL033C	No	Methionine-S-Sulfoxide Reductase	Response To Chemical
AKR2	YOR034C	No	Ankyrin Repeat-Containing Protein	Miscellaneous
ARP8	YOR141C	No	Nuclear Actin-Related Protein Involved In Chromatin Remodeling	Chromatin Organization
UBX2	YML013W	No	Bridging Factor Involved In Er-Associated Protein Degradation (Erad)	Proteolysis Involved In Cellular Protein Catabolic Process
SAT4	YCR008W	No	Ser/Thr Protein Kinase Involved In Salt Tolerance	Mitotic Cell Cycle
ASE1	YOR058C	No	Mitotic Spindle Midzone-Localized Microtubule Bundling Protein	Mitotic Cell Cycle
SER1	YOR184W	No	3-Phosphoserine Aminotransferase	Miscellaneous
	YMR010W	No	Putative Protein Of Unknown Function	Biological_Process
MAK31	YCR020C-A	No	Non-Catalytic Subunit Of N-Terminal Acetyltransferase Of The Natc Type	Miscellaneous
VP55	YOR069W	No	Nexin-1 Homolog	Miscellaneous
SAS5	YOR213C	No	Subunit Of The Sas Complex (Sas2P, Sas4P, Sas5P)	Miscellaneous
BN14	YNL233W	No	Targeting Subunit For Gic7P Protein Phosphatase	Miscellaneous
SLM1	YIL105C	No	Phosphoinositide Pi4,5P(2) Binding Protein, Forms A Complex With Slm2P	Signaling
APL6	YGR261C	No	Beta3-Like Subunit Of The Yeast Ap-3 Complex	Protein Targeting
PAC1	YOR269W	No	Involved In Nuclear Migration, Part Of The Dynein/Dynactin Pathway	Miscellaneous
URE2	YNL229C	No	Nitrogen Catabolite Repression Transcriptional Regulator	Response To Chemical
RP11	YIL119C	No	Transcription Factor, Allelic Differences Between S288C And Sigma1278B	Transcription From Rna Polymerase Ii Promoter
ERV29	YGR284C	No	Protein Localized To Copii-Coated Vesicles	Golgi Vesicle Transport
GPA1	YHR005C	Yes	Subunit Of The G Protein Involved In Pheromone Response	Response To Chemical
MGS1	YNL218W	No	Protein With DNA-Dependent Atpase And Ssdna Annealing Activities	Cellular Response To DNA Damage Stimulus
FLX1	YIL134W	No	Protein Required For Transport Of Flavin Adenine Dinucleotide (Fad)	Miscellaneous
SIS2	YKR072C	No	Negative Regulatory Subunit Of Protein Phosphatase 1 (Pp21P)	Mitotic Cell Cycle
SET4	YIL105W	No	Protein Of Unknown Function, Contains A Set Domain	Biological_Process
GCR2	YNL199C	No	Transcriptional Activator Of Genes Involved In Glycolysis	Transcription From Rna Polymerase Ii Promoter
IMP2*	YIL154C	No	Transcriptional Activator Involved In Maintenance Of Ion Homeostasis	Transcription From Rna Polymerase Ii Promoter
UBX4	YMR067C	No	Ubx Domain-Containing Protein That Interacts With Cdc48P	Proteolysis Involved In Cellular Protein Catabolic Process
SIR3	YLR442C	No	Silencing Protein	Chromatin Organization
YCK2	YNL154C	No	Palmitoylated Plasma Membrane-Bound Casein Kinase I Isoform	Response To Chemical
IST3	YIR005W	No	Component Of The U2 Snrnp	Miscellaneous
NAM7	YMR080C	No	Atp-Dependent Rna Helicase Of The Sfi Superfamily	Protein Modification By Small Protein Conjugation Or Removal
NTO1	YPR031W	No	Subunit Of The Nua3 Histone Acetyltransferase Complex	Chromatin Organization
SAC1	YKL212W	No	Phosphatidylinositol Phosphate (Ptdinsp) Phosphatase	Lipid Metabolic Process
LAT1	YNL071W	No	Dihydrolipoyamide Acetyltransferase Component (E2) Of The Pdc	Miscellaneous
PAP2	YOL115W	No	Non-Canonical Poly(A) Polymerase	Cellular Response To DNA Damage Stimulus
SIF2	YBR103W	No	Wd40 Repeat-Containing Subunit Of Set3C Histone Deacetylase Complex	Chromatin Organization
SHB17	YKR043C	No	Sedoheptulose Bisphosphatase Involved In Riboneogenesis	Miscellaneous
OCA1	YNL099C	No	Putative Protein Tyrosine Phosphatase	Response To Chemical
UBP9	YER098W	No	Ubiquitin-Specific Protease That Cleaves Ubiquitin-Protein Fusions	Protein Modification By Small Protein Conjugation Or Removal
BMT2	YBR141C	No	Nucleolar S-Adenosylmethionine-Dependent Rna Methyltransferase	Biological_Process
CHL4	YDR254W	No	Outer Kinetochores Protein Required For Chromosome Stability	Mitotic Cell Cycle
ORM1	YGR038W	No	Protein Of Unknown Function	Response To Chemical
COG8	YML071C	No	Component Of The Conserved Oligomeric Golgi Complex	Protein Targeting
SEC66	YBR171W	No	Non-Essential Subunit Of Sec63 Complex	Protein Targeting
RTT103	YDR289C	No	Protein Involved In Transcription Termination By Rna Polymerase Ii	Cellular Response To DNA Damage Stimulus
EAP1	YKL204W	No	Eif4E-Associated Protein, Competes With Eif4G For Binding To Eif4E	Miscellaneous
PML39	YML107C	No	Protein Required For Nuclear Retention Of Unspliced Pre-Mmas	Miscellaneous
LHP1	YDL051W	No	Rna Binding Protein Required For Maturation Of Trna And U6 Snrna	Miscellaneous
PIB1	YDR313C	No	Ring-Type Ubiquitin Ligase Of The Endosomal And Vacuolar Membranes	Protein Modification By Small Protein Conjugation Or Removal
AS11	YMR119W	No	Putative Integral Membrane E3 Ubiquitin Ligase	Proteolysis Involved In Cellular Protein Catabolic Process
MVP1	YMR004W	No	Protein Required For Sorting Proteins To The Vacuole	Protein Targeting
THI3	YDL080C	No	Regulatory Protein That Binds Pdc2P And Thi2P Transcription Factors	Transcription From Rna Polymerase Ii Promoter
SWR1	YDR334W	No	Swi2/Snf2-Related Atpase	Chromatin Organization
RIF1	YBR275C	No	Protein That Binds To The Rap1P C-Terminus	Cellular Response To DNA Damage Stimulus
RPL15B	YMR121C	No	Ribosomal 60S Subunit Protein L15B	Miscellaneous
PMT1	YDL095W	No	Protein O-Mannosyltransferase Of The Er Membrane	Response To Chemical
CKA1	YIL035C	No	Alpha Catalytic Subunit Of Casein Kinase 2 (Ck2)	Cellular Response To DNA Damage Stimulus
THR4	YCR053W	No	Theonine Synthase	Miscellaneous
DSS4	YPR017C	No	Guanine Nucleotide Dissociation Stimulator For Sec4P	Golgi Vesicle Transport
STP1	YDR463W	No	Transcription Factor	Transcription From Rna Polymerase Ii Promoter
HAP5	YOR358W	No	Subunit Of The Hap2P/3P/4P/5P Ccaat-Binding Complex	Transcription From Rna Polymerase Ii Promoter
YUR1	YIL139C	No	Mannosyltransferase Involved In Protein N-Glycosylation	Carbohydrate Metabolic Process
SLM6	YBR266C	No	Protein With A Potential Role In Actin Cytoskeleton Organization	Miscellaneous
UBP16	YPL072W	No	Deubiquitinating Enzyme Anchored To The Outer Mitochondrial Membrane	Protein Modification By Small Protein Conjugation Or Removal
GPB1	YOR371C	No	Multistep Regulator Of Camp-Pka Signaling	Response To Chemical
PEX30	YLR324W	No	Peroxisomal Integral Membrane Protein	Miscellaneous
UBCS	YDR059C	No	Ubiquitin-Conjugating Enzyme	Protein Modification By Small Protein Conjugation Or Removal
SUR1	YPL057C	No	Mannosylinositol Phosphorylceramide (Mipc) Synthase Catalytic Subunit	Lipid Metabolic Process
TOP1	YOL006C	No	Topoisomerase I	Transcription From Rna Polymerase Ii Promoter
ORM2	YLR350W	No	Protein Of Unknown Function	Response To Chemical
SNF11	YDR073W	No	Subunit Of The Swi/Snf Chromatin Remodeling Complex	Transcription From Rna Polymerase Ii Promoter
ELC1	YPL046C	No	Elongin C, Conserved Among Eukaryotes	Cellular Response To DNA Damage Stimulus
ESC8	YOL017W	No	Protein Involved In Telomeric And Mating-Type Locus Silencing	Miscellaneous
MDM30	YLR368W	No	F-Box Component Of An Scf Ubiquitin Protein Ligase Complex	Protein Modification By Small Protein Conjugation Or Removal
UBC13	YDR092W	No	E2 Ubiquitin-Conjugating Enzyme	Cellular Response To DNA Damage Stimulus
CTF19	YPL018W	No	Outer Kinetochores Protein, Needed For Accurate Chromosome Segregation	Mitotic Cell Cycle
NOP12	YOL041C	No	Nucleolar Protein Involved In Pre-25S Rrna Processing	Miscellaneous
IK13	YLR384C	No	Subunit Of Elongator Complex	Transcription From Rna Polymerase Ii Promoter
TRM1	YDR120C	No	Trna Methyltransferase	Miscellaneous
SCD6	YPR129W	No	Repressor Of Translation Initiation	Miscellaneous
APM4	YOL062C	No	Mu2-Like Subunit Of The Clathrin Associated Protein Complex (Ap-2)	Miscellaneous
CDC73	YLR418C	No	Component Of The Paf1P Complex	Transcription From Rna Polymerase Ii Promoter
	YDR131C	No	F-Box Protein Subunit Of Scf Ubiquitin Ligase Complex	Proteolysis Involved In Cellular Protein Catabolic Process
MET16	YPR167C	No	3'-Phosphoadenylylsulfate Reductase	Miscellaneous
CLN2	YPL256C	No	G1 Cyclin Involved In Regulation Of The Cell Cycle	Response To Chemical
YPT6	YLR262C	No	Rab Family Gtpase	Miscellaneous
LSM6	YDR378C	No	Lsm (Like Sm) Protein	Miscellaneous
ERJ5	YFR041C	No	Type I Membrane Protein With A J Domain	Miscellaneous
NEW1	YPL226W	No	Atp Binding Cassette Protein	Miscellaneous
	YLR287C	No	Putative Protein Of Unknown Function	Biological_Process
SHE9	YDR393W	No	Protein Required For Normal Mitochondrial Morphology	Miscellaneous
HIR1	YBL008W	No	Subunit Of The Hir Complex	Transcription From Rna Polymerase Ii Promoter
GUP2	YPL189W	No	Probable Membrane Protein	Miscellaneous
BUD6	YLR319C	No	Actin- And Formin-Interacting Protein	Mitotic Cell Cycle
PPM1	YDR435C	No	Carboxyl Methyltransferase	Protein Complex Biogenesis
	YBL036C	No	Putative Non-Specific Single-Domain Racemase	Biological_Process
REV3	YPL167C	No	Catalytic Subunit Of DNA Polymerase Zeta	Cellular Response To DNA Damage Stimulus
NBP2	YDR162C	No	Protein Involved In The Hog (High Osmolarity Glycerol) Pathway	Signaling
YEF1	YEL041W	No	Atp-Nadh Kinase	Miscellaneous
UBP13	YBL067C	No	Ubiquitin-Specific Protease That Cleaves Ub-Protein Fusions	Miscellaneous
POC4	YPL144W	No	Component Of A Heterodimeric Pdc4P-Irc25P Chaperone	Protein Complex Biogenesis

HST4	YDR191W	No	Member Of The Sir2 Family Of Nad(+)-Dependent Protein Deacetylases	Chromatin Organization
PRB1	YEL060C	No	Vacuolar Proteinase B (Yscb)	Miscellaneous
BOI1	YBL085W	No	Protein Implicated In Polar Growth	Miscellaneous
KAP120	YPL125W	No	Karyopherin Responsible For The Nuclear Import Of Rfp1P	Protein Targeting
HTA1	YDR225W	No	Histone H2A	Transcription From Rna Polymerase Ii Promoter
PAC2	YER007W	No	Microtubule Effector Required For Tubulin Heterodimer Formation	Protein Complex Biogenesis
COG7	YGL005C	No	Component Of The Conserved Oligomeric Golgi Complex	Protein Targeting
SR52	YJL092W	No	DNA Helicase And DNA-Dependent Atpase	Cellular Response To DNA Damage Stimulus
PEX14	YGL153W	No	Central Component Of The Peroxisomal Protein Import Machinery	Protein Complex Biogenesis
	YCL001W-A	No	Putative Protein Of Unknown Function	Biological_Process
IKI1	YHR187W	No	Subunit Of Hexameric RecA-Like Atpase Elp456 Elongator Subcomplex	Miscellaneous
LAS21	YJL062W	No	Integral Plasma Membrane Protein	Lipid Metabolic Process
PMR1	YGL167C	No	High Affinity Ca2+/Mn2+ P-Type Atpase	Miscellaneous
RHB1	YCR027C	No	Putative Rheb-Related Gtpase	Miscellaneous
HUT1	YPL244C	No	Protein With A Role In Udp-Galactose Transport To The Golgi Lumen	Miscellaneous
AIM22	YJL046W	No	Putative Lipote-Protein Ligase	Miscellaneous
SAE2	YGL175C	No	Endonuclease Involved In Processing Hairpin DNA Structures	Cellular Response To DNA Damage Stimulus
	YCR050C	No	Non-Essential Protein Of Unknown Function	Biological_Process
NUC1	YJL208C	No	Major Mitochondrial Nuclease	DNA Recombination
BUB1	YGR188C	No	Protein Kinase Involved In The Cell Cycle Checkpoint Into Anaphase	Mitotic Cell Cycle
YCK3	YER123W	No	Palmitoylated Vacuolar Membrane-Localized Casein Kinase I Isoform	Protein Phosphorylation
PAT1	YCR077C	No	Deadenylation-Dependent Mrna-Decapping Factor	Miscellaneous
SRB4	YER022W	Yes	Subunit Of The Rna Polymerase Ii Mediator Complex	Transcription From Rna Polymerase Ii Promoter
SRB2	YHR041C	No	Subunit Of The Rna Polymerase Ii Mediator Complex	Transcription From Rna Polymerase Ii Promoter
	YER156C	No	Putative Protein Of Unknown Function	Biological_Process
PET130	YJL023C	No	Protein Required For Respiratory Growth	Biological_Process
ESS1	YJR017C	Yes	Peptidylprolyl-Cis/Trans-Isomerase (Ppiase)	Transcription From Rna Polymerase Ii Promoter
EAF6	YJR082C	No	Subunit Of The Nua4 Acetyltransferase Complex	Chromatin Organization
GRX4	YER174C	No	Glutathione-Dependent Oxidoreductase	Response To Chemical
POL32	YJR043C	No	Third Subunit Of DNA Polymerase Delta	Cellular Response To DNA Damage Stimulus
POL30	YBR088C	Yes	Proliferating Cell Nuclear Antigen (Pcna)	Mitotic Cell Cycle
SIR1	YKR101W	No	Protein Involved In Silencing At Mating-Type Loci Hml And Hmr	Chromatin Organization
FKH1	YIL131C	No	Yorkhead Family Transcription Factor	Transcription From Rna Polymerase Ii Promoter
CYK3	YDL117W	No	Sh3-Domain Protein Located In The Bud Neck And Cytokinetic Actin Ring	Miscellaneous
MED8	YBR193C	Yes	Subunit Of The Rna Polymerase Ii Mediator Complex	Transcription From Rna Polymerase Ii Promoter
HMG2	YLR450W	No	Hmg-Coa Reductase	Lipid Metabolic Process
PTC2	YER089C	No	Type 2C Protein Phosphatase (Pp2C)	Cellular Response To DNA Damage Stimulus
CLB3	YDL155W	No	B-Type Cyclin Involved In Cell Cycle Progression	Mitotic Cell Cycle
TAF13	YML098W	Yes	Tfiid Subunit (19 Kda)	Transcription From Rna Polymerase Ii Promoter
LIA1	YJR070C	No	Deoxyhypusine Hydroxylase	Cytoskeleton Organization
PET123	YOR158W	No	Mitochondrial Ribosomal Protein Of The Small Subunit	Miscellaneous
PUB1	YNL016W	No	Poly (A)+ Rna-Binding Protein	Miscellaneous
RPB7	YDR404C	Yes	Rna Polymerase Ii Subunit B16	Transcription From Rna Polymerase Ii Promoter
VPS70	YJR126C	No	Protein Of Unknown Function Involved In Vacuolar Protein Sorting	Protein Targeting
RPB9	YGL070C	No	Rna Polymerase Ii Subunit B12.6	Transcription From Rna Polymerase Ii Promoter
COG6	YNL041C	No	Component Of The Conserved Oligomeric Golgi Complex	Protein Targeting
ARP4	YJL081C	Yes	Nuclear Actin-Related Protein Involved In Chromatin Remodeling	Transcription From Rna Polymerase Ii Promoter
BYE1	YKL005C	No	Negative Regulator Of Transcription Elongation	Transcription From Rna Polymerase Ii Promoter
PER1	YCR044C	No	Protein Of The Endoplasmic Reticulum	Lipid Metabolic Process
ALG12	YNR030W	No	Alpha-1,6-Mannosyltransferase Localized To The Er	Carbohydrate Metabolic Process
TAF8	YML114C	Yes	Tfiid Subunit (65 Kda)	Transcription From Rna Polymerase Ii Promoter
ARF1	YDL192W	No	Adp-Ribosylation Factor	Golgi Vesicle Transport
NRP1	YDL167C	No	Putative Rna Binding Protein Of Unknown Function	Biological_Process
HHF1	YBR009C	No	Histone H4	Transcription From Rna Polymerase Ii Promoter
EPL1	YFL024C	Yes	Subunit Of Nua4, An Essential Histone H4/H2A Acetyltransferase Complex	Transcription From Rna Polymerase Ii Promoter
PMT2	YAL023C	No	Protein O-Mannosyltransferase Of The Er Membrane	Response To Chemical
SER2	YGR208W	No	Phosphoserine Phosphatase Of The Phosphoglycerate Pathway	Miscellaneous
RKR1	YMR247C	No	Ring Domain E3 Ubiquitin Ligase	Chromatin Organization
ELM1	YKL048C	No	Serine/Threonine Protein Kinase That Regulates Cellular Morphogenesis	Mitotic Cell Cycle
DEP1	YAL013W	No	Component Of The Rpd3L Histone Deacetylase Complex	Transcription From Rna Polymerase Ii Promoter
GOS1	YHL031C	No	V-Snare Protein Involved In Golgi Transport	Golgi Vesicle Transport
SCS7	YMR272C	No	Sphingolipid Alpha-Hydroxylase	Lipid Metabolic Process
MUD2	YKL074C	No	Protein Involved In Early Pre-Mrna Splicing	Miscellaneous
NUP60	YAR002W	No	Fg-Nucleoporin Component Of Central Core Of The Nuclear Pore Complex	Cellular Response To DNA Damage Stimulus
OPI1	YHL020C	No	Transcriptional Regulator Of A Variety Of Genes	Transcription From Rna Polymerase Ii Promoter
AEP2	YMR282C	No	Mitochondrial Protein	Miscellaneous
HSL1	YKL101W	No	Nim1P-Related Protein Kinase	Mitotic Cell Cycle
KNS1	YLL019C	No	Protein Kinase Involved In Negative Regulation Of Poliii Transcription	Protein Phosphorylation
PIH1	YHR034C	No	Component Of The Conserved R2Tp Complex (Rvb1-Rvb2-Tah1-Pih1)	Miscellaneous
DYN3	YMR299C	No	Dynein Light Intermediate Chain (Lic)	Miscellaneous
TGL1	YKL140W	No	Steryl Ester Hydrolase	Lipid Metabolic Process
RPL8B	YLL045C	No	Ribosomal 60S Subunit Protein L8B	Miscellaneous
KSP1	YHR082C	No	Serine/Threonine Protein Kinase	Signaling
KRE1	YNL322C	No	Cell Wall Glycoprotein Involved In Beta-Glucan Assembly	Miscellaneous
CNB1	YKL190W	No	Calcineurin B	Response To Chemical
SRL2	YLR082C	No	Protein Of Unknown Function	Miscellaneous
YCK1	YHR135C	No	Palmitoylated Plasma Membrane-Bound Casein Kinase I Isoform	Response To Chemical
MON2	YNL297C	No	Protein With A Role In Endocytosis And Vacuole Integrity	Protein Targeting
PAC10	YGR078C	No	Part Of The Heteromeric Co-Chaperone Gimc/Prefoldin Complex	Protein Complex Biogenesis
HRT3	YLR097C	No	Putative Scf-Ubiquitin Ligase F-Box Protein	Response To Chemical
STB5	YHR178W	No	Transcription Factor	Transcription From Rna Polymerase Ii Promoter
GIS2	YNL255C	No	Translational Activator For Mrnas With Internal Ribosome Entry Sites	Miscellaneous
CLB1	YGR108W	No	B-Type Cyclin Involved In Cell Cycle Progression	Mitotic Cell Cycle
NTE1	YML059C	No	Serine Esterase	Lipid Metabolic Process
RER1	YCL001W	No	Protein Involved In Retention Of Membrane Proteins	Golgi Vesicle Transport
ERP4	YOR016C	No	Member Of The P24 Family Involved In Er To Golgi Transport	Golgi Vesicle Transport
AZF1	YOR113W	No	Zinc-Finger Transcription Factor	Transcription From Rna Polymerase Ii Promoter
RAD52	YML032C	No	Protein That Stimulates Strand Exchange	Cellular Response To DNA Damage Stimulus
GF2D	YCL036W	No	Protein Of Unknown Function	Biological_Process
SHE4	YOR035C	No	Protein Containing A Ucs (Unc-45/Cro1/She4) Domain	Cytoskeleton Organization
ELG1	YOR144C	No	Subunit Of An Alternative Replication Factor C Complex	Mitotic Cell Cycle
ERV25	YML012W	No	Member Of The P24 Family Involved In Er To Golgi Transport	Golgi Vesicle Transport
RVS161	YCR009C	No	Amphiphysin-Like Lipid Raft Protein	Cytoskeleton Organization
CKA2	YOR061W	No	Alpha' Catalytic Subunit Of Casein Kinase 2 (Ck2)	Cellular Response To DNA Damage Stimulus
IES4	YOR189W	No	Component Of The Ino80 Chromatin Remodeling Complex	Cellular Response To DNA Damage Stimulus
ERG5	YMR015C	No	C-22 Sterol Desaturase	Lipid Metabolic Process
DCN1	YLR128W	No	Scaffold-Type E3 Ligase	Protein Modification By Small Protein Conjugation Or Removal
GYP1	YOR070C	No	Cis-Golgi Gtpase-Activating Protein (Gap) For Yeast Rabs	Miscellaneous
RUD3	YOR216C	No	Golgi Matrix Protein	Golgi Vesicle Transport
FAR8	YMR029C	No	Protein Involved In Recovery From Arrest In Response To Pheromone	Response To Chemical
RNH203	YLR154C	No	Ribonuclease H2 Subunit	Miscellaneous
OST3	YOR085W	No	Gamma Subunit Of The Oligosaccharyltransferase Complex Of The Er Lumen	Protein Complex Biogenesis
DSE3	YOR264W	No	Daughter Cell-Specific Protein, May Help Establish Daughter Fate	Biological_Process
JJJ1	YNL227C	No	Co-Chaperone That Stimulates The Atpase Activity Of Ssa1P	Miscellaneous
KGD1	YIL125W	No	Subunit Of The Mitochondrial Alpha-Ketoglutarate Dehydrogenase Complex	Miscellaneous

YAP5	YIR018W	No	Basic Leucine Zipper (Bzip) Iron-Sensing Transcription Factor	Transcription From Rna Polymerase Ii Promoter
SYC1	YOR179C	No	Subunit Of The Apt Subcomplex Of Cleavage And Polyadenylation Factor	Transcription From Rna Polymerase Ii Promoter
IES2	YNL215W	No	Protein That Associates With The Ino80 Chromatin Remodeling Complex	Biological_Process
TPM2	YIL138C	No	Minor Isoform Of Tropomyosin	Cytoskeleton Organization
AIM29	YKR074W	No	Putative Protein Of Unknown Function	Biological_Process
PBS2	YJL128C	No	Map Kinase Kinase Of The Hog Signaling Pathway	Signaling
WHI3	YNL197C	No	Rna Binding Protein That Sequesters Cln3 Mrna In Cytoplasmic Foci	Miscellaneous
UBP7	YIL156W	No	Ubiquitin-Specific Protease That Cleaves Ubiquitin-Protein Fusions	Protein Modification By Small Protein Conjugation Or Removal
AVO2	YMR068W	No	Component Of A Complex Containing The Tor2P Kinase And Other Proteins	Signaling
SMA2	YML066C	No	Meiosis-Specific Prospore Membrane Protein	Meiotic Cell Cycle
PEX1	YKL197C	No	Aaa-Peroxin	Signaling
MSL1	YIR009W	No	U2B Component Of U2 Snrnp	Miscellaneous
AIP1	YMR092C	No	Actin Cortical Patch Component	Protein Complex Biogenesis
RPL43A	YPR043W	No	Ribosomal 60S Subunit Protein L43A	Miscellaneous
DOA1	YKL213C	No	Wd Repeat Protein Required For Ubiquitin-Mediated Protein Degradation	Cellular Response To DNA Damage Stimulus
RNH201	YNL072W	No	Ribonuclease H2 Catalytic Subunit	Miscellaneous
MSN1	YOL116W	No	Transcriptional Activator	Transcription From Rna Polymerase Ii Promoter
PHO88	YBR106W	No	Probable Membrane Protein	Miscellaneous
NAP1	YKR048C	No	Histone Chaperone	Transcription From Rna Polymerase Ii Promoter
INP52	YNL106C	No	Polyphosphatidylinositol Phosphatase	Lipid Metabolic Process
CAF130	YGR134W	No	Subunit Of The Ccr4-Not Transcriptional Regulatory Complex	Transcription From Rna Polymerase Ii Promoter
SLI15	YBR156C	No	Subunit Of The Conserved Chromosomal Passenger Complex (Cpc)	Regulation Of Cell Cycle
RMD5	YDR255C	No	Component Of Gid Complex That Confers Ubiquitin Ligase (U3) Activity	Protein Modification By Small Protein Conjugation Or Removal
PIL1	YGR086C	No	Primary Protein Component Of Eisosomes	Protein Phosphorylation
GIM5	YML094W	No	Subunit Of The Heterohexameric Cochaperone Prefoldin Complex	Transcription From Rna Polymerase Ii Promoter
NHP10	YDL002C	No	Protein Related To Mammalian High Mobility Group Proteins	Chromatin Organization
SSD1	YDR293C	No	Translational Repressor With A Role In Polar Growth And Wall Integrity	Miscellaneous
TOF2	YKR010C	No	Protein Required For Rdna Silencing And Mitotic Rdna Condensation	Mitotic Cell Cycle
	YML108W	No	Protein Of Unknown Function	Biological_Process
SLC1	YDL052C	No	1-Acyl-Sn-Glycerol-3-Phosphate Acyltransferase	Lipid Metabolic Process
IPK1	YDR315C	No	Inositol 1,3,4,5,6-Pentakisphosphate 2-Kinase	Miscellaneous
PTC4	YBR125C	No	Cytoplasmic Type 2C Protein Phosphatase (Pp2C)	Miscellaneous
MUB1	YMR100W	No	Mynd Domain-Containing Protein	Protein Modification By Small Protein Conjugation Or Removal
RPL13A	YDL082W	No	Ribosomal 60S Subunit Protein L13A	Miscellaneous
MSN5	YDR335W	No	Karyopherin	Miscellaneous
SAF1	YBR280C	No	F-Box Protein Involved In Proteasome-Dependent Degradation Of Aah1P	Proteolysis Involved In Cellular Protein Catabolic Process
PKR1	YMR123W	No	V-Atpase Assembly Factor	Protein Complex Biogenesis
LR54	YDR439W	No	Nucleolar Protein That Forms A Complex With Csm1P	Mitotic Cell Cycle
CS26	YIL036W	No	Basic Leucine Zipper (Bzip) Transcription Factor, In Atf/Creb Family	Transcription From Rna Polymerase Ii Promoter
SED4	YCR067C	No	Integral Er Membrane Protein That Stimulates Sar1P Gtpase Activity	Protein Complex Biogenesis
RLF2	YPR018W	No	Largest Subunit (P90) Of The Chromatin Assembly Complex (Caf-1)	Chromatin Organization
PKH3	YDR466W	No	Protein Kinase With Similarity To Mammalian Pdk1 And Yeast Pkh1P/Phk2P	Signaling
DFG10	YIL049W	No	Probable Polyprenol Reductase	Lipid Metabolic Process
HCR1	YLR192C	No	Eif3J Component Of Translation Initiation Factor 3 (Eif3)	Miscellaneous
MAK3	YPR051W	No	Catalytic Subunit Of The Natc Type N-Terminal Acetyltransferase	Miscellaneous
PKH1	YDR490C	No	Serine/Threonine Protein Kinase	Signaling
PHO80	YOL001W	No	Cyclin	Transcription From Rna Polymerase Ii Promoter
CH55	YLR330W	No	Component Of The Exomer Complex	Mitotic Cell Cycle
	YDR061W	No	Protein With Similarity To Abc Transporter Family Members	Biological_Process
LGE1	YPL055C	No	Protein Of Unknown Function	Chromatin Organization
MDM12	YOL009C	No	Mitochondrial Outer Membrane Protein	Protein Complex Biogenesis
BUD8	YLR353W	No	Protein Involved In Bud-Site Selection	Mitotic Cell Cycle
PPH3	YDR075W	No	Catalytic Subunit Of Protein Phosphatase Pp4 Complex	Cellular Response To DNA Damage Stimulus
SSN3	YPL042C	No	Cyclin-Dependent Protein Kinase	Transcription From Rna Polymerase Ii Promoter
TLG2	YOL018C	No	Syntaxin-Like T-Snare	Protein Targeting
ROM2	YLR371W	No	Gdp/Gtp Exchange Factor (Gef) For Rho1P And Rho2P	Signaling
GIS1	YDR096W	No	Histone Demethylase And Transcription Factor	Transcription From Rna Polymerase Ii Promoter
CHL1	YPL008W	No	Probable DNA Helicase	Mitotic Cell Cycle
PEX15	YOL044W	No	Tail-Anchored Type Ii Integral Peroxisomal Membrane Protein	Signaling
VAC14	YLR386W	No	Enzyme Regulator	Lipid Metabolic Process
DPB4	YDR121W	No	Subunit Of DNA Pol Epsilon And Of Isw2 Chromatin Accessibility Complex	Chromatin Organization
MSS18	YPR134W	No	Nuclear Encoded Protein Needed For Splicing Of Mitochondrial Intron	Miscellaneous
MET22	YOL064C	No	Bisphosphate-3'-Nucleotidase	Miscellaneous
RPN13	YLR421C	No	Subunit Of The 19S Regulatory Particle Of The 26S Proteasome Lic	Proteolysis Involved In Cellular Protein Catabolic Process
MKC7	YDR144C	No	Gpi-Anchored Aspartyl Protease	Miscellaneous
VP54	YPR173C	No	Aaa-Atpase Involved In Multivesicular Body (Mvb) Protein Sorting	Protein Complex Biogenesis
HF11	YPL254W	No	Adaptor Protein Required For Structural Integrity Of The Saga Complex	Transcription From Rna Polymerase Ii Promoter
RPS28B	YLR264W	No	Protein Component Of The Small (40S) Ribosomal Subunit	Miscellaneous
RPP2B	YDR382W	No	Ribosomal Protein P2 Beta	Protein Phosphorylation
RMD8	YFR048W	No	Cytosolic Protein Required For Sporulation	Biological_Process
THI6	YPL214C	No	Thiamine-Phosphate Diphosphorylase And Hydroxyethylthiazole Kinase	Miscellaneous
RPS30A	YLR287C-A	No	Protein Component Of The Small (40S) Ribosomal Subunit	Miscellaneous
SXM1	YDR395W	No	Nuclear Transport Factor (Karyopherin)	Miscellaneous
SCT1	YBL011W	No	Glycerol 3-Phosphate/Dihydroxyacetone Phosphate Sn-1 Acyltransferase	Lipid Metabolic Process
MNR1	YBL184C	No	Rna-Binding Protein That May Be Involved In Translational Regulation	Chromatin Organization
MMS22	YLR320W	No	Subunit Of E3 Ubiquitin Ligase Complex Involved In Replication Repair	Cellular Response To DNA Damage Stimulus
GIM4	YEL003W	No	Subunit Of The Heterohexameric Cochaperone Prefoldin Complex	Protein Complex Biogenesis
PSY4	YBL046W	No	Regulatory Subunit Of Protein Phosphatase Pp4	Cellular Response To DNA Damage Stimulus
SET6	YPL165C	No	Set Domain Protein Of Unknown Function	Biological_Process
CWC15	YDR163W	No	Non-Essential Protein Involved In Pre-Mrna Splicing	Miscellaneous
GDA1	YEL042W	No	Guanosine Diphosphatase Located In The Golgi	Carbohydrate Metabolic Process
RPS8A	YBL072C	No	Protein Component Of The Small (40S) Ribosomal Subunit	Miscellaneous
FRK1	YPL141C	No	Protein Kinase Of Unknown Cellular Role	Protein Phosphorylation
NUP42	YDR192C	No	Fg-Nucleoporin Component Of Central Core Of The Nuclear Pore Complex	Protein Targeting
CIN8	YEL061C	No	Kinesin Motor Protein	Mitotic Cell Cycle
	YBL086C	No	Protein Of Unknown Function	Biological_Process
VPS30	YPL120W	No	Subunit Of Phosphatidylinositol (Ptdins) 3-Kinase Complexes I And Ii	Protein Targeting
RTN1	YDR233C	No	Reticulon Protein	Protein Complex Biogenesis
ISC1	YER019W	No	Inositol Phosphosphingolipid Phospholipase C	Lipid Metabolic Process
PUF4	YGL014W	No	Member Of The Puf Protein Family	Chromatin Organization
SSE1	YPL106C	No	Atpase Component Of Heat Shock Protein Hsp90 Chaperone Complex	Miscellaneous
KEX1	YGL203C	No	Cell Death Protease Essential For Hypochlorite-Induced Apoptosis	Miscellaneous
JHD1	YER051W	No	JmjC Domain Family Histone Demethylase Specific For H3-K36	Chromatin Organization
SCW11	YGL028C	No	Cell Wall Protein With Similarity To Glucanases	Miscellaneous
	YJL055W	No	Putative Protein Of Unknown Function	Response To Chemical
HUR1	YGL168W	No	Protein Of Unknown Function	Miscellaneous
RPS14A	YCR031C	No	Protein Component Of The Small (40S) Ribosomal Subunit	Miscellaneous
GYP8	YFL027C	No	Gtpase-Activating Protein For Yeast Rab Family Members	Miscellaneous
SNX4	YJL036W	No	Sorting Nexin	Protein Targeting
SWI4	YER111C	No	DNA Binding Component Of The Sbf Complex (Swi4P-Swi6P)	Transcription From Rna Polymerase Ii Promoter
	YCR061W	No	Protein Of Unknown Function	Miscellaneous
SDS3	YIL084C	No	Component Of The Rpd3L Histone Deacetylase Complex	Transcription From Rna Polymerase Ii Promoter
HSE1	YHL002W	No	Subunit Of The Endosomal Vps27P-Hse1P Complex	Protein Targeting
SAK1	YER129W	No	Upstream Serine/Threonine Kinase For The Snf1 Complex	Protein Phosphorylation
SRB8	YCR081W	No	Subunit Of The Rna Polymerase Ii Mediator Complex	Transcription From Rna Polymerase Ii Promoter

TAF12	YDR145W	Yes	Subunit (61/68 Kda) Of Tfiid And Saga Complexes	Transcription From Rna Polymerase Ii Promoter
HTD2	YHR067W	No	Mitochondrial 3-Hydroxyacyl-Thioester Dehydratase	Lipid Metabolic Process
SPT2	YER161C	No	Protein Involved In Negative Regulation Of Transcription	Transcription From Rna Polymerase Ii Promoter
APS3	YJL024C	No	Small Subunit Of The Clathrin-Associated Adaptor Complex Ap-3	Protein Targeting
CDC27	YBL084C	Yes	Subunit Of The Anaphase-Promoting Complex/Cyclosome (Apc/C)	Protein Modification By Small Protein Conjugation Or Removal
EMC2	YJR088C	No	Member Of Conserved Er Transmembrane Complex	Miscellaneous
BMH1	YER177W	No	14-3-3 Protein, Major Isoform	Transcription From Rna Polymerase Ii Promoter
ISY1	YJR050W	No	Member Of The Nineteen Complex (Ntc)	Miscellaneous
RPB3	YIL021W	Yes	Rna Polymerase Ii Third Largest Subunit B44	Transcription From Rna Polymerase Ii Promoter
NFT1	YKR103W	No	Putative Transporter Of The Mrp Subfamily	Miscellaneous
DJP1	YIR004W	No	Cytosolic J-Domain-Containing Protein	Protein Targeting
UBP1	YDL122W	No	Ubiquitin-Specific Protease	Protein Modification By Small Protein Conjugation Or Removal
TFB3	YDR460W	Yes	Subunit Of Tfiih And Nucleotide Excision Repair Factor 3 Complexes	Transcription From Rna Polymerase Ii Promoter
SST2	YLR452C	No	Gtpase-Activating Protein For Gpa1P	Response To Chemical
DEG1	YFL001W	No	Trna:Pseudouridine Synthase	Miscellaneous
UGA3	YDL170W	No	Transcriptional Activator For Gaba-Dependent Induction Of Gaba Genes	Transcription From Rna Polymerase Ii Promoter
TAF4	YMR005W	Yes	Tfiid Subunit (48 Kda)	Transcription From Rna Polymerase Ii Promoter
MOG1	YJR074W	No	Conserved Nuclear Protein That Interacts With Gtp-Gsp1P	Protein Targeting
VRP1	YLR337C	No	Proline-Rich Actin-Associated Protein	Mitotic Cell Cycle
HDA1	YNL021W	No	Putative Catalytic Subunit Of A Class Ii Histone Deacetylase Complex	Transcription From Rna Polymerase Ii Promoter
POL2	YNL262W	Yes	Catalytic Subunit Of Dna Polymerase (Ii) Epsilon	Mitotic Cell Cycle
MNS1	YJR131W	No	Alpha-1,2-Mannosidase	Proteolysis Involved In Cellular Protein Catabolic Process
GIM3	YNL153C	No	Subunit Of The Heterohexameric Cochaperone Prefoldin Complex	Transcription From Rna Polymerase Ii Promoter
YIP3	YNL044W	No	Protein Localized To Copii Vesicles	Golgi Vesicle Transport
CDC20	YGL116W	Yes	Activator Of Anaphase-Promoting Complex/Cyclosome (Apc/C)	Mitotic Cell Cycle
SPE4	YLR146C	No	Spermine Synthase	Miscellaneous
BUD31	YCR063W	No	Component Of The Sf3B Subcomplex Of The U2 Snrnp	Mitotic Cell Cycle
SSK2	YNR031C	No	Map Kinase Kinase Kinase Of Hog1 Mitogen-Activated Signaling Pathway	Regulation Of Organelle Organization
TAF7	YMR227C	Yes	Tfiid Subunit (67 Kda)	Transcription From Rna Polymerase Ii Promoter
ACK1	YDL203C	No	Protein That Functions In The Cell Wall Integrity Pathway	Signaling
VMA1	YDL185W	No	Subunit A Of The V1 Peripheral Membrane Domain Of V-Atpase	Dna Recombination
RTG3	YBL103C	No	Bhh/Zip Transcription Factor For Retrograde (Rtg) And Tor Pathways	Transcription From Rna Polymerase Ii Promoter
RPB8	YOR224C	Yes	Rna Polymerase Subunit Abc14.5	Transcription From Rna Polymerase Ii Promoter
GCS1	YDL226C	No	Adp-Ribosylation Factor Gtpase Activating Protein (Arf Gap)	Cytoskeleton Organization
CGR1	YGL029W	No	Protein Involved In Nucleolar Integrity And Processing Of Pre-Rrna	Miscellaneous
OLA1	YBR025C	No	P-Loop Atpase With Similarity To Human Ola1 And Bacterial Ychf	Biological_Process
CDC34	YDR054C	Yes	Ubiquitin-Conjugating Enzyme (E2)	Mitotic Cell Cycle
SWC3	YAL011W	No	Protein Of Unknown Function	Chromatin Organization
OCAs	YHL029C	No	Cytoplasmic Protein Required For Replication Of Brome Mosaic Virus	Biological_Process
ZDS1	YMR273C	No	Protein With A Role In Regulating Swe1P-Dependent Polarized Growth	Mitotic Cell Cycle
SMY1	YKL079W	No	Protein That Interacts With Myo2P	Miscellaneous
SWD1	YAR003W	No	Subunit Of The Compass (Set1C) Complex	Chromatin Organization
YAP3	YHL009C	No	Basic Leucine Zipper (Bzip) Transcription Factor	Transcription From Rna Polymerase Ii Promoter
RIT1	YMR283C	No	2'-O-Ribosyl Phosphate Transferase	Miscellaneous
HAP4	YKL109W	No	Transcription Factor	Transcription From Rna Polymerase Ii Promoter
SPA2	YLL021W	No	Component Of The Polarisome	Mitotic Cell Cycle
MSC7	YHR039C	No	Protein Of Unknown Function	Organelle Fission
UBP15	YMR304W	No	Ubiquitin-Specific Protease Involved In Protein Deubiquitination	Protein Modification By Small Protein Conjugation Or Removal
DBR1	YKL149C	No	Rna Lariat Debranching Enzyme	Miscellaneous
BRE2	YLR015W	No	Subunit Of Compass (Set1C) Complex	Chromatin Organization
NAM8	YHR086W	No	Rna Binding Protein, Component Of The U1 Snrnp Protein	Miscellaneous
SKP2	YNL311C	No	F-Box Protein Of Unknown Function	Miscellaneous
ACB1	YGR037C	No	Acy-Coa-Binding Protein	Miscellaneous
EMP70	YLR083C	No	Protein With A Role In Cellular Adhesion And Filamentous Growth	Miscellaneous
CHS7	YHR142W	No	Protein Of Unknown Function	Carbohydrate Metabolic Process
RIM21	YNL294C	No	Ph Sensor Molecule, Component Of The Rim101 Pathway	Meiotic Cell Cycle
SLX9	YGR081C	No	Protein Required For Pre-Rrna Processing	Miscellaneous
APC9	YLR102C	No	Subunit Of The Anaphase-Promoting Complex/Cyclosome (Apc/C)	Chromatin Organization
OYE2	YHR179W	No	Conserved NADPH Oxidoreductase Containing Flavin Mononucleotide (Fmn)	Miscellaneous
TEX1	YNL253W	No	Protein Involved In Mrna Export	Miscellaneous
CLB6	YGR109C	No	B-Type Cyclin Involved In Dna Replication During S Phase	Mitotic Cell Cycle
CMP2	YML057W	No	Calcineurin A	Response To Chemical
STP22	YLC008C	No	Component Of The Escrt-I Complex	Protein Modification By Small Protein Conjugation Or Removal
AHC1	YOR023C	No	Subunit Of The Ada Histone Acetyltransferase Complex	Chromatin Organization
TRS33	YOR115C	No	One Of 10 Subunits Of The Transport Protein Particle (Trapp) Complex	Protein Complex Biogenesis
USA1	YML029W	No	Scaffold Subunit Of The Hrd1P Ubiquitin Ligase	Protein Complex Biogenesis
SRO9	YCL037C	No	Cytoplasmic Rna-Binding Protein	Miscellaneous
HIR2	YOR038C	No	Subunit Of Hir Nucleosome Assembly Complex	Transcription From Rna Polymerase Ii Promoter
SLP1	YOR154W	No	Glycosylated Integral Er Membrane Protein Of Unknown Function	Miscellaneous
ERG6	YML008C	No	Delta(24)-Sterol C-Methyltransferase	Lipid Metabolic Process
POL4	YCR014C	No	Dna Polymerase Iv	Cellular Response To Dna Damage Stimulus
YNG1	YOR064C	No	Subunit Of The Nua3 Histone Acetyltransferase Complex	Chromatin Organization
ULS1	YOR191W	No	Protein Involved In Proteolytic Control Of Sumoylated Substrates	Chromatin Organization
SOK2	YMR016C	No	Nuclear Protein That Negatively Regulates Pseudohyphal Differentiation	Miscellaneous
ACE2	YLR131C	No	Transcription Factor Required For Septum Destruction After Cytokinesis	Transcription From Rna Polymerase Ii Promoter
SKI7	YOR076C	No	Coupling Protein For The Ski Complex And Cytoplasmic Exosome	Miscellaneous
MK11	YOR231W	No	Mapkk Involved In The Protein Kinase C Signaling Pathway	Signaling
IMP2	YMR035W	No	Catalytic Subunit Of Mitochondrial Inner Membrane Peptidase Complex	Protein Targeting
	YLR177W	No	Putative Protein Of Unknown Function	Biological_Process
VPS21	YOR089C	No	Endosomal Rab Family Gtpase	Protein Targeting
HUA2	YOR284W	No	Cytoplasmic Protein Of Unknown Function	Biological_Process
RPS16A	YMR143W	No	Protein Component Of The Small (40S) Ribosomal Subunit	Miscellaneous
RPL37A	YLR185W	No	Ribosomal 60S Subunit Protein L37A	Miscellaneous
ISW2	YOR304W	No	Atp-Dependent Dna Translocase Involved In Chromatin Remodeling	Transcription From Rna Polymerase Ii Promoter
PEX17	YNL214W	No	Peroxisomal Membrane Peroxin And Subunit Of Docking Complex	Protein Complex Biogenesis
REV7	YIL139C	No	Accessory Subunit Of Dna Polymerase Zeta	Cellular Response To Dna Damage Stimulus
MSA2	YKR077W	No	Putative Transcriptional Activator	Transcription From Rna Polymerase Ii Promoter
MLP1	YKR095W	No	Myosin-Like Protein Associated With The Nuclear Envelope	Transcription From Rna Polymerase Ii Promoter
CHS1	YNL192W	No	Chitin Synthase I	Miscellaneous
BNR1	YIL159W	No	Formin	Protein Complex Biogenesis
MOT3	YMR070W	No	Transcriptional Repressor And Activator With Two C2-H2 Zinc Fingers	Transcription From Rna Polymerase Ii Promoter
POP2	YNR052C	No	Rnase Of The Dedd Superfamily	Transcription From Rna Polymerase Ii Promoter
LOS1	YKL205W	No	Nuclear Pore Protein	Miscellaneous
SNF3	YDL194W	No	Plasma Membrane Low Glucose Sensor, Regulates Glucose Transport	Response To Chemical
HXT17	YNR072W	No	Hexose Transporter	Miscellaneous
SPT7	YBR081C	No	Subunit Of The Saga Transcriptional Regulatory Complex	Chromatin Organization
VPS1	YKR001C	No	Dynamin-Like Gtpase Required For Vacuolar Sorting	Organelle Fission
MKS1	YNL076W	No	Pleiotropic Negative Transcriptional Regulator	Transcription From Rna Polymerase Ii Promoter
DYN2	YDR424C	No	Cytoplasmic Light Chain Dynein, Microtubule Motor Protein	Mitotic Cell Cycle
IML3	YBR107C	No	Outer Kinetochores Protein And Component Of The Ctf19 Complex	Mitotic Cell Cycle
DYN1	YKR054C	No	Cytoplasmic Heavy Chain Dynein	Mitotic Cell Cycle
YAF9	YNL107W	No	Subunit Of Nua4 Histone H4 Acetyltransferase And Swr1 Complexes	Chromatin Organization
SNF6	YHL025W	No	Subunit Of The Swi/Snf Chromatin Remodeling Complex	Transcription From Rna Polymerase Ii Promoter
IFA38	YBR159W	No	Microsomal Beta-Keto-Reductase	Lipid Metabolic Process
RKM4	YDR257C	No	Ribosomal Lysine Methyltransferase	Miscellaneous

NNF2	YGR089W	No	Protein That Exhibits Physical And Genetic Interactions With Rpb8P	Biological_Process
RAD10	YML095C	No	Single-Stranded DNA Endonuclease (With Rad1P)	Cellular Response To DNA Damage Stimulus
PTC1	YDL006W	No	Type 2C Protein Phosphatase (Pp2C)	Response To Chemical
DPL1	YDR294C	No	Dihydrosphingosine Phosphate Lyase	Signaling
IRS4	YKR019C	No	Eh Domain-Containing Protein	Signaling
NAB6	YML117W	No	Putative Rna-Binding Protein	Biological_Process
MBP1	YDL056W	No	Transcription Factor	Transcription From Rna Polymerase Ii Promoter
MCM21	YDR318W	No	Component Of The Kinetochore Sub-Complex Coma	Mitotic Cell Cycle
CCZ1	YBR131W	No	Protein Involved In Vacuolar Assembly	Protein Targeting
	YMR102C	No	Protein Of Unknown Function	Biological_Process
RPS16B	YDL083C	No	Protein Component Of The Small (40S) Ribosomal Subunit	Miscellaneous
INP51	YIL002C	No	Phosphatidylinositol 4,5-Bisphosphate 5-Phosphatase	Lipid Metabolic Process
APM3	YBR288C	No	Mu3-Like Subunit Of The Clathrin Associated Protein Complex (Ap-3)	Protein Targeting
SAS2	YMR127C	No	Histone Acetyltransferase (Hat) Catalytic Subunit Of The Sas Complex	Chromatin Organization
DOT1	YDR440W	No	Nucleosomal Histone H3-Lys79 Methylase	Mitotic Cell Cycle
PRM2	YIL037C	No	Pheromone-Regulated Protein	Miscellaneous
TUP1	YCR084C	No	General Repressor Of Transcription	Transcription From Rna Polymerase Ii Promoter
CSR2	YPR030W	No	Nuclear Ubiquitin Protein Ligase Binding Protein	Transcription From Rna Polymerase Ii Promoter
SDC1	YDR469W	No	Subunit Of The Compass (Set1C) Complex	Chromatin Organization
SEC28	YIL076W	No	Epsilon-Cop Subunit Of The Coatomer	Golgi Vesicle Transport
DCR2	YLR361C	No	Phosphoesterase	Mitotic Cell Cycle
NHP6A	YPR052C	No	High-Mobility Group (Hmg) Protein, Binds To And Remodels Nucleosomes	Transcription From Rna Polymerase Ii Promoter
PUF6	YDR496C	No	Pumilio-Homology Domain Protein	Miscellaneous
PRK1	YIL095W	No	Protein Serine/Threonine Kinase	Cytoskeleton Organization
YMD8	YML038C	No	Putative Nucleotide Sugar Transporter	Miscellaneous
ROX1	YPR065W	No	Heme-Dependent Repressor Of Hypoxic Genes	Transcription From Rna Polymerase Ii Promoter
GNP1	YDR508C	No	High-Affinity Glutamine Permease	Miscellaneous
PLB3	YOL011W	No	Phospholipase B (Lysophospholipase) Involved In Lipid Metabolism	Lipid Metabolic Process
RSC2	YLR357W	No	Component Of The Rsc Chromatin Remodeling Complex	Transcription From Rna Polymerase Ii Promoter
RAD55	YDR076W	No	Protein That Stimulates Strand Exchange	Cellular Response To DNA Damage Stimulus
	YPL041C	No	Protein Of Unknown Function Involved In Maintenance Of Telomere Length	Biological_Process
TAT2	YOL020W	No	High Affinity Tryptophan And Tyrosine Permease	Miscellaneous
SUR4	YLR372W	No	Elongase	Lipid Metabolic Process
MSH6	YDR097C	No	Protein Required For Mismatch Repair In Mitosis And Meiosis	Cellular Response To DNA Damage Stimulus
HAT1	YPL001W	No	Catalytic Subunit Of The Hat1P-Hat2P Histone Acetyltransferase Complex	Chromatin Organization
PSK2	YOL045W	No	Pas-Domain Containing Serine/Threonine Protein Kinase	Protein Phosphorylation
RPS29A	YLR388W	No	Protein Component Of The Small (40S) Ribosomal Subunit	Miscellaneous
KIN1	YDR122W	No	Serine/Threonine Protein Kinase Involved In Regulation Of Exocytosis	Protein Phosphorylation
CTF4	YPR135W	No	Chromatin-Associated Protein	Mitotic Cell Cycle
INP54	YOL065C	No	Phosphatidylinositol 4,5-Bisphosphate 5-Phosphatase	Lipid Metabolic Process
ECM22	YLR228C	No	Sterol Regulatory Element Binding Protein	Transcription From Rna Polymerase Ii Promoter
SWI5	YDR146C	No	Transcription Factor That Recruits Mediator And Swi/Snf Complexes	Transcription From Rna Polymerase Ii Promoter
	YPR174C	No	Protein Of Unknown Function	Biological_Process
VIK1	YPL253C	No	Protein That Forms A Kinesin-14 Heterodimeric Motor With Kar3P	Mitotic Cell Cycle
NEJ1	YLR265C	No	Protein Involved In Regulation Of Nonhomologous End Joining	Cellular Response To DNA Damage Stimulus
NKP1	YDR383C	No	Central Kinetochore Protein And Subunit Of The Ctf19 Complex	Biological_Process
HXK1	YFR053C	No	Hexokinase Isoenzyme 1	Carbohydrate Metabolic Process
LEA1	YPL213W	No	Component Of U2 Snrnp Complex	Miscellaneous
GUF1	YLR289W	No	Mitochondrial Matrix Gtpase	Miscellaneous
SI21	YDR409W	No	Sumo/Smr3 Ligase	Protein Modification By Small Protein Conjugation Or Removal
FUS3	YBL016W	No	Mitogen-Activated Serine/Threonine Protein Kinase Involved In Mating	Response To Chemical
CTI6	YPL181W	No	Component Of The Rpd3L Histone Deacetylase Complex	Miscellaneous
NUM1	YDR150W	No	Protein Required For Nuclear Migration	Organelle Fission
MIT1	YEL007W	No	Transcriptional Regulator Of Pseudohyphal Growth	Biological_Process
EDE1	YBL047C	No	Endocytic Protein	Response To Chemical
BEM4	YPL161C	No	Protein Involved In Establishment Of Cell Polarity And Bud Emergence	Signaling
HSP42	YDR171W	No	Small Heat Shock Protein (Shsp) With Chaperone Activity	Cytoskeleton Organization
	YEL043W	No	Predicted Cytoskeleton Protein Involved In Intracellular Signaling	Biological_Process
SSA3	YBL075C	No	Atpase Involved In Protein Folding And The Response To Stress	Protein Targeting
MKK2	YPL140C	No	Mapkk Involved In The Protein Kinase C Signaling Pathway	Signaling
UME6	YDR207C	No	Component Of The Rpd3L Histone Deacetylase Complex	Transcription From Rna Polymerase Ii Promoter
NPR2	YEL062W	No	Subunit Of Sea (Seh1-Associated), Npr2/3, And Iml1P Complexes	Response To Chemical
RPL23A	YBL087C	No	Ribosomal 60S Subunit Protein L23A	Miscellaneous
DBP1	YPL119C	No	Putative Atp-Dependent Rna Helicase Of The Dead-Box Protein Family	Miscellaneous
HOS2	YGL194C	No	Histone Deacetylase And Subunit Of Set3 And Rpd3L Complexes	Chromatin Organization
GPA2	YER020W	No	Nucleotide Binding Alpha Subunit Of The Heterotrimeric G Protein	Response To Chemical
KAP122	YGL016W	No	Karyopherin Beta	Protein Targeting
ELP4	YPL101W	No	Subunit Of Hexameric Recla-Like Atpase Elp456 Elongator Subcomplex	Transcription From Rna Polymerase Ii Promoter
VAM7	YGL212W	No	Vacuolar Snare Protein	Miscellaneous
HOM3	YER052C	No	Aspartate Kinase (L-Aspartate 4-P-Transferase)	Miscellaneous
RPL24A	YGL031C	No	Ribosomal 60S Subunit Protein L24A	Miscellaneous
PCH2	YBR186W	No	Hexameric Ring Atpase That Remodels Chromosome Axis Protein Hop1P	Organelle Fission
VID30	YGL227W	No	Central Component Of Gid Complex, Involved In Fbpase Degradation	Proteolysis Involved In Cellular Protein Catabolic Process
PTP3	YER075C	No	Phosphotyrosine-Specific Protein Phosphatase	Response To Chemical
TIF4632	YGL049C	No	Translation Initiation Factor Eif4G	Miscellaneous
MAD2	YJL030W	No	Component Of The Spindle-Assembly Checkpoint Complex	Mitotic Cell Cycle
BOI2	YER114C	No	Protein Implicated In Polar Growth, Functionally Redundant With Boi1P	Signaling
HCM1	YCR065W	No	Forkhead Transcription Factor	Transcription From Rna Polymerase Ii Promoter
GEF1	YJR040W	No	Voltage-Gated Chloride Channel	Miscellaneous
NEM1	YHR004C	No	Probable Catalytic Subunit Of Nem1P-Spo7P Phosphatase Holoenzyme	Lipid Metabolic Process
RTR1	YER139C	No	Ctd Phosphatase	Transcription From Rna Polymerase Ii Promoter
AHC2	YCR082W	No	Component Of The Ada Histone Acetyltransferase Complex	Chromatin Organization
APC4	YDR118W	Yes	Subunit Of The Anaphase-Promoting Complex/Cyclosome (Apc/C)	Protein Modification By Small Protein Conjugation Or Removal
PFS1	YHR185C	No	Sporulation Protein Required For Prospore Membrane Formation	Meiotic Cell Cycle
RAD4	YER162C	No	Protein That Recognizes And Binds Damaged DNA (With Rad23P) During Ner	Cellular Response To DNA Damage Stimulus
SPC1	YJR010C-A	No	Subunit Of The Signal Peptidase Complex (Spc)	Protein Targeting
TFG1	YGR186W	Yes	Tfiif (Transcription Factor Ii) Largest Subunit	Transcription From Rna Polymerase Ii Promoter
MCM22	YJR135C	No	Outer Kinetochore Protein And Component Of The Ctf3 Subcomplex	Mitotic Cell Cycle
PDA1	YER178W	No	E1 Alpha Subunit Of The Pyruvate Dehydrogenase (Pdh) Complex	Miscellaneous
RAD7	YJR052W	No	Protein That Binds Damaged DNA During Ner	Cellular Response To DNA Damage Stimulus
STH1	YIL126W	Yes	Atpase Component Of The Rsc Chromatin Remodeling Complex	Transcription From Rna Polymerase Ii Promoter
ATG17	YLR423C	No	Scaffold Protein Responsible For Phagophore Assembly Site Organization	Protein Phosphorylation
BRE1	YDL074C	No	E3 Ubiquitin Ligase	Transcription From Rna Polymerase Ii Promoter
HNT1	YDL125C	No	Adenosine 5'-Monophosphoramidase	Miscellaneous
RSC58	YLR033W	Yes	Component Of The Rsc Chromatin Remodeling Complex	Transcription From Rna Polymerase Ii Promoter
FMP27	YLR454W	No	Putative Protein Of Unknown Function	Biological_Process
MSH4	YFL003C	No	Protein Involved In Meiotic Recombination	Organelle Fission
AIR2	YDL175C	No	Rna-Binding Subunit Of The Tramp Nuclear Rna Surveillance Complex	Miscellaneous
CDC39	YCR093W	Yes	Component Of The Kinetochore-Associated Ndc80 Complex	Transcription From Rna Polymerase Ii Promoter
	YJR084W	No	Protein That Forms A Complex With Thp3P	Response To Chemical
BDF1	YLR399C	No	Protein Involved In Transcription Initiation	Chromatin Organization
SSN8	YNL025C	No	Cyclin-Like Component Of The Rna Polymerase Ii Holoenzyme	Transcription From Rna Polymerase Ii Promoter
NUT2	YPR168W	Yes	Subunit Of The Rna Polymerase Ii Mediator Complex	Transcription From Rna Polymerase Ii Promoter
SGM1	YJR134C	No	Protein Of Unknown Function	Biological_Process
MNN10	YDR245W	No	Subunit Of A Golgi Mannosyltransferase Complex	Carbohydrate Metabolic Process

SFB2	YNL049C	No	Component Of The Sec23P-Sfb2P Heterodimer Of The Copii Vesicle Coat	Protein Complex Biogenesis
CDC48	YDL126C	Yes	Aaa Atpase	Mitotic Cell Cycle
ERV41	YML067C	No	Protein Localized To Copii-Coated Vesicles	Golgi Vesicle Transport
YSY1	YJL004C	No	Integral Membrane Protein Of The Golgi	Protein Targeting
PPG1	YNR032W	No	Putative Serine/Threonine Protein Phosphatase	Carbohydrate Metabolic Process
FCP1	YMR277W	Yes	Carboxy-Terminal Domain (Ctd) Phosphatase	Transcription From Rna Polymerase Ii Promoter
RTN2	YDL204W	No	Reticulon Protein	Miscellaneous
ECM33	YBR078W	No	Gpi-Anchored Protein Of Unknown Function	Miscellaneous
HHT1	YBR010W	No	Histone H3	Mitotic Cell Cycle
ESA1	YOR244W	Yes	Catalytic Subunit Of The Histone Acetyltransferase Complex (Nua4)	Transcription From Rna Polymerase Ii Promoter
PTP1	YDL230W	No	Phosphotyrosine-Specific Protein Phosphatase	Miscellaneous
ROX3	YBL093C	No	Subunit Of The Rna Polymerase Ii Mediator Complex	Transcription From Rna Polymerase Ii Promoter
RPL4A	YBR031W	No	Ribosomal 60S Subunit Protein L4A	Miscellaneous
TAF3	YPL011C	Yes	Tfiid Subunit (47 Kda)	Transcription From Rna Polymerase Ii Promoter
MAF1	YDR005C	No	Highly Conserved Negative Regulator Of Rna Polymerase Iii	Transcription From Rna Polymerase Ii Promoter
PUS4	YNL292W	No	Pseudouridine Synthase	Miscellaneous
MUM2	YBR057C	No	Protein Essential For Meiotic DNA Replication And Sporulation	Organelle Fission
CDC23	YHR166C	Yes	Subunit Of The Anaphase-Promoting Complex/Cyclosome (Apc/C)	Protein Modification By Small Protein Conjugation Or Removal
BUD14	YAR014C	No	Protein Involved In Bud-Site Selection	Protein Complex Biogenesis
QCR10	YHR001W-A	No	Subunit Of The Ubiquinol-Cytochrome C Oxidoreductase Complex	Miscellaneous
YKU70	YMR284W	No	Subunit Of The Telomeric Ku Complex (Yku70P-Yku80P)	Chromatin Organization
KTI12	YKL110C	No	Protein That Plays A Role In Modification Of Trna Wobble Nucleosides	Transcription From Rna Polymerase Ii Promoter
SSA2	YLL024C	No	Atp-Binding Protein	Protein Targeting
SSF1	YHR066W	No	Constituent Of 66S Pre-Ribosomal Particles	Miscellaneous
GAS1	YMR307W	No	Beta-1,3-Glucanosyltransferase	Miscellaneous
ELF1	YKL160W	No	Transcription Elongation Factor With A Conserved Zinc Finger Domain	Transcription From Rna Polymerase Ii Promoter
POM34	YLR018C	No	Subunit Of The Transmembrane Ring Of The Nuclear Pore Complex (Npc)	Protein Complex Biogenesis
GGA2	YHR108W	No	Protein That Regulates Arf1P, Arf2P To Facilitate Golgi Trafficking	Protein Targeting
STB1	YNL309W	No	Protein With Role In Regulation Of Mbf-Specific Transcription At Start	Transcription From Rna Polymerase Ii Promoter
	YGR054W	No	Eukaryotic Initiation Factor (Eif) 2A	Miscellaneous
ARP6	YLR085C	No	Actin-Related Protein That Binds Nucleosomes	Chromatin Organization
MTG6	YHR151C	No	Protein Of Unknown Function	Biological_Process
MID1	YNL291C	No	N-Glycosylated Integral Membrane Protein Of The Er And Plasma Membrane	Miscellaneous
RPL11B	YGR085C	No	Ribosomal 60S Subunit Protein L11B	Miscellaneous
HOG1	YLR113W	No	Mitogen-Activated Protein Kinase Involved In Osmoregulation	Transcription From Rna Polymerase Ii Promoter
PTH1	YHR189W	No	One Of Two Mitochondrially-Localized Peptidyl-Trna Hydrolases	Miscellaneous
VP575	YML246W	No	Nap Family Histone Chaperone	Chromatin Organization
RPS23A	YGR118W	No	Ribosomal Protein 28 (Rp28) Of The Small (40S) Ribosomal Subunit	Miscellaneous
SPC2	YML055W	No	Subunit Of Signal Peptidase Complex	Protein Targeting
SFG29	YCL010C	No	Component Of The Hat/Core Module Of The Saga, Slik, And Ada Complexes	Transcription From Rna Polymerase Ii Promoter
HST3	YOR025W	No	Member Of The Sir2 Family Of Nad(+)-Dependent Protein Deacetylases	Chromatin Organization
LEO1	YOR123C	No	Component Of The Paf1 Complex	Transcription From Rna Polymerase Ii Promoter
TSA1	YML028W	No	Thioredoxin Peroxidase	Cellular Response To DNA Damage Stimulus
EMC1	YCL045C	No	Member Of Conserved Endoplasmic Reticulum Membrane Complex	Miscellaneous
CKB2	YOR039W	No	Beta' Regulatory Subunit Of Casein Kinase 2 (Ck2)	Cellular Response To DNA Damage Stimulus
NF1	YOR156C	No	Sumo E3 Ligase	Protein Modification By Small Protein Conjugation Or Removal
YAP1	YML007W	No	Basic Leucine Zipper (Bzip) Transcription Factor	Transcription From Rna Polymerase Ii Promoter
CWH43	YCR017C	No	Putative Sensor/Transporter Protein Involved In Cell Wall Biogenesis	Lipid Metabolic Process
CY1	YOR065W	No	Cytochrome C1	Miscellaneous
SLK19	YOR195W	No	Kinetochores-Associated Protein Required For Chromosome Segregation	Mitotic Cell Cycle
PEP8	YJL053W	No	Vacuolar Protein Component Of The Retromer	Miscellaneous
CKI1	YLR133W	No	Choline Kinase	Lipid Metabolic Process
BUD21	YOR078W	No	Component Of Small Ribosomal Subunit (Ssu) Processosome	Miscellaneous
KIN4	YOR233W	No	Serine/Threonine Protein Kinase	Mitotic Cell Cycle
MIH1	YMR036C	No	Protein Tyrosine Phosphatase Involved In Cell Cycle Control	Mitotic Cell Cycle
SAM1	YLR180W	No	S-Adenosylmethionine Synthetase	Miscellaneous
SNF2	YOR290C	No	Catalytic Subunit Of The Swi/Snf Chromatin Remodeling Complex	Transcription From Rna Polymerase Ii Promoter
MPD1	YOR288C	No	Member Of The Protein Disulfide Isomerase (Pdi) Family	Miscellaneous
NUP53	YMR153W	No	Fg-Nucleoporin Component Of Central Core Of Nuclear Pore Complex (Npc)	Mitotic Cell Cycle
MMR1	YLR190W	No	Phosphorylated Protein Of The Mitochondrial Outer Membrane	Miscellaneous
SLY41	YOR307C	No	Protein Involved In Er-To-Golgi Transport	Golgi Vesicle Transport
RCY1	YJL204C	No	F-Box Protein Involved In Recycling Endocytosed Proteins	Golgi Vesicle Transport
SPT21	YMR179W	No	Protein With A Role In Transcriptional Silencing	Transcription From Rna Polymerase Ii Promoter
ENT2	YLR206W	No	Epsin-Like Protein Required For Endocytosis And Actin Patch Assembly	Cytoskeleton Organization
RPL20B	YOR312C	No	Ribosomal 60S Subunit Protein L20B	Miscellaneous
RPS22A	YJL190C	No	Protein Component Of The Small (40S) Ribosomal Subunit	Miscellaneous
NPR1	YNL183C	No	Protein Kinase	Lipid Metabolic Process
SGN1	YIR001C	No	Cytoplasmic Rna-Binding Protein	Miscellaneous
IRC21	YMR073C	No	Putative Protein Of Unknown Function	Response To Chemical
	YPR022C	No	Putative Transcription Factor, As Suggested By Computational Analysis	Biological_Process
ADD66	YKL206C	No	Protein Involved In 20S Proteasome Assembly	Protein Complex Biogenesis
IOC3	YFR013W	No	Subunit Of The Isw1A Complex	Chromatin Organization
MSH2	YOL090W	No	Protein That Binds To DNA Mismatches	Cellular Response To DNA Damage Stimulus
UBC4	YBR082C	No	Ubiquitin-Conjugating Enzyme (E2)	Protein Modification By Small Protein Conjugation Or Removal
MEH1	YKR007W	No	Component Of The Ego And Gse Complexes	Miscellaneous
TPM1	YNL079C	No	Major Isoform Of Tropomyosin	Cytoskeleton Organization
VHR2	YER064C	No	Non-Essential Nuclear Protein	Miscellaneous
AIM3	YBR108W	No	Protein Interacting With Rvs167P	Protein Complex Biogenesis
RHO4	YKR055W	No	Non-Essential Small Gtpase	Regulation Of Organelle Organization
NCS2	YNL119W	No	Protein Required For Uridine Thiolation Of Lys(Uuu) And Glu(Uuc) Trnas	Protein Modification By Small Protein Conjugation Or Removal
SVP26	YHR181W	No	Integral Membrane Protein Of The Early Golgi Apparatus And Er	Carbohydrate Metabolic Process
TOS1	YBR162C	No	Covalently-Bound Cell Wall Protein Of Unknown Function	Biological_Process
SWM1	YDR260C	No	Subunit Of The Anaphase-Promoting Complex (Apc)	Mitotic Cell Cycle
DBF2	YGR092W	No	Ser/Thr Kinase Involved In Transcription And Stress Response	Organelle Fission
VP59	YML097C	No	Guanine Nucleotide Exchange Factor (Gef)	Protein Targeting
SLX5	YDL013W	No	Subunit Of The Slx5-Slx8 Sumo-Targeted Ubiquitin Ligase Complex	Cellular Response To DNA Damage Stimulus
SUR2	YDR297W	No	Sphinganine C4-Hydroxylase	Lipid Metabolic Process
SAP190	YKR028W	No	Protein That Forms A Complex With The Sit4P Protein Phosphatase	Mitotic Cell Cycle
	YML119W	No	Putative Protein Of Unknown Function	Biological_Process
RAD59	YDL059C	No	Protein Involved DNA Double-Strand Break Repair	Cellular Response To DNA Damage Stimulus
SWA2	YDR320C	No	Auxilin-Like Protein Involved In Vesicular Transport	Miscellaneous
TBS1	YBR150C	No	Putative Protein Of Unknown Function	Biological_Process
YKU80	YMR106C	No	Subunit Of The Telomeric Ku Complex (Yku70P-Yku80P)	Chromatin Organization
ASM4	YDL088C	No	Fg-Nucleoporin Component Of Central Core Of Nuclear Pore Complex (Npc)	Mitotic Cell Cycle
TIR3	YLO111W	No	Cell Wall Mannoprotein	Biological_Process
SNF5	YBR289W	No	Subunit Of The Swi/Snf Chromatin Remodeling Complex	Transcription From Rna Polymerase Ii Promoter
POM152	YMR129W	No	Glycoprotein Subunit Of Transmembrane Ring Of Nuclear Pore Complex	Protein Complex Biogenesis
SSN2	YDR443C	No	Subunit Of The Rna Polymerase Ii Mediator Complex	Transcription From Rna Polymerase Ii Promoter
TED1	YIL039W	No	Conserved Phosphoesterase Domain-Containing Protein	Golgi Vesicle Transport
ABP1	YCR088W	No	Actin-Binding Protein Of The Cortical Actin Cytoskeleton	Protein Complex Biogenesis
SRO7	YPR032W	No	Effector Of Rab Gtpase Sec4P	Signaling
PEX29	YDR479C	No	Peroxisomal Integral Membrane Peroxin	Miscellaneous
AIR1	YIL079C	No	Zinc Knuckle Protein	Miscellaneous
ARC18	YLR370C	No	Subunit Of The Arp2/3 Complex	Cytoskeleton Organization
SMK1	YPR054W	No	Middle Sporulation-Specific Mitogen-Activated Protein Kinase (Mapk)	Meiotic Cell Cycle

ITR1	YDR497C	No	Myo-Inositol Transporter	Miscellaneous
URM1	YIL008W	No	Ubiquitin-Like Protein Involved In Thiolation Of Cytoplasmic Trnas	Response To Chemical
VP571	YML041C	No	Nucleosome-Binding Component Of The Swr1 Complex	Chromatin Organization
HOS1	YPR068C	No	Class I Histone Deacetylase (Hdac) Family Member	Transcription From Rna Polymerase Ii Promoter
EMI1	YDR512C	No	Non-Essential Protein Of Unknown Function	Transcription From Rna Polymerase Ii Promoter
RPL34B	YIL052C	No	Ribosomal 60S Subunit Protein L34B	Miscellaneous
CSM3	YMR048W	No	Replication Fork Associated Factor	Mitotic Cell Cycle
OPY2	YPR075C	No	Integral Membrane Protein That Acts As A Membrane Anchor For Ste50F	Response To Chemical
CUE3	YGL110C	No	Protein Of Unknown Function	Biological_Process
MDM38	YOL027C	No	Mitochondrial Protein	Protein Complex Biogenesis
VID22	YLR373C	No	Glycosylated Integral Membrane Protein Localized To Plasma Membrane	Miscellaneous
BMH2	YDR099W	No	14-3-3 Protein, Minor Isoform	Mitotic Cell Cycle
ISR1	YPR106W	No	Predicted Protein Kinase	Biological_Process
GSH2	YOL049W	No	Glutathione Synthetase	Miscellaneous
ATP10	YLR393W	No	Assembly Factor For The F0 Sector Of Mitochondrial F1F0 Atp Synthase	Protein Complex Biogenesis
ECM18	YDR125C	No	Protein Of Unknown Function	Biological_Process
TAZ1	YPR140W	No	Lyso-Phosphatidylcholine Acyltransferase	Protein Complex Biogenesis
RTG1	YOL067C	No	Transcription Factor (Bhlh) Involved In Interorganelle Communication	Transcription From Rna Polymerase Ii Promoter
EST1	YLR233C	No	Tlc1 Rna-Associated Factor Involved In Telomere Length Regulation	Miscellaneous
GGA1	YDR358W	No	Golgi-Localized Protein With Homology To Gamma-Adaptin	Protein Targeting
SKI3	YPR189W	No	Ski Complex Component And Tpr Protein	Miscellaneous
GAL4	YPL248C	No	DNA-Binding Transcription Factor Required For Activating Gal Genes	Transcription From Rna Polymerase Ii Promoter
PDR8	YLR266C	No	Transcription Factor	Transcription From Rna Polymerase Ii Promoter
EFT2	YDR385W	No	Elongation Factor 2 (Ef-2), Also Encoded By Eft1	Miscellaneous
HSV2	YGR223C	No	Phosphatidylinositol 3,5-Bisphosphate-Binding Protein	Miscellaneous
PUS1	YPL212C	No	Trna:Pseudouridine Synthase	Miscellaneous
SEC72	YLR292C	No	Non-Essential Subunit Of Sec63 Complex	Protein Targeting
ERD1	YDR414C	No	Predicted Membrane Protein Required For Luminal Er Protein Retention	Carbohydrate Metabolic Process
PEP1	YBL017C	No	Type I Transmembrane Sorting Receptor For Multiple Vacuolar Hydrolases	Protein Targeting
TCO89	YPL180W	No	Subunit Of Torc1 (Tor1P Or Tor2P-Kog1P-Lst8P-Tco89P)	Signaling
ENT5	YDR153C	No	Protein Containing An N-Terminal Epsin-Like Domain	Golgi Vesicle Transport
VAC8	YEL013W	No	Phosphorylated And Palmitoylated Vacuolar Membrane Protein	Protein Targeting
PIN4	YBL051C	No	Protein Involved In G2/M Phase Progression And Response To DNA Damage	Mitotic Cell Cycle
TGS1	YPL157W	No	Trimethyl Guanidine Synthase, Conserved Nucleolar Methyl Transferase	Organelle Fission
ARG82	YDR173C	No	Inositol Polyphosphate Multikinase (Ipmk)	Transcription From Rna Polymerase Ii Promoter
FRD1	YEL047C	No	Soluble Fumarate Reductase	Response To Chemical
ATG8	YBL078C	No	Component Of Autophagosomes And Cvt Vesicles	Protein Targeting
UME1	YPL139C	No	Component Of Both The Rpd3S And Rpd3L Histone Deacetylase Complexes	Transcription From Rna Polymerase Ii Promoter
RAD9	YDR217C	No	DNA Damage-Dependent Checkpoint Protein	Transcription From Rna Polymerase Ii Promoter
AVT2	YEL064C	No	Putative Transporter	Miscellaneous
TEL1	YBL088C	No	Protein Kinase Primarily Involved In Telomere Length Regulation	Chromatin Organization
HOS3	YPL116W	No	Trichostatin A-Insensitive Homodimeric Histone Deacetylase (Hdac)	Transcription From Rna Polymerase Ii Promoter
GCN1	YGL195W	No	Positive Regulator Of The Gcn2P Kinase Activity	Miscellaneous
CHZ1	YER030W	No	Histone Chaperone For Htz1P/H2A-H2B Dimer	Chromatin Organization
CKB1	YGL019W	No	Beta Regulatory Subunit Of Casein Kinase 2 (Ck2)	Cellular Response To DNA Damage Stimulus
ATG21	YPL100W	No	Phosphoinositide Binding Protein	Protein Targeting
SKI8	YGL213C	No	Ski Complex Component And Wd-Repeat Protein	Organelle Fission
CEM1	YER061C	No	Mitochondrial Beta-Keto-Acyl Synthase	Lipid Metabolic Process
MIG1	YGL035C	No	Transcription Factor Involved In Glucose Repression	Transcription From Rna Polymerase Ii Promoter
AIM4	YBR194W	No	Protein Proposed To Be Associated With The Nuclear Pore Complex	Biological_Process
SHE10	YGL228W	No	Protein Involved In Outer Spore Wall Assembly	Meiotic Cell Cycle
GET2	YER083C	No	Subunit Of The Get Complex	Golgi Vesicle Transport
ERV14	YGL054C	No	Copii-Coated Vesicle Protein	Mitotic Cell Cycle
NGR1	YBR212W	No	Rna Binding Protein That Negatively Regulates Growth Rate	Miscellaneous
RTF1	YGL244W	No	Subunit Of Rnapii-Associated Chromatin Remodeling Paf1 Complex	Transcription From Rna Polymerase Ii Promoter
PEX4	YGR133W	No	Peroxisomal Ubiquitin Conjugating Enzyme	Protein Modification By Small Protein Conjugation Or Removal
SGF73	YGL066W	No	Saga Complex Subunit	Transcription From Rna Polymerase Ii Promoter
STP2	YHR006W	No	Transcription Factor	Transcription From Rna Polymerase Ii Promoter
PEA2	YER149C	No	Coiled-Coil Polarosome Protein	Mitotic Cell Cycle
CSM1	YCR086W	No	Nucleolar Protein That Mediates Homolog Segregation During Meiosis I	Mitotic Cell Cycle
TAF10	YDR167W	Yes	Subunit (145 Kda) Of Tfiid And Saga Complexes	Transcription From Rna Polymerase Ii Promoter
MDM31	YHR194W	Yes	Mitochondrial Protein That Have A Role In Phospholipid Metabolism	Lipid Metabolic Process
CHD1	YER164W	No	Chromatin Remodeler That Regulates Various Aspects Of Transcription	Transcription From Rna Polymerase Ii Promoter
	YJR011C	No	Putative Protein Of Unknown Function	Biological_Process
TFA1	YKL028W	Yes	Tfiie Large Subunit	Transcription From Rna Polymerase Ii Promoter
SRP40	YKR092C	No	Nucleolar Serine-Rich Protein	Miscellaneous
FAR3	YMR052W	No	Protein Of Unknown Function	Response To Chemical
BFA1	YJR053W	No	Component Of The Gtpase-Activating Bfa1P-Bub2P Complex	Mitotic Cell Cycle
CKS1	YBR135W	Yes	Cyclin-Dependent Protein Kinase Regulatory Subunit And Adaptor	Mitotic Cell Cycle
TUS1	YLR425W	No	Guanine Nucleotide Exchange Factor (Gef) That Modulate Rho1P Activity	Signaling
SNF1	YDR477W	No	Amp-Activated Serine/Threonine Protein Kinase	Protein Phosphorylation
RPP1B	YDL130W	No	Ribosomal Protein P1 Beta	Protein Phosphorylation
RGR1	YLR071C	Yes	Subunit Of The Rna Polymerase Ii Mediator Complex	Transcription From Rna Polymerase Ii Promoter
SAM37	YMR060C	No	Component Of The Sorting And Assembly Machinery (Sam) Complex	Protein Complex Biogenesis
BLM10	YFL007W	No	Proteasome Activator	Protein Complex Biogenesis
	YDL176W	No	Protein Of Unknown Function	Biological_Process
APC11	YDL008W	Yes	Catalytic Core Subunit, Anaphase-Promoting Complex/Cyclosome (Apc/C)	Protein Modification By Small Protein Conjugation Or Removal
IME1	YJR094C	No	Master Regulator Of Meiosis That Is Active Only During Meiotic Events	Transcription From Rna Polymerase Ii Promoter
DOC1	YGL240W	No	Processivity Factor	Mitotic Cell Cycle
CRZ1	YNL027W	No	Transcription Factor, Activates Transcription Of Stress Response Genes	Transcription From Rna Polymerase Ii Promoter
MET30	YIL046W	Yes	F-Box Protein Containing Five Copies Of The Wd40 Motif	Transcription From Rna Polymerase Ii Promoter
HOM6	YJR139C	No	Homoserine Dehydrogenase (L-Homoserine:Nadp Oxidoreductase)	Miscellaneous
LPD1	YFL018C	No	Dihydroipoamide Dehydrogenase	Miscellaneous
SWM2	YNR004W	No	Protein With A Role In Snrna And Snorna Cap Trimethylation	Miscellaneous
RPB11	YOL005C	Yes	Rna Polymerase Ii Subunit B12.5	Transcription From Rna Polymerase Ii Promoter
TCB3	YML072C	No	Cortical Er Protein Involved In Er-Plasma Membrane Tethering	Lipid Metabolic Process
MAD3	YJL013C	No	Subunit Of Spindle-Assembly Checkpoint Complex	Mitotic Cell Cycle
COQ2	YNR041C	No	Para Hydroxybenzoate Polyphenyl Transferase	Miscellaneous
MED4	YOR174W	Yes	Subunit Of The Rna Polymerase Ii Mediator Complex	Transcription From Rna Polymerase Ii Promoter
NOP6	YDL213C	No	Rna-Binding Protein Required For 40S Ribosomal Subunit Biogenesis	Miscellaneous
NAT1	YDL040C	No	Subunit Of Protein N-Terminal Acetyltransferase Nata	Miscellaneous
MNN2	YBR015C	No	Alpha-1,2-Mannosyltransferase	Carbohydrate Metabolic Process
HRT1	YOL133W	Yes	Ring-H2 Domain Core Subunit Of Multiple Ubiquitin Ligase Complexes	Mitotic Cell Cycle
OST4	YDL232W	No	Subunit Of The Oligosaccharyltransferase Complex Of The Er Lumen	Carbohydrate Metabolic Process
CYC8	YBR112C	No	General Transcriptional Co-Repressor	Transcription From Rna Polymerase Ii Promoter
HTM1	YBR034C	No	Nuclear Sam-Dependent Mono- And Asymmetric Methyltransferase	Transcription From Rna Polymerase Ii Promoter
APCS	YOR249C	Yes	Subunit Of The Anaphase-Promoting Complex/Cyclosome (Apc/C)	Chromatin Organization
GAL3	YDR009W	No	Transcriptional Regulator	Transcription From Rna Polymerase Ii Promoter
SAP30	YMR263W	No	Component Of Rpd3L Histone Deacetylase Complex	Transcription From Rna Polymerase Ii Promoter
UBP14	YBR058C	No	Ubiquitin-Specific Protease	Proteolysis Involved In Cellular Protein Catabolic Process
MED7	YOL135C	Yes	Subunit Of The Rna Polymerase Ii Mediator Complex	Transcription From Rna Polymerase Ii Promoter
FMP21	YBR269C	No	Putative Protein Of Unknown Function	Biological_Process
MRPL36	YBR122C	No	Mitochondrial Ribosomal Protein Of The Large Subunit	Miscellaneous
TAT1	YBR069C	No	Amino Acid Transporter For Valine, Leucine, Isoleucine, And Tyrosine	Miscellaneous
BST1	YFL025C	No	Gpi Inositol Deacylase Of The Endoplasmic Reticulum (Er)	Proteolysis Involved In Cellular Protein Catabolic Process

ENT4	YLL038C	No	Protein Of Unknown Function	Cytoskeleton Organization
NMD2	YHR077C	No	Protein Involved In The Nonsense-Mediated Mrna Decay (Nmd) Pathway	Miscellaneous
RPD3	YNL330C	No	Histone Deacetylase, Component Of Both The Rpd3S And Rpd3L Complexes	Transcription From Rna Polymerase Ii Promoter
TPK3	YKL166C	No	Camp-Dependent Protein Kinase Catalytic Subunit	Signaling
IRC25	YLR021W	No	Component Of A Heterodimeric Poc4P-Irc25P Chaperone	Protein Complex Biogenesis
UBA4	YHR111W	No	Protein That Activates Urm1P Before Urmylation	Response To Chemical
MSG5	YNL053W	No	Dual-Specificity Protein Phosphatase	Response To Chemical
RSC1	YGR056W	No	Component Of The Rsc Chromatin Remodeling Complex	Transcription From Rna Polymerase Ii Promoter
CSF1	YLR087C	No	Protein Required For Fermentation At Low Temperature	Miscellaneous
RTT107	YHR154W	No	Protein Implicated In Mms22-Dependent DNA Repair During S Phase	Cellular Response To DNA Damage Stimulus
CAF40	YNL288W	No	Component Of The Ccr4-Not Transcriptional Complex	Transcription From Rna Polymerase Ii Promoter
ASK10	YGR097W	No	Component Of Rna Polymerase Ii Holoenzyme	Transcription From Rna Polymerase Ii Promoter
AVL9	YLR114C	No	Conserved Protein Involved In Exocytic Transport From The Golgi	Golgi Vesicle Transport
RPN10	YHR200W	No	Non-Atpase Base Subunit Of The 19S Rp Of The 26S Proteasome	Proteolysis Involved In Cellular Protein Catabolic Process
RRP6	YOR001W	No	Nuclear Exosome Exonuclease Component	Miscellaneous
	YGR122W	No	Protein That May Be Involved In Ph Regulation	Transcription From Rna Polymerase Ii Promoter
GAL80	YML051W	No	Transcriptional Regulator Involved In The Repression Of Gal Genes	Transcription From Rna Polymerase Ii Promoter
GBP2	YCL011C	No	Poly(A+) Rna-Binding Protein	Miscellaneous
BUB3	YOR026W	No	Kinetochore Checkpoint Wd40 Repeat Protein	Mitotic Cell Cycle
UBP2	YOR124C	No	Ubiquitin-Specific Protease	Protein Modification By Small Protein Conjugation Or Removal
OST6	YML019W	No	Subunit Of The Oligosaccharyltransferase Complex Of The Er Lumen	Protein Complex Biogenesis
APA1	YCL050C	No	Ap4A Phosphorylase	Miscellaneous
CUE5	YOR042W	No	Ubiquitin-Binding Protein	Biological_Process
SEY1	YOR165W	No	Dynamin-Like Gtpase That Mediates Homotypic Er Fusion	Miscellaneous
YPT7	YML001W	No	Rab Family Gtpase	Regulation Of Organelle Organization
MAK32	YCR019W	No	Protein Necessary For Stability Of L-A Dsrna-Containing Particles	Miscellaneous
ALG8	YOR067C	No	Glucosyl Transferase	Lipid Metabolic Process
PTP2	YOR208W	No	Phosphotyrosine-Specific Protein Phosphatase	Signaling
UBC7	YMR022W	No	Ubiquitin Conjugating Enzyme	Chromatin Organization
SLX4	YLR135W	No	Endonuclease Involved In Processing DNA	Cellular Response To DNA Damage Stimulus
DIA2	YOR080W	No	Origin-Binding F-Box Protein	Protein Modification By Small Protein Conjugation Or Removal
RPL33B	YOR234C	No	Ribosomal 60S Subunit Protein L33B	Miscellaneous
SUB1	YMR039C	No	Transcriptional Coactivator	Transcription From Rna Polymerase Ii Promoter
VTA1	YLR181C	No	Multivesicular Body (Mvb) Protein	Protein Complex Biogenesis
TIM18	YOR297C	No	Component Of The Mitochondrial Tim22 Complex	Response To Chemical
HXT8	YJL214W	No	Protein Of Unknown Function With Similarity To Hexose Transporters	Miscellaneous
HUJ1	YMR161W	No	Co-Chaperone For Hsp40P	Proteolysis Involved In Cellular Protein Catabolic Process
PEX13	YLR191W	No	Integral Peroxisomal Membrane Protein	Protein Complex Biogenesis
SNU66	YOR308C	No	Component Of The U4/U6.U5 Snrnp Complex	Miscellaneous
PHO90	YJL198W	No	Low-Affinity Phosphate Transporter	Miscellaneous
HSC82	YMR186W	No	Cytoplasmic Chaperone Of The Hsp90 Family	Protein Complex Biogenesis
HRD3	YLR207W	No	Er Membrane Protein That Plays A Central Role In Erad	Proteolysis Involved In Cellular Protein Catabolic Process
PMT3	YOR321W	No	Protein O-Mannosyltransferase	Carbohydrate Metabolic Process
SWE1	YJL187C	No	Protein Kinase That Regulates The G2/M Transition	Mitotic Cell Cycle
CIK1	YMR198W	No	Kinesin-Associated Protein	Mitotic Cell Cycle
CPR6	YLR216C	No	Peptidyl-Prolyl Cis-Trans Isomerase (Cyclophilin)	Miscellaneous
SNC2	YOR327C	No	Vesicle Membrane Receptor Protein (V-Snare)	Golgi Vesicle Transport
SWI3	YJL176C	No	Subunit Of The Swi/Snf Chromatin Remodeling Complex	Transcription From Rna Polymerase Ii Promoter
EMC3	YKL207W	No	Member Of Conserved Er Transmembrane Complex	Miscellaneous
COG5	YNL051W	No	Component Of The Conserved Oligomeric Golgi Complex	Protein Targeting
TRM10	YOL093W	No	Trna Methyltransferase	Miscellaneous
PHO5	YBR093C	No	Repressible Acid Phosphatase	Miscellaneous
VPS51	YKR020W	No	Component Of The Garp (Golgi-Associated Retrograde Protein) Complex	Protein Targeting
EOS1	YNL080C	No	Protein Involved In N-Glycosylation	Response To Chemical
	YER077C	No	Putative Protein Of Unknown Function	Biological_Process
RAD16	YBR114W	No	Protein That Binds Damaged DNA During Ner	Cellular Response To DNA Damage Stimulus
TIF1	YKR059W	No	Translation Initiation Factor Eif4A	Miscellaneous
RPL41B	YDL133C-A	No	Ribosomal 60S Subunit Protein L41B	Miscellaneous
RAD5	YLR032W	No	DNA Helicase/Ubiquitin Ligase	Cellular Response To DNA Damage Stimulus
YSY6	YBR162W-A	No	Protein Of Unknown Function	Miscellaneous
PEX10	YDR265W	No	Peroxisomal Membrane E3 Ubiquitin Ligase	Protein Modification By Small Protein Conjugation Or Removal
RPS21B	YJL136C	No	Protein Component Of The Small (40S) Ribosomal Subunit	Miscellaneous
TS11	YML100W	No	Large Subunit Of Trehalose 6-Phosphate Synthase/Phosphatase Complex	Carbohydrate Metabolic Process
RPN4	YDL020C	No	Transcription Factor That Stimulates Expression Of Proteasome Genes	Transcription From Rna Polymerase Ii Promoter
CPR5	YDR304C	No	Peptidyl-Prolyl Cis-Trans Isomerase (Cyclophilin) Of The Er	Biological_Process
SET3	YKR029C	No	Defining Member Of The Set3 Histone Deacetylase Complex	Chromatin Organization
GTR1	YML121W	No	Cytoplasmic Gtpase	Signaling
RPS29B	YDL061C	No	Protein Component Of The Small (40S) Ribosomal Subunit	Miscellaneous
PEX3	YDR329C	No	Peroxisomal Membrane Protein (Pmp)	Protein Targeting
PEX32	YBR168W	No	Peroxisomal Integral Membrane Protein	Miscellaneous
MYO5	YMR109W	No	One Of Two Type I Myosins	Mitotic Cell Cycle
NUR1	YDL089W	No	Protein Of Unknown Function	Miscellaneous
EMC5	YIL027C	No	Member Of Conserved Er Transmembrane Complex	Miscellaneous
RIM1	YCR028C-A	No	Ssdna-Binding Protein Essential For Mitochondrial Genome Maintenance	Miscellaneous
REC114	YMR133W	No	Protein Involved In Early Stages Of Meiotic Recombination	Organelle Fission
ADA2	YDR448W	No	Transcription Coactivator	Transcription From Rna Polymerase Ii Promoter
APQ12	YIL040W	No	Protein Required For Nuclear Envelope Morphology	Lipid Metabolic Process
FIG2	YCR089W	No	Cell Wall Adhesin, Expressed Specifically During Mating	Response To Chemical
THP3	YPR045C	No	Protein That May Have A Role In Transcription Elongation	Miscellaneous
CWC21	YDR482C	No	Protein Involved In Rna Splicing By The Spliceosome	Miscellaneous
CST9	YLR394W	No	Sumo E3 Ligase	Organelle Fission
BRR1	YPR057W	No	Snrnp Protein Component Of Spliceosomal Snrnps	Miscellaneous
RPL37B	YDR500C	No	Ribosomal 60S Subunit Protein L37B	Miscellaneous
NOT3	YIL038C	No	Subunit Of Ccr4-Not Global Transcriptional Regulator	Transcription From Rna Polymerase Ii Promoter
PRM6	YML047C	No	Potassium Transporter That Mediates K+ Influx	Miscellaneous
SPE3	YPR069C	No	Spermidine Synthase	Miscellaneous
KRE28	YDR532C	No	Subunit Of A Kinetochore-Microtubule Binding Complex	Biological_Process
HXT10	YFL011W	No	Putative Hexose Transporter	Miscellaneous
CIN4	YMR138W	No	Gtp-Binding Protein Involved In Beta-Tubulin (Tub2P) Folding	Protein Complex Biogenesis
	YPR084W	No	Putative Protein Of Unknown Function	Biological_Process
SNF4	YGL115W	No	Activating Gamma Subunit Of The Amp-Activated Snf1P Kinase Complex	Transcription From Rna Polymerase Ii Promoter
RTT10	YPL183C	No	Wd40 Domain-Containing Protein Involved In Endosomal Recycling	Miscellaneous
LSM1	YJL124C	No	Lsm (Like 5m) Protein	Miscellaneous
SCS3	YGL126W	No	Protein Required For Inositol Prototrophy	Lipid Metabolic Process
GAL11	YOL051W	No	Subunit Of The Rna Polymerase Ii Mediator Complex	Transcription From Rna Polymerase Ii Promoter
SKI2	YLR398C	No	Ski Complex Component And Putative Rna Helicase	Miscellaneous
SWF1	YDR126W	No	Palmitoyltransferase That Acts On Transmembrane Proteins	Meiotic Cell Cycle
KAR3	YPR141C	No	Minus-End-Directed Microtubule Motor	Mitotic Cell Cycle
HST1	YOL068C	No	Nad(+)-Dependent Histone Deacetylase	Chromatin Organization
TOP3	YLR234W	No	DNA Topoisomerase Iii	Mitotic Cell Cycle
EAF1	YDR359C	No	Component Of The Nua4 Histone Acetyltransferase Complex	Chromatin Organization
SEM1	YDR363W-A	No	Component Of Lid Subcomplex Of 26S Proteasome Regulatory Subunit	Protein Complex Biogenesis
BOP2	YLR267W	No	Protein Of Unknown Function	Biological_Process
MUS81	YDR386W	No	Subunit Of Structure-Specific Mms4P-Mus81P Endonuclease	Cellular Response To DNA Damage Stimulus
DIE2	YGR227W	No	Dolichyl-Phosphoglucose-Dependent Alpha-1,2 Glucosyltransferase	Carbohydrate Metabolic Process

OXR1	YPL196W	No	Protein Of Unknown Function Required For Oxidative Damage Resistance	Response To Chemical
UBC12	YLR306W	No	Enzyme That Mediates The Conjugation Of Rub1P	Protein Modification By Small Protein Conjugation Or Removal
HXR1	YDR420W	No	Mucin Family Member That Functions As An Osmosensor In The Hog Pathway	Mitotic Cell Cycle
HAP3	YBL021C	No	Subunit Of The Hap2P/3P/4P/5P Ccaat-Binding Complex	Transcription From Rna Polymerase Ii Promoter
CB2C	YPL178W	No	Small Subunit Of The Heterodimeric Cap Binding Complex With Sto1P	Miscellaneous
CPR1	YDR155C	No	Cytoplasmic Peptidyl-Prolyl Cis-Trans Isomerase (Cyclophilin)	Chromatin Organization
EDC3	YEL015W	No	Non-Essential Conserved Protein With A Role In Mrna Decapping	Miscellaneous
SAS3	YBL052C	No	Histone Acetyltransferase Catalytic Subunit Of Nua3 Complex	Chromatin Organization
KIP2	YPL155C	No	Kinesin-Related Motor Protein Involved In Mitotic Spindle Positioning	Regulation Of Organelle Organization
NGG1	YDR176W	No	Subunit Of Chromatin Modifying Histone Acetyltransferase Complexes	Chromatin Organization
TCA17	YEL048C	No	Subunit Of Trappii	Protein Complex Biogenesis
NUP170	YBL079W	No	Subunit Of The Inner Ring Of The Nuclear Pore Complex (Npc)	Mitotic Cell Cycle
MFBI	YDR219C	No	Mitochondria-Associated F-Box Protein	Proteolysis Involved In Cellular Protein Catabolic Process
NOP16	YER002W	No	Constituent Of 66S Pre-Ribosomal Particles	Miscellaneous
AIM44	YPL158C	No	Protein That Regulates Cdc42P And Rho1P	Miscellaneous
BEM3	YPL115C	No	Rho Gtpase Activating Protein (Rhogap)	Signaling
DSD1	YGL196W	No	D-Serine Dehydratase (Aka D-Serine Ammonia-Lyase)	Miscellaneous
FIR1	YER032W	No	Protein Involved In 3' Mrna Processing	Miscellaneous
PGD1	YGL025C	No	Subunit Of The Rna Polymerase Ii Mediator Complex	Transcription From Rna Polymerase Ii Promoter
SWD3	YBR175W	No	Essential Subunit Of The Compass (Set1C) Complex	Chromatin Organization
KIP3	YGL216W	No	Kinesin-Related Motor Protein Involved In Mitotic Spindle Positioning	Mitotic Cell Cycle
MOT2	YER068W	No	Ubiquitin-Protein Ligase Subunit Of The Ccr4-Not Complex	Transcription From Rna Polymerase Ii Promoter
DST1	YGL043W	No	General Transcription Elongation Factor Tfiis	Transcription From Rna Polymerase Ii Promoter
MSI1	YBR195C	No	Subunit Of Chromatin Assembly Factor I (Caf-1)	Chromatin Organization
TAN1	YGL232W	No	Putative Trna Acetyltransferase	Miscellaneous
PPT1	YGR123C	No	Protein Serine/Threonine Phosphatase	Miscellaneous
RAD6	YGL058W	No	Ubiquitin-Conjugating Enzyme (E2)	Transcription From Rna Polymerase Ii Promoter
HPC2	YBR215W	No	Subunit Of The Hir Complex	Transcription From Rna Polymerase Ii Promoter
RMR1	YGL250W	No	Protein Required For Meiotic Recombination And Gene Conversion	Organelle Fission
PRE9	YGR135W	No	Alpha 3 Subunit Of The 20S Proteasome	Protein Complex Biogenesis
NPY1	YGL067W	No	Nadh Diphosphatase (Pyrophosphatase)	Miscellaneous
TDP1	YBR223C	No	Tyrosyl-DNA Phosphodiesterase I	Cellular Response To DNA Damage Stimulus
HXK2	YGL253W	No	Hexokinase Isoenzyme 2	Response To Chemical
GTR2	YGR163W	No	Putative Gtp Binding Protein	Transcription From Rna Polymerase Ii Promoter
DBP3	YGL078C	No	Rna-Dependent Atpase, Member Of Dexe/H-Box Family	Miscellaneous
RIM13	YMR154C	No	Calpain-Like Cysteine Protease	Miscellaneous
DNF1	YER166W	No	Aminophospholipid Translocase (Flippase)	Miscellaneous
RAV1	YJR033C	No	Subunit Of Rave Complex (Rav1P, Rav2P, Skp1P)	Protein Complex Biogenesis
TAF9	YMR236W	Yes	Subunit (17 Kda) Of Tfiid And Saga Complexes	Transcription From Rna Polymerase Ii Promoter
PTR2	YKR093W	No	Integral Membrane Peptide Transporter	Miscellaneous
STV1	YMR054W	No	Subunit A Of The Vacuolar-Atpase V0 Domain	Miscellaneous
KCH1	YJR054W	No	Potassium Transporter That Mediates K+ Influx	Miscellaneous
SRB7	YDR308C	Yes	Subunit Of The Rna Polymerase Ii Mediator Complex	Transcription From Rna Polymerase Ii Promoter
TDAS	YLR426W	No	Putative Protein Of Unknown Function	Response To Chemical
SSK1	YLR006C	No	Cytoplasmic Response Regulator	Regulation Of Organelle Organization
PPH21	YDL134C	No	Catalytic Subunit Of Protein Phosphatase 2A (Pp2A)	Mitotic Cell Cycle
APC1	YNL172W	Yes	Largest Subunit Of The Anaphase-Promoting Complex/Cyclosome	Mitotic Cell Cycle
BRE5	YNR051C	No	Ubiquitin Protease Cofactor	Protein Modification By Small Protein Conjugation Or Removal
IES1	YFL013C	No	Subunit Of The Ino80 Chromatin Remodeling Complex	Chromatin Organization
PPH22	YDL188C	No	Catalytic Subunit Of Protein Phosphatase 2A (Pp2A)	Mitotic Cell Cycle
TFB4	YPR056W	Yes	Subunit Of Tfiib Complex	Transcription From Rna Polymerase Ii Promoter
STE24	YJR117W	No	Highly Conserved Zinc Metalloprotease	Miscellaneous
RM11	YPL024W	No	Subunit Of The Recq (Sgs1P) - Topo Iii (Top3P) Complex	Mitotic Cell Cycle
HHF2	YNL030W	No	Histone H4	Chromatin Organization
DPB2	YPR175W	Yes	Second Largest Subunit Of DNA Polymerase Ii (DNA Polymerase Epsilon)	Chromatin Organization
HIR3	YJR140C	No	Subunit Of The Hir Complex	Transcription From Rna Polymerase Ii Promoter
BUL2	YML111W	No	Component Of The Rsp5P E3-Ubiquitin Ligase Complex	Protein Modification By Small Protein Conjugation Or Removal
VPS27	YNR006W	No	Endosomal Protein That Forms A Complex With Hse1P	Protein Targeting
SGT1	YOR057W	Yes	Cochaperone Protein	Protein Complex Biogenesis
HOT1	YMR172W	No	Transcription Factor For Glycerol Biosynthetic Genes	Transcription From Rna Polymerase Ii Promoter
CPR7	YJR032W	No	Peptidyl-Prolyl Cis-Trans Isomerase (Cyclophilin)	Miscellaneous
FPK1	YNR047W	No	Ser/Thr Protein Kinase	Response To Chemical
DPB11	YJL090C	Yes	DNA Replication Initiation Protein	Mitotic Cell Cycle
HBT1	YDL223C	No	Shmoo Tip Protein, Substrate Of Hub1P Ubiquitin-Like Protein	Response To Chemical
NOT5	YPR072W	No	Subunit Of Ccr4-Not Global Transcriptional Regulator	Transcription From Rna Polymerase Ii Promoter
POA1	YBR022W	No	Phosphatase That Is Highly Specific For Adp-Ribose 1"-Phosphate	Miscellaneous
TFB2	YPL122C	Yes	Subunit Of Tfiib And Nucleotide Excision Repair Factor 3 Complexes	Transcription From Rna Polymerase Ii Promoter
AAD4	YDL243C	No	Putative Aryl-Alcohol Dehydrogenase	Miscellaneous
GCN5	YGR252W	No	Catalytic Subunit Of Ada And Saga Histone Acetyltransferase Complexes	Transcription From Rna Polymerase Ii Promoter
CSG2	YBR036C	No	Endoplasmic Reticulum Membrane Protein	Lipid Metabolic Process
SUA7	YPR086W	Yes	Transcription Factor Tfiib	Transcription From Rna Polymerase Ii Promoter
RAD61	YDR014W	No	Subunit Of A Complex That Inhibits Sister Chromatid Cohesion	Mitotic Cell Cycle
MCK1	YNL307C	No	Dual-Specificity Ser/Thr And Tyrosine Protein Kinase	Mitotic Cell Cycle
TRM7	YBR061C	No	2'-O-Ribose Methyltransferase	Miscellaneous
ORC1	YML065W	Yes	Largest Subunit Of The Origin Recognition Complex	Miscellaneous
UBX7	YBR273C	No	Ubx (Ubiquitin Regulatory X) Domain-Containing Protein	Proteolysis Involved In Cellular Protein Catabolic Process
DER1	YBR201W	No	Endoplasmic Reticulum Membrane Protein	Proteolysis Involved In Cellular Protein Catabolic Process
RDH54	YBR073W	No	DNA-Dependent Atpase	Cellular Response To DNA Damage Stimulus
LDB18	YLL049W	No	Component Of The Dynactin Complex	Mitotic Cell Cycle
DPB3	YBR278W	No	Third-Largest Subunit Of DNA Polymerase Ii (DNA Polymerase Epsilon)	Chromatin Organization
CBF1	YJR060W	No	Basic Helix-Loop-Helix (Bhh) Protein	Transcription From Rna Polymerase Ii Promoter
EAF7	YNL136W	No	Subunit Of The Nua4 Histone Acetyltransferase Complex	Transcription From Rna Polymerase Ii Promoter
UBA3	YPR066W	No	Protein That Activates Rub1P (Nedd8) Before Neddylatation	Protein Modification By Small Protein Conjugation Or Removal
PDC1	YLR044C	No	Major Of Three Pyruvate Decarboxylase Isozymes	Carbohydrate Metabolic Process
BZZ1	YHR114W	No	Sh3 Domain Protein Implicated In Regulating Actin Polymerization	Protein Complex Biogenesis
RPS19B	YNL302C	No	Protein Component Of The Small (40S) Ribosomal Subunit	Miscellaneous
PEF1	YGR058W	No	Penta-Ef-Hand Protein	Mitotic Cell Cycle
ALT1	YLR089C	No	Alanine Transaminase (Glutamic Pyruvic Transaminase)	Miscellaneous
LIN1	YHR156C	No	Non-Essential Component Of U5 Snrnp	Biological_Process
CAF120	YNL278W	No	Part Of The Ccr4-Not Transcriptional Regulatory Complex	Transcription From Rna Polymerase Ii Promoter
PCP1	YGR101W	No	Mitochondrial Serine Protease	Regulation Of Organelle Organization
SRN2	YLR119W	No	Component Of The Escrt-I Complex	Protein Targeting
RPS4B	YHR203C	No	Protein Component Of The Small (40S) Ribosomal Subunit	Miscellaneous
ALG6	YOR002W	No	Alpha 1,3 Glucosyltransferase	Lipid Metabolic Process
RAS1	YOR101W	No	Gtpase Involved In G-Protein Signaling In Adenylate Cyclase Activation	Signaling
AIM32	YML050W	No	Putative Protein Of Unknown Function	Biological_Process
DCC1	YCL016C	No	Subunit Of A Complex With Ctf8P And Ctf18P	Mitotic Cell Cycle
STI1	YOR027W	No	Hsp90 Cochaperone	Miscellaneous
RGA1	YOR127W	No	Gtpase-Activating Protein For Polarity-Establishment Protein Cdc42P	Response To Chemical
PSF2	YML017W	No	Asn Rich Cytoplasmic Protein That Contains Rgg Motifs	Biological_Process
PEX34	YCL056C	No	Protein That Regulates Peroxisome Populations	Miscellaneous
WHI2	YOR043W	No	Protein Required For Full Activation Of The General Stress Response	Cytoskeleton Organization
LCB4	YOR171C	No	Sphingoid Long-Chain Base Kinase	Signaling
AIM34	YMR003W	No	Protein Of Unknown Function	Biological_Process
PET18	YCR020C	No	Protein Of Unknown Function	Miscellaneous

VAM10	YOR068C	No	Protein Involved In Vacuole Morphogenesis	Miscellaneous
NPT1	YOR209C	No	Nicotinate Phosphoribosyltransferase	Miscellaneous
PEX12	YMR026C	No	C3Hc4-Type Ring-Finger Peroxin And E3 Ubiquitin Ligase	Protein Targeting
STM1	YLR150W	No	Protein Required For Optimal Translation Under Nutrient Stress	Signaling
WHI5	YOR083W	No	Repressor Of G1 Transcription	Transcription From Rna Polymerase Ii Promoter
PUS7	YOR243C	No	Pseudouridine Synthase	Miscellaneous
ARG80	YMR042W	No	Transcription Factor Involved In Regulating Arginine-Responsive Genes	Transcription From Rna Polymerase Ii Promoter
SWI6	YLR182W	No	Transcription Cofactor	Transcription From Rna Polymerase Ii Promoter
CPA1	YOR303W	No	Small Subunit Of Carbamoyl Phosphate Synthetase	Miscellaneous
ECM5	YMR176W	No	Subunit Of The Snt2C Complex	Response To Chemical
YKE2	YLR200W	No	Subunit Of The Heterohexameric Gim/Prefoldin Protein Complex	Transcription From Rna Polymerase Ii Promoter
DGK1	YOR311C	No	Dialcylglycerol Kinase	Lipid Metabolic Process
UBP12	YJL197W	No	Ubiquitin-Specific Protease	Biological_Process
SGS1	YMR190C	No	Nucleolar DNA Helicase Of The Recq Family	Mitotic Cell Cycle
CLB4	YLR210W	No	B-Type Cyclin Involved In Cell Cycle Progression	Mitotic Cell Cycle
LDB19	YOR322C	No	Protein Involved In Ubiquitin-Dependent Endocytosis	Miscellaneous
MNN11	YJL183W	No	Subunit Of A Golgi Mannosyltransferase Complex	Carbohydrate Metabolic Process
CLN1	YMR199W	No	G1 Cyclin Involved In Regulation Of The Cell Cycle	Regulation Of Cell Cycle
MSC3	YLR219W	No	Protein Of Unknown Function	Organelle Fission
MIP1	YOR330C	No	Mitochondrial DNA Polymerase	Miscellaneous
SET2	YJL168C	No	Histone Methyltransferase With A Role In Transcriptional Elongation	Chromatin Organization
RAD14	YMR201C	No	Protein That Recognizes And Binds Damaged DNA During Ner	Cellular Response To DNA Damage Stimulus
RSA3	YLR221C	No	Protein With A Likely Role In Ribosomal Maturation	Miscellaneous
UBC11	YOR339C	No	Ubiquitin-Conjugating Enzyme	Protein Modification By Small Protein Conjugation Or Removal
HAL5	YJL165C	No	Putative Protein Kinase	Protein Phosphorylation
DBP7	YKR024C	No	Putative Atp-Dependent Rna Helicase Of The Dead-Box Family	Miscellaneous
PMS1	YNL082W	No	Atp-Binding Protein Required For Mismatch Repair	Cellular Response To DNA Damage Stimulus
DOT6	YER088C	No	Protein Involved In Rrna And Ribosome Biogenesis	Transcription From Rna Polymerase Ii Promoter
MUD1	YBR119W	No	U1 Ssrnp A Protein	Miscellaneous
KTR2	YKR061W	No	Mannosyltransferase Involved In N-Linked Protein Glycosylation	Carbohydrate Metabolic Process
HMO1	YDR174W	No	Chromatin Associated High Mobility Group (Hmg) Family Member	Transcription From Rna Polymerase Ii Promoter
RIC1	YLR039C	No	Protein Involved In Retrograde Transport To The Cis-Golgi Network	Miscellaneous
ARL1	YBR164C	No	Soluble Gtpase With A Role In Regulation Of Membrane Traffic	Protein Targeting
HEL2	YDR266C	No	Ring Finger Ubiquitin Ligase (E3)	Chromatin Organization
RPL17B	YJL177W	No	Ribosomal 60S Subunit Protein L17B	Miscellaneous
CUE4	YML101C	No	Protein Of Unknown Function	Biological_Process
RTK1	YDL025C	No	Putative Protein Kinase, Potentially Phosphorylated By Cdc28P	Biological_Process
	YDR306C	No	F-Box Protein Of Unknown Function	Proteolysis Involved In Cellular Protein Catabolic Process
ERP1	YAR002C-A	No	Member Of The P24 Family Involved In Er To Golgi Transport	Golgi Vesicle Transport
PHO84	YML123C	No	High-Affinity Inorganic Phosphate (Pi) Transporter	Miscellaneous
PEX19	YDL065C	No	Chaperone And Import Receptor For Newly-Synthesized Class I Pmps	Protein Targeting
UBX5	YDR330W	No	Ubx Domain-Containing Protein That Interacts With Cdc48P	Proteolysis Involved In Cellular Protein Catabolic Process
TEC1	YBR083W	No	Transcription Factor Targeting Filamentation Genes And Ty1 Expression	Transcription From Rna Polymerase Ii Promoter
	YMR111C	No	Protein Of Unknown Function	Biological_Process
UBX3	YDL091C	No	Subunit Of The Dsc Ubiquitin Ligase Complex	Biological_Process
CAP2	YIL034C	No	Beta Subunit Of The Capping Protein Heterodimer (Cap1P And Cap2P)	Protein Complex Biogenesis
SNT1	YCR033W	No	Subunit Of The Set3C Deacetylase Complex	Chromatin Organization
SUT2	YPR009W	No	Putative Transcription Factor Of The Zn2Cys6 Family	Transcription From Rna Polymerase Ii Promoter
YHP1	YDR451C	No	Homeobox Transcriptional Repressor	Transcription From Rna Polymerase Ii Promoter
AGE2	YIL044C	No	Adp-Ribosylation Factor (Arf) Gtpase Activating Protein (Gap) Effector	Golgi Vesicle Transport
TP52	YDR074W	No	Phosphatase Subunit Of The Trehalose-6-P Synthase/Phosphatase Complex	Carbohydrate Metabolic Process
MCM16	YPR046W	No	Component Of The Ctf19 Complex And The Coma Subcomplex	Mitotic Cell Cycle
PAC11	YDR488C	No	Dynein Intermediate Chain, Microtubule Motor Protein	Mitotic Cell Cycle
ICE2	YIL090W	No	Integral Er Membrane Protein With Type-iii Transmembrane Domains	Protein Complex Biogenesis
APT1	YML022W	No	Adenine Phosphoribosyltransferase	Miscellaneous
	YPR063C	No	Er-Localized Protein Of Unknown Function	Biological_Process
PSP1	YDR505C	No	Asn And Gln Rich Protein Of Unknown Function	Biological_Process
SYG1	YIL047C	No	Plasma Membrane Protein Of Unknown Function	Signaling
HMG1	YML075C	No	Hmg-Coa Reductase	Lipid Metabolic Process
MED1	YPR070W	No	Subunit Of The Rna Polymerase Ii Mediator Complex	Transcription From Rna Polymerase Ii Promoter
ARC1	YGL105W	No	Protein That Binds Trna And Methionyl- And Glutamyl-Trna Synthetases	Miscellaneous
BUD27	YFL023W	No	Unconventional Prefoldin Protein Involved In Translation Initiation	Protein Complex Biogenesis
MBF1	YOR298C-A	No	Transcriptional Coactivator	Transcription From Rna Polymerase Ii Promoter
ASR1	YPR093C	No	Ubiquitin Ligase That Modifies And Regulates Rna Pol Ii	Response To Chemical
MON1	YGL124C	No	Protein Required For Cvt-Vesicle/Autophagosome Fusion With The Vacuole	Protein Targeting
AGX1	YFL030W	No	Alanine:Glyoxylate Aminotransferase (Agt)	Miscellaneous
COS6	YGR295C	No	Protein Of Unknown Function	Biological_Process
MTC1	YJL123C	No	Protein Of Unknown Function That May Interact With Ribosomes	Biological_Process
SOH1	YGL127C	No	Subunit Of The Rna Polymerase Ii Mediator Complex	Transcription From Rna Polymerase Ii Promoter
HAC1	YFL031W	No	Basic Leucine Zipper (Bzip) Transcription Factor (Atf/Creb1 Homolog)	Transcription From Rna Polymerase Ii Promoter
SSM4	YIL030C	No	Ubiquitin-Protein Ligase Involved In Er-Associated Protein Degradation	Proteolysis Involved In Cellular Protein Catabolic Process
ALB1	YJL122W	No	Shuttling Pre-60S Factor	Miscellaneous
SNT2	YGL131C	No	Subunit Of Snt2C Complex, Ring Finger Ubiquitin Ligase (E3)	Transcription From Rna Polymerase Ii Promoter
REX4	YOL080C	No	Putative Rna Exonuclease	Miscellaneous
FAR10	YLR238W	No	Protein Involved In Recovery From Arrest In Response To Pheromone	Response To Chemical
ESC2	YDR363W	No	Sumo-Like Domain Protein	Mitotic Cell Cycle
UBP5	YER144C	No	Putative Ubiquitin-Specific Protease	Protein Modification By Small Protein Conjugation Or Removal
CIN2	YPL241C	No	Gtpase-Activating Protein (Gap) For Cin4P	Protein Complex Biogenesis
SEC22	YLR268W	No	R-Snare Protein	Golgi Vesicle Transport
RVS167	YDR388W	No	Actin-Associated Protein With Roles In Endocytosis And Exocytosis	Miscellaneous
PHB2	YGR231C	No	Subunit Of The Prohibitin Complex (Phb1P-Phb2P)	Miscellaneous
APL5	YPL195W	No	Delta Adaptin-Like Subunit Of The Clathrin Associated Protein Complex	Protein Targeting
	YLR312C	No	Putative Protein Of Unknown Function	Biological_Process
ARO80	YDR421W	No	Zinc Finger Transcriptional Activator Of The Zn2Cys6 Family	Transcription From Rna Polymerase Ii Promoter
NCL1	YBL024W	No	S-Adenosyl-L-Methionine-Dependent Trna: MSC-Methyltransferase	Response To Chemical
CUP9	YPL177C	No	Homeodomain-Containing Transcriptional Repressor	Transcription From Rna Polymerase Ii Promoter
RPA14	YDR156W	No	Rna Polymerase I Subunit A14	Miscellaneous
SPF1	YEL031W	No	P-Type Atpase, Ion Transporter Of The Er Membrane	Miscellaneous
SHP1	YBL058W	No	Ubx (Ubiquitin Regulatory X) Domain-Containing Protein	Mitotic Cell Cycle
RRD2	YPL152W	No	Peptidyl-Prolyl Cis/Trans-Isomerase	Mitotic Cell Cycle
SAS4	YDR181C	No	Subunit Of The Sas Complex (Sas2P, Sas4P, Sas5P)	Miscellaneous
MAK10	YEL053C	No	Non-Catalytic Subunit Of N-Terminal Acetyltransferase Of The Natc Type	Miscellaneous
	YBL081W	No	Non-Essential Protein Of Unknown Function	Biological_Process
HHO1	YPL127C	No	Histone H1, Linker Histone With Roles In Meiosis And Sporulation	DNA Recombination
GTB1	YDR221W	No	Glucosidase Ii Beta Subunit, Forms A Complex With Alpha Subunit Rot2P	Carbohydrate Metabolic Process
YND1	YER005W	No	Apyrase With Wide Substrate Specificity	Carbohydrate Metabolic Process
CDH1	YGL003C	No	Activator Of Anaphase-Promoting Complex/Cyclosome (Apc/C)	Mitotic Cell Cycle
	YPL113C	No	Glyoxylate Reductase	Miscellaneous
MDS3	YGL197W	No	Putative Component Of The Tor Regulatory Pathway	Signaling
CAU1	YER048C	No	Nuclear Type Ii J Heat Shock Protein Of The E. Coli DnaJ Family	Miscellaneous
CWH41	YGL027C	No	Processing Alpha Glucosidase I	Carbohydrate Metabolic Process
RP568	YBR181C	No	Protein Component Of The Small (40S) Ribosomal Subunit	Miscellaneous
OST5	YGL226C-A	No	Zeta Subunit Of The Oligosaccharyltransferase Complex Of The Er Lumen	Carbohydrate Metabolic Process
VTC1	YER072W	No	Subunit Of The Vacuolar Transporter Chaperone (Vtc) Complex	Miscellaneous
BEM1	YBR200W	No	Protein Containing Sh3-Domains	Response To Chemical

	YGL242C	No	Putative Protein Of Unknown Function	Biological_Process
SYF2	YGR129W	No	Member Of The Nineteen Complex (Ntc)	Miscellaneous
YBP2	YGL060W	No	Central Kinetochore Associated Protein	Mitotic Cell Cycle
PDB1	YBR221C	No	E1 Beta Subunit Of The Pyruvate Dehydrogenase (Pdh) Complex	Miscellaneous
RTG2	YGL252C	No	Sensor Of Mitochondrial Dysfunction	Transcription From Rna Polymerase Ii Promoter
CHO2	YGR157W	No	Phosphatidylethanolamine Methyltransferase (Pemt)	Lipid Metabolic Process
AFT1	YGL071W	No	Transcription Factor Involved In Iron Utilization And Homeostasis	Transcription From Rna Polymerase Ii Promoter
SLX1	YBR228W	No	Endonuclease Involved In DNA Recombination And Repair	Miscellaneous
ZRT1	YGL255W	No	High-Affinity Zinc Transporter Of The Plasma Membrane	Miscellaneous
TRS65	YGR166W	No	Subunit Of Trappii	Protein Complex Biogenesis
	YGL081W	No	Putative Protein Of Unknown Function	Biological_Process
ROT2	YBR229C	No	Glucosidase Ii Catalytic Subunit	Miscellaneous
CUL3	YGR003W	No	Ubiquitin-Protein Ligase	Protein Modification By Small Protein Conjugation Or Removal
PSD2	YGR170W	No	Phosphatidylserine Decarboxylase Of The Golgi And Vacuolar Membranes	Lipid Metabolic Process
GUP1	YGL084C	No	Plasma Membrane Protein Involved In Remodeling Gpi Anchors	Lipid Metabolic Process
UBP11	YKR098C	No	Ubiquitin-Specific Protease	Biological_Process
BUB2	YMR055C	No	Mitotic Exit Network Regulator	Mitotic Cell Cycle
PTK2	YJR059W	No	Putative Serine/Threonine Protein Kinase	Mitotic Cell Cycle
MED6	YHR058C	Yes	Subunit Of The Rna Polymerase Ii Mediator Complex	Transcription From Rna Polymerase Ii Promoter
CRN1	YLR429W	No	Coronin	Protein Complex Biogenesis
CCS1	YMR038C	No	Copper Chaperone For Superoxide Dismutase Sod1P	Miscellaneous
RD11	YDL135C	No	Rho Gdp Dissociation Inhibitor	Regulation Of Organelle Organization
TFB1	YDR311W	Yes	Subunit Of Tfiiv And Nucleotide Excision Repair Factor 3 Complexes	Transcription From Rna Polymerase Ii Promoter
FRE4	YNR060W	No	Ferric Reductase	Miscellaneous
RIM15	YFL033C	No	Protein Kinase Involved In Cell Proliferation In Response To Nutrients	Response To Chemical
UFD2	YDL190C	No	Ubiquitin Chain Assembly Factor (E4)	Response To Chemical
RSC3	YDR303C	Yes	Component Of The Rsc Chromatin Remodeling Complex	Transcription From Rna Polymerase Ii Promoter
ILM1	YJR118C	No	Protein Of Unknown Function	Miscellaneous
SMI1	YGR229C	No	Protein Involved In The Regulation Of Cell Wall Synthesis	Mitotic Cell Cycle
HHT2	YNL031C	No	Histone H3	Mitotic Cell Cycle
MPE1	YKL059C	Yes	Essential Conserved Subunit Of Cpf Cleavage And Polyadenylation Factor	Miscellaneous
CTK3	YML112W	No	Gamma Subunit Of C-Terminal Domain Kinase I	Protein Phosphorylation
CSE2	YNR010W	No	Subunit Of The Rna Polymerase Ii Mediator Complex	Transcription From Rna Polymerase Ii Promoter
RPB2	YOR151C	Yes	Rna Polymerase Ii Second Largest Subunit B150	Transcription From Rna Polymerase Ii Promoter
RPL35A	YDL191W	No	Ribosomal 60S Subunit Protein L35A	Miscellaneous
ECM21	YBL101C	No	Protein Involved In Regulating Endocytosis Of Plasma Membrane Proteins	Miscellaneous
CDC4	YFL009W	Yes	F-Box Protein Required For Both The G1/S And G2/M Phase Transitions	Mitotic Cell Cycle
WHI4	YDL224C	No	Putative Rna Binding Protein	Miscellaneous
RPS27B	YHR021C	No	Protein Component Of The Small (40S) Ribosomal Subunit	Miscellaneous
CHS3	YBR023C	No	Chitin Synthase Iii	Meiotic Cell Cycle
ARP7	YPR034W	Yes	Component Of Both The Swi/Snf And Rsc Chromatin Remodeling Complexes	Transcription From Rna Polymerase Ii Promoter
RAD57	YDR004W	No	Protein That Stimulates Strand Exchange	Cellular Response To DNA Damage Stimulus
MRPL10	YNL284C	No	Mitochondrial Ribosomal Protein Of The Large Subunit	Miscellaneous
FAT1	YBR041W	No	Very Long Chain Fatty Acyl-Coa Synthetase And Fatty Acid Transporter	Lipid Metabolic Process
CDC16	YKL022C	Yes	Subunit Of The Anaphase-Promoting Complex/Cyclosome (Apc/C)	Protein Modification By Small Protein Conjugation Or Removal
RPS11A	YDR025W	No	Protein Component Of The Small (40S) Ribosomal Subunit	Miscellaneous
MMS4	YBR098W	No	Subunit Of Structure-Specific Mms4P-Mus81P Endonuclease	Cellular Response To DNA Damage Stimulus
ECM2	YBR065C	No	Pre-Mrna Splicing Factor	Miscellaneous
CHK1	YBR274W	No	Serine/Threonine Kinase And DNA Damage Checkpoint Effector	Cellular Response To DNA Damage Stimulus
BUD3	YCL014W	No	Protein Involved In Bud-Site Selection	Mitotic Cell Cycle
ECM8	YBR076W	No	Non-Essential Protein Of Unknown Function	Biological_Process
UBR2	YLR024C	No	Cytoplasmic Ubiquitin-Protein Ligase (E3)	Protein Modification By Small Protein Conjugation Or Removal
DUG2	YBR281C	No	Component Of Glutamine Amidotransferase (Gatase Ii)	Miscellaneous
TMA23	YMR269W	No	Nucleolar Protein Implicated In Ribosome Biogenesis	Miscellaneous
FPR1	YNL135C	No	Peptidyl-Prolyl Cis-Trans Isomerase (Ppiase)	Chromatin Organization
VP53	YJL029C	No	Component Of The Garp (Golgi-Associated Retrograde Protein) Complex	Golgi Vesicle Transport
SSH1	YBR283C	No	Subunit Of The Ssh1 Translocon Complex	Protein Targeting
LSM7	YNL147W	No	Lsm (Like Sm) Protein	Miscellaneous
TEP1	YNL128W	No	Pten Homolog With No Demonstrated Inositol Lipid Phosphatase Activity	Meiotic Cell Cycle
RIM8	YGL046W	No	Merged Open Reading Frame	Miscellaneous
RIM8	YGL045W	No	Protein Involved In Proteolytic Activation Of Rim101P	Miscellaneous
LAG1	YHL003C	No	Ceramide Synthase Component	Lipid Metabolic Process

Query strains

NOTE: Gene description taken from the SGD Database (March 17th, 2007). Essentiality status taken from Saccharomyces Genome Deletion Project.

NOTE: The Primary Functional category was defined by the the top ranked GO term in the list of the 25 most frequently found GO slim terms (taken from SGD) for all array and query genes.

Gene	ORF	Essential?	Description	Primary Functional Category
ASF1	YJL115W	No	Nucleosome Assembly Factor	Histone Modification
RTT101	YJL047C	No	Cullin Subunit Of A Roc1P-Dependent E3 Ubiquitin Ligase Complex	Proteolysis Involved In Cellular Protein Catabolic Process
NUP133	YKR082W	No	Subunit Of Nup84P Subcomplex Of Nuclear Pore Complex (Npc)	Protein Targeting
RTT109	YLL002W	No	Histone Acetyltransferase	Histone Modification
RAD5	YLR032W	No	DNA Helicase/Ubiquitin Ligase	Protein Modification By Small Protein Conjugation Or Removal
RAD52	YML032C	No	Protein That Stimulates Strand Exchange	DNA Recombination
SGS1	YMR190C	No	Nucleolar DNA Helicase Of The Recq Family	DNA Recombination
MRE11	YMR224C	No	Nuclease Subunit Of The Mrx Complex With Rad50P And Xrs2P	DNA Recombination
YKU70	YMR284W	No	Subunit Of The Telomeric Ku Complex (Yku70P-Yku80P)	DNA Recombination
RPD3	YNL330C	No	Histone Deacetylase, Component Of Both The Rpd3S And Rpd3L Complexes	DNA Recombination
TOF1	YNL273W	No	Subunit Of A Replication-Pausing Checkpoint Complex	DNA Repair
PSY2	YNL201C	No	Subunit Of Protein Phosphatase Pp4 Complex	Signaling
HTZ1	YOL012C	No	Histone Variant H2Az	Chromatin Organization
HST3	YOR025W	No	Member Of The Sir2 Family Of Nad(+)-Dependent Protein Deacetylases	Histone Modification
EXO1	YOR033C	No	5'-3' Exonuclease And Flap-Endonuclease	DNA Recombination
ARP8	YOR141C	No	Nuclear Actin-Related Protein Involved In Chromatin Remodeling	DNA Recombination
RAD17	YOR368W	No	Checkpoint Protein	DNA Recombination
MRC1	YCL061C	No	S-Phase Checkpoint Protein Required For DNA Replication	Regulation Of Cell Cycle
DCC1	YCL016C	No	Subunit Of A Complex With Ctf8P And Ctf18P	Organelle Fission
RAD18	YCR066W	No	E3 Ubiquitin Ligase	Protein Modification By Small Protein Conjugation Or Removal
BRE1	YDL074C	No	E3 Ubiquitin Ligase	DNA Recombination
SLX5	YDL013W	No	Subunit Of The Slx5-Slx8 Sumo-Targeted Ubiquitin Ligase Complex	Protein Modification By Small Protein Conjugation Or Removal
PPH3	YDR075W	No	Catalytic Subunit Of Protein Phosphatase Pp4 Complex	DNA Recombination
UBC13	YDR092W	No	E2 Ubiquitin-Conjugating Enzyme	Protein Modification By Small Protein Conjugation Or Removal
RAD9	YDR217C	No	DNA Damage-Dependent Checkpoint Protein	Regulation Of Cell Cycle
SWR1	YDR334W	No	Swi2/Snf2-Related Atpase	Chromatin Organization
DOT1	YDR440W	No	Nucleosomal Histone H3-Lys79 Methylase	DNA Recombination
SLX8	YER116C	No	Subunit Of Slx5-Slx8 Sumo-Targeted Ubiquitin Ligase (Stubl) Complex	Protein Modification By Small Protein Conjugation Or Removal
RAD24	YER173W	No	Checkpoint Protein	DNA Recombination
SAE2	YGL175C	No	Endonuclease Involved In Processing Hairpin DNA Structures	DNA Recombination
RSC1	YGR056W	No	Component Of The Rsc Chromatin Remodeling Complex	DNA Repair
DDC1	YPL194W	No	DNA Damage Checkpoint Protein	DNA Recombination
mec1-100	YBR136W	yes	Genome integrity checkpoint protein and PI kinase superfamily member	cellular response to DNA damage stimulus
rfa1-t11	YAR007C	yes	Subunit of heterotrimeric Replication Protein A (RPA)	cellular response to DNA damage stimulus
sgs1-r1	YMR190C	no	RecQ family nucleolar DNA helicase	mitotic cell cycle

CURRICULUM VITAE

Davidsbodenstrasse 34
CH-4056 Basel
Switzerland
T: +41 61 5344190

Friedrich Miescher Institute for Biomedical Research
Maulbeerstrasse 66
CH-4058 Basel
Switzerland
T: +41 61 697 5583
nicole.hustedt@fmi.ch

EDUCATION

GRADUATE STUDIES since 6/2010

PhD thesis
Thesis advisor: Susan M. Gasser
Friedrich Miescher Institute for Biomedical Research, Basel, Switzerland
Title: Regulation of Mec1 (ATR) signalling in budding yeast

UNDERGRADUATE STUDIES

4/2009 - 12/2009

Diploma thesis
Thesis advisor: Silke Hauf
Friedrich Miescher Laboratory of the Max Planck Society, Tuebingen, Germany
Title: Aurora B function in the spindle assembly checkpoint

10/2004 - 12/2009

Degree in biochemistry (core areas: immunology, pharmaceutical chemistry, cell biology, structural biology, protein biochemistry)
Eberhard Karls University, Tübingen, Germany
Grade: 1.0 on a scale of 1 (best) to 6 (worst)

SCHOOL

06/2004

A level (Abitur) in biology, chemistry, politics and latin
Hermann-Billing-Gymnasium, Celle, Germany
Grade: 1.0 on a scale of 1 (best) to 6 (worst), best of class

SCIENTIFIC EXPERIENCE

since 6/2010

PhD student, group of Susan Gasser
Friedrich Miescher Institute for Biomedical Research, Basel, Switzerland
Topic: Regulation of Mec1 (ATR) signalling in budding yeast
Techniques used: budding yeast genetics, molecular biology (PCR, cloning, mutagenesis), biochemistry (radioactivity and non-radioactivity based *in vitro* kinase assays), cell biological techniques (immunoblotting, immunoprecipitation, yeast-two-hybrid assay, chromatin immunoprecipitation) tissue culture (culturing of cancer cell lines, transfection, gene knockdown with siRNA oligos, FACS), high-throughput techniques (yeast genetic interaction screen, suppressor screen, non-labelled phosphoproteomics), programming in R (basic knowledge)

4/2009 - 05/2010

Diploma student/research assistant, group of Silke Hauf
Friedrich Miescher Laboratory of the Max Planck Society, Tuebingen, Germany
Topic: Aurora B function in the spindle assembly checkpoint
Techniques used: fission yeast genetics, cell biological techniques (immunoblotting, immunoprecipitation, immunostaining, protein sample preparation for mass spectrometry), microscopy (wide field fluorescence imaging of living and fixed cells)

- 08/2008 - 09/2008 **internship**, group of Stefan Stevanović
Department of Immunology, Eberhard Karls University, Tuebingen, Germany
Topic: Methods in immunology
- 04/2008 - 03/2009 **research assistant**, group of Silke Hauf
Friedrich Miescher Laboratory of the Max Planck Society, Tuebingen, Germany
Topic: Creating analog-sensitive kinase alleles
- 02/2008 - 03/2008 **lab rotation**, group of Klaus Wanner
Department of Pharmaceutical Chemistry, Ludwigs Maximilian University, Munich
Topic: Establishment of a LC-MS/MS method for quantification of substances in biological matrices
- 11/2007 - 01/2008 **lab rotation**, group of Stefan Jentsch
Department of Molecular Cell Biology MPI for Biochemistry, Martinsried, Germany
Topic: Genetic and biochemical analysis of Mgs1 in DNA damage bypass
- 10/2007 - 11/2007 **lab rotation**, group of Reinhard Fässler
Department of Molecular Medicine, MPI for Biochemistry, Martinsried, Germany
Topic: Generation of α integrin fluorescent reporter protein constructs
- 04/2007 - 09/2007 **research assistant**, group of Andrei Lupas
Department of Protein Evolution, MPI for Developmental Biology, Tübingen, Germany
Topic: Isolation of chaperone proteins
- 11/2006 - 12/2006 **research assistant**, group of Volker Lipka
Center for Plant Molecular Biology, Eberhard Karls University Tübingen, Germany
Topic: Molecular biological work in *A. thaliana* and *E. coli*

PUBLICATIONS

Hustedt N, Seeber A, , Sack R, Tsai M, Bhupinder B, van Leeuwen F, Guenole A, van Attikum H, Srivas R, Ideker T, Shimada K, Gasser SM
Yeast PP4 interacts with ATR homologue Ddc2-Mec1 and regulates checkpoint signaling.
in revision at Molecular Cell

Seeber A*, Hegnauer A*, **Hustedt N**, van Leeuwen F, van Attikum H, Srivas R, Ideker T, Pasero P, Vogel M, Amsler P, Thomae N, Shimada K, Gasser SM
RFA1 recruits MRX to forks and double strand breaks in budding yeast. *in preparation*
*These authors contributed equally to this work

Hustedt, N., and Shimada, K. (2014). Analyzing DNA replication checkpoint in budding yeast. *Methods Mol Biol* 1170, 321-341.

Heinrich S, Sewart K, Windecker H, Langegger M, Schmidt N, **Hustedt N**, Hauf S (2014) Mad1 contribution to spindle assembly checkpoint signalling goes beyond presenting Mad2 at kinetochores. *EMBO Rep* 15: 291-298

Hustedt N, Gasser SM, Shimada K (2013) Replication Checkpoint: Tuning and Coordination of Replication Forks in S Phase. *Genes* 4: 388-434

Hegnauer AM*, **Hustedt N***, Shimada K, Pike BL, Vogel M, Amsler P, Rubin SM, van Leeuwen F, Guenole A, van Attikum H, Thoma NH, Gasser SM (2012) An N-terminal acidic region of Sgs1 interacts with Rpa70 and recruits Rad53 kinase to stalled forks. *EMBO J* 31: 3768-3783
*These authors contributed equally to this work.

Heinrich S, Windecker H, **Hustedt N**, Hauf S (2012) Mph1 kinetochore localization is crucial and upstream in the hierarchy of spindle assembly checkpoint protein recruitment to kinetochores. *J Cell Sci* 125: 4720-4727

CONFERENCE PRESENTATIONS

Abcam conference on Maintenance of Genome Stability 2014, St Kitts

Title: Protein Phosphatase 4: A new player in ATR/Mec1 regulation. (talk)

Cold Spring Harbor Eukaryotic DNA Replication & Genome Maintenance meeting 2013,
Cold Spring Harbor, USA

Title: Genetic and physical interaction between the ATR kinase and PP4 phosphatase in yeast. (poster)

Keystone symposium on Genomic Instability and DNA Repair 2013, Banff, Canada

Title: Mec1 checkpoint kinase regulation by the PP4 phosphatase. (poster)

Yeast Systems Biology Workshop 2012

Fribourg, Switzerland

Swiss meeting on Genome Stability and Chromatin Dynamics 2012, Weggis, Switzerland

Title: Exploring the S-phase function of the Mec1 checkpoint kinase: Genetic and biochemical analysis of a S-phase defective Mec1 mutant. (poster)

Cold Spring Harbor Eukaryotic DNA Replication & Genome Maintenance meeting 2011

Cold Spring Harbor, USA

Title: Mec1 dependent phosphorylation of Sgs1 facilitates replication checkpoint activation by direct interaction with Rad53 at stalled forks. (poster)

TEACHING EXPERIENCE

- | | |
|-------------------|---|
| 02/2014 - 03/2014 | Supervising and teaching undergraduate student in yeast genetics and molecular biology techniques |
| 06/2012 - 08/2012 | Supervising and teaching undergraduate student in yeast genetics and molecular biology techniques |
| 04/2006 - 07/2006 | Teaching a practical course in chemistry for students of human medicine |

GRANTS

- | | |
|------|---|
| 2013 | travel grant from Swiss Society for Molecular and Cellular Biosciences
to to attend a scientific conference |
|------|---|

PROFESSIONAL MEMBERSHIPS

- | | |
|-------------------|--|
| since 03/2012 | Swiss Society for Molecular and Cellular Biosciences |
| 06/2010 - 10/2012 | Image DNA damage response (EU training network) |

OTHER SKILLS / INTERESTS

SOFT SKILLS

- 02/2014 Project Management Workshop
Friedrich Miescher Institute, Basel, Switzerland
- 08/2012 Team Work, Career planning and Leadership Competencies Workshop
Friedrich Miescher Institute, Basel, Switzerland
- 06/2012 Effective Scientific Communication Workshop
University of Basel, Basel, Switzerland

ORGANIZATION SKILLS

since 11/2011 Initiation and organization of literature seminar (Journal Club)

since 06/2010 Organization of lab events (lab hikes, ski days)

LANGUAGE SKILLS:

German:	native speaker
English:	fluent
Spanish:	basic knowledge
Latin:	advanced certificate (Großes Latinum)

NON-SCIENTIFIC INTERESTS:

Outdoor Sports (hiking, climbing, alpine skiing)
Running (e.g. Dreilaenderlauf 2011- 13, Lucerne Marathon 2011)

Dr. Susan Gasser

Friedrich Miescher Institute for Biomedical Research
Maulbeerstrasse 66
P.O. Box 3775
4002 Basel
Switzerland
T: +41 61 69 75025

susan.gasser@fmi.ch

Dr. John Diffley

London Research Institute
44 Lincoln's Inn Fields
London
WC2A 3LY
United Kingdom
T: +44 1707 625869

john.diffley@cancer.org.uk

Dr. Silke Hauf

Virginia Bioinformatics Institute
1015 Life Science Circle (MC 0477)
Blacksburg, VA 24061
United States
T: +1 540 231 7318

silke.hauf@vt.edu

Dr. Fred van Leeuwen

The Netherlands Cancer Institute
Postbus 90203
1006 BE Amsterdam
The Netherlands
31 20 512 1973

fred.v.leeuwen@nki.nl

ACKNOWLEDGEMENTS

It would not have been possible to write this doctoral thesis without the help of Susan Gasser. Her mentoring, continuous support and insightful discussions as well as that of my thesis committee John Diffley, Philippe Pasero and Marc Bühler ensured that I had a successful PhD. Special thanks go to Kenji Shimada for introducing me to the world of yeast genetics and providing much needed brainstorming sessions and essential technical support. Sharing thoughts and ideas with him repeatedly helped me set my priorities.

The communicative atmosphere of the Gasser lab is one characteristic that makes the lab a great place to work. Scientific discussions, technical help as well as proof-reading each other's abstracts, reports and manuscripts shapes this collaborative spirit. It is my pleasure to thank all members of the Gasser lab for their help and support, especially Susan who facilitates such an atmosphere. I would like to specifically mention that I am deeply grateful to Monika Tsai and Razel Arpagaus for maintaining the lab in a clean and well-organized way, which provides a solid base for our research.

The FMI features a number of high-quality technical platforms without which many cutting-edge experiments would not be possible. Among them, I would like to especially thank Ragna Sack from the Protein Analysis Facility for mass spectroscopy analysis and her insights on possibilities and limitations of this technique. Also, Hubertus Kohler from the Cell Sorting and FACS facility greatly supported my work. In addition, Tim Roloff and Sophie Dessus-Babus (Functional Genomics Facility) and Michael Stadler (Computational Biology Facility) provided their know-how for genome sequencing and analysis.

Finally I am very thankful to Bhupinder Bhullar, Haico van Attikum, Aude Guenole, Trey Ideker, Rohith Srivas, Fred van Leeuwen and Hanneke Vlaming for their fruitful research collaborations